APPROVED FOR RELEASE: 2007/02/09: CIA-RDP82-00850R000500010010-4

FOR OFFICIAL USE ONLY

JPRS L/10212

23 December 1981

Translation

OPTICAL CAVITIES AND THE PROBLEM OF DIVERGENCE OF LASER EMISSION

By

Yuriy Alekseyevich Anan'yev

FBIS FOREIGN BROADCAST INFORMATION SERVICE

FOR OFFICIAL USE ONLY

APPROVED FOR RELEASE: 2007/02/09: CIA-RDP82-00850R000500010010-4

APPROVED FOR RELEASE: 2007/02/09: CIA-RDP82-00850R000500010010-4

NOTE

JPRS publications contain information primarily from foreign newspapers, periodicals and books, but also from news agency transmissions and broadcasts. Materials from foreign-language sources are translated; those from English-language sources are transcribed or reprinted, with the original phrasing and other characteristics retained.

Headlines, editorial reports, and material enclosed in brackets [] are supplied by JPRS. Processing indicators such as [Text] or [Excerpt] in the first line of each item, or following the last line of a brief, indicate how the original information was processed. Where no processing indicator is given, the information was summarized or extracted.

Unfamiliar names rendered phonetically or transliterated are enclosed in parentheses. Words or names preceded by a question mark and enclosed in parentheses were not clear in the original but have been supplied as appropriate in context. Other unattributed parenthetical notes within the body of an item originate with the source. Times within items are as given by source.

The contents of this publication in no way represent the policies, views or attitudes of the U.S. Government.

COPYRIGHT LAWS AND REGULATIONS GOVERNING OWNERSHIP OF MATERIALS REPRODUCED HEREIN REQUIRE THAT DISSEMINATION OF THIS PUBLICATION BE RESTRICTED FOR OFFICIAL USE ONLY.

APPROVED FOR RELEASE: 2007/02/09: CIA-RDP82-00850R000500010010-4

APPROVED FOR RELEASE: 2007/02/09: CIA-RDP82-00850R000500010010-4

JPRS L/10212

23 December 1981

OPTICAL CAVITIES AND THE PROBLEM OF DIVERGENCE OF LASER EMISSION

Moscow OPTICHESKIYE REZONATORY I PROBLEMA RASKHODIMOSTI LAZERNOGO IZLUCHENIYA in Russian 1979 (signed to press 29 Oct 79) pp 2-328

[Book by Yuriy Alekseyevich Anan'yev, Izdatel'stvo, 4,000 copies, 328 pages, UDC 539.1]

CONTENTS

Annotation 1
Preface 2

Introduction. Development of Concepts of the Optical Cavity as a Device for Producing Narrowly Directional Emission 4

CHAPTER 1. GENERAL INFORMATION 12

§ 1.1. Laws of Propagation of Light Beams and Angular Divergence of Radiation 12
The Huygens-Fresnel Principle (12). Distribution in the Far Zone (14). The Ideal Emitter (24). Arbitrary Monochromatic Emitter (19). Nonmonochromatic Emitter (25). Some Conclusions. Measurement of Divergence (26).

§ 1.2. Optical Cavities and Classification of Them. 28
Initial Information. A Little History (28). Passage of Light Beams Through Optical Systems. The Beam Matrix (30). Classification of Resonators by the Properties of Their Beam Matrices (35). Conditions of Resonator Equivalence (40).

§ 1.3. Modes of an Empty Ideal Resonator and Their Use for Describing the Laser Situation 42
Classification of Natural Oscillations (42). Integral Equation and Natural Oscillations of an Arbitrary Empty Resonator (46). Resonator With Active Layer (48). Suitability of the Standard Model of an Open Optical Cavity for Describing Real Lasers (50).

§ 1.4. Efficiency of Excitation Energy Conversion in Laser Resonators 52
Efficiency of Energy Conversion in an Element of Volume of the Medium (53). Accounting for Nonuniformity of the Distribution of Laser Radiation Lengthwise of the Cavity (56). General Excitation Energy and Stimulated Emission Balance (58). The Meaning and Possibilities of Applying the Derived Relations (61).

APPROVED FOR RELEASE: 2007/02/09: CIA-RDP82-00850R000500010010-4

APPROVED FOR RELEASE: 2007/02/09: CIA-RDP82-00850R000500010010-4

CHAPTER 2. RADIATION DIVERGENCE OF LASERS WITH STABLE AND FLAT CAVITIES 64

§ 2.1. Modes of Oscillations of Empty Stable Resonators 64
Eigenfunctions and Frequencies of a Stable Resonator with Infinite Mirrors (64). Spacial Structure of Natural Oscillations (67). Stable Resonators with Mirrors of Finite Dimensions (71)

§ 2.2. Edge Diffraction and Modes of Oscillations of an Empty Flat Optical Cavity 74
Auxiliary Diffraction Problem (74). Reflection From the Open Edge of a Waveguide. Natural Oscillations of a Resonator Made up of Strip or Rectangular Mirrors (78). Flat Cavity Made of Circular Mirrors (82). Polarization of Radiation of Natural Modes (85).

§2.3. Some Experimental Research Results 87
Early Observations of Stimulated Emission of Solid-State Lasers (88). Divergence of Radiation of Solid-State Lasers (90).

§2.4. Multimode Lasing in Ideal Optical Cavities 92
Mechanism of Multimode Lasing (92). Procedure and Some Results of Calculations of the Multimode Lasing Regime (96). Competition of Transverse Modes in Lasers with Flat Cavities (99). Deficiencies of the Model and the Possibilities of Improving It. (101).

§ 2.5. Influence of Resonator Deformations on Field Configuration of Individual Modes 103
Some General Remarks. Perturbation Theory (103). Flat Cavities with Minor Aberrations (105). Flat Cavities with Aberrations of Significant Magnitude (109).

§ 2.6. Methods of Angle Selection of Emission 112
Attempts to Solve the Problem of Divergence on the Basis of Resonators with Small Diffraction Losses (112). Lasers with Flat Cavities and Angle Selectors (115). Angle Selection of Emission of Lasers with Flat Cavities by Reducing the Number of Fresnel Zones (119). Flat Cavities of Large Effective Length (121). Multistage Lasers (124).

CHAPTER 3. ELEMENTS OF THE THEORY OF UNSTABLE RESONATORS 127

§ 3.1. Some Initial Information 127
Brief Historical Survey (127). Elementary Examination of the Ideal Unstable Resonator (128). Properties of Convergent Waves (133).

§ 3.2. Resonators with Slightly Inhomogeneous Medium 137
Simplest Method of Accounting for Inhomogeneities of the Medium (137). Aberrational Coefficients (139). Some Comments on the Possibilities of the Geometric Optics Approximation (142).

§ 3.3. Edge Effects and Spectrum of Natural Oscillations 145
Equivalence of Unstable Resonators and Interrelation of the Solutions for Different Types (145). Unstable Cavities with Completely "Smoothed" Edge (147). Unstable Resonators with Sharp Edge (150). Specifics of Edge Effects Under Real Conditions (154).

§ 3.4. Unstable Resonators with Central Coupling Aperture 160
Initial Premises. Oscillations of a Two-Dimensional Resonator that Have a Caustic (160). Two-Dimensional Resonator with Central Aperture (163). Three-Dimension Resonator with Coupling Aperture. Discussion of Results (166).

APPROVED FOR RELEASE: 2007/02/09: CIA-RDP82-00850R000500010010-4

APPROVED FOR RELEASE: 2007/02/09: CIA-RDP82-00850R000500010010-4

§ 3.5. Some Problems of Multiple-Mirror and Prism Unstable Resonators 170
Problem of Monodirectional Lasing Mode (170). Stabilizing the Direction of Radiation in Prism Resonators (175).
§ 3.6. Unstable Resonators with Field Reversal 179
Operation of Cross Section Reversal and Polarization Characteristics of Radiation (179). Aberration Characteristics of Unstable Resonators with Field Reversal (182). Resonators with Compact Output Aperture (185).

CHAPTER 4. APPLICATIONS OF UNSTABLE RESONATORS 189
§ 4.1. Unstable Resonators in Pulsed Free-Running Lasers 189
Selection of the Type and Parameters of the Resonator (189). Results of Experiments with Neodymium Glass Lasers (195). Gas Pulsed Lasers with Unstable Resonators. Problem of Steadying Oscillations (201).
§ 4.2. Unstable Resonators in Continuous Lasers 204
Survey of Experimental Work (204). Methods of Calculating the Efficiency of Flow Lasers (206). Simplest Model of a Gas Dynamic Laser Medium (210). Problem of Forming Uniform Field Distribution Over the Cavity of a Flow-Through Laser (215).
§ 4.3. Unsteady Resonators in Laswers with Controlled Spectral-Temporal Emission Characteristics 218
Simplest Types of Lasers with Control Elements (218). Lasers with Three-Mirror Optical Cavity (221). External Signal-Controlled Lasers (224). Multipass Amplifiers (226).

CHAPTER 5. OPTICAL INHOMOGENEITY OF ACTIVE MEDIA AND METHODS OF CORRECTING WAVE FRONTS 230
§ 5.1. Thermal Deformations of Solid-State Laser Cavities 231
Origin and Magnitude of Thermal Aberrations in the Case of Circular Active Rods (231). Consequences of Aberrations and Attempts to Correct Them (235). Various Methods of Reducing Cavity Deformations (238). Lasers Using Active Elements with Elongated Rectangular Cross Section (241).
§ 5.2. Phase Correction of Wave Fronts. Dynamic Holography and Stimulated Scattering 245
Optical-Mechanical Correction Systems (245). Holographic Correction Principles (247). Conditions of Realizing the Process of Holographic "Transfer" and its Energy Efficiency. "Transfer" on Thermal Gratings (250). Relation of the Idea of Dynamic Holography to the Phenomena of Stimulated Scattering. Lasers Based on Various Forms of Stimulated Scattering (255).
§ 5.3. Method of Wave Front Reversal 258
The Idea and Theoretical Possibilities of the Method (258). "Reversal" in Stimulated Backscattering (261). "Reversal" by Methods of Classical Optics and Holography (264). "Reversal" in Parametric Amplification of Light (267).

BIBLIOGRAPHY 269

APPROVED FOR RELEASE: 2007/02/09: CIA-RDP82-00850R000500010010-4

APPROVED FOR RELEASE: 2007/02/09: CIA-RDP82-00850R000500010010-4

UDC 539.1

OPTICAL CAVITIES AND THE PROBLEM OF DIVERGENCE OF LASER EMISSION

Moscow OPTICHESKIYE REZONATORY I PROBLEMA RASKHODIMOSTI LAZERNOGO IZLUCHENIYA in Russian 1979 (signed to press 29 Oct 79) pp 2-328

[Book by Yuriy Alekseyevich Anan'yev, Izdatel'stvo, 4000 copies, 328 pages]

[Text] The book gives the basics of the theory of optical cavities, and examines the factors that determine divergence of laser emission. Major emphasis is given to the problem of producing narrowly directed radiation; various methods are outlined for reducing angular divergence. The properties of lasers with so-called unstable optical cavities are considered in greatest detail. Methods of calculating and optimizing them are outlined, and the particulars of designs used in a variety of laser devices are discussed. The book also gives some information on factors giving rise to optical inhomogeneities in an active medium, the nature of wuch inhomogeneities, and methods by which their influence can be reduced. Figures: 112, tables 3, references 343.

APPROVED FOR RELEASE: 2007/02/09: CIA-RDP82-00850R000500010010-4

APPROVED FOR RELEASE: 2007/02/09: CIA-RDP82-00850R000500010010-4

PREFACE

The work of Nobel Prize winners N. G. Basov, A. M. Prokhorov and C. Townes (United States) has led to the creation of coherent light generators — lasers. Operating lasers appeared in 1960. Among the astonishing characteristics that attracted general attention, first of all it is necessary to mention divergence of the emission — the degree of directionality of a coherent light beam is theoretically limited only by diffraction at the exit aperture of the laser, and many people have held the opinion that there is no obstacle to achieving this maximum directionality. The literature of that time was full of optimistic predictions with respect to the possibilities for using lasers in super-long communication lines (including space), for long-distance power transmission, and so on. All of these predictions were, as a rule, based on simple manipulations with the known formula for the diffraction limit of divergence of emission $\phi_0 = 1.2\ \lambda/D$, where λ is the emission wavelength and D is the coherent light beam diameter. Actually, for ruby lasers ($\lambda = 0.694$ micron) which appeared first, the value of ϕ_0 is $4 \cdot 10^{-5}$ radian or 8 angular seconds for an easily attainable crystal diameter! However, the first observations of stimulated emission of such lasers, the active media of which were 6 to 10 mm in diameter, demonstrated that the angular divergence of their emission was appreciably greater than expected (usually by one or two orders).

Analysis of the causes of such behavior on the part of lasers and influencing them in the required direction turned out to be far from a simple matter. Countless experiments, the development of the theory of real resonators with active medium which, to a great extent, is based on the theory of ideal empty resonators developed in 1961-1966, and so on were required for this purpose. All of this spilled into the overall area of quantum electronics combining a great variety of methods of controlling the spatial characteristics of laser emission. Many of these methods are of great theoretical interest; as for practical importance of work aimed at decreasing the angular divergence of emission, it can hardly be over-estimated. Therefore it is no surprise that an enormous number of publications are devoted to the problem of divergence. However, up to the present time there has been no serious effort to discuss the fundamental concepts of the given problem as a whole. In all of the books on laser theory and laser engineering, in the best case the results of the theory of ideal resonators with optically homogeneous active medium (or empty resonators) are presented. The several surveys which have investigated individual special problems have not filled the gap. The present book would appear to be useful in this respect, and to what degree it has served this purpose can be best determined by its readers, whose suggestions will be appreciated and receive immediate attention.

APPROVED FOR RELEASE: 2007/02/09: CIA-RDP82-00850R000500010010-4

APPROVED FOR RELEASE: 2007/02/09: CIA-RDP82-00850R000500010010-4

We have presented only the most general information from the theory of empty ideal resonators which is needed to understand the following material. A somewhat more detailed study has been made of the problem of the divergence of emission in resonators with small diffraction losses, primarily in the most widespread resonator with flat mirrors. The discussion of this problem does not claim to be especially complete: a laser with a flat cavity is in essence a highly complicated oscillatory system with an enormous number of resonance frequencies subjected to the powerful influence of the most minute disturbance. Therefore the problem of the emission divergence of lasers with flat cavities, which is closely related to a still more complicated and general problem of their kinetics is truly inexhaustible. The book contains only information which suffices to explain the general situation and which is needed to read specialized literature.

Lasers with so-called unstable resonators are then discussed. The building of these lasers is the result of an area of research, representatives of which have tried not so much to provide an exhaustive description of systems with an enormous number of degrees of freedom as to limit the number of degrees of freedom. Although not everyone has become accustomed to lasers with unstable resonators, they are, in essence, much simpler than traditional lasers with flat cavities. They do not have such an abundance of Q-similar modes and sensitivity to the most minute disturbances. Therefore the theory of lasers with unstable resonators has already advanced farther than the theory of other types of lasers that appeared much earlier. The results of this theory will be discussed in considerable detail; attention has also been given to the most important experimental papers.

In conclusion, there is a brief study of the problem of optical inhomogeneity of active media, and some efforts to solve this problem are discussed.

The author is deeply indebted to N. A. Sventsitskaya, V. Ye. Sherstovitov, O. A. Shorokhov, N. I. Grishmanov, V. P. Kalinin, L. V. Koval'chuk and other of his colleagues for their participation in joint work with the author, the discussion of the results of which constitutes a significant part of this monograph, and for their assistance in preparing the manuscript for publication. There were useful discussions of individual topics with V. V. Lyubimov, M. S. Soskin. The author is also indebted to P. V. Zarubin and Ye. N. Sukharev, whose suggestions led to many editorial corrections.

The author found the constant attention and active support of Rem Viktorovich Khokhlov in the writing of this monograph especially meaningful. The monograph is dedicated to the memory of Rem Viktorovich Khokhlov.

Leningrad, August 1977 Yu. Anan'yev

APPROVED FOR RELEASE: 2007/02/09: CIA-RDP82-00850R000500010010-4

APPROVED FOR RELEASE: 2007/02/09: CIA-RDP82-00850R000500010010-4

INTRODUCTION

Development of Concepts of the Optical Cavity as a device for Producing Narrowly Directional Emission

The first papers on the feasibility of making resonators in the optical band for stimulated emission of coherent radiation were published by Prokhorov, and also by Shawlow and Townes in 1958. These papers to a great extent predetermined the course of research that led to the development of lasers.

As we know, laser action is based on the capacity of certain media under certain conditions to amplify luminous radiation passing through them. Therefore there is no doubt that a major role is played by the properties of the active medium itself and the method of stimulating it; however, the properties of the resonant cavity in which this medium is located also have an enormous influence on many characteristics of stimulated emission. Taking a central place among such characteristics is the angular divergence of emission. Here the resonator plays a truly decisive role: without a resonator, the active medium in itself as a rule is capable of amplifying the radiation passing through it to equal advantage no matter what the direction of propagation.

Optical oscillators made their appearance much later than rf and microwave oscillators. Therefore the concepts and terminology borrowed from these related fields are extensively used in describing optical oscillators, and we will continue this practice.

To convert an oscillator to an amplifier, it is necessary, in the language of electronics, to close the output of the amplifier to its input, to set up a feedback circuit (Figure 1, a). The essence of the feedback circuit is that part of the amplified radiation goes back into the system, is amplified again and so on, in this way maintaining a continuous signal — oscillation. Oscillators in the optical band amplify a light beam rather than an electric signal. In this connection, the feedback circuit must meet new requirements: after transmission through the feedback circuit the beam mustretain its original direction of propagation and structure. The simplest analog of Figure 1, a that meets these requirements is the optical resonance shown in Figure 1, b. Actually, such resonators, called ring cavities, have found some application. However, the first resonator in optics was a conventional Fabry-Perot interferometer made up of two flat mirrors (Figure 1, c). One mirror is partly transparent, and the stimulated emission is coupled out through it. The principal difference of this resonator from the ring cavity is that the feedback circuit passes through the same active medium, and the emission is repeatedly amplified.

APPROVED FOR RELEASE: 2007/02/09: CIA-RDP82-00850R000500010010-4

APPROVED FOR RELEASE: 2007/02/09: CIA-RDP82-00850R000500010010-4

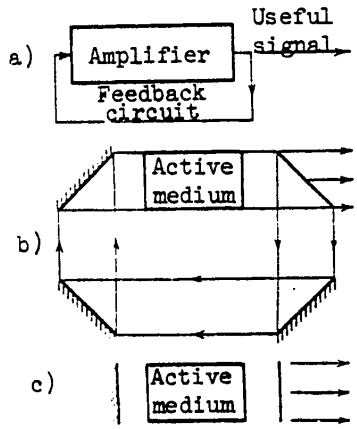

Figure 1. Diagrams of oscillators: a) oscillator in electronics; b) oscillator in optics; c) laser with flat optical cavity.

The Fabry-Perot interferometer has been such a successful resonator system that even today it is the most widely used type of laser cavity. Such popularity is due not only to extreme simplicity, but also to the capability of attaining high energy characteristics of output emission (the reasons for this will be taken up in section 1.4). However, the situation with regard to divergence of emission stimulated in flat-mirror cavities was trivial. The origin of comparatively large divergence is explained to a great extent by theoretical analysis of the properties of the flat optical cavity, which can be done by methods developed previously for resonant cavities in the microwave band. Such analysis shows that transmission through the feedback circuit in a flat cavity reproduces not just any beam directed along the axis and nearly parallel with it, but only a beam with strictly defined distribution of the amplitude and phase of the wave front. This beam is called the fundamental wave form (mode) of the cavity. What is more remarkable however, is that there are also beams (modes) that are reproduced with somewhat greater attenuation in which emission propagates at small but nonetheless noticeable angles to the axis of the cavity. These beams form a discrete set; the angle of inclination to the axis for modes that are neighbors in classification differs by approximately half the diffraction angle.

Thus, a flat cavity in some sense (and, of course, within certain limits) is indifferent to the direction of emission propagating through it. The roots of such indifference are in the fact that upon passage through the feedback circuit the oblique beams, like the axial beam, retain their original directions of propagation; they are prevented from "walking off" by edge diffraction. The mechanism of such diffraction will be taken up in section 2.2.

Because of differences in attenuation, the different off-axis modes have somewhat different thresholds of excitation; however, because of nonlinearity of the medium, these modes can be present simultaneously in the stimulated emission (Chapter 2), which should lead to a large angular divergence of the beam. For this reason, flat cavities with large aperture cannot give small beam divergence even when the medium is highly homogeneous.

APPROVED FOR RELEASE: 2007/02/09: CIA-RDP82-00850R000500010010-4

APPROVED FOR RELEASE: 2007/02/09: CIA-RDP82-00850R000500010010-4

Such is the situation in the idealized case of an optically homogeneous medium. An even greater disadvantage of the flat cavity from the standpoint of the directionality of radiation is the extremely sharp dependence of the field distribution in the cavity on slight distortions of shape (deformation). This can be explained by the simple example of a misaligned cavity. Nonparallelism of the mirrors is equivalent to insertion of an optical wedge in the feedback circuit that changes the beam direction by an angle δ that is twice the angle of misalignment. If we send a parallel beam into such a cavity, it will be turned through an angle δ after the first pass, through 2δ after the second and so on. Its displacement in the transverse direction will increase even faster, and a considerable part of the radiation will begin to leave the system, missing the mirrors. After a certain number of passes (a fairly large number for small δ), the beam shape is distorted so much that it becomes impossible to analyze the process of further propagation without consideration of diffraction effects. Therefore it is no simple matter to represent the steady-state field distribution in graphic form. In essence this distribution is the result of equilibrium between processes of diffraction and beam rotation. We emphasize that this equilibrium is reached after a process of accumulation of aberrations over a number of passes. It is also noteworthy, as shown by analysis (section 2.5), that there is a rapid rise in the number of passes over which aberrations accumulate with an increase in the cross sectional dimensions of the optical cavity. Therefore flat cavities with mirrors of large dimensions are particularly sensitive to slight aberrations.

The situation is similar, but even more complicated in the case of irregular deformations of the cavity. In general, the sources of such deformations are extremely varied: they include errors of manufacture and alignment of mirrors, initial optical inhomogeneity of the active medium, inhomogeneity induced during pumping due to nonuniform excitation and heating of the medium, scattering of light by microscopic inclusions, mechanical vibrations of the active element, turbulence of gas flow, and the list could be extended. It is no wonder that a great many papers have dealt with the problem of a nonideal flat resonator, most of them published in 1965-1969. The results of research dealing with the most common principles of behavior of lasers with nonideal optical cavities will be given in section 2.5. Of course, none of this research could eliminate the fundamental flaws of the flat optical cavity, but it has been very useful for an understanding of the processes that take place in a real cavity.

In these same years, as much research was done to find some new solution of the laser beam divergence problem. Two areas of such research can be distinguished.

Representatives of one of these areas tried without giving up the flat cavity to put into the feedback circuit so-called angle selectors: filters that transmit radiation only in a narrow range of angles. Such filters can be made by different methods: on the basis of total internal reflection, by additional Fabry-Perot étalons, by a combination of lenses and irises. All these methods were tried; however, subsequently because of considerable complications and a number of fundamental difficulties that will be taken up in section 2.6, they found only a few special applications.

Proponents of the other area of research have attempted to solve the problem of divergence (or at least single-mode lasing) by altering the shape of the mirrors rather than by complications in the design of the optical cavity. In particular, there has been a thorough investigation of lasers with so-called stable resonators,

FOR OFFICIAL USE ONLY

APPROVED FOR RELEASE: 2007/02/09: CIA-RDP82-00850R000500010010-4

APPROVED FOR RELEASE: 2007/02/09: CIA-RDP82-00850R000500010010-4

in which one or both mirrors are slightly curved (the equivalent of placement of a weak positive lens in the feedback circuit). Obviously in such a system a steady-state beam with approximately uniformly distributed amplitude and phase and a front close to planar should have such a small cross section that the focusing effect of the mirrors is compensated by the defocusing of the beam due to diffraction. This is the source of the main disadvantage of stable resonators: they are capable of single-mode lasing only with very small volumes of the active medium. And it is in lasers with small volumes of the working medium that stable resonators are still being used; an example is the ordinary helium-neon laser. If the volume of the medium is large, wide beams are produced in stable resonators with a complicated beam structure corresponding to an angular divergence larger than in flat cavities under the same conditions (sections 2.3 and 2.4).

Some other forms of optical cavities with small diffraction losses have also been investigated (section 2.6), but these were also failures.

This situation led to the general opinion that the problem of directionality of radiation could not be solved by improving the optical cavity, and that the only possible way was to make multistage systems of a maser laser and amplifiers (since amplifiers are not troubled with the effect of multiple accumulation of aberrations, like the flat cavity). A way out of this dilemma was suggested by Siegman's research with a simplified analysis of an "unstable resonator (in the accepted classification; section 1.2), which is formed by two convex mirrors. This analysis showed that in such a resonator, just as in the ideal flat optical cavity, there is a solution in the geometric approximation, only diverging rather than parallel beams propagate in both directions along the cavity, and part of the radiation passes the mirrors (section 3.1). At first Siegman's paper did not stir up any particular interest: some researchers were already working with unstable resonators, and were getting only undesirable side effects rather than encouraging results (see the beginning of section 3.1). And Siegman himself even switched his attention to the unusual features of edge effects in unstable resonators, devoting some years to the study of this problem, which is interesting, but as we will show below is far from decisive. From the standpoint of directionality of radiation, the most interesting peculiarities of unstable resonators were discovered ony with analysis of the influence of aberrations on steady-state field distribution. It was as a result of such an analysis that it became clear that the resonator considered by Siegman was only the first of an extensive class of cavities in which feedback conforms to a totally new algorithm that has a number of fundamental advantages.

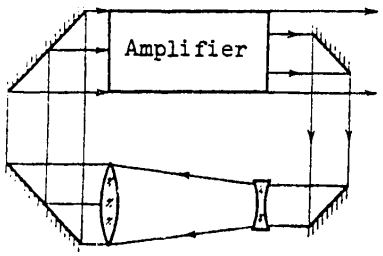

Figure 2. Diagram of a laser with unstable resonator.

APPROVED FOR RELEASE: 2007/02/09: CIA-RDP82-00850R000500010010-4

APPROVED FOR RELEASE: 2007/02/09: CIA-RDP82-00850R000500010010-4

The essence of this new algorithm is clarified by Figure 2. In the flat cavity, part of the radiation from the entire cross section of the output beam was introduced into the feedback loop (see Figure 1, b). In the unstable resonator as a rule all the radiation is fed back, but only from part of the cross section. For reproducibility of the process, the feedback circuit obviously has to be made in such a way that the beam is widened. In Figure 2, the wave front is planar and the beam is expanded by a telescopic system, but quite different versions are possible. In particular, the dimensions of the cross section of a parallel beam are also altered when it is reflected from a diffraction grating, and when it passes obliquely through the interfaces of media with different indices of refraction. Thus lenses and spherical mirrors are not at all obligatory equipment for an unstable resonator.

Now let us examine what advantages could be realized by what would seem to be such a minor change in the algorithm. As in the case of a flat cavity, let an optical

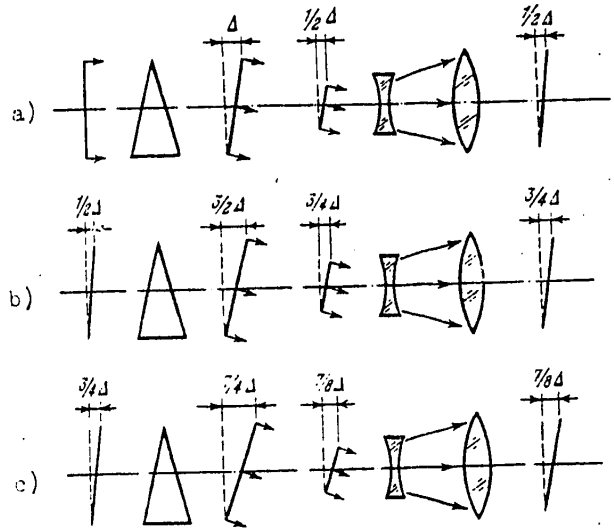

Figure 3. Accumulation of wave aberrations in an unstable resonator when an optical wedge is inserted.

wedge be inserted within the system, leading to rotaton of the beam, and let this rotation correspond to a magnitude of wave aberrations Δ (Figure 3,a). Part of the beam goes to the feedback loop; in the case shown in the figure, its transverse dimension is half the size of the entire beam. On this part of the cross section, the magnitude of the wave aberrations is of course equal to 1/2 Δ. When the cross section of the beam is stretched out by the methods enumerated above, the magnitude of the wave aberrations does not change; therefore by the beginning of the next cycle a beam arrives at the input of the system with aberration of 1/2 Δ, rather than Δ as in the case of a flat cavity. Upon passage through the system, another Δ is added (see Figure 3,b) and by the end of the second cycle the magnitude of the wave aberrations becomes 3/2 Δ. By the beginning of the third cycle it is 3/4 Δ, by the end -- 7/4 Δ (Figure 3,c) and so on. It can be seen that this quantity at the limit approaches 2Δ. Thus, the wave aberrations in the steady state are found to be only twice the level in a single pass. In this situation, shifting of the beam in the transverse direction does not generally play any particular part; it

APPROVED FOR RELEASE: 2007/02/09: CIA-RDP82-00850R000500010010-4

APPROVED FOR RELEASE: 2007/02/09: CIA-RDP82-00850R000500010010-4

leads only to slight redistribution of the fractions of the beam passing to different sides of the output mirror, but the feedback loop remains completely filled.

In the case of arbitrarily distributed sources of aberrations, of course there are changes in the quantitative factors, but the qualitative patterns remain the same: the accumulation of wave aberrations of the beam takes place over the calculated number of passes (see section 3.2). As the fraction of the beam cross section directed into the feedback loop decreases, this number approaches unity, a quantity typical of single-stage amplifiers.

We can also conclude from the example given in Figure 3 that in the unstable resonator there is only one form of wave front that is retained after the beam passes through the feedback loop. Actually the direction of the light beam admitted to the optical cavity rapidly approaches the unique equilibrium direction (which in the case of Figure 3 corresponds to steady-state wave aberrations 2Δ). Thus in contrast to the flat optical cavity, the unstable resonator displays rigorous selectivity with respect to the direction of emission; it would seem that here the effects of multimode lasing should have no influence on the magnitude of angular divergence.

These encouraging deliberations concerning the properties of unstable resonators, implied by the simplest geometric approximation, are confirmed as well by more thorough analysis in the diffraction approximation (section 3.3). Moreover, detailed acquaintance with the properties of unstable resonators allows us to formulate the following statement: if the operation of a laser in which a large volume of comparatively homogeneous active medium has been used is strongly influenced by diffraction, this means that errors have been made in its creation. At first glance this statement seems to be paradoxical; in all previously used optical cavities the beam structure has been determined in the final analysis by diffraction. However, this statement has a firm logical basis. The final goal is to produce a laser with minimum angular beam divergence; this goal is fully attainable in a homogeneous medium. Beams with minimum divergence are those for which the wave front is flat or spherical; it is well known that the propagation of such beams to short distances is beautifully described by the geometric approximation, without resorting to the concept of diffraction.

This covers the conceptual aspect, and we turn now to practice.

The scheme with two convex mirrors considered in Siegman's first paper was never used in that form, remaining a favorite subject of research for theoreticians in view of its symmetry. But then, a number of specialized schemes enabling solution of some problems in laser technology by much simpler means than before became popular.

Among these problems, of course, is the very problem of constructing simple laser emitters with high efficiency and low angular divergence of radiation. In most cases of practical importance, the so-called telescopic cavity (section 4.1) is suitable for solving this problem, being an asymmetric confocal system made up of a convex and a concave mirror. In this system the path of the rays differs from that of Figure 2 only in the spatial congruence of two oppositely directed beams, that is, in the same way that the scheme of Figure 1,c differs from that of Figure 1,b. Also of interest is the ring version of the telescopic cavity, wherein conditions are readily brought about such that the radiation flux propagating along the ring

APPROVED FOR RELEASE: 2007/02/09: CIA-RDP82-00850R000500010010-4

APPROVED FOR RELEASE: 2007/02/09: CIA-RDP82-00850R000500010010-4

to one side, without the use of nonreciprocal devices, should be many times greater than the flux following in the reverse direction (section 3.5).

There are a number of new possibilities associated with the idea of utilizing the particular role that is associated with the paraxial region in the unstable resonator. This idea is as follows. If we trace the path of the rays in an unstable resonator over several cycles, we can see that radiation "spreads out" over the entire cross section from a small area that is contiguous with the line that is the axis of the resonator. By introducing emission into the region with predetermined temporal and spectral characteristics, we can obviously accomplish effective control of the radiation of the entire laser. When the "seed" radiation is taken from an external source and coupled in through an aperture in the mirror on the axis of the optical cavity, our device becomes simply a multipass amplifier with very high gain (section 4.3). As the emission intensifies, the cross section of the beam expands, which facilitates attainment of the limiting possible energy characteristics. Control of radiation properties on the basis of this principle can also be realized by making single lasers that have the valuable property that the cross sections of the control elements that are used in them (shutters, spectral selectors) are many times less than the cross sections of the output apertures.

Some special problems can be successfully solved by a slight modification of the feedback algorithm. As an example, we can cite the problem of stabilizing the direction of radiation; this problem arises in the widely encountered case where there is an optical wedge inside the resonator with a size that changes during the lasing pulse (that is, because of mechanical vibrations of the active element). To strongly attenuate the influence of the wedge, it is sufficient to construct a feedback loop such that the beam is reversed in addition to the expansion of the cross section. If this change is made in the version shown in Figure 3, by the beginning of the second cycle the magnitude of wave aberrations is equal to -0.5Δ, by the end of the cycle it is $-0.5\Delta + \Delta$; by the beginning of the third cycle it is -0.25Δ, and by the end it is $+0.75\Delta$ and so on. In the final analysis a front is set up at the output of the system with aberration of 0.67Δ, that is, one-third of the value in the case of Figure 3. Let us note that both Figure 3 and the example now being considered are essentially different types of telescopic ring cavities. In the case of non-ring systems where the beam in following the feedback loop passes through the same wedge, designs can be developed with even better stability of the direction of the output beam (section 3.5).

Finally, we must not fail to mention problems that arise with the appearance of a number of new types of lasers. For example in the so-called fast-flow lasers the active medium passes through the optical cavity in the transverse direction, often with excitation beforehand rather than in the cavity. This leads to radiation field distribution patterns that are totally different from those of previously existing lasers; in particular, when flat mirrors are used, lasing can be localized in a narrow zone close to the edge of the cavity where the active medium enters. The density of the stimulated emission there is naturally extremely high. A completely analogous situation occurs in the transversely pumped Raman lasers. Difficulties of this kind are easily overcome by using unstable resonators: a kind of self-balanced mode arises, and the radiation flux is distributed more or less uniformly over the cross section of the cavity (section 4.2).

All these possibilities were quite quickly realized in specific devices (see Chapter 4). Thus within only a few years after the publication of the first report on experimental observation of angle selection in an unstable resonator it became

APPROVED FOR RELEASE: 2007/02/09: CIA-RDP82-00850R000500010010-4

APPROVED FOR RELEASE: 2007/02/09: CIA-RDP82-00850R000500010010-4

completely clear that this was the optical cavity that is optimum for the most diverse forms of lasers with narrow-beam emission.

All the aspects mentioned above, as well as some other facets of the problem of divergence will be dealt with more rigorously and consistently later. Before we go into this, let us note one interesting feature of the history of this problem. We have just spoken of the extent to which solution of the problem of divergence is obstructed by appreciable inhomogeneities of the active medium. The results of considerable research in the early sixties (section 2.3) showed that difficulties also pile up rapidly with increasing diameters of the lasing beams: the diffraction limit of divergence is difficult to attain only in the case where the diameter of the active element is large, and the limit is correspondingly small. If beam diameter is reduced (that is, by irising the cavity) to a size on the order of 1 mm or smaller, the beam divergence as a rule is on the diffraction level even when no special steps are taken.

The first gas lasers, typified by the pre-eminent helium-neon laser, operated on an active medium confined in a rather slender discharge tube, and produced a light beam of small diameter. The mixture itself was quite rarefied, and a negligible amount of power (by present-day standards of laser technology) was expended on excitation; therefore the active medium was nearly ideally homogeneous. Due to this confluence of circumstances, the developers of gas lasers did not come up against the problem of divergence in earnest for many years. It might seem to the superficial observer that this problem is specific in general to solid-state lasers, and arose primarily because of the imperfectness of solid active media. However, in recent years the intense development of gas laser physics has led to new types of lasers such as chemical, gasdynamic and other types, with power many orders of magnitude greater than that of the familiar helium-neon lasers. The rise in radiation power is being achieved by an increase in the pressure of the working medium, the dimensions of the space that it occupies, and specific energy inputs on excitation. All this entails considerable optical inhomogeneities of the medium. Thus, the problem of beam divergence has turned out to be a problem of all lasers with high emission power, not just solid-state lasers. The developers of high-power gas lasers are now coming up against just about the same difficulties as were previously encountered by the developers of the solid-state laser, and they are using just about the same methods of solving them. For this reason, research in the field of gas lasers has not added much new information on methods of angle selection. Most of the research that has played a large part in solution of the problem of divergence, and that will be used in this book, has been on solid-state lasers.

APPROVED FOR RELEASE: 2007/02/09: CIA-RDP82-00850R000500010010-4

APPROVED FOR RELEASE: 2007/02/09: CIA-RDP82-00850R000500010010-4

CHAPTER 1. GENERAL INFORMATION

§ 1.1. Laws of Propagation of Light Beams and Angular Divergence of Radiation

Huygens-Fresnel Principle. We shall use the scalar theory of diffraction to study the propagation laws of laser-generated coherent light beams. The essence of this approximation consists in the fact that the different transverse components of an electric or magnetic field are considered to be independent of each other, and they are considered separately.

The conditions of applicability of the scalar theory of diffraction are discussed in detail in [6]. In the previously investigated situations where the transverse dimensions of light beams and the paths traveled by them are many times (frequently even several orders) greater than the wavelength, these conditions are automatically satisfied.

The most important expression of scalar diffraction theory, which is one of the possible mathematical formulations of the Huygens-Fresnel principle, follows:

$$u(x_2, y_2) = \frac{1}{2i\lambda}\int\int\frac{\exp(ikr_{12})}{r_{12}}[1+\cos(n, r_{12})]\,u(x_1, y_1)\,dx_1dy_1. \qquad (1)$$

Here, x_1, y_1, x_2, y_2 are the transverse coordinates of points in the source plane and the observation plane parallel to it (Figure 1.1), r_{12} is the radius vector joining these points, n is the common normal to the planes, $k = 2\pi/\lambda$; finally, the function of the transverse coordinates u(x, y) which varies slightly at distances of $\sim\lambda$ is the complex field amplitude.

Expression (1) allows calculation of the field $u(x_2, y_2)$ in the second plane by the given field distribution in the first plane $u(x_1, y_1)$; the medium is considered to be homogeneous, the source is considered to be strictly monochromatic with time-dependence of the type $\exp(-i\omega t)$ such that $u(x, y, t) = u(x, y)\exp(-i\omega t)$, and the actual value of the field intensity is equal to $\mathrm{Re}[u(x, y)\exp(-i\omega t)]$. Let us note that the conversion from the field intensity u(x, y, t) to the emission intensity I(x, y) will be made hereafter by the formula $I(x, y) = \langle|u(x, y, t)|^2\rangle$, where the angular brackets denote averaging over an infinite time interval. For a monochromatic source $I(x, y) = |u(x, y)|^2$.

The transverse dimensions of the region in which the field is nonzero will almost always be considered limited and not too large. In cases where an opaque screen with a hole in it is located in the first plane, and the field sources themselves

APPROVED FOR RELEASE: 2007/02/09: CIA-RDP82-00850R000500010010-4

APPROVED FOR RELEASE: 2007/02/09: CIA-RDP82-00850R000500010010-4

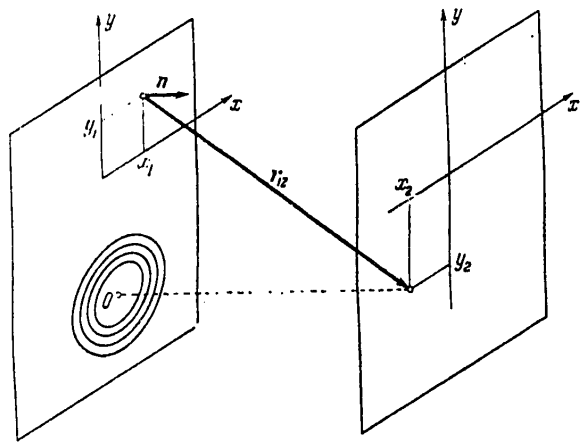

Figure 1.1. Huygens-Fresnel principle.

are located to the left of this screen, we shall adhere to Kirchhoff's principle. According to Kirchhoff's principle, when calculating the field in the second plane, integration in (1) must be performed only over the area of the hole. It is assumed that the presence of the screen has no influence on the field distribution in the hole vicinity (which is valid when the hole dimensions are significantly greater than λ).

As a rule, in the theory of optical resonators it is necessary to consider so-called paraxial beams, the angles of inclination of which to the system axis are small. This allows replacement of cos (n, r_{12}) in expression (1) by one.

Then, in the overwhelming majority of cases of practical importance, it is possible to replace the exact value of $r_{12}=\sqrt{z^2+(x_2-x_1)^2+(y_2-y_1)^2}$ in the exponent by the approximate value $r_{12}= z+(x_2-x_1)^2/2z+(y_2-y_1)^2/2z$, and it is possible to replace r_{12} in the denominator of the expression under the integral sign simply by the spacing between the planes z. Thus,

$$u(x_2, y_2) = \frac{\exp(ikz)}{i\lambda z}\int\int \exp\left\{ik\left[\frac{(x_2-x_1)^2}{2z}+\frac{(y_2-y_1)^2}{2z}\right]\right\} u(x_1, y_1)\, dx_1 dy_1. \qquad (2)$$

Formula (2) is usually called the Fresnel approximation. A detailed investigation of its limits of applicability appears in many optics handbooks (see, for example, [7]). We shall discuss only one important item here.

Although the assumption of limited transverse dimensions of the source was used in deriving (2), formulas of this type will sometimes be used hereafter for infinite integration limits. In order to understand how these formulas apply in this case, let us use (2) to derive the propagation laws of an infinite plane wave. Let this wave be directed along the z-axis so that the plane xy is its equiphasal surface: $u(x_1, y_1) = C = \text{const}$. Then (2) acquires the form

APPROVED FOR RELEASE: 2007/02/09: CIA-RDP82-00850R000500010010-4

APPROVED FOR RELEASE: 2007/02/09: CIA-RDP82-00850R000500010010-4

$$u(x_2, y_2) = \frac{C \exp(ikz)}{i\lambda z} \int_{-\infty}^{\infty}\int_{-\infty}^{\infty} \exp\left\{ik\left[\frac{(x_2 - x_1)^2}{2z} + \frac{(y_2 - y_1)^2}{2z}\right]\right\} dx_1 dy_1.$$

The improper interval in the form in which it appears in the right-hand side, does not converge in general. Actually, we shall break down the integration surface into so-called Fresnel zones, inside the first of which the phase of the expression under the integral sign varies from 0 to π, and inside the second, from π to 2π, the third, from π to 3π, and so on. As is easy to see, the Fresnel zone boundaries form a system of concentric circles with the center at the point 0 located opposite the observation point (see Figure 1.1). Their radii r_n are defined in the given case by the relations $(k/2z)r_n^2 = n\pi$ or $r_n = \sqrt{n\lambda z}$. Representing our surface integral in the form of a sum Σ of all integrals over individual Fresnel zones and performing the integration (for which it is more convenient to convert from cartesian coordinates to polar coordinates with the center at the point 0), in the final analysis we obtain the following expression: $\Sigma = (2i/\pi)(s_1 - s_2 - s_4 + \ldots)$, where s_1, s_2, s_3, ... are areas of the corresponding Fresnel zones. Inasmuch as $s_1 = s_2 = \ldots = \pi\lambda z$, the sum of this series does not approach a limit; hence, we have the corresponding statement with respect to the initial integral.

In order to overcome this difficulty, it is sufficient to consider that formula (1), which is more exact than (2), contains a factor in its expression under the integral sign which decreases slowly as the direction of the emission diverges from the normal to the source plane. Therefore in reality, in increasing order the terms of the series must decrease slowly, but regularly. In this case the sum of the series approaches a defined limit which does not in practice depend on the law by which the terms of the series decrease, and is equal to the half of the first of them (see, for example, [6], § 8, 2). Thus, $\Sigma = is_1/\pi$. In the final analysis we obtain the correct result: $u(x_2, y_2) = C \exp(ikz)$.

The presented arguments indicate that the operation of intermediate integration in infinite limits is entirely regular. This operation is necessary, for example, if the field in the plane of the source depends on only one of the cartesian coordinates. Then integration over the other coordinate leads to the following analog of formula (2) for the two-dimensional problem:

$$u(x_2) = \frac{\exp(ikz)}{\sqrt{i\lambda z}} \int \exp\left[ik\frac{(x_2 - x_1)^2}{2z}\right] u(x_1)\, dx_1. \tag{2a}$$

Distribution in the Far Zone. Now let us proceed to the primary topic of this section -- the problem of angular divergence of emission. Using (2), let us investigate the field distribution at large distances from the source z such that the inequality

$$z \gg \frac{k}{2}(x_1^2 + y_1^2)_{\max} \tag{3}$$

is satisfied. Then it is possible to neglect the terms with x_1^2 and y_1^2 in the expression under the integral sign. Also taking the terms with x_2^2, y_2^2 out to the common phase factor in front of the integral, we obtain

APPROVED FOR RELEASE: 2007/02/09: CIA-RDP82-00850R000500010010-4

APPROVED FOR RELEASE: 2007/02/09: CIA-RDP82-00850R000500010010-4

$$u(x_2, y_2) = \frac{\exp\left[ik\left(z + x_2^2/2z + y_2^2/2z\right)\right]}{i\lambda z} \times \iint \exp\left[-\frac{ik}{z}(x_1x_2 + y_1y_2)\right] u(x_1, y_1)\, dx_1 dy_1. \quad (4)$$

Finally, if we characterize the position of the observation point not by its cartesian coordinates but by the slope angles $\alpha_x = x_2/z$, $\alpha_y = y_2/z$ and the distance of z from the source, we obtain the especially descriptive formulas:

$$u(\alpha_x, \alpha_y, z) = \exp\left[ikz\left(1 + \alpha_x^2/2 + \alpha_y^2/2\right)\right] \times$$
$$\times \frac{1}{i\lambda z} \iint \exp\left[-ik(\alpha_x x_1 + \alpha_y y_1)\right] u(x_1, y_1)\, dx_1 dy_1, \quad (5)$$

$$I(\alpha_x, \alpha_y, z) = \frac{1}{z^2} F(\alpha_x, \alpha_y),$$
$$F(\alpha_x, \alpha_y) = \left| \frac{1}{\lambda} \iint \exp\left[-ik(\alpha_x x_1 + \alpha_y y_1)\right] u(x_1, y_1)\, dx_1 dy_1 \right|^2. \quad (6)$$

From these formulas it follows that the forms of emission distribution in the planes at different distances sufficiently removed from the source coincide, except the distribution scale increases proportionally to the distance z, and the density varies, correspondingly, $\propto 1/z^2$. Here, according to (5), the angular amplitude distribution is the Fourier transform of the amplitude distribution over the source cross section calculated for spatial frequencies $f_x = \alpha_x/\lambda$, $f_y = \alpha_y/\lambda$ with accuracy to the factor in front of the integral (for more details see [7]). The value of $F(\alpha_x, \alpha_y)$ introduced in (6) is none other than the radiation flux per unit solid angle. In classical photometry, this value was usually called the luminous intensity in the given direction; adhering to the presently more popular terminology, we shall call the function $F(\alpha_x, \alpha_y)$ the angular distribution of the radiation intensity (or the intensity distribution in the far zone), and we shall keep the term axial luminous intensity only for F(0, 0). We shall use the same notation for the angular distribution of the emission and nonmonochromatic sources, although formulas (5), (6) cease to be applicable here.

The intensity distribution width in the far zone is also the angular divergence of the light beam. Most frequently, when discussing divergence, we mean the so-called "divergence with respect to the 0.5 intensity level"; this is the width of the range of angles in which the intensity is no less than 0.5 of the maximum value. However, real emitters frequently have broad distribution "wings," for which a significant part of the power is required. Therefore the magnitude of the divergence with respect to the 0.5 intensity level, that is, in essence, the width of the central distribution maximum, is not very indicative unless the fraction of the total power contained in this maximum is known. The value usually called the divergence with respect to the 0.5 energy level has greater practical significance; this is the angular diameter of a circle in the far zone which encompasses half of the total radiation flux.

Before we proceed with analysis of specific examples, let us note the following characteristic features of the angular distribution of a monochromatic emitter which are a consequence of the Fourier transformation characteristics:

1) if the field distribution over the emitter aperture $u(x_1, y_1)$ can be represented in the form $u_x(z_1)u_y(y_1)$, then the expression for the angular distribution breaks down into the product of two cofactors

APPROVED FOR RELEASE: 2007/02/09: CIA-RDP82-00850R000500010010-4

APPROVED FOR RELEASE: 2007/02/09: CIA-RDP82-00850R000500010010-4

$$F(\alpha_x, \alpha_y) = F_x(\alpha_x)\, F_y(\alpha_y); \tag{7}$$

2) if one of the emitter dimensions is increased by K times while maintaining the form of the distribution over the aperture, the divergence of the emission in this direction decreases by K times.

Now let us proceed with the investigation of some important cases which will be encountered in the following sections.

The Ideal Emitter. We shall consider the emitter ideal if its complex field amplitude is constant in the exit cross section (aperture). It is possible to use only a hole in an opaque screen lighted by a point light source arranged so that the beam in the vicinity of the hole will be sufficiently uniform with respect to density and have plane wave front, as the optical system of such an emitter. Therefore, previously we talked about diffraction at the corresponding hole instead of an emitter of one form or another. Now the semitransparent end of a laser rod frequently plays the role of the ideal emitter.

It is easy to see that the maximum angular intensity distribution for an ideal emitter is always in the axial direction. An extraordinarily simple formula for the axial luminous intensity follows directly from (6):

$$F(0, 0) = \left| \frac{1}{\lambda} \int\int u_0 dx_1 dy_1 \right|^2 = \frac{|u_0|^2 S^2}{\lambda^2},$$

where u_0 is the field amplitude at the exit aperture of the emitter, S is the aperture (hole) area. If we consider that the value of $u_0^2 S$ is none other than the radiation flux through the entire exit aperture or the emitter power P, then

$$F(0, 0) = PS/\lambda^2. \tag{8}$$

Thus, for given power of the ideal emitter, its axial luminous intensity is directly proportional to the area of the exit aperture, and it does not depend on the shape of the exit aperture.

For emitters having identical power and aperture shape, but different transverse dimensions, the proportionality F(0, 0) of the area is trivial, and it follows directly from the already noted decrease in divergence with increase in transverse dimensions. Although the form of the emitter does not count in (8), it is possible to use (8) to develop the critierion for estimating the form of the emitter beginning with requirements imposed on the emitter when combining it with an external emission shaping system [8]. The fact is that in all cases where it is necessary to obtain maximum range (light ranging and detection, distance measurement, and so on), the basic element of the shaping system is the telescope turned with its eyepiece in the direction of the emitter (Figure 1.2). The telescope enlarges the transverse dimensions of a narrowly directional light beam by $K = f_2/f_1$ times, where f_1 and f_2 are the focal lengths of the objective and the eyepiece, K is the power of the telescope; the form of the complex amplitude distribution of the field in the first approximation is maintained. As was pointed out above, with this procedure the divergence of the emission decreases by K times. The axial luminous

APPROVED FOR RELEASE: 2007/02/09: CIA-RDP82-00850R000500010010-4

APPROVED FOR RELEASE: 2007/02/09: CIA-RDP82-00850R000500010010-4

intensity increases by K^2 times, respectively; in the case of the ideal emitter, even after the telescope, the luminous intensity continues to be defined by expression (8) (the emission wave front remains plane), except now S acquires significance of the beam cross sectional area at the exit from the telescope.

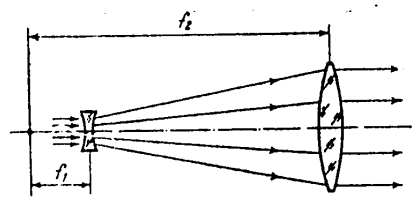

Figure 1.2. Galileo telescope.

If the objective dimensions are given and the vignetting losses are not permitted, the maximum axial luminous intensity is reached for the telescope power where the light beam cross section is exactly "inscribed" in the objective cross section, which is usually a circle. This situation is illustrated by Figure 1.3 where the cross sections of two emitters (a, b) and light beams at the telescope exit (c, d) are depicted on the same scale. Let us note that the forms of the emitters presented in the figure correspond to the same laser with different resonator systems (see § 4.2). From the figure it is clear that the axial luminous intensity in such devices is independent of the dimensions of the ideal emitter and can be defined by the formula

$$F(0, 0) = \frac{S_0}{\lambda^2} P\gamma, \tag{9}$$

where S_0 is the area of the telescopic objective, P is as before the emitter power (after subtracting the losses in the telescope), γ is the filling factor which depends only on the form of the emitter and is equal to the ratio of the emitter area to the area of the described circle (this circle is none other than the required cross section of the telescope eyepiece). When comparing ideal emitters of equal power, preference must be given to the emitters having larger γ (in our case, the emitter depicted in Figure 1.3,b). Sometimes for the sake of increasing axial

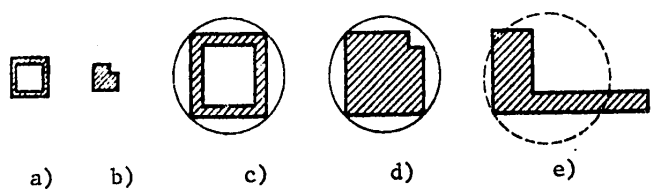

Figure 1.3. Influence of the form of the ideal emitter on the axial luminous intensity in the presence of an external shaping system: a), b) ideal emitters of identical area but different form; c), d) light beam cross sections at the exit of the shaping system; e) selection of shaping system for an emitter of irregular shape.

APPROVED FOR RELEASE: 2007/02/09: CIA-RDP82-00850R000500010010-4

APPROVED FOR RELEASE: 2007/02/09: CIA-RDP82-00850R000500010010-4

luminous intensity, it is even possible to relinquish part of the radiation power if γ can be increased significantly as a result. Thus, in the case illustrated in Figure 1.3,e, it is expedient to use only that part of the beam cross section located inside the dotted curve.

Let us conclude the investigation of ideal emitters by presenting data on the emission divergence with the simplest aperture shapes — rectangle, circle, ring. In the case of a 2a × 2b rectangle, performing the integration in (6) within the corresponding limits ($-a \leq x \leq a$, $-b \leq y \leq b$), we obtain

$$\frac{F(\alpha_x, \alpha_y)}{F(0, 0)} = \left[\frac{\sin(ka\alpha_x)}{ka\alpha_x}\right]^2 \left[\frac{\sin(kb\alpha_y)}{kb\alpha_y}\right]^2.$$

Thus, in accordance with (7), the expression for the intensity distribution in the far zone breaks down into the product of two cofactors here. Each of them depends on only one angular coordinate, and it is the distribution for a source in the form of an infinite strip (slot) of width h, equal to 2a or 2b, respectively; the form of this distribution is presented in Figure 1.4. This figure does not require special comment; let us only note that the width of the maximum with respect to the 0.5 intensity level is $\sim 0.9\ \lambda/h$.

For a circular aperture the distribution in the far zone is naturally axisymmetric, and it is described by the formula

$$\frac{F(\alpha)}{F(0)} = 4\left[\frac{J_1(ka\alpha)}{ka\alpha}\right]^2,$$

where $\alpha = \sqrt{\alpha_x^2 + \alpha_y^2}$ is the angle between the observation direction and the axial direction, a is the radius of a circle, J_1 is the Bessel function. The form of the distribution is presented in Figure 1.5 (curve I). The angular dimensions of the far-field pattern, as always, are inversely proportional to the emitter dimensions. The pattern itself consists of a central light spot surrounded by a system of concentric light circles (distribution peaks) with dark intervals (minima) separating them. The intensity of the light circles diminishes rapidly with an increase in radius (in order to reproduce two more peaks, except the central peak, it is necessary to increase the scale on the pattern, beginning with $\alpha = \lambda/2a$, by tenfold). In contrast to the case of a rectangle, the maxima and minima are not equidistant; on going away from the center, the spacing between adjacent rings asymptotically approaches the value of $\lambda/2a$. The angular radius of the first peak is $1.22\lambda/2a$; thus, the central spot occupies a region with angular width of $2.44\lambda/2a$. This region requires 84% of the total power of the circular emitter, the first ring (more precisely, the region between the first and second minima) requires 7%, and the second, 3%.

In the case of an emitter in the form of a ring with the same outside radius a and inside radius εa

$$\frac{F(\alpha)}{F(0)} = \frac{4}{(1-\varepsilon^2)^2}\left[\frac{J_1(ka\alpha)}{ka\alpha} - \varepsilon^2\frac{J_1(\varepsilon ka\alpha)}{\varepsilon ka\alpha}\right]^2.$$

APPROVED FOR RELEASE: 2007/02/09: CIA-RDP82-00850R000500010010-4

APPROVED FOR RELEASE: 2007/02/09: CIA-RDP82-00850R000500010010-4

The distribution graphs for two such ring emitters with ring width $a(1 - \varepsilon)$ differing by a factor of two, are presented in the same Figure 1.5 (curve II, $\varepsilon = 0.6$, and curve III, $\varepsilon = 0.8$). For convenience of comparison, all the curves are shown on the same scale, the powers of all three emitters are identical; the axial luminous intensity of the first (circular) emitter is taken as the unit luminous intensity.

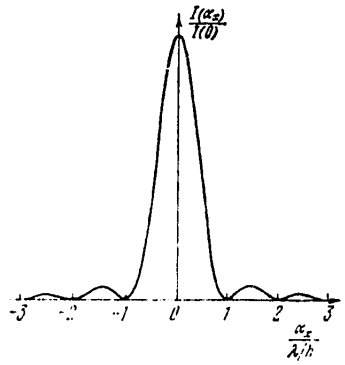

Figure 1.4. Intensity distribution in the far zone for a source in the form of an infinite strip with constant amplitude.

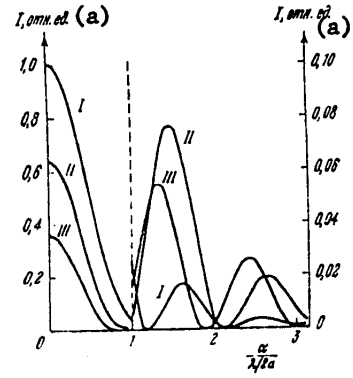

Figure 1.5. Intensity distribution in the far zone for ideal emitters with exit cross section in the form of a circle (I) and rings with ratios of the inside diameters to outside diameters of 0.6 (II) and 0.8 (III).

Key: a. I, relative units

In accordance with (8), the axial luminous intensity of ring emitters decreases with the area occupied by them, and in the adopted units it is equal to $1 - \varepsilon^2$, which is 0.64 for the second emitter and 0.36 for the third. Thus, the height of the central peak drops significantly; the width of this peak also is somewhat less than for a circular emitter (it can be shown that the width of this peak is determined by the average distance between different sections of the emitting surface which is greater for the ring than for the circle). Therefore the fraction of the total power required for the central peak drops sharply, amounting to 37% for the second emitter and only 17% for the third emitter. The radiation intensity at large angles to the axis increases correspondingly: in the second emitter 35 and 15% of the total power is required for the first two distribution rings in the far zone (instead of 7 and 3% for the first emitter), and for the third emitter, 20 and 18% of the total power are required.

It is worth while to note the following: for our three emitters the angular divergence measured with respect to the 0.5 intensity level is 1.03 $\lambda/2a$, 0.87 $\lambda/2a$ and 0.79 $\lambda/2a$, respectively; with respect to 0.5 power level (see above) the angular divergence is 1.06 $\lambda/2a$, 2.9 $\lambda/2a$ and 5.25 $\lambda/2a$. With this instructive example, we conclude our analysis of the emission divergence of systems with a plane wave front and uniform intensity distribution over the exit aperture.

Arbitrary Monochromatic Emitter. The axial luminous intensity of an arbitrary monochromatic emitter is, in accordance with (6) equal to $F(0, 0) = \left|\frac{1}{\lambda}\iint u(x_1, y_1)\,dx_1 dy_1\right|^2$.

APPROVED FOR RELEASE: 2007/02/09: CIA-RDP82-00850R000500010010-4

APPROVED FOR RELEASE: 2007/02/09: CIA-RDP82-00850R000500010010-4

Introducing the total emitter power $P = \iint |u(x_1, y_1)|^2 dx_1 dy_1$ and the area of the exit aperture S, we can represent this expression as follows: $F(0, 0) = \frac{PS}{\lambda^2}\gamma'$, where

$$\gamma' = \frac{|(1/S)\iint u(x_1, y_1)\, dx_1 dy_1|^2}{(1/S)\iint |u(x_1, y_1)|^2 dx_1 dy_1} = \frac{|\bar{u}|^2}{\overline{|u|^2}}. \tag{10}$$

As is known, for an arbitrary complex function u, the relation $|\bar{u}|^2/|u|^2 \leq 1$ is valid. Equality is achieved only when u = const. Hence, it follows directly that out of all possible emitters having identical powers and areas of exit aperture, the one in which the complex field amplitude at the exit cross section is constant, that is, the ideal emitter, has the greatest axial luminous intensity (this is why we call it the ideal emitter). This is, perhaps, the only general conclusion of interest to us which can be formulated with respect to the properties of the angular distribution for arbitray emitters (not considering the above-mentioned still more general law that the distribution in the far zone is a Fourier transform of the distribution with respect to the exit aperture or in the near zone). Therefore let us proceed with investigation of the most important special cases.

The emitters in which only the intensity distribution in the near zone is nonuniform and the phase is constant (the wave front is plane) differ little from ideal emitters with respect to their properties. For the mentioned nonideal emitters $u(x_1, y_1) = e^{i\phi_0}A(x_1, y_1)$, where A is not a complex coordinate function, but a real, nonnegative coordinate function. From (6) it is easy to see that in this case, just as for ideal emitters, the maximum of the intensity distribution in the far zone is in the axial direction. The dimensionless coefficient γ' which enters into the expression for the axial luminous intensity as a factor is equal to $\gamma' = (\bar{A})^2/\overline{A^2} < 1$, and it acquires the meaning of the fraction of the aperture area effectively filled with emission. If the aperture over which averaging is carried out when calculating γ', is circular, this parameter becomes entirely analogous to the parameter γ introduced for real emitters. In particular, under the condition of replacing γ by γ', formula (9) remains valid for the axial luminous intensity after the external shaping system.

It is important that the coefficient γ' becomes significantly less than one only for very large nonuniformity of the field distribution with respect to aperture. Let us present the following numerical example. Let the exit aperture of the emitter consist of two zones of identical area, over one of which the fraction ε of the total radiation flux is distributed uniformly, and over the other, the remaining flux is also uniformly distributed. For such an emitter (10) leads to the formula $\gamma' = 0.5 + \sqrt{\varepsilon(1 - \varepsilon)}$; for $\varepsilon = 0.2$ the parameter γ' is 0.9; for $\varepsilon = 0.1$, $\gamma' = 0.8$.

Let us consider another example. Let the radiation density at the exit aperture assume all values from 0 to some maximum with equal probability. In this case $\gamma' = \left[\int_0^1 \sqrt{x}\, dx\right]^2 \left[\int_0^1 x\, dx\right]^{-1} = 0{,}89$. From these examples it obviously follows that the nonuniformity of the field amplitude distribution is felt comparatively weakly on the magnitude of the axial luminous intensity (and the emission divergence along with it).

APPROVED FOR RELEASE: 2007/02/09: CIA-RDP82-00850R000500010010-4

APPROVED FOR RELEASE: 2007/02/09: CIA-RDP82-00850R000500010010-4

Phase inconstancy in the exit cross section has much greater influence on the distribution in the far zone. We shall investigate the frequently encountered case of quadratic dependence of the phase on the transverse coordinates in the greatest detail. This corresponds (if the coefficients on x_1^2 and y_1^2 are equal) to a spherical wave front. Thus, $u(x_1, y_1) = A(x_1, y_1)\exp\left[\frac{ik}{2\rho}(x_1^2 + y_1^2)\right]$; here $A(x_1, y_1)$ is a real, nonnegative coordinate function, ρ is the radius of curvature of the wave front. For $\rho > 0$ the wave front has convex shape (a diverging beam), and for $\rho < 0$, concave (the beam constricts at first).

Substituting this expression for $u(x_1, y_1)$ in (6), we obtain

$$F(\alpha_x, \alpha_y) = \left|\frac{1}{\lambda}\iint A(x_1, y_1)\exp\left[\frac{ik}{2\rho}(x_1^2 + y_1^2) - ik(\alpha_x x_1 + \alpha_y y_1)\right]dx_1 dy_1\right|^2 = \left|\frac{1}{\lambda}\iint \exp\left\{ik\left[\frac{(x_1 - \rho\alpha_x)^2}{2\rho} + \frac{(y_1 - \rho\alpha_y)^2}{2\rho}\right]\right\} A(x_1, y_1)\,dx_1 dy_1\right|^2.$$

From a comparison of this formula with (2) it follows that for a wave front with a radius of curvature of $\rho > 0$, the form of the angular distribution coincides with the density distribution pattern $I(x_2, y_2)$ on the observation plane removed a distance $z = \rho$ from the source with the same amplitude $A(x_1, y_1)$, but plane wave front (the conversion from a linear scale to angular is made by formulas $\alpha_x = x_2/\rho$, $\alpha_y = y_2/\rho$). If we change the sign on ρ, the similarity of these patterns is retained except one of them turns out to be inverted with respect to the other.

The results of beam diffraction with plane wave fronts have been investigated in sufficient detail in optics. At short distances ($z \ll a^2/\lambda$, where a is the characteristic size of the source), the shape and sizes of the spot quite precisely reproduce the shape and sizes of the source. For $z \gg a^2/\lambda$ the spot, on the contrary, can "blur" completely, and we have a far zone -- the shape of the spot repeats the angular distribution of the emission.

As applied to the case of a spherical wave front of interest to us, this information is interpreted as follows. For $|\rho| \ll a^2/\lambda$ or $a^2/\lambda|\rho| \gg 1$, the width of the angular distribution is simply equal to the source dimensions divided by $|\rho|$; this is none other than the angle between the edge beams normal to the wave front. Thus, the divergence of the emission here has a purely "geometric" origin. For $a^2/\lambda|\rho| \ll 1$, the curvature of the wave front, on the contrary, is so insignificant that it ceases to be felt in the emission divergence (the deflection of the wave front can be less than λ); here it is possible to talk about purely "diffraction" divergence. If we consider that the parameter $a^2/\lambda|\rho|$ is equal to the ratio of the "geometric" divergence $a/|\rho|$ to the "diffraction" divergence λ/a, the meaning of what has been said becomes entirely obvious. It remains only to trace in specific examples how the "geometric" and "diffraction" divergences change relative to each other as the steepness of the wave front changes.

This is done most simply in the case of a so-called gaussian beam, the axisymmetric amplitude distribution of which is described by a gaussian function $A(r) = A_0\exp[-(r/w)^2]$, where $r = \sqrt{x^2 + y^2}$, w is the beam radius defined as the distance at which the field amplitude decreases by e times by comparison with its value on the axis (Figure 1.6). Let us note that the intensity is cut in half at a distance $w\sqrt{(1/2)\ln 2}$ from the axis; thus, the total beam width with respect to the 0.5 intensity level is $w\sqrt{2\ln 2} \approx 1.2w$.

APPROVED FOR RELEASE: 2007/02/09: CIA-RDP82-00850R000500010010-4

APPROVED FOR RELEASE: 2007/02/09: CIA-RDP82-00850R000500010010-4

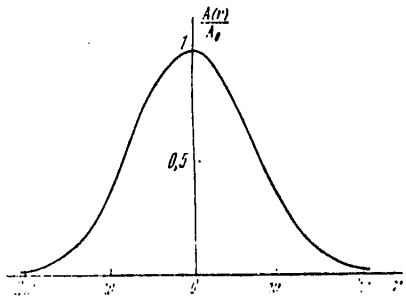

Figure 1.6. Amplitude distribution with respect to the gaussian beam cross section.

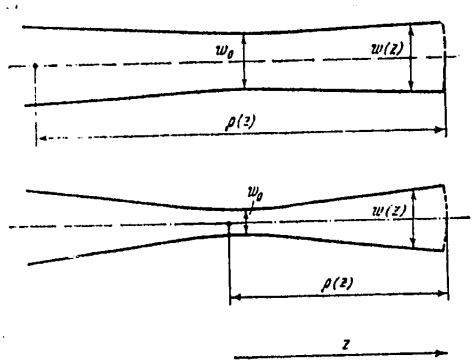

Figure 1.7. Propagation of gaussian beams in free space.

As we see below, gaussian beams play an important role in the theory of "stable" resonators. A most remarkable feature of such beams is the extraordinary simplicity of the laws of their diffraction propagation. Actually, when using (2) it is easy to see that at any distance from the source with a spherical wave front and gaussian amplitude distribution the beam remains gaussian as before with a spherical wave front; only the curvature of the front and the beam radius w vary. The minimum transverse dimension is reached at the "constriction" (neck), where the wave front is plane (Figure 1.7). Of course, the "neck" occurs in reality only when the beam has negative radius of curvature at the source exit, that is, it is constricted; for $\rho > 0$ the beam has an imaginary neck, the location of which is uniquely determined by its parameters.

If the general phase lead (see § 2.1) is neglected, the propagation of gaussian beams in free space is exhaustively described by the following two expressions, an illustration of which is presented in Figure 1.7:

$$w^2(z) = w_0^2\left[1 + (\lambda z/\pi w_0^2)^2\right], \tag{11}$$

$$\rho(z) = z\left[1 + (\pi w_0^2/\lambda z)^2\right]. \tag{12}$$

APPROVED FOR RELEASE: 2007/02/09: CIA-RDP82-00850R000500010010-4

APPROVED FOR RELEASE: 2007/02/09: CIA-RDP82-00850R000500010010-4

Here w is the beam radius at a distance z from the neck, w_0 is its value at the neck, ρ is the radius of curvature of the wave front.

By using these expressions it is easy to find the radiation divergence of a gaussian beam with spherical wave front of interest to us. Knowing ρ and w, it is possible to reproduce the position of the neck and the radius of the beam in it. However, it is still simpler to use the fact that, as was noted above, the far field pattern for a beam with radius of curvature of the wave front ρ is similar to the emission distribution pattern at a distance ρ from an analogous source with plane front. In accordance with (11), at a distance ρ from the source of the gaussian beam of radius w and with plane front the beam radius is $w\sqrt{1 + (\lambda\rho/\pi w^2)^2}$; proceeding from the linear dimension to angular, we find that the angular radius of gaussion distribution in the far zone is $(w/\rho)\sqrt{1+(\lambda\rho/\pi w^2)^2} = \sqrt{(w/\rho)^2 + (\lambda/\pi w)^2}$. Hence, it follows that angular divergence with respect to the 0.5 intensity level is $\ln 2 \cdot \sqrt{(w/\rho)^2 + (\lambda/\pi w)^2} = \sqrt{\left(\ln 2 \cdot \frac{w}{\rho}\right)^2 + \left(\frac{\ln 2}{\pi}\frac{\lambda}{w}\right)^2}$. It is easy to see that $\ln 2(w/\rho)$ is "geometric" divergence, and $(\ln 2/\pi)(\lambda/w)$ is "diffraction" divergence. Thus, in the given case the square of the resultant divergence is equal to the sum of the squares of the geometric and diffraction distribution widths.

Let us consider another example of a beam with uniform intensity distribution with respect to a rectangular aperture. In this case $F(\alpha_x, \alpha_y)$ decays into the product of two like co-factors, each of which is the angular distribution of the source emission in the form of an infinite strip with cylindrical shape of the wave front. Figure 1.8 shows the results of numerical calculations of the intensity distribution in the far zone for such a source for different relations between the geometric divergence h/ρ and the diffraction divergence λ/ρ (h is the strip width). The radiation density in the far zone is taken the same in all cases, and the axial luminous intensity of an ideal "strip" source with plane wave front ($\rho = \infty$) is taken as the unit for measuring the intensity in the far zone. Here the shapes of the geometric and diffraction distributions, in contrast to the preceding case, do not coincide, and the resultant pattern is much more complicated than for a gaussian beam.

Let us emphasize the following. As is easy to see, the geometric and diffraction divergences are equal to each other when the deflection of the wave front is a total of $\lambda/8$. For deflection λ, the geometric divergence is eight times the diffraction divergence and completely predominates over it. As follows from a comparison of curves 1 and 4 in Figure 1.8, the presence of this deflection with respect to only one of the coordinates causes a decrease in the axial luminous intensity by more than 11 times as compared to an ideal source; if analogous deflection occurred also in the other direction, the axial luminous intensity would decrease by as many times! This again demonstrates the enormous influence on the distribution in the far zone felt from even such small phase disturbances.

Now let us proceed to another type of source which we must deal with hereafter. We are again talking about beams with plane equiphasal surface, but the real amplitude of the field on this surface will be a sign-variable value. Let us limit ourselves to the simplest case of uniform distribution of the complex amplitude of the type

APPROVED FOR RELEASE: 2007/02/09: CIA-RDP82-00850R000500010010-4

APPROVED FOR RELEASE: 2007/02/09: CIA-RDP82-00850R000500010010-4

$$u_m(x) = \begin{cases} \cos\frac{(m+1)\pi x}{2a}, & m = 0, 2, 4, \ldots, \\ \sin\frac{(m+1)\pi x}{2a}, & m = 1, 3, 5, \ldots, \end{cases} \quad -a \leqslant x \leqslant a. \tag{13}$$

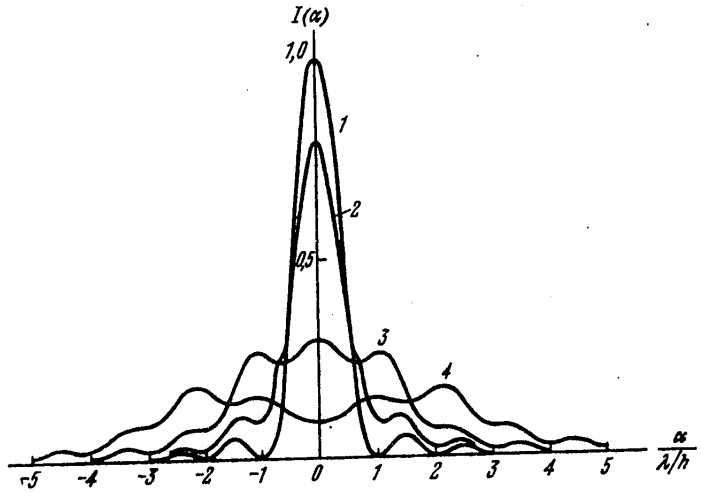

Figure 1.8. Angular emission distributions of sources with uniformly distributed amplitude and spherical wave front: 1 — "geometric" divergence is missing (the plane wave front is the same curve as in Figure 1.4); 2 — $h/\rho = 2\lambda/h$ (the deflection of the wave front is $\lambda/4$); 3 — $h/\rho = 4.5\lambda/h$ (the deflection of the wave front $9\lambda/16$); 4 — $h/\rho = 8\lambda/h$ (the wave front deflection is λ).

These functions assume zero values at the ends of the interval, and they each have m zeros inside; thus, all of them, except the first, are sign-variable. Let us write them as follows:

$$u_m(x) = \cos\left\{\frac{\pi}{2}\left[\frac{(m+1)x}{a} + m\right]\right\} = \\ = \frac{1}{2}\exp\left\{\frac{i\pi}{2}\left[\frac{(m+1)x}{a} + m\right]\right\} + \frac{1}{2}\exp\left\{-\frac{i\pi}{2}\left[\frac{(m+1)x}{a} + m\right]\right\}. \tag{14}$$

The field with complex amplitude of the type C exp(ikxα) for $\alpha \ll 1$ is a plane wave inclined at an angle α with respect to the axis. Therefore $u_m(x)$ is a superposition of two mutually coherent plane waves, the directions of propagation of which make the angles ±(m + 1)/2)(/2a). Calculating $\int_{-a}^{a} \exp(-ik\alpha_x x)\, u_m(x)\, dx$ (см. (6)), we obtain

$$F_m(\alpha_x) \infty \left\{ \frac{\sin\left[ka\left(\alpha_x - \frac{m+1}{2}\frac{\lambda}{2a}\right)\right]}{ka\left(\alpha_x - \frac{m+1}{2}\frac{\lambda}{2a}\right)} + (-1)^m \frac{\sin\left[ka\left(\alpha_x + \frac{m+1}{2}\frac{\lambda}{2a}\right)\right]}{ka\left(\alpha_x + \frac{m+1}{2}\frac{\lambda}{2a}\right)} \right\}^2$$

APPROVED FOR RELEASE: 2007/02/09: CIA-RDP82-00850R000500010010-4

APPROVED FOR RELEASE: 2007/02/09: CIA-RDP82-00850R000500010010-4

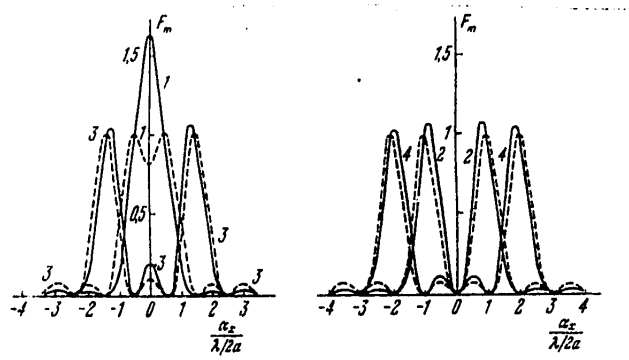

Figure 1.9. Distributions in the far zone for coherent and noncoherent superpositions of two plane waves. Solid curves — source with amplitude distribution of the type (13); dotted curves — incoherent sum of the same waves; curves 1, 2, 3, 4 — for m = 0, 1, 2, 3, respectively.

The graphs of $F_m(\alpha_x)$ for the first four functions are presented in Figure 1.9 (solid curves). We shall return to this figure soon, but let us note meanwhile that the sign-variable nature of the amplitude leads not only to growth of the divergence, but also to decay of the angular distribution into individual spots with comparable intensity (in our example when considering the analogous distribution with respect to the second coordinate $yF(\alpha_x, \alpha_y)$ there would be four peaks of equal magnitude). The angular distances between the spots are $\sim\lambda/\Delta$, where Δ is the distance between the amplitude distribution nodes in the near zone.

Nonmonochromatic Emitter. Let our source emit a set of monochromatic waves with different frequencies simultaneously:

$$u(x_1, y_1, t) = u_1(x_1, y_1)\exp(-i\omega_1 t) + u_2(x_1, y_1)\exp(-i\omega_2 t) + \ldots$$

Thanks to the superposition principle the field at any distance from the source can be written in analogous form:

$$u(x_2, y_2, t) = u_1(x_2, y_2)\exp(-i\omega_1 t) + u_2(x_2, y_2)\exp(-i\omega_2 t) + \ldots,$$

where the complex amplitude $u_i(x_2, y_2)$ of each component is calculated by substitution of $u_i(x_1, y_1)$ in the standard expressions presented at the beginning of this item. In accordance with the formula there, let us calculate the emission intensity averaged over a large time interval (the indices on x and y are omitted, the * will denote complex conjugation):

$$\begin{aligned} I(x, y) &= \langle |u(x, y, t)|^2 \rangle = \langle u(x, y, t)\, u^*(x, y, t) \rangle = \\ &= \langle [u_1 \exp(-i\omega_1 t) + u_2 \exp(-i\omega_2 t) + \ldots] \times \\ &\quad \times [u_1^* \exp(i\omega_1 t) + u_2^* \exp(i\omega_2 t) + \ldots] \rangle = \\ &= |u_1(x, y)|^2 + |u_2(x, y)|^2 + \ldots \end{aligned}$$

APPROVED FOR RELEASE: 2007/02/09: CIA-RDP82-00850R000500010010-4

APPROVED FOR RELEASE: 2007/02/09: CIA-RDP82-00850R000500010010-4

All of the cross terms oscillate with difference frequencies; therefore when averaging over a large time interval they do not contribute to the general sum. Thus, the total field intensity turns out to be equal to the sum of the intensities of individual monochromatic waves.

Let us again consider Figure 1.9. Graphs of the functions

$$F'_m(\alpha_x) = \left\{\frac{\sin\left[ka\left(\alpha_x - \frac{m+1}{2}\frac{\lambda}{2a}\right)\right]}{ka\left(\alpha_x - \frac{m+1}{2}\frac{\lambda}{2a}\right)}\right\}^2 + \left\{\frac{\sin\left[ka\left(\alpha_x + \frac{m+1}{2}\frac{\lambda}{2a}\right)\right]}{ka\left(\alpha_x + \frac{m+1}{2}\frac{\lambda}{2a}\right)}\right\}^2$$

are plotted on it as dotted curves for the same m as the solid curves. Thus, if the solid curves correspond to the case of coherent addition of two plane waves figuring in (14), the dotted curves correspond to incoherent addition of the same waves which could occur at different frequencies.

From this example it is obvious that the coherent and incoherent additions can lead to significantly different results. On the other hand, it is possible to see that the differences here are small except in cases where both added waves have noticeable intensity. This is understandable inasmuch as coherent addition differs from incoherent by consideration of the cross terms which include the amplitude cofactors of different waves.

We have paid definite attention to what would appear to be a quite elementary problem, for an unclear distinction between the concepts of coherent and incoherent additions is also encountered in the literature on optical resonators. Most frequently the confusion arises when using a standard procedure consisting in expansion of the field distribution of a real device in a series with respect to the eigenfunctions of an ideal system (see, for example, § 2.5). Such a series frequently contains high-order terms which, if taken separately, correspond to very great beam divergence. This appears to be a sign that the total divergence is large, but in reality it can be quite the opposite. Let us present an instructive example. Let the amplitude distribution u = C = const which is rectangular in the interval $-a < x < a$ be expanded in a series with respect to the functions of (13); $u = \frac{4C}{\pi}\left(u_0 - \frac{u_2}{3} + \frac{u_4}{5} - \frac{u_6}{7} + \ldots\right)$. Here, as a result of coherent addition successive consideration of terms of higher and higher order does not lead to an increase in the total divergence, but to a decrease (to be convinced of this, it is sufficient to compare the solid curve 1 in Figure 1.9 which pertains to the first term of the sum with Figure 1.4 which corresponds to the final result of summation).

Some Conclusions. Measurement of Divergence. The above investigation of the angular divergence of the emission of different sources is not at all exhaustive, but it should make it easier to understand how certain factors considered hereafter influence the divergence. The primary conclusion which can be drawn is that for systems with narrowly directional emission it is necessary first of all to strive for maximum uniform phase distribution of the emission with respect to the exit aperture. Nonuniformity of the amplitude distribution is far from so terrible (the case of sign-variable amplitude which would seem to be exempt from this rule can be interpreted as the case where there are phase jumps of π). Even multifrequency is dangerous only when a significant portion of the total energy goes to the components either with great divergence or with different directions of propagation.

APPROVED FOR RELEASE: 2007/02/09: CIA-RDP82-00850R000500010010-4

APPROVED FOR RELEASE: 2007/02/09: CIA-RDP82-00850R000500010010-4

In conclusion, let us consider the problem of measuring the angular divergence. On analysis of expression (2), we saw that the transition to the far zone where the form of the distribution ceases to depend on the distance is related to the possibility of neglecting the terms containing x_1^2 and y_1^2 in the phase factor of the expression under the integral sign. Under ordinary conditions, for this purpose it is necessary that the inequality (3) be satisfied, which, as a rule, requires significant removal from the emission source. Thus, for $\lambda = 0.5$ micron (green light) and a source diameter of 3-5 cm, the far zone is completely formed only at a distance on the order of several kilometers. However, it is easy to achieve complete absence of the mentioned terms also in direct proximity to the emission source. For this purpose, it is necessary to install the so-called quadratic phase corrector at the source exit; the simplest device of this type is an ordinary thin lens with spherical surfaces. The fact is that with small thickness of the lens, the field amplitude distribution does not change on passing through the lens. The curvature of the wave front only changes discontinuously, which is equivalent to the addition of a phase factor of the type of $\exp[i\gamma(x^2 + y^2)]$. It is easy to calculate the coefficient γ knowing the index of refraction of the lens material and radius of curvature of its surfaces; however, it is possible to proceed more simply. Actually, it is known of a positive lens ($f > 0$) that it converts a spherical wave front from a point source at its focal point to a plane front. The radius of curvature of a spherical front at the approach to the lens will be f in this case; the complex amplitude of the field with such a wave front has, as we already know, the phase factor $\exp[(ik/2f)(x^2 + y^2)]$. The phase is constant at the plane wave front; thus, passage through a lens with a focal length f leads to multiplication of the complex field amplitude by $\exp[(-ik/2f)(x^2 + y^2)]$ (a small total phase lead plays no role in this investigation).

Now let us return to expression (2). Multiplication of $u(x_1, y_1)$ by $\exp[-(ik/2f)(x_1^2 + y_1^2)]$ leads to mutual reduction of the terms containing x_1^2 and y_1^2 if the distance to the observation plane z is equal to f. Hence, we have the simplest formula of distribution observation in the far zone which everything follows: at the source exit a lens (or more complex optical system) is installed with focal length $f > 0$. The pattern in the focal plane is entirely like the distribution in the far zone; for transition to the angular scale it is necessary to divide the linear scale by f[1]. Inasmuch as the angular distribution of the emmision at any distance from the source remains the same, the distance from the source to the measuring lens plays no special role; it is also necessary to see that the lens always "encompasses" the entire light beam.

When there are grounds to assume that the wave front has a spherical component, the compensation of which causes a decrease in the divergence, it is worth while to measure the beam width d not only in the focal plane, but also at other distances ℓ from the lens. In order to understand what information such measurements give, let us mentally divide the lens into two components with focal lengths $f' = (1/f - 1/\ell)^{-1}$ and $f'' = \ell$, respectively. Inasmuch as the observation plane is the focal plane for the second of these components, it becomes clear that the ratio d/ℓ is none other

---

[1] A similar situation has already been encountered when analyzing beam divergence with a spherical wave front: transition from a spherical front with $\rho > 0$ to a plane front is equivalent to passage of the beam through a lens with $f = \rho$.

APPROVED FOR RELEASE: 2007/02/09: CIA-RDP82-00850R000500010010-4

APPROVED FOR RELEASE: 2007/02/09: CIA-RDP82-00850R000500010010-4

than the divergence of the source emission with the first component as the exit corrector. Finding the distance ℓ_0 at which the ratio d/ℓ passes through a minimum, we at the same time determine the focal power of the optimal corrector $1/f - 1/\ell_0$ and the divergence achieved when using it.

§ 1.2. Optical Cavities and Classification of Them

Initial Information. A Little History. Now let us proceed with the investigation of the most important sources of highly coherent narrowly directional emission-lasers. One of the basic laser elements, along with the active medium and the system for stimulating it, is the resonator. The standard requirement imposed on the resonator is the presence of comparatively high-Q (slowly damping) characteristic oscillations, the frequencies of which fall into the amplification band of the active medium. On the other hand, it is desirable that there not be too many oscillations with approximately the same Q-factor -- similtaneous stimulation of too large a number of them can lead to almost incoherent emission.

Optical-band cavities are characterized by the fact that their dimensions usually are several orders greater than the operating wavelength. This excludes the use of closed resonators in the form of a closed cavity with reflecting walls: the number of high-Q oscillations on optical frequencies would be extremely large in such cavities. Therefore open resonators which do not have side walls are used. The simplest of such resonators consist of two mirrors installed opposite to each other with the active medium between them. The placement of the mirrors leads to isolation of the predominant direction of propagation of the emission which must sharply decrease the number of high-Q modes by comparison with closed resonators. Actually, light beams traveling along the axis of the system (the common normal to the mirrors) are reflected alternately from the mirrors and obviously damp more slowly than others; inclined beams exit from the system, and this occurs faster the larger the angle they make with the axis.

Similar arguments led Prokhorov [1] to the basic idea of the prospectiveness of using open resonators. On the other hand, it is still impossible to extract information from these arguments as to whether such resonators have natural oscillations. It is possible only to conclude that these oscillations must be found in the form of a superposition of light beams directed along the resonator axis or slightly inclined to it. Only a careful analysis such as will be performed in this book can answer the questions of what sort of oscillations these are, how they are influenced by the presence of an active medium, how many of them will be present in the stimulated emission and, finally, what the resultant divergence of the emission will be. This analysis is for the most part based on the results of the theory of empty (that is, containing no active medium), open resonators.

The primary period of development of the theory of empty, open resonators extends from 1961 to 1966. The famous paper by Fox and Li [9] marked the beginning. The problem of the existence and properties of the lowest (that is, the highest-Q) modes of an empty open resonator was stated and solved numerically for several special examples for the first time in the paper by Fox and Li. The concept of diffraction losses was introduced for the first time. Diffraction losses can be defined as the fraction of the total radiation flux scattered as a result of diffraction and passing by the mirrors. For a number of reasons, this concept is much more useful as applied to optical-band cavities than the Q-factor concept,

APPROVED FOR RELEASE: 2007/02/09: CIA-RDP82-00850R000500010010-4

APPROVED FOR RELEASE: 2007/02/09: CIA-RDP82-00850R000500010010-4

and at this time it has almost completely displaced the Q-factor concept.

After reference [9] came the articles by Boyd, Gordon and Kogelnik [10, 11], in which a more general study was made of open resonators consisting of two spherical mirrors with arbitrary radii of curvature, and a classification of such resonators with respect to magnitude of the diffraction losses was presented. It was discovered that in a defined range of geometric parameters of the resonator (radii of curvature of the mirrors and spacing between them), the diffraction losses are very small, but on going outside this range, these losses increase extremely sharply. During those years it appeared that stable lasing could be achieved only in resonators with small diffraction losses; therefore such resonators were called stable; as we shall soon see, a system of two slightly concave mirrors can serve as a characteristic example of such resonators. For this reason, resonators with large losses which include, for example, a system of convex mirrors, were called unstable, and researchers did not consider them for several years.

A further significant step forward was made when references [12, 13] appeared. The general methods of analysis of complex devices consisting of an arbitrary number of optical elements with plane and spherical surfaces were developed in these papers. As a result, it turned out to be possible to reduce almost any complex resonator to the equivalent two-mirror system with the same field distributions of the natural oscillations on the mirrors and the same diffraction losses.

Papers by Soviet scientists -- V. P. Bykov, V. I. Talanov, et al. -- made an important contribution to the development of the given field of science. Among them a special role is played by the brilliant research cycle of L. A. Vaynshteyn which was summed up in the monograph [3] which was already mentioned in the introduction. Previously, he developed powerful, universal methods of analyzing microwave systems. The application of these methods to open optical-band cavities permitted Vaynshteyn to obtain simple analytical expressions for field distributions and losses in many cases where other researchers were forced to resort to machine calculations. His formulas were also suitable for high-order modes and for large-mirror resonators, that is, they even encompassed cases where machine methods were useless in view of the extraordinary awkwardness of the calculations.

All of the above-mentioned studies pertained to flat and "stable" resonators which had small diffraction losses. The results of these papers, that is, the theory of empty resonators with small losses, have also been reflected quite completely in almost all monographs on quantum electronics. Accordingly, we shall not go into a detailed restatement of the methods of solving certain problems or the results of calculations performed for a great variety of systems (a significant part of which did not find application subsequently). We shall only present a minimum amount of information which we need for the following discussion. We shall try to systematize this information as much as possible and avoid numerous "historical features" which would only complicate the discussion.

Open resonators are first of all divided into ring and linear cavities (see Figure V. 1). Ring cavities are made up of at least three (most frequently four) mirrors or other elements which change the direction of a light beam; they are used in a small number of types of special laser devices (laser gyroscopes, and so on). Ring resonators are almost never used in lasers with narrowly directional emission: they do not have any special advantages from the point of view of divergence of the

APPROVED FOR RELEASE: 2007/02/09: CIA-RDP82-00850R000500010010-4

APPROVED FOR RELEASE: 2007/02/09: CIA-RDP82-00850R000500010010-4

emission, and they are complicated to adjust; at the same time, the requirements on adjustment precision increase as the emission divergence decreases. Therefore linear cavities will be the primary subject of our analysis although the results of the analysis can be extended to the case of ring systems without difficulty.

Although a linear cavity contains fewer mirrors than a ring cavity, as a rule the linear cavity is an integral optical system. The mirrors themselves are frequently not plane, but spherical; an active element made of a material with an index of refraction different from one (but still variable with respect to cross section) is placed between the mirrors; if necessary polarizers, shutters, lenses, and so on are also placed between the mirrors. Therefore first of all we must discuss the laws of transmission of light beams through optical systems made of elements with spherical or plane surfaces.

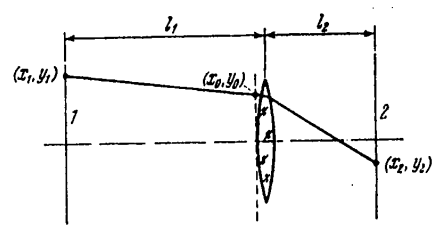

Figure 1.10. Thin lens between source and observation planes: 1 — source plane; 2 — observation plane.

Passage of Light Beams Through Optical Systems. Beam Matrix. First let us consider the simplest example where there is only one thin lens with focal length f between a monochromatic source and the observation plane; the distance from this thin lens to the source is ℓ_1, and the distance to the observation plane is ℓ_2 (Figure 1.10). According to (2), the field at the point with transverse coordinates x', y' in the reference plane located directly in front of the lens is

$$u(x', y') = \frac{\exp(ikl_1)}{i\lambda l_1} \int \exp\left\{ik\left[\frac{(x'-x_1)^2}{2l_1} + \frac{(y'-y_1)^2}{2l_1}\right]\right\} u(x_1, y_1)\, dS_1;$$

here $dS_1 = dx_1 dy_1$, $u(x_1, y_1)$ is as before the complex amplitude of the field on the reference plane of the source.

After passage through the lens, the complex amplitude is multiplied by exp $\left[-ik\frac{(x')^2+(y')^2}{2f}\right]$; finally, applying (2) again, we obtain the expression for the field distribution $u(x_2, y_2)$ in the observation plane:

$$u(x_2, y_2) = \frac{\exp[ik(l_1+l_2)]}{(i\lambda)^2 l_1 l_2} \iint \exp\left\{ik\left[\frac{(x'-x_1)^2}{2l_1} + \frac{(y'-y_1)^2}{2l_1} - \right.\right.$$
$$\left.\left. - \frac{(x')^2+(y')^2}{2f} + \frac{(x_2-x')^2}{2l_2} + \frac{(y_2-y')^2}{2l_2}\right]\right\} u(x_1, y_1)\, dS_1 dS'.$$

APPROVED FOR RELEASE: 2007/02/09: CIA-RDP82-00850R000500010010-4

APPROVED FOR RELEASE: 2007/02/09: CIA-RDP82-00850R000500010010-4

In order to express $u(x_2, y_2)$ directly in terms of $u(x_1, y_1)$, it is necessary to change the order of integration and take the integral over the surface of the lens S'; here we shall consider that the lens more than "encompasses" the entire light beam, and integration can be performed within infinite limits.

Thus, our problem reduced to calculation of the integral

$$\int\limits_{(S')} \exp\left\{ik\left[\frac{(x'-x_1)^2}{2l_1}+\frac{(y'-y_1)^2}{2l_1}-\right.\right.$$
$$\left.\left.-\frac{(x')^2+(y')^2}{2f}+\frac{(x_2-x')^2}{2l_2}+\frac{(y_2-y')^2}{2l_2}\right]\right\}dS' =$$
$$= \exp\left\{\frac{ik}{2}\left[\frac{x_1^2+y_1^2}{l_1}+\frac{x_2^2+y_2^2}{l_2}-\left(\frac{1}{l_1}+\frac{1}{l_2}-\frac{1}{f}\right)(x_0^2+y_0^2)\right]\right\}\times$$
$$\times\int\limits_{(S')}\exp\left\{\frac{ik}{2}\left(\frac{1}{l_1}+\frac{1}{l_2}-\frac{1}{f}\right)[(x'-x_0)^2+(y'-y_0)^2]\right\}dS',$$

where $x_0=\left(\frac{1}{l_1}+\frac{1}{l_2}-\frac{1}{f}\right)^{-1}\left(\frac{x_1}{l_1}+\frac{x_2}{l_2}\right)$, $y_0=\left(\frac{1}{l_1}+\frac{1}{l_2}-\frac{1}{f}\right)^{-1}\left(\frac{y_1}{l_1}+\frac{y_2}{l_2}\right)$ are the coordinates of a point on the surface of the lens at which the beam should be directed from the point (x_1, y_1) so that after refraction in the lens it will hit the point (x_2, y_2) (see the figure).

The last integral is similar to the ones investigated by us when discussing formula (1.2) at the beginning of § 1.1 and also is equal to half the integral over the first Fresnel zone. The center of a system of concentric circles which form the boundaries of the Fesnel zones (see Figure 1.1) is in the given case located at the point (x_0, y_0); the radii of the zones are equal to $r_n=\sqrt{n\lambda/(1/l_1+1/l_2-1/f)}$. After all of the transformations, we arrive at the desired formula:

$$u(x_2, y_2)=\frac{\exp[ik(l_1+l_2)]}{i\lambda(l_1+l_2-l_1l_2/f)}\int\exp\left\{\frac{ik}{2(l_1+l_2-l_1l_2/f)}\times\right.$$
$$\times\left[(1-l_2/f)(x_1^2+y_1^2)+(1-l_1/f)(x_2^2+y_2^2)-\right.$$
$$\left.\left.-2(x_1x_2+y_1y_2)\right]\right\}u(x_1, y_1)\,dS_1. \qquad (15)$$

Let us know that the sum $\ell_1+\ell_2$ in the exponent in front of the phase factor integral must be replaced by the optical distance L_0 between the source and observation planes measured along the system axis when considering finite thickness of the lens. The exponent in the expression under the integral sign has the form $ik\Delta(x_1, y_1; x_2, y_2)$, where Δ is the difference between the optical distance from (x_1, y_1) to (x_2, y_2) measured along the beam passing through these points and L_0.

In the investigated example we have not considered partial reflection of light from the lens surface. Consideration of this phenomenon would in the given situation only lead to a small decrease in the intensity of the emission passing through the

APPROVED FOR RELEASE: 2007/02/09: CIA-RDP82-00850R000500010010-4

APPROVED FOR RELEASE: 2007/02/09: CIA-RDP82-00850R000500010010-4

lens (if we neglect the slight influence of multiple reflection). However, inside an optical cavity light beams originating at the interfaces are superposed on the primary beam reflected from the end mirror. This can lead to consequences which cannot be neglected in spite of the apparently negligible intensity of the scattered light. Let us present a simple numerical example. Let a coherent beam with intensity $0.04\ I_0$ (the reflection coefficient equal to 4% has an interface between the air and glass with index of refraction of 1.5 for normal incidence) be added to the primary beam having intensity I_0 and, consequently, field amplitude $u_0 = \sqrt{I_0}$. The amplitude of this beam is $\sqrt{0.04 I_0} = 0.2u_0$; at the peak formed as a result of superposition of the interference pattern beams, the intensity is equal to $(1.2\ u_0)^2 = 1.44\ I_0$, at the minimum, $(0.8\ u_0)^2 = 0.64\ I_0$. It is unnecessary to comment on these figures. Therefore in the following analysis, in addition to the specially stipulated cases, the interfaces will always be considered coated. In order to get away from the influence of the interfaces in the experiments they are frequently not coated, but inclined slightly. Then the reflected emission leaves the resonator immediately and has no influence on the structure of the output beam, only slightlydecreasing its intensity.

Now let us proceed with investigation of more complex optical systems. It would be possible, of course, simply to perform an intermediate integration over every interface or thin lens inside the resonator; that is how Collins proceeded in reference [12], which was one of the first articles in the given field. This method is highly universal, but awkward. In the case of paraxial (slightly inclined) beams that are of interest in our case in systems with spherical and plane interfaces, the beam matrix method is more suitable. Kogelnik and Li [13, 14] developed this method in detail as applied to resonator theory.

The beam matrix is especially convenient in that it is calculated in the geometric approximation, but as we shall see later, knowing its elements makes it possible, if necessary, to describe the transmission of the light beam through the optical system also in the diffraction approximation. The beam or ABCD-matrix relates the values of the transverse coordinate x, y and slopes α_x, α_y of the light beams at the entrance and exit of the optical system:

$$\begin{Vmatrix} x_2 & y_2 \\ \alpha_{2x} & \alpha_{2y} \end{Vmatrix} = \begin{Vmatrix} A & B \\ C & D \end{Vmatrix} \cdot \begin{Vmatrix} x_1 & y_1 \\ \alpha_{1x} & \alpha_{1y} \end{Vmatrix}, \tag{16}$$

where the index 1 corresponds to the input plane, 2 corresponds to the output plane (Figure 1.11). The matrix product in (16) and hereafter is calculated in accordance with its standard definition. Being written for any one of two coordinate pairs, this formula acquires the form

$$\begin{vmatrix} x_2 \\ \alpha_{2x} \end{vmatrix} = \begin{Vmatrix} A & B \\ C & D \end{Vmatrix} \cdot \begin{vmatrix} x_1 \\ \alpha_{1x} \end{vmatrix}, \quad \text{or} \quad x_2 = Ax_1 + B\alpha_{1x}, \quad \alpha_{2x} = Cx_1 + D\alpha_{1x}.$$

The beam matrix elements are uniquely related to the focal length of the optical system F and the position of its principal planes. In particular, $C = -1/F$.

APPROVED FOR RELEASE: 2007/02/09: CIA-RDP82-00850R000500010010-4

APPROVED FOR RELEASE: 2007/02/09: CIA-RDP82-00850R000500010010-4

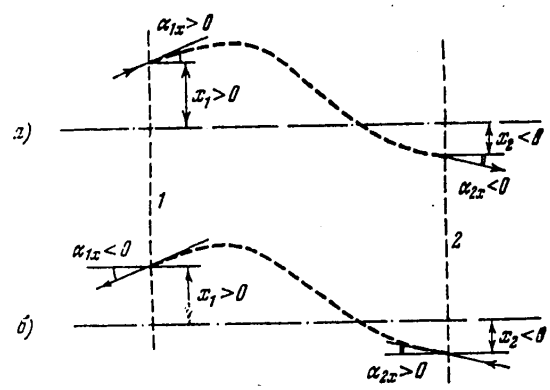

Figure 1.11. Definition of a beam matrix for the beam path in the forward (a) and return (b) directions. The arrows indicate the beam at the entrance and exit from the system; 1 — entrance plane, 2 — exit plane.

If the exit plane of the optical system with a beam matrix $\begin{Vmatrix} A_1 & B_1 \\ C_1 & D_1 \end{Vmatrix}$ is matched to the entrance plane of the system having the matrix $\begin{Vmatrix} A_2 & B_2 \\ C_2 & D_2 \end{Vmatrix}$, then the following matrix corresponds to passage through both of these systems:

$$\begin{Vmatrix} A_2 & B_2 \\ C_2 & D_2 \end{Vmatrix} \cdot \begin{Vmatrix} A_1 & B_1 \\ C_1 & D_1 \end{Vmatrix} = \begin{Vmatrix} A_2A_1 + B_2C_1 & A_2B_1 + B_2D_1 \\ C_2A_1 + D_2C_1 & C_2B_1 + D_2D_1 \end{Vmatrix},$$

and so on.

Let us proceed to another table of beam matrices for several optical systems (Table 1.1). The first of these systems is simply a segment of empty space of length ℓ, and the second is a layer of homogeneous medium of thickness ℓ and with index of refraction n. The third matrix corresponds to a single thin lens, the fourth matrix corresponds to the more complex case of a layer of medium of thickness ℓ with index of refraction varying by the law $n = n_0 - (1/2)n_2r^2$, where $r = \sqrt{x^2 + y^2}$ is the distance from the axis. Any optical systems of interest to us (in particular, presented at the end of the table) can be represented in the form of combinations of these four optical systems, and their matrices are equal to the corresponding products. The determinants of all of the first four matrices are equal to one; inasmuch as the determinant of the matrix product is equal to the product of the determinants of the individual matrices, the following relation is satisfied for any optical system

$$AD - BC = 1. \tag{17}$$

Setting $f_2 = \infty$ (no second lens) in the last of the matrices presented in the table, we obtain the beam matrix for the above-investigated case of a single lens between two reference planes at finite distances from it:

$$\begin{Vmatrix} 1 - l_2/f & l_1 + l_2 - l_1l_2/f \\ -1/f & 1 - l_1/f \end{Vmatrix}.$$

APPROVED FOR RELEASE: 2007/02/09: CIA-RDP82-00850R000500010010-4

APPROVED FOR RELEASE: 2007/02/09: CIA-RDP82-00850R000500010010-4

Table 1.1. Beam matrices of several of the simplest optical systems

No.	Optical system	Beam matrix
1	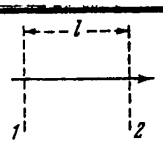	$\begin{Vmatrix} 1 & l \\ 0 & 1 \end{Vmatrix}$
2	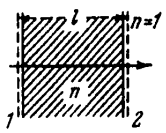	$\begin{Vmatrix} 1 & \frac{l}{n} \\ 0 & 1 \end{Vmatrix}$
3	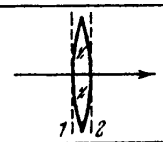	$\begin{Vmatrix} 1 & 0 \\ -\frac{1}{f} & 1 \end{Vmatrix}$
4	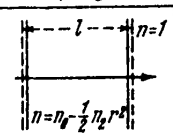	$\begin{Vmatrix} \cos\left(l\sqrt{\frac{n_2}{n_0}}\right) & \frac{1}{\sqrt{n_2 n_0}}\sin\left(l\sqrt{\frac{n_2}{n_0}}\right) \\ -\sqrt{n_0 n_2}\sin\left(l\sqrt{\frac{n_2}{n_0}}\right) & \cos\left(l\sqrt{\frac{n_2}{n_0}}\right) \end{Vmatrix}$
5	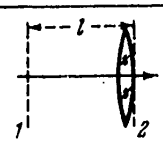	$\begin{Vmatrix} 1 & l \\ -\frac{1}{f} & 1-\frac{l}{f} \end{Vmatrix}$
6	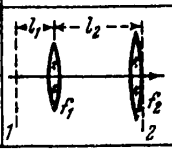	$\begin{Vmatrix} 1-\frac{l_2}{f_1} & l_1+l_2-\frac{l_1 l_2}{f_1} \\ -\frac{1}{f_1}-\frac{1}{f_2}+\frac{l_2}{f_1 f_2} & 1-\frac{l_1}{f_1}-\frac{l_2}{f_2}-\frac{l_1}{f_2}+\frac{l_1 l_2}{f_1 f_2} \end{Vmatrix}$

Comparing this matrix with formula (15), we see that the latter can be represented in the following form:

$$u(x_2, y_2) = \frac{\exp(ikL_0)}{ikB} \int\limits_{(S_1)} u(x_1, y_1) \exp\left\{\frac{i\pi}{\lambda B}\left[A(x_1^2 + y_1^2) + D(x_2^2 + y_2^2) - 2(x_1 x_2 + y_1 y_2)\right]\right\} dS_1. \tag{18}$$

As can be seen by direct checking, the same correspondence between the diffraction approximation formulas and the elements of the beam matrices also exists for other of the simplest systems presented in Table 1.1. It only remains to prove that formula (18) remains valid also for any combination of these systems. Let us do the proof by the induction method.

APPROVED FOR RELEASE: 2007/02/09: CIA-RDP82-00850R000500010010-4

APPROVED FOR RELEASE: 2007/02/09: CIA-RDP82-00850R000500010010-4

Let two optical systems exist, for each of which the integral expression relating the fields at the input and output, is written in terms of the elements of a beam matrix of the type of (18), and let the exit of the first of them be matched with the entrance of the second. Then, substituting the expression for the field at the exit of the first system in the integral relation of the second system, we represent the field at the exit of the second system, just as in our example with a lens, in the form of a double integral. Performing the integration with respect to the separating system of the intermediate plane, we obtain the desired integral relation relating the fields at the entrance and exit of a combination of two systems. It is possible to see that, as before, it will have the form of (18) with coefficients equal to the elements of the product of beam matrices of our two systems, that is, the matrix of the composite system as a whole. Adding another system, we obviously obtain the same result, and so on.

Thus, knowledge of the beam matrix permits transition to the diffraction approximation at any time if required; only the optical length of the system L_0 defining the magnitude of the total phase lead is not represented in terms of matrix elements. Now it is possible to proceed with investigation of optical cavities.

Classification of Resonators by the Properties of Their Beam Matrices. In trying to apply a beam matrix to the description of a resonator, as before we encounter the fact that this matrix in its standard definition relates the parameters of light beams at the entrance and exit surfaces of the optical system which are considered plane. At the same time the end mirrors of the resonator frequently have not plane, but spherical surfaces. In order to overcome this small difficulty, it is sufficient to represent each spherical end mirror with radius of curvature R (for a concave mirror $R > 0$, and a convex mirror, $R < 0$) in the form of a combination of a plane mirror and a thin lens with focal length $f = R$ installed beside it equivalent to the spherical end mirror (Figure 1.12; focal length of the spherical mirror, as is known, is $R/2$; in turn, the light beam passes through the lens of the equivalent combination on reflection from this combination twice). As a result of this substitution we obtain an equivalent resonator with plane end mirrors. The transmission of light between them is usually described using a standard ABCD-matrix which we shall consider to be the matrix and the initial resonator. As an example let us write the matrix elements for each case of a two-mirror resonator which can be obtained, setting $\ell_1 = 0$, $\ell_2 = \ell$, $f_1 = R_1$ and $f_2 = R_2$ in the last matrix of Table 1.1:

$$A = 1 - l/R_1, \quad B = l, \quad C = -\frac{1}{R_1} - \frac{1}{R_2} + \frac{l}{R_1 R_2}, \quad D = 1 - l/R_2; \tag{19}$$

here R_1 and R_2 are the radii of curvature of the left-hand and right-hand mirrors, ℓ is the distance between them.

If the elements of the beam matrix of an arbitrary resonator introduced in this way are substituted in (18), we obtain an integral transformation relating the distributions of the complex amplitude directly on the surface of the end mirrors. In this case it is possible to ignore whether we are dealing with the initial resonator (Figure 1.12, a) or the resonator equivalent to it (Figure 1.12,b): the integral transformation of the fields on the mirrors is the same in either case. If we use such light beam parameters as the inclinations of the beams and curvatures of the

APPROVED FOR RELEASE: 2007/02/09: CIA-RDP82-00850R000500010010-4

APPROVED FOR RELEASE: 2007/02/09: CIA-RDP82-00850R000500010010-4

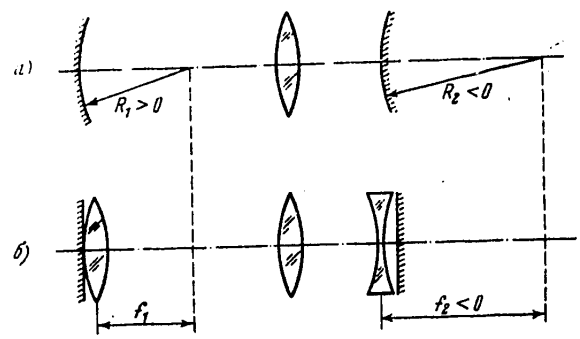

Figure 1.12. Determination of a beam matrix for a resonator with spherical end mirrors: a) initial cavity; b) equivalent resonator with plane mirrors.

wave fronts, on transition from the equivalent resonator to the initial one it is necessary to introduce the corresponding corrections (we shall present an example of this operation soon).

Finally, let us proceed to classification of optical cavities: this classification is based on the properties of their natural oscillations. Natural oscillations of a linear cavity, in turn, can be represented in the form of a set of two light beams propagated opposite to each other. On reflection from the end mirrors these beams transform into each other, which insures reproducibility of the process in time. Thus, the problem of finding the natural oscillation reduces to finding a light beam such that after complete passage through the cavity in both directions it retains its initial structure. For general classification of optical cavities the most superficial investigation of this problem in the geometric approximation which we shall proceed with now is sufficient. Let us only note that this solution by the beam matrix method was found for the first time to be essentially correct, but highly scholastic in the paper by Kahn [15].

If the optical system has an ABCD-matrix for passage of light through it from left to right, then passage from right to left is described by the beam matrix DBCA. It can be obtained from the inverse matrix (that is, the matrix realizing the opposite transformation to (16)), considering that when going back along the trajectory the linear coordinates have the former value, and the angles of inclination change sign (the direction of reckoning the angles of inclination is discussed in Figure 1.11).

On reflection from a plane end mirror, the linear and angular beam coordinates are retained. Therefore plane mirrors of an equivalent cavity (see Figure 1.12,b) perform the functions of planes separating the optical systems with ABCD and DBCA matrices, and complete passage through the resonator in both directions is described by the product of these matrices. If we take the right-hand mirror as the beginning, then the complete round-trip matrix has the form

$$\begin{Vmatrix} A & B \\ C & D \end{Vmatrix} \cdot \begin{Vmatrix} D & B \\ C & A \end{Vmatrix} = \begin{Vmatrix} AD+BC & 2AB \\ 2CD & AD+BC \end{Vmatrix}. \tag{20}$$

APPROVED FOR RELEASE: 2007/02/09: CIA-RDP82-00850R000500010010-4

APPROVED FOR RELEASE: 2007/02/09: CIA-RDP82-00850R000500010010-4

For any other choice of reference point, the full round-trip matrix changes, but the final result of the analysis of course remains the same. The choice made is convenient in that it permits us to obtain the form of the solution near the right-hand mirror, that is, at the exit aperture of the laser, immediately: by the tradition established in laser literature, we shall always depict lasers as having emission output to the right.

The solution of the geometric approximation will be found in the form of spherical waves with centers on the system axis. First of all let us find the law of transformation of the radii of curvature of such waves on passage of them through an arbitrary optical system. Each spherical wave with center on the axis and radius of curvature ρ corresponds to the family of beams $x/\alpha_x = \rho$ (here and hereafter we shall write all the relations for one of the two coordinate pairs). Thus, the beam with the coordinates x_1, α_{1x} entering the system belongs to the family of wave beams with $\rho_1 = x_1/\alpha_{1x}$. After passage through the system, the radius of curvature of this wave obviously becomes equal to $\rho_2 = x_2/\alpha_{2x}$, where x_2, α_{2x} are the coordinates of the same beam at the system exit. Substituting the values of x_2 and α_{2x} here, we obtain the desired law of transformation of the radius of curvature of a spherical wave in an arbitrary optical system: $\rho_2 = (A\rho_1 + B)/(C\rho_1 + D)$.

Using matrix (20) and this law, let us compile the equation for reproduction of the wave curvature after complete round-trip through the resonator:

$$\frac{(AD + BC)\rho' + 2AB}{2CD\rho' + AD + BC} = \rho'. \tag{21}$$

This equation has the solution $\rho'_{1,2} = \pm\sqrt{AB/CD}$.

Now it is time to remember that we are in the general case dealing with the matrix of an equivalent resonator (Figure 1,12,b) and we have obtained the solution for it. In order to proceed with the solution for the initial resonator with spherical exit mirror, as is easy to see, it is necessary to add the curvature of the exit mirror of the initial resonator $1/R_2$ to the obtained wave curvature. Thus, we obtain the final expression for the radii of curvature ρ of the waves which are solutions in the initial resonator:

$$1/\rho_{1,2} = 1/R_2 \pm \sqrt{CD/AB}. \tag{22}$$

As has been stated, it is obvious even by the naked eye that the properties of the resonator depend decisively on the sign of the ratio AB/CD which coincides with the sign of the product ABCD. Let us first consider the case where ABCD > 0. Then (21) has two different real solutions. It is possible to see that on passage through the resonator the coordinates of each beam belonging to the families of beams of the two found waves turn out to be multiplied by $\mu_{1,2} = AD + BC \pm 2\sqrt{ABCD}$. Obviously in this respect the transverse dimensions of the region occupied by each wave vary. Inasmuch as $\mu_1\mu_2 = (AD + BC)^2 - 4ABCD = (AD - BC)^2 = 1$ (see (17)), the absolute magnitude of one of the values of μ is always greater than one, and the other is always less than one. The transverse dimensions of the region occupied by the wave with $|\mu| < 1$ decrease from pass to pass. For any initial dimensions of the transverse cross section in the final analysis this wave "contracts" to a

APPROVED FOR RELEASE: 2007/02/09: CIA-RDP82-00850R000500010010-4

APPROVED FOR RELEASE: 2007/02/09: CIA-RDP82-00850R000500010010-4

point and, in spite of the formal reproducibility of the curvature of its front, it cannot serve as a steady solution.

The wave cross section with $|\mu| > 1$, conversely, expands by $|\mu|$ times on each pass. As a result of the finite dimensions of the mirrors, this expansion is not unlimited: part of the emission simply leaves the resonator, bypassing the mirrors, which predetermines the greater part of the losses. This wave, in combination with the wave generated by it, proceeding in the opposite direction, is also a steady state solution for resonators with ABCD > 0; as a result of the great magnitude of the losses, the given resonators, as we have already mentioned, have been called unstable. A detailed investigation of these resonators and the lasers based on them appears in Chapters 3 and 4, from which it follows that in the given case the geometric approximation gives an entirely satisfactory description of the resonator properties.

In the intermediate case of ABCD = 0 there is only one μ equal to +1 or -1. The nature of the solution essentially depends on which of the matrix elements is equal to zero. If this is B or C, then as follows from (17), the product AD, and with it, also μ are equal to one. This means that after complete passage through the resonator, the beam trajectory closes, and the beam again follows the same path. The path of the beams in these two cases, however, is quite different.

For B = 0, from (22), we obtain $\rho = 0$; thus, the center of curvature of the wave front is located directly at the exit mirror -- the radiation turns out to be focused at a point on this mirror. The wave going in the opposite direction is focused at a point on the other mirror (Figure 1.13, a). This is also understandable: the entrance and exit planes of the optical system with B = 0 are conjugate, the system projects the image of one of them on the other. In the given case expression (18) becomes meaningless; at the end of this section we shall deal with the problem of what to replace this relation with, but we shall not go into a detailed investigation of the properties of resonators with B = 0, for such resonators are almost never used.

On the contrary, the resonators with C = 0 are the most widespread. In this case, $\rho = R_2$ -- the right-hand mirror is an equiphasal surface of the wave front; it is easy to demonstrate that the left-hand mirror is too. Each beam follows the same path in the forward and return directions, being incident normally on both end mirrors. In particular, the layers of empty space or space filled with a homogeneous medium (see Table 1.1) have a matrix with C = 0 ($F = \infty$); therefore the given category includes the well-known flat cavity (see Figure 1.13, b), the concentric cavity similar to the flat cavity in many respects ($R_1 + R_2 = \ell$, Figure 1.13, c, d) and a family of resonators similar to them (the latter will be considered separately in § 2.6).

For resonators with A = 0 or D = 0 the value of μ is -1, and after complete roundtrip through the resonator the beam goes to the other side with respect to its axis; after a second roundtrip of the resonator, it returns to the initial position. In empty two-mirror resonators A = 0 for $R_1 = \ell$, D = 0 for $R_2 = \ell$; thus, the center of curvature of one of the mirrors is located on the other. The same point serves as the center of curvature of the spherical wave in the geometric approximation; the second mirror is an equiphasal surface of this wave (Figure 1.13, e, f). Among such resonators a special role is played by a symmetric confocal resonator with A = D = 0

APPROVED FOR RELEASE: 2007/02/09: CIA-RDP82-00850R000500010010-4

APPROVED FOR RELEASE: 2007/02/09: CIA-RDP82-00850R000500010010-4

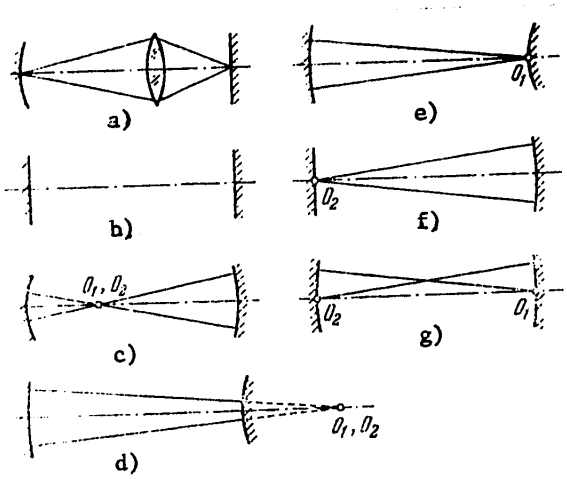

Figure 1.13. Different types of optical cavities with ABCD = 0: a) resonator with B = 0; b) flat cavity (C = 0); c), d) concentric cavities (C = 0); e) cavity with A = 0; f) semiconcentric cavity with D = 0; g) symmetric confocal cavity (A = D = 0); O_1, O_2 — centers of curvature of the left and right mirrors.

($R_1 = R_2 = \ell$, Figure 1.13, g); a wave with any initial curvature is reproduced in it.

All of the laws of the behavior of resonators with ABCD = 0 discovered with the help of geometric analysis to a defined degree depict the true picture of the field distribution of the highest-Q oscillations. Thus, in the resonator depicted in Figure 1.13, f, which is usually called semiconcentric, the lower mode field is actually similar to the sum of two spherical waves for which the second mirror is an equiphasal surface; on the first mirror the emission is concentrated at the diffraction "point" with dimensions $\sim\lambda\ell/a_2$, where a_2 is the transverse dimension of the second mirror.

It is only necessary to remember that when ABCD = 0 the slightest deviations from the ideal configuration of the cavity are sufficient for the field distribution to change sharply, and for the geometric approximation to become invalid (thus, for misalignment of a flat cavity there is no geometric solution). We shall discuss this in more detail in § 2.5.

Finally, for ABCD < 0 the "geometric" equation (21) has no real solution under any conditions. Analysis in the diffraction approximation (see § 2.1) shows that the lower-mode field of such cavities is primarily concentrated near the axis of the system and decreasec exponentially on going away from the axis. It is obvious that for sufficiently large mirrors a negligible portion of the total radiation flux will bypass the mirrors, and the diffraction losses will be extremely small. This led in its time to the name "stable" resonators as the opposite of "unstable" with ABCD > 0. The argument leading to such names have not withstood the test of time, but this terminology has become widespread, being a source of numerous misunderstandings among nonspecialists (the author knows of a case where the term "unstable

APPROVED FOR RELEASE: 2007/02/09: CIA-RDP82-00850R000500010010-4

APPROVED FOR RELEASE: 2007/02/09: CIA-RDP82-00850R000500010010-4

laser resonator" was translated in an abstract collection as "laser with falling mirrors"). In view of general acceptance, we, too, have been unable to avoid this unfortunate terminology.

Inasmuch as ABCD = AD(AD - 1), the "stability" condition (that is, the condition of smallness of the diffraction losses) can be written in the form AD(AD - 1) < 0 or 0 < AD < 1. For empty two-mirror resonators $A = 1 - \ell/R_1$, $D = 1 - \ell/R_2$ (see (19)). In the theory of such resonators created before the theory of multielement systems, the notation $1 - \ell/R_1 \equiv g_1$, $1 - \ell/R_2 \equiv g_2$ was adopted for these parameters. Thus, the two-mirror resonators are "stable" for $0 < g_1 g_2 < 1$; in this form the "stability" criterion also figured in the mentioned papers by Kogelnik and Li and many that followed.

Conditions of Resonator Equivalence. The problem of classifying optical resonators also includes the problem of selecting equivalent resonators, the solution of which, in particular, makes it possible to reduce the complex multicomponent systems to simpler two-mirror systems. We shall consider this problem in the diffraction approximation. Here, first of all, it is necessary to consider that the integral relation (18) is valid for the component system only when integration over all of the intermediate surfaces is performed within infinite limits. Hence, it follows directly that in the general case where both end mirrors have finite dimensions and actually limit the light beam cross section, it is impossible to use the matrix of total passage through the resonator described in (20) to compile the diffraction approximation equation. Therefore let us consider another expression of (18), considering that A, B and D are elements of a beam matrix describing passage through the resonator in one direction, and the indices 1 and 2 pertain to the left and right end mirrors.

The simplest formula for reducing an arbitrary multicomponent system to a two-mirror system with the same sizes of end mirrors follows directly from comparison of (18) and (19). For this purpose it is sufficient to install these mirrors at a distance $L_{equiv} = B$ from each other and give them radii of curvature $R_1 = L_{equiv}/(1 - A)$ and $R_2 = L_{equiv}/(1 - D)$. Making use of the meaning which an element of the beam matrix B has acquired, it is possible to realize the condition of "stability" in a very interesting form. Actually, on going from the inequality 0 < AD < 1 to the equivalent inequality -1 < BC < 0 or 1/BC < -1 and substituting $B = L_{equiv}$ and $C = -1/F$, we obtain $F/L_{equiv} > 1$. With this notation the relation of the "stability criterion" to the properties of a resonator as an optical system with focal length F is especially clearly obvious.

Although any resonator can be thus reduced to a two-mirror resonator, the number of parameters characterizing it will still remain too large even if we consider that the end mirrors have given shape (circular, square, and so on). There are 5 such parameters: any three elements of the beam matrix (the fourth can be found using (17)) and the transverse dimensions of the mirrors a_1, a_2. In order to decrease this number let us introduce the dimensionless coordinates $X_i = x_i/a_i$, $Y_i = y_i/a_i$, and let us write the field distribution functions in these coordinates: $U(X_i, Y_i) = u(a_i X_i, a_i Y_i)$. Then (18) acquires the form

APPROVED FOR RELEASE: 2007/02/09: CIA-RDP82-00850R000500010010-4

APPROVED FOR RELEASE: 2007/02/09: CIA-RDP82-00850R000500010010-4

$$U(X_2, Y_2) = \frac{a_1}{a_2} N \frac{\exp(ikL_0)}{i} \int\int \exp\{i\pi N[G_1(X_1^2 + Y_1^2) + G_2(X_2^2 + Y_2^2) - 2(X_1X_2 + Y_1Y_2)]\} U(X_1, Y_1)\, dX_1 dY_1. \quad (23)$$

Only three dimensionless generalized parameters remain: $G_1 \equiv \frac{a_1}{a_2} A$, $G_2 \equiv \frac{a_2}{a_1} D$ and $N \equiv \frac{a_1 a_2}{\lambda B}$; the last of them is usually called the Fresnel number — this parameter is equal to the geometric mean between the numbers of the Fresnel zones on the surface of the first mirror when observing from the center of the second ($a_1^2/\lambda B$) and on the surface of the second when observing from the center of the first ($a_2^2/\lambda B$). The factor a_1/a_2 in front of the integral sign simply describes the variation of the average emission density on transition of the beam to a mirror of another size.

Resonators with identical values of the parameters G_1, G_2 and N are entirely equivalent in the diffraction approximation. Equivalence indicates that the laws of integral transformation of the field given in one of the mirrors (in dimensionless coordinates) into the field at the other are entirely identical. Hence, in particular, it follows that the equivalent resonators have entirely identical field distributions of the natural oscillations at the mirrors and equal diffraction losses.

If one of the mirrors is so large that it covers the entire light beam, the number of equivalence parameters decreases to two. Then we shall always consider the "infinite" mirror located on the left; then for transition to the diffraction approximation it is possible to make direct use of the matrix (20). From (18) we obtain an integral relation describing the field transformation after complete round trip through the resonator in both directions:

$$u_2(x, y) = \frac{\exp(2ikL_0)}{2iAB\lambda} \int\int \exp\left\{\frac{i\pi}{2AB\lambda}[(AD + BC)(x^2 + y^2 + x'^2 + y'^2) - 2(xx' + yy')]\right\} u_1(x', y')\, dx' dy'. \quad (24)$$

In dimensionless coordinates, (24) acquires the form

$$U_2(X, Y) = N \frac{\exp(2ikL_0)}{i} \int\int \exp\{i\pi N[(AD + BC)(X^2 + Y^2 + X'^2 + Y'^2) - 2(XX' + YY')]\} U_1(X', Y')\, dX' dY'. \quad (24a)$$

Here the indices 1 and 2 pertain to the field distribution not on different mirrors, but on the same mirror — on the right-hand mirror before and after complete round trip through the resonator; $N \equiv a^2/(2AB\lambda)$, a is the dimension of this mirror; A, B, C and D are elements of the beam matrix of passage through the resonator from the left mirror to the right mirror; the values of X, Y, U have the previous meaning.

As one of the equivalence parameters it is natural to select the Fresnel number N; as is obvious from (24a) the other parameter can be the sum AD + BC or any of the values uniquely related to it. It is also possible to select AD, BC and ABCD and one of the μ as such a parameter.

In addition to N, stable resonators are usually characterized by the product AD ($g_1 g_2$); for unstable resonators, hereafter a combination of a large μ with respect

APPROVED FOR RELEASE: 2007/02/09: CIA-RDP82-00850R000500010010-4

APPROVED FOR RELEASE: 2007/02/09: CIA-RDP82-00850R000500010010-4

to absolute magnitude which we shall call the magnification of the resonator and denote by M, with N or $N_{equiv} \equiv (N/2)(M - 1/M)$ will be used (see Chapter 3).

It still remains to mention cases where the beam cross section is limited in the resonator not by mirrors, but by an iris located between them. In particular, this category includes the resonator with B = 0 in Figure 1.13; in this resonator the beam cross section is primarily limited not by mirrors, but by a lens. In such cases it is expedient to construct integral relations, beginning the round trip through the resonator not with one of the end mirrors, but directly with the element limiting the beam cross section. If the initial resonator is symmetric, it is possible to construct a symmetric resonator equivalent to it in which the beam cross section will be limited by the end mirrors; the method of construction is explained by Figure 1.14. An asymmetric resonator with internal iris does not reduce to an ordinary two-mirror resonator.

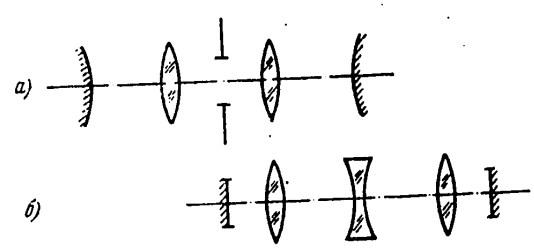

Figure 1.14. Construction of a resonator equivalent to a symmetric resonator with internal iris; a) initial resonator; b) equivalent resonator.

§ 1.3. Modes of an Empty Ideal Resonator and Their Use for Describing the Laser Situation

Just as the preceding section, this section will not contain detailed information about the structure of the natural oscillations of different specific types of resonators; it will be necessary to return to this discussion in the following chapters. In this section we shall only become familiar with the generally accepted approach to the classification of the natural oscillations of empty open resonators. In addition, there will be a discussion of the most important problem of when and to what degree information about the modes of empty ideal resonators can be suitable for description of real devices with an active medium. However strange, in laser literature the given problem has received immeasurably fewer pages of attention than the mindless use of the results of empty resonator theory even where it is clearly impossible to do this.

Classification of Natural Oscillations. The principles of the classification of natural oscillations are approximately identical for the majority of types of open resonators. Let us explain them in the example of a resonator made up of two completely reflecting plane rectangular mirrors 2a × 2b in size ($-a \leq x \leq a$, $-b \leq y \leq b$) installed at a distance ℓ from each other ($0 \leq z \leq \ell$). As will be demonstrated in the second chapter, the field of high-Q types of oscillations of such a resonator with very large Fresnel numbers ($a^2/\lambda\ell \gg 1$, $b^2/\lambda\ell \gg 1$) has in the first approximation the form of standing waves with respect to all three directions:

APPROVED FOR RELEASE: 2007/02/09: CIA-RDP82-00850R000500010010-4

APPROVED FOR RELEASE: 2007/02/09: CIA-RDP82-00850R000500010010-4

$$u_{mnq}(x, y, z, t) = \exp(-i\omega_{mnq}t)\sin\frac{q\pi z}{l}u_m(x)u_n(y), \tag{25}$$

where

$$u_m(x) = \begin{pmatrix}\cos\\ \sin\end{pmatrix}\frac{(m+1)\pi x}{2a}, \quad m = \begin{matrix}0, 2, 4, \ldots,\\ 1, 3, 5, \ldots,\end{matrix}$$

$$u_n(y) = \begin{pmatrix}\cos\\ \sin\end{pmatrix}\frac{(n+1)\pi y}{2b}, \quad n = \begin{matrix}0, 2, 4, \ldots,\\ 1, 3, 5, \ldots,\end{matrix}$$

are functions of the type of (13), m and n are small integers called transverse indi-indices, $q \approx 2\ell/\lambda$ is also an integer, but an extremely large number (10^4–10^7) called the axial index.

Let us rewrite (25) in the form

$$u_{mnq} = \frac{1}{2i}u_m(x)u_n(y)\left[\exp i\left(\frac{q\pi z}{l} - \omega t\right) - \exp i\left(-\frac{q\pi z}{l} - \omega t\right)\right],$$

from the standing wave we obtain the customary sum of two coherent light beams following along the z-axis in opposite directions and having field distribution $\infty u_m(x)\,u_n(y)$ on any reference plane perpendicular to the z-axis.

We have already become partly familiar with the properties of such light beams in § 1.1. Each beam consists of four plane waves, the propagation directions of which are characterized by angles of inclination $\alpha_x = \pm\frac{m+1}{2}\frac{\lambda}{2a}$, $\alpha_y = \pm\frac{n+1}{2}\frac{\lambda}{2b}$ (see Figure 1.15). All four angles between these directions and the z-axis are identical and are $\alpha = \sqrt{\alpha_x^2 + \alpha_y^2} = \frac{\lambda}{4}\sqrt{\left(\frac{m+1}{a}\right)^2 + \left(\frac{n+1}{b}\right)^2}$.

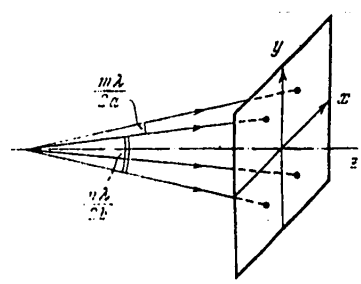

Figure 1.15. Directions of plane waves entering into the oscillation mode of a flat cavity.

The expressions for the angles of inclination (just as the formulas for the complex field amplitude of light beams making up the cavity modes presented in § 2.1 and more precise than (25)) include, in addition to the transverse indices m and n, the wavelength of the natural oscillation λ which also depends on the axial index q. However, remembering that all of this information in the final analysis is required

APPROVED FOR RELEASE: 2007/02/09: CIA-RDP82-00850R000500010010-4

APPROVED FOR RELEASE: 2007/02/09: CIA-RDP82-00850R000500010010-4

to describe a laser, it is only possible to be interested in oscillations, the wavelength of which falls in the amplification band of the active medium. In the majority of media the amplification band width $\Delta\lambda$ is so narrow that expression $\Delta\lambda \ll \lambda$ is satisfied (with significant "reserve"); therefore in the formulas for the transverse field structure it is possible to consider the wavelength fixed and equal to the wavelength at the center of the amplification band λ_0. Hence, it follows that the field distribution of the transverse direction and, with it, the radiation divergence are uniquely related to the transverse mode indices, and they do not depend on the axial index.

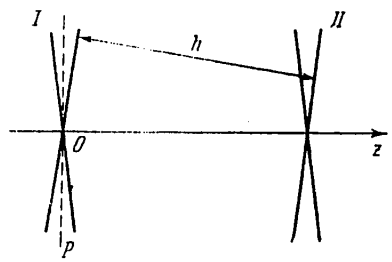

Figure 1.16. Determination of the phase velocity of the beam which is a superposition of plane waves: I, II -- initial and final positions of isolated fronts.

Now let us consider the problem of phase relations in a resonator and natural oscillation frequencies. We shall not write out the finished formulas, but derive them beginning with the field distribution (25) and at the same time becoming familiar with some of the properties of light beams which we have still not touched on. For this purpose, let us turn to Figure 1.16, where for simplicity two out of four of the plane waves making up a single beam are represented. Let us isolate one of the points in the space O at which the phases of these two waves coincide. Wave fronts first occupying the position I intersect at this point. It is easy to see that the surface on which the total field phase has the same value as at point O is the plane P passing through this point and normal to the z-axis.

In some time interval Δt both waves travel a distance $h = \Delta t$, and the fronts are shifted from position I to position II; the point of their intersection can travel a distance greater than h and equal to $c\,\Delta t/\cos\alpha$, where α is the angle which the normals to the wave fronts make with the z-axis. Together with the point O, the equiphasal surface of the total light beam is also shifted by the same distance. The shift rate of this surface is called the phase velocity; it determines the distance between nodes of a standing wave formed as a result of interference of two identical counter beams. In the given case the phase velocity is greater than the speed of light c in the ratio of $1/\cos\alpha \approx 1 + \alpha^2/2$; in this ratio twice the distance between the standing wave nodes $2\ell/q$ exceeds the wavelength $\lambda_{mnq} = 2\rho c/\omega'_{mnq}$. Considering what the angles of inclination α are equal to for plane waves entering into the mode (25), we obtain the desired formula

$$\frac{2l}{\lambda_{mnq}} = q + \frac{1}{2\pi}\delta_{mn}, \tag{26}$$

APPROVED FOR RELEASE: 2007/02/09: CIA-RDP82-00850R000500010010-4

APPROVED FOR RELEASE: 2007/02/09: CIA-RDP82-00850R000500010010-4

or

$$\omega'_{mnq} = \frac{c}{2l}\left(2\pi q + \delta'_{mn}\right), \tag{27}$$

where $\delta'_{mn} = \frac{\pi\lambda_0 l}{2}\left[\left(\frac{m+1}{2a}\right)^2 + \left(\frac{n+1}{2b}\right)^2\right]$.

Formulas (26) and (27) describe the natural oscillation spectrum; theoretically, they could be derived from the standard relation for the oscillations of mode (25) inside a rectangular parallelepiped $\ell \times 2a \times 2b$:

$$\frac{2}{\lambda_{mnq}} = \sqrt{\left(\frac{q}{l}\right)^2 + \left(\frac{m+1}{2a}\right)^2 + \left(\frac{n+1}{2b}\right)^2}.$$

Let us analyze these formulas. In our case of a flat cavity with $a^2/\lambda\ell \gg 1$, $b^2/\lambda\ell \gg 1$, the value of $\delta'_{mn}/2\pi$ with small m, n (that is, for the lowest modes) is small and has the nature of a correction to the integral q. The meaning of this correction becomes clear if we rewrite (26) as follows: $4\pi\ell/\lambda_{mnq} - \delta'_{mn} = 2\pi q$. Here $4\pi\ell/\lambda_{mnq}$ is the phase lead which would occur on a complete round trip through the resonator (that is, on the path 2ℓ) if the phase velocity were equal to c; $2\pi q$ is the true phase lead which obviously must be a multiple of 2π for self-imaging of the beam. Hence, it is obvious that δ'_{mn} is the amount by which the phase lead is diminished as a result of the fact that the phase velocity exceeds c. This phase correction, as should be expected (as a result of the fact that the transverse structure of the field and, with it, the phase velocity are constant along the length of the cavity) is proportional to ℓ; it increases quickly with a decrease in characteristic dimensions of the field structure in the transverse direction $2a/(m + 1)$, $2b/(n + 1)$.

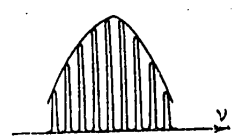

Figure 1.17. Amplification bands of the active medium and oscillation modes of a cavity with different axial indices q.

Thus, the resonance frequencies are determined primarily by the axial index q and they are grouped around values of $q\pi c/\ell$ which form an equidistant "comb" in the frequency scale with an interval between adjacent lines of $\Delta\omega = \pi c/\ell$ (or $\Delta\nu = c/2\ell$). For ordinary cavity lengths, this interval is so small that for the amplification band of the medium, as a rule, there are many lines with different q (Figure 1.17). The number of frequencies at which lasing is theoretically realizable is still greater if we consider the possible versions of the transverse indices m, n.

Let us present a brief discussion of the adopted terminology. For oscillations of the type of (25), usually the notation TEM_{mnq} is used; if we are talking about only

APPROVED FOR RELEASE: 2007/02/09: CIA-RDP82-00850R000500010010-4

APPROVED FOR RELEASE: 2007/02/09: CIA-RDP82-00850R000500010010-4

the transverse structure of the field, the index q is omitted. Thus, TEM_{00} is the lowest mode with m = n = 0 having the least divergence of the emission (see § 1.1). Analogous notation is also used for stable resonators with rectangular mirrors; the first two indices as before denote the numbers of the nodes of the field distribution function with respect to the corresponding areas. If the mirrors have a different form, then the modes are numbered differently (for circular mirrors its principles are discussed in §§ 2.1, 2.2); therefore in the general case we shall frequently designate the mode by one transverse index m.

When reading laser literature it is still necessary to consider that in the first papers on the theory of optical cavities, the lowest oscillations of the TEM_{00q} type were called, by analogy with the microwave band, axial, and the rest (with nonzero transverse indices), transverse. Subsequently, when describing the spectral or angular emission characteristics of multimod oscillators, a somewhat different meaning began to be attached to the terms "axial" and "transverse." We shall discuss this in more detail in § 2.4; now let us only note that when we are talking about the angular structure of emission, usually all the modes are called transverse without putting TEM_{00} in a special category.

Integral Equation and Natural Oscillations of an Arbitrary Empty Resonator. Although the above-presented analysis is also instructive, it in no way can be considered sufficiently complete; in it we even failed to mention the most important problem of diffraction losses, but this was done purposely: whereas the phase relations from which formulas of the type of (26), (27) follow can be obtained from very simple arguments, the situation is immeasurably more complicated with diffraction losses of flat cavities. It is true that Schawlow and Townes [2] made elementary estimates of losses based on calculating the number of passes which an inclined light beam can make before leaving the cavity completely, and based on identity of the time expended on this with the average lifetime of the photons in the cavity. As a result of the obviousness of it, this simplified procedure was at first definitely of value, but the calculations by Fox and Li [9] demonstrated that it is in essence entirely unjustifiable: not only the absolute magnitude of the true losses, but the entire nature of their dependence on the cavity parameters and slopes of the light beams making up the modes differ sharply from the results of such estimates. After publication of a series of articles by Vaynshteyn, it became clear that calculation of the number of passes of an inclined beam must be supplemented at least by calculation of what proportion of the emission approaching the edge of the resonator is reflected back (inside the cavity) as a result of edge diffraction. As will be obvious in § 2.2, these calculations are hardly primitive; therefore we have still not begun to deal with the problem of diffraction losses; going somewhat ahead, let us only note that in a flat cavity with fixed configuration the losses increase with the transverse indices of the modes, just as the phase corrections.

Thus, let us proceed to a stricter investigation of an arbitrary empty resonator. In accordance with [16], as the basis for the analysis let us use the universal expression describing passage of an arbitrary light beam through just as arbitrary an empty resonator (in both directions) having the form

$$u_2(x, y) = \exp(2ikL_0)\,\hat{P}u_1(x, y); \tag{28}$$

APPROVED FOR RELEASE: 2007/02/09: CIA-RDP82-00850R000500010010-4

APPROVED FOR RELEASE: 2007/02/09: CIA-RDP82-00850R000500010010-4

here $u_1(x, y)$ and $u_2(x, y)$ is the complex field amplitude on any selected reference surface before and after passage through the resonator in both directions, $\exp(ikL_0)\hat{P}$ is the integral conversion operator including all the necessary operations (for example, ingegration over intermediate surfaces, and so on). As an example of an expression of the type of (28) it is possible to use formula (24), where the operator is described for the special case of a resonator made of elements with spherical surfaces and with infinitely large left-hand mirror.

The exponential factor, the magnitude of which depends on the exact value of the emission wavelength corresponds to the total phase lead in twice the optical length of the resonator $2L_0$. The result of the effect of the operator $\hat{P}$ remaining after subtraction of this factor on any complex amplitude distribution function $u(x, y)$, can be considered independent of the wavelength if it does not go beyond the limits of the amplification band of the active medium (after the above-investigated example of a flat cavity, this does not require special explanations).

In addition to the total phase lead in the length of the resonator, in (28) it would also be necessary to consider the phase discontinuities on reflection of the beam from end mirrors. If the mirrors are metallic, the phase discontinuity will be π; this case also corresponds to a standing wave of the type of (25) (the "nodes" on the mirrors are formed as a result of the fact that the counter nodes are in opposite phase here). Inasmuch as on a complete round trip through the resonator there are two reflections from the mirrors, the total phase lead on their account is 2π and can be neglected (which would make it possible not to consider the phase discontinuities on the mirrors when compiling expression (24)). If the reflecting mirrors have multilayered dielectric coatings, the phase discontinuities are not equal to π. In order not to consider them separately, it is possible when performing the analysis to consider the resonator to consist not only of dielectric mirrors, but metallic mirrors, the surfaces of which are located where the field node closest to the dielectric mirror was located.

From formula (28) it follows that the integral equation for finding the natural modes, which is a condition of reconstructing the beam after a total round trip through the resonator, can be written in the form

$$\gamma u(x, y) = \exp(2ikL_0)\hat{P}u(x, y). \tag{29}$$

Obviously, u must be an eigenfunction of the integral operator $\hat{P}$. Let this operator have a set of eigenfunctions u_m and eigenvalues corresponding to them $\beta_m = \exp(-i\delta'_m - \delta''_m)$ so that $\hat{P}u_m = \exp(-i\delta'_m - \delta''_m)u_m$. Substituting u_m in (29), we obtain

$$\gamma_m = \exp(-\delta''_m)\exp[i(2kL_0 - \delta'_m)]. \tag{30}$$

In order that the complex amplitude distribution be reproduced not only with respect to form, but also have the previous phase, the value of γ_m must be real. Hence, it follows that the total phase lead $2kL_0 - \delta'_m$ must be $2\pi q$, where q is an integer. Thus, the phase condition $2kL_0 - \delta'_m = 2\pi q$ has the same form as (26), (27), and δ'_m is the phase correction known to us (in other resonators it can, of course, assume quite different values than in a flat cavity). The emission intensity after a round

APPROVED FOR RELEASE: 2007/02/09: CIA-RDP82-00850R000500010010-4

APPROVED FOR RELEASE: 2007/02/09: CIA-RDP82-00850R000500010010-4

trip through the resonator turns out to be multiplied by $\exp(-2\delta''_m)$, and the value of $1 - \exp(-2\delta''_m)$ is none other than the diffraction emission losses.

When calculating the mode structure many authors do not use the above-discussed procedure based on analysis of passage of a light beam through a cavity, but they find steady solutions of the differential field equations, imposing the corresponding boundary conditions on the mirrors. The emission attenuation caused by the presence of diffraction losses is described in this case by introduction of the complex frequency $\omega = \omega' - i\omega''$, so that the dependence of the field on time acquires the form $\exp(-i\omega t) = \exp(-i\omega' t - \omega'' t)$ (ω' and ω'' are real). The relation of ω' and ω'' to the eigenvalues of the operator $\hat{P}$ is very easy to establish. Obviously, the real part ω' of the complex frequency figures in the phase conditions such that for ω' formula $\omega'_{mq} = (c/2\ell)(2\pi q + \delta'_m)$ is valid as before. Finally, inasmuch as the field amplitude varies by $\exp(-\delta''_m)$ times on a complete round trip through the resonator, that is, in the time $2L_0/c$, then $\delta''_m = 2L_0/c)\delta''_m$ or $\omega''_m = (c/2L_0)\delta''_m$.

Resonator with Active Layer. Let us proceed with a study of the problem of how the resonator properties vary on introduction of an amplifying medium into it; here, just as when analyzing the properties of an ordinary empty resonator, we shall proceed in accordance with reference [16].

In order to explain the relation between the spatial distribution of the emission in real lasers and in empty resonators, let us consider the ideal case of an infinite plane-parallel active layer of thickness ℓ placed in an arbitrary open resonator (Figure 1.18); the resonator will be depicted as the two-mirror resonator for simplicity). We shall consider that the emission gain with respect to intensity k_{gain} (cm^{-1}) is distributed uniformly with respect to the layer; the index of refraction of the layer material n_0 is also constant and can differ from one (the surfaces of the layer are transparent in the latter case). Let also only one of the mirrors have the reflection coefficient equal to one as before; the reflection coefficient of the second will be $R' < 1$.

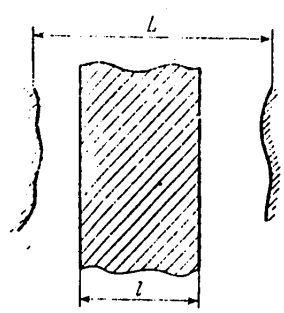

Figure 1.18. Active layer in an open resonator.

First, let us consider the transmission of a light wave through the active layer. The field distribution $u(x_2, y_2)$ on the second surface of the layer can be expressed in terms of the field distribution on the first surface $u(x_1, y_1)$ using formula (2) from § 1.1 if we substitute $z = \ell$ in it and replace the wavelength in the empty space λ by the wavelength in the layer $\lambda' = \lambda/n_0$, and k, by the complex propagation

APPROVED FOR RELEASE: 2007/02/09: CIA-RDP82-00850R000500010010-4

APPROVED FOR RELEASE: 2007/02/09: CIA-RDP82-00850R000500010010-4

constant $2\pi/\lambda' - ik_{gain}/2$. Neglecting the terms $k_{gain}(x_2 - x_1)^2/4\ell$ and $k_{gain}(y_2 - y_1)^2 4\ell$ in the exponent of the expression under the integral sign and proceeding to the wavelength in empty space λ, we obtain

$$u(x_2, y_2) = \frac{\exp\left(\frac{k_{yc}}{2} l + i\frac{2\pi}{\lambda} n_0 l\right)}{i\lambda l/n_0} \int\int \exp\left\{\frac{2\pi i}{\lambda}\left[\frac{(x_2 - x_1)^2}{2l/n_0} + \frac{(y_2 - y_1)^2}{2l/n_0}\right]\right\} \times$$
$$\times\, u(x_1, y_1)\, dx_1 dy_1.$$

From this relation it is obvious that the form of the wave front on passage through an active layer of thickness ℓ is transformed just as on traveling the distance ℓ/n_0 in empty space; the optical thickness of the layer $n_0\ell$ determines only the magnitude of the total phase lead; the field amplitude is multiplied by $\exp(k_{gain}\ell/2)$ (the first of these derivations also follows from the form of the beam matrix for a plane-parallel layer of dielectric; see Table 1.1).

Now let us construct an empty resonator equivalent to the given one, that is, having the same transverse structure of the oscillations. Let us do this as follows: let us replace the mirror with $R' < 1$ by a mirror of the same shape but totally reflecting; let us remove the active medium; finally, let us decrease the length of the section in which the layer was located by $\ell(1 - 1/n_0)$ (in the case depicted in Figure 1.18 it is simply necessary to install mirrors at the distance $L_{equiv} = L - \ell(1 - 1/n_0)$ from each other). From the above-performed analysis of transmission of a beam through the active layer it follows that the integral equation of the resonator with active medium will differ from the equation of an empty resonator constructed in this way only by the constant factor in the right-hand side:

$$\gamma u(x, y) = \sqrt{R'} \exp(2ikL_0 + k_{yc}l)\, \hat{P} u(x, y). \tag{29a}$$

Here L_0 is the total optical length of the resonator with the medium (for the case of Figure 1.18, equal to $L + \ell(n_0 - 1)$, $\hat{P}$ is the integral operator of the equivalent empty resonator, the eigenvalues of which will be denoted as before as $\beta_m = \exp(i\delta'_m - \delta''_m)$.

It is remarkable that neither introduction of a uniformly amplifying medium or replacement of the totally reflecting mirror by a semitransparent one implies alteration of the transverse structure of the natural oscillations. Their spectrum is subjected to significant retuning. Using the same arguments as in the case of an empty resonator, we obtain the following formulas defining the spectrum of the natural frequencies of the resonator with the active medium:

$$\omega'_{mq} = \frac{c}{2L_0}(2\pi q + \delta'_m),$$
$$\omega''_m = \frac{c}{2L_0}\left[\delta''_m + \ln\frac{1}{R'} - k_{yc}l\right]. \tag{31}$$

The first of them, it would appear, does not differ from the formulas for ω' already known to us; however, here the optical length of the resonator includes the optical length of the active layer $n_0\ell$ as a term, which changes the situation somewhat. The fact is that the index of refraction of the amplifying medium essentially depends on the position of the line inside the amplification band; this can cause disturbance

APPROVED FOR RELEASE: 2007/02/09: CIA-RDP82-00850R000500010010-4

APPROVED FOR RELEASE: 2007/02/09: CIA-RDP82-00850R000500010010-4

of the equidistance of the frequencies in view of their "pulling" (see, for example, [17]). As a rule, the divergence of the emission is not influenced by effects of this type, and therefore they will not be considered here.

The second formula arouses great interest. According to this formula, the introduction of the active medium has an enormous effect on the damping rate of the natural oscillations. This leads to a complete change in the picture of the resonance properties of the system as a whole.

Actually, the condition of overlap of the resonance curves corresponding to two adjacent resonance frequencies of the system ω_1 and ω_2 can be written in the form [3]

$$|\omega_1' - \omega_2'| < (\omega_1'' + \omega_2'')/2. \tag{32}$$

If the active medium in the optical cavity is absent or is not excited, this condition is almost always satisfied, for the natural frequencies of the individual modes are comparatively close together, and the losses causing damping usually are not so small (their basic source frequently is not the diffraction effects, but inactive absorption in the medium and exit of the emission through a semitransparent mirror). Satisfaction of the given condition, in turn, means that when testing the use of this system as a passive filter its resonance properties were not manifested at all, and it would be meaningless to talk about the existence of individual types of oscillations.

The situation is quite different in the presence of an excited active medium. In accordance with (31), the values of ω'' decrease; on approaching the lasing threshold, some of them approach zero. As a result, under conditions of regenerative gain, the resonance properties of the system can be manifested fully in spite of satisfaction of condition (32) in the absence of stimulation of the active medium. The resonance properties of the system are expressed still more sharply during steady lasing when one or several values of ω'' are equal to zero (generally speaking, as a result of a continuous "makeup" of the lasing by spontaneous emission, they also are very slightly different from zero here, but this can almost always be neglected).

Thus, in the case of a lasing laser the situation is not at all similar to that which would occur if the laser resonator were used as a passive filter and were excited by an external source. Therefore when describing the operation of a laser it is not worthwhile to use concepts connected with the attenuation rate in an empty resonator such as the Q-factor and resonance width of the line. Practice demonstrates that this only leads to every imaginable error: one gets the idea that in lasers with large losses per pass, the lasing process is of a "nonresonant" nature. Therefore we shall not introduce the given concepts or use them.

Suitability of the Standard Model of an Open Optical Cavity for Describing Real Lasers. Analysis of the above-presented example makes it possible to formulate conditions, the satisfaction of which permits direct use of the results of the theory of open, empty resonators to describe the field structure in real lasers. The most important of these conditions are as follows [16]:

1. High optical uniformity of the active medium is required.

Passage of the wave front through an inhomogeneous medium cannot be reduced to traveling the corresponding path in empty space; the selection of the equivalent

APPROVED FOR RELEASE: 2007/02/09: CIA-RDP82-00850R000500010010-4

APPROVED FOR RELEASE: 2007/02/09: CIA-RDP82-00850R000500010010-4

empty resonator is complicated, and in many cases it becomes impossible in general.

2. In the case of a resonator with external mirrors, the effect of the light reflected from the end surfaces of the active element must be excluded. We have already discussed the importance of this condition in the preceding section; in the presence of transmitting coatings usually it is possible to consider that this condition is satisfied. In individual cases (see § 4.1) even such measures turn out to be insufficient, and in order to eliminate side effects it is necessary to incline the interfaces with respect to the direction of propagation of the emission.

3. When deriving equation (29a), a model of an infinite uniform layer was used. For its applicability it is theoretically necessary that the index of refraction and the inverse population be constant not only directly between the mirrors, but also in the entire region where the emission field has noticeable intensity. The influence of the lateral surfaces of the active elements, the cell walls, the surfaces of the discharge excitation electrodes, and so on should not be manifested.

In real lasers, the latter condition is almost never satisfied. Moreover, the role of the aperture irises limiting the lasing zone frequently is played not by mirrors, but by the side surfaces of an active rod or the cell walls. In order at least to exclude the appearance of any type of additional beams observed in the first experiments with solid-state lasers [18, 19] and arising as a result of total internal reflection from the lateral surfaces, these surfaces are usually frosted (more rarely, the rod is submerged in an immersion medium). Usually partial scattering of the diffracting radiation still occurs, and the open resonator model is not entirely correct. However, models of the type of the "ideal dielectric rod between infinite mirrors" or "ideal dielectric cylinder inside a circular infinite wave guide" are entirely inapplicable for the description of real lasers; it is surprising that papers dealing with the study of such models as applied to the laser situation are sometimes still encountered.

Inasmuch as the decrease in the role of light scattered on the lateral surfaces is accompanied by an increase in the degree of directionality of the emission, during estimates of the limiting system characteristics it is still legitimate to make use of the open resonator model, which we shall continue to do hereafter.

4. In order that the laser emission field distribution be able in general to be described by the natural solutions of a steady integral equation, it is necessary that the lasing conditions remain unchanged for a sufficiently long time. This requirement is again far from always satisfied. Thus, in the 1960's, in a number of theoretical [20, 21] and experimental [22, 23] papers it was demonstrated that during giant pulse operation of a laser with flat cavity and comparatively homogeneous medium, the spatial distribution of the gain and the emission field changes extremely rapidly (during the time 10^{-9} to 10^{-8} sec). In such a situation it is inconceivable to consider the spatial structure of the emission unrelated to the lasing kinetics. The most fundamental papers on this relation for the case of a flat cavity belong to Suchkov and Letokhov [24, 25].

The operating conditions of the majority of types of lasers are nonsteady also in the absence of Q-switching of the resonator (here we are primarily dealing with the presence of characteristic emission "spikes" which are well known to specialists in solid-state lasers). A detailed theoretical description of the time-space

APPROVED FOR RELEASE: 2007/02/09: CIA-RDP82-00850R000500010010-4

APPROVED FOR RELEASE: 2007/02/09: CIA-RDP82-00850R000500010010-4

structure of the emission turns out to be possible only in certain simplest cases (for example, [24]), never realized in reality. Therefore in the overwhelming majority of papers the quasisteady approximation is used which does not take into account the peculiarities of the lasing kinetics. The nature of the errors made here is clear if we consider that in real lasers the role of the "seed" in shaping the individual lasing pulses ("spikes") is almost always played by the spontaneous noise emission. The light beam becomes narrowly directional only after multiple passage of the "seed" emission through the resonator (for lasers with unstable resonators this process will be considered in § 4.1). Therefore the departures from the quasisteady state of the operating conditions, as a rule, lead to some increase in the emission divergence.

In spite of this fact, the quasisteady approximation is in many cases efficient.

If departures from the ideal resonator (and with them, also angular divergence in the quasisteady approximation) are large, then the peculiarities of the kinetics, for obvious reasons, are felt little in the resultant width of the radiation pattern. In particular, the angular distribution of the emission begins to coincide approximately in the giant-pulse and ordinary lasing conditions.

For the case of ordinary free lasing conditions using the quasisteady multimodal approximation, it is possible to achieve satisfactory description of the properties even of lasers with highly homogeneous medium ([26], see § 2.4).

Thus, having set forth all the necessary stipulations with respect to the possibility of using the open resonator model in the quasisteady approximation, let us consider another aspect of the "resonator and active medium" problem.

§ 1.4. Efficiency of Excitation Energy Conversion in Laser Resonators

One of the basic requirements imposed on a laser resonator is high conversion efficiency of the energy stored in the excited active medium to stimulated emission energy. In order to achieve this, it is necessary:

1) to select the general configuration of the resonator (the placement of the mirrors and their transverse dimensions) so that the entire volume of the active medium will be filled with laser emission or, in flow lasers, the entire medium passes through the stimulated beam. This condition is trivial (although laser builders are not always sufficiently careful to see that it is satisfied);

2) to select the optimal magnitude of the emission losses. In the case of flat or stable cavities, the emission losses are the transmission coefficient of the exit mirror $1 - R'$; in the case of unstable resonators, the emission losses are the parameter $1 - 1/M^2$ which has a similar role, where M is the magnification of the resonator.

In this section we shall discuss the meaning and the method of selecting optimal losses. This question is the subject of a very broad literature. Methods of calculating ordinary type laser efficiencies (for lasers with stationary medium in which an inverse population is created) as a function of the properties of the medium and the value of the exit mirror transmission coefficient were developed generally in 1962-194, and they are discussed in a number of monographs and surveys [27, 28,

APPROVED FOR RELEASE: 2007/02/09: CIA-RDP82-00850R000500010010-4

APPROVED FOR RELEASE: 2007/02/09: CIA-RDP82-00850R000500010010-4

17]. The results of the majority of experiments pertain to the case of a flat cavity and are based on formal solution of the equations of emission transport of the type

$$\frac{dI_+}{dz} = (k_{\underset{(a)}{\text{ус}}} - \sigma_0) I_+, \quad \frac{dI_-}{dz} = -(k_{\underset{(a)}{\text{ус}}} - \sigma_0) I_-,$$

Key: a. gain

where I_+ and I_- are the intensities of the emission fluxes going to the exit mirror and in the opposite direction; k_{gain} is the emission gain in the medium, σ_0 is the so-called coefficient of "harmful" losses; in totally reflecting ($z = 0$) and exit ($z = \ell$) mirrors the following boundary conditions are imposed: $I_+|_{z=0} = I_-|_{z=0}$, $I_-|_{z=\ell} = R' I_+|_{z=\ell}$. This method is insufficiently clear and, as we shall see later, it is not always applicable; let us consider the given problem by somewhat different methods.

Efficiency of Energy Conversion in an Element of Volume of the Medium. Let us first define the maximum possible energy removal per unit volume of active medium; the operating conditions will be considered quasisteady, and the excitation conditions of the medium will be considered given. For solution of this problem it is necessary first of all to know how the number of photons which are produced in the indicated volume per unit time as a result of resonance interaction of the laser emission with the active medium depends on the laser emission flux density I (photon·cm^{-2}·sec^{-1}). This number is equal to $Ik_{gain}(I)$. The standard form of the dependence of Ik_{gain} on I is represented by the curve I in Figure 1.19. First comes the linear section, the slope of which is determined by the magnitude of the unsaturated gain of the weak signal k^0_{gain}. Then saturation begins to be manifested, and the gain decreases. For large I the product $Ik_{gain}(I)$ obviously approaches the limit P_{incl} equal to the number of acts of filling the inverse population as a result of pumping. It is clear that the form of the curve I cannot depend strongly on such specific characteristics of the medium as the system of levels, the nature of broadening of the operating transition line, and so on.

Let us consider the processes of nonresonance ("inactive") absorption of the laser emission on admixtures occurring in the same unit volume. The number of these processes is equal to $I\sigma_0$, where σ_0(cm^{-1}) is the same coefficient of "harmful" losses as in the above-presented equations for the radiation transfer (sometimes the absorption losses in the resonator mirrors also play a noticeable role, but they, as a rule, can be considered distributed over the entire length in the calculations, and it is possible to introduce the corresponding correction to σ_0). Two straight lines are plotted in Figure 1.19, one of which (II) corresponds to $\sigma_0 = k^0_{gain}/5$, and the other (III), $\sigma_0 = k^0_{gain}/50$.

The contribution of the investigated unit volume to the overall balance of the number of photons in the entire device is $Ik_{gain}(I) - I\sigma_0$. From the figure it is obvious that this difference is maximal for defined laser emission density; both

APPROVED FOR RELEASE: 2007/02/09: CIA-RDP82-00850R000500010010-4

APPROVED FOR RELEASE: 2007/02/09: CIA-RDP82-00850R000500010010-4

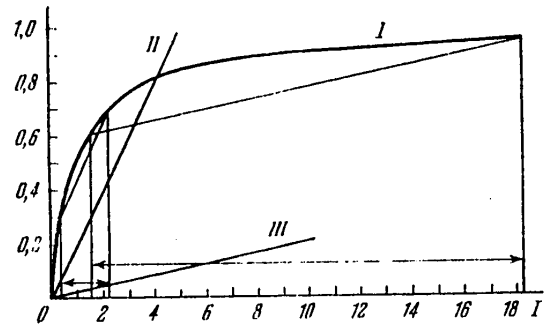

Figure 1.19. Number of elementary processes in an active medium as a function of emission density (the values of Ik_{gain}, $I\sigma_0$ are plotted on the y-axis.

the height of the peak and its width increase with an increase in the ratio k^0_{gain}/σ_0 (in the figure the arrows indicate the dangers of the flux densities for which the contribution is no less than 80% of its maximum value).

Now it is possible to estimate the efficiency of the energy conversion. It is conveniently characterized by the value of $X \equiv [Ik_{gain}(I) - I\sigma_0]/P_{pump}$; this is the ratio of the real contribution to the photon balance to the contribution in the case of an ideal laser in which the "harmful" losses are absent ($\sigma_0 = 0$), and I is so large that the entire inverse population is "processed" into laser emission. For exact calculation of X, it is necessary to know the form of the function $k_{gain} = k_{gain}(I)$, which varies, first of all, with the nature of broadening of the operating transition line. In the case of uniform broadening when all of the atoms in the upper laser level participate identically in the amplification process, it is extremely simple to establish this relation. Actually, in the steady-state mode it is necessary to realize equilibrium between the processes of filling the inverse population and its decay. In the important case of the most effective four-level media with "frozen" lower level of the operating transition (see [17]), the equilibrium condition has the simplest form $P_{pump} = Ik_{gain} + Ak_{gain}/\tau$, where A is the proportionality factor between the inverse population and k_{gain}, τ is the spontaneous decay time of the excited state. Hence, it follows that

$$k_{\text{ус}} = \frac{P_{\text{нак}}}{I + A/\tau} = \frac{\tau P^{(a)}_{\text{нак}}/A}{1 + I\tau/A}.$$

Key: a. pump

Inasmuch as for $I = 0 k_{gain} = k^0_{gain}$, then $\tau P_{pump}/A = k^0_{gain}$; the ratio τ/A in the denominator is called the nonlinearity coefficient and usually is denoted by the letter α [27]. Thus,

APPROVED FOR RELEASE: 2007/02/09: CIA-RDP82-00850R000500010010-4

APPROVED FOR RELEASE: 2007/02/09: CIA-RDP82-00850R000500010010-4

$$k_{\text{yo}}(I) = \frac{k^0_{\text{yo}}}{1+\alpha I}. \quad (33)$$
(a)

Key: a. gain

Considering these relations, the resultant formula for X acquires the form

$$X(I) = \frac{\alpha I}{1+\alpha I} - \frac{\sigma_0}{k^0_{\text{yo}}}\alpha I. \quad (34)$$

The value of X determined by this formula reaches its maximum value X_{max} for $\alpha I = \sqrt{k^0_{gain}/\sigma_0} - 1$; this value is

$$X_{\max} = \left(1 - \sqrt{\sigma_0/k^0_{\text{yo}}}\right)^2. \quad (35)$$

The graph of the dependence of X_{max} on k^0_{gain}/σ_0 following from (35) is presented in Figure 1.20 (curve I).

If the pumping power and the density of the laser emission are not distributed too nonuniformly with respect to the volume of the active medium, formula (35) gives an estimate of X_{max} for the entire device as a whole; as we shall see, in this case X_{max} is wholly determined by the ratio k^0_{gain}/σ_0. It is remarkable that the attained efficiency of energy conversion does not at all depend on the fact that the active medium is used in the lasing or amplifying system, but it is determined only by the characteristics of the medium and the conditions of its excitation. It is only necessary for any laser to insure optimal density of the stimulated or amplified emission.

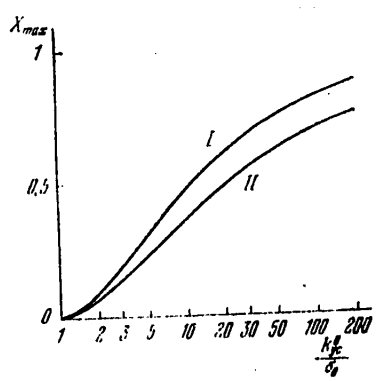

Figure 1.20. Energy conversion efficiency in a laser medium as a function of the ratio k^0_{gain}/σ_0.

The primary subject of investigation in this book is lasers. The meaning of the parameter k^0_{gain}/σ_0 for them is well known: it is none other than the ratio of the

APPROVED FOR RELEASE: 2007/02/09: CIA-RDP82-00850R000500010010-4

APPROVED FOR RELEASE: 2007/02/09: CIA-RDP82-00850R000500010010-4

pumping intensity to the value where k^0_{gain} is equal to σ_0 (that is, the lasing threshold is reached in the absence of "useful" emission losses). This ratio usually is called exceeding the lasing threshold and is denoted by n_0. Then (35) begins to coincide with the corresponding factor in the known formulas for laser efficiency [29, 17] which, in addition to this factor, also include the efficiency of the system for exciting the medium and other similar parameters (much later than in [29], formula (35) was also obtained by Rigrod [30]).

Accounting for Nonuniformity of the Distribution of Laser Radiation Lengthwise of the Cavity. There are a number of causes which can give rise to nonuniformity of the distribution of stimulated emission with respect to the volume of the active medium even for entirely uniform excitation of it. Let us begin with the fact that it is possible to do away with the presence of a "fine" structure of the intensity distribution with respect to length only during operation of the laser on a large number of modes with different axial indices (which also usually occurs). The fact is that only superposition of many standing waves of the type of $\sin q\pi z/L$ with different q gives more or less uniform total emission distribution with respect to length; in other words, for a broad emission spectrum it is possible to neglect the interference of the emission fluxes following with respect to the laser in the forward and return directions and to consider that I is simply equal to the sum of the densities of these fluxes. For a flat cavity, lasing is also usual in many transverse modes; this, by analogous arguments, permits departure from the transverse mode structure (see § 2.4).

Another reason causing nonuniformity of the distribution I in the medium is the presence of high gain on its length. It is clear that the uniformity of the distribution with respect to length increases as the reflection coefficient of the exit mirror R' approaches one; however, here the average emission density inside the resonator increases rapidly, sooner or later beginning to exceed the optimal value.

It is again possible to determine the most advantageous reflection coefficient R' from the point of view of achieving maximum output emission power using formulas (33), (34). Substituting the optimal flux density $I_{opt} = (\sqrt{k^0_{gain}/\sigma_0} - 1)/\alpha$ in (33), we obtain $k_{gain} = \sqrt{\sigma_0 k^0_{gain}}$. Obviously, once the total flux density is inevitably nonuniform with respect to length it is advantageous that it fluctuate around I_{opt}; here k_{gain} must fluctuate around $\sqrt{\sigma_0 k^0_{gain}}$, and the average value with respect to length of the laser $\overline{k_{gain}}$ can be taken equal to this value.

The condition of steady-state conditions in our case has the form

$$R' \exp\left[2\left(\overline{k_{\text{ус}}} - \sigma_0\right) l\right] = 1, \tag{36}$$

where ℓ is the length of the specimen (the diffraction losses of a flat cavity can be neglected in the given investigation). Substituting $k_{gain} = \sqrt{\sigma_0 k^0_{gain}}$, we obtain

$$\ln\left(1/R'_{\text{опт}}\right) = 2\sigma_0 l\left(\sqrt{k^0_{\text{ус}}/\sigma_0} - 1\right). \tag{37}$$

Knowing R'_{opt} it is easy to estimate the degree of nonuniformity of the distribution I with respect to length. Actually, let the flux density incident on the exit

APPROVED FOR RELEASE: 2007/02/09: CIA-RDP82-00850R000500010010-4

APPROVED FOR RELEASE: 2007/02/09: CIA-RDP82-00850R000500010010-4

mirror of the resonator be equal to I_0; the density of the flux reflected from it is $R'I_0$. Then the density of the flux incident on the totally reflecting mirror is $R'I_0 \exp[(\bar{k}_{gain} - \sigma_0)\ell] = I_0\sqrt{R'}$. Hence, it follows that the ratio of the total flux densities at the exit mirror and the totally reflecting mirror of a flat cavity is $(1 + R')/2\sqrt{R'}$.

It is easy to see that the total flux assumes extremal values near the end mirrors. Thus, it is possible to consider that the maximum I is larger than the minimal I by $(1 + R'_{opt})/2\sqrt{R'_{opt}}$ times where R'_{opt} is defined by the formula (36). It only remains to use Figure 1.19 to check whether the different densities go beyond the limits of the region inside which X is sufficiently close to X_{max}. If they do not go outside the region, then formulas (35), (37) can be used without considering the nonuniformity of the emission distribution with respect to length of the resonator. In the overwhelming majority of cases, that is the way it is. There are two reasons for this. First, the ratio $(1 + R')/2\sqrt{R'}$ greatly exceeds one only for very small R'. Thus, if R' = 0.1, then $(1 + R')/2\sqrt{R'} = 1.74$, and the total flux is distributed not too nonuniformly. Secondly, from formula (37) it is obvious that R'_{opt} is very small, as a rule, for large k^0_{gain}/σ_0; in this case the maximum difference in Figure 1.19 is very broad. For these reasons formulas (35), (37) are valid in an enormous range of variation of the laser parameters. In reference [31] it was demonstrated that they cannot be used only for such large "harmful" losses on the length of the sample $\sigma_0\ell$ that the following inequality begins to be satisfied:

$$\left(1 - \sqrt{\frac{\sigma_0}{k^0_{yc}}}\right)^2 \geqslant \frac{1}{l}\int_0^l \exp[-\sigma_0(l - z)]\,dz = \frac{1 - \exp(-\sigma_0 l)}{\sigma_0 l}.$$

The value in the right-hand side of the inequality is a value of X averaged on the length of the sample, which would be reached if all the filling of the inverse population as a result of pumping were "processed" into lasing photons which would subsequently be lost only as a result of absorption on the path to the exit mirror.

Let us present another example of the use of formula (34) to estimate the efficiency of the laser. This time we shall consider that measures are taken for spectral selection of the emission and lasing is single-frequency. Then a standing wave with a period of $\lambda/2$ is set up along the active element. If the emission fluxes propagated in the forward and return directions do not differ very strongly with respect to density (R' is not too small), then the intensity modulation depth in a standing wave period approaches 100%. In this case it is necessary to perform averaging of X(I) over the flux densities in the interval from 0 to $2\bar{I}$, where $\bar{I}$ is the mean value of the density. Considering that in view of linearity the losses as a result of inactive absorption $\overline{I\sigma_0} = \sigma_0\bar{I}$, we obtain

$$X(\bar{I}) = \frac{1}{2\pi}\int_0^{2\pi} \frac{\alpha\bar{I}(1 - \cos\varepsilon)}{1 + \alpha\bar{I}(1 - \cos\varepsilon)}\,d\varepsilon - \frac{\sigma_0}{k^0_{yc}}\alpha\bar{I} = 1 - \frac{1}{\sqrt{1 + 2\alpha\bar{I}}} - \frac{\sigma_0}{k^0_{yc}}\alpha\bar{I} \qquad (34a)$$

APPROVED FOR RELEASE: 2007/02/09: CIA-RDP82-00850R000500010010-4

APPROVED FOR RELEASE: 2007/02/09: CIA-RDP82-00850R000500010010-4

(the factor $1 - \cos\varepsilon = 2\sin^2(\varepsilon/2)$ describes the emission intensity as a function of the coordinate in a standing wave period); the maximum of X is reached for $\alpha\bar{I} = (1/2)[(k^0_{gain}/\sigma_0)^{2/3} - 1]$,

$$X_{max} = 1 + \frac{1}{2}\sigma_0/k^0_{yc} - \frac{3}{2}\sqrt[3]{\sigma_0/k^0_{yc}}. \tag{35a}$$

The graph of this value as a function of k^0_{gain}/σ_0 is presented in Figure 1.20 (curve II). From the figure it is obvious that the energy conversion efficiency on making the transition from multimode to single-frequency lasing decreases noticeably even if the spectral selector which isolates one frequency is ideal and does not introduce additional losses.

Although all the preceding formulas of this section were derived for a defined type of active medium, they are easily extended to the case of media with the same uniform broadening of the operating transition line, but with arbitrary level diagram. For a different level diagram (in particular, for a three-level medium, an example of which is the ruby), the inverse population balance equation acquires a more complicated form, but the final formula (33) describing the dependence of k_{gain} on I remains the same; only the nonlinearity coefficient α is expressed in terms of the parameters of the medium otherwise [27]. In the right-hand sides of formulas (34) and (35) the factor $k^0_{gain}/\alpha P_{pump}$ appears which was equal to one for four-level media with "frozen" lower level of the laser transition, and in all other cases this factor turns out to be less than one. The reduction in conversion efficiency by comparison with the four-level medium is explained by the fact that in the presence of atoms on the lower level of the operating transition a part of the pumping power is spent on equalizing the populations of the upper and lower levels without causing the appearance of amplification.

If broadening of the operating transition line is nonuniform, the form of $k_{gain}(I)$ begins to depend on the signal spectrum and, in the general case, differs from (33). After replacement of (33) by the corresponding expresion, the entire subsequent analysis can be performed by the same scheme. It is not worthwhile to reproduce it here: we shall return somewhat later to the case of a nonuniformly broadened line, considering it by more efficient means.

The above-discussed approach is based on investigation of the energy balance in an element of volume of the active medium. This is convenient in that it permits estimation of the attainable energy conversion efficiency in a laser, in practice based on data on the properties of the medium and its excitation system. We have noted that it is possible to use formulas (34), (35) independently of whether the device is an oscillator or amplifier; the resonator parameters were introduced into the analysis in essence only to estimate the possible errors. If we are interested in more detail in the properties of the lasers themselves (in particular, the dependence of their efficiency on the transmission of the exit mirror), it will be more useful to consider a somewhat different approach which will now be discussed.

General Excitation Energy and Stimulated Emission Balance. The power expended on exciting the upper laser level is expended along two channels; for spontaneous and stimulated transitions. In turn, the photons created as a result of stimulated transitions can either be absorbed by sources of "harmful" losses or exit from the laser

APPROVED FOR RELEASE: 2007/02/09: CIA-RDP82-00850R000500010010-4

APPROVED FOR RELEASE: 2007/02/09: CIA-RDP82-00850R000500010010-4

successfully, forming a useful signal. In accordance with this system, the expression for the energy conversion efficiency can be represented in the form of the product of two co-factors: $X = (1 - p_1)(1 - p_2)$. Here p_1 is the proportion of the total number of processes of deactivation of the upper laser level going to spontaneous transitions, and p_2 is the proportion of the total number of photons generated by stimulated transitions which are then absorbed inside the laser by the sources of losses. The value of p_2 in a flat cavity depends in practice only on $\sigma_0 \ell$ and R'; let us consider it first.

The flux density of the emission incident on the exit mirror of the resonator will be denoted by I_0 as before. Then, as we have seen, the density of the flux incident on the totally reflecting mirror is $I_0\sqrt{R'}$. In order to calculate the number of photons absorbed inside the laser, it is necessary to be given the emission density along the length of the sample. The interference effects, if they exist, can be neglected in this case: in view of the noted linear nature of the losses, the averaging of the number of absorbed photons with respect to the standing wave period offers nothing new. Thus, it is sufficient to calculate the arithmetic sum of the two fluxes traveling in opposite directions. In estimates of this type each of these fluxes can be completely considered exponentially increasing along the length of the sample. Then the flux following from the totally reflecting ($z = 0$) to the exit ($z = \ell$) mirror is $I_+ = I_0\sqrt{R'} \exp[\ln(1/\sqrt{R'})z/\ell]$; the flux in the opposite direction, $I_- = I_0\sqrt{R'} \times \exp[-\ln(1\sqrt{R'})z/\ell]$. The total number of absorbed photons is

$$\sigma_0 \int_0^l [I_+(z) + I_-(z)]\, dz = 2I_0\sigma_0 l(1 - R')/\ln(1/R').$$

Inasmuch as $I_0(1 - R')$ photons exit from the resonator,

$$p_2 = \frac{2I_0\sigma_0 l(1 - R')/\ln(1/R')}{2I_0\sigma_0 l(1 - R')/\ln(1/R') + I_0(1 - R')} = \frac{2\sigma_0 l}{2\sigma_0 l + \ln(1/R')}. \quad (38)$$

With respect to meaning the right-hand side of (38) is the ratio of "harmful" losses $2\sigma_0 \ell$ to the total losses. Hence, it follows that it is more correct to call the emission losses not $1 - R'$ as is usually done, but $\ln(1/R')$ (for R' close to one, these two values in practice coincide).

Now let us consider the value of p_1. In the case of multimodal lasing (that is, in the absence of a standing wave) in a four-level medium with uniformly broadened line and populated lower operating level everything is quite simple. Actually, when there is no lasing, all of the excitation power of the upper operating level is spent on spontaneous transitions; the gain will be k^0_{gain} in this case. In the presence of lasing the gain decreases to some value $k_{gain} < k^0_{gain}$; the decrease in gain is a consequence of a proportional decrease in upper level population, which, in turn, is accompanied by proportional decrease in the number of spontaneous transitions. Thus, when a gain k_{gain} is maintained in the active medium under the counter effects of pumping and lasing, the proportion of the excitation power equal to k_{gain}/k^0_{gain} is consumed for spontaneous transitions. Considering the pumping power distributed uniformly with respect to volume and performing the averaging with respect to it, we obtain the final expression

APPROVED FOR RELEASE: 2007/02/09: CIA-RDP82-00850R000500010010-4

APPROVED FOR RELEASE: 2007/02/09: CIA-RDP82-00850R000500010010-4

$$p_1 = \bar{k}_{yc}/k^0_{yc}. \quad (39)$$
(a)

Key: a. gain

Expressing $\bar{k}_{gain}$ in terms of the system parameters using the steady state conditions of (36), we obtain $p_1 = [2\sigma_0\ell + \ln(1/R')]/2k^0_{gain}\ell$.

Now let us find the optimal gain R'_{opt} for which the maximum value of $X = 1 - p_1 - p_2 + p_1p_2$ is reached. In our case the product p_1p_2 is equal to σ_0/k^0_{gain} and does not depend on R'; thus, it is necessary to find conditions under which $p_1 + p_2$ is minimal. If the product of two positive values is given, their sum is minimal when they are equal to each other. Therefore it is appropriate to select R' so that the condition $p_1 = p_2$ will be satisfied. Hence, it follows that $[2\sigma_0\ell + \ln(1/R'_{opt})]^2 = 4\sigma_0k^0_{gain}\ell^2$ or $\ln(1/R'_{opt}) = 2\sigma_0\ell(\sqrt{k^0_{gain}/\sigma_0} - 1)$; $p_1 = p_2 = \sqrt{\sigma_0/k^0_{gain}}$; thus, we have arrived at the known formulas (37), (35).

This approach helps to understand other results already known to us. Thus, it is possible to show that in the case of media with arbitrary level diagram but, as before, uniformly broadened line $1 - p_1 = (k^0_{gain} - k_{gain})/\alpha P_{pump} = (k^0_{gain}/\alpha P_{pump})(1 - k_{gain}/k^0_{gain})$; hence, it is obvious that in the expression for X, just as before, the factor $k^0_{gain}/\alpha P_{pump} < 1$ appears. Let us write out the resultant formula for X for multimode lasing and arbitrary R':

$$X = \frac{k^0_{yc}}{\alpha P_{\text{нак}}}_{(b)} \frac{k^0_{yc} - \sigma_0 - \ln(1/R')/2l}{k^0_{yc}}_{(a)} \frac{\ln(1/R')}{\ln(1/R') + 2\sigma_0 l}. \quad (40)$$

Key: a. gain b. pump

The situation with calculation of laser efficiency in the case of uniform lasing turns out to be more complex: at first glance, it is even unclear in what phase of the analysis it is possible to consider the presence of a standing wave. A more careful investigation shows that all of the calculations to formula (39) remain valid, but it is impossible to substitute the value of $\bar{k}_{gain}$ calculated using the condition of steady-state nature of (36) in this formula. The reasons for this become clear if we consider that at the standing wave nodes the field is absent, there are no stimulated transitions, and a large number of excited atoms accumulate (the local value of the gain reaches k^0_{gain}). These atoms make a defined, and large, contribution to the total number of spontaneous decay processes and, unconditionally, must be considered when calculating p_1 by formula (39); on the other hand, they do not participate in the amplification process, and therefore they must not figure in the condition of reproducibility of the process of the type of (36). Hence it follows that the radiation transport equations presented at the beginning of this section from which we have (36) are inapplicable in the given case. It is obvious that in the presence of a standing wave, the condition of steady state conditions must be based on more careful calculation of the number of stimulated transitions; as

APPROVED FOR RELEASE: 2007/02/09: CIA-RDP82-00850R000500010010-4

APPROVED FOR RELEASE: 2007/02/09: CIA-RDP82-00850R000500010010-4

was done in (34a) it is necessary to average not k_{gain}, but $k_{gain}I$ over the standing wave period. Then we automatically arrive at the preceding results.

Meaning and Possibilities of Applying the Derived Relations. The above-discussed method of calculating the efficiency, in spite of its simplicity, at times turns out to be useful even in highly nontrivial situations. It is especially convenient in cases where certain factors exist that increase the number of processes of deactivation of the upper operating level undesirable from the point of view of lasing, and there is a possibility of estimating the effect of these factors independently. Let us present two such examples.

Sometimes so-called superluminescence plays a noticeable role. It consists in the fact that before leaving the active medium the spontaneous emission can be amplified, causing additional deactivation of the excited atoms at the same time. As a result, the number of decay processes of the excited state not contributing to lasing increases by $\gamma > 1$ times. The parameter γ can be calculated; it depends on the properties of the medium, the configuration of the active zone, the conditions on the surfaces bounding it and, in the first approximation, on the mean value of the gain with respect to volume [32]. Under steady state conditions the latter is determined by the magnitude of the resonator losses. Calculating γ, it is also possible to estimate the energy conversion efficiency in the resonator: $X = (1 - \gamma p_1)(1 - p_2)$ where p_1 is the proportion of the spontaneous decay processes calculated without considering superluminescence; p_2 retains its former value defined by formula (38).

The proportion of the spontaneous decay processes also increases in the case of a nonuniformly broadened operating transition line even if the superluminescence is negligibly small. Figure 1.21 explains how this occurs in the example of multimodal lasing in a four-level medium with unpopulated ("frozen") lower operating level. In this medium the shapes of the luminescence and gain lines coincide, which increases the descriptiveness of the study.

Figure 1.21, a corresponds to the case of uniform broadening of the line, and Figure 1.21, b, nonuniform broadening. The curves for I describe the spectral dependence of the gain (and luminescence intensity) when the medium is excited, and the resonator and lasing are absent; the gain at the peak of the line reaches k^0_{gain} in this case. Curves II describe the spectral relations of the same values in the presence of steady state lasing; for frequencies at which lasing is realized, the magnitude of the average gain with respect to volume $\bar{k}_{gain}$ is reduced to $\sigma_0 + \ln(1/R')/2\ell$ (see (36)).

Uniform broadening is talked aboutwhen each atom has the same form and position of the amplification line (and luminescence) coinciding with the shape and position of the resultant line of the entire set of atoms. In this case any variation in the number of excited atoms implies proportional variation of the height of the corresponding graph; the form always remains unchanged. For uniform broadening even multimodal lasing is realized in a narrow frequency band near the peak of the line (§ 2.4); the gain also turns out to be equal to the above-indicated threshold value of $\bar{k}_{gain}$ for which the lasing is steady state. The height of the graph increases proportionally to $\bar{k}_{gain}/k^0_{gain}$ while retaining its former shape (curve II in

APPROVED FOR RELEASE: 2007/02/09: CIA-RDP82-00850R000500010010-4

APPROVED FOR RELEASE: 2007/02/09: CIA-RDP82-00850R000500010010-4

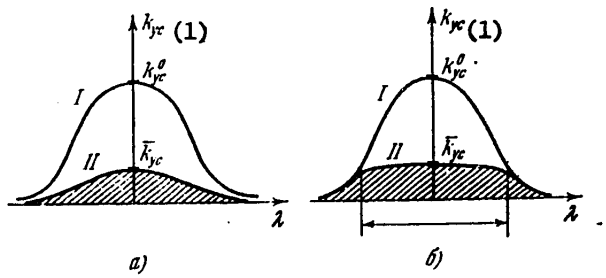

Figure 1.21. Problem of the influence of the nature of broadening of the operating transition line on the energy conversion efficiency in a laser resonator.

Key: 1. gain

Figure 1.21, a). Therefore, the number of acts of luminescence integrated with respect to frequency, being proportional to the area under the corresponding curve, decreases in the same ratio; hence, in the final analysis we have (39).

In the case of nonuniform broadening different atoms amplify at different frequencies, and therefore they are "responsible" for different segments of the overall amplification band. The shape of this band is not invariant — it depends on how the excited atoms are distributed with respect to frequencies. In this case lasing is set up over the entire frequency band noted in Figure 1.21, b by the arrows, inside which the gain of the weak signal exceeds the threshold value. Here the amplification band (and luminescence) assumes the form represented by curve II in the same figure. The area under the given curve, and with it, the number of spontaneous transitions, is 1.5 to 2 times greater than in the case of uniform broadening; p_1 increases also by as many times.

Thus, if in the case of a nonuniformly broadened line or in the presence of powerful superluminescence we select R' in accordance with (37), the proportion of the lasing power lost as a result of spontaneous transitions turns out to be larger than the proportion of power lost as a result of inactive absorption (let us remember that this choice of R' insured equality of p_1 and p_2 without considering the influence of the above-indicated factors increasing p_1). In this case it is expedient to use a resonator with somewhat larger R', at the same time approximating p_1 and p_2 to each other, which implies an increase in X.

Probably all of these examples would not be worthwhile considering in such detail if the results obtained were only valid for description of the truly steady-state lasing conditions. In reality, such conditions are encountered extremely rarely — even if Q-switching is absent, the lasing intensity, as a rule, experiences pulsations in time. One of the most frequently encountered is the "spike" lasing mentioned in § 1.3 where the time base of the intensity is a set of randomly distributed individual pulses — emission "spikes" — in the intervals between which lasing is in general absent. The possibility of using the above-derived formulas to estimate the efficiency of a laser operating under such conditions is far from obvious; This problem deserves separate consideration.

APPROVED FOR RELEASE: 2007/02/09: CIA-RDP82-00850R000500010010-4

APPROVED FOR RELEASE: 2007/02/09: CIA-RDP82-00850R000500010010-4

On transition from steady to "spike" conditions what can change? Obviously, the proportion p_2 of the total number of lasing photons absorbed inside the resonator must remain as before: it is determined simply by the ratio of the "harmful" losses to the total losses. At first glance it appears more complicated to calculate the number of photons coming during the "spikes" into the lasing channel; however, when averaging over a large time interval, it is possible, together with this, to estimate the number of spontaneous transitions in accordance with the above-developed approach. This presents no special difficulties.

The number of continuous decay processes of the excited state is at any point in time proportional to the instantaneous value of the inverse population; in the "spike" mode the latter naturally experiences oscillations. At the time of completion of the next "spike," it drops below the steady lasing threshold, from which it damps. In the inverval between "spikes," the inverse population increases monotonically as a result of incessant pumping until it begins to exceed the threshold level somewhat; then the next "spike" develops from the noise emission, and so on. Thus, the inverse population fluctuates around the threshold value; the scale of the fluctuations is relatively small, which is obvious from the fact that the spikes follow each other quite frequently -- in this short time the inverse population cannot increase sharply. As a result, the inverse population averaged over a long time interval and for a long time must be close to threshold; therefore the number of spontaneous processes remains approximately the same as under steady-state conditions.

The given analysis indicates that all the formulas of this section have much broader limits of applicability than can be initially indicated. In addition to everything else, they can be used not only for continuous, but also for pulse excitation of the active medium if the pulse duration exceeds the period required to set up steady oscillations in the resonator somewhat (or the average time interval between "spikes"). Only when calculating the output energy is it necessary to drop the initial and final sections of the pumping pulse in which lasing is absent (at the beginning, while the inverse population still does not reach the threshold value, and at the end when the pumping intensity drops below threshold).

The presented arguments and estimates explain the mechanism of the interrelation between the resonator parameters and energy characteristics of the laser emission. This analysis cannot claim to completeness; we have even not touched on one of the most widespread, if not the most widespread, case of giant pulse lasing. There is sufficient justification for this: the emission energy of a giant pulse laser depends on the choice of resonator parameters much less than on the type and characteristics of the shutter, on what measures are taken to control superluminescence in the inverse population accumulation stage, and so on.

Hereafter we shall consider the energy characteristics of lasers with unstable resonators. The specific nature of the analysis here consists in the fact that in unstable resonators, the radiation fluxes going to the exit mirror and back fill the active medium differently; in addition, the region adjacent to the resonator axis acquires a special role. The important case of a laser with medium moving in the direction perpendicular to the resonator axis will be investigated separately (§ 4.2).

APPROVED FOR RELEASE: 2007/02/09: CIA-RDP82-00850R000500010010-4

APPROVED FOR RELEASE: 2007/02/09: CIA-RDP82-00850R000500010010-4

CHAPTER 2. RADIATION DIVERGENCE OF LASERS WITH STABLE AND FLAT CAVITIES

§ 2.1. Modes of Oscillations of Empty Stable Resonators

The spatial characteristics of laser emission are determined to a great extent by the mode structure of the resonator used. We shall go into a more detailed study of it, but let us begin with the simplest case.

Eigenfunctions and Frequencies of a Stable Resonator with Infinite Mirrors. As we already know from § 1.2, resonators are called stable if the beam matrix elements satisfy the expression ABCD < 0. The integral equation for the complex field amplitude on one of the mirrors of such a resonator can be obtained directly from (1.24):

$$\gamma u(x, y) = \frac{\exp(2ikL_0)}{2iAB\lambda} \int\int \exp\left\{\frac{i\pi}{2AB\lambda}[(AD+BC)(x^2+y^2+ \right.$$
$$\left. + x'^2+y'^2) - 2(xx'+yy')]\right\} u(x', y')\, dx'dy'.$$

Solving this equation at infinite limits by the method of separation of variables and considering the relation between the coefficients of equation (1.17), we obtain the following set of eigenfunctions:

$$u_{mn}(x, y) = u_m(x)\, u_n(y),$$
$$u_j(t) = H_j(2t/w)\exp(-t^2/w^2), \tag{1}$$

where $H_j(v) = (-1)^j \exp\left(\frac{v^2}{2}\right)\frac{d^j}{dv^j}\exp\left(-\frac{v^2}{2}\right)$ are Hermite polynomials,

The graphs of several $u_j(v)$ are presented in Figure 2.1. All of the functions are real except the first $(j = 0)$ and sign-variable, having zeros with respect to j. The average distance between adjacent peaks of the functions decreases slowly with an increase in j. The width of the region in which the emission has noticeable intensity in this case increases just as slowly; at the edges of this region u_j decreases sharply. It is still worthwhile to note that for high-order functions, the amplitude oscillation scale varies little with respect to the beam cross section, increasing slowly toward its periphery. The envelope of these oscillations (the dotted curve in Figure 2.1, d) has its own "saddle" shape.

APPROVED FOR RELEASE: 2007/02/09: CIA-RDP82-00850R000500010010-4

APPROVED FOR RELEASE: 2007/02/09: CIA-RDP82-00850R000500010010-4

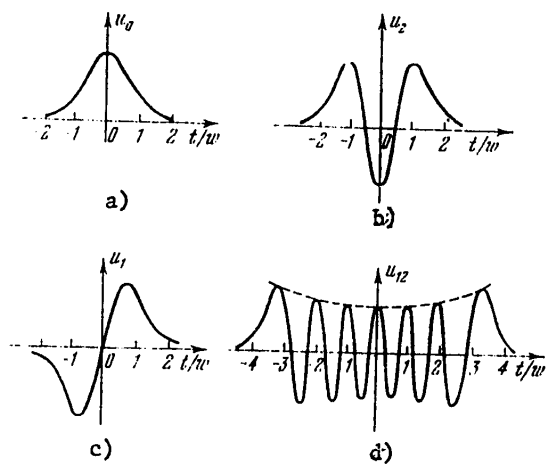

Figure 2.1. Form of the eigenfunctions (1) of a stable resonator with infinite mirrors. Cases a), b), c), d) for j = 0, 1, 2, 12, respectively.

The eigenfunctions (1) correspond to a set of eigenvalues of the equation of γ_{mn} with respect to which, by the procedure known to us from (§ 1.3), it is easy to find the natural oscillation frequencies ω_{mn}:

$$\omega_{mn} = \frac{c}{2L_0}(2\pi q + \delta_{mn}), \tag{2}$$

where $\delta_{mn} = (m + n + 1)\arccos\sqrt{AD}$; the sign of the root is determined by the sign of AB so that for AB > 0 the magnitude of the arcsine will be within the limits from 0 to $+\pi/2$; for AB < 0 it will be within the limits from + /2π to +π.

If the same integral equation is written not in a cartesian coordinate system, but cylindrical and we find the solution by the method of separation of variables in the form u(r, ϕ) = u(r) cos ℓϕ, we arrive at the following set of eigenfunctions and frequencies:

$$u_{pl}(r, \varphi) \sim (r/w)^l L_p^l(2r^2/w^2)\exp(-r^2/w^2)\cos l\varphi, \tag{3}$$

$$\omega_{pl} = \frac{c}{2L_0}(2\pi q + \delta_{pl}), \tag{4}$$

where $L_p^l(v) = v^{-l}\exp(v)\frac{d^p}{dv^p}[\exp(-v)v^{p+l}]$ are the generalized Laguerre polynomials, $\delta_{pl} = (2p + l + 1)\arccos\sqrt{AD}$, the parameter w retains its former value $(\lambda/\pi)^{1/2}(-AB/CD)^{1/4}$.

The form of the radial functions u(r) resembles to a known degree the form of the functions presented in Figure 2.1. In particular, $u_{p0}(r)$ has p roots; for $\ell \neq 0$ another root is added at the point r = 0; with an increase in the radial index p, the region of noticeable intensity shifts in the direction of larger r, and so on.

APPROVED FOR RELEASE: 2007/02/09: CIA-RDP82-00850R000500010010-4

APPROVED FOR RELEASE: 2007/02/09: CIA-RDP82-00850R000500010010-4

A very good idea about the structure of the beams described by formula (3) is provided by Figure 2.2 which we borrowed from the book [33].

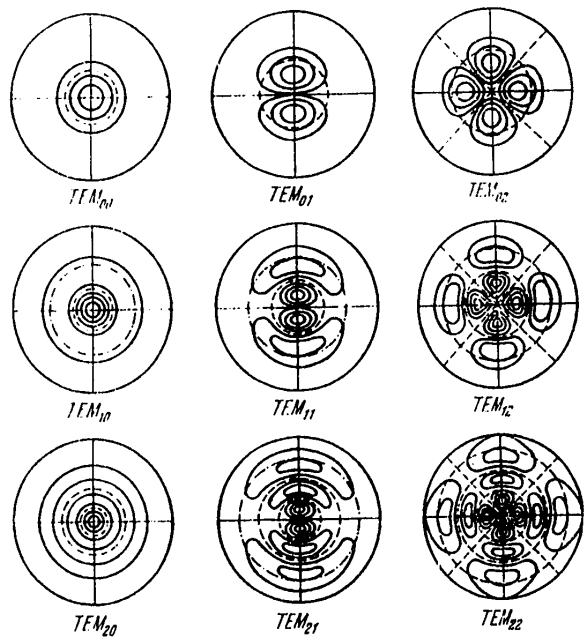

Figure 2.2. The field configuration of natural modes of oscillations of a stable resonator described by formula (3). On the solid closed lines the amplitude is 0.2, 0.5 and 0.8 of the maximum value; on the dotted lines the amplitude is equal to zero; the dash-dot line bounds the region inside which 86.5% of the total radiation flux is included.

The ambiguity of the choice of the systems of eigenfunctions, on the one hand, and the similarity of the behavior of these functions on the other, have a common basis. The fact is that all the functions of system (1), except the lowest ($m = n = 0$) are degenerate an infinite set of times; this means that there are as many different functions as one might like with the same natural frequency. Actually, it is little that the frequencies coincide for oscillations with different combinations of transverse indexes with identical sum of them $m + n$ (see (2)); it is possible to rotate the x and y axes as many times as one might like around the resonator axis. The same thing also pertains to functions of system (3): oscillations not only with equal $2p + \ell$ (see (4)), but also oscillations differing simply by the origin of reckoning of the azimuthal angle have identical frequency.

The superposition of any number of natural oscillations with identical complex frequencies (in the given case there is no damping and the frequencies are real) describes a strictly periodic process with the same frequency, that is, it is also a natural oscillation. Thus, for degenerate eigenfunctions it is possible to combine them arbitrarily, from which ambiguity of the choice of the systems of these functions arises. If desired it is possible to find how it is necessary to combine functions of the type of (1) in order to obtain (3) and vice versa.

APPROVED FOR RELEASE: 2007/02/09: CIA-RDP82-00850R000500010010-4

APPROVED FOR RELEASE: 2007/02/09: CIA-RDP82-00850R000500010010-4

Spatial Structure of Natural Oscillations. In order to understand the meaning of the obtained solutions, it is necessary to consider the propagation laws of the light beams making up these solutions. Inasmuch as the eigenfunctions (1) and (3) are real, the mirrors are equiphasal surfaces, and therefore the beams have spherical wave fronts near the mirrors. The lowest functions of the sets (1) ($m = n = 0$) and (3) ($p = \ell = 0$) coincide; this is the gaussian beam already known to us; its transverse radius, the definition of which is presented in § 1.1, is equal to w. For other beams the effective spot size, as is obvious from Figure 2.1, exceeds w the more, the larger their transverse indices; therefore we shall call w the linear distribution parameter in the general case and not the beam radius.

Using the Huygens-Fresnel principle (1.2), it is possible to see that the beams described by formulas (1), (3) have the same propagation laws as gaussian beams. In each such beam at any distance from the source the initial form of the amplitude distribution is reproduced; the wave front remains spherical; only the radius of curvature of the wave front ρ and the parameter w vary; this occurs in all of the beams identically in accordance with formulas (1.11), (1.12). Thus, Figure 1.7 can pertain to an equal degree to any beam from the families (1), (3) accept the distribution picture for which w gives the scale, and each beam has its own.

Inasmuch as on the exit mirror w and ρ are identical for all of the beams, they coincide in any segment of the length of the resonator. Figure 2.3 shows the law of evolution of w for such a family of beams. Any other characteristic dimension of the cross section of each beam varies exactly the same, in particular, the transverse dimensions of the region of high intensities outside which the field decreases exponentially. The surface bounding this region is called caustic; for beams of the type of (1), it has a rectangular cross section, (3) has a circular cross section. The volume included inside the caustic surface (or the caustic) naturally increases with the transverse mode indices. As an example, in the figure the dash-dot line depicts the caustic surface of the beam for which the field distribution with respect to the direction perpendicular to the axis lying in the plane of the figure is described by the function u_j with $j = 12$ (Figure 2.1, d). In the same figure 2.3, the dotted lines show the equiphasal surfaces which are common to all beams of the family; there is an infinite set of such surfaces. Installing the spherical mirrors with the same radii of curvature at the location of any two of these surfaces, we obtain an empty stable resonator, the solutions for which will be all of the beams of the given family. Using (1.11) and (1.12) to relate the resonator parameters and the families of beams, it is possible to obtain the following expression for the linear distribution parameter on the right-hand mirror of the resonator:

$$w_2^4 = \left(\frac{\lambda R_2}{\pi}\right)^2 \frac{R_1 - l}{R_2 - l} \frac{l}{R_1 + R_2 - l}$$

(all of the notation is the same as before). This expression is a special case of the more general expression $w_2 = (\lambda/\pi)^{1/2}(-AB/CD)^{1/4}$. The parameter w_1 on the left-hand mirror is defined by the same formulas, in which it is necessary only to exchange places with R_1 and R_2 or in the general case, A and D: $w_1 = (\lambda/\pi)^{1/2}(-BD/AC)^{1/4}$; hence, it follows that $w_1 w_2 = (\lambda/\pi)\sqrt{-B/C}$.

APPROVED FOR RELEASE: 2007/02/09: CIA-RDP82-00850R000500010010-4

APPROVED FOR RELEASE: 2007/02/09: CIA-RDP82-00850R000500010010-4

Finally, from the same Huygens-Fresnel principle, we have the following expressions for the phase lag $\Delta\Psi$ which occurs as a result of having the phase velocity exceed the speed of light (see § 1.3) on a path of length z, beginning with the "neck":

for type (1) beams $\Delta\Psi = (m + n + 1)\,\mathrm{arctg}\,(\lambda z/\pi w_0^2)$;

for type (3) beams $\Delta\Psi = (2p + l + 1)\,\mathrm{arctg}\,(\lambda z/\pi w_0^2)$;

here, just as in (1.11), (1.12), w_0 is the linear parameter at the "neck." If we use these relations to calculate the phase correction in an empty two-mirror resonator, we again arrive at the formulas which are special cases of the more general expressions (2), (4). As was already noted in § 1.3, the phase correction is larger, the smaller the characteristic dimension of the transverse beam structure. In the given case with an increase in the transverse indices, the distances between adjacent peaks of the amplitude distribution decrease (see Figure 2.1), and the phase correction increases correspondingly.

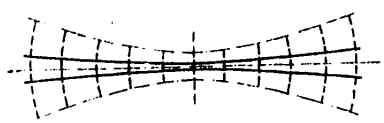

Figure 2.3. Evolution of the linear distribution parameter w for type (1) and (3) beams.

In order to trace the behavior of gaussian beams and, with them, the more complex beams type (1) and (3) inside an arbitrary resonator, it is possible to use the following procedure. The complex amplitude of a gaussian beam on an arbitrary reference plane is $\exp\left[-\frac{x^2+y^2}{w^2}\right]\exp\left[\frac{ik}{2\rho}(x^2+y^2)\right]$ (see § 1.1). It can be given the same form $\exp\left[\frac{ik}{2\tilde{\rho}}(x^2+y^2)\right]$, as for the complex amplitude of an ordinary spherical wave with uniformly distributed intensity. For this purpose it is sufficient to introduce the complex radius of curvature $\tilde{\rho}$, defining it using the expression

$$\frac{ik}{2\tilde{\rho}} = \frac{ik}{2\rho} - \frac{1}{w^2}, \quad \text{or} \quad \frac{1}{\tilde{\rho}} = \frac{1}{\rho} + \frac{i\lambda}{\pi w^2}.$$

This form of notation, of course, would not be of special interest if the conversion laws for $\tilde{\rho}$ in the optical systems did not compare exactly with the conversion laws of the radii of curvature of ordinary spherical waves. Actually, on passage through a lens with focal length f, the complex amplitude of any beams turns out to be multiplied by $\exp[-(ik/2f)(x^2 + y^2)]$ (see § 1.1). The value of $1/\tilde{\rho}$ in this case has $-1/f$ added to it; the curvature of ordinary spherical waves is transformed in the same way. Using (1.11), (1.12), it is also possible to see that as a result of traveling the distances z in empty space, z is added to $\tilde{\rho}$, just as to the radius of curvature of an ordinary wave. Thus, all of the relations which can be derived using geometric optics are valid for $\tilde{\rho}$; in particular, the conversion law of $\tilde{\rho}$ in an arbitrary optical system has the form (§1.2), $\tilde{\rho}_2 = (A\tilde{\rho}_1 + B)/(C\tilde{\rho}_1 + D)$. Hence, in turn, it follows that equation (1.21) and its solution (1.22) retain their meaning even for ABCD < 0. The radii of curvature in this case turn out to be purely imaginary

APPROVED FOR RELEASE: 2007/02/09: CIA-RDP82-00850R000500010010-4

APPROVED FOR RELEASE: 2007/02/09: CIA-RDP82-00850R000500010010-4

and equal to $\pm i\sqrt{-AB/CD}$. Waves with such radii of curvature have the following amplitude distribution:

$$u_{1,2}(x, y) \sim \exp\left[\left(ik/2\tilde{\rho}'\right)(x^2 + y^2)\right] = \exp\left[\pm (\pi/\lambda)\sqrt{-CD/AB}\,(x^2 + y^2)\right].$$

The amplitude of one of the waves increases without limit on going away from the axis; this wave is of interest to us. The second is a gaussian beam with radius $w = (\lambda/\pi)^{1/2}(-AB/CD)^{1/4}$. Inasmuch as the phase factor in the amplitude distribution is absent, the mirrors of the equivalent and, therefore, the initial resonator are equiphasal surfaces; thus, we have arrived at the solution already known to us.

Introduction of the complex radius of curvature permits the parameters of the gaussian beam to be traced without difficulty (and any beams of the type of (1), (3)) along the entire length of the arbitrary resonator. For maximum simplification of this procedure in its time special nomograms were compiled ("maps"); anyone who wishes to become familiar with them is referred to [12], [13]; we shall proceed to what goes on outside the resonator.

In the case of stable resonators, the radiation most frequently is output through the partially transparent exit mirror. As was demonstrated in § 1.3, the transverse structure of the natural oscillations does not depend on whether the reflection coefficient of the exit mirror is equal to one or is not equal to one (only that it be the same on the entire mirror surface). Therefore the semitransparent exit mirror of large transverse dimension originates beams with the amplitude of the type of (1), (3) for which it is an equiphasal surface.

For a gaussian beam with radius of curvature of the wave front R_2, the amplitude distribution in the far zone also has the form of a gaussian function with angular radius $\beta = \sqrt{(w/R_2)^2 + (\lambda/\pi w)^2}$ (§ 1.1). Inasmuch as the beams of the type of (1), (3) behave similarly to gaussian beams, in all of them the amplitude distribution in the far zone is described by the formulas (1), (3) in which x, y and r must be replaced by the slope angles α_x, α_y and $\alpha = \sqrt{\alpha_x^2 + \alpha_y^2}$, and the linear distribution parameter w must be replaced by the angular parameter β.

In the expression for β, the first term under the square root sign has a "geometric" origin, and the second term, "diffraction" origin (see § 1.1). The geometric term in stable resonators does not have theoretical significance, for it can easily be reduced to zero. For this purpose it is sufficient to install a lens with $f = R_e$ directly behind the exit mirror; this lens converts the spherical wave fronts of all the beams to plane fronts; the common angular parameter β decreases to the value $\beta_0 = \lambda/\pi w$, and the emission divergence decreases correspondingly. Hereafter, we shall always consider that this simplest measure with respect to decreasing the emission divergence at the output of a stable resonator has been adopted, and the geometric divergence is absent. For this reason it is necessary to note the following. It is easy to avoid geometric divergence so easily in this case only because the exit mirror of a stable resonator is clearly designated a spherical equiphasal surface common to all beams. The position of this equiphasal surface remains fixed even if a thermal "lens" occurs inside the resonator or there is some other disturbance of similar type -- even if the resonator continues to remain "stable." Unfortunately, the given property is almost the only advantage of stable resonators

APPROVED FOR RELEASE: 2007/02/09: CIA-RDP82-00850R000500010010-4

APPROVED FOR RELEASE: 2007/02/09: CIA-RDP82-00850R000500010010-4

from the point of view of beam divergence; for large apertures lasing takes place in them on high-order modes which correspond to very large diffraction divergence (§ 2.4). In all of the resonators which provide small diffraction divergence and are actually used in lasers with quite large aperture, the mirrors are not equiphasal surfaces; the shape of the wave front of the stimulated emission, as a rule, differs noticeably from an ideal sphere, and still worse, it frequently varies with time. Under these conditions the control of "geometric" divergence becomes, on the one hand, extraordinarily difficult, and on the other hand, it acquires primary significance. We shall discuss the methods of this control in the last chapter of the book.

As for diffraction divergence ψ of any of the beams (1), (3), it is possible to obtain a very useful formula for it if we use the fact that the relation between the angular dimension of a spot in the far zone and the angular parameter β_0 is equal to the ratio of analogous values in the near zone. Hence, we have the expression

$$\psi = \sqrt{-CD/AB}\,\Phi, \tag{5}$$

where Φ is the size of the spot in the near zone (at the exit mirror).

Now let us trace how the beam dimensions vary in the near and far zones on variation of the parameters of a stable resonator. Let us do this in the example of an empty two-mirror symmetric resonator with $R_1 = R_2 = R$, which is "stable" for $R > \ell/2$; the spacing between the mirrors ℓ will be considered fixed.

For a symmetric two-mirror resonator $-AB/CD = R^2\ell(R - \ell)/[2R - \ell)(R - \ell)]$. For $R \gg \ell$, the resonator is close to flat, $-AM/CD \approx R\ell/2$. Together with R, the cross sectional dimensions of all the beams in the near zone are comparatively large: $w \approx (^2R\ell/2\pi^2)^{1/4}$. The angular distribution parameter in the far zone $\beta_0 \approx (2\lambda^2/\pi^2R\ell)^{1/4}$ is correspondingly small. As R decreases and the resonator approaches confocal ($R = \ell$) - AB/CD decreases, approaching ℓ^2; w also decreases, approaching $\sqrt{\lambda\ell/\pi}$; the angular parameter β_0 increases correspondingly and approaches $\sqrt{\lambda/\pi\ell}$.

The beam dimensions behave the same way if R approaches ℓ from the other side: for $R \gtrsim \ell/2$, that is, when the resonator is "stable," but close to concentric, w is large, and β_0 is small. As R increases and approaches ℓ, the parameter $w \to \sqrt{\lambda\ell/\pi}$, $\beta_0 \to \sqrt{\lambda/\pi\ell}$. Thus, the beam dimensions of resonators with $\ell/2 < R < \ell$ and $R > \ell$ pass through the same value; why this can occur from is explained by Figure 2.4, a, b.

A symmetric confocal resonator is isolated from the others: the value of the ratio -AB/CD for $R = \ell$ will become undefined; therefore the beam cross sections on the exit mirror can have any transverse dimensions. Only the product of the linear parameters w_1 and w_2 on the left and right mirrors turns out to be fixed: $w_1w_2 = \lambda\ell/\pi$ (Figure 2.4, c). It is necessary to note that not only the above-investigated symmetric resonators, but any other two-mirror stable resonators have a large value of the given product. Actually, in the general case

$$w_1w_2 = \frac{\lambda}{\pi}\sqrt{-\frac{B}{C}} = \frac{\lambda}{\pi}\sqrt{\frac{l}{1/R_1 + 1/R_2 - l/R_1R_2}} = \frac{\lambda l}{\pi}\frac{1}{\sqrt{1 - g_1g_2}},$$

APPROVED FOR RELEASE: 2007/02/09: CIA-RDP82-00850R000500010010-4

APPROVED FOR RELEASE: 2007/02/09: CIA-RDP82-00850R000500010010-4

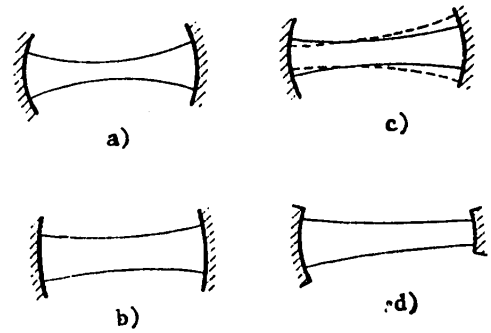

Figure 2.4. Natural oscillations of stable resonators. a), b) resonators with identical spot dimensions on the mirrors: a) resonator with $\ell/2 < R < \ell$, b) resonator with $R > \ell$; c), d) confocal resonator; c) two different beams with infinite mirrors, d) type of resonator oscillations with mirrors of finite dimensions.

where $g_{1,2} = 1 - \ell/R_{1,2}$; let us remember that only for a symmetric confocal resonator is $g_1 g_2 = 0$; for the remaining stable resonators $0 < g_1 g_2 < 1$. From the subsequent investigation it will be obvious that as a result of the indicated peculiarities a symmetric confocal resonator has the smallest diffraction losses among all possible empty two-mirror resonators with given transverse dimensions of the mirrors and distance between them.

Stable Resonators with Mirrors of Finite Dimensions. When considering finite dimensions of mirrors, degeneration of the eigenfunctions is removed to a significant degree; the "arbitrariness" of the selection disappears -- in the case of rectangular mirrors the solutions are only functions of the type of (1), and for circular mirrors, (3). The shape of the functions undergoes some changes; the equiphasal surfaces of all resonators except a symmetric confocal resonator cease to compare exactly with the surfaces of the finite mirrors. The spectrum of the eigenvalues also is subject to adjustment. The frequencies become complex: diffraction losses appear, and with them, damping of the natural oscillations. This adjustment to a significant degree involves various types of oscillations: the scales and nature of the variations are determined primarily by how the transverse dimensions of the mirrors relate to the dimensions of the region encompassing the caustic surface of given mode.

For such modes, the width of the caustic of which is noticeably less than the width of the mirrors, the field distribution remains almost the same as for infinite mirrors. The magnitude of the diffraction losses of the resonators not too close to confocal can in this case be calculated directly using formulas (1), (3): it is sufficient to calculate what portion of the total emission flux goes to the distribution "tails" which are beyond the boundaries of the mirror surface. Inasmuch as beyond the boundaries of the caustic the field decreases very sharply, as the caustic approaches the mirror dimensions, the losses increase rapidly, remaining nevertheless, very small with respect to absolute magnitude. Hence, it follows, that under other equal conditions the higher-order modes have greater losses -- they have broader caustics.

APPROVED FOR RELEASE: 2007/02/09: CIA-RDP82-00850R000500010010-4

APPROVED FOR RELEASE: 2007/02/09: CIA-RDP82-00850R000500010010-4

If the resonator is asymmetric, the basic contribution to the total losses is made by reflection from a mirror, the dimensions of which are closer to the dimensions of the corresponding caustic. This pertains to all stable resonators except a confocal one with $R_1 = R_2 = \ell$: inasmuch as for such a resonator it is not the spot dimensions on each mirror that are fixed, but only the magnitude of their product, these dimensions are redistributed for finite mirrors proportionally to the mirror dimensions (see Figure 2.4, d). As a result, the two mirrors make an identical — and small — contribution to the diffraction losses; the total losses turn out to be less than they would be for any other relation between the spot dimensions on the mirrors. If we consider that the product of the spot dimensions itself is minimal in the resonator of the given type, it becomes clear why it has record-small diffraction losses.

Now let us fix the configuration of the resonator and proceed successively to the modes with greater and greater transverse indices. Here the caustic sooner or later must approach closely to the edge of one or both mirrors. Beginning with this event, it is impossible to neglect the influence of the edge effects on the mode structure, and formulas (1)-(5) derived in the approximation of infinite mirrors become inapplicable. At the same time, the types of oscillations of still higher order still exist; their classification can be based as before on the number of distribution zeros with respect to the corresponding directions.

In order to understand the nature of the variations of the mode structure under the influence of the edge effects, it is best of all to trace the behavior of a specific type of oscillations in detail as the stable resonator gradually approaches a flat (or concentric) cavity. This analysis can be performed by the Vaynshteyn method; those desiring to become familiar in more detail with the mathematical aspect of the problem are referred to [34]; we shall only describe a qualitative picture of the phenomena. Let us do this in the example of a completely symmetric resonator consisting of two mirrors with $R_1 = R_2 > \ell$ and with identical transverse dimensions. The given dimensions and the spacing between the mirrors ℓ will be considered fixed; the initial curvature of the mirrors will be selected so large that the width of the caustic of the oscillations of the type of interest to us will be significantly less than the width of the mirrors (Figure 2.5,a). Now let us begin slowly to decrease the mirror curvature. The approach of the resonator to a flat cavity is, as we already know, accompanied by an increase in the linear parameter w; the transverse beam cross section increases with it. This process lasts until the beam begins to fill the mirrors entirely (Figure 2.5, b). A further decrease in curvature of the mirrors causes other consequences: the beam cross section remains almost unchanged, only the distribution peaks gradually become equidistant, and their heights equalize -- there is a gradual transition to the corresponding type of oscillations of the flat cavity (see Figure 2.5, c).

All of this can be given the following graphic interpretation. For the given "self-imaging" (type (1), (3)) structure of the light beam its cross sectional dimensions in a resonator with quite large mirrors (Figure 2.5,a) are established so that dynamic equilibrium is achieved between the processes of expansion of the beam as a result of diffraction divergence and focusing of it on reflection from concave finite mirrors. When the curvature of the mirrors decreases, their focusing effect is weakened, and the state of equilibrium shifts in the direction of the larger cross sections which correspond to smaller diffraction divergence. This is what happens until the situation depicted in Figure 2.5, b. Then, in

APPROVED FOR RELEASE: 2007/02/09: CIA-RDP82-00850R000500010010-4

APPROVED FOR RELEASE: 2007/02/09: CIA-RDP82-00850R000500010010-4

spite of the continuing attenuation of the focusing as a result of curvature of the mirrors, the beam cross section dimensions cease to grow, and the deflection divergence almost does not change. This can be given a unique explanation: a new factor is added that counteracts the divergence of the light beam; edge diffraction is a factor of this type. As the resonator subsequently approaches a flat cavity, the field at the mirror edge increases somewhat; the role of edge diffraction increases with it. Finally, in a flat cavity edge diffraction remains the only reason that the beam "does not walk out" of the system and does not have such large losses. Adhering to Vaynshteyn's terminology, it is possible to state that the field in a flat cavity is fixed not by the caustic as in stable resonators, but by the mirror edges (§ 2.2).

Edge diffraction still "contains" the field less efficiently than the caustic; therefore the diffraction losses of all types of oscillations on transition from a confocal resonator to a flat cavity (or concentric cavity) increase monotonically. Figure 2.6 can be used as a graphic illustration in which the relations are presented for the losses of two lowest types of oscillations of a symmetric resonator with circular mirrors as a function of the Fresnel number $N = a^2/\lambda\ell$ (2a is the mirror diameter) for different values of $|g|$ which vary from zero (the confocal resonator) to one (a flat or concentric cavity). We conclude the investigation of stable resonators with this. Let us only state that much more detailed information about the properties of empty, stable resonators, including the magnitudes of the diffraction losses, the phase corrections as a result of finiteness of the mirrors, and so on, can be found in the monograph on submillimeter wave engineering [33]. This is no accident: submillimeter resonators are excited by elementary dipoles or through an aperture in one of the mirrors; then the Q-factor of the system plays the decisive role, and resonators of the stable type fall into first place. On filling of the resonator with active medium as is done in the optical band, the initial Q-factor is not so important (§ 1.3), and the stable resonators

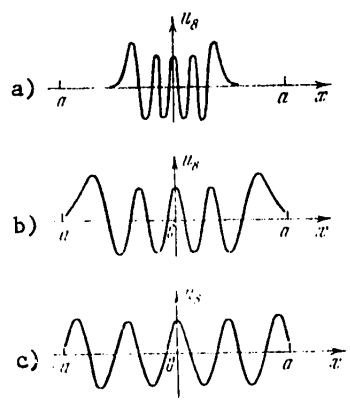

Figure 2.5. Evolution of a natural oscillation on transition from the symmetric stable resonator with transverse mirror dimensions of 2a to a flat cavity: a) stable resonator; b) stable resonator with smaller curvature of the mirrors; c) flat cavity.

APPROVED FOR RELEASE: 2007/02/09: CIA-RDP82-00850R000500010010-4

APPROVED FOR RELEASE: 2007/02/09: CIA-RDP82-00850R000500010010-4

lose their exclusiveness. In addition to everything else, it will become obvious that for achievement of small angular divergence of the exit emission of powerful lasers, in general they are not suitable; in order to arrive at this conclusion, the information which we already have at our disposal is entirely sufficient.

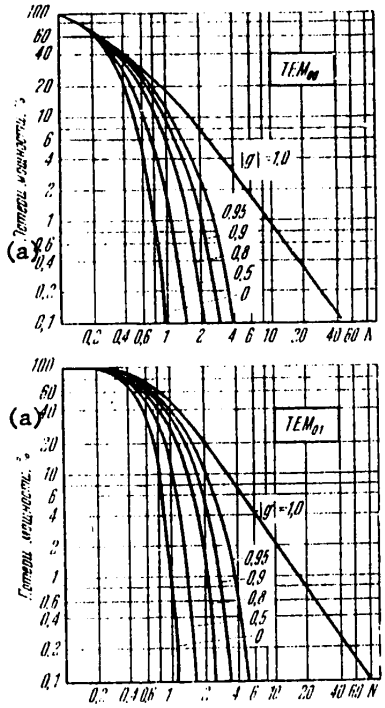

Figure 2.6. Losses of the two lowest types of oscillations of a symmetric resonator with circular mirrors as a function of the Fresnel number N for various values of $|g|$ (the magnitude of the losses is presented for passage through the resonator in one direction).

Key: a. power losses, %

§ 2.2. Edge Diffraction and Modes of Oscillations of an Empty Flat Optical Cavity

Auxiliary Diffraction Problem. Let us consider plane wave diffraction in a periodic structure made up of semiinfinite absorbing screens (Figure 2.7). The period of the structure is equal to ℓ; the direction of propagation of the wave incident on it makes a small angle α with the plane P passing through the edges of all of the screens.

Let us successively construct (beginning, of course, at the bottom) the field distributions on the reference planes normal to the direction of propagation of our wave and passing through the edges of the screens as shown in the figure. For this purpose let us use the Fresnel approximation (1.2a) for the two-dimensional case of interest to us:

APPROVED FOR RELEASE: 2007/02/09: CIA-RDP82-00850R000500010010-4

APPROVED FOR RELEASE: 2007/02/09: CIA-RDP82-00850R000500010010-4

$$u(x_2) = \frac{\exp(ikz)}{\sqrt{i\lambda z}} \int \exp\left[ik\frac{(x_2 - x_1)^2}{2z}\right] u(x_1)\, dx_1.$$

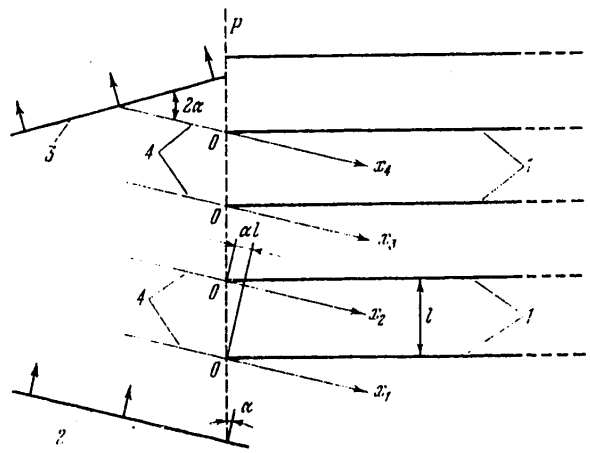

Figure 2.7. Plane wave diffraction on a periodic structure made of screens: 1 -- periodic structure made of absorbing screens, 2 -- initial plane wave, 3 -- reflected wave, 4 -- reference planes.

Let us remember that here z is the distance between the observation and source planes, the difference $x_2 - x_1$ has the meaning of the length of the projection of the radius-vector connecting the observation and source points on any of these planes.

In the investigated problem the transverse coordinate x, as illustrated in the figure, will be reckoned not from the common normal to the reference surfaces, but from the edge of the corresponding screen. Thus, the origin of the coordinates when making the transition to the next plane shifts in the transverse direction by $\alpha\ell$, and $x_2 - x_1$ must be replaced by $x_2 - \alpha\ell - x_1$. The distance between reference surfaces is $z = \ell\cos\alpha \approx \ell - \ell\alpha^2/2$. It is impossible to neglect the small correction term $\ell\alpha^2/2$ only in the rapidly varying phase factor exp(ikz) (see also § 1.1). In the final analysis we obtain the following recurrent formula relating the field distribution on two adjacent reference surfaces:

$$u_{n+1}(x) = \frac{\exp[ikl(1 - \alpha^2/2)]}{\sqrt{i\lambda l}} \int_{-\infty}^{0} \exp\left[ik\frac{(x - x' - \alpha l)^2}{2l}\right] u_n(x')\, dx'.$$

Introducing the dimensionless coordinate $\tau = \sqrt{k/\ell}x$ and omitting the common phase factor $\exp[il\ell(1 - \alpha^2/2)]$, we arrive at the final form of the recurrent formula for the functions $U(\tau) \equiv u(\sqrt{\ell/k}\tau)$:

$$U_{n+1}(\tau) = \frac{1}{\sqrt{2i\pi}} \int_{-\infty}^{0} \exp[i(\tau - \tau' - s)^2/2]\, U_n(\tau')\, d\tau', \qquad (6)$$

APPROVED FOR RELEASE: 2007/02/09: CIA-RDP82-00850R000500010010-4

APPROVED FOR RELEASE: 2007/02/09: CIA-RDP82-00850R000500010010-4

where $s \equiv \alpha\sqrt{k\ell}$; here and hereafter n will be the number of screens on which the wave has already been diffracted.

The lower reference plane is an equiphasal surface of an initial plane wave; thus, U_0 = const. In combination with formula (6) this means that the entire set of functions $U_n(\tau)$ (and with them, the complete picture of the diffraction in a periodic structure) is uniquely defined by the magnitude of the parameter s. The most interesting case is the one where the slope angles of the plane wave α are so small that the condition $s \ll 1$ is satisfied.

In Figure 2.8 results are presented from numerical calculations of the radiation intensity $|U_n(\tau)|^2$ on several reference surfaces for s = 0.3.[1] The function $|U_1(\tau)|^2$ (Figure 2.8, a) has the form well known in optics: it describes the diffraction pattern of the plane wave on a halfplane (see, for example, [6], Figure 8.37). The boundary of the geometric shadow is located at the point $\tau = s = 0.3$; although the edge of the second screen ($\tau = 0$) is located to the left of this point, the field amplitude and, with it, the radiation intensity turn out to be smaller near this edge than for the initial wave. Therefore near the edge of the next screen the intensity turns out to be even less (see Figure 2.8,b). With it the radiation energy in the region $\tau > 0$ absorbed in the screen decreases (the area under the curve decreases); here this area turns out to be less than it should be from geometric optics (the area of a rectangle). On making the transition to the subsequent mirrors, the absorbed energy continues to decrease, and in the final analysis it is established at a very low level. Hence, it follows that as a result of diffraction, the periodic structure of the screens basically does not absorb, but scatters the emission incident on it at small angles.

In the vicinity of $\tau < 0$ deep modulation of the amplitude develops with time; the modulation period gradually increases, approaching a defined limit (Figure 2.8,c, d, e; on the last graph, the field distribution was almost steady-state — variations on transition to subsequent screens are already small). This indicates that in scattered emission a discrete wave is formed, the interference of which with the initial wave leads to amplitude modulation; the great depth of modulation indicates that the intensity of this wave is comparable to the intensity of the initial wave.

The property of a plane (or spherical) wave undergoing diffraction on an opaque screen known in theoretical optics helps to understand the structure of scattered emission. This property consists in the fact that such a wave can be represented in the form of the sum of a wave which, being completely absent in the geometric shadow region, is not distorted by diffraction in the remaining space, and a wave, the fictitious source of which is the edge of the screen (see, for example, [6], § 8.9). Actually, in our example, after simple transformations the following expressions can be obtained for the field u_1 which arises as a result of diffraction on the first screen:

$$u_1(x) = \begin{cases} c - (c/\sqrt{i\pi})\, F\left[\sqrt{\pi/\lambda l}\,|x - \alpha l|\right], & x < \alpha l, \\ (c/\sqrt{i\pi})\, F\left[\sqrt{\pi/\lambda l}\,|x - \alpha l|\right], & x > \alpha l, \end{cases}$$

[1] The author takes this opportunity to express his appreciation to L. V. Koval'chuk who performed these calculations on a computer specially for this publication.

APPROVED FOR RELEASE: 2007/02/09: CIA-RDP82-00850R000500010010-4

APPROVED FOR RELEASE: 2007/02/09: CIA-RDP82-00850R000500010010-4

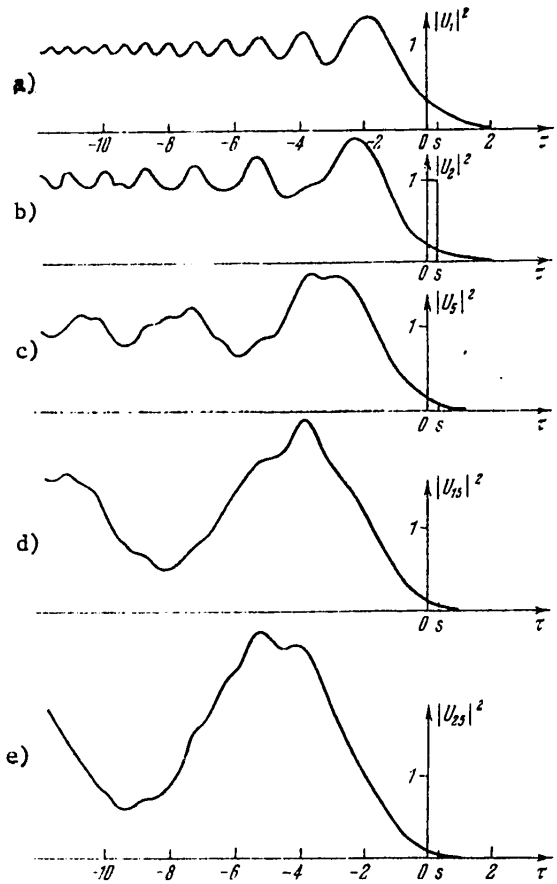

Figure 2.8. Result of successive diffraction of a plane wave on periodically arranged absorbing screens for s = 0.3.

where c is the amplitude of the initial plane wave, $F(a) \equiv \int_a^\infty \exp(it^2)\,dt \quad (a > 0)$ is the Fresnel integral. For the Fresnel integral it is possible to propose the following approximate expression giving a correct representation of the behavior of F(a) in the entire range of variation of the argument: $F(a) \approx \{[i/[2(a+\sqrt{i/\pi})]]\} \exp(ia^2)$. Substitution of this expression in the last formulas for $u_1(x)$ indicates that the field in the geometric shadow zone has the form $A(x)\exp[ik(x-\alpha l)^2/2l]$, where A(x) is a comparatively slowly varying function of the coordinate. A comparison with the expressions for spherical waves from § 1.1, indicates that the given relation describes a cylindrical wave that diverges from the edge of the first screen. The amplitude of this wave A(x) decreases on going away from the edge of the geometric shadow; the nature of the decrease is clear both from the above-presented expression for the Fresnel integral and from the upper graph in Figure 2.8. In the vicinity of $x < \alpha l$, in addition to the entirely analogous cylindrical wave, there is also an undistorted plane wave with initial amplitude c. It is the interference of a plane wave with a cylindrical wave that leads to the appearance of characteristic

APPROVED FOR RELEASE: 2007/02/09: CIA-RDP82-00850R000500010010-4

APPROVED FOR RELEASE: 2007/02/09: CIA-RDP82-00850R000500010010-4

amplitude modulation, the depth of which decreases on going away from the edge of the shadow together with the cylindrical wave amplitude.

Diffracting on the second screen, the undistorted plane wave generates a new cylindrical wave, the fictitious source of which is the edge of the second screen. In addition to the cylindrical wave, the resultant field contains, as before, an undistorted plane wave, diffraction of which on the next screen leads to the appearance of the next cylindrical wave, and so on.

Thus, the field of emission scattered as a result of edge diffraction is a superposition of cylindrical waves, the sources of which are the edges of all of the screens, and the amplitudes decrease identically as the direction of the emission deviates from the direction of the initial plane wave. As a result of the interference of many cylindrical waves succeeding in getting sufficiently far from the point of their generation, a number of discrete directions are isolated in which the amplitudes of these waves are summed (entirely similar to how this happens on exposure of a diffraction grating to a monochromatic plane wave, see [6], § 8.6). The angles θ which these directions make with the plane P satisfy the obvious condition $k\ell(1 - \alpha^2/2) - k\ell(1 - \theta_n^2/2) = 2n\pi$ ($\theta_n \ll 1$) or $\theta_n^2 = \alpha^2 + 2n\lambda/\ell$, $n = 0, 1, 2, \ldots$ Let us note that these formulas can be obtained directly from the known relation of diffraction grating theory $\sin\theta - \sin\theta_0 = \pm n\lambda/d$, where θ and θ_0 are angles which the incident and reflected wave make with the normal to the plane of the grating, and d is the grating period (in our case its role is played by ℓ). In the intermediate direction, mutual interference "extinguishing" of the cylindrical waves takes place. As for plane waves formed as a result of interference addition and propagated in the isolated directions, inasmuch as the scattered light intensity increases rapidly with an increase in θ, in the scattered emission the wave with the least θ predominates; this is the wave mirror "reflected" from the plane P ($\theta_0 = \alpha$). Its presence also causes deep amplitude modulation of the established field distribution with spatial period of $\lambda/2\alpha$ (in the dimensionless coordinates π/s). The remaining waves have significantly smaller amplitudes and lead only to small, fine-scale amplitude modulation.

Let us sum the results of the investigation of our auxiliary problem. If the angle of incidence of the plane wave on a periodic structure made of absorbing screens is sufficiently small, the greater part of the energy of the emission is not absorbed, but scattered as a result of diffraction. In the scattered emission, the primary role is played by the "reflected" wave, to which the greater part of the total intensity of the scattered emission goes; thus, the amplitude of the reflected plane wave is comparable to the amplitude of the initial incident wave, approaching it as α decreases.

Reflection from the Open Edge of a Wave Guide. Natural Oscillations of a Resonator made up of Strip or Rectangular Mirrors. The above-described phenomena are the basis for the mechanism of diffraction "containment" of the field inside the resonator that we mentioned in the preceding section. Actually, the problem of diffraction on a periodic structure of screens is entirely similar to the problem of diffraction on the edge of an open semiinfinite wave guide formed by two flat, totally reflecting mirrors installed at a distance ℓ from each other (Figure 2.9). The radiation absorbed in the screens here corresponds to the radiation leaving from the open edge of the wave guide. Of course, in both cases the nature of the setup processes depends on the initial conditions and can be quite different, but

APPROVED FOR RELEASE: 2007/02/09: CIA-RDP82-00850R000500010010-4

APPROVED FOR RELEASE: 2007/02/09: CIA-RDP82-00850R000500010010-4

the steady field distributions must coincide. It is only necessary to consider that in a wave guide not one, but a set of two plane waves go in the direction of the open edge, converting into each other on reflection from the mirrors (Figure 2.9). Inasmuch as the nodes of the total field distribution must be located in the mirrors, an additional condition $k\ell(1 - \alpha^2/2) = q\pi$ is imposed on the frequency, where q is a large (on the order of $2\ell/\lambda$) integer.

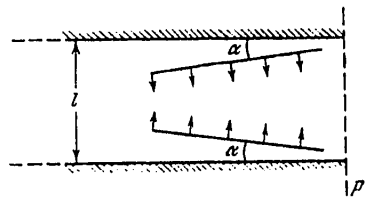

Figure 2.9. Set of two plane waves ("wave guide" wave) propagated in the direction of the open edge (P) of a flat, semiinfinite wave guide.

Using the wave guide approach, Vaynshteyn and his followers were able to obtain many valuable theoretical results not only for plane, but other open resonators; therefore we shall discuss the laws obtained above in the language of wave guide theory. The set of two waves that convert into each other on reflection from the wave guide walls, the frequency and angles of inclination of which satisfy the above-indicated condition, is the so-called wave-guide wave. It is propagated through a plane wave guide with ideally conducting (reflecting) walls as large a distance as one might like without damping. The waves for which the given condition is not satisfied can not be propagated through the wave guide and damp quickly.

The initial wave guide wave with $q = q_0$, being propagated from left to right, approaches the open edge of the wave guide; diffraction on the open edge leads to the fact that the emission almost does not exit to the outside and "is reflected" back. This reflected (or scattered) radiation, in turn, breaks down into a set of wave-guide waves, the angles of inclination of which β satisfy the same condition with $q = q_0, q_0 - 1, q_0 - 2, \ldots$ A wave with $q = q_0$ is similar to the initial wave and differs from it only by the opposite direction of propagation; it is called reflected, and the ratio of its amplitude to the amplitude of the initial wave is called the reflection coefficient from the edge; for small α the modulus of the reflection coefficient approaches one. Waves with $q \neq q_0$ are called transformed; in the case of interest to us for very small α, their amplitudes are small, and hereafter we shall not be especially interest in the transformed waves.

The field of the wave-guide wave propagated from left to right with constant amplitude in time has the form

$$\exp(-i\omega t)\exp(ik_x x)\begin{pmatrix}\cos\\ \sin\end{pmatrix}\frac{\pi q z}{l}, \quad -\frac{l}{2} \leqslant z \leqslant \frac{l}{2},$$

where sin is taken for even q, cos, for odd q (so that the field on the wave guide walls will be equal to zero), and the propagation constant $k_x = k\sin\alpha \simeq (\pi q/\ell)\alpha$ is related to the frequency by the expression

APPROVED FOR RELEASE: 2007/02/09: CIA-RDP82-00850R000500010010-4

APPROVED FOR RELEASE: 2007/02/09: CIA-RDP82-00850R000500010010-4

$$\left(\frac{\omega}{c}\right)^2 = k^2 = \left(\frac{\pi q}{l}\right)^2 + k_x^2. \tag{7}$$

For construction of the oscillation modes of a flat cavity, we need waveguide waves, the amplitude of which damps exponentially in time. Their fields are described by the same formula, except the frequency ω, and with it also the propagation constants k, k_x, become complex: $\omega = ck = \omega' - i\omega''$, $k_x = k_x' - ik_x''$

From (7) it follows that for damping oscillations ($\omega'' > 0$) the symbols k_x' and k_x'' coincide; hence it follows that the field amplitude of such a wave-guide wave at any fixed point in time increases along the direction of its propagation($\sim \exp(k_x'' x)$). In order to understand the meaning of this, it is sufficient to imagine that the wave is generated by a remote source that damps in time. The emission which is far from the source at the given point in time was generated by it obviously at earlier points in time when the source was more intense; therefore the field amplitude in remote sections also turns out to be large.

Now let us consider a segment of a wave guide open on both ends, which is a strip cavity with mirrors 2a wide ($-a \leq x \leq a$). Its natural oscillations will be found in the form of a sum of two wave guide waves propagated in opposite directions with identical natural frequencies and q. For diffraction reflection from the edge, each of them generates the other; a decrease in amplitude as a result of incomplete reflection is compensated for by the above-mentioned buildup along the direction of the wave propagation.

Omitting the factors describing the dependence of the field on t and z, for the total amplitude we have the expression $A \exp(ik_x x) + B \exp(-ik_x x)$. The first term corresponds to a wave propagated in the direction of the edge $x = +a$, where it generates the second one (the transformed waves occurring on reflection from the edge with different $|k_x|$ will be neglected); thus, the amplitudes of our two waves are related at the edge by the expression $R_{0,0} A \exp(ik_x a) = B \exp(-ik_x a)$, where $R_{0,0}$ is the coefficient of diffraction reflection from the edge. The condition at the edge $x = -a$ has the form $R_{0,0} B \exp(ik_x a) = A \exp(-ik_x a)$; from these two boundary conditions we have $A = \pm B$, $R_{0,0} \exp(2ik_x a) = \pm 1$. The last expression is the characteristic equation from which the set of natural frequencies of a strip resonator can be defined; the only thing left to do is to substitute the value of $R_{0,0}$ in it.

By using analytical methods, the investigation of which is far beyond the scope of this book, Vaynshteyn [35] obtained the following formula for the coefficient of diffraction reflection of a wave guide wave from the open edge:

$$R_{0,0} = -\exp[-\beta(1-i)s], \tag{8}$$

where $\beta = 0.824$, s is the parameter introduced above, which in the general case is equal to $\sqrt{\lambda\ell/2\pi}\, k_x$ and in the presence of damping becomes complex. The given formula is valid for $\ell \gg \lambda$, $|s| \ll 1$; in the optical band the first of these conditions is always satisfied, the second requires that damping in time and the angles of inclination of the plane waves entering into the wave guide wave be quite small; it is true that (8) remains satisfactorily accurate even when $s \lesssim 1$. Let us note that as s decreases, the modulus of $R_{0,0}$ approaches one; the presence of not only an

APPROVED FOR RELEASE: 2007/02/09: CIA-RDP82-00850R000500010010-4

APPROVED FOR RELEASE: 2007/02/09: CIA-RDP82-00850R000500010010-4

amplitude factor, but also a phase factor in the right-hand side of (8) corresponds to the fact that the minimum total field amplitude is located at some distance from the edge of the wave guide (returning to Figures 2.7, 2.8, it is possible to say that reflection takes place somehow from the plane parallel to P and located somewhat to the right).

Substituting (8) in the characteristic equation, expressing s in terms of k_x and representing ± 1 in the form of exp (imπ), m = 0, 1, 2, ..., for k_x we obtain the following set of values:

$$k_x = \frac{(m+1)\pi}{2a(1+\varepsilon)}, \tag{9}$$

where $\varepsilon = \beta(1+i)/\sqrt{8\pi N}$, $N \equiv a^2/\lambda\ell$ is the Fresnel number known to us from § 1.2. In order that the condition of smallness s be satisfied, the value of m must satisfy the inequality $m \ll \sqrt{8N/\pi}$.

Now let us compare the properties of an open strip resonator with the properties of an analogous closed resonator unbounded along the y-axis (the side reflecting walls with the coordinates $x = \pm a$ are added). For the latter $k^2 = (q\pi/\ell)^2 + [(m+1)\pi/2a]^2$, from which we have $\omega_{qm} \approx \frac{c}{2l}\left[2\pi q + \frac{\pi(m+1)^2}{8N}\right]$. For the open resonator, the expression defining the spectrum of the natural frequencies has the form $\omega_{qm} \approx \frac{c}{2l}\left[2\pi q + \frac{\pi(m+1)^2}{8N(1+\varepsilon)^2}\right]$. For ordinary mirror sizes $|\varepsilon| \ll 1$; therefore the frequency spectrum of an open resonator is very close to the frequency spectrum of a closed resonator. The theoretical difference consists only in the fact that as a result of complexity of ε for the open resonator, the frequencies turn out to be complex — and damping appears.

The wave guide approach made it possible also to calculate the natural frequency spectrum of a strip resonator and the field distribution of natural oscillation modes. Knowing all of this, it is easy to proceed with the more conventional method of description where we are not talking about wave guide waves propagated in transverse directions, but a light beam following the resonator axis. The interrelation between the complex oscillation frequency and the eigenvalues of $\beta_m = \exp(-i\delta'_m - \delta''_m)$ of the integral operator $\hat{P}$ describing the conversion of a transverse field structure on a complete round trip through the resonator in both directions, was established in § 1.3. As applied to the given case we have

$$\delta'_m = \mathrm{Re}\left[\frac{\pi(m+1)^2}{8N(1+\varepsilon)^2}\right] = \frac{\pi^2(m+1)^2 M(M+2\beta)}{[(M+\beta)^2+\beta^2]^2},$$
$$\delta''_m = -\mathrm{Im}\left[\frac{\pi(m+1)^2}{8N(1+\varepsilon)^2}\right] = \frac{2\pi^2(m+1)^2\beta(M+\beta)}{[(M+\beta)^2+\beta^2]^2}, \tag{10}$$

where $M = \sqrt{8\pi N} = \sqrt{\frac{8\pi}{\lambda l}}\,a$. Usually M >> 1, and $\delta'_m \approx \frac{\pi}{8N}(m+1)^2$, $\delta''_m \approx \beta\sqrt{\frac{\pi}{2}}\frac{(m+1)^2}{8N^{3/2}}$.

Finally, the diffraction losses of the emission on passage through the resonator in both directions are

APPROVED FOR RELEASE: 2007/02/09: CIA-RDP82-00850R000500010010-4

APPROVED FOR RELEASE: 2007/02/09: CIA-RDP82-00850R000500010010-4

$$1 - \exp(-2\delta_m'') \approx 2\delta_m'' \approx \beta \sqrt{\frac{\pi}{2}} \frac{(m+1)^2}{4N^{3/2}}.$$

The eigenfunctions oı a strip resonator can be described in the form

$$u_m(x) = \begin{pmatrix}\cos\\ \sin\end{pmatrix} \frac{\pi(m+1)x}{2a\left(1+\beta\frac{1+i}{M}\right)}, \quad m = \begin{matrix}0, 2, 4 \ldots,\\ 1, 3, 5 \ldots\end{matrix} \tag{11}$$

The form of u_0 and u_1 is presented in Figure 2.10, a, b for several different numbers of Fresnel zones N. In Figure 2.10, a, the dotted lines are used to plot the curves obtained in reference [9] for one of the same versions of a resonator by numerical solution of the corresponding integral equation. Small differences between the exact (the dotted line) and approximate solutions arise from the fact that when deriving (11), considering the process of diffraction reflection of the wave guide from the edge of the resonator, we considered only the reflected wave, and the remaining components of the emission scattering were neglected. For larger N the differences become entirely insignificant.

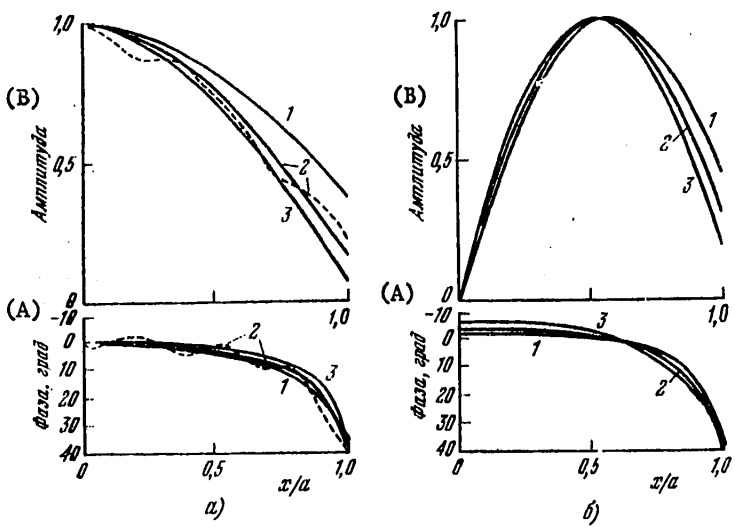

Figure 2.10. Lowest symmetric and antisymmetric eigenfunctions of a flat strip resonator: a) $u_0(x)$, 1 — N = 0.5, 2 — N = 2.5, 3 — N = 6.25; b) $u_1(x)$, 1 — N = 2 — N = 4, 3 — N = 10. The solid curves are the result of calculations by formula (11), and the dotted curves are the data from exact numerical calculations.

Kye: A. phase, degrees B. amplitude

APPROVED FOR RELEASE: 2007/02/09: CIA-RDP82-00850R000500010010-4

APPROVED FOR RELEASE: 2007/02/09: CIA-RDP82-00850R000500010010-4

In order to obtain an idea about the behavior of the higher-order eigenfunctions, it is possible to consider Figure 2.5, c in which the amplitude u_8 is depicted. As a result of complextity of the argument, this is not an entirely "pure" sine curve — the scale of the oscillations increases somewhat from the center to the periphery of the beam. In addition, at the distribution "nodes" the field amplitude differs somewhat from zero (as a result of inequality of the amplitudes of the two interfering wave guide waves); therefore the given figure is to some degree provisional.

By using the method of separation of variables, it is easy to obtain the eigenfunctions and eigenvalues for an open resonator made up of two flat rectangular mirrors 2a × 2b in size installed opposite each other:

$$u_{mn}(x, y) = \begin{pmatrix}\cos\\ \sin\end{pmatrix}\frac{(m+1)\pi x}{2a[1+\beta(1+i)/M_a]}\cdot\begin{pmatrix}\cos\\ \sin\end{pmatrix}\frac{(n+1)\pi y}{2b[1+\beta(1+i)/M_b]},$$

$$\delta'_{mn} = \delta'_m(M_a) + \delta'_n(M_b), \quad \delta''_{mn} = \delta''_m(M_a) + \delta''_n(M_b),$$

where $M_a = \sqrt{8\pi/\lambda l}\,a$, $M_b = \sqrt{8\pi/\lambda l}\,b$, δ' and δ'' are defined as before by formulas (10). Thus, in the case of rectangular mirrors the phase corrections and losses are equal to the sum of the phase corrections and losses of two strip resonators, the mirror width of each of which is equal to one of the sides of a rectangle.

Flat Cavity made of Circular Mirrors. It is first necessary, according to Vaynshteyn, again to resort to the wave guide approach. The solution is found in the form $\exp(-i\omega t) f(r, \varphi)\begin{pmatrix}\cos\\ \sin\end{pmatrix}\frac{\pi q z}{l}$, where $f(r, \varphi) = J_n(k_r r)\begin{pmatrix}\cos n\varphi\\ \sin n\varphi\end{pmatrix}$, $n = 0, 1, 2, \ldots$, J_n is a Bessel function, ℓ is, as before, the distance between mirrors. The given expression, just as the sum of two wave guide waves used when investigating a strip resonator, is the exact solution of the wave guide equation between flat mirrors of infinite dimensions. The oscillation frequency ω is related to the values of q, k_r just as it was related to the values of q, k_x in the preceding case.

At a sufficient distance from the center it is possible to use the asymptotic Hankel representation for the function $J_n(k_r r)$

$$J_n(k_r r) = \sqrt{2/\pi k_r r}\cos[k_r r - (2n+1)\pi/4] \sim$$
$$\sim \exp\{i[k_r r - (2n+1)\pi/4]\} + \exp\{-i[k_r r - (2n+1)\pi/4]\},$$

that is, it is possible to represent the solution in the form of the sum of two radial waves proportional to exp $(ik_r r)$ and exp $(-ik_r r)$. The amplitudes of these waves are related near the edge of the mirrors, just as before, by the coefficient of diffraction reflection from the edge, where it is considered that the magnitude of the reflection coefficient depends on k_r just as it depended on k_x. Thus, it is assumed that the curvature of the edge and the cylindricity of the wave are not felt

APPROVED FOR RELEASE: 2007/02/09: CIA-RDP82-00850R000500010010-4

APPROVED FOR RELEASE: 2007/02/09: CIA-RDP82-00850R000500010010-4

Table 2.1. Roots of the equation $J_n(\nu) = 0$

m \ n	0	1	2	3
0	2,40	3,83	5,14	6,38
1	5,52	7,02	8,42	9,76
2	8,65	10,17	11,62	13,01
3	11,79	13,32	14,80	16,22

in the diffraction reflection coefficient; it is possible to familiarize oneself with arguments in favor of this proposition and also a number of other mathematical fine points connected with the problem of circular mirrors in [3].

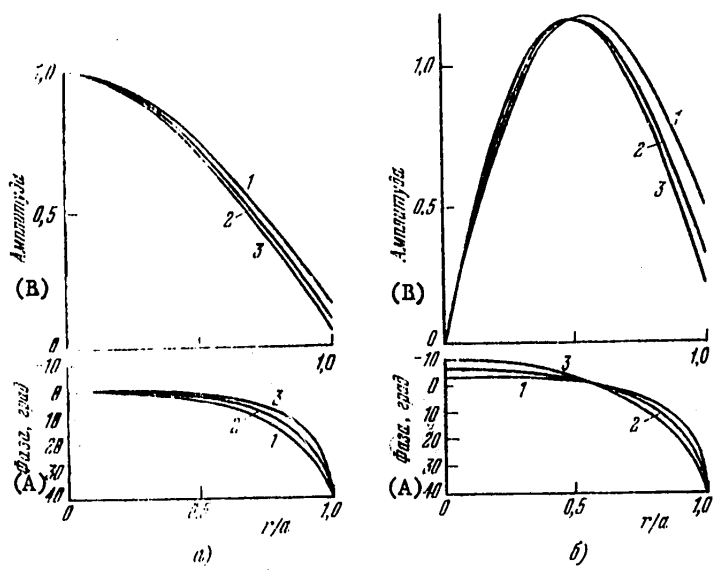

Figure 2.11. Radial eigenfunction factor of a flat optical cavity made of circular mirrors: a) $f_{00}(r)$; b) $f_{01}(r)$; 1 — N = 2, 2 — N = 5, 3 — N = 10.

Key: A. phase, degrees B. amplitude

APPROVED FOR RELEASE: 2007/02/09: CIA-RDP82-00850R000500010010-4

APPROVED FOR RELEASE: 2007/02/09: CIA-RDP82-00850R000500010010-4

The corresponding calculations lead to a discrete set $k_r = \nu_{mn}/a(1 + \varepsilon)$, where 2a is the mirror diameter, ε has the same value as in (9), ν_{mn} is the (m + 1)st positive root of the equation $J_n(\nu) = 0$ (Table 2.1). Hence, we have the following formulas for the eigenfunctions and eigenvalues of a resonator made of circular flat mirrors:

$$u_{mn}(r, \varphi) = f_{mn}(r)\begin{pmatrix}\cos n\varphi \\ \sin n\varphi\end{pmatrix} = J_n\left\{\frac{\nu_{mn} r}{a[1 + \beta(1 + i)/M]}\right\} \cdot \begin{pmatrix}\cos n\varphi \\ \sin n\varphi\end{pmatrix},$$

$$\delta'_{mn} = 4\nu_{mn}^2 \frac{M(M + 2\beta)}{[(M + \beta)^2 + \beta^2]^2}, \quad \delta''_{mn} = 8\nu_{mn}^2 \frac{\beta(M + \beta)}{[(M + \beta)^2 + \beta^2]^2},$$

where $M \equiv \sqrt{8\pi/\lambda\ell}\,a$. The diffraction losses for large M are equal to $16\beta\nu_{mn}^2 M^{-3} = \frac{\beta}{\pi\sqrt{2\pi}}\nu_{mn}^2 N^{-3/2}$; let us remember that $N = a^2/\lambda\ell$ is the number of Fresnel zones, $\beta = 0.824$.

The graphs of the functions $f_{00}(r)$ and $f_{01}(r)$ are presented in Figure 2.11, a, b. The nature of the difference between these functions and the exact solutions of the integral equation is the same as in the case of a strip resonator (see Figure 2.10,a).

Polarization of Radiation of Natural Modes. Without considering the systems investigated in § 3.6 with field reversal, the situation with polarization in all empty, open resonators is identical; the information presented below pertains to an equal degree both to the flat cavities investigated in this section and to resonators of other types (in particular, stable resonators which were discussed in the preceding section).

Inasmuch as from the very beginning we used scalar diffraction theory, there is no dependence on polarization direction in any of the derived formulas; in particular, the natural frequencies for oscillations with any linear polarization are identical. Hence, it follows automatically that the natural oscillations can not only have arbitrary linear polarization, but also be a superposition of oscillations with different linear polarization, that is, have circular or elliptic polarization. Hereafter, for more descriptiveness we shall represent the oscillations as linearly polarized; let us begin with the case of rectangular mirrors.

Figure 2.12 contains a schematic description of the field distributions of TEM_{00}, TEM_{10} and TEM_{01} oscillations with respect to their linear cross section with rectangular mirrors; on the dotted lines, the field will be equal to zero. In the general case of unequal sides of the rectangle, the frequencies of the TEM_{10} and TEM_{01} oscillations are different; for square mirrors they coincide — additional degeneration occurs. By superposition of such degenerate oscillations, oscillations with more complex field topology can be obtained as illustrated in Figure 2.13.

APPROVED FOR RELEASE: 2007/02/09: CIA-RDP82-00850R000500010010-4

APPROVED FOR RELEASE: 2007/02/09: CIA-RDP82-00850R000500010010-4

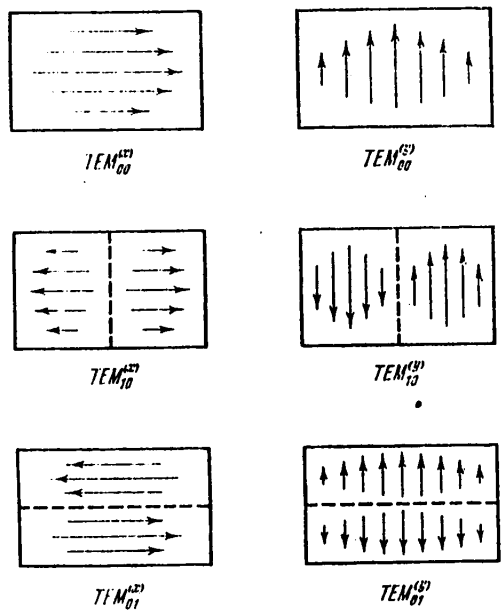

Figure 2.12. Field distribution with respect to resonator cross section with rectangular mirrors.

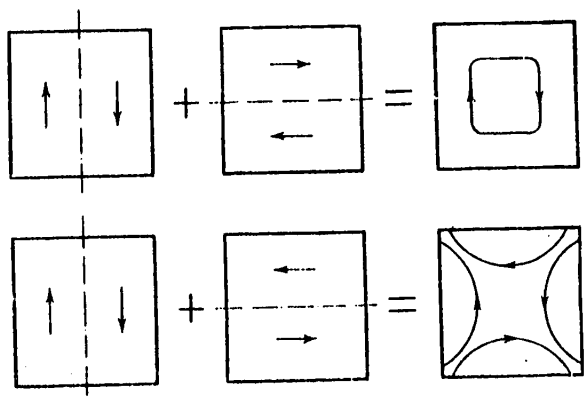

Figure 2.13. Formation of oscillations with complex field topology in a resonator with square mirrors [9].

APPROVED FOR RELEASE: 2007/02/09: CIA-RDP82-00850R000500010010-4

APPROVED FOR RELEASE: 2007/02/09: CIA-RDP82-00850R000500010010-4

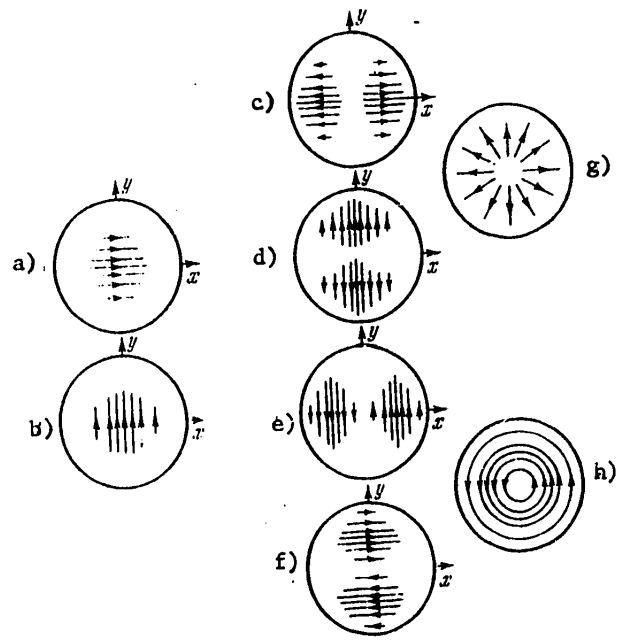

Figure 2.14. Field distribution with respect to resonator cross section with circular mirrors [3]: a) $TEM_{00}^{(x)}$; b) $TEM_{00}^{(y)}$; c) $TEM_{01}^{(x)}$, u ~ cos ϕ; d) $TEM_{01}^{(y)}$, u ~ sin ϕ; e) $TEM_{01}^{(y)}$, u ~ sin ϕ; f) $TEM_{01}^{(x)}$, u ~ sin ϕ; g) $TEM_{0.}^{(r)}$; h) $TEM_{01}^{(\phi)}$.

Finally, Figure 2.14 shows TEM_{00} and TEM_{01} oscillations of a resonator with circular mirrors; superposition of the oscillations depicted in Figure 2.14, c-f, leads to the natural oscillations TEM_{01} with radial (g) and azimuthal (h) directions of polarization.

With this, we complete the investigation of empty resonators with small diffraction losses.

§ 2.3. Some Experimental Research Results

It was already mentioned in the introduction that the first gas lasers had highly uniform and extremely weakly amplifying active medium; in addition, the active medium was included in long narrow cells which led to a small number of Fresnel zones N on the resonator mirrors. For small N, as will be demonstrated hereafter, the optical nonuniformity of the medium, imperfection of the resonator elements and gain saturation effects are most weakly manifested; for these reasons, the experimental data of the transverse field structure of gas lasers at that time did not offer too much to consider. It is possible to note, it is true, that when using "stable" resonators distribution patterns similar to the patterns predicted by the theory of ideal empty resonators were observed quite frequently. In the

APPROVED FOR RELEASE: 2007/02/09: CIA-RDP82-00850R000500010010-4

APPROVED FOR RELEASE: 2007/02/09: CIA-RDP82-00850R000500010010-4

case of flat mirrors (which were used comparatively rarely for gas lasers), small deviations from the ideal configuration led to sharp distortion of the form of the field distribution. Thus, in one of the first papers on investigation of continuous gas lasers written by Herriott [36] such distortions were observed for deviations from ideal planeness of the mirrors of $\sim\lambda/100$.

In the 1970's when powerful gas lasers with large volumes of optically nonuniform active medium began to be more and more widespread, the problem of the divergence of their emission was solved on the basis of unstable resonators rather than stable or flat cavities (see Chapter 4). Therefore the basic source of information on the transverse field structure in nonideal resonators with small diffraction losses remain the results of the studies of solid-state lasers performed in the 1960's.

Early Observations of Stimulated Emission of Solid-State Lasers. The first experiments demonstrated that the angular divergence of the emission of solid-state lasers was significantly greater (usually by one or two orders) than the expected value. In order to discover the causes of the comparatively large angular divergence of the emission, various studies were made of the spatial structure of the stimulated beam as a function of the degree of uniformity of the active medium, the pumping intensity, and so on. The greater part of this research pertains to the case of a resonator with flat mirrors.

When comparing experimental data with the results of the theory of empt open resonators, it was discovered very quickly that the reg lar spot distribut in the near or far zones corresponding to defined oscillation modes of an ideal resonator is almost never encountered. Even approximate similarity of the field distribution patterns with the oscillation modes of an ideal resonator is observed, as a rule, only when the lasing threshold is slightly exceeded, the medium is homogeneous to the maximum and under other exceptionally favorable conditions [37-40]. With an increase in pumping intensity, the number of oscillation modes present in the stimulated emission increases. Modes appear with more and more complicated structure and greater and greater divergence of the emission [37, 38, 40, 41]. In addition to everything else, the spatial distribution of the emission during a lasing pulse does not remain constant at all. Thus, if the stimulated emission pulse lasts more than 10^{-5} seconds, as a rule, it decays into a large number of already mentioned emission "spikes" randomly distributed in time; the field structure varies almost randomly from spike to spike. Therefore if we are able to observe individual modes of oscillations, then it is possible only with the help of high-speed photography, recording the field distribution for individual spikes. Even with high-speed photography, recognition among the other modes of the single, lowest mode which has diffraction divergence of the emission, is far from a frequent event.

When using active rods with noticeable optical inhomogeneities, identification of the individual modes of oscillations becomes impossible [42, 43, 39, 40]. In many experiments it was discovered that very small resonator aberrations with respect to magnitude are sufficient for complete distortion of the field distribution of the lowest-order modes. Thus, for example, in one case [44] such distortion was caused by elastic deformations of a ruby rod (as a result of especially applied forces), in another case it was caused by transition from samples with optical length variations $\Delta L \sim 0.1\lambda$ to samples with $\Delta L \sim 0.25\lambda$ [39]. Accordingly, in subsequent papers an effort was made to analyze the mechanism of the effect of optical inhomogeneities on the field structure.

APPROVED FOR RELEASE: 2007/02/09: CIA-RDP82-00850R000500010010-4

APPROVED FOR RELEASE: 2007/02/09: CIA-RDP82-00850R000500010010-4

The papers by Evtuhov and Neeland [38, 45] and, in particular, Leontovich and Veduta [46] were a significant step forward in understanding the essence of this mechanism. In these papers it was demonstrated that if a nonuniform active rod serves as the source of the second-order wave aberrations (of the positive lens type), then the resonator with flat mirrors is made equivalent to an empty resonator with concave mirrors. The observed field structure in such cases corresponds to the predictions of stable resonator theory. Thus, the concept of the equivalent resonator was used for the first time to interpret the experimental data.

In reference [46] an explanation was also presented for a number of laws observed when using stable resonators. When the threshold is slightly exceeded, only the lowest types of oscillations with least diffraction losses located near the axis of the sample are stimulated. The appearance of stimulated emission first in the central zone is promoted by the fact that the pumping emission density and, with it, the inverse population frequently reach the maximum value on the axis of the sample [47, 48]. With an increase in pumping power, the threshold of stimulated emission of higher-order oscillation modes is reached, and the region encompassed by the stimulated emission expands. Finally, when the threshold is exceeded by a great deal, the modes of such high order that the stimulated emission fills the entire active medium appear.

The above-described picture of replacement of the oscillation modes was actually observed in many papers (for example, [49, 50]); the argument that the maximum transverse index of the modes present in the stimulated emission is determined by the condition of filling the entire resonator cross section also found complete confirmation [51-53]. Let us note that resonator "stability" was insured in different experiments both by using concave mirrors [51, 53] or introducing positive lenses into the resonator with flat mirrors [52, 53] and by "lenticularity" of the sample itself [54]. It is also interesting that on appearance of modes with high transverse indices in the stimulated emission, the lowest oscillation modes of the stable resonator are "displaced" — they cease to be observed in the stimulated emission (for example, [49]).

The following is especially important for us. Inasmuch as with an increase in order of the modes, the emission divergence also increases, the radiation pattern of lasers with "stable" resonators not only does not become more constricted as the active zone diameter increases, but it even becomes broader. Thus, the situation here turns out to be quite clear, and it is extremely unfavorable from the point of view of achieving small emission divergence.

APPROVED FOR RELEASE: 2007/02/09: CIA-RDP82-00850R000500010010-4

APPROVED FOR RELEASE: 2007/02/09: CIA-RDP82-00850R000500010010-4

With a decrease in sphericalness of the mirrors and as the resonator approaches a flat cavity, information about the angular divergence of the emission becomes less and less systematic. The modes of oscillations observed in stimulated emission frequently have such an irregular structure that whatever it is, classification of them becomes impossible; frequently it is not even possible to trace the correlation between the width of the radiation pattern and the perfection of the resonator. This is all the more true, as numerous studies have demonstrated, in that in the case of a flat cavity the field structure turns out to be especially sensitive to intraresonator wave aberrations, the sources of which are highly varied. In spite of this fact, for large diameters of the active elements, the emission divergence, although it exceeds the diffraction limit significantly, is far from that in the case of stable resonators (for example [55]). Therefore lasers with flat mirrors remained the basic type of solid-state lasers for many years.

Divergence of the Radiation of Solid-State Lasers. Comparatively small emission divergence and, together with this, a variety of factors influencing it, have insured constant interest on the part of researchers in lasers with flat cavities. Let us present the basic results from numerous studies in which the causes limiting the axial luminous intensity of these lasers was investigated.

A significant part of the studies pertain to ruby lasers. Being the typical crystalline active medium, the ruby has an enormous number of randomly distributed micro- and macro inhomogeneities leading to significant scattering of light. The characteristic magnitude of the losses to low-angular light scattering is 0.01-0.1 cm^{-1} [56] for this material (just as also for many other crystalline active media [17]).

In the case of noticeable light scattering, the width of the central core in the angular distribution usually is 5-20'. The core is surrounded by a system of comparatively intense rings [57-60, 39, 46] with angular radii equal to the radii of the rings in the Fabry-Perot etalon for light with a wavelength equal to the emission wavelength in the central core (for example, [60]; let us note that the magnitudes of these angular radii form the same sequence as the slope angles of the transformed waves θ_n in the preceding section). According to some observations, the ring width in the angular distribution is determined by the same expressions as in the passive etalon, and it depends on the quality of the sample, respectively [39]. Finally, in the paper by Vanyukov, et al. [61] the relation of the indicated rings to the light dispersion was finnaly proved by introducing an additional scattering element into the resonator.

Observations of the spatial coherence [57-59] and emission spectra [62] led to the conclusion that the emission pertaining to individual oscillation modes is in practice distributed over the entire spot of the far-field pattern and the shape of the wave front at the exit from the laser has an extraordinarily complicated and irregular structure.

All of this does not fit within the framework of the concepts developed by the theory of ideal empty resonators. The interpretation of the observed phenomena is also complicated by the fact that in almost every specific case the influence of a great variety of types of resonator aberrations is exhibited. Nevertheless, in many of the experiments it was possible to trace a clear correlation between optical perfection of the active medium and the degree of directionality of the emission: with a decrease in uniformity of the sample, the angular divergence of both

APPROVED FOR RELEASE: 2007/02/09: CIA-RDP82-00850R000500010010-4

APPROVED FOR RELEASE: 2007/02/09: CIA-RDP82-00850R000500010010-4

the amplifiers [63] and lasers [63-68] increases. It is worth while especially to note the fact that with large angular divergence, the magnitude turns out to be close to the magnitude of the angular divergence of a high-parallel beam from an external source after single passage of it through the same sample [67-69].

In references [66-68], an experimental study was made of the peculiarities of the influence of such specific sources of light dispersion as the sliding surfaces, interfaces between modules, and so on. From the presented data it follows that for macroinhomogeneities, basically the light dispersion on the microinhomogeneities — on the distribution "wings" — is felt in the magnitude of the central angular distribution core.

The angular divergence and power of the emission as a function of length of a flat cavity for the case of a laser using a macroscopically uniform medium but having noticeable dispersion on microinhomogeneities ($CaF_2:Sm^{2+}$) was studied in [26]; it was demonstrated that the divergence of the emission is proportional to $L^{-1/2}$ in a very broad range of variation of L. It is noteworthy that with an increase in the resonator length, a decrease in divergence until it approaches the diffraction limit was accompanied only by insignificant reduction of the lasing power.

As has already been pointed out, the light scattering sources in crystalline active media are distributed more or less randomly with respect to volume. The aberrations caused by nonuniform heating of the active rod (so-called thermal deformations of the resonator) have an entirely different nature. Their source is the thermal variations of the index of refraction and the phenomenon of photoelasticity caused by the presence of thermal stresses [70, 71].

The given effect was detected in 1963 [72, 73] and was studied in detail in many subsequent papers. On the basis of their origin itself, in contrast to light dispersion, the thermal deformations reduce to the presence of an index of refraction gradient which varies slowly with respect to the cross section of the specimen.

The thermal deformations are especially large in active elements of lasers operating in the periodic [74, 75] or continuous [54] mode. However, even when the laser operates in the single spike mode, thermal deformations at the end of the pulse frequently reach noticeable magnitude and have a significant influence on the angular divergence of the emission. Thus, in one of the early papers by Vanyukov, et al. [76] pertaining to a comparatively small neodymium glass laser with pumping that is not very intense, a two-fold increase in the divergence at the end of the lasing pulse was observed which was correctly ascribed to thermal effects. Hereafter, as the size and power of solid state lasers increase, the control of the thermal deformations has become one of the most important problems of laser engineering. We shall discuss the methods of solving this problem and other aspects of the problem of optical nonuniformity of active media in more detail in Chapter 5. Now let us only note that analogous phenomena are also observed in powerful gas lasers: microinhomogeneities occurring during the process of excitation of the gas medium or during its turbulent motion frequently lead to noticeable light scattering; instead of the thermal deformations of the active element, here thermal deformations occur in the resonator mirrors.

In addition to the enumerated factors, the spatial structure of the beam is influenced by a number of other factors. Thus, great significance is attached to the

APPROVED FOR RELEASE: 2007/02/09: CIA-RDP82-00850R000500010010-4

APPROVED FOR RELEASE: 2007/02/09: CIA-RDP82-00850R000500010010-4

accuracy of alignment of the flat mirrors: if they are not parallel, the spot in the far zone is elongated in the misalignment direction, and in the case of sufficiently large misalignments, it breaks down into a number of individual spots [77-80]. Resonators with uniform active medium and correspondingly small emission divergence are especially sensitive to nonparallelness of the mirrors [80].

The relation was also noted for the angular divergence of the emission as a function of the nature of the distribution of the inverse population with respect to the cross section of the sample [81].

The set of many causes in the final analysis also leads to the fact that the magnitude of the angular divergence when using resonators with small diffraction losses usually is several angular minutes and greatly exceeds the diffraction limit even in the case of lasers with highly uniform active media.

From the point of view of the beam structure itself, the great magnitude of its angular divergence can be the fault of both the presence of a large number of oscillation modes in the stimulated emission and the fact that in systems with noticeable aberrations the emission wave front belonging to the highest Q-modes, can differ sharply from planar. The latter phenomenon is frequently called mode deformation; although this term is not entirely precise, it is convenient to use in many studies.

From the data presented in many articles [39-43, 57-59, 62, 77-80], it is possible to draw the qualitative conclusion that in the case of lasers with flat mirrors in the presence of noticeable aberrations the mode deformations are especially important. The decrease in aberrations is accompanied by an increase in the role of the effects connected with multimodality (for example [40]); finally, if special care is exercised in conducting the experiment and a uniform active medium is used, the angular divergence of the emission turns out to be primarily caused by multimodality of lasing.

Now let us proceed with a more consistent analysis of the phenomena. Let us begin with multimodal lasing. Its mechanism is so complex that for lasers with noticeable optical nonuniformities, noone has seriously studied it. Only the theory of multimode lasing in ideal resonators is more or less advanced. Judging by the experimentally observed trends, which we discussed above, this case is also of interest, and we shall investigate it in the following section.

§ 2.4. Multimode Lasing in Ideal Optical Cavities

Mechanism of Multimode Lasing. At the beginning of the 1960's, the approximation where the inverse population is considered uniformly distributed through the volume of the resonator was used to describe the operation of a laser. Within the framework of this approximation, multimode lasing is totally unexplainable. Actually, in the case of steady-state lasing, as we saw at the beginning of § 1.4, under the joint effect of pumping and stimulated emission, the inverse population is established at a level such that the gain in accuracy compensates for losses in the resonator. If such compensation occurs for the mode of oscillations with the lowest excitation threshold (the frequency is closest to the frequency of the maximum amplification band, the diffraction losses are minimal), then for the

APPROVED FOR RELEASE: 2007/02/09: CIA-RDP82-00850R000500010010-4

APPROVED FOR RELEASE: 2007/02/09: CIA-RDP82-00850R000500010010-4

remaining modes the gain turns out to be less than the losses, and the modes should not be excited.[1]

As we have seen, the results of experimental studies of the transverse field structure do not correspond to such representations. The data on the emission spectrum are, perhaps, more indicative: even for solid-state lasers based on media with uniformly broadened line, the lasing spectrum width frequently is comparable to the gain band width [17]. Thus, in Figure 2.15, the x's are used to plot the results of the measurement of the intensity distribution between oscillations with different axial indices q performed in [62] (the corrections to the frequency as a result of the transverse field structure were quite small in the given case); dotted lines are used to plot the luminescence line. From the figure it is obvious that the lasing spectrum has components so removed from the center of the line that the gain of their frequencies is noticeably less than maximum.

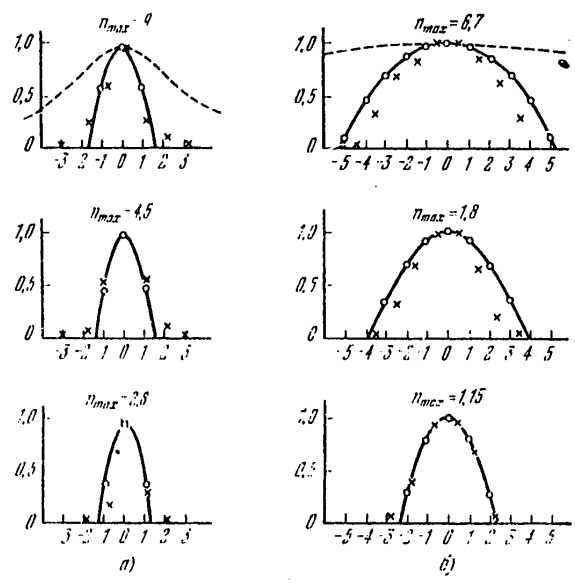

Figure 2.15. Lasing emission energy distribution among spectral bands with different axial indices (the value of $(\nu - \nu_0))c/2n_0\ell)^{-1}$ is plotted on the x-axis, where ν_0 is the frequency at the center of the luminescence line). Temperature of the specimen: a) 15° K, b) 40 K: n_{max} — the threshold is exceeded with respect to pumping intensity; x — experimental data (energy of the emission belonging to individual spectral bands, in relative units); ○ — calculated data; the dotted curve is the curve for the luminescence line.

[1]The effects expanding the lasing spectrum in the case of a nonuniformly broadened operating transition band or in the presence of factors causing mode synchronization will not be discussed here.

APPROVED FOR RELEASE: 2007/02/09: CIA-RDP82-00850R000500010010-4

APPROVED FOR RELEASE: 2007/02/09: CIA-RDP82-00850R000500010010-4

The data on the emission spectra also led to the idea that the primary cause of multimodality is the nonuniformity of the inverse population distribution with respect to the resonator volume arising under the effect of the stimulated emission field. The first paper in which it was demonstrated that in spite of the elementary theoretical predictions, the single-frequency lasing mode is unstable, was written by Kuznetsova and Rautian [82]. Soon Tang and Statz [83, 84] proposed a simple model of multimode lasing based on the proposition that with simultaneous excitation of several modes of oscillations, their frequency differences are sufficiently large that the inverse population does not change noticeably during the intermode beat period. When calculating the inverse population this permits summation not of the field amplitudes of individual modes, but their intensities directly (see § 1.1 on the addition of fields of several sources with different frequencies). On the basis of the given model which will be discussed below, Tang and Statz were able to find the steady state distribution of the lasing emission between modes with pumping intensities somewhat exceeding the threshold. As a result of this, the solution was extended to the case of exceeding the lasing threshold by large amounts [62, 85, 86].

Another fact is very important. The excitation thresholds of individual modes do not coincide as a result of two factors -- the presence of differences in the magnitudes of the diffraction losses and the fact that the gain depends on the position of the frequency inside the luminescence band. As for the diffraction losses, as is known, they depend on the axial index. When investigating angular divergence, this permits us to do away with the problem of the emission spectrum [84, 86]. As a result, it is possible to calculate the set of values of $A_m \equiv \sum_q A_{mq}$, where A_{mq} is the power scattered in the mode with transverse index m and axial index q, and the summation is carried out with respect to all possible q. The set of values of A_m usually is called the intensity distribution between transverse modes, although in essence we are not talking about individual modes, but groups of modes, each of which contains all the oscillations having identical transverse, but different axial indices.

In the case of a flat cavity, on the contrary, the oscillation frequency is basically determined by the axial index; the correction as a result of the transverse structure is usually small. In turn, this permits us to get away from the presence of the transverse structure of the field when calculating the emission spectrum; the calculation result is a set of values $A_{(q)} \equiv \sum_m A_{mq}$, which usually is called the distribution between the axial modes. For this reason, it is possible to make the remark made about the values of A_m.

Now let us explain the multimode lasing mechanism in the example of spectral distribution of the emission in a flat optical cavity. Here is it necessary to consider the field structure along the resonator axis; the transverse structure, as was demonstrated above, can be ignored.

Let us consider Figure 2.16. The curve in Figure 2.16,a provisionally depicts the intensity distribution of one of the types of oscillations along the resonator axis (in reality, of course, an immeasurably larger number of modulation periods equal to $\lambda/2$ are fitted into the length of the resonator than on the figure). We shall consider that the frequency of this oscillation mode fits the center of the luminescence line, and thus, it has the lowest excitation threshold.

APPROVED FOR RELEASE: 2007/02/09: CIA-RDP82-00850R000500010010-4

APPROVED FOR RELEASE: 2007/02/09: CIA-RDP82-00850R000500010010-4

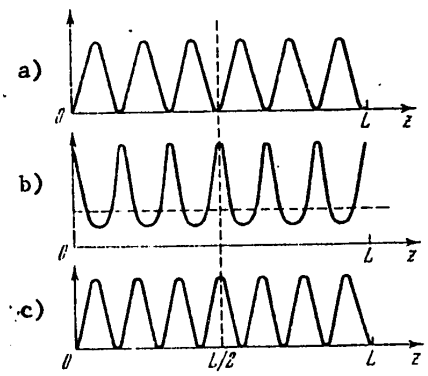

Figure 2.16. Induced spatial modulation of the inverse population as the cause of instability of the unimodal conditions; a), c) oscillation intensity distribution with different axial indices with respect to resonator length (provisionally depicted); b) induced spatial modulation of the inverse population during lasing on the first oscillation, the dotted line denotes the threshold level of the inverse population.

Let the pumping intensity be distributed uniformly along the length of the resonator. While it exceeds the threshold very little, the lasing intensity is negligibly small, the inverse population is distributed almost uniformly and is equal to the threshold (the dotted line in Figure 2.16, b). When the threshold is noticeably exceeded, the situation changes: the lasing power increases, stimulated transitions begin to play a significant role in the inverse population balance, and the distribution of the latter acquires the form represented by the solid curve in Figure 2.16,b. At the field distribution nodes, a large number of excited atoms accumulate which do not participate in the lasing process in the given oscillation mode. As a result, the inverse population averaged with respect to length turns out to be appreciably greater than the threshold value (this fact also leads to the situation where the laser efficiency during unimodal lasing is less than the efficiency for multimode lasing; see § 1.4, Figure 1.20).

It is obvious that sooner or later lasing will begin on modes with adjacent axial indices: although their frequencies do not fall in the center of the line, which decreases the gain, part of the intensity peaks are not at the inverse population distribution minima as in the first mode, but at the maxima (see Figure 2.16,c). With still higher pumping intensity the lasing power in these modes increases so much that they, similarly to the first, create unfavorable inverse population distribution for themselves; as a result, the lasing threshold can be reached on subsequent side frequencies, and so on.

As the number of modes of oscillations present in the stimulated emission increases, the total emission intensity distribution becomes more and more uniform. The inverse population averaged over the resonator length gradually approaches the threshold value. Obviously, sooner or later the time must come when the amount that the threshold population exceeds the threshold value cannot compensate for the decrease in gain on transition to the next side frequencies; therefore the

APPROVED FOR RELEASE: 2007/02/09: CIA-RDP82-00850R000500010010-4

APPROVED FOR RELEASE: 2007/02/09: CIA-RDP82-00850R000500010010-4

number of modes on which lasing is realized still remains finite and not too large with limited increase in the pumping intensity.

The mechanism of spatial competition of the transversed oscillation modes is entirely analogous. If the pumping intensity is distributed uniformly over the resonator cross section, the mode with least diffraction losses is excited first. As the lasing power increases, the inverse population distribution with respect to cross section becomes more and more nonunform; the average inverse population with respect to cross section increases until the excitation threshold of the next transverse mode is reached, and so on.

Thus, the multimodality arises first of all as a result of the fact that the emission intensity in individual modes of oscillations is distributed nonuniformly with respect to the resonator volume. This argument, clearly formulated in the mentioned articles by Tang and Statz, quickly found experimental confirmation. In a number of papers [87-89], various procedures were tested which made it possible to avoid modulation of the radiation intensity with respect to the resonator length (the simplest of them consists in using a traveling wave ring cavity [85]); in all cases a sharp decrease in width of the lasing spectrum was actually observed by comparison with ordinary type lasers.

Procedure and Some Results of Calculations of the Multimode Lasing Regime. In order to calculate the steady-state multimode lasing regime within the scope of the model discussed above, it is necessary to solve the system of equations, each of which is the condition of keeping the amplitude of one of the oscillation modes present in the stimulated emission constant in time. In the case of a four-level medium with unpopulated lower operating level, this system described as applied to the problem of finding the emission spectrum has the form

$$\frac{d\ln A_i}{dt} \sim \int_0^l \frac{k_{yc}^0 \chi_i (1-\cos 2q_i \pi z/l)}{1+\sum_k \chi_k A_k (1-\cos 2q_i \pi z/l)} - \sigma_0 l - \ln(1/\sqrt{R'}) \begin{cases} =0, & i=0, \pm 1, \pm 2, \ldots, \pm r, \\ <0, & |i|>r; \end{cases} \tag{12}$$

here $q_i = q_0 + i$ is the axial index, i is the mode number (reckoning from the center of the luminescence line where $q = q_0$); k^0_{gain} is the gain on the central frequency in the absence of lasing; $\chi_i = \chi(\nu_i)$, $\chi(\nu)$ is a function which describes the shape of the luminescence line (in the center line $\chi_0 = 1$; for the remaining frequencies $\chi < 1$); A_i is the energy dissipation power in the ith mode (including the emission power leaving the resonator) in the corresponding dimensionless units; $\sigma_0 \ell$ are the inactive losses, R' is the reflection coefficient of the exit mirror. Lasing is considered to be realized on 2r + 1 frequencies arranged symmetrically with respect to the center of the line.

In formulas (12), the factor $1 - \cos 2q_i \pi z/\ell = 2\sin^2 q_i \pi z/\ell$ describes the intensity distribution of the ith oscillation along the resonator length (R' is considered close to one); the expression $k^0_{gain}\left[1+\sum_k \chi_k A_k (1-\cos 2q_k \pi z/l)\right]^{-1}$ is the gain distribution on the central frequency established under the overall effect of the entire

APPROVED FOR RELEASE: 2007/02/09: CIA-RDP82-00850R000500010010-4

APPROVED FOR RELEASE: 2007/02/09: CIA-RDP82-00850R000500010010-4

lasing emission field. Hence, it is obvious that the integral in (12) is the gain averaged over the resonator length on the ith mode frequency calculated with weight equal to the intensity distribution function of the given mode. Thus, the idea of conditions (12) is quite obvious: for modes present in the stimulated emission the gain must be equal to the losses; for the remainder, less than the losses (otherwise the regime will be unstable). Let us also note that the method of averaging the gain used here is based on calculating the number of induced emission processes caused by the given mode field. Thus, formulas (12) are in essence the balance conditions of the number of photons in the individual modes.

As an example of how the results of the solution of system (12) look, let us present the figure 2.15 which is already familiar to us and in which the circles are used for the data on the emission spectrum calculated in [62] for the same conditions under which the experimental measurements were taken. It is obvious that the forms of the calculated and the experimentally obtained distributions are quite similar.

The system of conditions analogous to (12) can be written also as applied to the problem of finding the intensity distribution between the transverse modes of oscillations. Depending on the frequency, the factor χ can in this case be omitted; then it is necessary to add the diffraction losses which depend on the transverse index to the losses to inactive absorption and transmission of the exit mirror already considered in (12). The main change, of course, is that the expressions $1 - \cos 2q_i \pi z/\ell$ describing the intensity distributions along the resonator axis must be replaced by the distribution functions of the intensities of the different transverse modes with respect to the resonator cross section. Here we encounter one of the primary difficulties of the theory of filled resonators for the first time. The fact is that any nonuniformity of distribution of the gain with respect to the resonator volume (including that arising under the effect of the lasing field itself) must, generally speaking, cause a change in the individual mode field structure by comparison with the structure in the empty resonator. While the problem of spectral composition of the emission was considered, this could be ignored: the spatial modulation period of the gain along the resonator axis is so small ($\sim\lambda/2$) that no noticeable change in the flux densities in opposite directions takes place along its length. Hence, it follows that the result of interference of these fluxes is described with extraordinarily high accuracy as before by the expression $1 - \cos 2q\pi z/\ell$.

On making the transition to investigation of the angular divergence of the emission, the situation changes sharply: the spatial modulation period in the transverse direction of both the lowest mode fields and occurring in the presence of quite intense gain distribution fields will be compared with the mirror dimensions. Thus, the width of the zones inside which the gain predominates over the losses or vice-versa, is less, is not so small. Inasmuch as the light waves entering into the transverse modes are inclined very slightly with respect to the resonator axis, transmission across this zone corresponds to an incomparably longer path along the resonator axis. As a result, the light waves in the corresponding segments can acquire significant additional gain or attenuation by comparison with the case of an empty resonator. This, in turn, must cause significant changes in both the form of the field distribution and the magnitude of the diffraction losses.

Nevertheless, in a significant part of the papers devoted to specific calculations of the competition of transverse modes, the same values of the diffraction losses

APPROVED FOR RELEASE: 2007/02/09: CIA-RDP82-00850R000500010010-4

APPROVED FOR RELEASE: 2007/02/09: CIA-RDP82-00850R000500010010-4

and field distributions were used as in an empty resonator. This is most justified in the case of stable resonators: the characteristic dimensions of the transverse field in them are less than the characteristic dimensions in flat cavities (the causes of lower sensitivity of stable resonators to various types of excitations will also be discussed in the following section). Therefore the results of the papers on stable resonators theoretically will be reliable: let us begin with them.

Let us first note that in the case of stable resonators the natural oscillation frequency depends sharply not only on the axial, but the transverse indices (see § 2.1; the values of δ_{mn} and δ_{pl} usually are significantly superior to the phase corrections in a flat resonator). Therefore the problem of finding the emission spectrum will become more complicated; during lasing on a very large number of types of oscillations, the spectral width turns out to be appreciably less than would be expected from the solution of (12). As for the angular divergence of the emission, the basic argument about the possibility of estimating it without considering the presence of the field structure along the resonator axis remains valid.

The results of the corresponding papers [90, 91, 53] turned out to correspond completely to the experimental data. The first of these papers belongs to Fox and Li, and was done by exact numerical methods providing for automatic consideration also of the mode deformations as a result of nonuniform gain distribution and possible instability of the kinetic regime; the subsequent results were calculated by the above, less strict method permitting, however, estimates to be made in an immeasurably larger range of variation of the resonator parameters. In all cases, a gradual increase in the pumping intensity was accompanied by the process of successive "displacement" of the lower-order modes by the oscillation modes with higher transverse indices. This process is explained by the fact that in the case of stable resonators the emission of the high-order modes is distributed over greater volume than the emission of the lowest modes (see Figure 2.1, 2.2). As a result, the situation arises which is illustrated in Figure 2.17. Curve 2 in Figure 2.17 provisionally depicts the lowest mode field intensity distribution; curve 1 provisionally depicts the higher-order modes. If these two modes were excited simultaneously, as a result of the total effect of their fields, the gain distribution would assume the form of curve 3. It is clear that the mean "effective" value of the gain for the lowest mode will in this case turn out to be less than for the high-order mode which indicates impossibility of simultaneous excitation of them with comparable intensities.

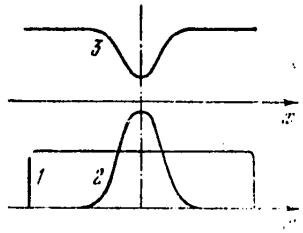

Figure 2.17. Competition of modes of different volume; 1, 2 — field distribution of different transverse modes with respect to the resonator cross section (depicted provisionally); 3 — gain distribution with simultaneous excitation of both modes.

APPROVED FOR RELEASE: 2007/02/09: CIA-RDP82-00850R000500010010-4

APPROVED FOR RELEASE: 2007/02/09: CIA-RDP82-00850R000500010010-4

Competition of the Transverse Modes in Lasers with Flat Cavities. Now let us proceed to the case of lasers with flat cavities which we shall discuss in somewhat more detail. There are no special grounds for assuming that the emission divergence with circular and square mirrors of the same area must differ significantly. As for square or, in the general case, arbitrary rectangular mirrors, within the framework of the above-discussed simplest model, the angular divergence with respect to any two mutually perpendicular directions can be calculated independently of the divergence with respect to the other [84, 86] (similarly to how the divergence and emission spectrum can be determined independently).

The solution of the system of equations of the type of (12) using the values of the diffraction losses, calculated for an empty resonator and the approximate intensity distribution functions with respect to cross section of the type of $|u_m(x)|^2 \sim \begin{pmatrix}\cos^2\\ \sin^2\end{pmatrix}\frac{(m+1)\pi x}{2a}$ (see (11)) leads to the following results [86]. If the pumping is uniform, the power A_m dissipated in individual transverse modes of oscillations of a strip resonator (in the case of rectangular mirrors $A_m \equiv \sum_n A_{mn}$) will turn out to distributed among them by the law $A_m = A_0 - B\delta''_m$, where $2\delta''_m$ are the diffraction losses (in the case of rectangular mirrors, the part of the diffraction losses which is connected with the field structure in the given direction, see § 2.2), A_0 and B are parameters which depend on the properties of the medium of the resonator and also the pumping intensity. The greatest power goes to the lowest mode with minimum diffraction losses. Thus, in flat resonators the excitation of high-order modes does not lead to displacement of the lower ones (as a result of the fact that the volumes of all the modes are approximately identical). The number of modes A in a two-dimensional resonator and, consequently, the magnitude of the angular divergence with respect to one of the directions $\Theta \sim K\lambda/2a$ are saturated extremely quickly as the pumping intensity above the threshold increases ($K \sim \sqrt[3]{(\chi - 1)/\chi}$ where χ is a parameter which is equal to the ratio of the pumping intensity to its threshold value for a four-level medium). With uniform distribution of sufficiently intense pumping and $K \gtrsim 3$, the following simple formulas are valid:

$$K \approx 1{,}5\sqrt[3]{\sigma_0 l + \ln(1/\sqrt{R'})}\, a/\sqrt{\lambda L_{\text{экв}}} \quad \text{(a)}$$

$$\Theta \sim 0{,}7\sqrt[3]{\sigma_0 l + \ln(1/\sqrt{R'})}\, \sqrt{\lambda/L_{\text{экв}}} \quad \text{(a)}$$

Key: a. equiv

where $L_{\text{equiv}} = L - \ell(1 - 1/n_0)$, L is the distance between the mirrors, ℓ is the length of the model with flat ends made of a medium with index of refraction n_0 (see the comments to Figure 1.18, § 1.3).

From these formulas it is obvious that inasmuch as $K \sim a$, with an increase in cross-section of the active elements the angular divergence of the emission does not decrease and is farther and farther from the diffraction limits; the correctness of this conclusion was confirmed, in particular, by direct experimental checking for the case of a neodymium glass laser [26].

APPROVED FOR RELEASE: 2007/02/09: CIA-RDP82-00850R000500010010-4

APPROVED FOR RELEASE: 2007/02/09: CIA-RDP82-00850R000500010010-4

Within the framework of the same model, it is also simple to consider the influence of the nonuniformity of the pumping distribution and the losses with respect to the resonator cross section [86]. Here, much depends on the specific form of these distributions. Without going into details, let us note the following trend: in a laser, generally speaking, an effort is made to establish the lasing emission field such that the resultant gain distribution will approach the loss distribution to the maximum (that is, the threshold condition will be approximately satisfied over the entire cross section). If this emission field is representable in the form of the sum of fields of several lowest modes, lasing will be realized in them. This indicates not only comparatively small emission divergence, but also that the calculated model itself is not so rough in the given case: on satisfaction of the threshold condition in the entire resonator cross section mode deformation is absent, and the use of the same formulas as in an empty resonator to describe the mode structure becomes valid. A simple analysis shows that this situation must be observed most frequently in cases where the ratio of the pumping intensity to the losses decreases smoothly from the center to the edge of the resonator; the lowest mode intensity in this case increases noticeably by comparison with the case of uniformly distributed pumping and losses.[1]

If the indicated ratio, on the contrary, increases on going away from the axis, this must be accompanied by noticeable mode deformations and must, as a rule, lead to large angular divergence. Finally, with sharply asymmetric pumping distribution (or loss distribution), both the mode deformations and the angular divergence of the emission must be especially large. Actually, the proposition that in the given case lasing can be realized on modes which are similar with respect to structure to the modes of an ideal empty resonator leads to logical contradiction. Indeed, the sum of the intensities of any number of modes of an ideal resonator is always distributed symmetrically with respect to cross section and cannot "correct" the asymmetry of the gain distribution caused by nonuniform pumping. This, in turn, can lead to significant mode deformation which contradicts the initial assumption.

All of the enumerated laws are actually observed when investigating lasers if measures are taken to reduce the phase aberrations of the resonator to a minimum. Thus, in reference [92], the greater pumping concentration on the axis of a cylindrical rod caused a decrease in angular divergence. The results of a carefully made comparison of the cases of symmetric and asymmetric pumping distributions with respect to resonator cross section are also of interest [81]; they can serve as a good illustration of the presented arguments (Figure 2.18). The object of investigation was a laser using an active element made of neodymium glass of rectangular cross section. The pumping distribution with respect to one of the directions — along the large cross sectional dimension — was uniform, and with respect to the other dimension, it varied (Figur e 2.18, a). This caused variations of the angular divergence of the emission with respect to the corresponding direction (Figure 2.18, b). Sharp asymmetry of the angular distribution in the case of asymmetric pumping distribution indicates high deformation of the modes, for the modes of an ideal resonator have symmetric far-field pattern.

---

[1] In real lasers such effects can be manifested only in complete absence of any resonator deformations, including thermal.

APPROVED FOR RELEASE: 2007/02/09: CIA-RDP82-00850R000500010010-4

APPROVED FOR RELEASE: 2007/02/09: CIA-RDP82-00850R000500010010-4

Deficiencies of the Model and the Possibilities of Improving It. In spite of the fact that the above-discussed simplest model of multimode lasing leads to plausible explanation of a number of experimentally observed laws, the possibility of using it for quantitative estimates of the angular divergence is far from obvious. Indeed, it is possible to use the field distributions of an empty resonator, as we have seen, only in certain special cases; in the remaining cases, it is impossible to neglect the mode deformations as a result of nonuniform distribution of the gain (or losses), generally speaking. The proposition that the frequency differences of the transverse modes participating in lasing are quite large in the case of a large number of Fresnel zones N also is not entirely justified. Finally, the steady intensity distribution of the emission between the individual modes predicted within the framework of the given approximation was never observed in practice, most frequently, as a result of the "spike" lasing regime. It is true that it was explained in § 1.4 why the energy characteristics of the laser must on averaging with respect to a sufficiently large number of "spikes" correspond to the calculation data in the steady-state approximation; the same arguments can be stated also in favor of correctness of the discussed model, but its deficiencies are still obvious.

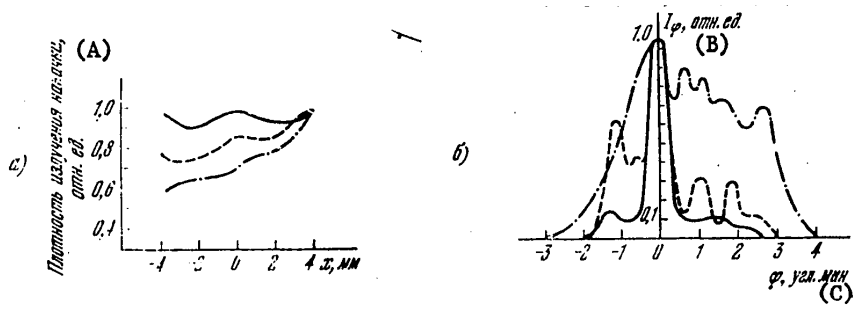

Figure 2.18. Angular distribution of laser emission during pumping that is nonuniform with respect to one of the directions in accordance with the pumping distribution [81].

Key: A. pumping emission density, relative units
B. I_ϕ, relative units
C. ϕ, angular minutes

Numerous efforts have been made at more complete consideration of all of the processes occurring in real lasers. Among them it is worthwhile to note the numerical calculations of the processes of establishment of the multimode lasing regime after inclusion of the previously absent pumping, performed in the previously mentioned papers by Tang and Statz [83, 84]. Expressions of the type of (12) were used in the calculations. Considering the dependence of A_i on time, these expressions are a system of differential equations of the type of $d \ln A_i/dt = F_i(A_0, A_1, \ldots)$. It turned out that although the steady intensity distribution between the individual modes is also established in the final analysis, the setup process lasts for an extremely long period of time, and the oscillations of total intensity occuring in this case are of an irregular nature and are similar to the experimentally observed

APPROVED FOR RELEASE: 2007/02/09: CIA-RDP82-00850R000500010010-4

APPROVED FOR RELEASE: 2007/02/09: CIA-RDP82-00850R000500010010-4

random "peaks." It became possible to understand that the smallest "failures" in operation of the laser caused by pumping instability, variation of the resonator parameters as a result of vibrations, thermal effects, and so on are sufficient for the intensity oscillations to last indefinitely. Subsequently, numerous experimental studies (for example, [93, 94]) demonstrated that the causes of the "spike" mode are indeed such.

We shall not discuss the results of other papers devoted to detailed study of multimode regimes and the emission kinetics of lasers with flat cavities in general. Although among these papers there are very interesting ones, either special cases are investigated everywhere or models are used which are only a little more perfected than the one discussed above. In addition to everything else, the behavior of real lasers with flat cavities depends to a high degree on such a large number of factors, frequently not controllable during the course of even the most careful experiments, that it is inconceivable to fully take them into account.

Let us present the following instructive example to confirm this argument. In any model of a laser with a flat cavity, boundary conditions are induced in one form or another at the edge of the resonator or diffraction losses defined by edge effects are given. In particular, when deriving the above-presented formulas for a number of simultaneously excited transverse modes and angular divergence, the values of the diffraction losses found in § 2.2 were used: $2\delta''_m = \beta\sqrt{\frac{\pi}{2}} \times \frac{(m+1)^2}{4N^{3/2}} \doteq 0{,}26\,(m+1)^2 a^{-3} (\lambda l)^{3/2}$. When the losses themselves were considered, it was assumed that the resonator mirrors are installed exactly opposite each other and are equal in size; if these conditions are not satisfied, all of the formulas become, in general, invalid.

In order to understand what deviations from ideal resonator configuration can lead to such an effect, let us return to Figures 2.7, 2.9. If the edge of one of the mirrors is shifted in the transverse direction with respect to the edge of the other by $\Delta a \approx \alpha l$, one of the mirrors begins to cover the second reflected wave generated by the edge, and the entire edge diffraction pattern is distorted significantly. The angles of inclination of the waves entering into the mode with transverse index m are $\alpha \approx ((m + 1)/2)(\lambda/2a)$; thus, for noticeable variation of the losses of this mode it is sufficient that inaccuracy in the mutual arrangement of the mirrors or inequality of their dimensions reached $\Delta a \approx \frac{m+1}{2}\frac{\lambda l}{2a} = \frac{m+1}{4N}a$. In particular, if the halfwidth of one of the mirrors exceeds the halfwidth of other by this amount, the given mirror can be considered infinitely large in the first approximation. Transmission of the light beam through this resonator in both directions is equivalent to trasmission in one direction through a symmetric flat resonator of double length; the diffraction losses reduced to a unit length increase in this case by $\sqrt{2}$ times.

Thus, for $N \gg 1$ very small deviations from resonator symmetry are sufficient for the diffraction losses of the lowest modes to become different. The magnitude of the losses can feel the frequently existing scattering of the light on the lateral surfaces of the active element or cell walls, and so on. It is true that in the case of large N usually many transverse modes are excited; the properties of the high-order modes are less subject to the effect of random causes (indeed the critical magnitude of the deviations from ideal configuration $\Delta a \sim m + 1$); therefore theoretical estimates of the total number of modes are still meaningful.

APPROVED FOR RELEASE: 2007/02/09: CIA-RDP82-00850R000500010010-4

APPROVED FOR RELEASE: 2007/02/09: CIA-RDP82-00850R000500010010-4

The efforts to create models of multimode lasing more adequate to the actual situation in a laser with a flat resonator are continuing. However, they can obviously lead only to deeper substantiation of the fact already long obvious to experimenters that flat cavities with a large number of Fresnel zones cannot insure minimum divergence of the emission even with an ideally uniform medium. Therefore it is best to proceed to an investigation of the effect of intraresonator aberrations.

§ 2.5. Influence of Resonator Deformations on Field Configuration of Individual Modes

In this section a study will be made of the problem of how the form of the field distribution of individual modes varies under the effect of various types of intraresonator aberrations. Inasmuch as in the final analysis we are interested in the possibility of achieving small divergence, special attention will be given to the case of comparatively small optical inhomogeneities.

Some General Remarks. Perturbation Theory. The analysis of mode deformations with small diffraction losses has been the subject of a broad literature. The majority of reasonable results were obtained either by a numerical iterative method proposed in the paper by Fox and Li [9] or by direct solution of differential equations for an electromagnetic field or, finally, using the expansion in a series with respect to eigenfunctions of an ideal resonator. The latter method is very descriptive and permits unique consideration of the influence of the most varied factors; we shall pay special attention to it.

The expansion of the arbitrary field distribution in a series with respect to eigenfunctions u_m of the operator of an ideal resonator $\hat{P}$ (see § 1.3) is possible, strictly speaking, only in the case where these functions form a complete system. Only stable resonators with infinite mirrors have a complete system of eigenfunctions; perturbation theory has been widely used to calculate them since 1964. [95, 96]. With finite dimensions of the mirrors, the eigenfunctions of open resonators, as Vaynshteyn demonstrated [3], do not form a complete system. This is all the more the case in that for modes of very high order even the scalar formulation of the Huygens-Fresnel principle on which all of our discussion is based, becomes unexceptable. However, the eigenfunctions corresponding to modes with small transverse indices coincide in the case of stable resonators with the functions of resonators made of infinite mirrors, and with flat mirrors they are very similar to the eigenfunctions of a closed resonator with flat mirrors which, as is known, form a complete set. In addition, the coefficients of the corresponding series usually decrease rapidly, and it is possible to get by with several of the first terms. Therefore the expansion in a series with respect to eigenfunctions of both stable and flat resonators is still valid (a more detailed discussion for the case of a flat cavity appears in [97]), and it leads to results which almost coincide with the data of much more tedious exact calculations. In the case of small aberrations, the methods of perturbation theory are applicable.

In the first approximation of perturbation theory the solutions of the equation $(\hat{P} + \hat{P}')u'_m = \beta'_m u'_m$ corresponding to a resonator with aberrations are described by the formulas

$$u'_m = u_m + \sum_k a_{mk} u_k, \quad a_{mk} = \frac{P'_{km}}{\beta_m - \beta_k},$$
$$\beta'_m = \beta_m + P'_{mm}. \tag{13}$$

APPROVED FOR RELEASE: 2007/02/09: CIA-RDP82-00850R000500010010-4

APPROVED FOR RELEASE: 2007/02/09: CIA-RDP82-00850R000500010010-4

Here $\hat{P}'$ is the perturbation operator, u'_m and $'_m$ are eigenfunctions and eigenvalues of a resonator with aberrations, $P'_{km} = \int u_k \hat{P}' u_m ds$ are matrix elements of the perturbation operator.

The mathematical aspect of perturbation theory is explained in any text on quantum mechanics. The only difference of the above-presented relations from the standard ones is that in the expression under the integral sign for P'_{km} the operation of complex conjugation of one of the eigenfunctions is absent (the substantiation of the expediency of this notation appears in [95, 96]). These relations have, in the given case, the following meaning. The matrix elements of the perturbation operator are none other than the relative amplitudes of light waves scattered as a result of perturbation from certain modes of an ideal resonator to others (it is possible to understand this when considering specific forms of the perturbation operator). The values of a_{mk} are the amplitudes of the induced oscillations; it is natural that they are inversely proportional to the frequency differences of the "inducing force" and the free oscillations of the system $\beta_m - \beta_k$. In the case of stable resonators usually these differences are many times greater than the differences for the case of flat mirrors (see also the remark in the preceding section on the emission spectrum of lasers with stable resonators).

The given fact is the basic cause for comparatively weak dependence of the form of the field distribution in stable resonators not only on misalignments of the mirrors, leading, primarily, to a shift of the resonator axis), but also on aberrations of other types. As a result, the angular divergence of the laser emission with a stable resonator, as a rule, is determined not by the influence of the aberrations, but the presence in the stimulated emission of higher order oscillation modes (see §§ 2.3, 2.4). Therefore those who desire to become familiar in more detail with the behavior of stable resonators in the presence of aberrations are referred to the available broad literature on the subject (for example [95, 96, 98, 99]), and we shall limit ourselves to further investigation of lasers with flat mirrors.

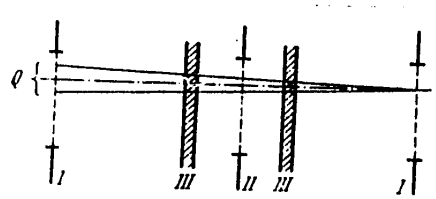

Figure 2.19. Equivalent diagram of a resonator with flat mirrors: I, II — mirrors, III — perturbation zone.

In the case of flat mirrors with a large number of Fresnel zones, the effect of the operator $\hat{P}$ reduces to a significant degree to parallel transfer of the wave front, the diffraction "displacement" is small. As follows from the comments presented in § 1.1 for formula (1.2), the field source at an arbitrary point on the surface of the resonator mirror (see the equivalent diagram in Figure 2.19) is, in essence, the initial wave field in the region Q around the same point encompassing several Fresnel zones. The given fact greatly facilitates calculation of the matrix elements of the perturbation operator.

APPROVED FOR RELEASE: 2007/02/09: CIA-RDP82-00850R000500010010-4

APPROVED FOR RELEASE: 2007/02/09: CIA-RDP82-00850R000500010010-4

Actually, let the perturbation source be concentrated in the zone occupying a small part of the length of the resonator (Figure 2.19); on passage through it, the wave amplitude is multiplied by the aberration factor f(r) which varies slowly with respect to the resonator cross section (in the general case this factor also includes the amplitude and phase corrections). If the variations of f(r) in the dimensions of the region Q are small, the field distribution of the wave passing through the entire resonator forward and backward turns out to be multiplied by $f^2(r)$ independently of the segment of resonator length the perturbation zone is located in. Therefore all such sources of aberrations (including the nonuniformly excited active medium) can be considered concentrated in narrow zones near the mirrors, which has been done in many papers (for example, [100, 101, 90, 86]).

Thus, the operator of a resonator with aberrations can be represented in the form of $F\hat{P}$, where F is a factor describing the total influence of all sources of aberrations; the perturbation operator $\hat{P}' = F\hat{P} - \hat{P} = (F-1)\hat{P}$; hence, it follows that

$$P'_{km} \approx \int u_k(r)\, u_m(r)\, [F(r) - 1]\, ds \tag{14}$$

(we used $\beta_m \approx 1$).

When calculating the expansion coefficients a_{mk} by formulas (13), (14), it is expedient to introduce another simplification, replacing the eigenfunctions and the eigenvalues by the corresponding values for a closed resonator. Indeed, inasmuch as when N >> 1 the value of β/M in formulas (11) is a small parameter, the eigenfunctions of the open strip resonator are close to the functions of a closed one $u_m^0(x) = \begin{pmatrix}\cos\\ \sin\end{pmatrix}\frac{\pi(m+1)x}{2a}$. As for the difference of the eigenvalues, for an open resonator it is determined by the magnitude of the phase corrections δ'_m with accuracy to terms of the same order of smallness. Phase corrections, in contrast to diffraction losses, in practice do not depend on random parallel shifts or inequality of the size of the mirrors (see the end of the preceding section) and coincide with the corrections for a closed resonator. In the two-dimensional case

$$\delta'_m \approx (m+1)\frac{\pi}{8N}, \quad \beta_m - \beta_k \approx (k^2 - m^2)\frac{\pi i}{8N}.$$

Hence, it follows that the result of the effect of the perturbations on the form of the field distribution depends little on random causes. Therefore information obtained using the above-discussed approximation can serve as an objective characteristic of the emission field of real lasers; calculation of the influence of the perturbations on the magnitude of the diffraction losses requires a much more complex analysis [for example, [102]).

Flat Cavities with Minor Aberrations. Let us proceed with the investigation of specific types of perturbations, beginning with purely phase aberrations. The results of this investigation pertain to some degree not only to empty resonators, but to the case of multimode lasing where the gain in the entire resonator cross section is close to threshold (see § 2.4) and the amplitude perturbations are therefore small.

APPROVED FOR RELEASE: 2007/02/09: CIA-RDP82-00850R000500010010-4

APPROVED FOR RELEASE: 2007/02/09: CIA-RDP82-00850R000500010010-4

The most widespread source of first-order wave aberrations (the optical wedge) is nonparallelness of the mirrors. In this case, for the two dimensional (strip) resonator

$$F(x) - 1 = \exp\left(i\frac{2\pi}{\lambda}2\varepsilon x\right) - 1 \approx i\frac{2\pi}{\lambda}2\varepsilon x$$

(ε is the angle between the mirrors). The perturbation operator is antisymmetric; accordingly, a_{mk} with odd $|m - k|$ are not equal to zero. A simple analysis shows that with an increase in the misalignment angle ε, the center of gravity of the field distribution shifts monotonically in the direction of more remote edges of the mirrors (the opposite conclusion in the monograph [3] is based on inaccuracy in the discussion). In particular, the expression for the eigenfunction of the lowest mode has the form $u_0' \approx u_0 + 4\frac{a\varepsilon}{\lambda}Nu_1$ ([97]; (Figure 2.20, a). In accordance with this expression, the fundamental mode turns out to be noticeably deformed even for extremely small misalignment angles. When ε reaches a value of $\lambda/4aN$, the angular divergence of the emission of the fundamental mode is approximately doubled [103]; the perturbation theory itself simultaneously ceases to be applicable for description of this mode.

Inasmuch as $\delta_m' \sim (m + 1)^2$, with a decrease in the transverse index the deformations of the modes of oscillations decrease sharply. Therefore, in the usual multimode regime, the total magnitude of the angular divergence turns out to be appreciably less sensitive to misalignments than the fundamental mode field configuration.

More detailed information about the field structure and the diffraction losses in resonators with flat misaligned mirrors can be found, for example, in [79, 80, 99, 102, 104-106]. In the last of the above-enumerated articles, the corresponding results were obtained by the Vaynshteyn method in analytical form. It it noteworthy that in accordance with the data of [102], with an increase in the angle of misalignment, the diffraction losses increase most rapidly for the lowest order modes (that is, with the least number of field distribution "nodes"). As a result, the curves on the graph representing the losses of different modes as a function of the misalignment angle intersect (Figure 2.21).

Analogous intersection of the curves was also observed in reference [107] when performing the calculations (by the iteration method) for a flat cavity with large irregular aberrations caused by thermal deformation of the active element in imperfect illumination systems. This fact demonstrated that in the case of resonators with large diffraction losses efforts to classify the modes by the magnitude of these losses can lead to complete confusion; we shall discuss an example of such confusion in § 3.3.

The properties of a flat cavity are also of interest in the presence of second-order aberrations (slightly concave or convex mirrors, small thermal lens, and so on). In the case of a strip resonator the perturbation operator with second-order aberrations has the form $F(x) - 1 \approx i\frac{2\pi}{\lambda}2h(x/a)^2$, where h is the difference in the distances between mirrors at the edge and in the center of the resonator (Figure 2.20, b, c). The operator is symmetric, $u_0' \approx u_0 - 0.6(h/\lambda)Nu_2$ [97].

APPROVED FOR RELEASE: 2007/02/09: CIA-RDP82-00850R000500010010-4

APPROVED FOR RELEASE: 2007/02/09: CIA-RDP82-00850R000500010010-4

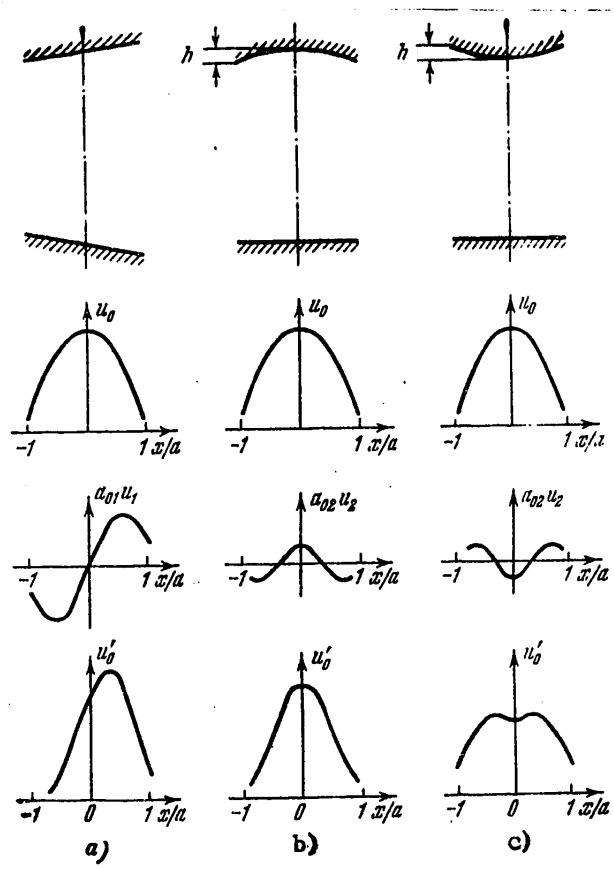

Figure 2.20. Effect of phase aberrations on the lowest mode field distribution: a) mirror misalignment; b) concave mirrors; c) convex mirrors.

For $h < 0$ (the mirrors are concave) the lowest mode field naturally is concentrated near the resonator axis ($a_{02} > 0$, see Figure 2.20, b). The diffraction losses decrease in this case [102, 104]. For deflections $|h| \gtrsim \lambda/10N$ in order to find the distribution in the fundamental mode usually it is quite possible to use the results of stable resonator theory.

For $h > 0$ (convex mirrors), the field distribution with respect to resonator cross section becomes more uniform (Figure 2.20, c); the diffraction losses increase sharply.

Now we see how the lowest mode fields vary in the presence of amplitude aberrations. The source of amplitude aberrations is nonuniform distribution of the inverse population or losses with respect to the resonator cross section. Kuznetsova [108] demonstrated that for amplitude aberrations a diffraction "makeup" of the zones with small inversion (or large losses) with radiation from the region in which the gain predominates over the losses takes place. As a result, the equiphasal surface begins to be distorted and even for the lowest mode the emission divergence can differ noticeably from the diffraction limit.

APPROVED FOR RELEASE: 2007/02/09: CIA-RDP82-00850R000500010010-4

APPROVED FOR RELEASE: 2007/02/09: CIA-RDP82-00850R000500010010-4

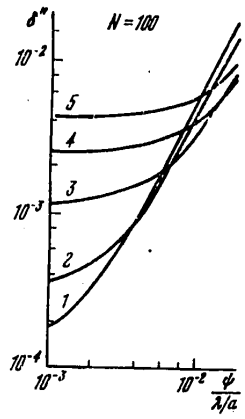

Figure 2.21. Diffraction losses in the resonator with circular flat mirrors of radius a as a function of the misalignment angle ψ [10]]: 1 — TEM_{00}, 2 — TEM_{01}, 3 — TEM_{11}, 4 — TEM_{21}, 5 — TEM_{31}.

It is of interest that the nonuniformity of distribution of the inverse population can lead to the presence not only of amplitude but also phase aberrations. Thus, if lasing is realized on frequencies noticeably distant from the center of the luminescent line, the phenomenon of anomalous dispersion begins to be felt (see, for example, [109]). As a result, the index of refraction turns out to depend on the magnitude of the inverse population; for frequencies in different directions from the center of the line, the variations of the index of refraction are opposite with respect to sign.

The same perturbation theory helps to understand the mechanism of the influence of amplitude aberrations, just as phase aberrations. The value of F - 1 defining the matrix elements of the perturbation operator is in the general case equal to [97]

$$\exp\underset{(a)}{(k_{yc}l)}(1-\rho)\exp\left[i\left(\eta k_{yc}l+\frac{4\pi}{\lambda}\Delta L\right)\right]-1\approx$$
$$\approx k_{yc}l-\rho+i\left(\eta k_{yc}l+\frac{4\pi}{\lambda}\Delta L\right),$$

Key: a, gain

where ρ is the total losses (including losses to passage through the mirrors), ΔL is the variations in optical length of the resonator as a result of phase distortions not connected with inverse population, $\eta k_{gain}\ell$ are the phase distortions as

APPROVED FOR RELEASE: 2007/02/09: CIA-RDP82-00850R000500010010-4

APPROVED FOR RELEASE: 2007/02/09: CIA-RDP82-00850R000500010010-4

a result of the presence of anomalous dispersion of the active medium.[1] For uniform Lorentian broadening $\eta = 2(\nu - \nu_0)/\Delta\nu_\ell$, where ν and ν_0 are the operating frequency and the frequency in the center of the luminescence lines, respectively, $\Delta\nu_\ell$ is the halfwidth of the luminescence line (see, for example, [109]).

If the phase aberrations are absent and the only source of perturbations is nonuniformity of distribution of k_{gain} and ρ with respect to the resonator cross section ($\eta = 0$), the matrix elements of the perturbation operator are real. Here the coefficients a_{mk}, just as $\beta_m - \beta_k$, turn out to be almost purely imaginary values (see (13)). For this reason the amplitude aberrations lead first of all not to amplitude, but to phase distortions of the eigenfunctions.

Within the framework of the first approximation of perturbation theory it is also possible to find the self-consistent solutions for the lasing regime using one lowest mode [97]. The reason for the nonuniformity of distribution of the inverse population in this case is the presence of a nonuniform lasing field itself. The corresponding analysis shows that for small phase aberrations of the type of a negative lens (convex mirrors), the range of pumping intensities for which the unimodal regime is stable expands by comparison with the case where the aberrations are absent (or, all the more, have opposite sign). This is also understandable: the volume of the lowest mode increases (see Figure 2.20), and it "burns up" the inverse population more uniformly with respect to the resonator cross section.

Flat Cavities with Aberrations of Significant Magnitude. Let us proceed to the cases where the modes of oscillations of a resonator with aberrations have so little in common with the modes of oscillations of an ideal empty resonator that it is necessary to forget perturbation theory. Thus, especially for small amounts of excess over the lasing threshold, the situation is widespread where emission of individual modes is not distributed over the entire resonator cross section but localized in a small zone of it. In the already mentioned papers by Kuznetsova [108], a study is made of the case where this situation is caused by sharp nonuniformity of distribution of the gain which for the greater part of the cross section is appreciably less than the threshold value and exceeds the latter only in a small segment where the lasing field is located. With sufficiently removed edges of the mirrors from this section, the diffraction on these edges can be neglected, which was done in [108]. Let us note that on the basis of the given model in [112] it was possible to explain some of the experimentally observed peculiarities of the energy characteristics of lasers with nonuniform pumping.

Soskin and Kravchenko [113, 80], using a model of a resonator with "stepped" mirrors, investigated the case where such localization was caused not by amplitude aberrations, but phase aberrations. For phase distortions of a random nature, the emission can turn out to be concentrated in several separate segments of the cross section (like "local stable resonators"); as a result of the presence of

---

[1] Generally speaking, the index of refraction depends on the degree of excitation of the active medium not only as a result of anomalous dispersion. In particular, for neodymium glass it is more important that the atoms in the ground and excited states have different polarizability [110]; the same effect is described for the case of a ruby, for example, in [111].

APPROVED FOR RELEASE: 2007/02/09: CIA-RDP82-00850R000500010010-4

APPROVED FOR RELEASE: 2007/02/09: CIA-RDP82-00850R000500010010-4

exponentially decreasing distribution "tails" a weak diffraction relation is realized between the segments. Using the given model, it is possible to explain a number of phenomena observed near the lasing threshold. However, when the threshold is exceeded little, the laser emission intensity distribution inevitably becomes much more uniform (as a result of the "equalizing" effect of the nonuniformity of the gain distribution induced by the lasing field). The experimental data mentioned in § 2.3 [58, 59, 62] also indicate that with intense pumping the emission of individual modes, although it has small-scale amplitude modulation, is distributed in practice over the entire operating cross section (in the sometimes observed intensity spikes -- filaments -- a negligible fraction of the total emission flux is concentrated). Therefore the models, the basis for which are the concepts of localization of the field in individual segments of the cross section, are unsuitable as a rule for estimating the angular divergence of the emission in ordinary lasing modes.

Efforts at strict investigation of the general case of arbitrary phase aberrations when considering the mutual effect of the distributions of the laser emission and inverse population on each other lead to extraordinarily awkward constructions. Therefore it turns out to be expedient to do away with the details of the inverse population distribution and only consider that, to a significant degree as a result of the effect of this distribution on the emission field the lasing is realized predominately in modes with maximum volume. In this way it is possible to obtain comparatively simple formulas which correspond to the experimentally observed laws to estimate the angular divergence of the laser emission as a whole. Let us present such formulas for two extreme cases -- where the source of the phase aberrations is dispersion of light on microinhomogeneities and where a slowly varying gradient of the index of refraction with respect to cross section exists. The most successful method of considering the effect of the randomly arranged small scale inhomogeneities was proposed in 1968 by Lyubimov [114], who made a large contribution to the development of the theory of empty resonators with phase aberrations. This method is based on the concept of the mode of oscillations of a real system as a complicated complex characterized by a single frequency which is a superposition of many modes of an ideal resonator with randomly distributed amplitudes and phases. The relation between individual modes is realized as a result of light dispersion; inasmuch as it is quite weak, the complex can include only modes with initial frequencies that do not differ too much. The estimates made by Lyubimov for the spectral width of the range in which these frequencies lie lead to the following resultant formula for the angular aperture θ of the emission of such complexes: $\theta \approx \rho_{disp}^{1/4}\sqrt{\lambda/L_{equiv}}$ [115].

The experimental data of [26, 115] pertaining to a fluorite and samarium laser where the macroinhomogeneities are absent and there is "pure" light dispersion on the microinhomogeneities (perceived as a halo when observing a point source of light through a crystal), at least do not contradict this formula. It is, however, necessary to exercise known caution with regard to the formula inasmuch as certain assumptions which are far from always justifiable were used in its derivation. In particular, it was assumed that the width of the light dispersion index is less than the width of the angular distribution of the lasing beam formulated in the presence of light dispersion. The following is also doubtful: the presence of a noticeable light dispersion leads to a sharp increase in angular divergence of the radiation, already not very small, in flat cavities with large N. The cause of

APPROVED FOR RELEASE: 2007/02/09: CIA-RDP82-00850R000500010010-4

APPROVED FOR RELEASE: 2007/02/09: CIA-RDP82-00850R000500010010-4

the light dispersion can be not only microinhomogeneities. Thus, sometimes an effort is made to use metal reflectors with a large number of small apertures as semitransparent mirrors for lasers in the far infrared range (see § 4.2). Diffraction in the aperture system leads to the appearance of a significant amount of scattered light, which in turn, causes the most undesirable consequences from the point of view of divergence of the emission [116].

Now let us proceed to the most important and widespread case where the optical length of the resonator varies slowly with respect to its cross section. The cause of this can be macroinhomogeneities of the active element, thermal deformations, errors in making the mirrors, and so on. This problem was investigated most comprehensively for arbitrary deformations equal to the wavelength with respect to order of magnitude in reference [117]. The authors use the following approach, the mathematical aspect of which will not be discussed. By solving the corresponding differential equation of the field for each of the waves traveling to the edge of the resonator, superposition of which forms a transverse mode, an equiphasal surface is constructed. According to the optical-geometric approximation, the normal to this surface at each point determines the direction of the emission originating from the given point (in § 1.1 in the example of a spherical wave front we saw that for deflections of $\sim\lambda$ the emission divergence can be completely estimated by this method). The resultant formula for the maximum angle between the direction of emission and the resonator axis has the form

$$\alpha_{max} = \{[2h/l + (\nabla h)^2/12]_{max} - [2h/l + (\nabla h)^2/12]_{min}\}^{1/2},$$

where h are the variations of optical length of the resonator caused by mirror distortions (the index of refraction of the medium was considered equal to one). If h varies within the limits of the cross section so slowly that it is possible to neglect the terms $(\nabla h)^2/12$, the formula acquires the form $\alpha_{max} = \sqrt{2\Delta\ell/\ell}$, where $\Delta\ell$ is the total variation of the optical length in the working cross section.

In the same paper [117], it was pointed out that terms with $(\nabla h)^2$ vanish pletely when the mirrors are flat and parallel, and variations of the optical length are caused by dependence of the index of refraction on the transverse coordinate (hence, it is clear what type of errors can occur as a result of "displacement" of the optical inhomogeneities along the resonator length). In this case the formula for the divergence can be derived by a very simple method. Actually, let us trace the trajectory of a beam multiply reflected from flat mirrors and gradually intersecting layers with different index of refraction as it moves across the resonator axis. Variations of the angle α' between the beam and the axis in this case are caused exclusively by the refraction at the boundaries between the layers and can be calculated directly by the sine theorem $\sin(\pi/2 - \alpha'_1)/\sin(\pi/2 - \alpha'_2) = n_2/n_1$, where α'_1 and α'_2 are values of α' in layers with index of refraction n_1 and n_2, respectively. Using $\alpha' \ll 1$, we obtain $(\alpha'_2)^2 - (\alpha'_1)^2 = 2(n_2/n_1 - 1)$. Now it remains only to consider that the mode encompassing the entire lasing region corresponds to a family of beams intersecting this entire region. Hence, it follows directly that in one of the segments of the cross section the angle α' reaches at least a value of $\alpha'_{max} = \sqrt{2\Delta n/n}$, where n is the total variation of the index of refraction within the limits of the lasting zone. Inasmuch as the angle in outer space α is related to α' by the expression $\alpha = n\alpha'$, we arrive at the final formula $\alpha_{max} = \sqrt{2n\Delta n}$.

APPROVED FOR RELEASE: 2007/02/09: CIA-RDP82-00850R000500010010-4

APPROVED FOR RELEASE: 2007/02/09: CIA-RDP82-00850R000500010010-4

Let us note that five years later another method of deriving the same formula based on similar arguments was published in [118] (instead of the sine theorem, the standard equation of a beam trajectory in a nonuniform medium borrowed from [119] was used).

It is time to sum up our investigation. The following fact is most remarkable. In flat cavities, as a result of the effect of multiple passage of the light through the same large-scale optical inhomogeneity, the resultant distortions of the wave front of the steady-state oscillations usually greatly exceed the distortions acquired on one pass. In particular, this pertains to cases where the magnitude of the aberrations in one pass is small, and the characteristic transverse dimensions of the optical inhomogeneities, on the contrary, are large. Actually, the variation of the optical length $\Delta\ell$ in the characteristic dimension b in the final analysis causes, as we have seen, deviation of the direction of the emission from axial by the amount $\sqrt{2\Delta\ell/\ell}$. At the same time, the deviation of the beam direction in one pass (that is, in the amplifying mode) is $\Delta\ell/b$; the ratio of these two values is $\sqrt{2b^2/\ell\Delta\ell}$

As a result, the "sensitivity" of a flat cavity to small phase aberrations turns out to be extremely high. Comparison of the formulas presented in this and the preceding section shows that for $\Delta\ell \sim \lambda$ the divergence of the emission of individual modes exceeds the divergence which would occur in the absence of aberrations as a result of multimodality of the lasing.

Thus, the theoretical elements, just as the set of experimental data (§2.3), indicate that in the overwhelming majority of cases the primary cause of comparatively large divergence of the emission of lasers with flat cavities is not multimodality of lasing, but deformation of the modes under the effect of intraresonator wave aberrations.

Section 2.6. Methods of Angle Selection of Emission

In this section an analysis will be made of the efforts to decrease the divergence of laser radiation with planar or stable resonators (or resonators similar to them; see below) which have been built at different times and with varying degrees of success. The majority of these methods are now only of historic interest; however, some of them are used even today.

Attempts to Solve the Problem of Divergence on the Basis of Resonators with Small Diffraction Losses. In a number of papers a study has been made of the possibility of creating resonators from mirrors with aspherical surface, the shape of which is selected in such a way that the diffraction losses in the lowest mode are just as small as for stable resonators, but they increase with the transverse index faster than for stable resonators. This theoretically facilitates the achievement of unimodal oscillation. Some systems of this type are presented in Figure 2.22.

The resonators depicted in Figure 2.22,a,b, were made from dihedral reflectors, the angle between the flat faces of which is $\pi - \alpha$ in the former case, and $\pi/2 - \alpha$ in the latter case ($\alpha \ll 1$). The effect of the first type of reflector on a narrow light beam to a certain extent is similar to the effect of a concave mirror; some "fine focusing" of the beam is realized. The reflector of the second type only adds "inversion" of the beam cross section to this effect; therefore resonators of these two types are equivalent to each other in the absence of aberrations. It is possible to see that the transverse dimensions of the light beams corresponding to individual transverse modes increase in them with the transverse index faster than in stable

APPROVED FOR RELEASE: 2007/02/09: CIA-RDP82-00850R000500010010-4

APPROVED FOR RELEASE: 2007/02/09: CIA-RDP82-00850R000500010010-4

resonators, which ensures greater selectivity for reflectors of finite dimensions. The properties of these resonators are described in more detail in [120, 121].

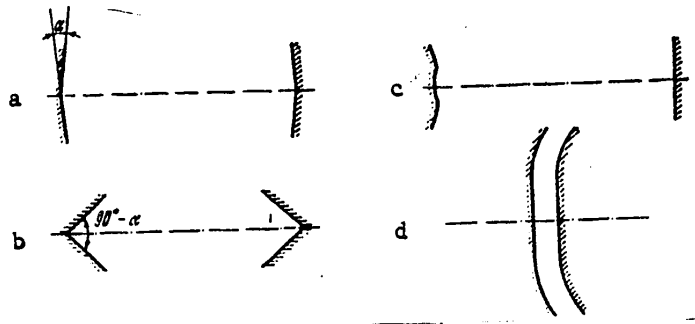

Figure 2.22. Some types of resonators with aspherical mirrors: a, b--resonators with dihedral reflectors [120, 121]; c--resonator with central "indentation" [122]; d--resonator proposed in [123].

Figure 2.22, c, depicts a resonator in which the eigenvalue spectrum is still more radically rarefied. The dimensions of the central section of the left-hand reflector--the "indentation"--can be taken so that they will be equal to the dimensions of the basic mode spot formed by this section and the right-hand mirror of a stable resonator. Then the losses of this mode will be small; broader beams corresponding to other modes will go beyond the limits of the central section and scatter quickly in the peripheral part of the resonator. This must lead to significant increase in the losses.

At first glance it may seem that an analogous effect is achieved by simple irising of the stable resonator. However, in the latter case as we have seen in Sections 2.1, 2.2, the high-order mode field begins to be confined inside the resonator by edge diffraction (the edge of the iris has the same effect on the light beam as the edge of a mirror); in the resonator depicted in Figure 2.22, c, the diffraction on the edge of the "indentation" turns out to be significantly attenuated as a result of the presence of halation. Vaynshteyn [3] indicated the possibility of using a similar procedure; the effort at practical implementation in the optical range (in the example of a helium-neon laser) is described in [122].

Sometimes proposals for a different plan are encountered in the literature. Thus, in [123] the properties of the resonator depicted in Figure 2.22, d, were analyzed. With a strictly defined form of the components of its reflectors, the equation for finding the natural oscillations has only one solution. However, in [123] a study was made only of the equation of an empty resonator made up of infinite mirrors; consideration of the edge effects and the introduction of an active medium should change the situation sharply--nothing may remain of "unimodality." In addition to everything else it is unclear how such reflectors would be made with the precision required in the optical range.

In contrast to the last-mentioned version, the possibility of using the resonators depicted in Figure 2.22, a-c, is unquestioned. However, they are all characterized by the same deficiency as the ordinary stable resonator itself: under

APPROVED FOR RELEASE: 2007/02/09: CIA-RDP82-00850R000500010010-4

APPROVED FOR RELEASE: 2007/02/09: CIA-RDP82-00850R000500010010-4

conditions of unimodal oscillation it is possible to make effective use of only a very small volume of the optically uniform medium (it is sufficient to point out that in the mentioned experimental work [122] the depth of the "indentation" was ~λ/10). Therefore the devices with aspherical reflectors are not able to compete with the stable resonators which are simple to make and align.

It must be noted that for cross section dimensions of the active medium not exceeding several millimeters, unimodal oscillation can be achieved using both stable and planar resonators. In particular, it is appropriate to note the successful method of empirical selection of the optimal parameters of the resonator near the "stability" boundary used for the first time in [124] and also used successfully in a number of subsequent experiments. The method is based on the application of a combination of plane and concave spherical mirrors, the distance between which L varies near a value equal to the radius of curvature of the concave mirror R. For L = R (or in the case of the presence of an active element of length ℓ with an index of refraction n_0, for $L_{equiv} = L - \ell(1 - 1/n_0) = R$) a so-called semiconcentric resonator is realized which is equivalent to the planar resonator and thus is at the "stability" limit (Section 1.2). For shorter lengths, the resonator is stable; it is important that for L ≈ R small variations in the distance between the mirrors lead, as it is easy to see, to significant simultaneous variation of the diffraction losses and spot dimensions of the fundamental and other transverse modes. This makes it easy to select the optimal combination of them from the point of view of the output characteristics of the laser. Obviously, when this choice is made empirically, the "lenticularness" of the sample is automatically taken into account if it exists, and so on.

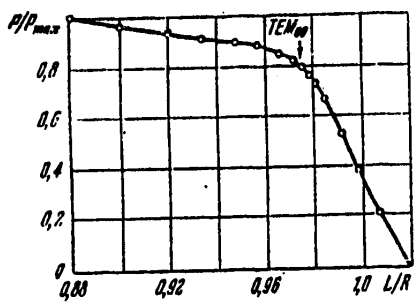

Figure 2.23. Results of experiments in oscillation selection in a resonator close to a semiconcentric resonator [128].

Figure 2.23 shows a standard graph for use of the indicated method borrowed from [28], where this method is discussed in great detail. The graph was obtained in experiments with a helium-neon laser; the ratio L/R is plotted along the x-axis, the line L/R = 1 is the "stability" limit. On approaching it from the left, the diffraction losses increase, the total oscillation power P decreases slowly, then the number of transverse modes present in the oscillations are reduced. At the point noted by the arrow, only the lowest mode TEM_{00} remains. The resonator length corresponding to this point can also be considered optimal: further movement toward the stability limit and transition to the region of instability

APPROVED FOR RELEASE: 2007/02/09: CIA-RDP82-00850R000500010010-4

APPROVED FOR RELEASE: 2007/02/09: CIA-RDP82-00850R000500010010-4

located to the right causes only a sharp decrease in power and then cessation of oscillation.

All of this is good, however, only in the case of lasers with small cross sections of the active medium for which the problem of radiation divergence in general is not acute. As for the lasers of primary interest to us which have a large exit aperture, for them the application of stable resonators leads, as has already been noted more than once, to oscillation on higher-order modes with a broad radiation pattern. Nevertheless, efforts have been renewed many times to solve the problem of divergence even in this case. In Chapter 5 there is a brief discussion of the conversion of light beams corresponding to the high-order modes to narrowly directional light beams by the methods of holographic correction. A search was also conducted for simpler methods; from the work in this direction there are some interesting papers (for example, [125]), but their practical significance is low. Therefore hereafter we shall limit ourselves to the investigation of the methods of angular selection (decreasing the angular divergence of the radiation) in planar resonators which has received significant development in its time.

Lasers With Planar Resonators and Angle Selectors. For constriction of the radiation pattern of a laser with planar resonator it is necessary in the general case also to decrease the number of modes in which lasing is realized and, what is usually even more important, the deformations of these modes. The number of modes is determined primarily by the ratio between the diffraction and nonselective losses. Therefore for angular selection in the hypothetical case of an ideally uniform medium where the mode deformations are small, it is necessary to try to increase the differences of the diffraction losses.

In the presence of aberrations of any type, the most important problem turns out to be decreasing the mode deformations; in accordance with perturbation theory (Section 2.5), for this purpose it is necessary to increase the differences of the eigenvalues of the operator $\hat{P}$, including the phase corrections.

Making this remark of a general nature, let us proceed with investigation of the specific methods of angular selection.

In order to obtain the desired effect usually additional elements called angle selectors are introduced into the resonator. They are essentially filters, the transmission of which depends sharply on the direction of propagation of the radiation. Historically, the first type of angle selector was a system of two confocal lenses and an iris with small aperture placed at their common focal point [126, 127]. A concentric resonator with an iris in the central plane [128, 129] (Figure 2.24, b) is entirely identical to a planar resonator with such a selector (Figure 2.24, a). The operating principle of such a selector is obvious. Instead of an iris a passive shutter can be used: part that clears first then acts as an iris aperture [130].

The effect of the selector based on the Fabry and Perot etalon [131, 132] is based on the fact that the transmission of the etalon depends not only on the

APPROVED FOR RELEASE: 2007/02/09: CIA-RDP82-00850R000500010010-4

APPROVED FOR RELEASE: 2007/02/09: CIA-RDP82-00850R000500010010-4

wavelength, but also the direction of propagation of the radiation. Inasmuch as for inclined incidence of the beam, this relation becomes sharper, the etalon is installed at an angle to the resonator axis (Figure 2.24, c). For realization of angular selection in both directions it is necessary to use two etalons.

Probably the method of selection based on using the dependence of the reflection coefficient at the interface of two media on the angle of incidence had the greatest popularity. Near the critical angle of total internal reflection, the indicated relation is especially sharp; therefore these angles of incidence are used. In order to eliminate the selective effect it is possible to make the light undergo multiple reflections (Figure 2.24, d). In the 1960's a large number of versions of selectors of this type [133-140] grouped under the general heading of total internal reflection selectors were proposed.

Let us consider the mechanism of the effect of the selectors on the angular divergence. From very general arguments it is clear that the presence of a filter, the transmission of which depends on the direction of propagation of the radiation is primarily felt in the magnitude of the losses of individual transverse modes. The phase corrections are determined for fixed configuration of the resonator in practice only by the number of angles of distribution of the amplitude with respect to cross section (that is, the transverse mode index), and in the presence of a selector, they must vary insignificantly (see Section 2.2 for the similarity of phase corrections in open and closed resonators). The results of strict calculations [141] confirm this obvious conclusion.

Let us present the data for the idealized case of a Gaussian selector, the shape of the passband of which is intermediate between the shapes of the bands of real selectors presented in Figure 2.24, and it is described by the formula $g^2(\phi) = \exp[-(\phi/\Delta\phi)^2]$ (Figure 2.25; see [141]); ϕ is the angle between the direction of propagation of the radiation and the resonator axis; $\Delta\phi$ is the passband width, g^2 is the transmission with respect to intensity. If we consider that the transverse modes with the index m correspond to values of $\phi = \pm(m + 1)\theta_{diff}/2$ (see Sections 2.2, 1.1; $\theta_{diff} = \lambda/2a$), the magnitude of the losses introduced by the selector follow directly $\Delta(2\delta''_m) = (m + 1)^2(\theta_{diff}/2\Delta\phi)^2$ (this same result was obtained in [141] by a stricter procedure).

Let us now trace how the magnitude of the angular divergence of the radiation must vary with the passband width of the selector.

In the absence of aberrations the role of the selector reduces to variation of the conditions of competition of the modes (Section 2.4) by increasing the loss differences. The losses introduced by the Gaussian selector turn out to be greater than the diffraction losses in an ideal empty resonator on satisfaction of the condition $2\Delta\phi/\theta_{diff} < (a^2/\lambda L)^{3/4}$. Inasmuch as for lasers with large cross section $a^2/\lambda L = N >> 1$, the angular divergence in the given idealized case can decrease sharply even for comparatively greater width of the selector passband. Estimation shows that to achieve the unimodal conditions with an ideal active medium it is sufficient to use a selector with $\Delta\phi$ several times greater than $\theta_{diff}/2$.

APPROVED FOR RELEASE: 2007/02/09: CIA-RDP82-00850R000500010010-4

APPROVED FOR RELEASE: 2007/02/09: CIA-RDP82-00850R000500010010-4

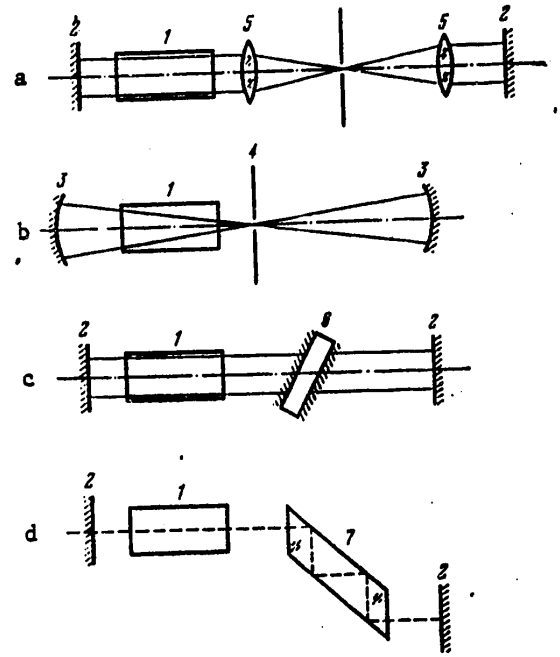

Figure 2.24. Diagrams of lasers with angle selectors: 1--active sample; 2--plane mirror; 3--spherical mirror; 4--iris with aperture; 5--lens; 6--Fabry and Perot etalon; 7--plane-parallel plate.

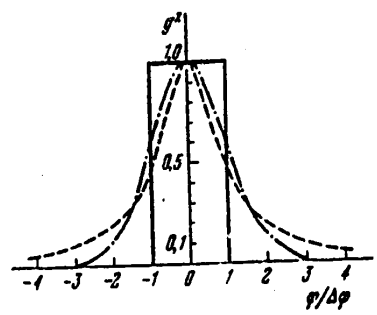

Figure 2.25. Shape of the passband of different angle selectors: Gaussian selector (dash-dot line), the selector based on the Fabry and Perot etalon (dotted line) and the ideal selector (solid line).

This possibility is based on the fact that the losses introduced by the given type of selector are even noticeable for $\phi \ll \Delta\phi$ (see Figure 2.25). Among real selectors, only the selector based on the Fabry and Perot etalon (see Figure 2.24, c) has this (quadratic) form of the function $g(\phi)$. The selectors with an opening (Figure 2.24, a, b) and the total internal reflection selectors (Figure

FOR OFFICIAL USE ONLY

APPROVED FOR RELEASE: 2007/02/09: CIA-RDP82-00850R000500010010-4

APPROVED FOR RELEASE: 2007/02/09: CIA-RDP82-00850R000500010010-4

2.24, d) have a passband with shape approaching a rectangle ("ideal" selectors according to the terminology of [141, 142]). In this case, just as should be expected, the presence of a selector is felt noticeably in the value of the losses only for the modes, the indices of which are close to the value of $2\Delta\phi/\theta_{diff}$ [141]; therefore the selectors of the given type can decrease the amount of angular divergence only to a value approximately equal to $\Delta\phi$.

In the presence of noticeable aberrations the basic function of the selector must be to decrease the deformations of the oscillation with the highest Q. Let us remember that the mode deformations themselves can be interpreted as the result of the presence of induced oscillations in the modes of an ideal resonator (see the preceding section). Beginning with this fact, it is easy to see that in order to decrease the mode deformations the losses introduced by the selector must turn out to be larger in magnitude not only than the diffraction losses, but also the phase corrections in the empty resonator. Hence, it follows that for noticeable aberrations (that is, in practice always) only selectors with sufficiently narrow passband, independently of its shape, can turn out to be useful.

When using angular selectors, just as in the case of angular selection by increasing the length of the resonator which will be considered a little later, not only the angular radiation characteristics are of interest, but also the energy characteristics of the radiation. The possibility of decreasing the width of the radiation pattern without significant gain in radiation power is connected with the magnitude and the nature of the aberrations. This relation is exhibited most clearly when investigating the shape of the scattering index of a coherent light beam.

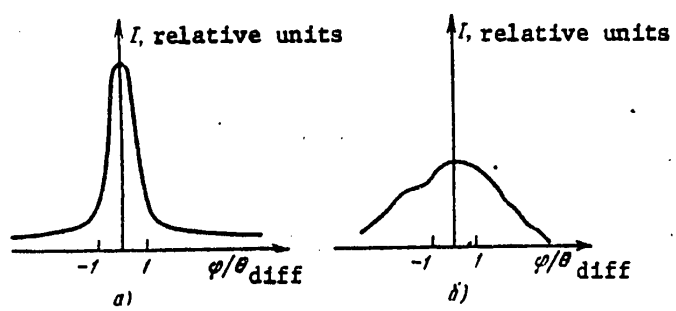

Figure 2.26. Radiation patterns after single passage of the light through the active medium: a--light dispersion on microinhomogeneities; b--low-order wave aberrations as a result of the presence of macroinhomogeneities.

Figure 2.26 contains a schematic representation of two radiation patterns of a light beam after single transmission through an active sample (at the entrance to the sample the wave front is planar). These patterns directly characterize the angular divergence of the beam at the exit from the laser system using the given sample as the final amplifier (of course, if a well-collimated beam is fed to its input).

FOR OFFICIAL USE ONLY

APPROVED FOR RELEASE: 2007/02/09: CIA-RDP82-00850R000500010010-4

APPROVED FOR RELEASE: 2007/02/09: CIA-RDP82-00850R000500010010-4

The first of them (Figure 2.26, a) pertains to the case of weak light dispersion on microinhomogeneities. The greater part of the energy of the light passing through the sample (on the order of $1 - \rho_{dis}$, the presence of secondary diffraction peaks is neglected) is concentrated in the central core having diffraction width. The remainder of the radiation is distributed in a comparatively wide range of angles.

Figure 2.26, b, corresponds to the presence of low-order wave aberrations (refraction on macroinhomogeneities). Primarily the most central core of the pattern expands, the axial luminous intensity decreases significantly. From the Rayleigh number it follows that the core width begins to exceed the diffraction limit noticeably when the aberrations exceed $\lambda/4$.

It is obvious that the effort to realize angular selection will lead to essentially different results in the cases of Figures 2.26, a, and 2.26, b. The light dispersion on the microinhomogeneities does not prevent achievement of the diffraction limit; the power of the generated radiation in this case, if the pumping intensity is sufficiently high, decreases insignificantly (the effective losses increase by approximately ρ_{dis} [26]). In the case of Figure 2.26, b, an effort to constrict the angular divergence to less than the width of the central core of the scattered light indicatrix is coupled with unavoidable significant energy losses.

The experimental data correspond quite well to the above-discussed arguments. First of all, it must be noted that when using all types of angle selectors a decrease in angular divergence and an increase in the axial luminous intensity were actually observed. Nevertheless, the angle selectors have not found broad application. The reason for this lies both with the high requirements on the precision of their manufacture and alignment and a number of specific deficiencies characteristic of each type of selector.

The basic deficiency of systems with an iris (see Figure 2.24, a, b) is undesirable concentration of the radiation in a small section of the cross section. In lasers of comparatively low power this leads to rupture of the diaphragm or electric breakdown near its surface (see, for example, [129]). Angle selection using the Fabry and Perot etalons is greatly complicated as a result of the presence of a large number of transmission peaks; therefore no one has followed the example of the authors of [131, 132] who were able to realize it in low-power ruby lasers. Only total internal reflection selectors have found some application in powerful pulsed lasers, but even they in the final analysis disappeared from the scene as a result of the extraordinary requirements on the precision of manufacture and alignment and also the degree of finish of the working surfaces.

Angle Selection of Emission of Lasers with Flat Cavities by Reducing the Number of Fresnel Zones. If we do away with angle selectors, it remains only to increase the selective properties of the planar resonator itself by decreasing the number of Fresnel zones N. This can be achieved by reducing the cross section or by increasing the length of the resonator.

APPROVED FOR RELEASE: 2007/02/09: CIA-RDP82-00850R000500010010-4

APPROVED FOR RELEASE: 2007/02/09: CIA-RDP82-00850R000500010010-4

A significant decrease in the active cross section by irising the resonator, of course, must lead to a corresponding drop in the output power, and therefore cannot be considered among the efficient selection procedures. Some movement in this direction is still possible. The fact is that a light beam always broadens somewhat on passage through a planar resonator (as a result, diffraction losses appear). If we use an exit mirror with cross section only somewhat less than the cross section of the active element, the latter will still be completely filled by the irised beam. It only remains to use the radiation exiting from the laser through a narrow circular zone around the mirror as the useful signal along with the radiation passing through the semitransparent exit mirror. Thus, it is possible to decrease N somewhat, almost without relinquishing output power. This procedure was described for the first time in [143]; the name of diffraction yield of radiation was attached to it. The same method was used with slight modifications in [144]; the given direction reached a logical conclusion in the laser described by Kalinin et al., the reflection coefficient of the exit mirror of which decreased smoothly from the center to the periphery [145]. In all of the enumerated cases, just as should be expected, an increase in the degree of directionality and a decrease in the sensitivity to the misalignment of the mirrors were observed (as a result of a decrease in the total or effective size of the exit mirror), but with intense pumping the angular divergence significantly exceeded the diffraction limit.

Let us note that lasers with mirror transmission that is variable with respect to cross section are a clear example of systems having extraordinary dependence of the mode structure on the excitation conditions. In the case of uniform distribution of pumping slightly exceeding the lasing threshold, the field configuration of the individual types of oscillations will be close to the configuration predicted by the theory of the corresponding empty resonators [146]. If the amount the threshold is exceeded is large, then as a result of the competition of the transverse modes the distribution of the gain with respect to cross section approaches the loss distribution, and the structure of the individual modes will become similar to the structure in lasers with ordinary mirrors.

A much more radical decrease in N without reduction of the working volume can be achieved by a simple increase in the distance between mirrors. This method of angular selection is the most natural and, in addition, very effective: here, in contrast to the case of the application of angular selectors, not only the losses increase, but also the phase corrections, which leads to a rapid decrease in the mode deformation. In addition, it is simpler by far to vary the length of the resonator than to introduce a selector and change the passband width; therefore the given method of constricting the radiation pattern has been studied most systematically.

The most important result of numerous studies was solid establishment of the fact that on variation of L within very broad limits the angular divergence of the radiation varies with a high degree of accuracy proportionally to $L^{-1/2}$—indeed the theoretical estimates based on any models pertaining to mode deformations and to multimode oscillations (Sections 2.4, 2.5) lead to the same relation! This relation has been exemplified by lasers of the most varied types: a ruby laser (the resonator length was varied by approximately 15 times) [147],

FOR OFFICIAL USE ONLY

APPROVED FOR RELEASE: 2007/02/09: CIA-RDP82-00850R000500010010-4

APPROVED FOR RELEASE: 2007/02/09: CIA-RDP82-00850R000500010010-4

a neodymium glass laser (~15 times), a fluorite laser with samarium (~10^3 times) [26], and an alkyliodide molecule photodissociation laser (~30 times, [148]. The following is characteristic. If the medium has a comparatively high amount of optical nonuniformity, increasing the length of the resonator above some limit is accompanied by quite rapid decrease in power to complete cessation of oscillation, although it may still be far to diffraction divergence. As a result, the axial luminous intensity, initially increasing with resonator length, goes through a peak, the position and height of which depend on the degree of optical nonuniformity of the medium. This fact was noted for the first time by Sventsitskaya and Khazov in [147] (in this paper, the method of representing data on the angular distribution of radiation in the form of the dependence of the proportion of the beam energy included inside the axial cone on the angle at the apex of this cone, see Figure 4.4, 4.7, which has acquired deserved popularity was introduced). It is of interest that when the sharp lasing power drop begins, the angular divergence begins to decrease with an increase in L even faster than $L^{-1/2}$ [148]. This is explained by the fact that as a result of a sharp increase in the threshold, the lasing begins to be localized in individual sections of the cross section with the largest gradient of the index of refraction [147, 148]--the "effective" value of Δn decreases.

As the optical uniformity of the medium increases, it is possible to come closer and closer to diffraction divergence without noticeable loss of power (it is true in this case the requirements on the necessary precision of alignment of the resonator increase). Finally, when the medium is so uniform that $\Delta L < \lambda/4$, the diffraction limit can be reached. For this purpose the distance between the mirrors must be usually so large that N exceeds 1 somewhat. Herein lies the basic deficiency of the given selection method: for lasers in the visible range even with diameters of the active elements only 5-8 mm, the required resonator length is several meters. If we consider that for maintenance of the same N the length must increase proportionately to the square of the linear dimensions of the working cross section, it becomes clear that in the case of powerful lasers it is entirely unreasonable to solve the problem by a simple increase in distance between the mirrors. It is also necessary to consider that for short lasing pulses long length of the resonator is in general unacceptable inasmuch as the pulse development time increases together with the length.

The way out of the indicated difficulty consists in using resonators that have short actual length, but equivalent to the planar resonator with small N. This method of angular selection is of definite interest not only from the practical point of view, but also from the procedural point of view; therefore let us discuss it in somewhat more detail.

Flat Cavities of Large Effective Length. In Figure 2.27 several versions of devices of this type are presented. The first of them was used to decrease the angular divergence in 1963 [149], but correct notions of its properties were still not developed at that time. Using the methods discussed in Section 1.2, the corresponding analysis will be performed without special difficulty. However, we shall not consider the beam matrices of these resonators as a whole, but we shall use a more obvious procedure which will also be useful hereafter to consider unstable resonators.

APPROVED FOR RELEASE: 2007/02/09: CIA-RDP82-00850R000500010010-4

APPROVED FOR RELEASE: 2007/02/09: CIA-RDP82-00850R000500010010-4

A common characteristic of all resonators equivalent to the planar resonator (including the ones depicted in the figure) is the fact that in the geometric approximation all of the beams normal to the surface of one of the terminal mirrors, on passing through the resonator, are incident normally on the surface of the second terminal mirror and follow back along the same path. Accordingly, such resonators can be broken down entirely into sections, each of which is bounded by a pair of parallel planes or concentric spheres. The boundaries of the edge sections are the terminal mirrors themselves; the intermediate thin lenses can be considered, as usual, phase correctors, passing through which leads only to the corresponding change in curvature of the wave front (see Figure 2.27).

The result of passage of the light through these sections in the wave approximation can be calculated by using the apparatus of beam matrices or directly from the Huygens-Fresnel principle. Here it is expedient to give the distributions of the complex amplitude directly on the surfaces bounding the sections and in dimensionless coordinates r/a, where $2a$ is the difference between the edge beams in the geometric approximation (thus changing the scale on transition to the sections with another beam cross section). Then it is possible to arrive at the following simple laws.

On passage through a type I section (plane boundaries) $2a$ wide and L long, the complex distribution of the amplitude is transformed just as on passage through a section of the same type $2a_0$ wide and $L_{eff} = La_0^2/a^2$ long (this is understandable--the number of Fresnel zones N is the same in them). The passage through the type II section with light beam width in the geometric approximation at the entrance and exit surfaces $2a_1$ and $2a_2$ is equivalent to passing through a type I section of width $2a_0$ and length $L_{eff} = La_0^2/a_1a_2$; as a result of variation of the cross section, only an additional amplitude factor a_1/a_2 is acquired (see also (1.23)); the general phase multiplier $\exp(ikL)$ plays no special role in our investigation.

By this procedure, the passage through all of the type I and II sections reduces to passage through the corresponding distances of type I sections of the same width $2a_0$. Inasmuch as passage through several such sections, in turn, is equivalent to passage through a section of total length, the L_{eff} defined in this way for all type I and II sections can be simply added.

It is easy to demonstrate that passage through the type III sections with entrance and exit widths of $2a_1$ and $2a_2$ is equivalent to returning a distance $L_{eff} = La_0^2/a_1a_2$ in a type I section; inversion of the beam and variation of the amplitude in the ratio a_1/a_2 also occur. Therefore the effective lengths of the type III sections are subtracted from the total sum (the growth of the angular divergence of the radiation caused by this on introduction of the type III section into the system was observed experimentally, and it was explained in [115]). If we also consider the extraordinary energy concentration at the constriction points, it becomes obvious that the presence of such sections inside the resonator, as a rule, is undesirable.*

* In powerful amplifiers, on the contrary, such sections then called "optical relays" sometimes are specially introduced, for a decrease in L_{eff} helps to prevent self-focusing [330].

APPROVED FOR RELEASE: 2007/02/09: CIA-RDP82-00850R000500010010-4

APPROVED FOR RELEASE: 2007/02/09: CIA-RDP82-00850R000500010010-4

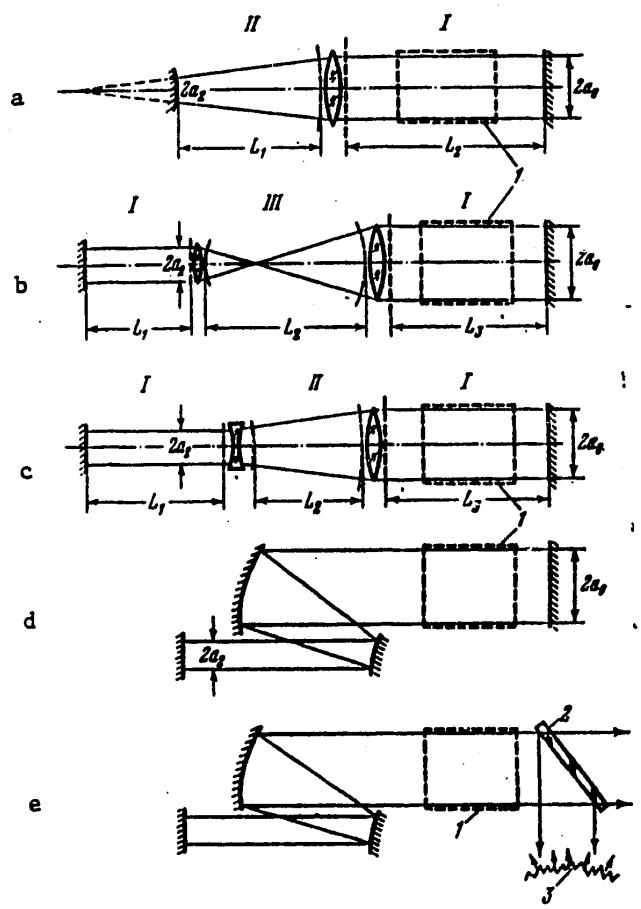

Figure 2.27. Resonators with long effective length: a--resonator described in [149]; b-d--planar resonators with telescope located inside them; e--resonator with telescope and nonresonant feedback; 1--active element; 2--partially reflecting plate; 3--diffuser.

Thus, all of the systems depicted in Figure 2.27 are equivalent to planar resonators with easily calculated effective length (let us note that if such a resonator is used as the Fabry-Perot interferometer, the angular distance between rings in it will be determined by this effective length). For the case of Figure 2.27, a, L_{eff} is equal to $L_2a_0/a_2 + L_1$; for Figure 2.27, b, $L_3 - L_2a_0/a_2 + L_1a_0^2/a_2^2$; for Figure 2.27, c, $L_3 + L_2a_0/a_2 + L_1a_0^2/a_2^2$. The width of the equivalent resonator $2a_0$ is selected in all cases equal to the beam width on the extreme right section where the active medium must be placed. It is obvious that the presence of sections with small beam cross section leads to a sharp increase in the effective length; the effective value of the parameter N decreases correspondingly (in the case most advantageous from this point of view in Figure

APPROVED FOR RELEASE: 2007/02/09: CIA-RDP82-00850R000500010010-4

APPROVED FOR RELEASE: 2007/02/09: CIA-RDP82-00850R000500010010-4

2.27, c, it is $N_{eff} = [(\lambda L_3/a_0^2) + (\lambda L_2/a_0 a_2) + (\lambda L_1/a_2^2)]^{-1}$). If such a section occupies the greater part of the length of the system, the effective length of the resonator turns out to be significantly greater than the actual length, approximately in the ratio of a_0^2/a_2^2. This leads to a gain in the amount of the angular divergence by a_0/a_2 times (let us note that in the case of Figure 2.27, b, c, the ratio a_0/a_2 is equal to the multiplicity of the telescope formed by the lenses). In the final analysis this gain is achieved as a result of concentration of the entire light flux in small sections, but nevertheless the increase in the radiation density here is not so large as in the case of selectors with a diaphragm (Figure 2.24, a, b). In addition, for attenuation of this undesirable effect it is possible to use the fact that the radiation flux incident on a totally reflecting mirror of a planar resonator is less than the flux incident on the semitransparent exit mirror with reflection coefficient R' by $(R')^{-1/2}$ times (Section 1.4). Thus, in order to decrease the radiation flux in the sections with a small cross section it is sufficient to realize the energy yield from the opposite (right) end of the resonator. The reflection coefficient of the exit mirror R' must be selected as small as possible [148]. This choice becomes possible when using active media with sufficiently large amplification coefficient.

We have given so much attention to the methods of angle selection in lasers with planar resonator primarily because there are situations where it is not possible to get along without a planar resonator. Thus, pulsed lasers exist in which the excitation occurs nonsimultaneously in the different parts of the resonator cross section. In such cases the use of unstable resonators which are now a commonly recognized means of achieving small divergence is impossible--lasers with unstable resonators operate satisfactorily only under condition of simultaneous and not too nonuniform excitation of the entire operating volume. Planar resonators with small N can turn out to be more advantageous than unstable resonators also in the case of the presence of noticeable light dispersion with indicatrix of the type depicted in Figure 2.25, a--as we have seen, it does not prevent achievement of minimum divergence in planar resonators with large L (or L_{eff}), but can have a sharply negative effect on the parameters of lasers with unstable resonators (Section 4.1). For these reasons, both the system depicted in Figure 2.27, c, and the angle selection system entirely equivalent to it with a mirror telescope (Figure 2.27, d) proposed by one of the authors of [148]--Danilov--at the end of the 1960's are sometimes used at the present time. The version of such systems with nonresonant feedback [118] (Figure 2.27, e) which can be used for enormous amplification in the active medium is also of noticeable interest. The nonresonant coupling makes the laser in practice nonmisalignable and sharply increases the stability of its operation under the conditions of optical nonuniformities which are variable in time.

Multistage Lasers. There is another truly universal method of obtaining narrowly directional emission which, although it is not a resonator method, on the basis of its traditionalness it deserves mention in this chapter. This method consists in using a master oscillator and a number of subsequent amplification stages. The master oscillator can be low-power and have low efficiency, the achievement of unimodality under such conditions presents no difficulty. The emission of the laser is directed toward a telescopic system which increases the

APPROVED FOR RELEASE: 2007/02/09: CIA-RDP82-00850R000500010010-4

APPROVED FOR RELEASE: 2007/02/09: CIA-RDP82-00850R000500010010-4

light beam diameter and then, to amplification stages with gradually increasing cross section. Matching telescopes are again placed between the amplifying stages. Gradual expansion of the beam cross section theoretically also keeps the density of the amplified radiation at a level that is not too high and reduces angular divergence.

The use of almost all of the active material when operating in a purely amplifying mode has obvious advantages from the point of view of divergence of the radiation--indeed here there is no multiple transmission of light with respect to the same nonuniformity leading to accumulation of aberrations as in the planar resonator (Section 2.5). In spite of this fact, only powerful monopulse lasers, primarily solid-state lasers, are now being made multistage.

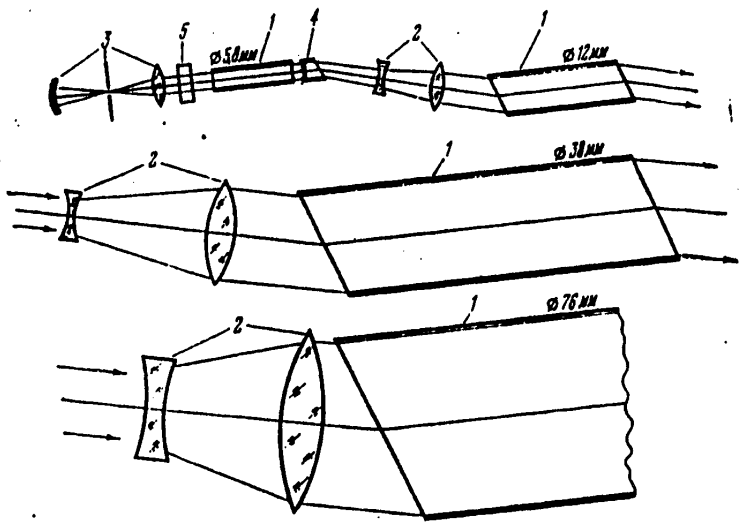

Figure 2.28. Example of a multistage system [129]: 1--active element; 2--telescopic system; 3--angle selector of the master oscillator with diamond diaphragm; 4--semitransparent mirror of the master oscillator based on a prism with Brewster angle; 5--shutter.

One of the first systems of this type assembled by the simplest "classical" system is depicted in Figure 2.28. Modern lasers for experiments in the field of laser thermonuclear fusion appear immeasurably more complex--they consist of a minimum of six parallel channels (for comprehensive illumination of the target), and they contain a truly enormous number of active rods, elements for splitting and reduction of the light beams, "decouplers" between the stages for separation of superluminescence, and so on. However, the main thing is that quite different factors determine the radiation divergence: as a result of extraordinarily high radiation density in the amplifying channel nonlinear processes develop leading to expansion of the radiation pattern and, in the final analysis, to self-focusing of the radiation inside the active material which is disastrous for such devices. Therefore the control of these processes acquires a decisive

APPROVED FOR RELEASE: 2007/02/09: CIA-RDP82-00850R000500010010-4

APPROVED FOR RELEASE: 2007/02/09: CIA-RDP82-00850R000500010010-4

role: In order that they not develop, the above-mentioned "optical relays" and other spatial filters are installed between the stages, which determines the angular divergence of the output radiation. Thus, the breakdown of the system into a set of stages here essentially pursues highly specific goals.

This situation is quite characteristic--the application of multistage devices turns out to be justified only in certain special cases and also when it is desirable to achieve record output parameters with universality of the device. Actually, in this way it is possible to obtain radiation density in the entire exit aperture close to the rupture threshold of the optical materials. The master oscillator is a small part of the system, and for mode changing it can simply be replaced by another one.

In the most frequently encountered cases where although not record, but very close to record parameters are required in combination with simplicity, modest size and weight characteristics, and so on, the lasers which are made with a single-oscillator system and one version or another of an unstable resonator take first position. We shall now proceed with a discussion of these lasers.

APPROVED FOR RELEASE: 2007/02/09: CIA-RDP82-00850R000500010010-4

APPROVED FOR RELEASE: 2007/02/09: CIA-RDP82-00850R000500010010-4

Chapter 3. Elements of the Theory of Unstable Resonators

Section 3.1. Some Initial Information

Brief Historical Survey. In 1965 the article by Siegman [4] was published which established the beginning of the entire field of quantum electronics. This article discussed the possibility of the practical application of unstable resonators with large diffraction losses.

At that time the idea that resonators with large diffraction losses must have high selective properties began to win general recognition. This was promoted to a high degree by the explanation of the nature of multimode lasing presented by Tang and Statz (Section 2.4), from which it followed that in order to decrease the number of simultaneously excited transverse modes it is necessary to increase the differences of the diffraction losses (and not their ratios as was first assumed). The loss differences can be large obviously only when the losses themselves are large.

It was known that the transition from stable resonators to planar resonators is accompanied not only by an increase in volume of the lowest modes, but also an increase in the diffraction loss differences; both promote the achievement of lasing on a small number of the lowest transverse modes. The results of a few theoretical works (for example, [104]) also indicated that on passing through the stability limit and proceeding deep into the instability region the losses of the lowest mode continued to increase; this made it possible to hope that the losses of the other modes grow still more rapidly, and the selective properties of the resonator improve.

However, the transition to the instability region must, it would appear, also be accompanied by highly undesirable phenomena, above all, an increase in the threshold and corresponding reduction of the lasing power. In addition, numerical calculations have demonstrated that as a result of the growth of the field amplitude on the edge of the resonator and amplification of the edge diffraction the field distribution in the resonators with weakly convex mirrors is much more "cut up" than in the planar ones. What happens with field distribution with an increase in the curvature of the convex mirrors was unclear; by analogy with the planar misaligned resonator it seemed that it should become entirely unfavorable.

The results of the individual experiments in which variation of the parameters of the resonators near the stability limit was realized were not at all hopeful. Thus, in [150] when going into the instability region, a sharp decrease in the

APPROVED FOR RELEASE: 2007/02/09: CIA-RDP82-00850R000500010010-4

APPROVED FOR RELEASE: 2007/02/09: CIA-RDP82-00850R000500010010-4

lasing power and an increase in the angular divergence of the radiation were observed. In [124] which was already referenced in Section 2.6, the transition to unstable resonators was accompanied only by a sharp decrease in the lasing power; the graph borrowed from [124, 28] and presented in Figure 2.23 could not point to the idea of the expediency of the application of unstable resonators with large diffraction losses.

Against this background Siegman's article stood out sharply. The precariousness of the basic objections to the application of unstable resonators with large losses was demonstrated in it. The primary point of the paper was investigation of them in the geometric approximation. It led to results already known to us according to Section 1.2--a set of two spherical waves propagated in opposite directions converting into each other on reflection from the end mirrors can be found in an unstable resonator. The geometric investigation was strengthened by a very important argument that with large losses the influence of the edge diffraction can turn out to be weak, and the strict solution will differ little from the geometric solution. The fact is that although the peripheral part of the light beam is sharply disturbed by diffraction, as a result of significant expansion of the beam cross section on passing through the resonator, it then passes by the mirrors and the field distribution in them has little distortion. Running somewhat ahead, we see that the situation in reality turned out to be not so simple; the conditions under which edge diffraction does not play a special role and lasing is realized in a single transverse mode well described by the geometric approximation were finally discovered only in 1971 [151]. We shall discuss this in more detail in Section 3.3.

Siegman also pointed out that in the case of unstable resonators with large diffraction losses it is expedient to realize diffraction output of the radiation, that is, use that part of the beam which bypasses the exit mirror as the useful signal (see also Section 2.6). Here it is possible to replace the semitransparent exit mirror by a totally reflecting one, thus leaving the total losses and the lasing threshold on the same level as in planar resonators. The adoption of these measures should help to avoid a sharp drop in the radiation power which previously appeared to be unavoidable.

Of course, all of these arguments needed comprehensive checking. It was even unclear whether the unstable resonators with large diffraction losses are actually selective; Siegman himself stated the fear that the losses for the lowest and subsequent modes in such systems turn out to be approximately identical. Finally, the problem of sensitivity of the field distribution to the effect of intraresonator aberrations which is decisive for the problem of angular divergence of the radiation (see Chapter 2) is in general not discussed in this or all subsequent papers by Siegman. It was investigated in 1968-1970 [152, 153]; it was only after this that the advantages of the unstable resonators with large diffraction losses in narrowly directional lasers were clearly recognized.

Elementary Examination of the Ideal Unstable Resonator. Let us proceed with a systematic study of the properties of unstable resonators. First we shall perform an analysis within the framework of the simplest optical-geometric approximation: then it will be obvious that as applied to resonators of the given class frequently more precise determination of the conditions of achieving unimodal lasing is left to diffraction theory.

APPROVED FOR RELEASE: 2007/02/09: CIA-RDP82-00850R000500010010-4

APPROVED FOR RELEASE: 2007/02/09: CIA-RDP82-00850R000500010010-4

Let us begin with ideal resonators formed by spherical or flat, totally reflecting mirrors and having spherical interfaces between media with different indices of refraction (or a "lens-like" medium). Let us explain the meaning of the general solution of the geometric approximation found for such resonators in §1.2 in the specific example of the resonator depicted in Figure 3.1, a, consisting of two flat mirrors and a lens with focal length f placed between them. Inasmuch as this resonator consists of a total of three simplest elements, it is possible not to resort to the formal apparatus of beam matrices and find the solution by the more graphic method first used in [4].

As a result of incidence of a spherical wave on a mirror, a reflected spherical wave is produced, the center of curvature of which is located at a point which is the image of the center of curvature of the incident wave. Therefore two spherical waves propagated in opposite directions make the transition into each other after reflection from the end mirrors under the condition of mutual reflection of the centers of their curvature O_1 and O_2. In the given case these conditions have the form (see Figure 3.1, a, b)

$$\frac{1}{l_1+x}+\frac{1}{l_2-y}=\frac{1}{f},\qquad \frac{1}{l_2+y}+\frac{1}{l_1-x}=\frac{1}{f}. \tag{1}$$

The solution of the system leads to the expressions

$$x_{1,2}=\pm\sqrt{\frac{l_1-f}{l_2-f}[l_1l_2-f(l_1+l_2)]},\quad y_{1,2}=\frac{l_2-f}{l_1-f}x_{1,2}.$$

If one of the inequalities $f<\ell_1\ell_2/(\ell_1+\ell_2)$ or $\ell_1<f<\ell_2$ is satisfied (for determinacy we shall consider $\ell_1<\ell_2$), then the values of $x_{1,2}$ and $y_{1,2}$ are real, and the resonator is unstable.

The path of the beams for the case of $0<f<\ell_1\ell_2/(\ell_1+\ell_2)$ is presented in Fig 3.1, a, b, and for the case of $f<0$ (a scattering lens), in Figure 3.1, c. The first solution (x and y are positive) corresponds to the beam path indicated by the solid arrows, and the second solution, directly opposite (the dotted arrows).

Let us first consider the solution describing a spherical wave, the cross section of which expands on passage through the resonator; from the figure it is obvious that this is the first solution. For the first solution the coordinate of each beam on the path from the mirror 1 to mirror 2 varies in the ratio

$\frac{l_1+x_1}{x_1}\frac{-y_1}{l_2-y_1}\equiv M'$; from mirror 2 to mirror 1, in the ratio $\frac{l_2+y_1}{y_1}\frac{-x_1}{l_1-x_1}\equiv M''$.

The values of M' and M'' are negative in the given case inasmuch as the transverse coordinate changes sign on intersection of the beam with the axis. After final passage through the resonator in both directions the coordinate turns out to be multiplied by $M'M''\equiv M$, where $M=\frac{1+\sqrt{1-f^2/(l_1-f)(l_2-f)}}{1-\sqrt{1-f^2/(l_1-f)(l_2-f)}}$.

APPROVED FOR RELEASE: 2007/02/09: CIA-RDP82-00850R000500010010-4

APPROVED FOR RELEASE: 2007/02/09: CIA-RDP82-00850R000500010010-4

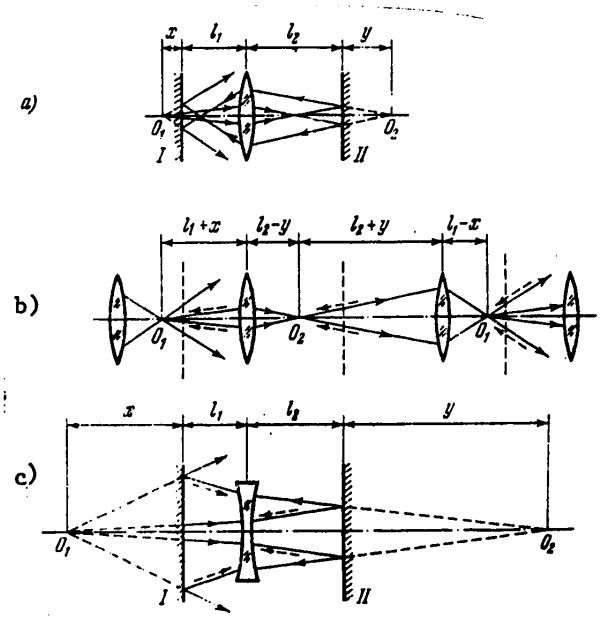

Figure 3.1. Path of beams in an unstable resonator made of two flat mirrors (I and II) and a lens: a) resonator with positive lens; b) its equivalent diagram; c) resonator with negative lens. The solid arrows indicate the first solution (a basic diverging wave), the dotted arrows indicated the second solution (a converging wave).

The parameter M which will hereafter be called the magnification of the resonator is already known to use from §1.2: this is a larger value of μ with respect to absolute magnitude. In both cases depicted in Figure 3.1 M is positive (for the resonator in Figure 3.1, c, M', M''>0). However, there are also resonators with negative M -- after a full round trip in both directions the beam turns out to be on the other side of the axis (see, for example, Figure 3.3, b, c).

Thus, as a result of complete passage through the resonator from one end mirror to the other and back, the transverse dimensions of the cross sections of one of the two possible beams with reproducible curvature of the wave front increased by $|M|>1$ time. It is easy to see that the cross section of this beam increases as much not only in the mirror planes, but also along the entire length of the resonator. Thus, the emission density inside the resonator decreases by $|M|$ times for the two-dimensional case (a cylindrical wave) and by M^2 times for the three-dimensional case (a spherical wave). In the case of multiple passage through the resonator the beam cross section naturally does not grow without limit, but it turns out to be bounded as a result of finiteness of the mirror dimensions for other resonator elements playing the role of aperture diaphragms. Here part of the emission exits from the resonator. The emission flux inside the system decreases together with its density after each complete pass by $|M|$ or M^2 times.

APPROVED FOR RELEASE: 2007/02/09: CIA-RDP82-00850R000500010010-4

APPROVED FOR RELEASE: 2007/02/09: CIA-RDP82-00850R000500010010-4

It is noteworthy that the magnitude of the relative losses equal to $1-1/|M|$ or $1-1/M^2$ is entirely determined by the resonator configuration, that is, in the given case, by the values of ℓ_1, ℓ_2 and f. Only the place where the emission exits from the system depends on the transverse dimensions of the resonator elements, more precisely, their relation. Thus, if the lens is sufficiently large and the dimensions a_1 and a_2 of the mirrors 1 and 2 satisfy the inequality $|M'|a_1>a_2>a_1/|M''|$, the emission exits partially from both sides: the fraction of the beam cross section equal to $a_2/|M'|a_1$ hits mirror 2, and the fraction equal to $a_1/|M''|a_2$ hits mirror 1 (Figure 3.2, a). If one of the mirrors covers the entire radiation flux propagated in its direction, the emission exits only from the opposite end of the resonator (Figure 3.2, b).

Now let us return to the second solution of system (1). We shall hereafter call the wave corresponding to it converging: on passage through the resonator its cross section does not increase, but decreases by the same $|M|$ times. If the resonator is not excited from any external source, this decrease takes place without limit. Thus, after passing through the resonator, the converging wave is reconstructed only with respect to curvature, but not with respect to radiation distribution, and it is impossible to use it to construct the steady-state field distribution in the geometric approximation.

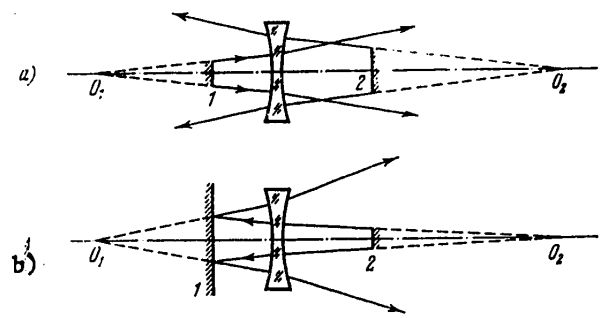

Figure 3.2. Diffraction emission output: a) two-way, b) one-way

Generally speaking in the example of resonators with stable configuration it is known that in itself the absence of a solution in the geometric approximation still does not mean that there is no solution when considering the diffraction effects. In some phase of the beam constriction, apparently equilibrium can occur between the focusing effect of the resonator and the defocusing influence of the diffraction (see §2.1). However, in the given case this possibility is excluded: in contrast to a stable resonator, an unstable one has defined focusing properties only with respect to a converging wave of geometric approximation. The smallest departures from it (in particular, caused by diffraction) lead to fast defocusing, the beam expands and gradually becomes a stable diverging wave corresponding to the first solution of system (1). At the end of this section such processes will be considered in more detail.

From §2.1, we already know that the enumerated laws occur not only in the investigated specific case, but also for any unstable resonators. It is always possible to compile and solve a system of equations analogous to (1) (for multielement

APPROVED FOR RELEASE: 2007/02/09: CIA-RDP82-00850R000500010010-4

APPROVED FOR RELEASE: 2007/02/09: CIA-RDP82-00850R000500010010-4

resonators this is conveniently done by the beam matrix method; the solutions have the form of (1.22) in the general case). One of the system solutions leads to an unstable converging wave, and the other, to a stable diverging wave which in essence describes the field distribution of the fundamental resonator mode.

In particular, two-mirror resonators turn out to be unstable if one of the inequalities $(1-\ell/R_1)(1-\ell/R_2)>1$ or $(1-\ell/R_1)(1-\ell/R_2)<0$ is satisfied, where R1 and R_2 are the radii of curvature of the mirrors, ℓ is the distance between them. The formulas for the magnification M and position of the centers of curvature of the diverging and converging wave are in the general case awkward; let us present information only about certain types of resonators which have found or can find application (Figure 3.3).

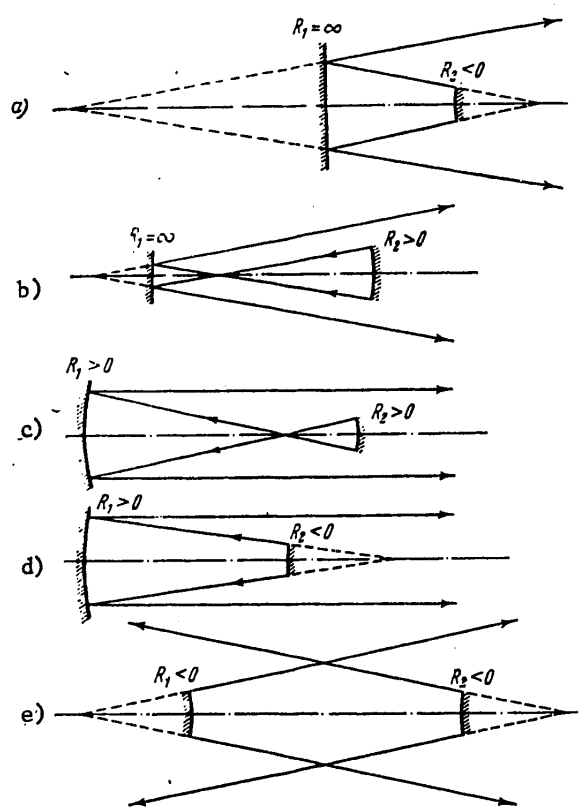

Figure 3.3. Diagrams of unstable resonators: a) resonator made of flat and convex mirrors; b) resonator made of flat and concave mirrors ($\ell>R_2$); c) asymmetric confocal resonator made of concave mirrors; d) confocal resonator made of concave and convex mirrors (telescopic resonator); e) symmetric resonator made of convex mirrors

APPROVED FOR RELEASE: 2007/02/09: CIA-RDP82-00850R000500010010-4

APPROVED FOR RELEASE: 2007/02/09: CIA-RDP82-00850R000500010010-4

If one of the mirrors is flat ($R_1=\infty$), the center of curvature of the diverging wave moving in the direction of the other mirror is located at a distance $\sqrt{\ell^2-\ell R_2}+\ell$ from it; $M=(\sqrt{\ell^2-\ell R_2}+\ell)/(\sqrt{\ell^2-\ell R_2}-\ell)$. For $R_2<0$ (the mirror is convex), the centers of both waves are located outside the cavity (Figure 3.3, a). For $R_2>0$ (the mirror is concave) and $\ell>R_2$, the resonator is also unstable; one of the centers is located inside the resonator (Figure 3.3, b).

The asymmetric confocal systems ($R_1+R_2=2\ell$, $R_1\neq R_2$ are interesting versions of unstable resonators; for determinacy we shall consider $R_1>R_2$). Both the confocal resonator made of concave mirrors ($R_1>R_2>0$; Figure 3.3, c) and the resonator made of concave and convex mirrors usually called telescopic [153] ($R_1>0$, $R_2<0$; Figure 3.3, d). In both cases $M=-R_1/R_2$; the wave propagated in the direction of the second mirror is plane.

For obvious arguments in practical developments usually one-way output of the emission is used (Figure 3.3, a-d). However, the subject of the majority of articles on diffraction theory of empty unstable resonators is a symmetric system made up of two identical convex mirrors (Figure 3.3, e). In contrast to the notation introduced earlier for it, the magnification coefficient of the wave cross section on passage through the resonator in one direction is called the magnification coefficient (that is, $M'=M''\equiv M$ instead of $M'M''\equiv M$). It turns out to be possible to limit ourselves to investigation of this system as a result of the fact that passage through it in one direction is entirely equivalent to passage through any resonator with one-way output and the same values of the parameters M, N_{equiv} in both directions (for the definition of N_{equiv} see §3.2). One such resonator with one-way output equivalent to that depicted in Figure 3.3, e is, as is easy to see, the resonator of halflength made by the diagram in Figure 3.3, a, and having identical convex mirror. Thus, for the case of Figure 3.3, e

$$M=\frac{\sqrt{l^2/4-lR/2}+l/2}{\sqrt{l^2/4-lR/2}-l/2}=\frac{\sqrt{l^2+2l|R|}+l}{\sqrt{l^2+2l|R|}-l},$$

and the center of the diverging wave is located at a distance $x=(1/2)(\sqrt{\ell^2+2\ell|R|}-\ell)$ from the near mirror.

Properties of Convergent Waves. Let us discuss another peculiarity of unstable resonators very important to their practical applications. In real devices there are almost always certain sources of light dispersion (for example, interfaces). If they generate a converging (or close to it) wave even with negligibly small initial intensity, frequently this is sufficient for sharp alteration of the field structure. This phenomenon was observed for the first time in [153]; it was demonstrated there that it can be explained beginning with the laws of evolution of light beams during multiple passage through a resonator, and these laws have been derived for the special case of a telescopic resonator. Let us consider them, limiting ourselves just as in [153], to spherical waves, the centers of which are located on the system axis; these include the converging and diverging waves.

Let us begin with the geometric approximation. Let the curvatures of the diverging and converging waves in an arbitrary reference plane inside an unstable resonator

APPROVED FOR RELEASE: 2007/02/09: CIA-RDP82-00850R000500010010-4

APPROVED FOR RELEASE: 2007/02/09: CIA-RDP82-00850R000500010010-4

be equal to $1/\rho_p \equiv c_p$ and $1/\rho_c \equiv c_c$, respectively. A resonator with magnification M can be both a linear and a ring cavity. Knowing c_p, c_c and M, it is easy to construct the beam matrix describing a complete round trip through the resonator beginning with the indicated reference plane (and ending, of course, with it). Actually, inasmuch as a beam with the coordinate x and the slope α_x belongs to a family of wave beams of the indicated class with curvature $c=\alpha_x/x$, the conversion laws of arbitrary x and c have the form (see §1.2)

$$x_N = Ax_{N-1} + Bc_{N-1}x_{N-1}, \quad c_N x_N = Cx_{N-1} + Dc_{N-1}x_{N-1},$$

or

$$\frac{x_N}{x_{N-1}} = A + Bc_{N-1}, \quad c_N = \frac{C + Dc_{N-1}}{A + Bc_{N-1}}, \tag{2}$$

where x_{N-1}, c_{N-1}, x_N, c_N are beam parameters before and after the N-th pass through the resonator.

The curvature of the diverging wave remains as before on passage through the resonator, and the coordinates of each beam are multiplied by M; thus,

$$A + Bc_p = M; \quad \frac{C + Dc_p}{A + Bc_p} = c_p, \text{ or } C + Dc_p = Mc_p.$$

For converging wave, in the same way we obtain $A+Bc_c=1/M$, $C+Dc_c=c_c/M$. The solution of these four equations with respect to A, B, C, D leads to the formulas

$$A = \frac{(c_p/M) - Mc_c}{c_p - c_c}, \quad B = \frac{M - 1/M}{c_p - c_c}, \quad C = -c_p c_c B,$$
$$D = \frac{Mc_p - c_c/M}{c_p - c_c}.$$

Substituting them in (2) and introducing $q \equiv (c-c_p)/(c-c_c)$, it is possible to see the validity of the following recurrent relations:

$$x_N/x_{N-1} = M(1 - q_N)/(1 - q_{N-1}), \; q_N = q_{N-1}/M^2.$$

Hence, we have the desired formulas describing the variations in the transverse cross directional dimensions and curvatures after N complete passes through the cavity:

$$x_N/x_0 = M^N(1 - q_N)/(1 - q_0), \; q_N = q_0/M^{2N}. \tag{3}$$

From these formulas it follows that when $c_0 \neq c_c$, c_p the parameter q is finite and decreases quickly; as it decreases the wave approaches a diverging wave (q=0). Waves close to converging have large initial $|q_0|$; when $|q|$ exceeds $|M|$, the wave cross section decreases on the next pass through the resonator. Sooner or later $|q|$ becomes less than $|M|$, and the cross section begins to increase.

APPROVED FOR RELEASE: 2007/02/09: CIA-RDP82-00850R000500010010-4

APPROVED FOR RELEASE: 2007/02/09: CIA-RDP82-00850R000500010010-4

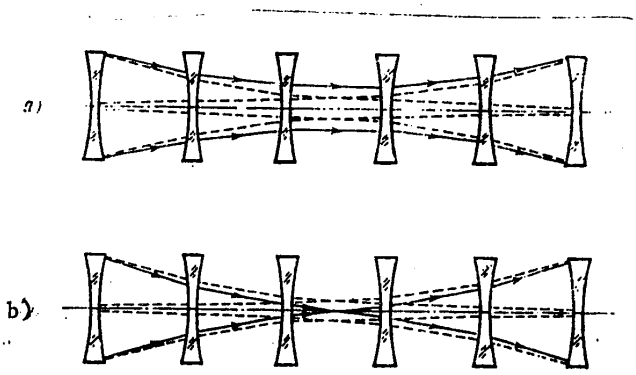

Figure 3.4. Passage of spherical waves close to a converging wave through a symmetric resonator made of convex mirrors along the equivalent optical line

As an illustration of what has been said we can use Figure 3.4 in which passage of light beams along the optical line equivalent to a symmetric unstable resonator made of convex mirrors is depicted. The beam path for converging and diverging waves is plotted with a dotted line; the solid lines pertain to waves close to converging with large positive (a) and negative (b) values q_0. At first the wave with negative values of q_0 is constricted even faster than a converging wave, but after several passes it is focused at a point and then diverges rapidly (x changes sign after focusing).

From the figure it is clear that if for any reason a wave close to a converging wave arises in the resonator, for example, as a result of light dispersion, then for several first passes the scattered emission forming it remains entirely inside the resonator. The number of these passes N_0 can be determined from the condition $|x_{N_0}/x_0|=1$ and for large $|q_0|$ the number of passes $N_0 \sim \ln|q_0|/\ln|M|$. In this time the flux density of the emission belonging to the main diverging wave decreases by $M^{2N_0}=q_0^2$ times; as a result, the relative intensity of the scattered light increases correspondingly*.

These estimates made within the framework of the geometric approximation indicate that as c_0-c_c decreases, the role of the scattered emission in unstable resonators increases rapidly. For $c_0=c_c$ it is necessary to use the diffraction approximation: the geometric approximation predicts an infinitely long process of contraction of the beam in this case and is obviously meaningless.

Let us consider the evolution of a converging wave in the diffraction approximation in the example of the telescopic resonator depicted in Figure 3.3, d;

---

*In the presence of an excited active medium this light is amplified not only with respect to relative intensity, but also with respect to absolute intensity.

APPROVED FOR RELEASE: 2007/02/09: CIA-RDP82-00850R000500010010-4

APPROVED FOR RELEASE: 2007/02/09: CIA-RDP82-00850R000500010010-4

for this purpose it is most convenient to use the effective length method discussed in §2.6.

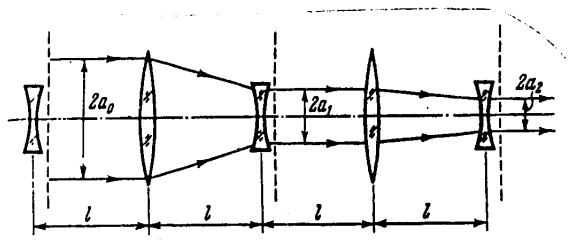

Figure 3.5. Passage of a converging wave through the optical line equivalent to a telescopic resonator. The dotted lines separate the segments of the line, each of which corresponds to a complete pass through the resonator in both directions.

The process of propagating a converging wave generated near a convex mirror of a telescopic resonator is analogous to the process of passage of a parallel light beam through an optical line depicted in Figure 3.5. The segments of the line, each of which corresponds to a signal pass through the resonator are separated from each other by dotted lines; the solid lines indicate the path of the beams in the geometric approximation.

In the first segment the complex amplitude distribution in dimensionless transverse coordinates is transformed just as when traveling the distance $\ell+\ell a_0^2/a_0a_1=\ell(1+M)$ in empty space (see §2.6; ℓ is half the length of the segment, equal to the cavity length); in the second segment the transformation is like traveling the distance $(\ell a_0^2/a_1^2)+\ell a_0^2/a_1a_2=\ell(M^2+M^3)$, and so on. Thus, traveling through the resonator N times corresponds to $L_{eff}=\ell(1+M+M^2+\ldots+M^{2N-1})=\ell(M^{2N}-1)/(M-1)$. On such a path in empty space the cross sectional dimension of the beam would increase as a result of diffraction convergence from the initial value of $2a_0$ approximately to $2a_0+(\lambda/2a_0)L_{eff}=2a_0+(\lambda\ell/2a_0)(M^{2N}-1)/(M-1)$.

For transition from empty space to the case of interest to us it is necessary to consider that in calculations with L_{eff}, the scale of the transverse distribution varies proportionately to the width of the parallel beam in the geometric approximation. After traveling N elements of the line, the width decreases by M^N times. Thus, the true size of the spot after the converging wave travels through the resonator N times is $2a_N=\frac{1}{M^N}[2a_0+(\lambda l/2a_0)(M^{2N}-1)/(M-1)]$.

For the usually satisfied condition $4a_0^2(M-1)/\lambda\ell>>1$, the number of passes N_0, after which the cross section of the converging wave passing through the constriction stage, expands as a result of diffraction and reaches the former dimensions of $2a_0$, is equal to $N_0\sim\ell n[4a_0^2(M-1)/\lambda\ell]/\ell nM$; in this time the emission density of the diverging wave decreases by $M^{2N_0}=[4a_0^2(M-1)/\lambda\ell]^2$ times. For real lasers, M^{2N_0} can reach extremely large value; thus, for the neodymium glass laser described in [153] with a rod diameter of 45 mm, this value was more than 10^6. Therefore it is no surprise that the presence of a converging wave even with very small initial intensity can change the operating conditions of the laser as a whole sharply.

APPROVED FOR RELEASE: 2007/02/09: CIA-RDP82-00850R000500010010-4

APPROVED FOR RELEASE: 2007/02/09: CIA-RDP82-00850R000500010010-4

Hereafter, we shall become familiar with the consequences to which the formation of a converging wave leads as a result of edge diffraction (§3.3) or as a result of partial reflection of light from the interfaces inside the resonator (§4.1).

It remains only to estimate for what departures from the converging wave it becomes possible to use the formulas of the geometric approximation (3). Obviously, for this purpose it is necessary that it be possible to replace the diffraction divergence by geometric when analyzing passage of a beam through an optical line. In §1.1 it was demonstrated that the geometric divergence predominates over diffraction even when the deflection of the spherical wave front is $\sim\lambda/2$, which corresponds to curvature of the front of $\sim\lambda/a_0^2$. Thus, for a telescopic resonator the geometric investigation is valid for $|c_0|\gtrsim\lambda/a_0^2$. In the general case of an arbitrary unstable resonator this condition acquires the form $|c_0-c_c|\gtrsim\lambda/a_0^2$; hence, it follows that the diffraction approximation is required only while the deviations of the scattered waves from converging are extremely small.

§3.2. Resonators with Slightly Inhomogeneous Medium

As has already been noted, the properties of real systems are determined not so much by how the field distribution looks in the ideal empty resonator as to what degree the given distribution is distorted in the presence of different types of disturbances. Later it will be demonstrated that unstable resonators differ advantageously from flat cavities in this respect.

From the general arguments it follows that the presence of nonuniformities of the medium of the type of an optical wedge or a small lens must play a significantly smaller role in unstable resonators than in flat cavities. Actually, in the case of spherical mirrors the presence of an optical wedge only leads to corresponding shift of the resonator axis. It is easy to see that a small nonuniformity in the medium of the lens type causes certain changes in the value of M and curvature of the wave leaving the resonator.

In the general case of a medium with an index of refraction that varies slowly with respect to volume, the laws are more complicated, but the "sensitivity" of unstable resonators to aberrations remains, as before, incomparably less than for flat cavities. In the final analysis this is connected with very fast establishment of the steady field distribution (let us remember that in the special case of spherical waves departures from the exact solution decrease by M^2 times with each pass through the resonator; see §3.1). It is obvious that if a spherical diverging wave of an ideal system is "released" into a resonator with slightly nonuniform medium, after several passes the solution in practice is established. Hence, it is obvious that in the case of unstable resonators the influence of inhomogeneity of the medium is accumulated over a countable number of passes, and therefore it is small.

Simplest Method of Accounting for Inhomogeneities of the Medium. For lasers that produce narrowly directional emission usually active media with minimal optical nonuniformities are used. In this case it is possible to use the especially graphic approach widely used during interferometric studies of slightly nonuniform media.

APPROVED FOR RELEASE: 2007/02/09: CIA-RDP82-00850R000500010010-4

APPROVED FOR RELEASE: 2007/02/09: CIA-RDP82-00850R000500010010-4

This method consists in the fact that the beam path is considered to coincide with the beam path with an ideally uniform medium, and the magnitude of the wave front distortion occurring as a result of nonuniformity of the distortion, is equal to the optical path difference by the corresponding trajectories. The given approach makes it possible easily to establish the fundamental qualitative [153] and quantitative [154] laws of the behavior of unstable resonators with slightly nonuniform medium.

Let us consider the passage of the basic diverging wave over an optical line equivalent to a telescopic resonator with active element made of a slightly nonuniform medium; this process is depicted in Figure 3.6, a. As is obvious from the figure, the radiation filling the entire cross section of the active element "spreads" before this from a small central segment of the cross section over the extent of several passes. The dimensions of this central segment of the cross section decrease on going away from the exit cross section in the geometric progression and they are quickly made sufficiently small that it is possible to neglect the wave aberrations within the limits of the cross section.

Hence, it follows that the accumulation of aberrations actually takes place here only for several passes. The number of passes making a noticeable contribution to the deformations of the established wave front decreases with an increase in multiplicity of the telescopic system M (or in the general case, with modulus M). If the nonuniformity of the medium reduces to the presence of a slowly varying gradient of the index of refraction (for example, as a result of thermal effects, see §5.1), the finite magnitude of the aberrations of the steady-state front can easily be found by simple summation; let us do this, finding the field distribution u(r) on the reference surface coinciding with an equiphasal surface of an ideal resonator. It is convenient to locate this surface, just as in §1.2, near the exit mirror; then u(r) describes the form of the wave leading the resonator directly. In the case of a telescopic resonator the reference surface is a plane (plotted in Figure 3.6 by the dotted line).

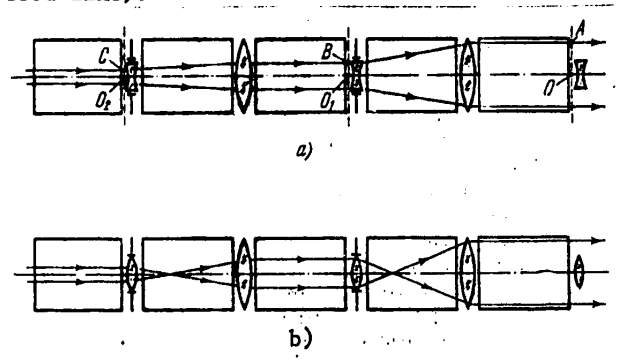

Figure 3.6. Passage of a diverging wave over optical lines equivalent to a telescopic (a) and asymmetric confocal resonator made of concave mirrors (b). The dotted lines indicate the reference planes.

APPROVED FOR RELEASE: 2007/02/09: CIA-RDP82-00850R000500010010-4

APPROVED FOR RELEASE: 2007/02/09: CIA-RDP82-00850R000500010010-4

In accordance with the adopted estimation procedure

$$u(r) \sim \exp\left\{i\frac{2\pi}{\lambda}\left[\int\limits_{ABC\ldots} n(s)\,ds - \int\limits_{OO_1O_2} n(s)\,ds\right]\right\}, \tag{4}$$

where n is the index of refraction of the medium; integration is carried out over the distance along the corresponding beam; thus, the expression in brackets is the difference of the optical paths with respect to the beam ABC ..., ending at the point A with transverse coordinate r and with respect to the beam OO_1O_2... traveling along the resonator axis occurring as a result of nonuniformity of the medium.

Let us introduce the path difference in one period of the equivalent diagram

$$\Delta L(r) = \int\limits_{AB} n(s)\,ds - \int\limits_{OO_1} n(s)\,ds$$

and the value

$$F(r) = \exp\left[i\frac{2\pi}{\lambda}\Delta L(r)\right]$$

(with a uniform medium $\Delta L(r) \equiv 0$, $F(r)=1$). Then considering that the coordinates of the points A, B, C ... are equal to r, r/M, r/M^2,..., it is possible to write (4) in the form

$$u(r) \sim \exp\left\{i\frac{2\pi}{\lambda}\left[\Delta L(r) + \Delta L\left(\frac{r}{M}\right) + \Delta L\left(\frac{r}{M^2}\right) + \ldots\right]\right\} = \\ = F(r)\,F\left(\frac{r}{M}\right)F\left(\frac{r}{M^2}\right)\cdots \tag{5}$$

With an increase in k the values of $\Delta L(r/M^k)$ approach zero, and $F(r/M^k)$, correspondingly, approaches one. Accordingly, the product in the righthand side of (5) approaches a defined limit which is the desired solution with unlimited increase in the number of terms.

Let us note that the introduction of the complex index of refraction permits unique consideration not only of the phase, but also amplitude distortions occurring as a result of nonuniform distribution of the gain. In addition, the value of F(r) can include factors that describe the nonuniform distribution of the reflection coefficient with respect to the mirror surface (see the following section).

Aberrational Coefficients. Let us use the above-discussed method for investigation of the case frequently encountered in practice where nonuniformities are distributed uniformly over the entire length of the resonator and n can be represented in the form $n(r)=n_0+n_1r+n_2r^2+\ldots$ Then

$$\Delta L(r) = L\left[n_1 r + n_2 r^2 + \ldots + \frac{1}{r - r/M}\int\limits_{r/M}^{r}(n_1 r' + n_2 r'^2 + \ldots)\,dr'\right] = \\ = L\sum_{k=1}^{\infty} n_k\left[1 + \frac{1}{k+1}\frac{M^{k+1}-1}{(M-1)M^k}\right]r^k.$$

APPROVED FOR RELEASE: 2007/02/09: CIA-RDP82-00850R000500010010-4

APPROVED FOR RELEASE: 2007/02/09: CIA-RDP82-00850R000500010010-4

In the brackets of the last expression the one corresponds to the half of the period of the equivalent diagram which the beam passes through, being parallel; the second term corresponds to the remaining half (cross section expansion phase).

Now let us calculate the sum $\Delta L(r)+\Delta L(r/M)+\ldots$ It is easy to see that for this, in the last formula it is sufficient to replace r^k by r^k на $r^k+\left(\frac{r}{M}\right)^k+\left(\frac{r}{M^2}\right)^k+\ldots=\frac{1}{1-1/M^k}r^k$. Thus,

$$\Delta L(r)+\Delta L\left(\frac{r}{M}\right)+\ldots=L\sum_{k=1}^{\infty}\alpha_k(M)\,n_k r^k,$$
$$\alpha_k(M)=\left[1+\frac{1}{k+1}\frac{M^{k+1}-1}{(M-1)M^k}\right]\frac{1}{1-1/M^k}. \tag{6}$$

The equivalent diagram of the unstable confocal resonator made of concave mirrors depicted in Figure 3.3, c is divided exactly the same into sections which the light beam passes through, being parallel and sections in which the beam coordinates vary by M times (Figure 3.6, b). Therefore for the given resonator all the above-presented calculations remain valid; formulas (6) are also valid (of course, under the condition of substitution of the corresponding, already negative values of M in them).

Let us remember that the wave front distortions which occur in the case of single passage of a parallel beam through the given medium are equal to $L\sum_{k=1}^{\infty}n_k r^k$. Hence, the meaning of the coefficients α_k figuring in (6) is clear. These coefficients will be called aberration coefficients hereafter: their values indicate how many times the given type of nonuniformity appears more strongly in unstable resonators than in single-pass amplifiers.

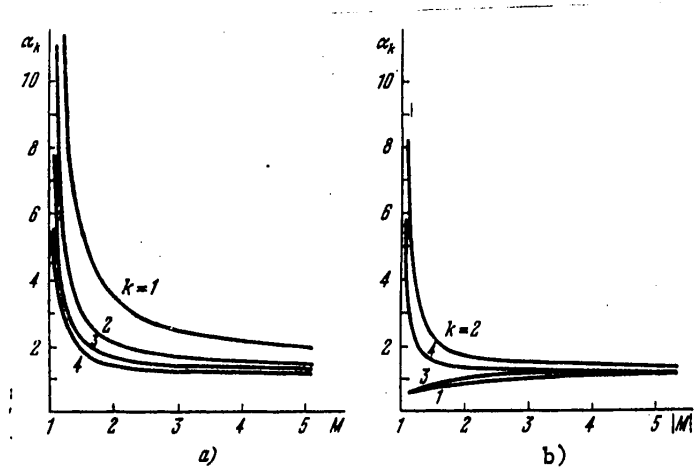

Figure 3.7. α_k as a function of M: a) theoretical resonator; b) asymmetric confocal resonator made of concave mirrors

APPROVED FOR RELEASE: 2007/02/09: CIA-RDP82-00850R000500010010-4

APPROVED FOR RELEASE: 2007/02/09: CIA-RDP82-00850R000500010010-4

The dependence of the first few α_k on the magnification M is presented in Fig 3.7. It is obvious that in the case of a telescopic resonator (M>1, Figure 3.7, a) all terms of the series (6) decrease monotonically. The nonuniformity of the type of an optical wedge is manifested comparatively strongly (k=1; first-order wave aberrations): for values of M=2 to 5 which are characteristic of many types of lasers (see Chapter 4), the beam at the exit from the resonator is deflected from its initial direction by an angle exceeding the angle of inclination by 3.5 to 2 times on a single pass through the introduced wedge. The effect of a nonuniformity of the lens type (k=2, second-order wave aberrations) in the same variation range of M turns out to be greater than in the case of a single-pass amplifier by only 2-1.5 times; higher-order wave aberrations are manifested still more weakly.

The confocal resonator made of concave mirrors (M<-1, Figure 3.7, b) is significantly less sensitive to the presence of odd-order wave aberrations than the telescopic resonator. For $|M|<3$, the beam direction at the output of this system turns out to be even more stable with respect to introduction of the wedge than in the amplifiers ($\alpha_1<1$). It is easy to see that the reason for this is "reversal" of the beam on passage of the period of the equivalent diagram, as a result of which each off-axis beam alternately passes through zones with larger and smaller index of refraction (Figure 3.6, b; we shall familiarize ourselves in more detail with phenomenona of this type in §3.5). The reaction to the fourth-order aberration on "reversal" of the beam does not change, and therefore remains approximately the same as in a telescopic resonator (a small difference arises as a result of half the equivalent diagram period in which broadening of the beam cross section takes place).

Inasmuch as in the case of the most frequently used telescopic resonator all the aberration coefficients α_k decrease monotonically with an increase in M, the angular divergence of the emission in this case decreases as a rule. However, if the series $\Sigma\alpha_k n_k r^k$ is sign-variable, a nonproportional decrease in its coefficient can theoretically lead to the situation where the distribution becomes less favorable. Therefore for individual specific forms of n(r), the intermediate values of M can turn out to be advantageous instead of the larger ones. A similar example

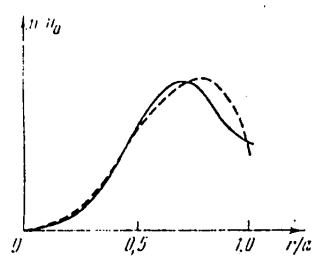

Figure 3.8. Index of refraction as a function of radius. The solid curve is the function used in [155].

was presented in reference [155]: machine calculations in the above-discussed approximation demonstrated that for the case where $n(r)-n_0$ has the form depicted

APPROVED FOR RELEASE: 2007/02/09: CIA-RDP82-00850R000500010010-4

APPROVED FOR RELEASE: 2007/02/09: CIA-RDP82-00850R000500010010-4

by the solid curve in Figure 3.8*, the angular divergence of the radiation does not decrease, but increases with an increase in M. Analyzing this case, it is easy to see that the form of n(r) is selected so that the aberrations occurring on different passes will compensate for each other. It is sufficient to alter the form of the function n(r) somewhat (for example, go to the dotted curve in Figure 3.8) for the indicated effect to disappear; therefore, the given example is not typical -- as a rule it is still useful that the aberrations were summed for the smallest possible number of passes through a nonuniform medium.

Some Comments on the Possibilities of the Geometric Optics Approximation. First, let us discuss the problem of the applicability of the above-discussed method of estimating u(r). Obviously, it is valid only for a small optical nonuniformity of the medium which does not cause significant alteration of the path of the beams by comparison with the case of an ideal resonator. For this purpose it is necessary that in any section of the cross section of the beam incident on the mirror, the angle between the normal to its wave front and the normal to the wave front of the diverging wave of the ideal resonator will be much less than the angle between the latter and the normal to the mirror surface (Figure 3.9). Mathematically, for a two-dimensional or axisymmetric problem this condition is formulated as follows:

$$\left|\frac{d}{dr}\left[\Delta L(r)+\Delta L\left(\frac{r}{M}\right)+\Delta L\left(\frac{r}{M^2}\right)+\ldots\right]\right| \ll \frac{d}{dr}\left|h(r)\right|, \text{ where } h(r)=(r^2/2\rho)-(r^2/2R_2)$$

is the distance between the mirror surface and the equiphasal surface of the diverging wave adjacent to it. Using expression (1.22) to find the curvature of the last ρ, we obtain $\text{см}\ \frac{1}{\rho}-\frac{1}{R_2}=\pm\sqrt{\frac{CD}{AB}}=\pm\frac{1}{AB}\sqrt{ABCD}=\frac{1}{2}\frac{\lambda N}{a^2}\left(M-\frac{1}{M}\right)$,

where $N\equiv a^2/(2AB\lambda)$ is the parameter introduced at the end of §1.2. Thus, $h(r)=\frac{\lambda N}{4}\left(M-\frac{1}{M}\right)\frac{r^2}{a^2}$, , and our condition acquires the form

$$\left|\frac{d}{dr}\left[\Delta L(r)+\Delta L\left(\frac{r}{M}\right)+\ldots\right]\right| \ll \frac{d}{dr}\left|N_{\text{экв}}\frac{\lambda}{2}\frac{r^2}{a^2}\right|, \tag{7}$$

where

$$N_{\text{экв}}=\frac{N}{2}\left(M-\frac{1}{M}\right). \tag{8}$$

(1)

Key: 1. equiv

Let us note that the value of $N_{equiv}\lambda/2$ is equal to h(a), that is, the distance between the equiphasal surface of the diverging wave of an ideal resonator and

*The shape of the curve in Figure 3.8 differs somewhat from that depicted in the figure in reference [155], but it is reproduced by the numerical data presented there.

APPROVED FOR RELEASE: 2007/02/09: CIA-RDP82-00850R000500010010-4

APPROVED FOR RELEASE: 2007/02/09: CIA-RDP82-00850R000500010010-4

the edge of the mirror (Figure 3.9). The parameter N_{equiv} introduced in this way plays an important role in the diffraction theory of unstable resonators (see the next section). As is easy to see, this parameter is, similarly to M, an algebraic value: in the situation depicted in Figure 3.9, $N_{equiv}>0$; if the wave front first touches the edge and not the center of the mirror, $N_{equiv}<0$. For confocal systems $\rho=\infty$ and $N_{equiv}=2h_0/\lambda=(M-1)a^2/2\lambda L$, where h_0 is the deflection of the exit mirror (in the case of a telescopic resonator $N_{equiv}>0$, for a resonator made of concave mirrors $N_{equiv}<0$). For an empty symmetric resonator depicted in Figure 3.3, e, $N_{equiv}=(a^2/2\lambda L)\ (M-1/M)$.

In the light of criterion (7), the fact attracts attention that as $|M|$ approaches one the limits of applicability of the developed model constrict sharply, inasmuch as here, on the one hand, $|N_{equiv}|$ decreases, and on the other hand, the greater part of the aberration coefficients α_k increases sharply (Figure 3.7). Finally, in the limiting case of a plane (M=1), concentric (M=1, Figure 1.13, c, d) or semiconcentric (M=-1, Figure 1.13, f) resonator the presence of small disturbances as convenient as one might like is sufficient for the sum in (5) to diverge and the optical-geometric approximation to become disadvantageous. Thus, we obtained another explanation of extraordinary sensitivity of a plane resonator to a different type of aberrations.

For performance of specific calculations in the case of a noticeably nonuniform medium, it is possible to use an improved Eikonal method within the framework of the optical-geometric approximation [6, 156]. In particular, here the redistribution of the emission intensity with respect to the beam cross section caused by the deflection of the beams as a result of phase inhomogeneities is already taken into account; it is true, as it was shown in §1.1, the nonuniformity of the amplitude distribution has very little influence on the angular divergence of the emission.

Although the Eikonal method has broader limits of applicability than the above-discussed simplest approximation, no new behavior laws of unstable resonators have been discovered by using [156]. Inasmuch as this method, in addition, is less descriptive and requires machine calculations, we shall not use it hereafter.

In conclusion, let us discuss another aspect of the optical-geometric approximation. Over the extent of the period of the equivalent line, the field amplitude varies in the ratio $K(0)\rho(0)/|M|^p$ along the beam running along its axis, where $K(0)\equiv\exp[(1/2)k_{gain}(0)\ell]$ and $\rho(0)\equiv\sqrt{R'(0)}$ are the amplitude gains in the medium and the reflection coefficient of the exit mirror on the system axis (a large cross-section mirror in asymmetric resonators will always be considered completely reflecting; for the definition of k_{gain} and R', see §1.4); $|M|^p$ is a factor which describes the decrease in the amplitude as a result of broadening of the beam; in the two-dimensional case p=1/2; in the three-dimensional case p=1.

The field source at the point r is the field at the point r/M (see Figure 3.6). In accordance with the definition of the aberration function F(r) the complex field amplitude along this beam varies in the ratio $\frac{K(0)\rho(0)}{|M|^p}F(r)$.

This calculation permits the following equation to be compiled

$$\gamma u(r)=\frac{K(0)\rho(0)}{|M|^p}F(r)\,u\left(\frac{r}{M}\right), \tag{9}$$

APPROVED FOR RELEASE: 2007/02/09: CIA-RDP82-00850R000500010010-4

APPROVED FOR RELEASE: 2007/02/09: CIA-RDP82-00850R000500010010-4

where γ is the eigenvalue. Using the substitution

$$u(r) = \tilde{u}(r) F(r) F\left(\frac{r}{M}\right) F\left(\frac{r}{M^2}\right) \ldots, \quad \gamma = \gamma' K(0) \rho(0)$$

equation (9) reduces to the equation of an ideal resonator which was presented for the first time in such form by Siegman and Arrathoon [157]:

$$\gamma' \tilde{u}(r) = \frac{1}{|M|^p} \tilde{u}\left(\frac{r}{M}\right). \tag{9a}$$

This equation formally has solutions of the type $\tilde{u}(r) \sim r^m$ with eigenvalues $\gamma' = (1/M)^{p+m}$, where m is any number. Siegman and Arrathoon arrived at the conclusion that m can assume values of 0, 1, 2, 3, ...; here they began with the requirements that the function $\tilde{u}(r)$ and all of its derivatives at the point r=0 be limited. However, this conclusion, generally speaking, did not have solid ground to stand on: it is known that the optical-geometric approximation is applicable only when the relative variations of u(r) in the dimensions of the Fresnel zone $\sqrt{\lambda L}$ are small, that is, for

$$\sqrt{\lambda L} \left| \frac{d \ln u}{dr} \right| \ll 1. \tag{10}$$

Condition (10) at the point r=0 is satisfied only by a trivial solution of the equation (9a) $\tilde{u}$=const (m=0) which leads to formula (5), which is therefore the solution to equation (9) with eigenvalue

$$\gamma = K(0) \rho(0) / |M|^p. \tag{11}$$

For final solution of the problem of the mode spectrum of an unstable resonator, diffraction approximation is required. In addition, in the case of sharply outlined mirrors condition (10) is not satisfied even near the edge of the beam, which leads to a number of characteristic features of such resonators. Let us proceed with investigation of these problems.

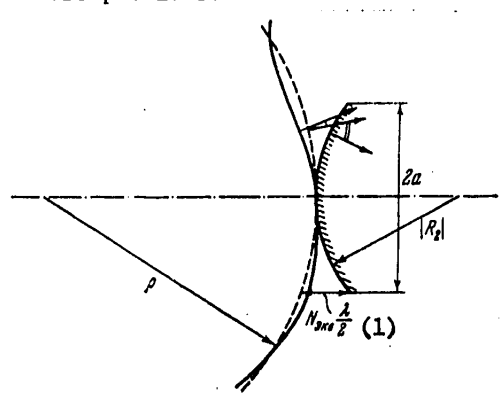

Figure 3.9. Wave front near the exit mirror of a resonator with aberrations. The equiphasal surface for an ideal resonator is plotted by the dotted line.

Key: (1) N_{equiv}

APPROVED FOR RELEASE: 2007/02/09: CIA-RDP82-00850R000500010010-4

APPROVED FOR RELEASE: 2007/02/09: CIA-RDP82-00850R000500010010-4

Section 3.3. Edge Effects and Spectrum of Natural Oscillations.

Equivalence of Unstable Resonators and Interrelation of the Solutions for Different Types. In the diffraction approximation the field distribution of unstable resonators, just as resonators of other types, is described by the eigenfunctions of a system of two integral equations relating the fields on the mirrors using the Huygens-Fresnel principle. For resonators with one-sided radiation output, when one of the mirrors is quite large and is totally reflecting (see Figure 3.3, a-d), it is possible to use the integral expression (1.24) or (1.24a) permitting a single equation to be compiled containing only the field distribution function on the other mirror.

If we go from field distribution on the exit mirror to the distribution on the equiphasal surface of the diverging wave of the geometric approximation (see above, Section 3.2), the desired equation acquires an especially obvious form [157]. Actually, substituting in (1.24a) $U(X, Y) = \chi(X, Y)\exp[i\pi N_{equiv}(X^2 + Y^2)]$ (by which the indicated transition is realized) and considering that $AD + BC = (M + 1/M)/2$, we obtain the following integral equation:

$$\gamma_m \chi_m(X, Y) = N\frac{\exp(2ikL_0)}{i}\iint \exp\left\{i\pi NM\left[\left(X' - \frac{X}{M}\right)^2 + \left(Y' - \frac{Y}{M}\right)^2\right]\right\}\chi_m(X', Y')\,dX'\,dY'. \tag{12}$$

Let us write out the analogous equation for the two-dimensional case which will basically be considered; here we shall consider that the exit mirror has a peak reflection coefficient $\rho(x)$ which is variable with respect to cross section; the phase factor $\exp(2ikL_0)$ will be omitted:

$$\gamma_m \chi_m(X) = \sqrt{N/i}\int_{-\infty}^{\infty} \rho_1(X')\exp\left[i\pi NM\left(X' - \frac{X}{M}\right)^2\right]\chi_m(X')\,dX'. \tag{13}$$

Here, just as in (12), γ_m is the eigenvalue, $X \equiv x/a$ is the dimensionless coordinate; 2a is the characteristic size of the mirror; the parameter N_{equiv} used on making the transition to the new reference surface is, as before, related to N and M by the expression $N_{equiv} = (N/2)(M - 1/M)$; finally, $\rho_1(X) \equiv \rho(aX)$; for the case of a finite totally reflecting mirror

$$\rho_1(X) = \begin{cases} 1, & |X| \leqslant 1, \\ 0, & |X| > 1. \end{cases}$$

The equation for the symmetric resonator has the same form (Figure 3.3, e)* under the condition that the reflection coefficient of both of its mirrors is described by the same function $\rho_1(X)$.

* In this case the value of γ_m, just as M (see Section 3.1), pertains to passage through the resonator not at the bottom, but to one side.

APPROVED FOR RELEASE: 2007/02/09: CIA-RDP82-00850R000500010010-4

APPROVED FOR RELEASE: 2007/02/09: CIA-RDP82-00850R000500010010-4

Thus, all unstable resonators with one-sided radiation output equal to N and M (or M and N_{equiv}) and the same law of variation of the reflection coefficient of the exit mirror are equivalent to each other (for the special case of totally reflecting mirrors this result was obtained already in Section 1.2). Moreover, the eigenfunctions and the values for the resonators in which any two parameters out of three (N, M, N_{equiv}) are negative can be expressed in terms of the eigenfunctions and values of the resonator with the same with respect to absolute magnitude but positive parameters (it is true that for this when $M < 0$ it is necessary that the condition $\rho(-x) = \rho(x)$ be satisfied--indeed on changing the sign of M, the influence of only symmetrically distributed aberration sources can remain invariant; see Section 3.2). Let us demonstrate this in the example of resonators with $N > 0$, $M < 0$, $N_{equiv} < 0$ (these include, in particular, the confocal resonator depicted in Figure 3.3, c). On making the transition from (13) to the complex conjugate equation, replacing X' under the integral sign by -X' and using $\rho_1(-X') = \rho_1(X')$ and $M = -|M|$ we obtain

$$\frac{\gamma^*}{i}\chi^*(X) = \sqrt{\frac{N}{i}}\int_{-\infty}^{\infty}\rho_1(X')\exp\left[i\pi N|M|\left(X' - \frac{X}{|M|}\right)^2\right]\chi^*(-X')\,dX'$$

(the * indicates, just as everywhere, complex conjugation).

It is known that the eigenfunctions of such resonators are symmetric (χ_s) or antisymmetric (χ_a). Substituting the expression $\chi^*_{s,a}(-X') = \pm\chi^*_{s,a}(X')$ in the latter we obtained equations distinguished only by the factor for γ and for the rest coinciding entirely with the equation of the resonator having the parameters N, $|M|$. In the final analysis we have

$$\gamma_{s,a}(N, -|M|) = \mp i\gamma^*_{s,a}(N, |M|),$$
$$\chi_{s,a}(N, -|M|, X) = \chi^*_{s,a}(N, |M|, X).$$

For resonators with $N < 0$, $M > 0$, $N_{equiv} < 0$ (as an example we can use the symmetric resonator made of two sharply concave mirrors)

$$\gamma(-|N|, M) = \gamma^*(|N|, M), \quad \chi(-|N|, M, X) = \chi^*(|N|, M, X).$$

Finally, for $N < 0$, $M < 0$, $N_{equiv} > 0$ (for example, the confocal resonator made of concave mirrors in which a mirror with large R is used as the exit mirror)

$$\gamma_{s,a}(-|N|, -|M|) = \pm i\gamma_{s,a}(|N|, |M|),$$
$$\chi(-|N|, -|M|, X) = \chi(|N|, |M|, X).$$

From the presented formulas it is obvious that for all types of unstable resonators with identical N, M and N_{equiv} with respect to absolute magnitude, the eigenvalues are distinguished by phase factors, but they coincide with respect to modulus; thus, all of them have identical diffraction losses. The eigenfunctions recorded on the equiphasal surface of the diverging wave of the geometric approximation turn out to be complex-conjugate for resonators with $N_{equiv} < 0$

FOR OFFICIAL USE ONLY

APPROVED FOR RELEASE: 2007/02/09: CIA-RDP82-00850R000500010010-4

APPROVED FOR RELEASE: 2007/02/09: CIA-RDP82-00850R000500010010-4

with respect to the eigenfunctions of resonators with $N_{equiv} > 0$. Inasmuch as the transition from the indicated reference surface to the surface of the mirrors is realized by multiplication by $\exp(i\pi N_{equiv}X^2)$, the distributions on the mirror surface are also complex-conjugate.

All of this permits us hereafter to limit ourselves to the investigation of any one type of resonator. We shall illustrate everything in the example of a resonator made up of two identical convex mirrors (Figure 3.3, e; $N > 0$, $M > 0$, $N_{equiv} > 0$), limiting ourselves, as a rule, to the investigation of the two-dimensional case and departing from this rule only when the transition to three dimensional leads to a qualitative change in the oscillation spectrum.

Unstable Cavities With Completely "Smoothed" Edge. Initially, following [151, 154], let us consider the properties of such unstable resonators for which the edge diffraction effects are insignificant. From the general arguments it is clear that this occurs in the case where the reflection coefficient of the mirrors, and with it also the field amplitude, smoothly decrease toward the edge of the system. From the materials presented in Section 3.2, it also follows that the field distribution of the fundamental mode in such resonators must be described well by the formula for the opticogeometric approximation (5) which satisfies equation (9). The relation between the equations of the diffraction approximation (13) and the opticogeometric approximation (9) is quite obvious. Actually, the factor $\exp[i\pi NM(X' - X/M)^2]$ for large values of $X' - X/M$ oscillates rapidly. Therefore if the product $\rho_1\chi$ is a slowly variable function of X' the magnitude of the integral in (13) is in practice determined only by the behavior of this function in the vicinity of the point X/M (see also Section 1.1). Expanding it near this point in a Taylor series

$$\rho_1(X')\chi(X') = \rho_1\left(\frac{X}{M}\right)\chi\left(\frac{X}{M}\right) + \left(X' - \frac{X}{M}\right)\frac{d(\rho_1\chi)}{dX'}\bigg|_{X'=X/M} + \cdots$$

and limiting ourselves to the terms written out, after integration we immediately obtain (9) with the aberration function $F(X) = \rho_1(X/M)/\rho_1(0)$ (in the case of an empty resonator $K \equiv 1$).

In order to discover what the mode spectrum of unstable resonators with smoothed edge is, let us consider their properties in the diffraction approximation in the example of a resonator with Gaussian distribution of the mirror reflection coefficient:

$$\rho(x) = \exp(-2x^2/a^2), \quad \rho_1(X) = \exp(-2X^2).$$

This case is especially interesting in that the mirrors with Gaussian distribution ρ can be considered to have an ideally smoothed edge: As a result of reflection of the light beams from them with an amplitude having Gaussian or uniform distribution, the Gaussian beams are generated, the far-field pattern of which does not have additional peaks. In addition, for resonators with such mirrors there is an exact analytical solution [3]. When the transverse dimensions of the mirrors and the diffraction losses are not too small (more

FOR OFFICIAL USE ONLY

APPROVED FOR RELEASE: 2007/02/09: CIA-RDP82-00850R000500010010-4

APPROVED FOR RELEASE: 2007/02/09: CIA-RDP82-00850R000500010010-4

precisely, on satisfaction of the condition $\pi N_{equiv}(M - 1/M) >> 1$), after transition to the normal coordinates this solution acquires the form [151]*

$$u_m(x) \sim u_0(x)\, H_m\left(2\sqrt{-i\pi N_{\text{экв}}}\,\frac{x}{a}\right), \quad m = 0, 1, 2, \ldots, \qquad \dagger = \text{equiv} \tag{14}$$

$$\gamma_m \approx \left(\frac{1}{M}\right)^{m+\frac{1}{2}}, \tag{15}$$

where $u_0(x) = \exp(-[2/(M^2 - 1)][x^2/a^2])$, $H_m(t) = (-1)^m \exp(t^2/2) \times (d^m/dt^m) \times \exp(-[t^2/2])$ are Hermite polynomials. Inasmuch as $H_0(t) = 1$, the function u directly describes the field distribution of the lowest mode; it is easy to see that it satisfies the opticogeometric equation (9) and can be found using formula (5):

$$u_0(x) = \rho\left(\frac{x}{M}\right)\rho\left(\frac{x}{M^2}\right)\ldots = \exp\left(-\frac{2x^2}{M^2a^2} - \frac{2x^2}{M^4a^2} - \ldots\right) = \exp\left(-\frac{2}{M^2-1}\frac{x^2}{a^2}\right).$$

Now let us consider the Hermite polynomials. All of them contain the term t^m; in the first two polynomials it is unique ($H_0(t) = 1$, $H_1(t) = t$); the rest, in addition to it, also contain the terms of lower orders ($H_2(t) = t^2 - 1$, $H_3(t) = t^3 - 3t$, and so on). These additional terms play a significant role only for small values of the argument H_m; from (14) it is obvious that this occurs in the investigated case of large N_{equiv} only on the small central section of the resonator cross section. Thus, the first two modes on the entire resonator cross section, and the subsequent ones, on the larger part of it are described by the functions $u_0(x)(x/a)^m$ which are solutions of the opticogeometric equation (9) (see the end of Section 3.2). The exponents on x/a actually turn out to be integral, except, in spite of the proposition of Siegman and Arrathoon , this does not follow from any conditions on the resonator axis (where the geometric approximation ceases to be valid), but from the requirement of the bounding of $u_m(x)$ at infinity [151].

An example of the field distribution of several lowest modes for M = 2 and $\pi N_{equiv} = 50$ is presented in Figure 3.10. The field amplitude of the fundamental mode (m = 0) decreases on going away from the center of the mirrors by a Gaussian law, the characteristic size of the "spot" in the plane of the mirror is $2a\sqrt{M^2 - 1}$. The fields of the other modes fill the central region of the resonator less uniformly. With an increase in the transverse index m the zone of larger amplitude shifts away from the center. The equiphasal surfaces of the modes with m = 0, 1 naturally coincide with the surface of the spherical wave of the geometric approximation (Figure 3.10, b). In the wave fronts of the higher-order modes near the center of the mirrors noticeable deviations from the spherical shape are observed--it turns out that the Hermite polynomials contain, in addition to t^m, also other terms.

* On comparison with the published data it is necessary to consider that in a number of papers, including [151, 154], the dependence of the field on time $\exp(i\omega t)$ was used and not $\exp(-i\omega t)$ as in the present publication (as a result, the sign on i changes everywhere).

FOR OFFICIAL USE ONLY

APPROVED FOR RELEASE: 2007/02/09: CIA-RDP82-00850R000500010010-4

APPROVED FOR RELEASE: 2007/02/09: CIA-RDP82-00850R000500010010-4

Nevertheless, the most interesting for us now is not the specific form of the solutions in the resonator with Gaussian mirrors, but the fact that in expressions (14), (15) the form of the distribution $\rho(x)$ essentially determines only the factor $u_0(x)$ common to all eigenfunctions (inasmuch as $N_{equiv} \sim a^2$, the value of the argument H_m does not depend on a). It is also remarkable that the eigenvalues in accordance with (15) do not depend on the sizes of the mirrors and coincide with the eigenvalues which were obtained by formal methods in references [158, 159] for resonators with mirrors of infinite dimensions.

We have already seen that within the framework of the opticogeometric approximation the isolation of the factor describing the field distribution of the fundamental mode for any form of aberration function $F(x)$ reduces the corresponding equation to the equation of an ideal resonator (see the transition from (9) to (9a)). By analogy it is possible to propose that in the diffraction approximation the eigenfunctions have the form (14) not only for Gaussian mirrors, but also in the general case of many unstable resonators with well-smoothed edge. The field distribution of the fundamental mode u_0 which figures in (14) here must be considered using (5); the eigenvalues must be equal to the following (see (11))

$$\gamma_m = K(0)\rho(0)(1/M)^{m+1/2}. \tag{15a}$$

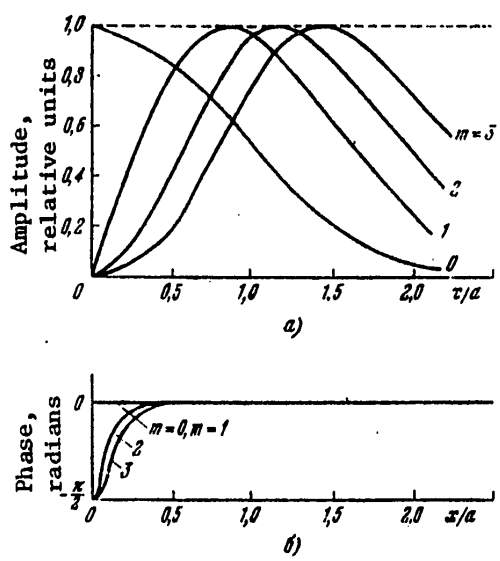

Figure 3.10. Field distributions of the lowest modes in a resonator with Gaussian mirrors ($M = 2$, $\pi N_{equiv} = 50$): a--amplitude distribution; b--phase distribution (the origin is the spherical wave of the geometric approximation).

Then it will be obvious that these arguments formulated in [151] are basically true; however, it is still necessary to become familiar with the properties of resonators, the mirrors of which have regular geometric shape with sharply outlined edge.

APPROVED FOR RELEASE: 2007/02/09: CIA-RDP82-00850R000500010010-4

APPROVED FOR RELEASE: 2007/02/09: CIA-RDP82-00850R000500010010-4

Unstable Resonators With Sharp Edge. As we have already mentioned in Section 3.1, in Siegman's first paper [4] he stated the argument that in unstable resonators with large losses the edge diffraction must influence only the peripheral part of the beam immediately exiting from the resonator. Hence, it follows that the field distribution on the mirrors (or with one-sided output, on the output mirror) and the magnitude of the losses must not noticeably depend on the edge effects; the analogous conclusion regarding the properties of unstable resonators with large losses can also be found in Vaynshteyn ([3], problem No 8 for Chapter 4). However, precise machine calculations performed by Sigmen and Arratun [157] by the iterative method demonstrated that the picture of the properties of unstable resonators with totally reflecting mirrors of finite dimensions is far from simple. It was discovered that the field distribution for oscillations with the least losses does not differ too strongly, but nevertheless, noticeably, from the predictions of the geometric approximation (Figure 3.11). It turned out that the nature of this distribution and the magnitude of the losses depend in a complex way on the transverse dimensions of the mirrors, revealing explicit periodic dependence with variation of N_{equiv} for fixed M. The typical form of the relation calculated in [157] for the losses as a function of N_{equiv} is presented in Figure 3.12, a (the procedure used made it possible simultaneously to find the losses of the two highest Q modes).

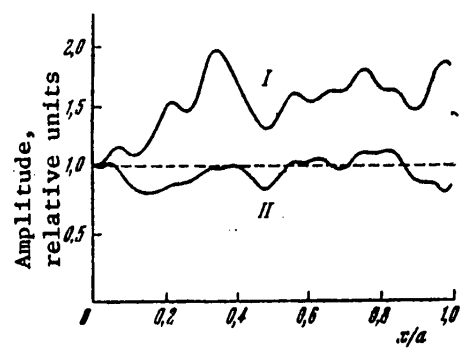

Figure 3.11. Amplitude distribution of modes with least losses near the degeneration point in the resonator with sharp edge (M = 1.86, $N_{equiv} \approx 5$) [157]. Curve I--$N_{equiv} \leq 5$; curve II--$N_{equiv} \geq 5$.

The work by Siegman and Arrathoon was a major contribution to the theory of unstable resonators with a sharp edge; in particular, the parameter N_{equiv} was introduced here. However, the physical meaning of this parameter remained unclear; in addition, when interpreting the calculated data the authors of [157] erroneously considered that the lower "wavy" line GHJ ... corresponds to one mode of the lowest order, and the V-type branches AGB, CHD and EJF ..., another symmetric mode. In reality, as was indicated in [152] and confirmed by the results of the latest machine calculations [160, 161] the apparent periodicity of the variation of the losses is caused by the fact that as N_{equiv} grows, the types of oscillations having the highest Q-factor alternately exchange places (similarly to how this occurs in Figure 2.21). This exchange takes place near

FOR OFFICIAL USE ONLY

APPROVED FOR RELEASE: 2007/02/09: CIA-RDP82-00850R000500010010-4

APPROVED FOR RELEASE: 2007/02/09: CIA-RDP82-00850R000500010010-4

the integral values of N_{equiv} for which the modes turn out to be doubly degenerate with respect to losses (but not with respect to frequencies). Let us note that the configurations of the fields of two adjacent modes near the degeneration point are presented in Figure 3.11.

In Figure 3.12, b, c, a more complete picture of the behavior of the natural oscillations of a two-dimensional resonator [160] and a three-dimensional resonator with circular mirrors [161] is depicted. It is obvious that in the final analysis there are a small number of modes, the losses of which vary with N_{equiv} quasiperiodically so that these oscillations alternately become the highest Q. In the three-dimensional case these laws are also maintained for large N_{equiv} at the same time as in the two-dimensional case, beginning with a defined value of N_{equiv}, the curves cease to intersect--the degeneration of the modes with respect to the losses is removed.

Without going into a detailed analysis of these phenomena, it is possible directly to draw the conclusion that the edge effects in unstable resonators are still manifested although only the central and it would appear, almost undisturbed part of the beam as a result of diffraction is incident on the exit mirror. In order to understand the cause of this, it is necessary to consider that as a result of diffraction, in addition to the undistorted reflected wave, an additional wave also appears, the fictitious source of which is the edge of the mirror (see Section 2.2). Although the amplitude of the additional wave decreases sharply with removal from the direction of the reflected wave (Figure 3.13), some part of the radiation scatters also at large angles, including in the direction opposite to the direction of the incident wave (noted in the figure by the dotted arrows). This radiation gives the beginning of the converging wave, the properties of which were investigated in detail in Section 3.1. Let us remember the basic characteristic feature of the converging wave: at the same time as the intensity of the basic wave decreases on a single pass through the resonator by M or M^2 times, the radiation pertaining to the converging wave remains entirely inside the resonator for many passes. As a result, the converging wave, in spite of its negligible intensity near the edge of the system where it is formed, is amplified as it approaches the resonator axis to such a degree that it has a significant influence on the entire field structure.

The discussed picture, although primitive, nevertheless permits understanding of the role of the parameter N_{equiv} [154]. For this purpose let us return to Figure 3.9. In Figure 3.9 the dotted line depicts the equiphasal surface of the diverging wave moving in the direction of the mirror for the presently investigated case of an ideal resonator (the medium is absent or uniform). It is easy to see that this surface is equiphasal also for a converging wave moving away from the mirror. Therefore the radiation of the diverging wave incident on the edge of the mirror and then forming the converging wave passes between the equiphasal surfaces of these waves a total distance $N_{equiv}\lambda$. Thus, on variation of N_{equiv} by one, the phase difference between the diverging wave and the converging wave occurring as a result of edge diffraction varies by 2π, which also leads to quasiperiodicity of the properties of unstable resonators.

FOR OFFICIAL USE ONLY

APPROVED FOR RELEASE: 2007/02/09: CIA-RDP82-00850R000500010010-4

APPROVED FOR RELEASE: 2007/02/09: CIA-RDP82-00850R000500010010-4

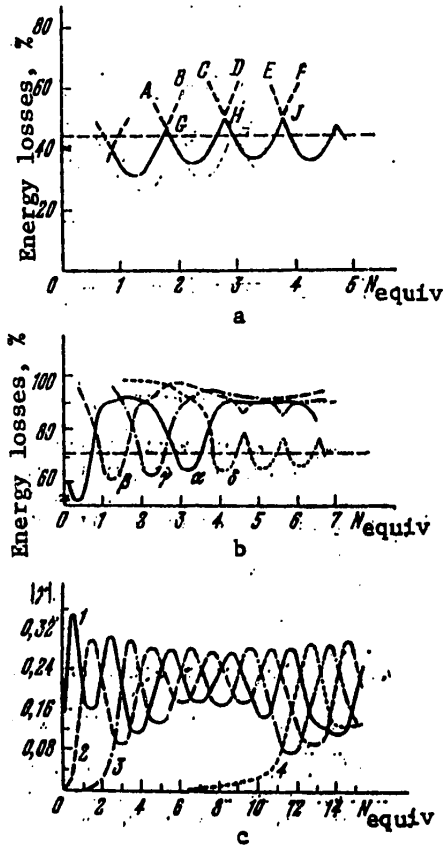

Figure 3.12. Losses and eigenvalues as a function of N_{equiv}: a--losses in the two-dimensional resonator, M = 1.86 [157]; b--losses in the two-dimensional resonator, M = 3.3 [160] (the dotted line is used to plot the losses for the lowest resonator mode with smoothed edge); c--the eigenvalues in the three-dimensional resonator with spherical mirrors, M = 5, the azimuthal mode index is equal to zero (there is no dependence on the azimuthal angle) [161].

Let us note that it is possible always to determine N_{equiv} by the distance between the equiphasal surfaces of the diverging and converging waves near the element bounding the beam cross section in the resonator, whereas the definition of N_{equiv} given in Figure 3.9 sometimes makes no sense. This occurs primarily in ring cavities and also in systems in which the beam cross section is limited not only by the exit mirror, but by the iris placed at a noticeable distance from it.

A more careful investigation of the properties of unstable resonators with a sharp edge can be made by the analytical methods of Vaynshteyn similarly to how this was done in Section 2.2 for the case of a planar resonator. We shall

FOR OFFICIAL USE ONLY

APPROVED FOR RELEASE: 2007/02/09: CIA-RDP82-00850R000500010010-4

APPROVED FOR RELEASE: 2007/02/09: CIA-RDP82-00850R000500010010-4

become somewhat familiar with the mathematical aspect of the question in the following section where there is a discussion of the properties of resonators with central beam hole: the solution in the geometric approximation is in general absent there, and it is not possible to get along without the Vaynshteyn approach. Now we only note that as a result of considering the interference effects the radiation scattered by edge diffraction inside the resonator turns out to be distributed not with respect to all, but with respect to a number of discrete directions. Just as in Section 2.2, one of them corresponds to the wave "reflected" from the edge, and the rest, to the "transformed" waves; only inasmuch as the angle of incidence of the initial wave on the edge of the mirror α (see Figure 2.7) is very large here, among the "transformed" waves there are waves which are scattered not only at angles larger than the "reflected" one (that is, with $\theta > \alpha$), but also at smaller angles ($\theta < \alpha$). A comparison of Figures 3.13 and 2.7 shows that in the case of unstable resonators, when a divergent wave is incident on the edge, the wave that is "reflected" from the edge is indeed convergent. The approximate calculations made by Lyubimov et al. [162, 163] demonstrated that the above-described complex laws actually are explained by interaction of the fundamental wave with the "reflected" wave and the one or two "transformed" waves closest to it. The radiation scattered in other directions quickly exits from the resonator, and therefore plays no significant role.

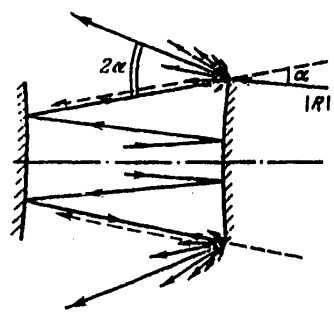

Figure 3.13. The formation of scattered waves during edge diffraction.

Subsequent foreign publications in which the Vaynshteyn methods were still used (see, for example, [164]) do not add anything theoretically new to the results obtained in [162, 163]. It must be noted that in a case of unstable resonators such calculations, especially considering at least one "transformed" wave, require extraordinarily awkward calculations and in the final analysis it is not possible to get around a machine solution of the systems of transcendental equations. Therefore their results are very difficult to see and are not clear. In addition, later it will be obvious that the problem of classification of the natural oscillations in unstable resonators, in general, and in those with a sharp edge, in particular, is primarily of academic interest. In practice only the nature of the behavior of the modes with the least losses turns out to be important, and it is entirely clear from the results of references [157, 152, 160, 161] in which the numerical iterative method was used (see Figure 3.12). Therefore we shall consider this problem in more detail and proceed to a discussion of the properties of real systems.

APPROVED FOR RELEASE: 2007/02/09: CIA-RDP82-00850R000500010010-4

APPROVED FOR RELEASE: 2007/02/09: CIA-RDP82-00850R000500010010-4

Specifics of Edge Effects Under Real Conditions. The resonators with significant cross sectional dimensions and not too small $|M| - 1$ are of the greatest interest from the point of view of the problems of divergence of the radiation; obviously for them $|N_{equiv}| >> 1$ is satisfied. The specific nature of the diffraction effects in such resonators primarily consists in the fact that the fundamental diverging wave is incident on the edge of the mirror at a comparatively large angle α defined by the geometry of the system (see Figure 3.13). From the radiation scattered as a result of diffraction only that part remains in the resonator which is deflected from the reflected beam at angles exceeding α. We have already seen that even in this part of the radiation the primary role is played by the converging wave corresponding to the angle of deviation 2α. It is easy to show that the values of α and N_{equiv} are related by the expression $\alpha = N_{equiv}\lambda/a$. In real resonators of powerful lasers N_{equiv} usually varies from several tens to many thousands (see Chapter 4); here the angles 2α reach several degrees.

At the same time it is known that the intensity of the diffraction scattering of light at large angles depends strongly on the nature of the edge of the mirrors [165]. The above-enumerated theoretical papers in which the effects of the mode degeneration with respect to losses, and so on were observed essentially pertain to the hypothetical case where the edge of the mirrors is ideally sharp and precisely outlined along a straight line or curve with center on the axis of the resonator. Such a model is entirely admissible when we are talking, for example, about the lowest modes of planar resonators which correspond to small angles of incidence of radiation on the edge of the mirror. For unstable resonators it is impossible to neglect the natural "blurring" of the edge and imperfection of the mirror outlines; both of these factors lead to attenuation of the diffraction scattering of the light at large angles and, consequently, to a decrease in the intensity of the converging wave. If this decrease is significant, the degeneration with respect to losses is removed and the eigenvalues approach the values predicted by formula (15).

Let us estimate what the deviations from the ideal conditions should be in order that the intensity of the converging wave decrease sharply. This is done most frequently for the case where the mirror reflection coefficient decreases from one to zero not discontinuously, but over the extent of a zone of finite width d (a similar situation occurs, in particular, when using mirrors with multilayered interference coatings). Actually, significant variation of the amplitude of the beam reflected from the mirror at the characteristic dimension d indicates that in the expansion of the amplitude in a Fourier series there are components present with spatial frequencies of $\sim 1/d$. Inasmuch as the angular distribution of the radiation is the Fourier type of distribution in the near zone (Section 1.1), these components correspond to the angles of inclination of $\sim\lambda/d$. Hence it follows that in order that the light be scattered primarily at angles less than $2\alpha = 2N_{equiv}\lambda/a$, it is necessary to satisfy the condition $d > d_0 \equiv a/2N_{equiv}$ [151]. Let us note that the situation here is entirely the same as in radio engineering where a decrease in the steepness of the pulse front is accompanied by the corresponding constriction of the signal spectrum.

FOR OFFICIAL USE ONLY

APPROVED FOR RELEASE: 2007/02/09: CIA-RDP82-00850R000500010010-4

APPROVED FOR RELEASE: 2007/02/09: CIA-RDP82-00850R000500010010-4

A more careful calculation of the decrease in intensity of the scattered waves can be made as follows. Let us break down the entire "smoothing" zone in a series of sections Δx wide each. Replacing the "smooth" function $\rho(x)$ by a step function, we obtain the set of "steps" of height $-(d\rho/dx)\Delta x$. Each "step" obviously generates edge waves with relative amplitude $-(d\rho/dx)\Delta x$ (see Section 2.2). Adding them in the far zone considering the phase relations and replacing the summation with respect to all "steps" by integration, we find that the intensity of the edge waves scattered at an angle ψ is proportional to

$$B(\psi) = -\int_{a-d/2}^{a+d/2} \exp\left(i\frac{2\pi}{\lambda}\psi x\right) \times \frac{d\rho}{dx}\,dx \quad [166];$$

let us note that $B(\psi)$ is the angular spectrum of a source of width d with amplitude distribution $-(d\rho/dx)$. If we consider that for $d \to 0$ the value of $B(\psi) \to 1$, it becomes clear that replacement of the sharp edge by a smoothed edge causes a decrease in the amplitude of the radiation scattered at an angle ψ by $1/|B(\psi)|$ times.

The estimates made using these relations in [166] demonstrated that the parameter d_0 introduced above is actually the critical width of the "smoothing" zone, on achievement of which the diffraction "reflection" from the edge turns out to be significantly attenuated. With a further increase in zone width, the intensity of the converging wave continues to decrease rapidly (in some cases experiencing pulsations; the specific form of the dependence of $1/|B(2\alpha)|$ on d/d_0 naturally is determined by the law of decrease of ρ inside the zone).

In the same paper [166], Sherstobitov and Vinokurov performed the corresponding calculations for two-dimensional resonators made of cylindrical mirrors with comparatively small N_{equiv}. The calculations were performed by the numerical method of Fox-Li; the "smoothing" of the edge was introduced by direct assignment of the form of $\rho(x)$. It was found that smoothing does entail elimination of degeneration of the lowest modes with respect to losses. As an illustration Figure 3.14 shows the losses of the two lowest symmetric modes as a function of N_{equiv} in the resonator in which ρ decreases to zero in a region of width $\sim d_0$ by a linear law. It is obvious that the degeneration is completely removed, and the losses are close to the losses in a resonator with ideally smoothed edge (dotted lines). The field distribution of the basic mode u_0 in this case is excellently described by the formula (5); the distribution of the second mode, although not so good, still satisfactorily coincides with the results of the calculations by formula (14) with substitution in it of the same u_0 (see Figure 3.15).

Let us note that in general on making the transition to the higher-order modes, the effect of the converging wave regularly increases and for elimination of it, a greater and greater degree of smoothing of the edge is required. This is easy to understand if we begin with the field distribution in the resonator with ideally smoothed edge and introduce the partially smoothed edge of a disturbance leading to the formation of a converging wave. The initial field of the high-order modes is comparatively high on the periphery of the resonator and small on its axis (see Figure 3.10). Therefore with an increase in the transverse index,

FOR OFFICIAL USE ONLY

APPROVED FOR RELEASE: 2007/02/09: CIA-RDP82-00850R000500010010-4

APPROVED FOR RELEASE: 2007/02/09: CIA-RDP82-00850R000500010010-4

on the one side, the initial intensity of the converging wave increases, and on the other, its influence on the field structure in the central part of the resonator increases. Hereafter we shall not touch on the problem of higher modes, but limit ourselves to analysis of behavior of modes with the least losses.

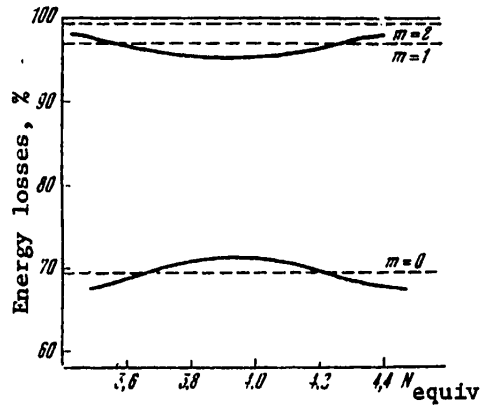

Figure 3.14. Losses of two lowest symmetric modes as a function of N_{equiv} in a resonator with partially smoothed edge [166]; the dotted lines are the values of the losses in the resonator with completely smoothed edge; M = 3.3.

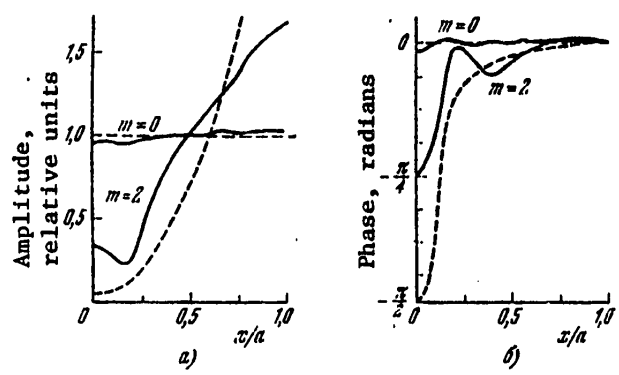

Figure 3.15. Field distributions of the lowest symmetric modes in a resonator with partially smoothed edge for M = 3.3, $N_{equiv} \approx 4$ [166]: a--amplitude distribution; b--phase distribution (the origin is the spherical wave of the geometric approximation). The solid lines represent the machine calculations, and the dotted lines, the calculation by formulas (14), (5).

Thus, for removal of the degeneration of the lowest modes of the two-dimensional unstable resonators with small N_{equiv} slight smoothing of the edge is sufficient (let us remember that for large N_{equiv} the degeneration in the two-dimensional resonators is absent even without any smoothing). This conclusion can be

FOR OFFICIAL USE ONLY

APPROVED FOR RELEASE: 2007/02/09: CIA-RDP82-00850R000500010010-4

APPROVED FOR RELEASE: 2007/02/09: CIA-RDP82-00850R000500010010-4

directly generalized to the case of a three-dimensional resonator with spherical rectangular mirrors, for in such resonators, as we have seen many times in Chapter 2, the variables are easily separated.

In resonators with circular spherical mirrors the edge effects are manifested significantly more strongly: Here, in contrast to the three-dimensional resonators with cylindrical mirrors, a simple increase in N_{equiv} in the presence of a sharp edge does not lead to removal of the degeneration of the lowest modes (see Figure 3.12). The reasons for this consist in the fact that the density of the converging wave increases as it approaches the center more sharply for spherical mirrors than for cylindrical mirrors (it is known that the diffraction structure at the center of the pattern is expressed more strongly with diffraction on a circular hole than on a slit of the same transverse dimension). In references [163, 338], the Vaynshteyn method was used to show that for removal of the degeneration in resonators with circular spherical mirrors it is necessary to decrease the amplitude of the converging wave by comparison with the case of a sharp edge by approximately $e^{\ln(2\pi N_{equiv})/\ln M}$ times. This corresponds to a not so small width of the smoothing zone: for the most favorable decreasing law

$$\rho\left(\rho(r)=\frac{1}{2}-\frac{1}{\sqrt{\pi}}\int_0^{(r-a)/d}\exp\left(-\frac{t^2}{2}\right)dt\ [166]\right)$$

it will be $(d_0/\pi)\sqrt{1+\ln[\ln(2\pi N_{equiv})/\ln M]}$, in the case of a linear law and laws close to it [166] it reaches $\sim 0.5 d_0 \ln(2\pi N_{equiv})/\ln M$. Nevertheless, for large N_{equiv} this is only a small portion of the total size of the mirrors.

Finally, the time has come to see what relation the case of the resonator with partially smoothed edge discussed by us has to the properties of the real systems. The parameters of solid-state lasers described in the following chapter correspond to the widths of the smoothing zone required for removal of the degeneration of the lowest modes by losses 0.1-1 mm; this blurring of the edge occurs quite frequently.

There are other factors which can lead to attenuation of the influence of the edge effects. Thus, for the smallest misalignments of the resonator the values of N_{equiv} measured from different sides of the system axis begin to differ from each other; these differences also arise as a result of the influences of aberrations (see Figure 3.9). Finally, the edge of the mirrors can be inexactly outlined. All of this leads to the fact that the waves beginning in different sections of the mirror loop arrive at the axis with different phases and therefore are mutually extinguishing (it is known that using the diaphragm with uneven edge, it is possible completely to blur the diffraction pattern far from the boundary of the geometric shadow). The meaning of the parameter d_0 here becomes entirely clear: For variation of the distance from the axis to the edge within the limits from $a - d_0/2$ to $a + d_0/2$ the value of N_{equiv} varies by one, the phase difference between the diverging and converging waves, by 2π.

FOR OFFICIAL USE ONLY

APPROVED FOR RELEASE: 2007/02/09: CIA-RDP82-00850R000500010010-4

APPROVED FOR RELEASE: 2007/02/09: CIA-RDP82-00850R000500010010-4

Everything that has been stated together with certain other results of the above-enumerated experiments suffices for drawing the following basic conclusion: The degeneration of the lowest modes of real resonators with $N_{equiv} >> 1$, as a rule, is absent, and if necessary it can be reliably prevented by using such simple measures as the application of a bevel to the edge of the mirror (for more information about the suppression of edge effects by this method see [3]), the application of a serrated iris, and so on. Of course, we are talking only about cases where the degeneration is caused by diffraction on the edge of the mirror and not light dissipation in the active medium or on interfaces (the effect of the light dissipation will be briefly considered in Section 4.1).

The removal of the degeneration with respect to losses is accompanied by the fact that the field distribution begins to be described with a high degree of accuracy by the formulas of the opticogeometric approximation (it is only necessary to consider that manifestations of diffraction remain in the peripheral part of the beam leaving the resonator with small smoothing of the edge). The applicability of the opticogeometric approximation in turn indicates that the operation of the laser will be reliably realized on one transverse mode. Actually, the condition of steady-state lasing on the fundamental mode has the form $\gamma = K(0)\rho(0)/|M|^P = 1$ (see (11), (15a)). Hence it follows that the amplification coefficient of the medium on the system axis for any intensity and distribution of the pumping in the free lasing mode is equal to $|M|^P/\rho(0)$, which in accordance with the same formula (15a) is appreciably less than the amplification coefficient required for excitation of the other modes. Thus, the lasing regime can cease to be unimodal only in the presence of such large disturbances that the formulas (14), (15) become inapplicable even for the lowest modes. A special case of such disturbances is, as we have seen, the presence of an ideally sharp and exactly outlined edge of the mirrors.

All of these problems pertaining to edge effects in unstable resonators are of unquestioned cognitive interest. However, from the practical point of view in itself the problem of degeneration of the modes with respect to losses is not so important as can be demonstrated. From the numerical calculations performed in [157, 153, 162] and other papers, it follows that for small N_{equiv} the degenerate modes correspond in practice to the same angular radiation distribution, especially in the case of nontransparent mirrors, although only the outer part of the beam will exit from the resonator (see also Figure 3.11). With an increase in N_{equiv}, the fields of the highest Q oscillations, independently of the presence or absence of degeneration, differ less and less from the spherical wave field of the geometric approximation undergoing single diffraction on the mirror aperture. In addition, even for an ideally sharp edge if N_{equiv} is sufficiently large these differences are of an almost irregular nature (Figure 3.16). Thus, degeneration cannot be essentially felt in the angular divergence of the radiation, and it is undesirable only when constructing single-frequency lasers.

If the transverse dimensions of the cross section of the active medium are so small that N_{equiv} cannot exceed a few units, for achievement of the single-frequency lasing it is possible to select, in accordance with Siegman's recommendations [167], resonator parameters such that N_{equiv} will be close to the a half-integer. In this case the difference of the losses of the two highest

APPROVED FOR RELEASE: 2007/02/09: CIA-RDP82-00850R000500010010-4

APPROVED FOR RELEASE: 2007/02/09: CIA-RDP82-00850R000500010010-4

Q modes turns out to be comparatively large even for a sharp edge (see Figure 3.12). It is only necessary to consider that the field distribution in the resonators with small N_{equiv}, as a rule, is highly nonuniform, which prevents the achievement of the maximum high output parameters of the lasers (for more information see Sections 1.4, 4.1).

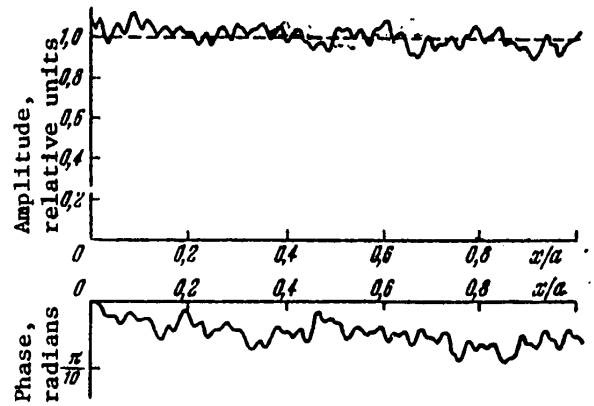

Figure 3.16. Amplitude and phase distribution of the basic mode of a two-dimensional resonator for $N_{equiv} = 30$, $M = 2.38$ [166].

In conclusion let us note that the above-discussed arguments were basically stated in [151, 154], and with minimum corrections, they are confirmed by the results of the numerical calculations in [166, 163, 338]. Thus, the problem of suppression of nonuniformity of the field distribution occurring as a result of the edge diffraction, first acquired urgency and found theoretical solution as applied to the problem of optical resonators. Some time later the same problem arose for the creators of powerful laser amplifiers. The fact is that when the density of the amplified radiation approaches the self-focusing threshold occurring under the effect of any factors the nonuniformity of the distribution can lead to the fact that at any point this threshold will be exceeded, and the active element damaged. One such factor can be edge diffraction; for suppression of its effect, the same procedures in essence were used as were discussed in [151] (the so-called anodizing of the aperture).

FOR OFFICIAL USE ONLY

APPROVED FOR RELEASE: 2007/02/09: CIA-RDP82-00850R000500010010-4

APPROVED FOR RELEASE: 2007/02/09: CIA-RDP82-00850R000500010010-4

§3.4. Unstable Resonators with Central Coupling Aperture

Initial Premises. Oscillations of a Two-Dimensional Resonator That Have a Caustic. An important property of unstable resonators is the fact that in them the emission somehow "spreads" from the central segment of the cross section (see Figure 3.6). As a result of this, the possibility appears for controlling the operation of the laser as a whole by influencing the indicated segment. In the last chapter there will be a discussion of amplifiers and lasers based on the given principle. Their characteristics are determined to a great extent by how efficiently control is realized; the latter, in turn, depends on to what degree the self-excitation threshold of the laser with an unstable resonator rises with shielding of the central segment of its cross section.

This section of the book is devoted to a theoretical analysis of the properties of unstable resonators with shielded central segment of the cross section or aperture in one of the mirrors which usually is called the coupling aperture. This analysis not only leads to useful practical conclusions, but also forces us to discuss a number of important items of the diffraction theory of unstable resonators in more detail which were discussed inadequately in the preceding section of the book. Some information which we shall use later can theoretically be extracted from the already quoted article [163]. However, in our discussion we shall fully adhere to reference [168] which was specially devoted to resonators with coupling aperture and was published almost simultaneously.

In reference [168] the question was investigated quite completely and consistently. It is impossible in practice to find exact solutions for an unstable resonator with coupling aperture in analytical form; therefore we shall limit ourselves to approximate estimates. The performance of these estimates can to a significant degree be based on analyzing the behavior of the eigenfunctions of the resonator without an aperture. The fact is that, as will be obvious later, among these functions there are those for which the field amplitude in some region adjacent to the resonator axis is negligibly small. With an increase in dimensions of the indicated region, the eigenvalues decrease (that is, the losses of the corresponding modes increase).

Inasmuch as the presence of a disturbance in the zone of a negligibly small field must not have significant influence on the field distribution as a whole, it is possible to talk about the existence of a class of functions which almost coincide in resonators with and without an aperture. Among them, the function in which the dimensions of the small-field region approximately coincide with the dimensions of the introduced aperture has the maximum eigenvalue. It is natural to assume that the given function also corresponds to the highest-Q mode of the resonator with aperture; then it will be obvious that this assumption is entirely justified.

Let us proceed with an analysis, which as we have already mentioned, can be made by the Vaynshteyn method. First let us consider the case of a symmetric two-dimensional resonator formed by two convex cylindrical mirrors.

In accordance with the Vaynshteyn method, for construction of the solution in a resonator with finite mirrors, the eigenfunctions of a resonator made up of unlimited mirrors are used. As was demonstrated in [162], the eigenfunctions and

APPROVED FOR RELEASE: 2007/02/09: CIA-RDP82-00850R000500010010-4

APPROVED FOR RELEASE: 2007/02/09: CIA-RDP82-00850R000500010010-4

eigenvalues of the integral equation of a resonator made of convex cylindrical mirrors of infinite dimensions have the form

$$F_\nu(\eta) = D_\nu\left(\pm e^{-i\pi/4}\eta\right), \tag{16}$$

$$\gamma_\nu = M^{-\left(\nu+\frac{1}{2}\right)}, \tag{17}$$

where $\eta \equiv \sqrt{4\pi N_{equiv}}x/a$ is a dimensionless coordinate, D_ν is the Weber function, and the index ν can assume an arbitrary complex value.

It is known that functions of the type of (16) satisfy the differential equation

$$\frac{d^2F_\nu(\eta)}{d\eta^2} + \left[\frac{\eta^2}{4} - \left(\nu + \frac{1}{2}\right)i\right]F_\nu(\eta) = 0 \tag{18}$$

and in the general case they describe a set of three waves. One of them, converging, is propagated in the direction of the resonator axis (depending on the sign of the argument D_ν in (16), from the larger positive or negative η direction); then it partially travels through the central region, partially is reflected from it and at the same time starts two expanding waves which spread in different directions from the resonator axis. For Im $\nu>0$, the greater part of the emission passes through the central zone of the resonator; for Im $\nu<0$, on the contrary, the radiation is basically reflected in the opposite direction.

We are interested in the latter case; when investigating the latter case, it is convenient to use the concept of a caustic surface, from which reflection is realized. Analysis shows that although the caustic here is greatly "diffused," for determinacy it can be considered to be located where $\mathrm{Re}[\eta^2/\underline{r-(}\nu+1/2)i]$ changes sign, that is, it can be assigned the coordinate $\eta_0(\nu)=\pm 2\sqrt{-\mathrm{Im}\nu}$. Hence, we have the following formula for the equivalent Fresnel number in the dimension of the zone next to the axis encompassed by the caustic:

$$N^0_{\text{экв}}(\nu) = -\mathrm{Im}\,\nu/\pi. \tag{19}$$

(1)

Key: 1. equiv

The indicated zone bounded by the points $\pm\eta_0$ is an analog of the potential barrier in quantum mechanics. With an increase in barrier width, that is, with an increase in $-\mathrm{Im}\,\nu$, the fraction of the emission passing through the barrier decreases rapidly. Estimates show that even for $-\mathrm{Im}\,\nu \geq 0.3$, the intensity of the diverging wave in the other half of the resonator will become negligibly small, and the modulus of the reflection coefficient from the caustic is in practice equal to one.

If the value of Im ν gives the position of the caustic, then the value of Re ν, in turn, defines the nature of variation of the amplitudes of all the waves at a noticeable distance from the caustic, and also, as follows from (17), the magnitude of the diffraction losses

$$1 - |\gamma_\nu|^2 = 1 - M^{-(2\mathrm{Re}\,\nu+1)}. \tag{20}$$

APPROVED FOR RELEASE: 2007/02/09: CIA-RDP82-00850R000500010010-4

APPROVED FOR RELEASE: 2007/02/09: CIA-RDP82-00850R000500010010-4

In the above-investigated solutions for a resonator with infinite mirrors, the source of the converging wave is located at infinity; the amplitude of this wave is uniquely related to the amplitude of the diverging wave reflected from the caustic only near the caustic itself. Far from the resonator axis, these waves do not interact, any ratio of their amplitudes is admissible, which gives rise to the arbitrariness in selecting ν.

On transition to a resonator with mirrors of finite dimensions, the situation changes. Upon hitting the edge of the mirror, the diverging wave undergoes diffraction scattering and, as we already know, generates a number of waves with different propagation directions. Among these waves there is a "reflected" wave -- a converging wave described by the same Weber function. For reasons which now should be entirely clear, this wave plays an especially important role. The remaining ("transformed") waves can be neglected in the first approximation; quantitative arguments in favor of this will be presented later.

Inasmuch as the only source of a converging wave in an empty resonator with mirrors of finite dimensions can be diffraction scattering of the diverging wave, the amplitudes of these waves turn out to be interrelated not only near the resonator axis, but at the edge of the mirrors. Their ratio near the edge must equal the reflection coefficient from the edge R_{refl} known to us from §2.2, which in accordance with the Vaynshteyn method can be calculated by an independent method [3, 162].

Analyzing the properties of resonators with coupling aperture, we shall limit ourselves to an investigation of oscillations with $-\mathrm{Im}\,\nu>0.3$ ($N_{equiv}(\nu)>0.1$), for which the resonator essentially breaks down into two independent halves. This greatly simplifies the calculations by comparison with the case of the highest-Q modes of ordinary unstable resonators, for which $|\mathrm{Im}\,\nu|$ is small, and the oscillations in both halves of the resonator are interrelated (let us note that for this reason the lowest symmetric modes which describe the synchronous oscillations in both halves of the resonator which sharply "make each other up," have significantly lower losses than all the remaining modes, including the lowest antisymmetric mode [162]).

Simplification of the calculations for caustics noticeably removed from the axis is also promoted by the fact that the diverging and converging waves W_1 and W_2 are described highly exactly in this case by the solutions of equation (18) in the VKB-approximation:

$$W_{1,2}(\eta)\sim\left[\frac{\eta^2}{4}-\left(\nu+\frac{1}{2}\right)i\right]^{-\frac{1}{4}}\exp\left\{\pm i\int_{\eta_0}^{\eta}\sqrt{\frac{\eta'^2}{4}-\left(\nu+\frac{1}{2}\right)i}\,d\eta'\right\}; \tag{21}$$

the boundary conditions have the form

$$\underset{(1)}{W_1(\eta_0)=R'_{\text{отр}}W_2(\eta_0)},\quad \underset{(2)}{W_2(\eta_{\text{кр}})=R''_{\text{отр}}W_1(\eta_{\text{кр}})}, \tag{22}$$

Key: 1. reflected; 2. edge

APPROVED FOR RELEASE: 2007/02/09: CIA-RDP82-00850R000500010010-4

APPROVED FOR RELEASE: 2007/02/09: CIA-RDP82-00850R000500010010-4

where R'_{refl} is the reflection coefficient from the caustic ($|R'_{refl}|=1$), η_{edge} is the dimensionless coordinate of the edge of the mirror. Let us note that in the general case the waves W_1 and W_2 are not spherical, although for small $|\nu|$ they are similar to the diverging and converging waves of the geometric approximation.

Substitution of (21) in (22) leads to the following equation for determining ν:

$$R'_{\text{отр}} R_{\text{отр}} \exp\left\{2i \int_{\eta_0}^{\eta_{\text{кр}}} \sqrt{\frac{\eta'^2}{4} - \left(\nu + \frac{1}{2}\right)} i \, d\eta'\right\} = 1. \tag{23}$$

Equation (23) is satisfied by a discrete series of values of ν; each of them corresponds to its own mode. It is possible to demonstrate that in the case of large mirrors ($N_{equiv} \gg 1$) and oscillations with caustics not too removed from the axis ($N^0_{equiv} \ll N_{equiv}$) the following laws exist:

1. On transition to each mixed mode the value of N^0_{equiv} increases by approximately $2/(\ln 4\pi N_{equiv})$, so that the caustics of the possible oscillations are located on the mirror surface very frequently, especially at a noticeable distance from the resonator axis.

2. The value of $|\gamma|$ directly determining the diffraction losses (see (20)) is related to the position of the caustic of the given mode $\eta_0 = \sqrt{4\pi N^0_{equiv}}$ by the approximate relationship

$$\ln|\gamma| = \frac{\ln M \ln|R^{(1)}_{\text{отр}}|}{1 + \ln\left|4\pi N_{\underset{(2)}{\text{экв}}} / \sqrt{(\pi N^0_{\underset{(2)}{\text{экв}}})^2 + \bar{1}}\right|}. \tag{24}$$

Key: 1. refl; 2. equiv

Now, in accordance with the arguments discussed at the beginning of this section, it is possible to trace how the losses of the lowest mode of a two-dimensional unstable resonator must vary as the dimensions of the introduced coupling aperture increase.

Two-Dimensional Resonator with Central Aperture. In a resonator without an aperture, as is known, the lowest symmetric mode has the greatest Q-factor. Its losses are similar to the value of 1-1/M predicted by the geometric approximation (see §3.3). On introduction of an aperture (more precisely, a slit) with small width corresponding to $N^0_{equiv}=0.1$, the resonator is broken down into two weakly connected halves, and the losses increase sharply to a value characteristic of the lowest antisymmetric oscillations. As the dimensions of the aperture of the lowest mode of such a resonator increase, the modes with caustics more and more remote from the center must grow alternately. Inasmuch as the spectrum of these modes is quite dense for large N_{equiv}, in the first approximation it is possible to neglect the "stepped nature" of the increase in the losses and consider that the formula (24) is valid for any N^0_{equiv} satisfying the condition $0.1 \leq N^0_{equiv} \ll N_{equiv}$. The value of N^0_{equiv} now acquires the meaning of the equivalent Fresnel number in the aperture dimensions.

APPROVED FOR RELEASE: 2007/02/09: CIA-RDP82-00850R000500010010-4

APPROVED FOR RELEASE: 2007/02/09: CIA-RDP82-00850R000500010010-4

The correctness of the adopted model was checked in the same paper [168] by performing numerical calculations on a computer by the Fox-Li method. Among the results of these calculations, the dependence of the losses of the lowest symmetric (that is, highest-Q) modes of the resonator with aperture on the aperture dimensions is of the greatest interest. An example of such a relation for the case of a sharply outlined edge of the mirrors, $M=2.38$ and $N_{equiv}=29.4$ is presented in Figure 3.17 (the solid curve). The dotted curve calculated by formula (24) on substitution of the following value in it is plotted on the same figure:

$$\underset{(1)}{|R_{\text{отр}}|} \approx \underset{(2)}{[2\pi N_{\text{экв}}(M-1/M)]^{-1}}. \tag{25}$$

Key: 1. refl; 2. equiv

The given expression for the coefficient of diffraction reflection from a sharply outlined mirror edge can be obtained from the corresponding formula of reference [3], and it is again valid on satisfaction of the conditions $N^0_{equiv} \ll N_{equiv}$ and $N_{equiv} \gg 1$ (see also [162]).

As follows from Figure 3.17, the behavior of the lowest modes of a resonator with aperture corresponds entirely to the developed concepts (at least in the case of a sharply outlined mirror edge). The presence of an aperture with $N^0_{equiv} \simeq 0.1$ causes growth of the losses to the value of $\sim(1-1/M^2)$ predicted by formulas (20), (24), (25) (it is easy to see that for $N_{equiv} \gg 1$, small N^0_{equiv} and $2 \lesssim M \lesssim 5$

$$\ln \frac{1}{\underset{(1)}{2\pi N_{\text{экв}}}(M-1/M)} \left[\ln \frac{4\pi N_{\text{экв}}}{\sqrt{(\underset{(1)}{\pi N^0_{\text{экв}}})^2+1}} + 1 \right]^{-1} \approx -1,$$

Key: 1. equiv

from which it follows that $|\gamma| \simeq 1/m$). As numerical calculations have demonstrated, the losses of the lowest antisymmetric and symmetric modes begin to coincide for such N^0_{equiv}.

After sharp initial increase in the losses, a further increase in aperture dimensions accompanied by comparatively slow growth of the losses which is described satisfactorily by formula (24). At the break points of the solid curve alternation of the highest-Q modes takes place. The mode switching process is analogous to the one observed with an increase in the mirror dimensions of an unstable resonator without aperture (see Figure 3.12): the modes at the switching points are degenerate with respect to losses, but they are distinguished by the field configuration.

Let us note that the differences between the solid and dotted curves in Figure 3.17 are essentially of a random nature, for the location of the pulsations on the solid curve varies with variation of N_{equiv}.

Now let us consider how the properties of a two-dimensional unstable resonator vary with the central coupling aperture when smoothing the edge of the mirrors (see the preceding section). The presence of smoothing leads to a decrease in amplitudes of

APPROVED FOR RELEASE: 2007/02/09: CIA-RDP82-00850R000500010010-4

APPROVED FOR RELEASE: 2007/02/09: CIA-RDP82-00850R000500010010-4

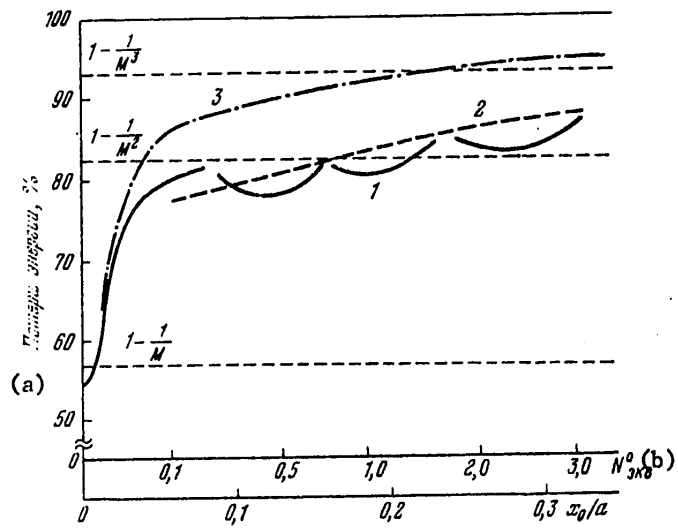

Figure 3.17. Lowest mode losses as a function of the size of the coupling aperture (two-dimensional resonator, M=2.38, N_{equiv}=29.4): 1 -- calculation of the losses of symmetric modes on a computer, 2 -- calculation by formulas (24), (25), 3 -- calculation by formula (24) in the case of a partially smoothed edge; $|R_{refl}|$ decreased by tenfold.

Key:

a. Energy losses, %

b. N^0_{equiv}

the scattered waves reduced on the edge, in particular, to a decrease in $|R_{refl}|$. Whereas this is felt very little in the magnitude of the losses of the highest-Q oscillations in resonators without apertures (they only become closer to a value of 1-1/M predicted by the geometric approximation), the losses in a resonator with aperture with edge smoothing increase significantly according to (24). Therefore in the graph of the losses as a function of the magnitude of the introduced aperture, the initial segment of the curve becomes still steeper (the dash-dotted curve in Figure 3.17); as the degree of smoothness of the edge increases, the steepness of this section continues to grow.

The numerical calculations performed in [168] demonstrated that the process of variation of the losses as the edge is smoothed is described satisfactorily by formula (24) while the width of the smoothing zone remains significantly less than the total mirror width. From the derivation of this formula it is obvious that in this case when the "edge" is extended to the greater part of the mirror, the developed approximation ceases to be applicable. In order to estimate to what values the losses can theoretically build in this case, let us consider the case of a resonator with ideally smoothed edge investigated in the preceding section, the mirrors of which have gaussian distribution of the amplitude coefficient of reflection ρ with respect to cross section ($\rho(x)=\exp(-2x^2/a^2)$). Let us remember that the field distributions of the various modes in the greater part of the cross section of such a resonator are described by the functions

APPROVED FOR RELEASE: 2007/02/09: CIA-RDP82-00850R000500010010-4

APPROVED FOR RELEASE: 2007/02/09: CIA-RDP82-00850R000500010010-4

$$u_m(x) \sim \exp\left(-\frac{2}{M^2-1}\frac{x^2}{a^2}\right)\left(\frac{x}{a}\right)^m, \quad m = 0, 1, 2, \ldots, \tag{26}$$

which are solutions of the equation of an unstable resonator in the optical-geometric approximation (9).

If the geometric approximations were completely valid, the presence of a central aperture of any size would automatically lead to equality of the field amplitude to zero over the entire resonator cross section, that is, to the absence of solutions. However, near the resonator axis the mode fields with $m \geq 2$ vary with respect to their relative intensity so critically that the geometric approximation ceases to be applicable (the condition (10) is not satisfied). This also leads in the final analysis to the fact that exact solutions of the diffraction approximation (14) include the Hermite polynomials as factors and not $(x/a)^m$. Inasmuch as they also contain lower order terms, it turns out that exact solutions with $m \geq 2$ in some zone adjacent to the axis have additional phase shift (Figure 3.10, b) and significantly greater amplitude than would be expected from (26) (although with respect to absolute magnitude it is less than the amplitude in segments of the cross section more removed from the axis).

If we investigate the mechanism of self-imaging of a steady-state field distribution using the Huygens-Fresnel principle, it is possible to see that as a result of diffraction the primary contribution to the field amplitude in the vicinity of the anomaly does not give a central segment as would be expected from the geometric approximation, but more intense peripheral parts of the beam. Accordingly, shielding the central segment in one of the mirrors should not lead to noticeable alteration of the field distribution in the other, and the admissible coupling aperture dimensions can be identical with the dimensions of the anomaly zone. It only remains to relate these dimensions to the magnitude of the losses of the corresponding modes. Having done this, we arrive at the following formula:

$$|\gamma(N^0_{\text{экв}})| \approx M^{-\left(\sqrt{8\pi N^0_{\text{экв}}}+1\right)}, \quad N^0_{\text{экв}} > 0{,}1. \tag{27}$$
(1) (1)

Key: 1. equiv

It is true that inasmuch as in the case of a resonator with gaussian mirrors the anomaly zone does not have clear boundaries of the caustic type, some arbitrariness is permissible in defining its dimensions. For this and other reasons, formula (27) is of an approximate nature, but the conclusion derived from it regarding extraordinarily large losses in resonators with gaussian mirrors and central aperture is indisputable.

Three-Dimensional Resonator with Coupling Aperture. Discussion of Results.
Let us proceed to the case of a resonator with spherical mirrors that is of practical importance. By using calculations analogous to those performed earlier, it is possible to see that for axisymmetric solutions in a three-dimensional resonator with circular mirrors and coupling apertures the same approximate formula (24) is valid as for a two-dimensional resonator. The formulas for R_{refl} in the two-dimensional and three-dimensional cases also coincide, and the losses in the two

APPROVED FOR RELEASE: 2007/02/09: CIA-RDP82-00850R000500010010-4

APPROVED FOR RELEASE: 2007/02/09: CIA-RDP82-00850R000500010010-4

and three-dimensional resonators with the same N_{equiv}, N^0_{equiv} (>0.1), M and identical nature of the edge of the mirror turn out to be identical. At the same time, the losses in a three-dimensional resonator without aperture amount to $\sim 1-1/M^2$ and greatly exceed the losses in the analogous two-dimensional resonator close to 1-1/M. Accordingly, introduction of a small aperture in a three-dimensional resonator does not lead to such a sharp increase in losses as in the two-dimensional resonator (Figure 3.18). The causes of the differences in behavior of the resonators with cylindrical and spherical mirrors become clear if we consider that the presence of an aperture in the two-dimensional case (that is, slits and a cylindrical mirror) led to breakdown of the resonator into two noninteracting parts. In the three-dimensional case, just as fast an increase in losses must be observed on introduction of a system of two mutually perpendicular slits breaking up the mirror into four parts instead of a circular aperture (it is with this system of slits and not with a square aperture that the variables in the problem of a resonator with square mirrors are separated).

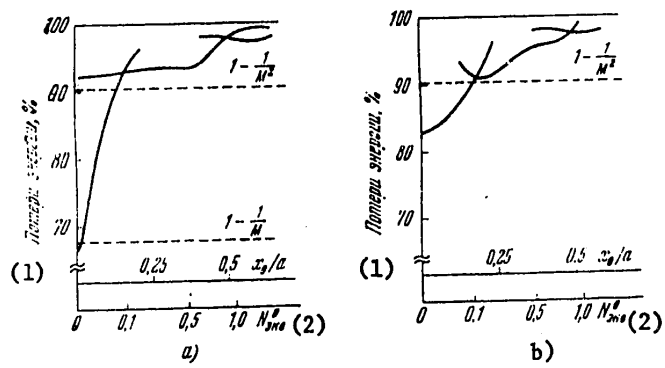

Figure 3.18. Losses of the lowest symmetric modes as a function of the size of the coupling aperture in the case of a sharp mirror edge (M=3.3, N_{equiv}=3.59): a) two-dimensional resonator, b) three-dimensional resonator with circular mirrors

Key:
1. Energy losses, %
2. N^0_{equiv}

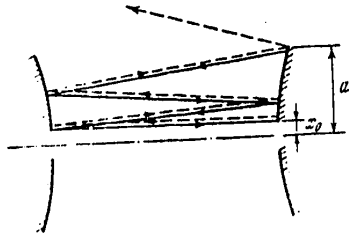

Figure 3.19. Path of beams in an unstable resonator with coupling aperture

APPROVED FOR RELEASE: 2007/02/09: CIA-RDP82-00850R000500010010-4

APPROVED FOR RELEASE: 2007/02/09: CIA-RDP82-00850R000500010010-4

Let us also explain the causes of approximate coincidence of losses in two-dimensional and three-dimensional resonators with apertures of sufficiently large size. For this purpose we shall use the not very strict, but very descriptive "semigeometric" approximation, the essence of which consists in the fact that the beam path inside the resonator is considered purely geometrically, and the coefficient of "reflection" from the edge is taken from diffraction theory. Accordingly, let us approximately construct the beam trajectory which, following from the edge of the mirror and alternately being reflected from both mirrors, approaches the resonator axis until it hits the surface of one of the mirrors near the edge of the aperture normally, after which it returns along the same path as shown in Figure 3.19. Using the current formulas of geometric optics (3), it is possible to find the expression that relates the number of passes of the beam between the mirrors n along its path from the edge of the mirror to the boundary of the aperture with mirror dimension a and hole size x_0: $x_0/a=2M^n/(M^{2n}+1)$. For $(x_0/a^2=N^0_{equiv}/N_{equiv}<<1$, we have $n\simeq\ln(4N_{equiv}/N^0_{equiv})/2\ \ln M$.

After every 2n passes, the beam hits the edge of the mirror, where it is reflected back with a reflection factor $|R_{refl}|$. If we consider that the damping process in the resonator takes places continuously and the amplitude varies with respect to modulus by $|\gamma|$ times during one pass, it is possible to write the equality $|\gamma|^{2n}=|R_{refl}|$ from which

$$\ln|\gamma| = \frac{\ln|R^{(1)}_{\text{отр}}|}{2n} = \frac{\ln|R_{\text{отр}}|\cdot\ln M}{\ln\left(4N_{\text{экв}}/N^0_{\text{экв}}\right)}. \qquad (28)$$

(2)

Key: 1. refl; 2. equiv

For $0.3<N^0_{equiv}<<N_{equiv}$, this formula in practice coincides with (24). All of the calculations performed when deriving it, and indeed, the path of the beams in two-dimensional and three-dimensional axisymmetric cases do not differ in any way (see Figure 3.19); therefore the final result is, of course, identical.

The semigeometric approximation also helps to understand why when analyzing the diffraction scattering of a diverging wave on the edge of the mirror it is possible in the first approximation to neglect all of the stimulated waves except the reflected wave having a caustic near the edge of the aperture. The fact is that the remaining waves either go farther to the center and exit from the resonator through the aperture or, on the contrary, they have caustics more removed from the resonator axis. The latter corresponds to smaller numbers of passes n and, consequently, a smaller lifetime of the emission in the resonator. Estimates show that the influence of these waves must be taken into account by multiplying $|R_{refl}|$ by a factor somewhat larger than one, but the logarithm of this factor is small by comparison with the logarithm of $|R_{refl}|$ itself, and the value of $|\gamma|$ calculated by formula [28] varies little. The results of machine calculations (see Fig 3.17) also indicate that the above-discussed approximation insures reliable accuracy for practical requirements.

It remains only to extend the results obtained in this section to the most important case of asymmetric resonators in practice. From the principle of equivalence (§3.3) it follows directly that the losses on a double pass of an asymmetric resonator with aperture in the exit mirror are exactly equal to the losses for a

APPROVED FOR RELEASE: 2007/02/09: CIA-RDP82-00850R000500010010-4

APPROVED FOR RELEASE: 2007/02/09: CIA-RDP82-00850R000500010010-4

symmetric resonator with the same values of N_{equiv}, N^0_{equiv} and the magnification M on one pass.

Other versions of the location of the coupling aperture are also possible. Thus, its functions can be performed by a small tilted mirror installed between the mirrors on the system axis (or a prism), which is an opaque screen for the main resonator. As indicated in §3.2, the magnitude of the parameter N^0_{equiv} corresponding to the sizes of this screen must be determined by the distance between equiphasal surfaces of spherical waves of the geometric approximation propagated in opposite directions (Figure 3.20). In particular, for the telescopic resonator, the corresponding formula has the form $N^0_{equiv} = x_0^2/2\lambda z$, where z is the distance from the screen to the common focal point of the mirrors.

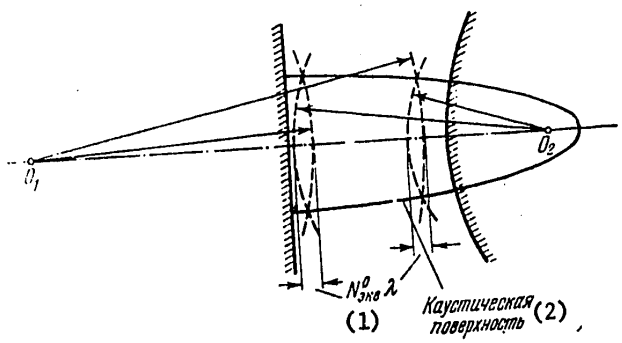

Figure 3.20. Problem of the value of N^0_{equiv} for various positions of the screen

Key:
1. N^0_{equiv}
2. Caustic surface

Analysis shows that the screens installed in different segments of length of the resonator but having equal N^0_{equiv} "rest" on the same caustic surface of the resonator (Figure 3.20), and therefore must have approximately the same influence on the magnitude of the losses. Hence, it follows that formulas (20), (24) are directly applicable for calculating the losses on a complete pass of the resonator with arbitrarily arranged screen or aperture.

Our theoretical investigation of systems with a central coupling aperture ends with this. These systems are perhaps the only version of unstable resonators for which the Vaynshteyn method leads to visible results even in the presence of a sharp edge. The oscillation pattern in resonators without a central aperture is much more complicated (we mentioned the causes for this at the beginning of this section). The cases where mirrors, in addition to everything else, are arranged asymmetrically with respect to the optical axis are especially difficult for analysis. The only effort to solve such a problem by the Vaynshteyn method was undertaken in [169]; the authors of the indicated paper were able to obtain reasonable results for two-dimensional resonators with a sharp edge, the mirrors of which on different sides of the axis have unequal N_{equiv}. If one of the two

APPROVED FOR RELEASE: 2007/02/09: CIA-RDP82-00850R000500010010-4

APPROVED FOR RELEASE: 2007/02/09: CIA-RDP82-00850R000500010010-4

values of N_{equiv} is sufficiently large and the other decreases gradually, the losses oscillate around the value predicted by the geometric approximation. This takes place until the smaller N_{equiv} reaches values of ~0.3; beginning at that point, further approximation of the edge to the axis causes monotonic growth of the losses. When the edge goes around the other side from the axis so that the latter ceases to intersect the mirror, the losses continue to increase. Finally, when the edge, moving in the former direction, goes beyond the axis so that N_{equiv} (measured on the other side) reaches ~0.3, the differences between the solutions for such a resonator and the above-investigated resonators with comparatively large central apertures disappear (let us remember that the oscillations in the different "halves" of resonators with apertures were considered independent of each other). Those desiring to become familiar in detail with the mathematical aspects of the matter are referred to [162, 163, 169]; unfortunately, the authors of the indicated articles use a set of parameters and notation system differing sharply from those used in the literature on unstable resonators, which greatly complicates the reading.

§3.5. Some Properties of Multimirror and Prism Unstable Resonators

In this section and the sections that follow, a number of interesting possibilities will be investigated which are connected with using unstable resonators including more than two mirror-reflecting surfaces. This gives us reason to discuss several problems which are of common interest and we did not touch on earlier. First of all, these include the problem of achievement of the unidirectional lasing mode in ring systems and the problem of the emission polarization state in anisotropic resonators. In addition, a study will be made of the properties of special layouts of unstable resonators with reduced sensitivity to aberrations and with maximum compact form of the exit aperture.

Problem of Monodirectional Lasing Mode. In a number of cases it is necessary that the entire stimulated emission flux pass through the ring cavity in only one of the two possible directions. As was pointed out in §2.4, this mode, which is called monodirectional (or the traveling wave mode) is useful, in particular, for achievement of a lasing spectrum that is as narrow as possible: the modulation of the intensity along the resonator axis, which is usually one of the causes of multifrequency lasing is absent here. In order to achieve the traveling wave mode, most frequently the so-called nonmutual filters are used. A number of transformations of the polarization state are realized in them (using a Faraday cup and other elements) such that the losses for the two directions of passage through the resonator turn out to be equal (see, for example, reference [87] which was cited in §2.4). More rarely, an additional mirror is installed behind the semitransparent mirror of the ring cavity for the same purposes as illustrated in Figure 3.21, a (for example, [170]). This leads to "pumping" of the emission going in the direction indicated by the dotted arrows into the wave with opposite direction of passage. Both methods insure very high degree of monodirectionality (that is, a high ratio of wave intensities with different directions of passage).

APPROVED FOR RELEASE: 2007/02/09: CIA-RDP82-00850R000500010010-4

APPROVED FOR RELEASE: 2007/02/09: CIA-RDP82-00850R000500010010-4

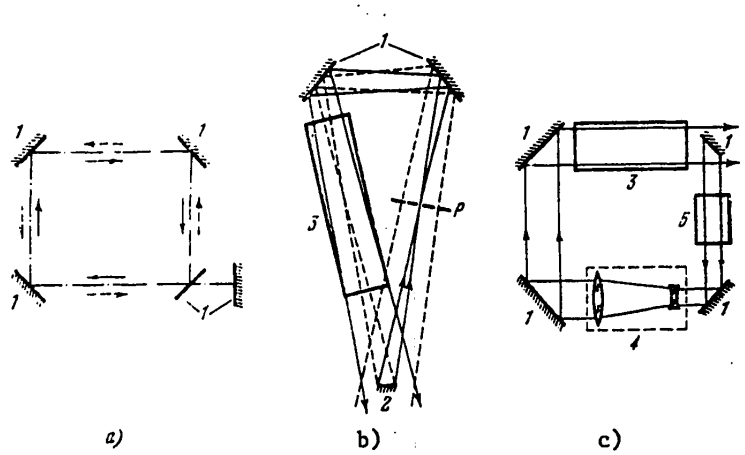

Figure 3.21. Ring cavities: a) flat cavity with additional mirror; b), c) unstable ring cavities; 1 -- flat mirror, 2 -- concave mirror, 3 -- active element, 4 -- telescope, 5 -- angle selector

Some peculiarities of unstable resonators have pointed to the idea that the arsenal of means for achieving the traveling wave can be supplemented with their help. The fact is that in resonators used earlier with small diffraction losses, the path of the beams is in the first approximation reversible (see §5.3 about conjugate waves); hence, it follows that the volumes of the waves propagated in opposite directions coincide. In unstable resonators, as a result of the large diffraction losses, the path of the beams is significantly irreversible (this is indicated at least by the fact that the lasing cannot be realized on one converging wave). As a result, as is obvious from Figure 3.21, b, waves with opposite directions of passage can fill the active medium quite differently.

In reference [152] the seemingly obvious argument was stated that the installation of an iris with small aperture at the "neck" of one of the waves (the plane P in Figure 3.21, b) should completely suppress the wave going in the opposite direction. The diagram of a telescopic ring cavity with emission angle selector presented in Figure 3.21, c is equivalent to the diagram in Figure 3.21, b (the iris with small aperture at the "neck" is one of the versions of angle selectors; see §2.6) and also apparently insures monodirectionality of the mode. Let us consider this situation in more detail in accordance with [171].

The diagram depicted in Figure 3.21, b with an iris installed in the P plane corresponds to the optical line presented in Figure 3.22. The symmetry of the lens with focal length f=R/2 corresponds to the surface of a concave mirror with radius of curvature R (in order for it to be possible to neglect the astigmatism occurring in the case of oblique incidence of the beam on the spherical mirror, it is necessary to insure a very small angle of incidence, as illustrated in the figure or replace the concave mirror by a flat mirror with a positive lens installed nearby). The small iris aperture is matched with the center of the spherical wave which is the solution in the geometric approximation. Thus, the planes of two adjacent irises are conjugate with respect to the lens placed between them and

APPROVED FOR RELEASE: 2007/02/09: CIA-RDP82-00850R000500010010-4

APPROVED FOR RELEASE: 2007/02/09: CIA-RDP82-00850R000500010010-4

are at distances of $\ell_{1,2}=(L/2)(1\pm\sqrt{1-4f/L}$ from it, where L is the period of the line (the total length of the resonator).

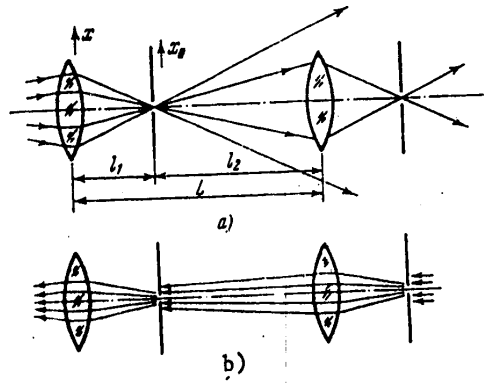

Figure 3.22. Optical line equivalent to a resonator in Figure 3.21, b: a) beam path for the Type I wave; b) beam path for Type II wave.

Let us limit ourselves to an investigation of the two-dimensional case. Here it is impossible to use the beam matrix of a complete round trip through the resonator to compile the integral equation inasmuch as the beam cross section is limited by, in addition to the exit mirror, one element -- the aperture in the iris (§1.2). Therefore it is necessary to express the distributions in the aperture of the adjacent lens and in the plane of the next iris successively in terms of the field distribution F(x) in the plane of one of the irises. Carrying out this standard procedure and integrating over the lens surface, we obtain the following equation for finding the steady-state field distribution of a wave propagated along the line from left to right (a type I wave):

$$\gamma F_{\mathrm{I}}(y)=\frac{1}{\sqrt{|M|}}\int_{-1}^{1}K(y,y')F_{\mathrm{I}}(y')\,dy', \tag{29}$$

where

$$K(y,y')=\frac{\sin\alpha\pi(y-y'/M)}{\pi(y-y'/M)}\times$$
$$\times\exp\left\{\frac{-ikb}{4f}\left[y^2\left(1+\sqrt{1-\frac{4f}{L}}\right)+y'^2\left(1-\sqrt{1-\frac{4f}{L}}\right)\right]\right\}.$$

Here the following notation is used: $y\equiv x/b$; 2b is the size of the iris aperture; $\alpha=b/b_0$, $b_0\equiv\ell_1\lambda/2a$, 2a is the transverse dimension of the lens (carrying out the analogy between the effect of the iris and the effect of the angle selector in the diagram in Figure 3.21, c, it is easy to see that α corresponds to the value of $\Delta\theta/(\lambda/2a)$, where $\Delta\theta$ is the pass band width of the selector); $M=-\ell_2/\ell_1=-(1+\sqrt{1-4f/L})/(1-\sqrt{1-4f/L}$ is the resonator magnification; finally, γ is the eigenvalue of the equation. The phase factor in front of the integral is omitted.

APPROVED FOR RELEASE: 2007/02/09: CIA-RDP82-00850R000500010010-4

APPROVED FOR RELEASE: 2007/02/09: CIA-RDP82-00850R000500010010-4

The analogous equation can be obtained also for distribution in the plane of the iris $F_{II}(y)$ of the field of the wave propagated along the line in the opposite direction (type II wave). It turns out that it differs from equation (29) only by the fact that the variables y and y' in the formulas for the kernel of the equation K change places. Such an equation is called associated with respect to (29); it is known that the associated equations have identical spectrum of eigenvalues [172]. Thus, waves with different directions of passage have the same diffraction losses. This law is of a universal nature and occurs in the case of any ring resonators without special "valve" devices of the type discussed above.

The given conclusion is at first glance paradoxical, especially as applied to the example investigated by us; therefore we shall continue the analysis and discover the spatial structure of the oscillations of interest to us.

For simplification of the calculations we shall consider the iris sufficiently small that the condition $kb^2/2f \ll 1$ is satisfied, which can be written in the form $a^2/\lambda L \gg \alpha^2/|M|$. Then the exponential factor in the formula for K can be omitted, and the kernel of the equation becomes real. It is possible to show that the equation for the field distribution $\phi_I(y_0)$ of the I type wave on a spherical equiphasal surface of the geometric solution located near the lens (plotted by the dotted line in Figure 3.22) simultaneously begins to coincide with the associated equation with respect to (29) for F_{II}, and the equation for the field distribution $\phi_{II}(y_0)$ of the type II wave on the same spherical surface, with the equation for F_I ($y_0 \equiv x_0/a$ is the dimensionless coordinate). Hence, it follows that the normalized distribution functions of the field amplitude on the lens and iris apertures corresponding to identical eigenvalues for waves propagated in different directions are pairwise equal: $F_I = \phi_{II}$, $F_{II} = \phi I$.

In the same paper [171], the iteration method was used to calculate the field distributions and eigenvalues γ_s and γ_a of the lowest symmetric and antisymmetric modes for a number of values of M and α. As always, it turned out that the antisymmetric mode has significantly greater losses; thus, for $M=3$ and $1 \leq \alpha \leq 5$ the values of $\gamma_s > 0.5$, $\gamma_a < 0.3$. Therefore the antisymmetric mode cannot participate explicitly in lasing, and hereafter we shall talk about only the lowest symmetric mode.

Calculations have demonstrated that with an increase in α, the eigenvalue γ_s approaches a value of $1/\sqrt{|M|}$ predicted by the geometric approximation, oscillating around it (without breaks characteristic of the dependence of the losses on N_{equiv} in the case of ordinary unstable resonators with a sharp edge, see Figure 3.12). The peaks of γ_s are located near the odd values of α; here the field amplitude ϕ_1 of the type I wave in the lens plane (and, correspondingly, the type II wave in the iris plane) decreases somewhat on going away from the resonator axis. For even α, the field increases to the periphery, γ_s is minimal; finally, for the half-integral α, the field distribution is almost uniform (Figure 3.23, a). With an increase in α the distribution becomes more uniform on the average.

At the same time, the type I and II waves are intense only in the central zones of the iris and lens, respectively. With an increase in α, the relative size of these zones decreases (Figure 3.23, b). Let us note that for fixed α with an increase in M the differences between the exact and geometric solutions decrease monotonically.

APPROVED FOR RELEASE: 2007/02/09: CIA-RDP82-00850R000500010010-4

APPROVED FOR RELEASE: 2007/02/09: CIA-RDP82-00850R000500010010-4

It is easy to see that the type I waves are close to the solutions in the usual unstable resonator (without an iris); the perturbation introduced by the iris decreases with an increase in α. The mechanism of their self-imaging is quite clear from Figure 3.22, a.

The mechanism of formation of the type II waves also permits graphical interpretation (Figure 3.22, b). The plane wave incident on the iris, as a result of diffraction, fills part of the lens. With an increase in the iris aperture, the diffraction angle and, with it, the region of intense exposure of the lens decreases. Here the finiteness of the lens dimensions turns out to be smaller and smaller, and the lens projects the emitting aperture on the plane of the other iris. with magnification $-\ell_2/\ell_1=M$, which leads to equality of losses for type I and II waves.

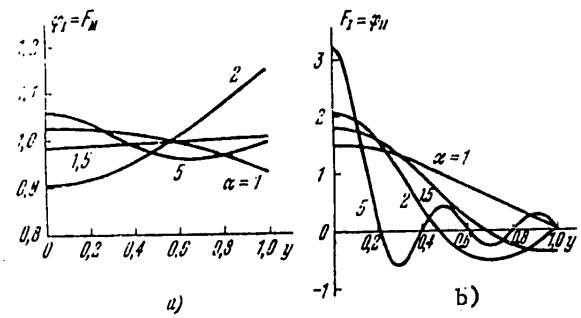

Figure 3.23. Field amplitude distribution in an unstable ring cavity for M=3 and different α

The situation for the resonators of the type of Figure 3.21, c is entirely analogous. The angular distribution in the selector corresponds to the emission distribution in the plane of the iris here.

Let us sum up the results. In unstable ring cavities with angle selection of the emission, complete monodirectionality is not achieved without taking additional measures: in addition to the waves with the desired direction of propagation there are also waves with opposite direction of passage through the resonator and the same losses. The emission of the first of them fills the entire resonator cross section; the losses in this case primarily are caused by the fact that part of the beam bypasses the mirror. The emission of the waves with opposite direction of propagation is intense only in the region with small transverse dimensions; the losses for them are caused predominantly by the fact that part of the emission is scattered on the selecting element (the iris, angle selector), but they have the former value. It is necessary to note that equality of the eigenvalues for these two types of waves follows from the most general properties of integral equations and cannot be violated even in the presence of a nonuniformly distributed inverse population.

It is true that it is possible to select the resonator parameters so that the ratio v of the volumes of the active medium filled with the wave emission with different directions of passage will be very large (as follows from Figure 3.21, b, the

APPROVED FOR RELEASE: 2007/02/09: CIA-RDP82-00850R000500010010-4

APPROVED FOR RELEASE: 2007/02/09: CIA-RDP82-00850R000500010010-4

value of $v_{-}M^2$ is insured even without selecting elements by simple selection of the location of the active sample [154]; this quite trivial possibility was also investigated in the much later paper [173] than [171, 154]). At the same time, significant magnitude of the ratio of the corresponding emission fluxes (of order 2v-1) is achieved. For certain applications this solution to the problem can be satisfactory, but achievement of single frequency, unfortunately, is not facilitated: indeed, in unstable resonators the emission spreads from the central segment of the cross section playing the role of the "master oscillator" (see Figure 3.6), and both waves are present there.

Completing the analysis of the unstable ring cavities with angle selection, let us note another interesting feature of them. The emission scattered at high angles is filtered by the angle selector; this is the fate, in particular, of the converging wave generated as a result of diffraction on the mirror edge. Therefore the given resonators even with sharp mirror edge behave similarly to the most usual (linear) ones with well "smoothed" edge; the proofs of this and discussion of the problem of optimal characteristics of the selector can be found in [174].

Stabilizing the Direction of Radiationin Prism Resonators. Now let us proceed from the problem of monodirectionality to analysis of the possibilities of creating resonators which are less sensitive with respect to the influence of intraresonator wave aberrations of lower order than the ordinary telescopic one. We have already encountered one type of them: in §3.2 it was demonstrated that a confocal unstable resonator made of two concave mirrors (see Figure 3.3, c) reacts weakly to odd-order aberrations as a result of the effect of "inversion" of the beam cross section. In spite of this valuable property, the practical use of a confocal resonator made of concave mirrors is frequently complicated as a result of extraordinary concentration of the emission at the common focal point of the mirrors. It is possible to get away from this deficiency and, at the same time, make use of the advantages accompanying inversion of the beam cross section by using totally internally reflecting prisms as the resonator elements (or two-sided or corner reflectors equivalent to them).

Two diagrams of such resonators which are of practical interest and were investigated in [175] are presented in Figure 3.24, a, b. They are both essentially diagrams of an ordinary telescopic resonator (Figure 3.24, c), for which one (the concave) or both mirrors are replaced by 90-degree prisms (we shall later discuss the peculiarities of such resonators following from whether the prisms are two-faced as depicted in the figure or triple prisms). The surfaces of these prisms turned toward the inside of the resonator are spherical; their radii of curvature are equal to $-(n-1)\ R_{1,2}$, where n is the index of refraction of the prism material, $R_{1,2}$ are the radii of curvature of the replaceable mirrors of the telescopic resonator. On passage through such prisms, the beam curvature is transformed just as on reflection from replaced mirrors, but the beam itself turns out to be inverted.

Analysis of the influence of aberrations on the resultant form of the wave front can be performed by the same method used in §3.2 for confocal unstable resonators with ordinary mirrors. Let us remember that the most descriptive result of the corresponding calculations is the magnitude of the aberration coefficients demonstrating how many times the presence of different types of wave aberrations is felt more strongly in the field distribution in the given unstable resonator than

APPROVED FOR RELEASE: 2007/02/09: CIA-RDP82-00850R000500010010-4

APPROVED FOR RELEASE: 2007/02/09: CIA-RDP82-00850R000500010010-4

in a single-pass amplifier (see formulas (6)). If, as in §3.2, we consider that an optically inhomogeneous medium fills the entire length of the resonator, where the index of refraction depends only on the transverse coordinate x and can be represented in the form $n_0+n_1x+n_2x^2+\ldots$, for the aberration coefficients β_k in the case of the two given types of prism resonators we obtain the following formula:

$$\beta_k = \left[1 + (-1)^k \frac{|M|^{k+1} - 1}{(k+1)(|M|-1)|M|^k}\right] \frac{1}{1 - 1/M^k}. \qquad (30)$$

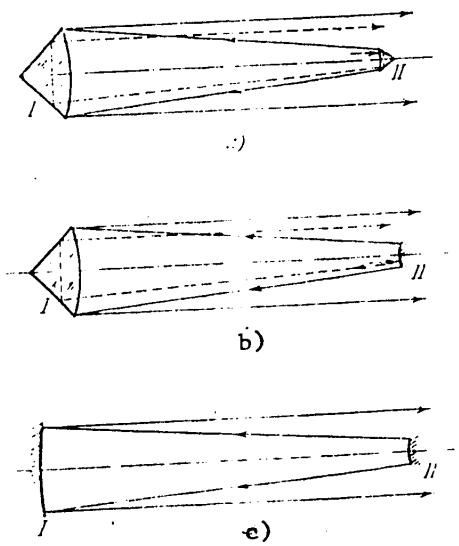

Figure 3.24. Diagrams of telescopic resonators: a) resonator made of prisms with convex and concave surfaces; b) resonator made of a prism with convex surface and convex mirror; c) ordinary telescopic resonator

The factor in brackets, just as in formulas (6) for aberration coefficients α_k in ordinary unstable confocal resonators corresponds to one complete round trip through the resonator. The trajectories of beams making such a round trip and having identical values of the transverse coordinate x at the end of the path are plotted on Figure 3.24 by dotted lines. It is obvious that in resonators with equal $|M|$, these beams travel the same paths through the active medium, from which the magnitude of the factor in brackets coincides for the given two diagrams. Another factor, $1/(1-(1/M^k))$, as before, describes the result of summation of the aberrations on many passes (see §3.2). Inasmuch as for the first of the diagrams $M>0$, and for the second $M<0$, for odd k this factor does not coincide for them. It is obvious that the second diagram has lower sensitivity to odd-order aberrations; its advantages are manifested more strongly as $|M|$ approaches one.

Comparison of (30) with (6) demonstrates that the effect of even-order wave aberrations in the prism resonators naturally is the same as in a telescopic resonator and somewhat greater than in a confocal system made of concave mirrors.

APPROVED FOR RELEASE: 2007/02/09: CIA-RDP82-00850R000500010010-4

APPROVED FOR RELEASE: 2007/02/09: CIA-RDP82-00850R000500010010-4

As for odd aberrations and, in particular, first-order ones (an optical wedge), here the prism resonators have explicit advantages not only over a telescopic resonator, but also over a confocal resonator made of concave mirrors. Thus, the values of β_3 for $2 \lesssim |M| \lesssim 5$ are less than the values of α_3 by 2-3 times. The role of the first-order aberrations in all of the mentioned resonators is clear from Table 3.1. It is obvious that the diagram in Figure 3.24, b has truly record small sensitivity to the presence of an optical wedge (or gain gradient constant with respect to cross section k_{gain}) in the active sample.

Table 3.1

$\|M\|$	α_1		β_1	
	$M>0$	$M<0$	$M>0$	$M<0$
1,5	5,5	0,7	0,5	0,10
2	3,5	0,83	0,5	0,17
3	2,5	1,0	0,5	0,25
5	2,0	1,17	0,5	0,33

The effect of an optical wedge can be estimated, of course, by a simpler method. The direction of the parallel beam exiting from the telescopic resonator is given by the direction of the resonator axis. In turn, the latter can be defined as the beam trajectory which after each reflection from a mirror prism returns along the same path. Beginning with this definition, it is easy to see that the resonator axis must pass through the centers of curvature of the mirror or the apexes of the prisms from which this resonator is made.

If the gradient of the index of refraction in the active sample is small, it is possible to consider the optical wedge thin and located in the middle of the element. On introduction of such a wedge, the optical axes of the resonators must be converted from straight lines to broken lines as shown in Figure 3.25. From this figure it is obvious that the angle of inclination ϕ' of the beam leaving the resonator is related to the angle of variation of the direction of passage through the wedge ψ by the expression $\phi'/\psi=\ell_1/(\ell_1+\ell_2)$, where ℓ_1 and ℓ_2 are the distances from the wedge to the centers of curvature of the mirrors or the apexes of the prisms. Finally, it remains to express the radii of curvature of the mirrors in terms of the distance between them L and magnification M: $R_1=2ML/(M-1)$, $R_2=-2L/(M-1)$. Now it is easy to calculate the ratio ϕ'/ψ for all cases of interest to us.

For a centrally located rod in a resonator made of two prisms $\ell_1=\ell_2=L/2$, $\phi'/\psi=0.5$; in a resonator made of a prism and convex mirror $\ell_1=L/2$, $\ell_2=L/2-R_2=L/2+2L/(|M|-1)$ (see Figure 3.25, a), $\phi'/\psi=0.5-1/(|M|+1)$. In both types of confocal resonators made of ordinary mirrors $\ell_1=-(R_1-L/2)$, $\ell_2=L/2-R_2$ (see Figure 3.25, b), $\phi'/\psi=1.5+2/(M-1)$. The expressions found by this method for ϕ'/ψ coincide with the previously presented formulas for β_1, α_1. Let us also

APPROVED FOR RELEASE: 2007/02/09: CIA-RDP82-00850R000500010010-4

APPROVED FOR RELEASE: 2007/02/09: CIA-RDP82-00850R000500010010-4

calculate ϕ'/ψ for a telescopic resonator made of a prism and a mirror in which the prism replaces not the concave mirror as in Figure 2.24, b, 2.25, a, but convex mirror: $\ell_1=-(R_1-L/2)$, $\ell_2=L/2$; $\phi'/\psi=1.5-1/(|M|+1)$. This value is appreciably greater than for the diagrams in Figure 3.24, a, b; therefore the given type of resonator is of no special interest.

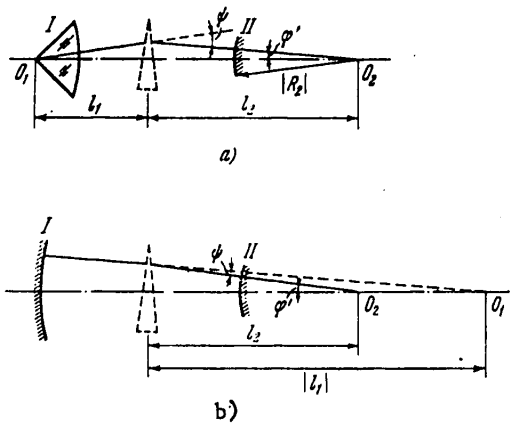

Figure 3.25. Variation of the direction of the emission on introduction of an optical wedge into a resonator:
a) resonator made of a prism with convex surface and convex mirror; b) ordinary telescopic resonator

Let us note that in the resonators depicted in Figure 3.24, a, b, as the active element approaches the prism with convex surface, β_1 decreases together with ℓ_1.

Among the important advantages of prism resonators is also low sensitivity to rotations of their elements. Actually, rotation of a mirror with radius of curvature R by the angle ε (in the plane of Figure 3.24, 3.25) causes transverse displacement of the center of its curvature by the distance εR. It is possible to demonstrate that this rotation of the prism with respect to its apex causes a transverse shift of the reference point through which the resonator axis passes only by the amount $\sim\varepsilon h(1-1/n)$, where n is as before the index of refraction of the prism material, h is its thickness along the direction of the resonator axis. Usually $h/R\sim10^{-2}$, and the requirements on the accuracy of orientation of the prisms turn out to be two or three orders lower than the requirements imposed in the case of mirrors. Finally, in the diagram in Figure 2.24, b, as a result of the large distance between reference points (Figure 2.25, a), rotation of the convex mirror also causes an appreciably smaller effect than in an ordinary telescopic resonator.

Another interesting characteristic of prism resonators is their polarization anisotropy. It occurs as a result of the fact that the linearly polarized emission as a result of reflection from some surface with significant angles of incidence acquires different phase leads depending on whether the polarization plane lies in the plane of incidence or perpendicular to it. Hence, in particular, it follows that if the initial polarization plane was oriented in an intermediate direction, after reflection the light acquires analytical polarization.

APPROVED FOR RELEASE: 2007/02/09: CIA-RDP82-00850R000500010010-4

APPROVED FOR RELEASE: 2007/02/09: CIA-RDP82-00850R000500010010-4

There is no special difficulty with analyzing the polarization characteristics of resonators with two-sided prisms depicted in Figure 3.24. Actually, the plane of incidence for all of the reflections here is the same and coincides with the plane of the figure. Therefore linearly polarized emission with polarization plane parallel to or perpendicular to the edges of the prisms preserves the initial state of polarization after a complete trip through the resonator. Hence, it follows that the natural oscillations of resonators with two-sided prisms can have one of these two directions of the polarization plane. As a result of different phase lead, they correspond to different natural frequencies; therefore there are no solutions with other polarizations states which are always a superposition of these two.

The picture of the properties of resonators with triple prisms is much more complicated. In order to discover this pattern, it is expedient to use the method of Jones polarization vectors (see, for example, [176]), but we shall explain the essence of this method somewhat later and in a simpler example; for the time being we shall only report the final results of the corresponding analysis [177]. It turns out that even in the most favorable cases where there is only one triple prism (or there are two of them, but with identically oriented sides), the resonator aperture is divided into three pairs of 60-degree sectors located opposite each other. Inside each pair its own polarization state is set up which differs from the states in the other sectors. This, just as the presence of faces of finite width on the edges of the prisms, weakens the relation between the adjacent pairs of sectors. Therefore in resonators with triple prisms simultaneously with some increase in lasing threshold (by comparison with ordinary systems) a trend can be manifested toward independent lasing in individual regions of the cross section, which decreases the spatial coherence of the emission.

The above-presented arguments permit completely defined determination of the possible applications of prism resonators. In particular, it is clear that the triple prisms proposed in [178] can turn out to be useful primarily in cases where exact alignment of the resonator elements is complicated, and the active medium is not too uniform, so that it is impossible to impose especially high requirements on the spatial coherence of the emission. If exact alignment is realizable (in at least one plane) and such high beam stability of the resonator elements is desired as in the case of triple prisms, a system of two two-faced prisms can be used. Finally, for high spatial coherence of the emission its direction can be stabilized with respect to one of the coordinates by combining a convex mirror and two-faced prism. We shall familiarize ourselves with examples of the use of prism resonators and similar resonators made of completly reflecting mirrors in the following chapter.

§3.6. Unstable Resonators with Field Reversal

Operation of Cross Section Reversal and Polarization Characteristics of Radiation. Up to now we have basically dealt with resonators after a complete round trip through which, the light beam cross section retains its initial orientation or is rotated 180° with respect to the system axis. The former include, for example, a telescopic resonator, and the latter, a confocal resonator made of concave mirrors, and only in a resonator with one two-sided prism (Figure 3.24, b) did the cross section turn out to be not rotated, but mirror-imaged with respect to the

APPROVED FOR RELEASE: 2007/02/09: CIA-RDP82-00850R000500010010-4

APPROVED FOR RELEASE: 2007/02/09: CIA-RDP82-00850R000500010010-4

plane passing through the axis and the edge of the prism. At the same time, there is an entire class of resonators on passage through which the cross section is rotated by an angle which is neither 0 nor 180°. In order to achieve such cross sectional rotation, it is sufficient in a four-mirror ring cavity such as, for example, depicted in Figure 3.21, a, to take one of the mirrors out of the plane of the figure and rotate this mirror and the two adjacent ones so that the light beam can as before pass through the resonator. This type of ring cavity, the axis of which is a closed broken line which does not lie in one plane, is called volumetric [179]. It is possible to see that after passage through it, the light beam cross section will be rotated by an angle δ which in the general case is an extremely complex function of the arrangement of mirrors [180]. Therefore we shall not derive the formulas for δ in the case of an arbitrary resonant cavity, but we shall limit ourselves to illustrating the possibility of rotating the cross section in the simplest example where four mirrors are combined pairwise into two two-sided corner reflectors installed opposite each other with "crossed" edges (mutually rotated with respect to the system axis; see Figure 3.26, a). Such a resonator is in essence not a ring cavity, but a linear one (as we see, the face between the prism and ring cavities is not so sharp). On reflection from each dihedron the beam cross section is mirror imaged with respect to the plane passing through the axis and the edge of a dihedron; as a result of two such mirror imagings, the cross section is rotated by an angle which is twice the angle between the edges of the reflectors (Figure 3.26, b). From this example it is obvious that by selecting the mutual arrangement of the mirrors it is possible to have δ assume any given value. Let us note that for resonant ring (or including corner reflectors) cavities with an odd number of reflections on a complete round trip, just as

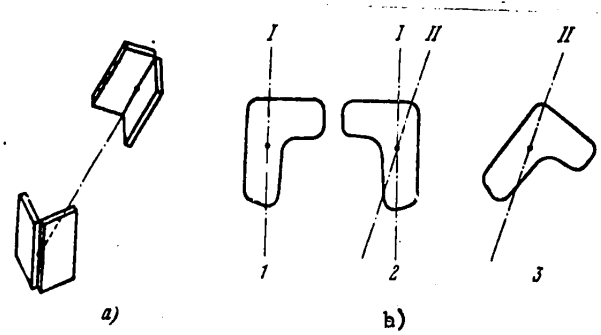

Figure 3.26. Field reversal in optical resonators:
a) simplest resonator made of two dihedral reflectors;
b) evolution of the beam cross section (1 -- initial cross section, 2 -- cross section after reflection from an element with side along I, 3 -- cross section after reflection from an element with side along II).

in the case of the simplest prism resonator (Figure 3.24, b) rotation is not achieved, but only mirror imaging of the cross section.

First, let us calculate the polarization characteristics of steady-state oscillations in resonators with field reversal [181]. For this purpose let us use the

APPROVED FOR RELEASE: 2007/02/09: CIA-RDP82-00850R000500010010-4

APPROVED FOR RELEASE: 2007/02/09: CIA-RDP82-00850R000500010010-4

above-mentioned Jones method. The state of polarization in the coordinate system connected with the light beam will be described by the polarization vector which is a set of complex field amplitudes with respect to two mutually perpendicular directions: $e = \begin{vmatrix} e_1 \\ e_2 \end{vmatrix}$. If the ratio e_1/e_2 is real, the light is linearly polarized; with complex value of this ratio the polarization is elliptic.

Each optical element corresponds to its own T matrix which describes the conversion of the polarization vector on passage through this element:

$$Te = \begin{vmatrix} T_{11} & T_{12} \\ T_{21} & T_{22} \end{vmatrix} \cdot \begin{vmatrix} e_1 \\ e_2 \end{vmatrix} = \begin{vmatrix} T_{11}e_1 + T_{12}e_2 \\ T_{21}e_1 + T_{22}e_2 \end{vmatrix}.$$

If the light passes successively through elements with matrices T_1 and T_2, the final polarization state is described by the vector T_2T_1e, and so on.

Let us apply the Jones method to the case of a resonator made of two dihedral prisms (or reflectors). Here we can get along with a total of the two simplest matrices. One of them describes the result of reflection from the dihedral prism in the case where the component e_1 lies in the plane of incidence, and the component e_2 is oriented, correspondingly, along the edge of the prism; this matrix has an obvious form

$$G(0) = \begin{Vmatrix} \exp(2i\Delta_1) & 0 \\ 0 & \exp(2i\Delta_2) \end{Vmatrix} = \exp(i\Delta_1 + i\Delta_2) \begin{Vmatrix} \exp(i\Delta) & 0 \\ 0 & \exp(-i\Delta) \end{Vmatrix},$$

where $\Delta \equiv \Delta_1 - \Delta_2$, Δ_1 and Δ_2 are the phase leads on reflection for radiation polarized parallel to and perpendicular to the plane of incidence, respectively (let us consider that the intensity losses on reflection are absent). Using the second matrix, the transition is made to the reference system rotated by an angle β with respect to the old one; this matrix is

$$S(\beta) = \begin{Vmatrix} \cos\beta & \sin\beta \\ -\sin\beta & \cos\beta \end{Vmatrix}.$$

Now it is possible to compile the reflection matrix $G(\beta)$ from a prism rotated by the angle β with respect to the reference system; actually, rotating the coordinate system itself by the same angle, we can use the matrix $G(0)$, after which it is necessary to return to the old coordinate system by repeated application of $S(\beta)$ (and not $S(-\beta)$, inasmuch as the direction of rotation with respect to variable direction of beam propagation turns out to be as before). Thus, $G(\beta)=S(\beta)G(0)S(\beta)$; finally, the matrix of the complete round trip through the resonator, if we begin with movement toward the prism oriented with respect to the initial reference system, has the form

APPROVED FOR RELEASE: 2007/02/09: CIA-RDP82-00850R000500010010-4

APPROVED FOR RELEASE: 2007/02/09: CIA-RDP82-00850R000500010010-4

$$T(\beta) = S(\beta)\,G(0)\,S(\beta)\,G(0) = \\ = \exp(2i\Delta_1 + 2i\Delta_2)\begin{Vmatrix} \cos^2\beta\cdot e^{2i\Delta} - \sin^2\beta & \sin 2\beta\cdot\dfrac{1+e^{-2i\Delta}}{2} \\ -\sin 2\beta\cdot\dfrac{1+e^{2i\Delta}}{2} & \cos^2\beta\cdot e^{-2i\Delta} - \sin^2\beta \end{Vmatrix}.$$

The natural oscillations of the resonator must have a polarization vector that satisfies the equation $T(\beta)\begin{vmatrix} e_1 \\ e_2 \end{vmatrix} = \gamma\begin{vmatrix} e_1 \\ e_2 \end{vmatrix}$ (inasmuch as the diffraction has identical influence on both components, when calculating the polarization state the diffraction can be neglected). Solving this equation, we obtain $\gamma_{1,2}=\exp(2i\Delta_1+2i\Delta_2\pm i\theta)$, where $\theta=\arccos(\cos^2\beta\cos 2\Delta-\sin^2\beta)$; finally,

$$\left(\frac{e_1}{e_2}\right)_{1,2} = e^{i\left(\frac{\pi}{2}+\Delta\right)}\,\frac{\cos^2\beta\sin 2\Delta \pm \sin\theta}{\sin 2\beta\cos\Delta}.$$

From the expressions obtained, it follows that in resonators with field rotation, elliptic polarization of the radiation is set up in the general case, which becomes linear only when $\beta=0$ or $\pi/2$, that is, when the angle of rotation of the cross section on a complete round through the resonator δ is equal to 0 or 180°. The modulus of the two eigenvalues is equal to one, which indicates the absence of any additional losses connected with polarization effects. This is a common property of all resonators which contain only elements leading to different phase shifts of the polarization components, rotations of the polarization plane, and so on. Losses can appear only on introduction of polarizers, that is, elements in which at least part of the radiation of one of the polarizations is absorbed or is coupled out.

Aberration Characteristics of Unstable Resonators with Field Reversal. Let us proceed to an investigation of the influence of optical inhomogeneities; for this purpose we shall use the former method of estimates in accordance with which we shall consider that the beam path coincides with the path in an ideal resonator. The basic difference from the previously encountered cases is the following: if in ordinary unstable resonators the beam, multiply reflected from mirrors and thus removed from the axis, does not go beyond the limits of one plane, then in resonators with field rotation the azimuthal angle ϕ varies by δ after each complete pass -- the beam is somehow "twisted" into a spiral. This leads to effective averaging of the azimuthal nonuniformities of the index of refraction and gain, as a result of which the influence of the nonuniformities on the steady field distribution turns out to be less than in ordinary resonators. The role of the nonuniformities distributed axisymmetrically remains, of course, as before.

It must be noted that the decrease in sensitivity to the influence of azimuthal nonuniformity of distribution n and k_{gain} on introduction of the field reversal operation is, of course, characteristic of all types of resonators. Flat cavities have this property to an even higher degree than unstable ones. The case of a flat cavity also includes the first experiments in which field reversal was used to increase the uniformity of the radiation distribution in the near zone [182, 183]. It is understandable that in the first of these experiments resonators with field reversal were proposed as alternatives to unstable resonators.

APPROVED FOR RELEASE: 2007/02/09: CIA-RDP82-00850R000500010010-4

APPROVED FOR RELEASE: 2007/02/09: CIA-RDP82-00850R000500010010-4

Let us proceed with the calculation; in order to simplify the calculations as much as possible, let us limit ourselves to the case where $\Delta n(r,\phi)$ is representable in the form of the sum of several terms of the type $n_{km}r^k\cos(m\phi+\phi_{km})$. The terms with m=0 describe the axisymmetric component of the distribution of optical inhomogeneities; the term with k=1, m=1 corresponds to an optical wedge oriented with respect to direction with azimuthal angle ϕ_{11}, and so on.

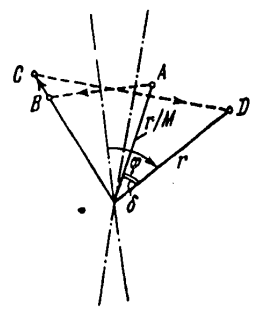

Figure 3.27. Beam trajectories for one complete round trip through a prism telescopic resonator with field reversal (given in the projection on the plane perpendicular to the resonator axis). The dotted lines are used to plot the projections of segments of the trajectory travelled inside the prisms.

Let our resonator with field reversal be telescopic and consist of the same two dihedral prisms as in Figure 3.24, a. The edge of the right -- exit -- prism will be considered oriented along the line $\phi=0$, and the left prism, $\phi=\delta/2$ (see Fig 3.27). Let us trace, as always, the trajectory of a beam undergoing a complete round trip through the resonator and having the transverse coordinates r,ϕ at the end of the path before the exit prism. Before making the pass, the beam had the coordinates r/M, $\phi-\delta$ (the point A in the figure); directly after reflection from the exit prism it had the coordinates $-r/M$, $\delta-\phi$ (point B). Then comes the inclined segment of the trajectory along the resonator axis, the projection of which is depicted by the segment BC; here the light beam expands, the coordinates before the second prism assume the value r, $\delta-\phi$. Finally, after reflection from the second prism the beam travels parallel to the axis in the direction of the exit prism having the coordinates r,ϕ (point D).

Summing the increments of the optical length with respect to two segments of the trajectory passing through the medium and considering that the inhomogeneous medium is distributed uniformly with respect to the entire resonator length, we obtain $\Delta L(r,\varphi)=L\sum_{k,m} n_{km}r^k\left[\cos(m\varphi+\varphi_{km})+\frac{M^{k+1}-1}{(k+1)(M-1)M^k}\cos(-m\varphi+m\delta+\varphi_{km})\right]$

(L is the distance between prisms).

The resultant distortions of the wave front are defined by the sum (see §3.2) $\Delta L(r,\ \varphi)+\Delta L(r/m,\ \varphi-\delta)+\Delta L(r/M^2,\ \varphi-2\delta)+\dots$ Considering that for

$|x|<1$

APPROVED FOR RELEASE: 2007/02/09: CIA-RDP82-00850R000500010010-4

APPROVED FOR RELEASE: 2007/02/09: CIA-RDP82-00850R000500010010-4

$$\cos\alpha + x\cos(\alpha+\beta) + x^2\cos(\alpha+2\beta) + \ldots = \\ = \mathrm{Re}\left[e^{i\alpha}\left(1 + xe^{i\beta} + x^2e^{2i\beta} + \ldots\right)\right] = \mathrm{Re}\,\frac{\exp(i\alpha)}{1 - x\exp(i\beta)},$$

in the final analysis we find that the desired sum is [181]

$$L\sum_{k,m} n_{km}\alpha_{km}(\varphi)\,r^k,$$

$$\alpha_{km}(\varphi) = \left[\cos(m\varphi + \varphi_{km} - \varphi'_{km}) + \right. \\ \left. + \frac{M^{k+1}-1}{(k+1)(M-1)M^k}\cos(-m\varphi + m\delta + \varphi_{km} + \varphi'_{km})\right] \times \\ \times \frac{1}{\left|1 - \frac{1}{M^k}\exp(im\delta)\right|},$$

where $\varphi'_{km} = \mathrm{arctg}\,\frac{\sin m\delta}{M^k - \cos m\delta}$. The first term in brackets, just as in the analogous formula (6), corresponds to total aberrations coming to the segments through which the light beam passes, being parallel (that is, traveling in the direction of the exit prism), and the second term, traveling in the opposite direction. Hence, it is obvious that if we were dealing not with a prism resonator, but with a monodirectional telescopic ring cavity, the first term would remain the same, and the second would be absent.

The entire first factor in the formula for $\alpha_{km}(\phi)$ is close to that which appears in the expression defining the magnitude of the aberrations on one pass ΔL (only phase shifts of $\pm\phi'_{km}$ are added); in this respect the given formula resembles (30), (6). The second factor, which appears as a result of summation of the aberrations on many passes, looks essentially different here; it is equal to $\frac{1}{|1-(1/M^k)\exp(im\delta)|}$ instead of $\frac{1}{1-1/M^k}$. Thus, the sensitivity to the aberrations of the investigated type on transition from ordinary resonator to systems with field reversal varies approximately in the ratio $c_{km} = \frac{1-1/M^k}{|1-(1/M^k)\exp(im\delta)|}$.

The values of c_{km} are always less than or equal to one, where equality is achieved only for $m\delta=2j\pi$, $j=0, 1, 2, \ldots$, that is in the trival cases where the index of refraction as a function of the azimuthal angle is absent or is periodic with a period equal to the angle of rotation δ or less by an integral number of times. The choice of δ is most favorable where the condition $m\delta=(2j+1)\pi$, $j=0,1,2, \ldots$ is satisfied for the predominant type of aberrations. If it is primarily required that the influence of the optical wedge be attenuated ($m=1$), it is expedient to choose $\delta=\pi$, that is, see that the beam cross section is inverted on passage through the resonator; as we have seen, this is easy to achieve even without two crossed prisms. A very frequently encountered type of aberration is astigmatism generated by the resonator elements having different focal power with respect to two mutually perpendicular directions ($m=2$); as is known, for quite large angles

APPROVED FOR RELEASE: 2007/02/09: CIA-RDP82-00850R000500010010-4

APPROVED FOR RELEASE: 2007/02/09: CIA-RDP82-00850R000500010010-4

of incidence the most ordinary spherical mirrors begin to have such properties. In order to suppress the astigmatism effect efficiently, it is necessary to insure $\delta=\pi/2$, which is achieved by mutual rotation of the edges of the prisms by 45°; it is possible to become familiar with an example of this type in [235].

More precisely defining our investigation, it is necessary to recognize that the most prospective area of application of unstable resonators with field reversal is lasers with weakly amplifying media [8]. Actually, with significant gain it is possible to use resonators with large M (see Chapter 4), the sensitivity of which to aberrations even without field reversal is quite low (§3.2). In the case of small gains, on the contrary, in order to insure satisfactory energy characteristics it is necessary to select the values of M close to one. The criticalness of resonators with such M with respect to the presence of optical inhomogeneities is so high that it is worthwhile to take all possible measures to reduce it; the introduction of the field reversal operation is, perhaps, the most effective of such measures. The gain achieved in this case increases as M approaches one: if the condition $m\delta\neq 2j\pi$ is satisfied, then for $M\to 1$ the values of $|c_{km}|$ decrease without limit.

Resonators with Compact Output Aperture. The field reversal operation permits the solution of another problem which arises when building lasers with weakly amplifying media and having great practical significance. We are talking about the problem of obtaining a compact shape of the exit aperture. The fact is that in ordinary unstable resonators with opaque mirrors and small magnification, the output beam is a narrow ring or other analogous figure with large dimensions and small area. This form of aperture is disadvantageous from the point of view of angular divergence of the emission; it is desirable to achieve a situation such that with the former area (for maintenance of the same losses to emission) its dimensions reduced to a maximum. In §1.1, it was demonstrated that in the presence of an external shaping optical system, this is advantageous even in the case where the wave front has an ideal plane form: although the axial luminous intensity at the laser exit remains as before, it increases at the shaping system exit (as a result of an increase in power of the telescope with the same dimensions of its objective). If the magnitude of the divergence has not so much diffraction origin as "configurational" origin (see §1.1), the reduction in the aperture dimensions in itself causes, as a rule, a decrease in angular divergence; with an external optical system , the advantage is greater.

The method of obtaining compact form of the exit aperture in unstable resonators with small M was proposed in [184]; let us discuss his idea.

In resonators consisting of standard optical elements with spherical and plane mirrors, the light beam in the plane of the exit mirror, completely covering the latter, necessarily has the cross sectional shape geometrically similar to the cross sectional shape of the exit mirror itself (with a scale of such transformation M). Thus, the cross section of a beam leaving the resonator is the result of "subtraction" of geometrically similar figures differing only with respect to dimensions from each other (a ring can be used as an example).

APPROVED FOR RELEASE: 2007/02/09: CIA-RDP82-00850R000500010010-4

APPROVED FOR RELEASE: 2007/02/09: CIA-RDP82-00850R000500010010-4

It is possible to see that with identical orientation of these two figures, the problem of obtaining compact "difference" of them does not have an acceptable solution; the mirror conversion of one of them also helps little. Let us consider the possibilities opened up by introducing the operation of rotation of the cross section.

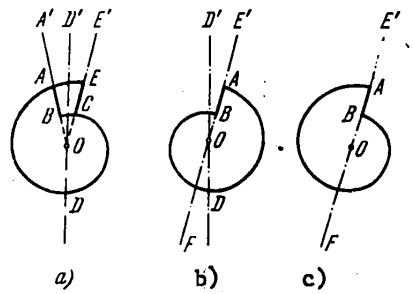

Figure 3.28. Evolution of the beam cross section in a prism resonator with field reversal and sectional output: a) beam before reaching the sectional output plate (ECDAE) and after passing through it (ABCDA); the plate occupies the section A'BCE'; b) beam after reflection from a prism with its edge along DD'; c) beam after reflection from a prism with its edge along FE'

The condition that part of the outline of the figure having the equation in polar coordinates $f=f(\phi)$ lie on the previous outline after rotation by an angle δ and magnification by M times, has the form $M\cdot f(\phi-\delta)=f(\phi)$. The simplest curve satisfying this condition is the logarithmic spiral $r=C\exp(\ln M\cdot(\phi/\delta))$. Actually, it is easy to construct the required combination of two geometrically similar figures, the common part of the outline of which is a logarithmic spiral. This combination is shown in Figure 3.28, a; the smaller the figures, ABCDA, corresponds to the exit mirror, the larger, ECDAE, to the cross section of the entire light beam in the plane of this mirror, the difference, ABCEA, corresponds to the cross section of the beam leaving the resonator. The resonator axis passes through the center of the spiral O, the angle between segments OE and OA is equal to the angle of rotation of the cross section with respect to passage through the resonator δ, the ratio of their lengths is equal to the resonator magnification M (in the figure $\delta=30°$, $M=1.06$).

In reality, it is not at all necessary to try to cut out the exit mirror in the shape of the figure ABCDA. It is better to make this mirror larger, to install an inclined reflecting plate inside the resonator near it to couple out the emission. In ordinary unstable resonators frequently such a procedure is followed; the reflecting plate in this case covers the entire resonator cross section and has an aperture for passage of the central part of the beam to the exit mirror (examples of such systems are presented in Figure 4.15a, b and 4.16). In our case the resonator with rotation of the cross section, the reflecting plate (more precisely, its projection on the plane normal to the resonator axis) must have the shape of the section A'BCE'. Successively rotating and magnifying ΔBOC, it is easy to see that the shape of the beam cross section depicted in the figure is obtained automatically in this case.

APPROVED FOR RELEASE: 2007/02/09: CIA-RDP82-00850R000500010010-4

APPROVED FOR RELEASE: 2007/02/09: CIA-RDP82-00850R000500010010-4

The use of a sectional reflecting plate is especially convenient in that the beam leaving the resonator turns out to be rigidly "associated" with a defined segment of the cross section. The variations of the magnification of the resonator M caused by deformation of the mirrors or inhomogeneity of the medium, small shifts of the resonator axis, and so on can cause only a shift of the outer boundary of the beam AE. At the same time, with ordinary ring output and M close to one, the simplest deformations of the mirrors are sufficient for the ring to convert to a "crescent" or decay into individual spots.

Let us explain how the evolution of the beam cross section looks in a resonator made of two crossed prisms when this method of coupling out the radiation is used. The edges of these prisms will be considered oriented as in Figure 3.27. The sectional reflecting plate must be installed directly in front of the prism which we have called the exit prism. In front of this plate the beam cross section has the form ECDAE (Figure 3.28, a); after this plate, the beam cross section is ABCDA. Then the light beam hits the prism installed immediately after the plate with edge directed along DD'; after reflection from it the cross section acquires a mirror converted form with respect to DD' (when observed from the same side) presented in Figure 3.28, b. The edge of the second prism is oriented along FE'; as a result of reflection from it, the beam cross section is again mirror imaged (now, with respect to FE') and it acquires the initial shape and orientation (Figure 3.28, c). A small decrease in area, which is a consequence of subtracting ABCE, is compensated for by "elongation" of the cross section by M times on the path to the second prism.

It is necessary, however, to make a small stipulation. In order that after reflection from the exit prism the light beam not fall on the back side of the reflecting plate, it is necessary that the edge of the last BC be symmetric with respect to DD'. This leads to the fact that the outline of the entire light beam in the prism resonator is not "smooth," as in the figure, but it has small "steps." In the given resonator with the extent of the greater part of its length, the cross sections of the beams propagated opposite to each other have forms very close to those depicted in Figure 3.28, b, c and they make an almost ideal circle when summed.

Let us calculate the shape of the beam ABCE leaving the resonator as a function of M and δ. Obviously, $AE \simeq OE \cdot 2 \sin(\delta/2)$; from the equation of a spiral it follows that $OC/OE = \exp(-2\pi/\delta) \ln M) = M^{-2\pi/\delta}$, $CE = OE\ (1 - M^{-2\pi/\delta})$. The maximum compact form is obviously reached for AE=CE, for which it is necessary to satisfy the condition $2 \sin(\delta/2) + M^{-2\pi/\delta} = 1$. Inasmuch as the losses to emission, and with them, also magnification M usually are selected beginning with purely energy arguments (see the next chapter), the given condition is in essence the equation for determing δ which always has a solution. Thus, the above-discussed method of constructing unstable resonators makes it possible by selection of the angle δ to achieve compact form of the exit aperture with filling coefficient γ on the order of 0.6 (for ordinary systems this coefficient, the definition of which is given in §1.1, does not exceed $1-1/M^2$) for losses to emission as small as one might like (M close to one). Let us note that when desired, by varying not only δ but also the configuration of the reflecting plate, it is possible to achieve an entirely different form of exit beam cross section than in Figure 3.28, for example, strictly rectangular.

APPROVED FOR RELEASE: 2007/02/09: CIA-RDP82-00850R000500010010-4

APPROVED FOR RELEASE: 2007/02/09: CIA-RDP82-00850R000500010010-4

All of the above-presented information on the properties of unstable resonators with field reversal were obtained using the geometric approximation. Diffraction theory of such systems has still not been constructed; it is possible to assume, however, that the criterion of suitability of the optical-geometric approximation here is the standard condition $N_{equiv} \gg 1$ (for calculation of N_{equiv} the distance from the O axis to the edge of the sectional plate BC must be taken as the characteristic transverse dimension a).

With this, we end the investigation of the most general problems of the theory of unstable resonators. A number of more special theoretical problems important for certain specific applications, will be considered in the following chapter when discussing these applications.

APPROVED FOR RELEASE: 2007/02/09: CIA-RDP82-00850R000500010010-4

APPROVED FOR RELEASE: 2007/02/09: CIA-RDP82-00850R000500010010-4

CHAPTER 4. APPLICATIONS OF UNSTABLE RESONATORS

§ 4.1. Unstable Resonators in Pulsed Free-running Lasers

The basic result of using unstable resonators usually is expected to be the achievement of small angular divergence while maintaining the same energy characteristics of the laser as in the case of using planar or unstable resonators. It is perhaps simplest of all to do this for pulsed lasers using large volumes of active medium that are not too nonuniform. Actually, in the case of pulsed excitation usually high amplification coefficients are achieved; as will be obvious later, this permits the application of resonators with quite large magnification M, which without any of the contrivances of the type described at the end of the preceding chapter have low sensitivity to the effect of optical nonuniformities. If the operating cross section of the active zone is large, the values of N_{equiv} also turn out to be large; therefore the edge effects almost have no influence on the mode structure and have no negative effect on the directionality of the radiation.

Selection of the Type and Parameters of the Resonator. The most important factors which determine the angular divergence of the radiation were investigated in the preceding chapter. Therefore now we shall primarily discuss the problems pertaining to the energy characteristics of lasers with unstable resonators: in the case of large volumes of the active medium, the problem of efficiency acquires primary significance. As for the efficiency of the lasers during their operation on a single transverse mode, unstable resonators here have explicit advantages over resonators of other types. Actually, it is known that the maximum efficiency of a laser is achieved usually when the laser radiation distribution in general features repeats the pumping distribution (§ 1.4). In planar resonators and, especially in resonators with stable configuration the field of one mode cannot uniformly fill a sufficiently large cross section, the correlation between the forms of distribution of the lasing and pumping fields is very weak (thus, in § 2.5 it was noted that the amplitude aberrations in a planar resonator primarily cause not amplitude, but phase distortions of the wave fronts). Accordingly, in lasers with such resonators usually the multimode oscillation mode is realized with large angular divergence of the radiation (§§ 2.3, 2.4).

Unstable resonators provide incomparably more favorable conditions for achievement of high efficiency in the presence of single-mode oscillation. With a uniform active medium and mirrors with reflection coefficient constant with respect to cross section, the field distribution of the lowest mode is close to Π-type. If the inverse population is nonuniform, then, as was noted in [152], in accordance with formula (5) the lasing field acquires a similar nature of distribution.

FOR OFFICIAL USE ONLY

APPROVED FOR RELEASE: 2007/02/09: CIA-RDP82-00850R000500010010-4

APPROVED FOR RELEASE: 2007/02/09: CIA-RDP82-00850R000500010010-4

However, for realization of the indicated prerequisite it is necessary that a number of conditions be satisfied. First of all, of course, it is necessary that the lasing radiation fill the cross section of the active zone well over its entire length. If this is not so, the output power of the laser decreases, frequently more sharply than in accordance with the proportion of the used volume: the region in which the medium is excited, and the lasing radiation is absent, is a powerful source of luminescence and, as a result of amplification of it (so-called superluminescence [32]) it can significantly decrease the inverse population in the remaining volume.

On the other hand, it is necessary to see that the lasing radiation does not hit the sidewalls of the active element or the cell in which the lasing is realized. In addition to decreasing the efficiency of the system, this can lead to an increase in angular divergence of the radiation as a result of the influence of the scattered light.

Thus, it is necessary that the configuration of the beam propagated to the exit mirror exactly coincide with the configuration of the active element (the beam propagated in the opposite direction has less volume for one-way output). This imposes restrictions on the type of resonator used.

Most frequently, the active zone has a cylindrical shape. In this case the beam going to the exit mirror must be at least close to parallel. If M exceeds one by very little, the given condition is more or less observed even when using the simplest resonator made up of a planar and convex mirrors (see Figure 3.3,a), the beam cross section in which on the path from the plane mirror to the convex mirror increases by $2M/(M + 1)$ times. However, with large losses to radiation, it becomes necessary to use the asymmetric confocal systems depicted in Figure 3.3,c,d. The transverse dimension of the exit mirror must be $|M|$ times less than the cross section of the active element. Here, its shape should obviously be similar to the shape of the cross section of the active zone (from reading the theoretical papers it appears that it must be circular or square; in reality, this is not so at all).

A confocal resonator made of concave mirrors is less sensitive to aberrations (§3.2); in addition, for the same $|M|$ and distance between the mirrors it has $(|M| + 1)/(|M| - 1)$ times larger value of $|N_{equiv}|$ than the telescopic one. On the other hand, it also has a very large deficiency: the center of the spherical wave reflected from the exit mirror is inside the resonator (Figure 3.3,c). As a result, the beam following from the exit mirror fills the resonator cross section worse than in the telescopic one; however, it is still more important that the beam density at the focal point reaches an extremely large value and can easily exceed not only the rupture threshold of the solid active medium, but also the threshold of formation of breakdown in the gas. For the indicated reasons, in the majority of practical applications the theoretical resonator proposed in [185, 152] is used.

Then the question arises of selecting the optimal magnification M. From the point of view of diminishing the effect of large-scale optical nonuniformities it is desirable that M be as large as possible. For this purpose it is expedient to destroy other sources of losses to radiation and use completely reflecting mirrors. Then the admissible value of M is determined by purely energy arguments. In order to understand what these arguments are, let us consider the dependence of the output power of a laser with telescopic resonator on M. Just as in § 1.4, we

FOR OFFICIAL USE ONLY

APPROVED FOR RELEASE: 2007/02/09: CIA-RDP82-00850R000500010010-4

APPROVED FOR RELEASE: 2007/02/09: CIA-RDP82-00850R000500010010-4

shall limit ourselves to the analysis of the simplest case where the pumping is uniformly distributed with respect to the volume of the active medium having a cylindrical shape, the interference phenomena between the radiation fluxes following in opposite directions do not appear, and the relation between the amplification coefficient and the total radiation has the form of (1.33). Introducing the radiation density in dimensionless units $\rho \equiv \alpha I$, let us rewrite (1.33) in the form

$$k_{yc} = k^0_{yc}/(1 + \rho^+ + \rho^-), \tag{1}$$

(a)

Key: a. amplification

where ρ^+ and ρ^- are the flux densities to the exit mirror and in the opposite direction, respectively (Figure 4.1).

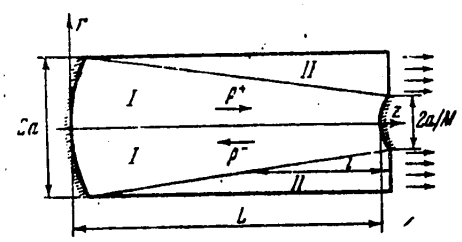

Figure 4.1. Radiation fluxes in a laser with telescopic resonator.

It is easy to see that inside the region I which is filled by the fluxes in both directions, the inverse population and the flux density itself vary only along the length $z (0 \leq z \leq L)$, and these values are constant with respect to cross section. Then for ρ^+ and ρ^- in the indicated region the obvious relations are valid:

$$\rho^+(z) = \rho^+(0) \exp\left\{\int_0^z [k_{yc}(z') - \sigma_0]\, dz'\right\},$$

$$\rho^-(z) = \rho^-(0) \exp\left\{-\int_0^z [k_{yc}(z') - \sigma_0]\, dz'\right\} \cdot \left(\frac{z_0}{z_0 - z}\right)^2, \tag{2}$$

where σ_0 is the coefficient of inactive losses; the factor $[z_0/(z_0 - z)]^2$ describes the decrease in the density of the diverging spherical wave on going away from an imaginary center z_0 coinciding with the common focal point of the mirrors.

Equations (1) and (2) must be solved jointly with respect to $\rho^+(z)$ and $\rho^-(z)$ considering the boundary conditions $\rho^+(0) = \rho^-(0)$ and $\rho^+(L) = \rho^-(L)$. Finding the exact solution in analytical form is impossible. For approximate solution it is convenient to use the fact that according to (2) $\sqrt{\rho^+(z)\rho^-(z)} = \rho(0)z_0/(z_0 - z)$.

Inasmuch as the sum $\rho^+ + \rho^-$ is with an accuracy to several percentages equal to $2\sqrt{\rho^+\rho^-}$ up to values of ρ^+ and ρ^- differing by two or three times (larger differences in practice do not exist) it is possible by the corresponding substitution to convert equation (1) as follows:

APPROVED FOR RELEASE: 2007/02/09: CIA-RDP82-00850R000500010010-4

APPROVED FOR RELEASE: 2007/02/09: CIA-RDP82-00850R000500010010-4

$$k_{yc} = k^0_{yc}[1 + 2\rho(0)z_0/(z_0 - z)]^{-1}. \tag{1a}$$

The substitution of (1a) in (2) with subsequent integration leads to the equation for determination of $\rho(0)$:

$$2\frac{M}{M-1}\rho(0)\ln\frac{[2\rho(0)+1]M}{2\rho(0)M+1} = 1 - \frac{\ln M + \sigma_0 L}{k^0_{yc}L},$$

where $M = z_0/(z_0 - L)$, as always, is the magnification of the resonator.

Finding $\rho(0)$, it is possible by using (2) to calculate the distribution $\rho^+(z)$ in the region I. When the part of the radiation flux remote from the axis ($r > a/M$, 2a is the diameter of the active element) intersects the boundary between the regions and goes into zone II where $\rho^- = 0$, further amplification of the flux is easily considered by the corresponding formula for the amplifying mode [186], which is a direct consequence of the radiation transport equation:

$$\ln\left(\frac{\rho_{\text{вых}}}{\rho}\right)^{(a)} = (k^0_{yc} - \sigma_0)l + \frac{k^0_{yc}}{\sigma_0}\ln\left[\frac{(k^0_{yc}/\sigma_0) - 1 - \rho_{\text{вых}}}{(k^0_{yc}/\sigma_0) - 1 - \rho}\right]^{(b)},$$

Key: a. out b. amplification

where ρ is the flux density at the entrance to region II; ρ_{out} is the flux density at the exit from the resonator as a function of the distance ℓ traveled by the flux in this region (see Figure 4.1). It is obvious that the value of ℓ, and with it also ρ_{out}, increase with an increase in r.

Figure 4.2 shows the graphs of the density distributions of the radiation leaving the resonator calculated in this way. As is obvious from Figure 4.2, with an increase in M the radiation density at the laser exit decreases, but the width of the radiating zone (a - a/M) naturally increases. For some value M_{opt} the power of the outgoing radiation will be maximal.

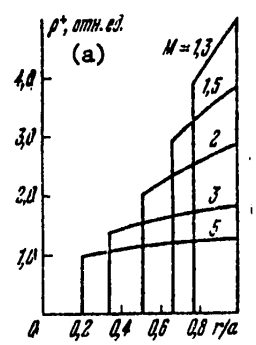

Figure 4.2. Density distribution of outgoing radiation with respect to cross section of the active element for the case $k^0_{amp}L = 3.0$, $\sigma_0 L = 0.12$ and different values of M.

Key: a. relative units

APPROVED FOR RELEASE: 2007/02/09: CIA-RDP82-00850R000500010010-4

APPROVED FOR RELEASE: 2007/02/09: CIA-RDP82-00850R000500010010-4

The effectiveness of the energy conversion and the resonator X introduced in § 1.4 can be calculated as the ratio of the number of lasing photons leaving the resonator $\int_{(S)} I\,dS$ (integration is performed over the area of the exit aperture) to the total number of acts of filling out the inverse population in the volume of the oscillator $\int_{(V)} P_{pump}\,dv$. Inasmuch as in the case of a four-level medium with uniformly broadened line and unpopulated lower level of the operating transition $P_{pump} = k^0_{amp}/\alpha$ (see § 1.4), we obtain $X = \left(\int_{(S)} \rho^+ ds\right) \Big/ \left(\int_{(V)} k^0_{yc}\,dv\right)$. In particular, for the case of a circular cylindrical element with uniform pumping

$$X = \frac{2}{\underset{(b)}{k^0_{yc}} La^2} \int_{a/M}^{a} \rho_{\underset{(a)}{out}}(r)\, r\, dr.$$

Key: a. out b. amplification

Figure 4.3 shows the efficiency of the resonator X calculated using the last formula as a function of the value of M for a number of values of $\sigma_0 L$ and $k^0_{amp} L$ (let us remember that in the case of a four-level medium the ratio k^0_{amp}/σ_0 is the amount the lasing threshold is exceeded in the absence of losses to radiation, that is, for M = 1). The data for a telescopic resonator are compared with the data pertaining to a planar resonator with the same total losses and lasing threshold (the reflection coefficient of the output mirror R' is $1/M^2$).

From Figure 4.3 it follows that the efficiency of the energy conversion in a telescopic resonator in the given case is somewhat less, but it is very close to the efficiency in the corresponding planar resonator. Thus, for a laser with a telescopic resonator, the formulas of § 1.4 can be used under the condition of replacement of R' in them by $1/M^2$. In particular, for $\sigma_0 L$ that is not too large, the value of X can be determined using the expression

$$X \approx \frac{\ln M}{\ln M + \sigma_0 L}\left(1 - \frac{\ln M + \sigma_0 L}{k^0_{yc} L}\right), \tag{3}$$

the optimal magnification of the resonator, by the formula

$$\ln M_{\underset{(a)}{opt}} \approx \sigma_0 L\left(\sqrt{k^0_{yc}/\sigma_0} - 1\right), \tag{4}$$

Key: a. opt

finally, the maximum value of X, just as in the case of a plane resonator is approximately equal to

$$X_{max} \approx \left(1 - \sqrt{\sigma_0/k^0_{yc}}\right)^2. \tag{5}$$

The above-discussed analysis was performed in reference [187], being the first example of calculation of the energy characteristics of lasers with unstable resonators. Later, more complex cases were investigated which require very awkward machine calculations (we shall touch on the methods of performing these calculations

APPROVED FOR RELEASE: 2007/02/09: CIA-RDP82-00850R000500010010-4

APPROVED FOR RELEASE: 2007/02/09: CIA-RDP82-00850R000500010010-4

in § 4.2). Thus, in [188] calculations were made of the efficiency for nonuniform distribution of the pumping with respect to cross section and large excesses over the threshold; it turned out that the formulas (3)-(5) remain in force under the condition of substitution of the value of k^0_{amp} averaged over the cross section in them. Analogous laws occur, as is known, also in the case of planar resonators.

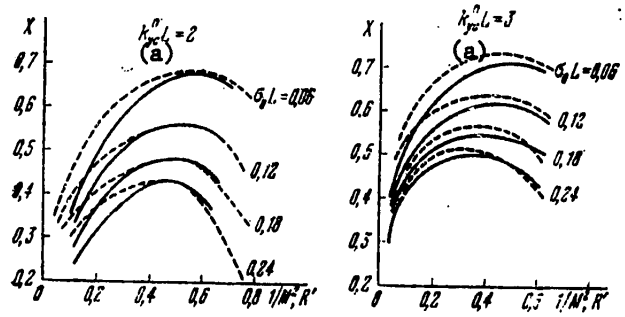

Figure 4.3. Efficiency of the resonator with telescopic (solid curves) and planar (dotted curves) resonators as a function of the values of $1/M^2$ and R', respectively, for $k^0_{amp}L = 2$ and 3.

Key: a. amplification

This similarity of behavior of the telescopic and planar resonators of course is no accident. Its causes consist in the fact that the nature of filling of the cylindrical active element with lasing radiation in these two types of resonators with identical losses to radiation is not so strongly distinguished as it appears at first glance. Actually, with equality of the losses in the medium, identical mean values of the amplification coefficient are established; consequently, the mean radiation densities approximately coincide. Then, along the path from the "blind" mirror to the exit mirror in a planar resonator, the radiation density increases by $1/\sqrt{R'}$ times (§ 1.4), in the telescopic resonator, by M times, that is, in the same ratio. Hence it is obvious that ρ^+ in these two resonators has similar values in the entire volume of the active medium. As for the radiation traveling in the opposite direction (ρ^-), in the telescopic resonator its distribution is less favorable: although the total radiation flux is approximately the same as in the planar resonator it is distributed not with respect to the entire cross section, but only with respect to part of it; worst of all is the filling near the exit mirror. As a result, the total density $\rho^+ + \rho^-$ is distributed over the active volume in the case of a telescopic resonator somewhat more nonuniformly, which leads to insignificant decrease in the efficiency.

Thus, the telescopic resonator insures an efficiency which is close to its maximum value defined by formula (5) if we select the radiation losses $1 - 1/M^2$ such as the optimal planar resonator would have. Moreover, the value of X in the vicinity of its maximum varies very slowly with M, and the variation of M within known limits is not related to a significant reduction in the efficiency of the system. This can be used so that when selecting M the arguments connected with divergence of the radiation are considered. For reduction of the divergence, it is, as a rule, expedient to use resonators with the largest possible M. Here the sensitivity of the resonator to the aberrations decreases (§ 3.2); in addition, the ring

APPROVED FOR RELEASE: 2007/02/09: CIA-RDP82-00850R000500010010-4

APPROVED FOR RELEASE: 2007/02/09: CIA-RDP82-00850R000500010010-4

at the exit will become less narrow. However, it is necessary to proceed to values of M significantly exceeding 2 with great caution. First of all, from § 3.3 it follows that single-mode lasing with uniform field distribution is achieved most reliably for large N_{equiv}. If the transverse dimensions of the active element are given, N_{equiv} reaches a maximum for M = 2. A futher increase in M, in spite of some increase in curvature of the mirrors causes a decrease in N_{equiv} as a result of a fast decrease in the transverse dimensions of the exit mirror.

Extremely large values of M can be disadvantageous also in the presence of light dispersion, especially at angles close to 180° (usually all possible interfaces are sources of this light dispersion). It is easy to understand the reason for this if we consider that with an increase in M the proportion of the radiation participating in the "regular" feedback channel decreases, and the light intensity mixed with it as a result of dispersion of the basic flux remains unchanged; thus, the role of the light dispersion increases.

The proper choice of the resonator parameters even in the case of uniform active medium still does not guarantee that a high axial luminous intensity will be obtained. From the information presented in the preceding chapter it is clear that for this to occur, it is necessary to exclude the formation of converging waves with noticeable initial intensity. In the case of a telescopic resonator, the purely converging wave is formed, as is easy to see, with partial reflection of the basic wave from the plane interfaces perpendicular to the resonator axis; therefore the interfaces existing in the laser (for example, the end surfaces of the rod) must be inclined noticeably.

Results of Experiments with Neodymium Glass Lasers. The above-discussed arguments about the choice of the type and the parameters of an unstable resonator and also a signficant part of the concepts developed in Chapter 3 regarding the properties of unstable resonators were developed during the course of experimental studies of neodymium glass resonators [5, 152, 189, 153, 190, 191, 1968, 192-197], and they were confirmed by the results of these studies. In the example of lasers of the given type a most detailed comparison was made between the characteristics of the lasers with planar and unstable resonators; in practice all of the new versions of the systems based on unstable resonators were tested and studied for the first time. Let us discuss the basic results of the experiments pertaining to the lasers with the simplest two-mirror resonators discussed in this section.

For a diameter of the neodymium rod of 10 mm and length of 120 mm, the application of an unstable resonator led only to a twofold gain in axial luminous intensity by comparison with the case of a planar resonator [152]. In the greater part of the subsequent experiments, a highly efficient laser based on a rod 45 mm in diameter and 600 mm long which was described in [198] was used. It served as a prototype for the series manufactured GOS-1001 lasers and various versions of them. Here the axial luminous intensity on replacement of the planar resonator by an unstable one increased by tens of times. The angular divergence of the radiation measured by the half intensity level decreased from 2' to 15-20"; with respect to the half energy level, from 5' to 40" (Figure 4.4, curve I) [152]. Let us note that this situation is quite characteristic: the larger the laser, the greater the effect from using an unstable resonator in it. The achieved gain in divergence also increases with an increase in optical uniformity of the active medium; in this respect the investigated laser was entirely satisfactory.

FOR OFFICIAL USE ONLY

APPROVED FOR RELEASE: 2007/02/09: CIA-RDP82-00850R000500010010-4

APPROVED FOR RELEASE: 2007/02/09: CIA-RDP82-00850R000500010010-4

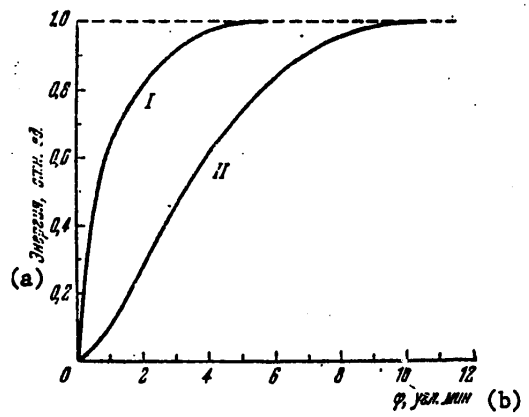

Figure 4.4. Angular distribution of the emission of a solid-state laser with telescopic resonator [152]: I — resonator without interfaces perpendicular to the axis; II — a coated glass plate was installed inside the resonator perpendicular to the axis. The proportion of the energy included in the cone with apex angle ϕ is plotted on the y-axis.

Key: a. energy, relative units
b. angular minutes

In the experiments with rods 45 mm in diameter the mirrors were totally reflecting. The losses to emission were equal to the optimal transmission factor for the case of planar mirrors, and they amounted to ~75% (M = 2). The use of a telescopic resonator insured approximately the same radiation energy as in the case of a planar resonator. In the case of a planoconvex system of mirrors, the output energy dropped by 1.5–2 times as a result of worse filling of the active element with the lasing radiation. After these experiments with large losses to emission, only telescopic resonators began to be used everywhere.

Subsequently, the output energy of an emission of a laser of the given type was brought to 4500 joules, and with series installation of two active elements in one resonator with M = 5, to 8000 joules [194]. The angular divergence of the radiation was: with respect to 0.5 intensity level, ~40"; with respect to half energy level, about 1'30".

Let us note the following important fact. In order to realize small angular divergence, in the case of a telescopic resonator it turned out to be necessary to incline the ends of the active element by 2–3° with respect to the resonator axis, which made it possible to avoid the converging waves generated by Fresnel reflection. The necessity for taking such measures was proved by the following demonstration experiment: a glass plate with coated surfaces was installed strictly perpendicular to the axis in a telescopic resonator with active element, the ends of which were inclined; the residual reflection of the coated surfaces did not exceed 0.3%. This turned out to be sufficient that the lasing pattern changed strikingly, and the angular divergence of the radiation increased so much that it approached the value characteristic of a planar resonator (curve II in Figure 4.4) [153]. The corresponding photographs are presented in Figure 4.5, a, b [photos not reproduced].

APPROVED FOR RELEASE: 2007/02/09: CIA-RDP82-00850R000500010010-4

APPROVED FOR RELEASE: 2007/02/09: CIA-RDP82-00850R000500010010-4

The mechanism responsible for poor directionality of radiation in such cases was studied in [197, 336]. It turned out that on introduction of a third planar mirror into the telescopic resonator, "spurious" modes appear which correspond to closed beam trajectories. Many passes through the active medium go with one reflection from this mirror. Therefore the "spurious" modes even for the smallest reflection coefficients of the planar mirror have lower excitation thresholds than the fundamental mode of a two-mirror resonator. Inasmuch as these modes, in addition, are characterized by high nonuniformity of the field distribution, some of them are excited immediately with all of the sad consequences following from this. And this is no surprise: in § 3.3 we encountered the situation where the presence of even a negligibly weak converging wave generated by edge diffraction leads to degeneration with respect to losses. Therefore the efforts sometime made to influence the lasing mode (in particular, lower its threshold) by artificial initiation of converging waves obviously always must lead to an increase in divergence of the radiation [336].

However, let us continue the discussion of the properties of lasers with "normal" unstable resonators not having sources of converging waves. Among the discovered peculiarities of such lasers, high stability of their output parameters is remarkable, including the form of the angular distribution of the radiation. Such phenomena characteristic of lasers with planar resonators as variation of the angular distribution from pulse to pulse, a gradual increase in angular divergence during aging of the active element, and so on were not observed. This property of lasers with unstable resonators is to one degree or another inherent in all systems with spherical mirrors, and it is frequently connected with their small criticalness with respect to the alignment precision. As the experiments have demonstrated, small rotations and shifts of the mirrors in the transverse direction cause only small changes in the beam direction. The magnitude of these variations corresponds completely to the predictions of the geometric approximation. The form of angular distribution is essentially distorted only for such large rotations of the mirrors that the axis of the resonator tightly approaches the flat surface of the sample [152] (an analogous cycle of studies for the case of a CO_2 laser was performed later in the paper by Krupke and Suya [199]).

Also in accordance with the geometric approximation, the displacements of one of the mirrors in the longitudinal direction cause variation of the curvature of the wave leaving the resonator. In the case of a telescopic resonator it is possible to use this means of focusing the beam at a given distance $d \gg L$ from the laser, increasing the distance between the mirrors by comparison with the distance L for confocal location of them by the amount $\sim(M + 1)L^2/(M - 1)d$ (focusing at the distance $d \sim L$ is also possible, but it is accompanied by a decrease in the output power as a result of "tapering" of the light beam in the active element).

In reference [152], a study was also made of the spectral and time characteristics of the emission of a neodymium glass laser with unstable resonators. There were no special differences from the characteristics of lasers with planar mirrors: the same random spikes, approximately the same integral width of the spectrum; only the duration of each spike turned out to be somewhat less, and the average time interval between them increased.

The reduction in duration of the spikes arose from the fact that the oscillations in unstable resonators are set up somewhat faster than in planar resonators. The

APPROVED FOR RELEASE: 2007/02/09: CIA-RDP82-00850R000500010010-4

APPROVED FOR RELEASE: 2007/02/09: CIA-RDP82-00850R000500010010-4

main reason for this is the presence of some mechanism of forced "spreading" of the emission over the cross section. We shall discuss this question in more detail at the end of this section when we are talking about lasers for which the rate of establishment of the oscillations plays the decisive role. As for the spectral distribution of the radiation, for planar and unstable resonators it is essentially the distribution of the radiation intensity between modes with different axial indices (see § 2.4). Near the axis of an unstable resonator the same interference of two counterflows and the formation of standing waves occur as in a planar resonator. Therefore the mechanism of the spatial competition of the axial modes in resonators of both types is identical in spite of the fact that in the unstable resonator the peripheral part of the active element is filled with radiation propagated in only one direction (see also the discussion of the problem of spectral selection in ring cavities in § 3.5).

The observations of the time expansion of the spatial distribution of the emission [152, 153, 192] demonstrated that during lasing, insignificant shifts of the center of symmetry of the angular disribution of the emission take place. In addition, the angular distribution also in individual spikes differed from the distribution for the ideal emitter. As a result, the integral width of the angular distribution with respect to time for the investigated lasers noticeably exceeded the diffraction limit. Obviously, this was a consequence of thermal deformations of the resonator, the vibrations of the samples, and so on. Taking measures against the effect of these factors led to a decrease in the radiation divergence.

In particular, the results of experiments with a laser based on an active element of great length and with rectangular cross section are indicative [192]. During the pumping pulse the sample underwent noticeable mechanical vibrations along the small dimension of the cross section. Accordingly, the center of gravity of the angular distribution completed complex oscillatory movement in the same direction; the divergence of the radiation with respect to this direction was four times greater than the diffraction limit, and it amounted to ~2'20". The replacement of the concave mirror by a dihedral prism with convex surface turned into the resonator and an edge parallel to the large dimension of the cross section led to complete correspondence to the ideas developed in § 3.5, almost total stabilization of the direction of radiation. The angular divergence decreased in this case to 1'. If a telescopic resonator made of two prisms was used, the degree of stabilization of the direction was somewhat less, and the divergence was ~1'10".

Extraordinarily high selective properties of unstable resonators with large Fresnel numbers were fully manifested in the test experiments performed in [190]. The manifestations of optical nonuniformity of the medium and other similar causes were completely eliminated here. A two-dimensional unstable resonator with M = 2 made of totally reflecting mirrors, one of which was planar and the other, convex cylindrical (Figure 4.6), was used. The active element, just as in the preceding case, was a rectangular parallelepiped, the location of the flashlamps insured high uniformity of distribution of pumping in the direction of the large dimension of the cross section. The curvature of the wave front emitting from the resonator was compensated for by an additional lens.

FOR OFFICIAL USE ONLY

APPROVED FOR RELEASE: 2007/02/09: CIA-RDP82-00850R000500010010-4

APPROVED FOR RELEASE: 2007/02/09: CIA-RDP82-00850R000500010010-4

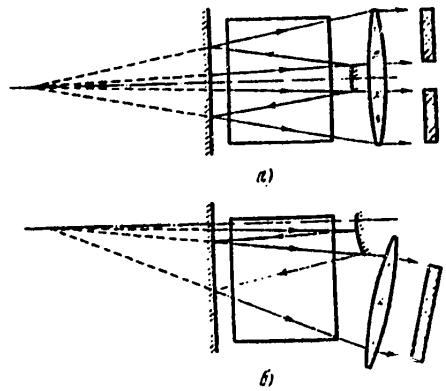

Figure 4.6. Diagram of a laser with rectangular active rod and two-dimensional unstable resonator: a) symmetric, b) asymmetric exit of the radiation (the crosshatched rectangles on the right depict the exit beam cross section).

Two methods of exiting this radiation from the laser were tested which are illustrated in Figure 4.6, a, b; N_{equiv} was ~1700 and ~7000, respectively. In the former case the integral angular distribution of the radiation with respect to pulse time along the direction in the plane of the figure coincided almost with the Fraunhofer diffraction pattern on two rectangular openings (Figure 4.5, c [photo not reproduced]; the long extent of the pattern with respect to the second direction is connected with the fact that in this direction the resonator was equivalent to a planar resonator; in addition, the compensating lens was not cylindrical as should be, but spherical). The band contrast is very close to one, which indicates high spatial coherence of the radiation (let us note that the distance between two beams leaving the resonator was ~120 mm).

Noticeable deviations from the results of the diffraction at the exit aperture of the laser and when using the system depicted in Figure 4.6, b with exit of the radiation in the form of a single beam in one direction from the axis of the resonator were not detected. As a result of increasing the aperture width, in this case the divergence was less than in the first case, and it was 2" or $1 \cdot 10^{-5}$ rad (Figure 4.5, d [photo not reproduced]).

After performing these experiments the thesis that unstable resonators with large N_{equiv} with uniform medium provide single-mode lasing with diffraction angle of divergence of the radiation could be considered proved. It was only left to establish whether departure of the divergence of the radiation of real lasers from the diffraction limit is a consequence of such prosaic causes as imperfection of the elements of the resonator, optical nonuniformity of the medium, or the "high-order modes" sometimes mentioned in the literature are at fault here. According to § 3.2, the wave front of a light beam which is the fundamental mode of an unstable resonator is formed in it just as on transmission of the beam through a multistage amplifier (Figure 3.6). Therefore the best answer to the stated problem can be given by direct experimental comparison of the divergence of the radiation of a real laser with an unstable resonator with divergence at the exit of the multistage amplifier

APPROVED FOR RELEASE: 2007/02/09: CIA-RDP82-00850R000500010010-4

APPROVED FOR RELEASE: 2007/02/09: CIA-RDP82-00850R000500010010-4

(see § 2.6) constructed from analogous active elements. This comparison was undertaken in [195].

The basic results of [195] are presented in Figure 4.7. Curve 1 corresponds to the angular distribution at the input of the final stage of amplification, curve 2, at the output of the multistage system. The data for the laser with telescopic resonator are plotted using x's; it is obvious that the multistage system in its "pure" form insures somewhat less divergence of the emission. However, if we cover the central part of the exit aperture of the multistage system so that the beam acquires the same circular cross section as in the case of a telescopic resonator the divergence of the radiation of the devices of both types comes close to coinciding (see curve 3).

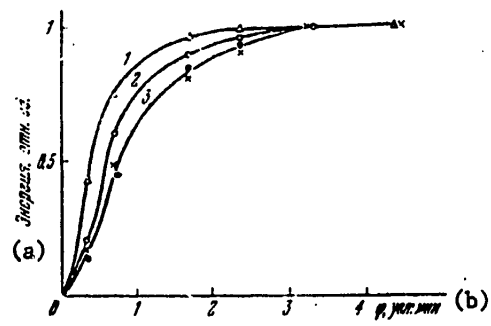

Figure 4.7. Angular distribution of the radiation energy (the proportion of the energy in a cone with apex angle ϕ is plotted on the y-axis): 1 — at the entrance of the final stage of a multistage system; 2 — at the exit of a multistage system with circular aperture; 3 — annular exit of the radiation; x — telescopic resonator, ● — multistage system with annular diaphragm.

Key: a. energy, relative units
b. angular minutes

Attention is attracted by the fact that the differences between curves 2 and 3 cannot be explained by purely diffraction phenomena: the halfwidth of the angular energy distribution as a result of diffraction of the plane front in a circular opening was 5" more under the conditions of [195], and in the annular opening, a total of 4" more. Obviously these differences were caused primarily by the fact that the optical uniformity of the central part of the pumped neodymium glass rod is higher than its periphery (information about the nonuniformity induced in such cases is presented in [200]); therefore the addition of the central part to the annular exit aperture also causes a noticeable decrease in the divergence.

From Figure 4.7 it is obvious that preliminary stages and the final amplifier in the given case make similar contributions to the total radiation divergence with respect to magnitude. From the materials of § 3.2 it follows that for a telescopic resonator used in [195] with M = 2 the distortions of the wave front coming as a result of large-scale nonuniformities before the last pass through the active rod and directly in this last pass are also similar with respect to magnitude. The analogy between the multistage system and the telescopic resonator is quite obvious here.

FOR OFFICIAL USE ONLY

APPROVED FOR RELEASE: 2007/02/09: CIA-RDP82-00850R000500010010-4

APPROVED FOR RELEASE: 2007/02/09: CIA-RDP82-00850R000500010010-4

Thus, carefully made unstable resonators are actually capable of insuring the same radiation divergence as multistage circuits (considering obvious corrections connected with the differences in the exit apertures). As will be obvious in §4.3, by using these resonators amplifiers can be constructed which provide enormous amplification of the weak signal in one standard active element (considerable work is required, in particular, in devices consisting of many channels synchronized by a single master oscillator). At the same time, the experience of [195] demonstrated that the problems pertaining to energy efficiency are solved on the basis of unstable resonators much more simply than when using multistage systems (as a result of a significantly smaller number of elements in the optical system of the device). Therefore the sphere of application of the awkward multistage systems primarily remains the rare cases where for the sake of achieving record radiation parameters any means are considered justifiable.

The entire research cycle discussed above which was performed in the example of pulsed neodymium glass lasers with free lasing permitted sufficiently complete discovery of the possibilities connected with the application of unstable resonators in their simplest version. This cycle was preceeded by a total of two articles with reports on experiments with similar resonators. The first of them is the initial paper by Siegman [4] which we have mentioned many times and in which, in addition to the formulation of a number of the most important theoretical arguments (§ 3.1), the preliminary results of studying a ruby laser with unstable resonator are also discussed; the second is the paper [201] on experiments with a pulsed argon laser having a discharge tube 7 mm in diameter. In both cases it was impossible to obtain any positive effect from transition to the unstable resonator.

Gas Pulsed Lasers with Unstable Resonators. Problem of Steadying Oscillations. Subsequent foreign publications about the application of unstable resonators in pulsed lasers began to appear only in 1972 [202, 203], and they pertained to the case of CO_2 lasers. No new information about the properties of unstable resonators was contained in these papers, and nothing special was presented on a purely technical level. Actually, among several of the first experiments the highest output parameters were achieved in [203]: for a pulse energy of 3.5 joules, the radiation divergence was $\sim 2 \cdot 10^{-4}$ radians, and the brightness was $\sim 2 \cdot 10^{13}$ watts/(cm^2-steradian). For comparison we mention that in Soviet lasers with telescopic resonator based on neodymium glass long before this the smaller angular divergence was "mastered" with an output energy of $\sim 10^3$ joules, and in 1971-1972 there were already lasers with brightness of $\sim 10^{17}$ watts/cm^2-steradian) [204, 205].

Beginning with that time, unstable resonators began to be used also with invariant success in lasers of almost all types. It is sufficient to mention, for example, the creation of an electroionization laser with a pulse energy of 7500 joules [206]. However, the results of experiments with metal vapor lasers are of the greatest cognitive interest [207]: the specific peculiarities of these lasers forced a new look at some theoretically known properties of unstable resonators. The fact is that the amplification coefficient of the medium is extraordinarily high here; on the other hand, the population inversion here exists for such a short time that during this time the light travels through the resonator only a few times. Since low divergence is desirable at all costs, it is of primary importance for the optical cavity to be capable of rapidly isolating the fundamental mode from noise radiation.

APPROVED FOR RELEASE: 2007/02/09: CIA-RDP82-00850R000500010010-4

APPROVED FOR RELEASE: 2007/02/09: CIA-RDP82-00850R000500010010-4

The problem of establishing oscillations in optical resonators was first encountered in 1961 by Fox and Li [9]: the iterative calculations that they performed to a significant degree simulate the processes occurring in real lasers; the initial field distribution written into the iterative procedure plays the role of the "nucleating center," the source of which in real lasers is spontaneous emission. Then Fox and Li noted the obvious relation between the rate of establishment of steady oscillations and the differences in the losses of the individual modes: actually, during the time of passage of the light through an empty resonator the intensity ratio of any two modes varies by $(1 - \Delta_1)/(1 - \Delta_2)$ times, where Δ_1 and Δ_2 are their diffraction losses. Obviously the intensity ratio will vary in the same way also in the presence of a medium with uniformly distributed amplification coefficient k_{amp} with respect to volume (the eigenvalues of the integral equation of the resonator turn out to be multiplied by the same coefficient $\exp(k_{amp}\ell)$ in this case, (see § 1.3). If the medium was uniformly excited at the time of beginning of development of lasing from the noise "nucleating center," the situation will be maintained until the lasing power builds up to such a degree that saturation level is reached.

Hence it follows that the more the losses of the individual modes differ, the faster the generation of certain modes against the background of the others will occur; in particular, the oscillations in unstable resonators must be set up much faster than in plane, and especially stable cavities. For these reasons the rate of establishment of the oscillations in the most unstable resonators increases with an increase in $|M|$.

Although all of these facts were well-known, the problem of calculating the time required for the diffraction directed beam to form in an unstable resonator from spontaneous emission was clearly stated only in [207], and it was gradually solved in [207-209]. It is true that the authors of the indicated papers for some reason considering the given situation exceptional tried to get around using the known results and methods of the theory of optical resonators, even such generally used ones as the introduction of the equivalent resonator. Accordingly, for this quite simple problem they obtained a very complex solution, making, in the course of the matter, an entire series of erroneous statements (for more details see [210]). In particular, their advice to select the resonator parameters so that the converging beam will expand to the former cross sectional dimensions invariably in an integral number of passes is meaningless. Therefore it is better to discuss a significantly simpler solution to the same problem presented in [210].

Let the active medium have the cross section 2a × 2a and be placed inside a telescopic resonator (Figure 4.8). Let us follow, for example, the fate of the nucleated radiation which at the initial point in time is emitted near the convex mirror in the direction of a concave mirror. We shall take the spherical equiphasal surface of the diverging wave located on the convex mirror, the center of curvature of which is at the common focal point of the mirrors as the reference surface. The complex amplitude of the nucleation field of one of the polarizations on this reference surface can be represented in the form of the series

$$u(x, y) = \sum_{k,l} u_{kl} \exp\left(k\pi i \frac{x}{a}\right) \exp\left(l\pi i \frac{y}{a}\right), \quad k, l = 0, \pm 1, \pm 2, \ldots$$

FOR OFFICIAL USE ONLY

APPROVED FOR RELEASE: 2007/02/09: CIA-RDP82-00850R000500010010-4

APPROVED FOR RELEASE: 2007/02/09: CIA-RDP82-00850R000500010010-4

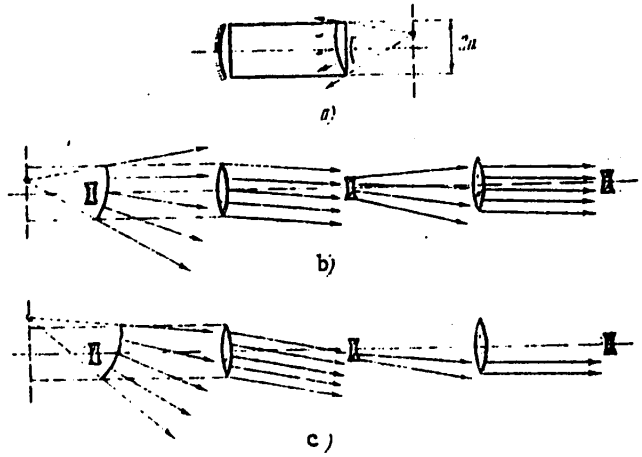

Figure 4.8. Transmission of spherical waves through a telescopic resonator: a) one of the "diverging" waves; b), c) transmission of diverging waves with centers of curvature near the zone 2a wide (b) and outside this zone (c) over an equivalent line.

This series corresponds to the set of spherical waves with randomly distributed amplitudes u_{kl}, the mean value of which can be calculated beginning with the power of the spontaneous radiation for a solid angle $(\lambda/2a)^2$. The centers of curvature of these waves lie in the focal plane and are shifted from the common focal point of the mirrors in two directions a distance $k\lambda f_2/2a$, $\ell\lambda f_2/2a$, where f_2 is the focal length of the convex mirror, k and ℓ are the wave indices. The centers of curvature of the waves, the radiation of which completely covers the concave mirror, fills a zone 2a × 2a in size (see the figure); the number of such waves, consequently, is equal to $(4a^2/\lambda f_2)^2$. As the figure shows, some of the radiation of waves lying near this zone also reaches the range of the laser; however, it very quickly leaves the confines of the optical cavity entirely. Therefore, except for the very earliest stages, the number of waves taking part in the process of lasing onset is $(4a^2/\lambda f_2)^2$, i.e. the spontaneous emission falling in a solid angle of $(2a/f_2)^2$.

Now let us trace the behavior of the waves; this is entirely possible within the framework of the geometric approximation until the divergence tightly approaches the diffraction limit. Obviously after the first reflection from the concave mirror part of the cross section of each wave equal to $1/M^2$ remains inside the resonator; the waves themselves go from spherical to planar with propagation directions inclined with respect to the axis at angles of $(k/M)(\lambda/2a)$; $(\ell/M)(\lambda/2a)$. The width of the entire range of angles, that is, the total divergence of the emission is $\frac{4a^2}{\ell f_2}\frac{1}{M}\frac{\lambda}{2a} = 2a/Mf_2$. After each subsequent passage through the resonator, the amount of radiation remaining in it decreases by M^2 times. The slopes of all the beams, and with them, also the total angle of divergence, decrease by M times.

Thus, after n passes through the resonator, the proportion of the radiation of all of the waves entering into the "nucleating center" equal to $1/M^{2n}$ remains in it,

APPROVED FOR RELEASE: 2007/02/09: CIA-RDP82-00850R000500010010-4

APPROVED FOR RELEASE: 2007/02/09: CIA-RDP82-00850R000500010010-4

and the total "geometric" divergence is $2a/M^n f_2$. The number of passes n_0 during which the "geometric" divergence decreases to $\lambda/2a$ and thus the formation of the diffraction diverging beam (the basic mode) is completed, is defined by the expression $2a/(M^{n_0} f_2) = \lambda/2a$ or $M^{n_0} = 4a^2/(\lambda f_2)$. By this time the proportion of primary "nucleating" radiation equal to $1/M^{2n_0} = (\lambda f_2/4a^2)^2$ remains inside the resonator. It is easy to see that this proportion corresponds to the radiation intensity which initially pertained on the average to one wave.

In spite of the primativeness, the given analysis leads to the same quantitative results which were obtained in [207-209] using somewhat more complex manipulations with the "compressing waves." Using these results, it is entirely possible to undertake specific calculations of the kinetics of such lasers. However, the most important conclusion can also be drawn without performing such calculations. From the above-presented relations it follows that the time of formation of a diffraction-directional beam with fixed dimensions of the resonator decreases slowly and monotonically with an increase in M (inasmuch as $n_0 = \ln [4(M - 1)a^2/\lambda L]/\ln M$). Thus, the thesis that to obtain the smallest possible divergence it is necessary, considering the stipulations made on page 53 to use unstable resonators with the largest possible magnifications, has received another, quite weighty substantiation.

This entire concept was checked experimentally in [207]. When using a telescopic resonator with M = 6 in a copper vapor pulse laser, the calculated time required for fundamental mode lasing turned out to be greater than the time during which the radiation density inside the given laser could grow from the noise density to the saturation level. As a result, the integral divergence with respect to the pulse duration exceeded the diffraction limit by almost an order. For M = 200 (!) this limit was reached, it is true, at the price of a sharp drop in radiation power as a result of the extraordinary rise in the lasing threshold. Probably for intermediate M it would be possible to achieve both small divergence and sufficient radiation energy[1]).

§ 4.2. Unstable Resonators in Continuous Lasers

Survey of Experimental Work. Somewhat later than in pulsed neodymium glass lasers, unstable resonators began also to be used in continuous gas lasers. Among the first publications only one short, but exceptionally interesting article [211] stands out which to a great extent anticipated the future development of the resonators of gas dynamic lasers; we shall return to this paper later. As for other studies in 1969-1973, their subjects were low-pressure electric discharge CO_2-lasers [199, 212, 213] and chemical lasers [214, 215]. The early paper by Krupke and Sooy [199] is isolated here. In this paper a telescopic resonator was used in practice for the first time; as a result of the carefulness of the experiment and the high optical uniformity of the active medium the authors were able to observe the diffraction structure of the distribution in the far zone with full width of the central peak on the order of 1' ($3.5 \cdot 10^{-4}$ radians)[2].

---

[1] This was done in the recent experiment [332].

[2] In this paper an analysis was made for the first time of the consequences of misalignment and variation of the curvature of the mirrors in two types of confocal unstable resonators.

APPROVED FOR RELEASE: 2007/02/09: CIA-RDP82-00850R000500010010-4

APPROVED FOR RELEASE: 2007/02/09: CIA-RDP82-00850R000500010010-4

It must be noted that in all of the enumerated studies except [211] not only the goals, but also the conditions differed sharply from the conditions of the experiments with neodymium lasers, primarily by the fact that in view of the modest dimensions of the resonator cross sections and the long wavelength, the Fresnel numbers N were quite small. The theoretical limit of the angular divergence of these lasers, on the other hand, was not small. Thus, in the same paper by Krupke and Sooy, the width of the radiation ring at the exit from the laser was ~1 mm; the angle into which half the energy went, although it was not measured, must have been equal to $5 \cdot 10^{-3}$ radians under these conditions. This divergence could be completely achieved also using a planar resonator. Therefore the basic positive result of the mentioned experiments is not the achievements in the field of angular selection, but experimental testing of a number of conclusions of the theory of unstable resonators pertaining to the magnitude of the losses, the nature of their dependence on N_{equiv}, and so on. A detailed summary of the results of testing the theory is available in the highly substantial survey by Siegman [216]. It is of interest that although the majority of researchers, in accordance with the recommendations of Siegman [167], have carefully selected the resonator parameters so that N_{equiv} will be close to a half integer, no article contains data indicating that this choice actually is useful from the point of view of angular divergence of the emission.

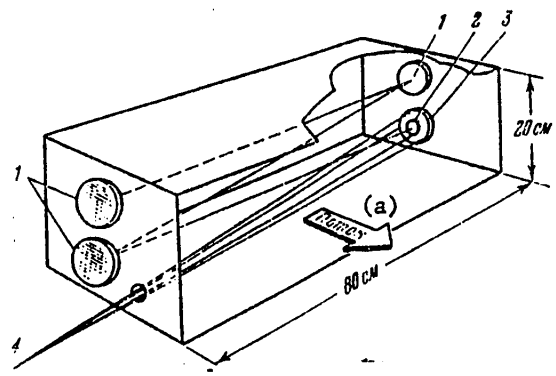

Figure 4.9. Schematic representation of the active zone and resonator of a powerful gas dynamic laser [211]: 1 — planar mirrors, 2 — convex exit mirror, 3 — external concave mirror, 4 — exit beam.

Key: a. flow

Now let us more carefully consider the results of [211]. This article is devoted to experiments with a powerful gas dynamic laser; the schematic representation of the active zone with the resonator borrowed from [211] is presented in Figure 4.9. As is obvious from the figure, the resonator is installed so that the lasing radiation will pass through the gas flow perpendicularly to the direction of motion of the flow itself. This arrangement of the cavity, which is called transverse, is adopted because the high average powers require large flow rates of the gas mix, and organization of uniform gas flows with large flow rates is possible only in the case here the resonator elements are beyond the limits of the flow cross section (in electric discharge lasers the same thing occurs also with the electrode assemblies).

APPROVED FOR RELEASE: 2007/02/09: CIA-RDP82-00850R000500010010-4

APPROVED FOR RELEASE: 2007/02/09: CIA-RDP82-00850R000500010010-4

Tests were run on a gas dynamic laser in [211] with resonators of two types. The first type was a stable resonator made of two large metal mirrors, in one of which a system of many holes 1.5 mm were made, the total area of which was on the order of 6% of the total area of the mirror. This procedure does not withstand any criticism from the point of view of divergence of the radiation (§ 2.5), but it permits realization of a resonator with given small losses to emission, and, as the experience of [211] shows, it can be used for experimental optimization of the energy characteristics of the laser. With this resonator the output power was 55 kilowatts.

The second type resonator is depicted in Figure 4.9. It was formed by four mirrors and was already unstable. One of the mirrors was convex, it served as the output mirror, and accordingly was smaller in diameter than the others. The beam passing near it fell on the additional concave mirror and was focused on the hole in the wall of the cavity through which it was taken outside. The use of a system with three passes through the active medium permitted, in spite of small amplification per pass, operation of the laser with magnification of the resonator $M = 1.6$; the output power was 30 kilowatts.

An almost twofold reduction in lasing power by comparison with the case of a stable resonator indicates that the achievement of the maximum efficiency of energy conversion in the gas dynamic laser resonator is not such a trivial problem as for pulsed lasers. It is necessary to consider that such a resonator consists, as a rule, of several carefully aligned (or even equipped with an automatic alignment system, see [217]) cooled mirrors and is, together with the fastenings, the aligning slides, and so on, a quite complicated device. It is part of a still more complicated engineering structure which is the fast-flow laser as a whole. Inasmuch as the purely empirical selection of the optimal resonator under such conditions becomes too thankless, the theoretical methods of analysis have been widely developed, the investigation of which we shall proceed with.

Methods of Calculating the Efficiency of Flow Lasers. It is necessary to distinguish two cases immediately. Whereas the fast-flow laser operates in the frequency mode where the excitation of the medium is realized by individual, periodically repeating pulses, the procedure for calculating its energy characteristics does not differ in any way from the procedure for calculating the efficiency of the resonator of ordinary pulsed lasers. Actually, one pumping pulse lasts, as a rule, 10^{-6} to 10^{-4} seconds; the medium during this time can travel such a short distance that it can be considered stationary during the pulse (the flow velocity in the frequency lasers usually does not exceed 100 m/sec. In pulsed lasers, as we know from §1.4, the state of the active medium in any elementary volume of it under the given pumping conditions is uniquely defined by the density of the lasing radiation passing through this volume. This makes it possible to talk not only about the efficiency of the laser as a whole, but also about the efficiency of energy conversion in any part of its volume, which significantly facilitates the understanding of the basic laws (§ 1.4). The local nature of the dependence of the amplification coefficient on the radiation density leads to significant simplification also of the quantitative calculations of lasers with unstable resonators. First, the equations describing the state of the medium themselves are simple in this case. Secondly, it is very easy by using the threshold condition to find the radiation density on the axis of the resonator before finding the distribution in the entire volume (see § 4.1), which greatly accelerates the convergence of the ordinarily used iterative procedure.

APPROVED FOR RELEASE: 2007/02/09: CIA-RDP82-00850R000500010010-4

APPROVED FOR RELEASE: 2007/02/09: CIA-RDP82-00850R000500010010-4

In continuous-wave flow lasers the situation is quite different. The concept of local efficiency here cannot exist in general: the previously excited active medium flows through an entire beam of generated radiation, and the number of atoms reacting with the beam can be calculated only beginning with knowledge of the radiation distribution as a whole. It is also more difficult to calculate the radiation density in advance on the system axis inasmuch as the inverse population on the axis depends not on this density, but on the entire history of the medium reaching here, in particular, the field density on its entire path.

Similar laws occur also in the case of side optical pumping of induced Raman scattering lasers frequently called Raman [combination] lasers or VKR[1]-converters[218]. On the other hand, the amplification coefficient of the lasing radiation on the combination frequency is proportional to the pumping radiation density on the initial frequency. On the other hand, the attenuation of the pumping radiation on passage through the medium is almost wholly determined by its interaction with the generated radiation — without lasing, the primary pumping radiation is poorly absorbed by the medium. It is easy to see that the pumping light density in Raman lasers is, from the point of view of resonator theory, the complete analog of the inverse population density in flow lasers; the residual absorption in the Raman laser medium corresponds to a decrease in the inverse population down stream with respect to the gas as a result of spontaneous relaxation of the active medium of the flow laser.

In 1968 Alekseyev and Sobel'man [219] pointed out that the application of a planar resonator in a Raman laser with side pumping is fraught with highly unpleasant consequences. Inasmuch as the amplification coefficient near the edge of the resonator from the side of which the pumping is realized, usually noticeably predominates over the losses on the combination frequency in the mirrors and the medium, the lasing radiation density here turns out to be extraordinarily high (if its growth does not prevent the beginning of lasing on subsequent combination frequencies, for which the radiation on the first combination frequency is itself pumping). At the same time, with an increase in the density of the converted (Raman) radiation, the attenuation coefficient of the primary radiation increases — the region of powerful lasing screens the remaining volume from the pumping radiation. Thus a tendency shows up for the lasing region to contract into a very narrow zone, and this is difficult to eliminate. Analogous phenomena must occur also in flow lasers although usually not in such sharply expressed form (we shall discuss the causes of this somewhat later).

In the case of an unstable resonator, independent development of lasing on the periphery of the converter or the flow laser is impossible, for the lasing radiation must come from the central section of the cross section. Extraordinary growth of the lasing radiation density on the axis of the system is impossible, for it causes rapid growth of the density also on the periphery, which leads to a decrease in the amplification on the axis. As a result, the regime turns out to be self-balanced; the lasing radiation fills the resonator cross section, its density is established on a level such that the number of pumping quanta reaching the axis in the Raman laser or excited atoms in the flow laser insures exact satisfaction of steady state conditions.

---

[1]The first letters of the Russian words that mean induced Raman scattering].

APPROVED FOR RELEASE: 2007/02/09: CIA-RDP82-00850R000500010010-4

APPROVED FOR RELEASE: 2007/02/09: CIA-RDP82-00850R000500010010-4

These arguments are formulated in [154], and they were confirmed by the experimental data of the above-quoted reference [211] (the nonuniformity of the intensity distribution observed there with respect to cross section of the unstable resonator did not exceed ±50%). In all of the subsequent theoretical papers devoted to estimation of the efficiency of the continuous lasers, a study is made of the self-balanced lasing regime on the lowest transverse mode.

It is true that in the experiment of [220] with defined resonance, a mathematical model of a flow laser was proposed from which it follows that the lasing regime must be not steady, but autooscillatory with an oscillation period on the order of the drift time of the gas flow through the resonator zone. If this model were correct, the autooscillations would be characteristic of even a broader class of lasers than the authors of [220] themselves proposed[1]. However, the medium was considered single-component in [220], the speed of light was considered infinite, and the geometric approximation, valid, even under the conditions where the properties of the medium vary sharply over the extent of small sections of the resonator cross section near its axis. Judging by the results of [221], it is sufficient to do away with the proposition of single-component mixture so that the trend toward the autooscillations will decrease sharply (and in real lasers, as a rule, mixtures are used which contain more than one component). Consideration of the fact that for the light to pass through the resonator takes a finite time is extremely important and must also lead to damping of the oscillations (from the papers at the beginning of the 1960's devoted to the kinetics of solid-state lasers it is known that neglecting this fact usually leads to absurd results). Thus, the deep autooscillation mode is hardly widespread. As for the ordinary and unavoidable oscillations of intensity caused by fluctuations of the resonator Q-factor, and so on, they can hardly lead to significant departure of the energy parameters of the laser averaged over a large time interval from the calculation results in the quasistationary approximation (see § 1.4).

In itself the calculation of the efficiency of a laser operating in the steady state mode in the general case reduces to finding a self-consistent combination of distributions of the amplification coefficient and the lasing field. The equations describing the dependence of the amplification coefficient distribution on the excitation conditions and the lasing field depend on the peculiarities of the medium and are quite different. As for the lasing field distribution, for it it turns out most frequently to be sufficient to use the geometric approximation. Actually, we have already discussed the causes by which it is possible to neglect the effect of the edge diffraction in lasers with large M_{equiv} (§ 3.3). The consideration of large-scale nonuniformities of the active medium does not require diffraction approximation (§ 3.2). Moreover, if the medium is not too nonuniform, it is possible also to take the path of the beams the same as would occur in an ideal resonator. Hence, it follows that weak optical nonuniformity of the active medium, just as the edge diffraction, can in general not be considered in the energy calculation. On the other hand, inasmuch as the angular divergence of the radiation depends primarily on the phase distribution at the laser output, and the nonuniformity of

---

[1]At the end of the indicated article, an additional factor is erroneously introduced to describe the phenomena of amplification saturation, at the same time as consideration of these phenomena is already built into the initial equations.

FOR OFFICIAL USE ONLY

APPROVED FOR RELEASE: 2007/02/09: CIA-RDP82-00850R000500010010-4

APPROVED FOR RELEASE: 2007/02/09: CIA-RDP82-00850R000500010010-4

the intensity distribution influences it weakly, the amplification saturation phenomenon must be felt little in its magnitude; this conclusion follows from the materials of § 1.1 and is confirmed by the results of sometimes undertaken specific calculations (for example, [222]). Therefore the width of the radiation pattern can be estimated in the first approximation without calculation of the energy characteristics of the laser.

In order to find the self-consistent solution most frequently an iterative method is used. The simplest iterative procedure used in the 1960's to study the phenomena of amplification saturation in planar and stable resonators [100, 90, 109] consists of the following. An initial field distribution (usually uniform) is taken; this distribution is substituted in the equations of the medium; the latter are solved, and the spatial distribution of the amplification coefficient is found. Then the new field distribution is calculated as a result of single passage of the initial beam through the resonator with the active medium. The newly obtained field distribution is substituted in the equations of the medium, and so on. As applied to the calculations of lasers with unstable resonators in a weakly nonuniform medium performed in the geometric approximation, the given procedure can be written as follows: $F_{n+1}(r) = f[u_n(r)]$, $u_{n+1}(r) = F_n(r)u_n(r/M)$, where F is the aberration function calculated considering the distribution of the amplification coefficient (see § 3.2), and the index denotes the number of the iteration. The calculations are quite tedious, for although only the field distribution at the exit mirror u(r) figures in the above formulas, for the calculation of F(r) it is necessary to deal with the amplification coefficient distributions (and, consequently, the field distribution) in the entire volume of the laser.

As was noted above, the convergence of the iterative procedure can be accelerated significantly by preliminary calculation of the radiation density and inverse population on the resonator axis. In the case of lasers considered in the preceding section, it was sufficient for this purpose to consider the conditions on the axis itself. Later it will be obvious that this problem is also solved for flow lasers, it is true, using more complex calculations. The data obtained on the magnitude of the field under the state of the medium on the resonator axis are used in the subsequent calculations; here the condition of stationarity of the regime turns out to be automatically satisfied in all phases of the iterative procedure. Finding the amplification coefficient distribution next, this makes it possible for us to not limit ourselves to single "transmission" of the beam through the resonator with the medium and to find the steady state field distribution corresponding to the given picture of the state of the medium. The iterative procedure acquires the form $F_{n+1}(r) = f[u_n(r)]$, $u_{n+1}(r) = u(0)F_n(r)F_n(r/M)F_n(r/M^2)\ldots$, where u(0) is the previously found field amplitude on the axis. As a result, the volume of the calculations is reduced noticeably, especially for complex mathematical models of the medium. The calculations of pulsed lasers with nonuniform optical pumping mentioned in § 4.1 [188] and the calculations of gasdynamic lasers discussed below were performed by approximately the same method.

Other procedures are also used which permit reduction of the volume of the calculations both when finding the field distribution by the given parameters of the resonator and state of the medium and for calculations of lasers as a whole. Although the authors of each of these procedures present very convincing arguments in its favor, it is now difficult to determine which of them is actually more

FOR OFFICIAL USE ONLY

APPROVED FOR RELEASE: 2007/02/09: CIA-RDP82-00850R000500010010-4

APPROVED FOR RELEASE: 2007/02/09: CIA-RDP82-00850R000500010010-4

effective. Therefore those who desire to familiarize themselves in more detail with the method of the calculations are referred to numerous corresponding articles [222-227, 188, 156], and so on); at the same time we shall limit ourselves to the fact that we shall explain some peculiarities of the calculations and the behavior of flow lasers in the example of gas dynamic lasers with two-mirror telescopic resonator investigated in [188, 228]. All of the basic laws here are the same as in the case of resonators of the type depicted in Figure 4.9 (if, of course, we compare lasers with identical amplification not on the beam width, but on the entire path from one terminal mirror of the resonator to another). Lasers with resonators, the axis of which is "broken" not across, but along the direction of the gas flow behave differently; we shall not consider them.

Simplest Model of a Gas Dynamic Laser Medium. Methods and Results of Energy Calculations of Gas Dynamic Lasers with Two-Mirror Resonator. In the overwhelming majority of gas dynamic lasers the inverse population is created, by the proposal of Konyukhov and Prokhorov [229], by adiabatic expansion of a gas mixture consisting primarily of CO_2 and N_2. These two components also play the primary role in the lasing process. CO_2 molecules are characterized by a comparatively short oscillatory relaxation time; the laser transition is also realized in them. Fast loss of the oscillatory energy reserves in this component is frequently compensated for by resonance transmission of excitation from the N_2 molecules on collision with them.

The relative molar concentration 1 - c of the second component of the mixture is larger than the first (c) and the majority of the total oscillatory energy reserves is concentrated in the second component, N_2, which is, therefore, a type of energy "reservoir." As a result of the long natural oscillatory relaxation time of the molecules of the second component, the energy from this reservoir is consumed primarily for excitation of molecules of the first component.

Although the atoms located on a quite large number of oscillatory levels of both components participate in the operation of the laser in one way or another, Konyukhov [230] proposed limiting ourselves to a system of a total of two equations for description of the relaxation processes of the medium occurring in the resonator zone. These equations, being reduced to the maximum convenient form for calculations of the resonators, have the form [188]

$$\frac{dk_1(x, s)}{dx} = \frac{ck_2 - (1-c)k_1}{h} - \frac{k_1}{h_1} - (\rho^+ + \rho^-)k_1,$$
$$\frac{dk_2(x, s)}{dx} = -\frac{ck_2 - (1-c)k_1}{h} - \frac{k_2}{h_2}.$$

Here k_1 is the amplification coefficient of the laser radiation; it is proportional to the oscillatory energy reserves in the first component (the population of the lower laser level is considered equal to zero, which usually does not lead to large errors); k_2 is the value having dimensionality (but not meaning) of the amplification coefficient and characterizing the oscillatory energy reserves in N_2; ρ^+ and ρ^-, just as in the preceding section, are the densities of the lasing radiation fluxes directed in opposite directions in the corresponding units; the designations of the coordinates are presented in Figure 4.10; h_1, h_2 are the distances during the time of passage of which by the flow of mixture oscillatory relaxation of the

FOR OFFICIAL USE ONLY

APPROVED FOR RELEASE: 2007/02/09: CIA-RDP82-00850R000500010010-4

APPROVED FOR RELEASE: 2007/02/09: CIA-RDP82-00850R000500010010-4

individual components will occur in the absence of resonance energy exchange; finally, h is the distance during the time of passage of which the processes of resonance energy exchange, neglecting processes of other types (oscillatory relaxation, induced emission), cause relaxation of the ratio of the energy stored in the components k_1/k_2 to the equilibrium value of $\sim c/(1 - c)$ (it is considered that on collision of two different molecules the probability of exchange of excitation does not depend on which of the molecules is excited before collision). Let us note that as a result of the fact that the energy exchange between the components is realized with finite velocity ($h \neq 0$), the total oscillatory energy reserve in the medium cannot decrease too rapidly with as high a density of the generated radiation as one might like. This should attenuate the manifestations of the mentioned trend toward "constriction" of the radiation in the case of a planar resonator.

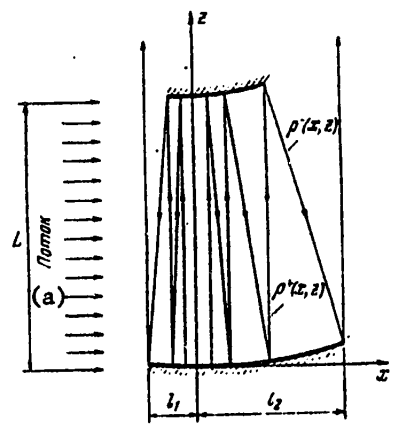

Figure 4.10. Diagram of a telescopic resonator in a flow laser.

Key: a. flow

It is possible to demonstrate that the transition from the density of the output radiation ρ^+ in the adopted units to the resonator efficiency X defined as the ratio of the number of quanta of output radiation to the total number of excited molecules at the entrance to the resonator should take place according to the formula

$$X = \int \rho^+(s)\, ds \left\{ \int [k_1(s') + k_2(s')]\, ds' \right\}^{-1},$$

where the first integral is taken with respect to the exit optical aperture of the resonator, and the second with respect to the flow cross section surface at its entrance to the resonator.

In spite of simplicity of the given model, its application insures satisfactory precision of the energy calculations of the gas dynamic laser in a defined range of variation of composition and parameters of the gas mixture [231]. In the greater part of the specific calculations performed with its help, the results of which will be discussed below, the following initial data standard for gas dynamic lasers were used: mixture composition 15% CO_2, 83.5% N_2, 1.5% H_2O; gas flow

APPROVED FOR RELEASE: 2007/02/09: CIA-RDP82-00850R000500010010-4

APPROVED FOR RELEASE: 2007/02/09: CIA-RDP82-00850R000500010010-4

velocity 1500 m/sec; gas pressure in the vicinity of the resonator 0.1 atm, temperature in the flow 350 K. These data correspond to the following values of the parameters which figure in the equations of the medium: $c = 0.15$, $h = 0.1$ cm, $h_1 = 4$ cm, $h_2 = 250$ cm. Let us also present the value of such an interesting characteristic of the active medium of the flow laser as the length H on which independent relaxation of the excitation is realized in the absence of the lasing field. As is known, any multicomponent mixture, the energy exchange rate between the components of which significantly exceeds the rates of the remaining processes, has such a unique relaxation length. For our medium this condition is satisfied ($h \ll h_1, h_2$); the total relaxation length is $H = [(c/h_1) + (1 - c)/h_2]^{-1} \approx 25$ cm.

At the entrance to the resonator the active medium was considered excited uniformly over the flow cross section and in equilibrium ($k_1^0/k_2^0 = c/(1 - c)$), the total magnitude of the application coefficient of the entrance to the resonator $k_1^0 L$ varied from 0.3 to 0.6 (L is the flow width of the medium). For maximum energy pickup for the location of the mirrors depicted in Figure 4.10, their shape obviously must be rectangular, which was assumed in the calculations. The reflection coefficient of each mirror was considered to be 98%.

The calculations were performed for resonators both made of cylindrical mirrors and made of spherical mirrors. In the first case the calculations were not too complicated inasmuch as all of the distributions are essentially two-dimensional. However, the resonator made of cylindrical mirrors can insure angular selection only with respect to one direction. In the case of spherical mirrors which in practice is more important the calculations are greatly complicated: the gas flow alternately intersects the planes passing through the axis of the resonator at different angles to the direction of motion of the flow, and the solutions in these planes turn out to be dependent on each other. Therefore when constructing the solution in the entire volume it is necessary in all steps of the iterations to manipulate the total three-dimensional field distributions and amplification coefficient distribution. The only exception is one plane passing through the resonator axis on which the solution can be found without constructing distributions in the remaining volume — the plane in Figure 4.10. The solution of the corresponding two-dimensional problem permits the field on the resonator axis to be found immediately, which greatly facilitates subsequent calculations.

It also turned out to be convenient to divide the resonator by the axial plane $x = 0$ into two parts having in the general case different lengths ℓ_1, ℓ_2, (see Figure 4.10) and to proceed with calculations of the distributions in the right-hand side only after the solution on the left-hand side has been completely constructed.

For optimization of the resonator, its magnification M, the widths of the left and right-hand sides ℓ_1 and ℓ_2 were varied. In addition to the effectiveness of the resonator X, for each version the values of the relative losses characteristic of flow lasers were also calculated — relaxation in the volume X_{rel}, removal from the resonator X_{rem} and absorption in the mirrors $X_{mir} = 1 - X - X_{rel} - X_{rem}$. Let us remember that X is the ratio of the number of quanta leaving the laser in the form of useful radiation to the total number of excited molecules entering the resonator at the same time; the relative relaxation and removal losses are

FOR OFFICIAL USE ONLY

APPROVED FOR RELEASE: 2007/02/09: CIA-RDP82-00850R000500010010-4

APPROVED FOR RELEASE: 2007/02/09: CIA-RDP82-00850R000500010010-4

fractions of this total number lost as a result of the processes of deactivation by collisions and as a result of removal of excited molecules that have incompletely interacted with the radiation from the resonator; the meaning of X_{mir} is entirely clear.

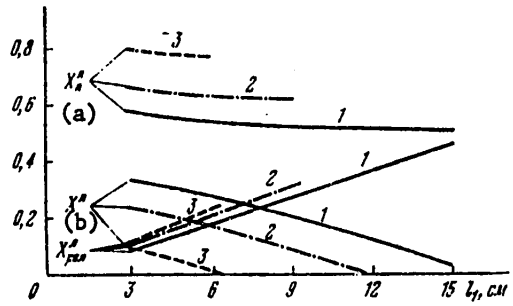

Figure 4.11. Efficiency of the left-hand side of the resonator X^m, the relative relaxation losses in its volume, X^{ℓ}_{rel} and the removal from it X^{ℓ}_{rem} as a function of the length of the left-hand side ℓ_1 for $M = 1.33$: curves 1, 2, 4 — for $k_1^0 L = 0.6$, 0.5 and 0.4, respectively.

Key: a. X^{ℓ}_{rem} b. X^{ℓ}_{rel}

Let us proceed with the investigation of the results of the calculations pertaining to the case of the resonator with spherical mirrors. The relations are presented in Figure 4.11 for the efficiency of the left-hand side of the resonator X^{ℓ} and relative losses X^{ℓ}_{rem}, X^{ℓ}_{rel} as a function of the width of this part with respect to the flow ℓ_1. As is obvious from the figure, with a decrease in ℓ_1 the losses to relaxation are reduced approximately proportionally to ℓ_1 at the same time as the losses to removal vary slowly; as a result, the efficiency X_{ℓ} increases. The meaning of these laws becomes clear if we consider the following peculiarity of the solution for the left-hand side. On the axial plane $x = 0$ separating the left and right sides of the resonator, the distributions and densities of the field and, what is especially important, the amplification coefficient turned out to be quite uniform in all of the calculated cases. Thus, over the extent of the left-hand side of the resonator the amplification coefficient with respect to the entire flow cross section decreases from the initial value of k_1^0 approximately to the threshold value $k_1^{\pi} = (\ln M - \ln R')/L$ (R' is the mirror reflection coefficient). It is necessary to add to this that for the selected mixture the energy exchange between components was so fast that the present radiation field could not significantly disturb the equilibrium ratio between the number of excited molecules CO_2 and N_2. Hence it follows that the losses to removal from the left-hand side of the resonator for any width must in the given case be close to k_1^{π}/k_1^0.

On the other hand, the less the width ℓ_1 becomes, the greater the fields must be insuring such a decrease in the amplification coefficient. This leads to an increase in the role of stimulated radiation processes by comparison with the role of the relaxation processes, that is, to an increase in X^{ℓ} as a result of a decrease in X^{ℓ}_{rel}.

APPROVED FOR RELEASE: 2007/02/09: CIA-RDP82-00850R000500010010-4

APPROVED FOR RELEASE: 2007/02/09: CIA-RDP82-00850R000500010010-4

Now let us proceed to the right-hand side. As we have seen, the state of the medium at the entrance to it can be considered in the first approximation uniquely defined by the resonator losses. Therefore the only parameter which depends on the conditions in the left-hand part of the resonator subject to variation when investigating the right-hand part remains the radiation flux density on the axis $\rho(0, 0)$; this makes it possible significantly to reduce the number of variants of the calculations of the right-hand side.

The construction of the solution in the right-hand side offers the possibility of calculating its efficiency X^{π} defined as the proportion of the excited molecules "processed" into outgoing radiation left after passage through the left-hand side. The results of the calculations X^{π} for $M = 1.33$ and three values of $\rho(0, 0)$ are presented in Figure 4.12. It is obvious that the dependence of X^{π} on ℓ_2 differs with respect to nature from the similar dependence for the left-hand side: with an increase in ℓ_2, the efficiency first increases rapidly, then more and more slowly and, finally, it reaches an extraordinarily gently sloping maximum. This is explained by the fact that on passage of the active medium through the right-hand side of the resonator the oscillatory energy reserve of the molecules is completely exhausted; as a result of a decrease in field density down stream this process takes place more and more slowly. The maximum efficiency is achieved when the amplification in the medium becomes so small that it compares with the losses on the mirrors. Of cours, it is possible in practice to limit ourselves to a significantly smaller width of the right-hand side, losing very little in efficiency, and on the other hand gaining significantly in size of the mirrors. For the above-indicated parameters of the medium, the value of $\ell_2 \sim 15$ cm (see [228] and also Figure 4.12) can be used which is also used in the subsequent calculations.

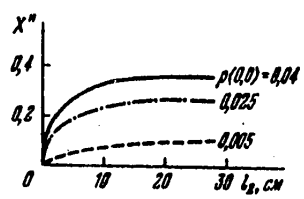

Figure 4.12. Efficiency of the right-hand side of the resonator as a function of its length ℓ_2 for $M = 1.33$ and three different $\rho(0, 0)$.

Now it is possible to proceed with investigation of the properties of the resonator as a whole. In Figure 4.13 we have the relations for its efficiency $X = X^{\ell} + X^{\ell}_{rem} X^{\pi}$ as a function of the magnification M and width of the left-hand part for $\ell_2 = 15$ cm. It is obvious that the given relation coincides with respect to nature with the analogous function for the left-side only (see Figure 4.11). This is also understandable: for small M and ℓ_1, $\rho(0, 0)$ increases, and as a result the efficiency not only in the left-hand side, but also the right-hand side increases, and together with them, the efficiency of the resonator as a whole. The growth of X with a decrease in M and ℓ_1 continues in the entire investigated range of parameters, slowing only in the case of $k_1^0 L = 0.6$ for $\ell_1 \sim 3$ cm and $M \sim 1.3$; at this time

APPROVED FOR RELEASE: 2007/02/09: CIA-RDP82-00850R000500010010-4

APPROVED FOR RELEASE: 2007/02/09: CIA-RDP82-00850R000500010010-4

X already reaches 60%. It makes no special sense to investigate the region of still smaller values of M and ℓ_1: for ordinary sizes of the active zone of a gas dynamic laser the geometric approximation ceases to be valid there, and therefore the direction of the radiation must become worse.

Thus, in order to achieve high efficiency of energy conversion it turns out to be sufficient to select a total resonator width which is not too much less than the relaxation length of the medium (let us remember that H = 25 cm), the width of the left-hand side is selected approximately an order less, and the resonator losses such that the threshold value of the amplification coefficient is approximately half the value at the entrance to the resonator. This choice has quite clear meaning and may fail to give the desired result only in case of inadequate energy exchange rate between the components of the mixture. Actually, then the total oscillatory energy reserve will not be able to keep up with the gain reduction in the presence of the field, and the losses to removal must increase.

In [228] a series of the corresponding calculations were made for mixtures with the compositions 5% CO_2, 90% N_2, 5% H_2O and 8% CO_2, 90% N_2, 2% H_2O; in both cases the value of k_1^0L was 0.8, the pressure was taken equal to 0.05 atm, and the remaining parameters were the same as in the above-investigated case. The energy exchange rate between the components for these mixtures was noticeably less (primarily as a result of reduced pressure). The calculations demonstrated that for analogous selection of the position of the axis and the dimensions of the mirrors, the efficiency on the order of 0.6-0.7 was achieved only when the threshold value of the amplification coefficient was less than the input value by 3 or 4 times. From the procedural point of view the following is networthy. Although the amplification coefficient in the plane x = 0 is as before close to threshold, the content of the excited molecules N_2 here also depends on the field density. Inasmuch as, in turn, in the entire indicated plane the field density is close to $\rho(0, 0)$, the value of $\rho(0, 0)$ even for mixtures with small energy exchange rate remains the only parameter subject to variation for calculations of the right-hand side.

Problem of Forming Uniform Field Distribution over the Cavity of a Flow-Through Laser. The above-investigated example is quite typical; it is clear from it what arguments must be and are being taken into account when selecting the resonator for a fast-flow laser. It is also obvious that even the

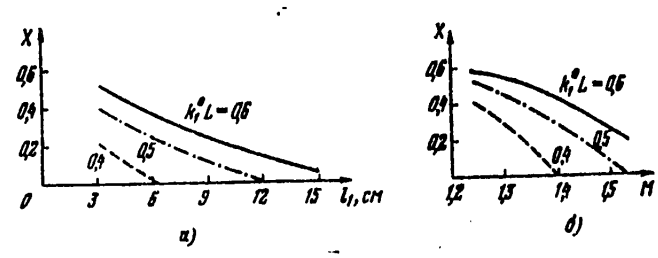

Figure 4.13. Efficiency X of a resonator as a whole as a function of its parameters with a length of the right-hand side ℓ_2 = 15 cm: a) dependence of the magnitude of X on the length of the left-hand side for M = 1.33; b) the value of X as a function of parameter M for ℓ_1 = 3 cm.

APPROVED FOR RELEASE: 2007/02/09: CIA-RDP82-00850R000500010010-4

APPROVED FOR RELEASE: 2007/02/09: CIA-RDP82-00850R000500010010-4

simplest unstable laser made up of spherical mirrors with accurate selection of its parameters can entirely insure satisfactory efficiency of the energy conversion. However, for practical applications it is almost as important to have more or less uniform distribution of the radiation intensity with respect to cross section (otherwise the local thermal loads of the mirrors and angular divergence of the radiation will increase). Although with uniformity of field distribution in the unstable resonators of this type things go better than in planar resonators, they are not sufficiently good. Thus, in Figure 4.14 we have the intensity distribution on a concave spherical mirror (curve 1) for the very case where efficiency of 60% ($k_1^0L = 0.6$, $\ell_1 = 3$ cm, $M = 1.3$) was achieved for a mixture with a pressure of 0.1 atmosphere. Here the graph is also plotted for a two-dimensional resonator (curve 2) for the same parameters of the medium, losses and position of the axis (let us note that under these conditions it has approximately the same efficiency). From the figure it is obvious that the field distribution is quite nonuniform, especially in the more important case of spherical mirrors (in the diffraction approximation a sharp distribution "peak" can smooth off somewhat, but the total nonuniformity will still be clearly noticeable). A more favorable form of distribution is observed only in versions with low efficiency, primarily with excessively large M when the field inside the resonator turns out to be insufficiently intense. This type of situation obviously occurred in the above-described experiments using a gas dynamic laser [211], which is indicated by the low efficiency of the resonator with satisfactory uniformity of distribution.

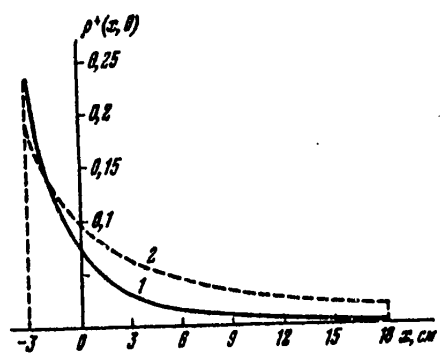

Figure 4.14. Field density distribution in a concave mirror: 1 — for spherical mirrors, M = 1.3; 2 — for cylindrical mirrors, M = 1.69.

The use of multipass systems of the type depicted in Figure 4.9 permits a sharp increase in M. As a result of the complication of the system, a noticeable positive effect is achieved, in particular, the actness of the exit aperture increases, and its filling factor γ increases (see 1.1, 3.6; Figure 1.3, a b corresponds to the single pass and one of the possible versions of multipass systems). However, it is still not possible to achieve a combination of high efficiency with high uniformity of the field distribution here.

In order to solve this most important problem it is possible to consider the prism resonators investigated in § 3.5 in which the effect of wave aberrations of odd order was significantly attenuated by comparison with the ordinary telescopic resonater. The effect of the amplification coefficient gradient directed across the

FOR OFFICIAL USE ONLY

APPROVED FOR RELEASE: 2007/02/09: CIA-RDP82-00850R000500010010-4

APPROVED FOR RELEASE: 2007/02/09: CIA-RDP82-00850R000500010010-4

axis is identical to the influence of the gradient of the index of refraction (wedge) and the wave phase, and it must be attenuated to the same degree.

It is true that in the far infrared range where the greater part of the flow lasers operate, transparent total internal reflection prisms analogous to those used in solid state lasers are hardly realizable. However, for low magnifications M which are characteristic of the flow lasers with single-pass resonators, the application of a confocal resonator becomes mandatory inasmuch as satisfactory filling of the operating cross section with lasing radiation is also achieved in a resonator made up of planar and slightly convex mirrors (see also § 4.1). Replacing the planar mirror by a dihedral 90-degree reflector made up of two planar mirrors, we obtain the desired resonator. For equalizing the intensity distribution, the edge of the reflector must be oriented obviously perpendicular to the plane of Figure 4.10.

This possibility was investigated experimentally in the example of the flow-type CO_2-laser of comparatively smaller power in reference [232]. The systems discussed above were tested (Figure 4.15, a, b); for convenience of selecting the optimal parameters of the resonator, the convex mirror was not spherical, but cylindrical with regulated curvature [233] so that the unstable resonator would be two-dimensional. For the same purpose the radiation was coupled out by two auxiliary mirrors, the position of which could be adjusted. The preliminary recordings of the radiation patterns of the amplification coefficient with respect to the resonator cross section [234] demonstrated that the medium in the given laser relaxes quickly, and the conditions are quite typical for continuous flow systems.

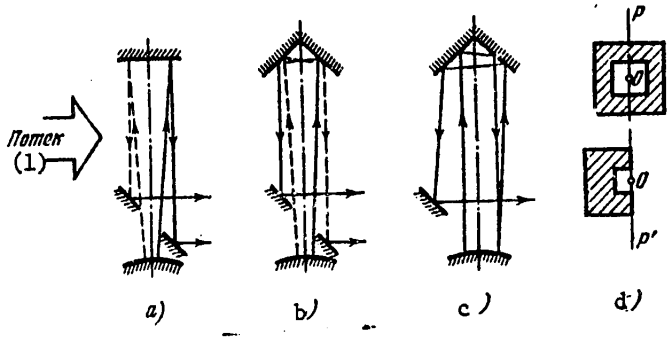

Figure 4.15. Unstable resonators in the flow-type lasers: a) resonator made of planar and convex mirrors; b), c) resonator made of a corner reflector and convex mirror; b) symmetric; c) asymmetric radiation output; d) various versions of the type of projection of the exit aperture on the plane perpendicular to the resonator axis; the axis passes through the point O, the line PP' is perpendicular to the plane of the figure; a) to c).

Key: 1. flow

The results of the experiments turned out to be highly hopeful. When using the system depicted in Figure 4.15, a a tenfold decrease in intensity downstream was observed inside the generated beam. The differences between the intensities and the left and right halves of the resonator with corner reflector (Figure 4.15, b) did not exceed 25%. Another interesting possibility is connected with the application of the corner reflector: in order to increase the compactness of the exit

FOR OFFICIAL USE ONLY

APPROVED FOR RELEASE: 2007/02/09: CIA-RDP82-00850R000500010010-4

APPROVED FOR RELEASE: 2007/02/09: CIA-RDP82-00850R000500010010-4

aperture it is sufficient to resort to asymmetric output of the radiation. In the case of a three-dimensional resonator this is done using an output mirror, the possible versions of the shape and arrangement of which are explained by Figure 4.15, d. In the two-dimensional resonator it is possible simply to remove one of the two output mirrors (Figure 4.15, c). Then the radiation which was incident earlier on this mirror and immediately left the resonator now makes an additional pass through the resonator and leaves from the opposite side. The width of the output zone approximately doubles, the radiation distribution in the far zone becomes more favorable.

From the results of the experiments and rough estimates [232] it is also possible to draw some conclusions relative to the energy characteristics of the flow lasers in which an unstable resonator with corner reflector is used. If we select magnification M and the width of the left-hand side the same as in the case of an ordinary resonator, the average radiation density here will remain as before; the efficiency of the left-hand side almost does not change. As for the right-hand side, its width in the systems with beam "inversion" is automatically close to the width of the left and, as a rule, falls far short of the optimal width of the right-hand side of the ordinary resonators. However, as a result of much greater radiation density the efficiency of the right-hand side also remains approximately on the former level. Thus, it is possible to hope that resonators with corner reflectors will permit insurance of the same efficiency of energy conversion as ordinary resonators with noticeably less width of the operating zone and greater compactness of the exit aperture.

The confocal unstable resonators made of two concave mirrors must have similar properties (see Figure 3.3, c), where "inversion" of the light beam is also realized. However, their use in many cases can cause undesirable phenomena at the common focal point of the mirrors where the radiation density reaches an enormous value.

On the other hand, the great prospectiveness of the application of unstable resonators investigated in § 3.6 with field rotation in continuous-action lasers is unquestioned. The quite recently published results of the corresponding experiments [235, 333] completely confirm the correctness of the arguments discussed in this regard in § 3.6. The introduction of the operation of rotation of the cross section actually cardinally equalizes the intensity distribution in the near zone. Sensitivity to astigmatism decreases so much that the latter is weakly manifested even when the corner reflectors forming the linear resonator include spherical mirrors, the angles of incidence of the light on which are, therefore, $\pi/4$. Finally, the use of a sectional output (see Figure 3.28) instead of annular not only increases the compactness of the exit aperture, but also leads to a significant decrease in divergence of the outgoing radiation without reducing its power.

It only remains to mention that sometimes reports appear in the literature and resonators, the elements of which have the shape of a surface differing sharply from spherical — conical, toroidal, and so on (see, for example, [236]). The possibility of obtaining a small angular divergence of the emission in this way still is far from obvious and we shall not analyze properties of such systems.

§ 4.3. Unsteady Resonators in Lasers with Controlled Spectral-Temporal Emission Characteristics

Simplest Types of Lasers with Control Elements. For many practical applications it is necessary that the stimulated emission have not only small divergence, but

FOR OFFICIAL USE ONLY

APPROVED FOR RELEASE: 2007/02/09: CIA-RDP82-00850R000500010010-4

APPROVED FOR RELEASE: 2007/02/09: CIA-RDP82-00850R000500010010-4

also given time-spectral characteristics. Their achievement usually is insured by the fact that the corresponding control elements are located inside the resonator.

The first publication on building a giant-pulse laser with unstable resonator belongs to the year of 1969 [189]. This was a solid state neodymium-doped glass laser; a passive shutter covered the entire cross section of the active element. The output energy was ~20 joules, the peak power was ~$1.5 \cdot 10^9$ watts, the angular divergence with respect to 0.5 intensity level was ~4"($2 \cdot 10^{-5}$ radians), but a significant part of the energy went to the "tails" of the angular distribution as a result of light dissipation in the shutter liquid. As a result of rapid "spread" of the emission over the cross section of the unstable resonators the pulse duration turned out to be noticeably shorter than when using a planar resonator.

Subsequently, giant pulse lasers with unstable resonators have always been constructed by one of two circuits depicted in Figure 4.16; here the shutter does not cover the entire cross section of the active element, but only the exit mirror. This leads to significant improvement of the output characteristics: the peripheral part of the beam running "to the exit" from the laser, bypasses the shutter and does not undergo additional absorption and dispersion in it [204]. In addition, possibilities are created for controlling the radiation flux having larger area using a small shutter. If we consider that the optically improved fast-acting shutters usually have small aperture, the prospectiveness of using such systems to construct spikeless, monopulsed and other controlled-Q lasers becomes obvious. Thus, at the beginning of the 1970's highly improved a giant-pulse neodymium glass lasers were built with radiation brightness of ~10^{17} watts/(cm^2-steradian) [204, 205]. Let us also note the achievement of the quasisteady lasing mode of an analogous laser in [237].

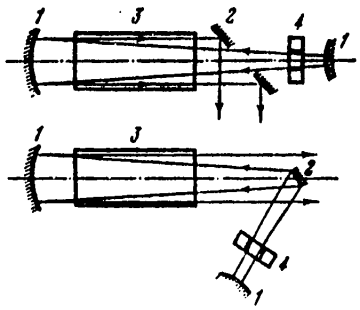

Figure 4.16. Diagrams of Q-switched lasers; 1 — resonator mirror, 2 — additional mirror, 3 — active sample, 4 — shutter

The entire resonator cross section or its exit mirror can be covered, of course, not only by the shutter, but also the spectral selector. It is necessary, however, when installing any controlling elements to deal with the specifics of unstable resonators which impose restrictions on the types and methods of placement of these elements. First of all it is necessary to take steps to prevent the occurrence of a converging wave. If the resonator is telescopic, the flat surfaces of the controlling elements must be also inclined with respect to the resonator axis just as any other interfaces (see § 4.1; in the light of this fact Figure 4.16 is provisional).

APPROVED FOR RELEASE: 2007/02/09: CIA-RDP82-00850R000500010010-4

APPROVED FOR RELEASE: 2007/02/09: CIA-RDP82-00850R000500010010-4

Another important characteristic of unstable resonators complicating the problem of controlling their emission is the fact that the introduction of a small optical wedge does not lead to sharply exceeding the lasing threshold, just as in a planar resonator, but it causes only a shift of the optical axis. As a result, it is necessary to depart from a number of traditional methods of control based on the application of an optical wedge which varies in time or depends on the wavelength. Thus, the placement of a dispersion prism inside an unstable resonator leads not to spectral selection of the emission, but only to the fact that the radiation spectrum will be expanded in the corresponding direction — in the far zone instead of one spot the spectral distribution image appears. Efforts to modulate the Q-factor using a rotating prism can hardly lead to good results.

Thus, in giant-pulse lasers with unstable resonators it is necessary to use predominately passive or electrooptical shutters[1]; for spectral selection primarily the Fabry and Perot etalons are suitable, on passage through which the value does not change its direction. However, even here it is necessary to consider the fact that in any linear, unstable resonator, not a plane wave, but a spherical wave will be propagated in at least one of the two opposite directions. Under these conditions the introduction of the etalon will not cause intensity modulation with respect to the resonator cross section except in the case where the angular width of the maximum transmission of the etalon will exceed the angle of opening of the spherical wave. The angular width of the maximum transmission of the etalon in turn is equal to the angular distance between adjacent rings divided by the number of inferfering beams N which depends on the reflection coefficient of the working surfaces of the etalon. As a result, we arrive at the following condition imposed on the magnitude of the etalon base t [196]:

$$t \leqslant \frac{\lambda}{2N \sin\varphi\, \Delta\varphi} = \frac{M}{M-1}\frac{\lambda L}{2ND \sin\varphi}, \tag{6}$$

where D is the diameter of the transverse cross section of the active element; M and L are the magnification and the equivalent length of the resonator; ϕ is the angle between the normal to the etalon surface and the resonator axis; finally, $\Delta\phi = (M - 1)D/ML$ is the angle of opening of the diverging beam in the telescopic resonator (when deriving (6), the inequality $\phi \gg \Delta\phi$ which usually is satisfied was considered to be valid).

Multiple beam reflection in an inclined etalon also leads to some "blurring" of the position of the resonator axis, which in turn can cause an increase in the radiation divergence. The corresponding calculations indicate that the condition of smallness of this increase by comparison with the diffraction angle again reduces to formula (6). Inasmuch as the etalon base determines the width of the region of its dispersion ($\Delta\lambda = \lambda^2/2t$), consequently the expression (6) limits the minimum width of the spectrum reached in the laser with direct placement of the selecting etalon in the telescopic resonator.

---

[1]Self-Q switching of unstable resonators described in [238] and a number of subsequent papers is realized only in the smallest lasers and leads to output parameters which are hardly recorded even for this class of laser.

FOR OFFICIAL USE ONLY

APPROVED FOR RELEASE: 2007/02/09: CIA-RDP82-00850R000500010010-4

APPROVED FOR RELEASE: 2007/02/09: CIA-RDP82-00850R000500010010-4

Lasers with Three-Mirror Optical Cavity. Further improvement of the methods of controlling the emission of lasers with unstable resonators is connected with the idea formulated and experimentally substantiated in [153] of the effect on the central section of the resonator cross section, from which the radiation "spreads." For normal course of the beams this section is the analog of the master oscillator, and the remaining part of the cross section, a multipass amplifier. In order to realize this idea, it is sufficient to make an opening at the center of one of the mirrors and install an auxiliary mirror behind it; the control elements of very small size can be conveniently placed in the narrow "appendix" formed in this way. This three-mirror resonator and the scheme equivalent to it without an opening in the mirror are depicted in Figure 4.17.

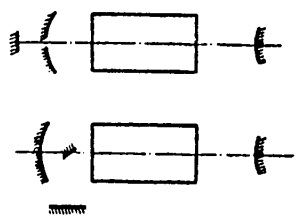

Figure 4.17. Diagrams of resonators with radiation control in the central section of the cross section.

The possibility of efficient radiation control using the given procedure is limited by the fact that, as follows from the materials of § 3.4, a laser with unstable resonator is capable of lasing even with a completely shielded central section of the cross section. Therefore, if in the "appendix," for example, the shutter and the axial section are "blocked" at a given point in time and the lasing threshold increases insignificantly, independent lasing which is not controlled, will develop in the remaining volume. Hence, it is clear what important practical significance the nature of the dependence of the lasing threshold on the dimensions of the covered central segment of the cross section has.

The results of the measurements of this relation performed in [191, 168, 193, 196] turned out to be entirely in correspondence to the theoretical representation developed in § 3.4. In the case of two-dimensional resonators the threshold increases with an increase in hole sizes (more precisely, the slit width) extraordinarily sharply. Thus, the shielding of the central section ~3 mm wide has approximately tripled the threshold intensity of the pumping of the laser described in § 4.1 based on a rectangular large active element with resonator made of planar and cylindrical mirrors (Figure 4.6) [168]. Therefore the control of the radiation characteristics of lasers with two-dimensional unstable resonators is realized without special difficulty. In particular, the use of the simplest disc modulator has made it possible to convert the mentioned laser to the regular "spike" mode with repetition of these spikes from 25 to 50 kilohertz [168]. In reference [193] special selection of the radiation of the same laser without a noticeable decrease in its output power was successfully produced by the introduction of the Fabry and Perot etalon into the "appendix."

Lsers with resonators made of spherical mirrors behave entirely differently. Their lasing threshold increases very slowly with the size of the central circular

APPROVED FOR RELEASE: 2007/02/09: CIA-RDP82-00850R000500010010-4

opening. Thus, in a laser with active neodymium doped glass element 45 mm in diameter and a telescopic resonator with magnification M = 2 for a hole diameter in the concave mirror of 4 mm, the pumping threshold intensity increased by 1.3 times; for a diameter of 8 mm, it approximately doubled by comparison with the case where the hole was absent. Even the presence of a hole with a diameter of 20 mm and almost reaching the diameter of the convex mirror (22 mm) caused onl ı triple increase in the self-excitation threshold [191].

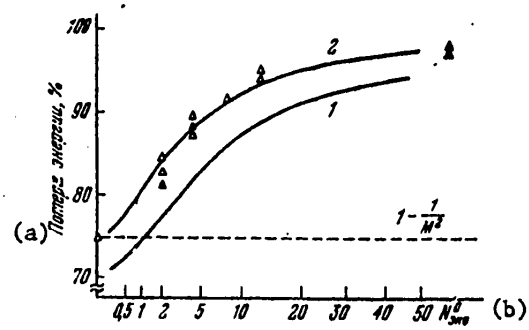

Figure 4.18. Losses of the lowest modes as a function of the size of the coupling hole in a three-dimensional resonator with circular mirrors (M = 2, N_{equiv} = 60). The dots represent the experimental data; 1 — the calculation for the case of a sharp mirror edge; 2 — analogous calculation in the presence of "smoothing" of the edge ($|R_{refl}|$ decreased by four times).

Key: a. energy losses, %
b. N_{equiv}

In Figure 4.18, the data on the dependence of the losses of the lowest mode on the size of the coupling hole calculated by the results of experimental observations and by formulas from § 3.4 in [168] are compared. As is obvious from the figure, the experimental points lie noticeably above curve 1 obtained on substitution of the value of the coefficient of diffraction reflection from the edge R_{refl} calculated by the formula for an ideally sharp edge (3.25) in expression (3.24). In order to achieve comparison of the calculated and the empirical data it is necessary to decrease the value of $|R_{refl}|$ substituted in (3.24) by four times (curves 2). For this decrease $|R_{refl}|$ in the given case there was sufficient "smoothing" of the edge (see § 3.3) in a zone ~0.1 mm wide, which, apparently, are curved in the experiment.

Inasmuch as the shielding of the small axial section here only causes an insignificant increase in the self-excitation threshold, the possibilities for controlling the radiation turn out to be more limited than in the case of two-dimensional resonators. In particular, it is explicitly impossible, when placing the controlling elements only in the "appendix" to realize giant pulse lasing or a lasing mode close to it. If the operating transition line is broadened nonuniformly, the spectral selection of the radiation is also complicated. Actually, in the loop

FOR OFFICIAL USE ONLY

APPROVED FOR RELEASE: 2007/02/09: CIA-RDP82-00850R000500010010-4

of this line with intense single-frequency lasing a "trough" arises, and the amplification coefficient on the side frequencies becomes noticeably larger than on the frequency at which lasing occurs. Therefore the isolation of one frequency using the selector in the "appendix" cannot prevent self-excitation of the lasing on the side frequencies in the remaining volume.

Nevertheless the problem of spectral selection in unstable resonators with spherical mirrors frequently can be solved even in the case of a nonuniformly broadened line. According to [196] it is necessary to try to install one etalon having a small base directly between the primary mirrors of the resonator so that it covers the entire operating cross section. The purpose of this etalon must be to isolate the band, the width of which does not exceed the width of the "trough" in the line contour. If this can be done without violating condition (6), for further constriction of the spectrum it is possible to use the "appendix."

The favorable situation actually occurred when performing the experiments described in [196] with a neodymium-doped glass laser with the active element 45 mm in diameter and 600 mm long. The telescopic laser had magnification of M = 2; the output power without spectral selection was 500 joules per pulse. The preliminary constriction of the spectrum from the width usual to neodymium lasers equal to several nanometers, to a value of ~0.5 nm was carried out using an etalon having a base of only 0.05 mm. Insmuch as all of the conditions were satisfied which were initially discussed, the introduction of this etalon did not cause any changes in the form of the angular distribution (its width with respect to the 0.5 intensity level was $8 \cdot 10^{-5}$ radians). Here the output power dropped to 400 joules. Subsequent introduction of the etalons with bases appreciably larger than in the first one into the "appendix" caused only further decrease in the width of the spectrum, reaching, in the final analysis, 0.003 nm; not only the radiation divergence, but also the output power remained constant.

The following is of interest. In these experiments the width of the opening beyond which the "appendix" with additional etalons was located and amounted to a total of 3 mm. The overlap of this small section of the cross section exceeded by only 10% the self-excitation threshold of the entire laser. In the central section taken separately, the lasing threshold, considering all of the introduced etalons, unconditionally would be higher. This demonstrates that the above-mentioned division into the "master oscillator" and "amplifier" is purely arbitrary inasmuch as the radiation control of the "amplifier" is realized when the self-excitation threshold of the latter was below the threshold in the "master oscillator." The fact is that, as the experiments demonstrated, with the "oscillator" and "amplifier" spatially combined in the three-mirror system, the radiation arrives not only from the first to the second, but also as a result of diffraction, from the second to the first. This increases the radiation density in the "appendix" especially for a small diameter of the appendix, and the role of the "appendix" turns out to be quite large.

The uniform part of the line broadening that determines the width of the "trough" was rather extensive in the silicate neodymium glass used in Ref. 196, which made it easier to pick out the precontraction etalon without violating condition (6). It might not be possible to pick out such an etalon in lasers based on media with a narrower uniform broadening band. What to do in such cases is still unclear; it is possible that it remains only to do away with the linear and resort to the unidirectional ring cavities for which condition (6) becomes invalid.

APPROVED FOR RELEASE: 2007/02/09: CIA-RDP82-00850R000500010010-4

APPROVED FOR RELEASE: 2007/02/09: CIA-RDP82-00850R000500010010-4

Ending with three-mirror resonator lasers, let us note that if there is too much absorption in the "appendix," its role can be significantly strengthened by placement of an additional small-cross section active element in it. It would appear that it is possible to achieve an analogous effect on introducing a special deflector (or orienting one of the interfaces perpendicular to the resonator axis) to produce a convergent wave that "overflows" to the center, but this leads to a sharp increase in the radiation divergence (see [196] and also § 4.1).

External Signal-Controlled Lasers. Now let us proceed to another method permitting the use of the special role of the central segment of the cross section of an unstable resonator. This method was proposed in 1969 [239], and it consists in the fact that radiation from an external source is input to the laser with unstable resonator through the central coupling hole. The properties of such a laser depend decisively on the relation between the amplification of the medium and the losses of the resonator with the coupling hole. If this relation is such that self-excitation of the system does not occur in the absence of an external signal, we are dealing with a "pure" amplifier capable of operating in the slave mode and thus, suitable for effective amplification of powerful short pulses and other purposes. If the self-excitation threshold is low and turns out to be exceeded, it is more correct to talk not about an amplifier, but about a laser controlled by an external signal. Let us first consider the latter case.

The control of laser radiation by an external signal is a well-known method of obtaining the given spectral-time characteristics. This method was used successfully in planar resonators (see, for example [240-243]), where the "nucleating center" from an external source was introduced, as a rule, immediately over the entire cross section of the resonator. Inasmuch as in unstable resonators the radiation quickly "spreads" from the central region, for such effective control here it is obviously sufficient to introduce a beam from an external source only into the region which permits us to go on with quite low power of it. Unfortunately, a comparison of the results achieved in practice obtained when using planar and ustable resonators is almost impossible inasmuch as these results pertain to entirely different cases. For planar resonators, a study was primarily made of the spectrum control mode of a giant pulse by injection of the "nucleating center" at the beginning of its development. As for unstable resonators, for them the control of the spectral-time characteristics of the emission was still realized only under conditions close to quasistationary although the possibility of controlling monopulse lasers also raises no doubt.

In order to obtain the same output power for a controlled laser operating in the quasistationary mode as for an ordinary laser it is obviously sufficient to use an unstable resonator for it with the same M and introduce radiation with the same density into the coupling hole which is developed inside the standard lasers without the coupling hole. However, for more reliable control it is expedient either to increase the density of the controlling signal (which both in the pulsed and in the flow lasers leads to a decrease in amplification on the axis) or noticeably increase M or, finally, do both. Then the system with the supplied external signal turns out to be significantly below its self-excitation threshold, which improves its controllability — in essence, the amplification mode occurs. It is only necessary, by increasing M_1, to see that this does not lead to a large decrease in the output power. This may occur especially quickly in flow lasers with low amplification. As for pulsed lasers using highly amplifying media, the parameters of their resonators can, as a rule, vary entirely "painlessly" within the broad

FOR OFFICIAL USE ONLY

APPROVED FOR RELEASE: 2007/02/09: CIA-RDP82-00850R000500010010-4

APPROVED FOR RELEASE: 2007/02/09: CIA-RDP82-00850R000500010010-4

limits, especially in the presence of a quasistationary controlled signal (we shall discuss the causes for this somewhat later).

Let us touch on the problem of selecting the size of the coupling hole. The losses of resonators made of spherical mirrors and the radiation density required from an external source to prevent self-excitation depend very slightly on the dimensions of the hole. Hence, it follows that the required control signal power is in the first approximation proportional to the area of the hole. Therefore it is advantageous to use quite small holes; however, they must not be so small that the resonator axis can go beyond their limits as a result of alignment errors, vibrations, and so on.

Beginning with these arguments, the parameters of an unstable resonator were selected for the first laser of the given class built in [191]. This laser, just as in many experiments described above, was built on the basis of an active element made of neodymium-doped glass 45 mm in diameter and 600 mm long. The telescopic resonator had magnification of M = 5 instead of the usual M = 2; the diameter of the coupling hole was determined by the precision of the alignment and it was 3 mm. The external master oscillator operated in the mode of random radiation "spikes" which is usual for solid-state lasers; its output power was more than two orders less than the output power of the basic laser which was several hundreds of joules for a pumping pulse duration of ~1.5 milliseconds. Although the presence of intervals between the "spikes" does not at all promote control reliability, complete synchrony of the "spikes" at the output of the master oscillator and the system as a whole was observed.

In [191], the requirements on the required accuracy of mutual alignment of the external oscillator and the control laser were also discovered, and it was demonstrated that they are not at all extraordinary: The admissible magnitude of the angle between the direction of the beam from the external oscillator and the axis of the powerful laser was in the given case ~1'.

One and a half years later a report appeared on work of a similar nature in the field of CO_2-lasers: under the effect of a weak signal introduced in the axial section with frequency corresponding to one of the rotational transitions of the CO_2 molecule, a powerful laser with unstable resonator began to generate on this frequency although without the input of the external signal it operated on another rotational transition [244]. In the same paper the argument was stated of the possibility of feeding the control beam not to the central but to the peripheral section of the cross section so that a converging wave amplified as it approached the axis was formed. Using this procedure, the required spectral characteristics probably can be obtained, but there will hardly be small divergence of the radiation simulataneously with this.

Now let us discuss one of the most remarkable peculiarities of pulsed lasers with unstable resonators operating under the effect of radiation from an external source. We are talking about the extraordinarily weak dependence of their output power on the resonator parameters and the control signal intensity if the latter was present. In this respect the results of the calculations of the energy characteristics of a controlled laser the parameters of which are typical of powerful neodymium-doped glass lasers performed in [245] are indicative. The diameter of the coupling hole in a concave mirror of a telescopic resonator was taken equal to the diameter of the convex mirror or less than it by M times so that the beam from the external

APPROVED FOR RELEASE: 2007/02/09: CIA-RDP82-00850R000500010010-4

APPROVED FOR RELEASE: 2007/02/09: CIA-RDP82-00850R000500010010-4

source during its expansion to filling the exit aperture completed three or five passes through the medium, respectively (if the given laser was not capable of self-excitation in the absence of an external signal it would be a "pure" three or five-pass amplifier). The value of M varied from 2 to 20 (M = 2 corresponded to the optimal value of the magnification calculated by formula (4) for an ordinary laser constructed on the given active element).

The calculations demonstrated that as M increases with fixed power of the external signals falling within reasonable limits, the efficiency of the controlled laser decreased monotonically, but noticeably more slowly than the efficiency of ordinary lasers. This is understandable: when M is so large that the lasing in an ordinary laser is completely curtailed, the laser with coupling hole operates as a multipass amplifier, and on supplying the external signal it has a finite output power frequently commensurate with maximum.

The efficiency of a controlled laser depends still less on the power of the external signal. It is sufficient to present the following data: in the entire above-indicated range of variation of M, the variation of the controlling signal power by more than three orders did not lead to a decrease in the efficiency below the level equal to 40% of its maximum value. This also has a simple explanation: it is known that the relative fluctuations of the power at the output of any laser amplifier operating in the quasistationary mode is always significantly less than the relative power fluctuations at its input as a result of amplification saturation. Here, as a result of the presence of several radiation passes through the medium, the given effect appears still more rarely.

The results of [245] permit some conclusions to be drawn which pertain to the properties not only of controlled but also ordinary lasers with unstable resonators. It happens that any disturbance on the central section of the cross section strongly reduces the losses of an empty resonator, and with them, the lasing threshold of the corresponding laser. Thus, the presence of even weak small-scale nonuniformities easily leads to the formation of local "stable" resonators near the axis with all of the consequences following from this [246]. It can be demonstrated that a significant reduction in the threshold arising from such causes must cause a significant increase in the lasing power. However, in reality the variation of the conditions on the small axial section can sharply influence the output power only in the case where the laser was quite close to the lasing threshold before this. If the threshold is greatly exceeded, the output parameters have little sensitivity to variations of the radiation density on a small segment of the cross section independently of whether these variations were caused by the influence of local disturbances or the radiation is supplied, as in a controlled laser, from an external source.

Multipass Amplifiers. In conclusion, let us briefly discuss the "pure" multipass amplifiers, the unstable resonators of which have such large losses that the self-excitation does not occur even in the absence of an external signal. Most frequently these amplifiers are constructed on the basis of a telescopic resonator; then they are called (at least in Soviet literature) telescopic. The possible versions of telescopic amplifiers are presented in Figure 4.19. As a result of the presence of several passes through the medium, one such amplifier is capable of replacing several single-pass amplifiers with telescopes between them (see §2.6, Figure 2.28) [239].

FOR OFFICIAL USE ONLY

APPROVED FOR RELEASE: 2007/02/09: CIA-RDP82-00850R000500010010-4

APPROVED FOR RELEASE: 2007/02/09: CIA-RDP82-00850R000500010010-4

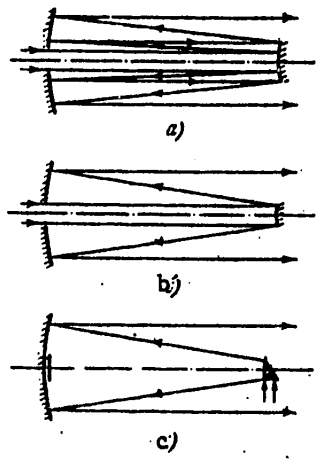

Figure 4.19. Telescopic amplifiers: a) multipass, b) three-pass, c) two-pass amplifiers; in the last amplifier the mirror aperture is replaced by an absorbing screen.

As a rule, amplifiers with unstable resonators are used in the intermediate stages of powerful giant-pulse lasers (e. g. [247, 248]; simple single-pass amplifiers are often preferred for the final stages, as they have greater radiation strength through elimination of the output mirror and concomitant radiation in the reverse direction). Therefore, the important thing here is not so much efficiency as it is the weak-signal gain, which preferably should be maximized.

The amplification of the weak signal in the n-pass amplifier is equal to K^n, where K is the amplification on one pass of the active medium. Therefore for the given K it is necessary to strive for the largest possible n; this promotes the achievement not only of high amplification but also satisfactory energy efficiency of the device.

If K is small, multipass systems of the type depicted in Figure 4.19, a can be used; let us begin with them. We shall consider that the radiation is fed through the coupling hole in a concave mirror as depicted in the figure; here n is odd, the beam cross section expands inside the amplifier by $M^{(n-1)/2}$ times. Hence it follows that $n = 1 + 2 \ln (D/d)/\ln M$, where d and D are the beam diameter at the input and the output of the amplifier, respectively. In order to obtain a large n it is obviously necessary to use a resonator with the lowest possible magnification M and minimum coupling hole diameter d.

Inasmuch as the self-excitation threshold of a laser with small coupling aperture is almost equal to the lasing threshold of an ordinary laser which is achieved for K = M, the least admissible value of M is equal to K. As for the diameter of the coupling hole, it is limited from below, as we have already pointed out, by the precision of the alignment. The latter, it is true, depends not only on the overall dimensions of the resonator, but also on M, but for the large M characteristic of the amplifiers this relation is very weak. Therefore we shall consider the minimum aperture diameter fixed and equal to d_0.

APPROVED FOR RELEASE: 2007/02/09: CIA-RDP82-00850R000500010010-4

APPROVED FOR RELEASE: 2007/02/09: CIA-RDP82-00850R000500010010-4

Thus, the maximum n is $n_{max} = 1 + 2 \ln(D/d_0)/\ln K$. Here amplification of the weak signal is achieved by $K^{n_{max}} = K(D/d_0)^2$ times [249] (exactly the same power transformation coefficient occurs also in controlled lasers operating in the quasistationary mode [191]). From the condition $n_{max} \geq 5$ we obtain the criterion of applicability of multipass systems: $K \leq \sqrt{D/d_0}$.

For large K three-pass systems can be used (Figure 4.19 b) insuring a general amplification coefficient K^3. Inasmuch as here $M = D/d$, even without considering the increase in the threshold as a result of the presence of the coupling hole, self-excitation should not begin until $K = D/d$. If we consider that the coupling hole diameter is no smaller than the convex mirror diameter and if necessary can be made as shown in the figure larger than the convex mirror diameter (at the price of insignificant decrease of output power), the admissible value of K increases as a result of a corresponding increase in the self-excitation threshold to values on the order of $(D/d)^{1.5 \text{ to } 2}$ [249]. Hence it follows that the criterion of applicability of three-pass systems has the form $K \lesssim (D/d_0)^{1.5}$.

In essence the two-pass system does not contain a resonator (Figure 4.19, c) and can be used for K as high as one might like. In order better to "decouple" the two-pass amplifier with the master oscillator, it is expedient to create a hole in the concave mirror with diameter equal to or somewhat larger than the diameter of the input beam (holes for the analogous purpose not in the concave mirror but in the convex mirror can also be made in the case of the systems depicted in Figure 4.19, a, b).

As all these estimates show, if the ratio D/d_0 is sufficiently large, extraordinarily high total amplification coefficients of the weak signal can be achieved in a wide range of variation of the amplification in one pass. Let us consider an experiment: in reference [249] indirect measurements were made of this parameter in the case of a powerful three-pass neodymium-doped glass amplifier; they led to a value of $2 \cdot 10^5$.

It is necessary, however, to consider that the amplification of any laser amplifier depends exponentially on the excitation energy stored in it, and it decreases extremely rapidly with depletion of the latter (a different, still sharper dependence is observed only in regenerative amplifiers). For example, it is sufficient that the inverse population be cut in half and the amplification coefficient of the weak signal will become equal to the square root of its initial value (under the conditions of [249], $4.5 \cdot 10^2$). Therefore when feeding a pulse with energy sufficient for removal of a significant part of the stored inverse population to the amplifier input, the amplification at the end of the pulse will become very small, and the pulse energy ratio at the output and input turns out to be much less than the initial amplification coefficient of the weak signal (hence it is obvious that the role of the latter should not be overestimated).

In spite of this fact, the telescopic amplifiers do not in practice provide large amplifications even in the case where they are measured with respect to the pulse energies. Thus, in [247], a pulse with an energy of 0.12 joules was fed to the input of the three-pass neodymium-doped glass amplifier; the output power was 15 joules. In [248] the analogous amplifier had an output power of 18 joules for an

FOR OFFICIAL USE ONLY

APPROVED FOR RELEASE: 2007/02/09: CIA-RDP82-00850R000500010010-4

APPROVED FOR RELEASE: 2007/02/09: CIA-RDP82-00850R000500010010-4

energy at the input of 0.03 joule (600 fold amplification with respect to energy). Let us again emphasize that in all the experiments with telescopic amplifiers (just as with controlled lasers) small divergence of the radiation characteristic of lasers with unstable resonators was observed.

In conclusion, let us note one deficiency of multipass systems which consists in the following. If the telescopic amplifier is assembled, for example, by the five-pass system, then thanks to the diffraction, the scattering of the light at the interfaces, on nonuniformities, and so on, some part of the radiation reaches the limits of the exit aperture, completing only three passes with respect to the active medium, and some, even a total of one pass. Thus, the scattered light arrives at the output of the amplifier before the basic flux. If we consider that the first "lots" of the radiation are subject to especially large amplification, this scattered light can turn out to be not so weak by comparison with the basic signal.

This deficiency can complicate (but not make impossible) the application of telescopic amplifiers in specific lasers for research in the field of thermonuclear fusion. There, the admissible radiation power incident on the target before the arrival of the basic pulse is extremely low. It is true that it not excluded that these phenomena are not so dangerous as it appears: the scattered radiation theoretically has a quite different radiation pattern and can simply not hit the target.

There are times when it may also be undesirable that part of the output cross section of telescopic amplifiers is covered by the convex mirror and not filled with radiation, which is detrimental to uniform exposure of the target in laser-driven fusion. However, even though telescopic amplifiers may not be used in such cases, in many other applications they may be extremely useful.

We conclude with this very interesting example of the use of unstable resonators for the construction of amplifying systems with unique properties. The materials of this chapter indicate that the most varied problems of laser engineering can be successfully solved using such resonators.

APPROVED FOR RELEASE: 2007/02/09: CIA-RDP82-00850R000500010010-4

APPROVED FOR RELEASE: 2007/02/09: CIA-RDP82-00850R000500010010-4

CHAPTER 5. OPTICAL INHOMOGENEITY OF ACTIVE MEDIA AND METHODS OF CORRECTING WAVE FRONTS

In the preceding sections of the book we are talking primarily about the search for optical systems that permit realization of the limiting energy and angular characteristics of laser emission for the given properties of the active medium. When such systems are found, the following result depends only on these properties. If the medium is optically nonuniform, the maximum small divergence of the radiation at the laser output in the general case is unattainable; it is only possible to decrease the effect of some of the simplest types of aberrations if their existence can be predicted in advance (see, for example, § 3.5). Therefore simultaneously with improvement of the optical systems — and on a much larger scale — studies were made of optical nonuniformities of various active media, and efforts were made at a comprehensive decrease in the these nonuniformities. At the same time, a persistent search was made for the universal methods which would permit us to obtain narrowly directional radiation also with arbitrarily nonuniform active medium. A brief discussion of the experiments on this level will be the subject of this chapter.

The most important cause of optical nonuniformity of active media is the fact that the process of excitation of the medium is always accompanied by the dispersion of a significant amount of energy in it which is spent on heating the medium, the formation of shock waves in it, and so on. The nature of the nonuniformities depends on the peculiarities of the medium and the method of its excitation; their value increases quickly with the laser power.

As for high-power gas lasers, the methods of excitation of certain gases and the types of induced optical nonuniformities are extremely varied. In pulsed electric discharge lasers the active medium at the time of occurrence of discharge is heated intensely, its subsequent expansion is accompanied by the formation of shock waves; nonuniformities caused by nonuniformity of the discharge itself are added to this. In pulsed chemical lasers nonuniformities can be manifested which are caused by nonsimultaneity of the occurrence of the reactions in the entire volume of the active medium, and so on.

The sources of aberrations of optical channels of high-power continuous-action gas lasers are highly varied. The thermal deformations of the mirrors, phase distortions in the windows used for output of the radidation from the resonator are added here to the specific phenomena occurring on transmission of light through fast gas flows (scattering on turbulent pulsations, and so on). In powerful flow lasers operating not in the continuous, but in the frequency-periodic mode,

FOR OFFICIAL USE ONLY

APPROVED FOR RELEASE: 2007/02/09: CIA-RDP82-00850R000500010010-4

APPROVED FOR RELEASE: 2007/02/09: CIA-RDP82-00850R000500010010-4

powerful sound waves caused by "pulsating" energy input are superposed on the already complex gas flow pattern.

This entire enormous complex of various phenomenon has still been studied very little, and it is almost impossible to classify the data available in the literature. Only one thing is clear — the most favorable situation is the one with optical nonuniformities in low-pressure gas lasers.

The situation is entirely different with regard to the problem of optical nonuniformities in solid-state lasers. The excitation method in practice in all types of them is the same — optical pumping — therefore the deformation pattern of the resonators is not distinguished by special variety; in addition, it is quite simple. If it is considered that the systematic work in this area started in the first half of the 1960's, it is no surprise that for a number of types of solid-state lasers the given problem has already been solved to a significant degree.

In the example of solid-state lasers it is quite obvious how large a variety of procedures there are which can be used to decrease the resonator deformations; at the same time what difficulties are caused by the solution of the problem of induced nonuniformities even in such a comparatively simple case is highly instructive. We shall limit ourselves to this example.

§ 5.1. Thermal Deformations of Solid-State Laser Cavities

Origin and Magnitude of Thermal Aberrations in the Case of Circular Active Rods. In § 2.3 we have already mentioned the thermal deformations of a resonator which occur as a result of nonuniform heating of the active element by pumping radiation. These aberrations are for the majority of types of solid-state lasers one of the main obstacles on the path to achievement of diffraction divergence of radiation, and for the most widespread glass lasers, they are in practice the only obstacle.

In the single pulse mode, the thermal deformations are a consequence of nonuniformity of distribution of heat release with respect to the volume of the sample, which occurs even when using the most modern illumination systems. In particular, for standard active elements of circular cross section, in the best case more or less axisymmetric pumping distribution can be achieved. The nonuniformity of distribution with respect to radius is in practice always present. Its nature is determined in the final analysis by two opposite factors. One of them is attenuation of the pumping radiation on approaching the axis as a result of absorption in the medium, the other one is "fine focusing" of this radiation on the axis as a result of refraction on passage of the active element through the cylindrical side surface. Depending on which of these factors predominates, the pumping radiation density on the axis can be both less than and greater than the density on the lateral surface [47, 48].

The heat release process in the medium takes place with almost zero lag; therefore the thermal deformations build up smoothly during a single pumping pulse, reaching imposing values in the case of high-power lasers (see, for example, [200]). Together with the deformations, the radiation divergence also increases by the end of the pulse.

As was noted in the same § 2.3, the thermal deformations of the resonators of continuous and frequency lasers are especially large. The thermal flux in the

FOR OFFICIAL USE ONLY

APPROVED FOR RELEASE: 2007/02/09: CIA-RDP82-00850R000500010010-4

APPROVED FOR RELEASE: 2007/02/09: CIA-RDP82-00850R000500010010-4

quasistationary mode here has entirely defined direction — from the axis of the element to its lateral surface, through which heat removal is realized. Therefore the steady-state temperature distribution in lasers of this type is of a quite regular nature even with noticeable nonuniformity of heat release. On going away from the axis the temperature decreases approximately by a quadratic law. The total temperature gradient with respect to the cross section usually approaches close to the limit after which the rupture of the material by the thermal stresses begins; in the majority of lasers of this type this limits the power of the pumping radiation introduced into the active element and, with it, the output lasing power.

Let us consider the phenomena occurring on transmission of light through a nonuniformly heated active element of circular cross section. We shall consider the temperature inside the element dependent only on the distance to its axis: $T(r, \phi, z) = T(r)$. In order not to deal with awkward tensors, we shall limit ourselves to the case of isotropic material, which glass also is.

The thermal deformations of the resonator are a consequence of the dependence of the index of refraction of the medium on the temperature and on the magnitude of the thermal stresses occurring in the active element:

$$n(T, \sigma_{\parallel}, \sigma_{\perp}) = n_0 + \beta(T - T_0) + C_1\sigma_{\parallel} + C_2\sigma_{\perp}, \tag{1}$$

where T_0 and n_0 are the average temperature of the medium and the index of refraction corresponding to it; $\beta = dn/dT$ is the thermal coefficient of absolute variation of the index of refraction in the absence of stresses; $C_1 \equiv \partial n/\partial\sigma_{\parallel}$ and $C_2 \equiv \partial n/\partial\sigma_{\perp}$ are the so-called photoelastic constants [250]; $\sigma_{\parallel}$ are the normal stresses on the polarization direction, $\sigma_{\perp}$ is the sum of the normal stresses with respect to two other directions (the normal stresses are the diagonal elements of the stress tensor; the positive sign is assigned to the tensile stress). As applied to our case

$$n_{r,\varphi}(r) = n_0 + \beta[T(r) - T_0] + C_1\sigma_{r,\varphi} + C_2(\sigma_z + \sigma_{\varphi,r}), \tag{1a}$$

where $n_{r,\phi}$ is the index of refraction for light polarized in the radial or tangential directions, respectively; σ_r, σ_ϕ, σ_z are the radial, tangential and longitudinal stresses.

Elasticity theory leads to the following expressions for the distribution of the thermal stresses inside a rod of unlimited length for axisymmetric distribution of the temperature [251]:

$$\begin{aligned} \sigma_r &= \frac{\alpha E}{2(1-\mu)}[T_0 - T_{\text{ср}}(r)], \\ \sigma_\varphi &= \frac{\alpha E}{2(1-\mu)}[T_0 + T_{\underset{(a)}{\text{ср}}}(r) - 2T(r)], \\ \sigma_z &= \frac{\alpha E}{1-\mu}[T_0 - T(r)]. \end{aligned} \tag{2}$$

Key: a. average

FOR OFFICIAL USE ONLY

APPROVED FOR RELEASE: 2007/02/09: CIA-RDP82-00850R000500010010-4

APPROVED FOR RELEASE: 2007/02/09: CIA-RDP82-00850R000500010010-4

Here α is the coefficient of thermal expansion, E is the Young's modulus, μ is the Poisson coefficient which fluctuates within the limits of 0.25 to 0.3 for the majority of materials; T_0 is the average temperature of the rod; $T_{ave}(r) = \frac{2}{r^2}\int_0^r T(r')r'dr'$ is the average temperature of the medium in the zone of radius r adjacent to the axis.

The substitution of (2) in (1a) leads to the known formulas for variations of the index of refraction inside the circular cylindrical active element first published in [70, 71]. Let us write out these formulas in the form in which they usually are used at the present time:

$$n_{r,\varphi}(r) = n_0 + P[T(r) - T_0] \pm Q[T(r) - T_{cp}(r)], \tag{3}$$

where $P = \beta - \frac{\alpha E}{2(1-\mu)}(C_1 + 3C_2)$, $Q = \frac{\alpha E}{2(1-\mu)}(C_1 - C_2)$ are the laser thermal optical constants introduced in [200]. From (3) it follows that the value of P characterizes the variations of the index of refraction average with respect to both polarizations, Q characterizes birefringence. As will be obvious later, these two constants remain meaningful and are sufficient for complete description of the resonator deformations also in the important case of active elements with strongly elongated rectangular cross section uniformly illuminated from both lateral surfaces.

The expediency of introducing new thermal optical constants arose from the following causes. Before lasers, optics dealt primarily with parts free of large internal stresses; their temperature could slowly vary with time, remaining, however, approximately identical throughout the entire volume. If the light beam travels a distance ℓ through such a part, on variation of the temperature of the entire part by ΔT the optical length of path inside it varies by $\Delta(n\ell) = n\Delta T\cdot\alpha\ell + \ell\Delta T\cdot\beta$. Inasmuch as the path traveled by the beam outside the part decreases in this case by $\Delta\ell$, the total increment of the optical path is $\Delta(n\ell) - \Delta\ell = W\ell\Delta T$, where $W = \beta (n - 1)\alpha$ is the thermal optical constant which was used earlier in optical instrument making [252].

In order not to return again to the question of thermal optical constants, let us note that already at the beginning of the 1970's some researchers preferred to be guided by the values not of P and Q, but W when selecting the optimal composition of the neodymium glass (for example, [253, 254]). This was frequently caused by the fact that for many laser glasses the numerical values of W and P are close to each other, and frequently by the fact that the authors [253] created a procedure for measuring W simpler and more convenient than the procedures developed in [200, 255, 256] for direct measurement of P and Q. However, numerous specific data [256, 257] indicate that the correlation between W and P on variation of the compositions of the glasses turns out to be not at all ideal. Therefore now in almost all of the papers devoted to the creation of the so-called athermal glass, only P and Q are used as the criterial thermal optical constants (for more details see [258]).

Let us continue the investigation of thermal deformations of resonators with circular cylindrical elements. Formula (3) describes the variations of the index of refraction inside an unlimited long rod. It is necessary to consider the possible role of the edge effects in real rods of finite length. This problem is nontrivial and is a source of numerous errors; therefore let us discuss it in somewhat more detail.

APPROVED FOR RELEASE: 2007/02/09: CIA-RDP82-00850R000500010010-4

APPROVED FOR RELEASE: 2007/02/09: CIA-RDP82-00850R000500010010-4

The nature of the distribution of the longitudinal normal stresses and edge effects in problems of this type is explained by Figure 5.1. Let us first imagine that a rod of length ℓ having flat ends in the unheated state is part of the freely supported (unreinforced) monolithic rod of unlimited length (Figure 5.1, a).

Now we shall heat the entire infinite rod uniformly over the entire length; for determinacy we shall consider the temperature monotonically decreasing on going away from the axis. From the arguments of asymetry it is clear that any cross section perpendicular to the axis which was planar in the unstressed rod of unlimited length remains planar also on axisymmetric heating of it. The two isolated cross sections separated by a distance ℓ do not constitute an exception. Hence, it follows that in the given case all of the layers of the rod located at different distance from the axis acquire the same relative elongation along the z-axis corresponding obviously to the average heating temperature. For cold layers this elongation is excessive, and for hot layers, it is insufficient, from which we have the distribution pattern σ_z depicted in Figure 5.1, a described by formula (2).

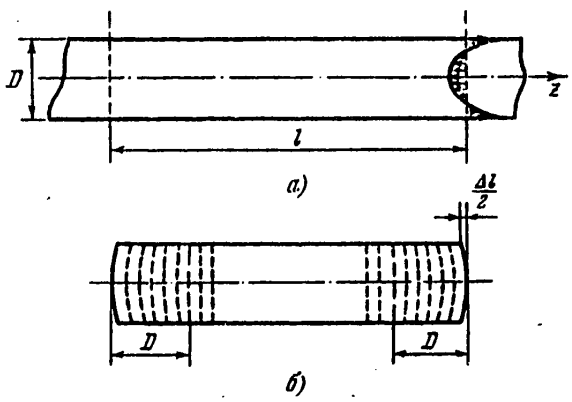

Figure 5.1. Distribution of longitudinal normal stresses and edge effects in an active element with axisymmetric temperature distribution: a) circular cylindrical rod of infinite length; b) rod of finite length.

Let us make sections through the isolated cross sections and thus produce our rod of finite length. Before this, a system of forces depicted in Figure 5.1, a was applied to both ends of the rod from the outside, which kept them flat in spite of nonuniform heating. Now these forces are removed and the ends are deformed. The magnitude of the deformations obviously will be the same as if we applied the same system of forces in the opposite direction (Figure 5.1, b) to each end of the unstressed rod. The results of these forces from each side is equal to zero; therefore in accordance with the Saint-Venant principle which is known in elasticity theory [251], they are capable of causing noticeable deformations only in the sections directly adjacent to the ends, the length of which does not exceed the rod diameter D. As a result, the total picture of longitudinal deformations of the rod acquires the form provisionally depicted in Figure 5.1, b (in reality, in addition to everything else not only the ends are distorted, but also the sections of the lateral surface of the rod adjacent to them). The cross sections which were flat in the unheated rod remain flat also after nonuniform heating of it over the extent of almost the entire length. Only small sections near the end freely expand in

FOR OFFICIAL USE ONLY

APPROVED FOR RELEASE: 2007/02/09: CIA-RDP82-00850R000500010010-4

APPROVED FOR RELEASE: 2007/02/09: CIA-RDP82-00850R000500010010-4

accordance with their individual temperature. Therefore the difference $\Delta\ell$ between the lengths of the rod obtained for measurements along the axis and along the generatrix (Figure 5.1, b) is not $\alpha\ell\Delta T$, as can be demonstrated, but a many times smaller value $\sim\alpha D\ \Delta T$ where ΔT is the total temperature gradient.

Although the conclusion obtained with the help of elasticity theory and confirmed by direct measurements that the amount of sag of the ends is nearly independent of ℓ and is very small, was published in 1966 [74] it was not possible at that time completely to do away with the invalid ideas of thermal deformations. As an example let us mention the paper [259] in which the estimate of the sag of the ends and analysis of the consequences following from this were performed beginning with the formula $\Delta\ell = \alpha\ell\Delta T$. Apparently, the same error prompted the authors of [253] to include the term $\alpha(n - 1)\ell\Delta T$ which should not be there in the initial formula for the resonator deformations.

It is possible to sum up the results. The stress and strain pattern in a rod of finite length differs from the pattern in an infinite rod only in small sections of length near the ends of the rod where the state of material is less stressed. If we consider that the mean variations of the optical path on transmission of light through the unstressed and thermally stressed parts are described by constants W and P that are not too different with respect to magnitude, it becomes clear that the edge effects in the given situation play a special role. Actually, in reference [200], they were not manifested noticeably even for $\ell/D \sim 4$. Thus, the deformations of the resonator with axisymmetrically heated rod of length ℓ can be found by simple multiplication of the equality (3) by ℓ. Then, however, we deal with the case where analogous edge effects will play a larger role.

Consequences of Aberrations and Attempts to Correct Them. From formula (3) it follows that for any form of $T(r)$, except the trivial $T(r) = \text{const}$, changes also take place in the average index of refraction for two polarizations of the index of refraction and birefringence. What the presence of an index of refraction gradient leads to, we already know from Chapters 2-4. For quadratic dependence of T on r which is characteristic of the frequency and continuous lasers, the average index of refraction is also a quadratic function of r — a powerful thermal "lens" is manifested. If this lens is in no way compensated for, the angular divergence of the radiation turns out to be very large. On introduction of the corresponding quadratic phase corrector into the resonator, the divergence decreases [54, 260].

This lens-like nature of a specimen is frequently observed also in the single flash mode. Its compensation naturally has the same effect on the angular divergence [261, 262]. However, the possibilities of this method of controlling the thermal "lenses" should not be overestimated. Actually, the dynamic correction of any distortions, including arbitrary "lenticularity" is a very difficult problem. Technically complicated correction methods which will be discussed in the next two sections have been developed only in very recent times, and they will be used obviously only in highly critical cases. If we are talking about comparatively simple means, it remains only to place the previously selected corrector inside the resonator, adjust the resonator, considering the subsequently manifested "lenticularity" (this is what was done, in particular, when creating the monopulse master oscillator in [129]), and so on. In this situation any variations of the thermal regime of the active element and pumping conditions are sufficient for compensation to be disturbed. Satisfactory correction in the powerful single pulse mode of free lasing where the magnitude of the deformations changes

APPROVED FOR RELEASE: 2007/02/09: CIA-RDP82-00850R000500010010-4

APPROVED FOR RELEASE: 2007/02/09: CIA-RDP82-00850R000500010010-4

significantly under the effect of the pulse is highly problematic. One of the many attempts to create a element capable of compensation for a thermal lens coming during the pulse was undertaken in [263]. This element was a mirror that absorbs a small portion of the lasing radiation incident on it in its mass and undergoes, therefore, thermal deflection. The mirror was successfully tested outside the resonator, but no special applications were found.

Double refraction also leads to highly unfavorable consequences. It is known that the results of transmission of planopolarized light through an isotropic medium, the optical axis of which is perpendicular to the direction of propagation essentially depends on the mutual orientation of the optical axis and the plane of the initial polarization. If they are parallel or perpendicular to each other, the light remains planopolarized. In all the remaining cases the polarization becomes elliptic -- a second linear component appears, and, as is said, the beam depolarizes. In a circular rod with axisymmetric temperature distribution, the local optical axes of an anisotropic medium as a result of the stress effect are directed along the radii. Therefore the depolarization with respect to passage through this element takes place in all sections of the cross section except the ones adjacent to the two straight lines passing through the axis of the element, one of which is parallel to the polarization plane of the initial beam, and the other is perpendicular to it (Figure 5.2, a).

If the resonator contains elements realizing the complete or partial polarization of the radiation, the double refraction leads to the highly characteristic "cross" pattern of the distribution of the polarized components with respect to the cross section. This picture was investigated theoretically and experimentally in [264, 265] for the case of weak double refraction in planar and telescopic resonators (in a telescopic resonator it turned out to be more favorable). However, even without detailed investigation it is clear that the depolarization of such resonators leads to a reduction in the lasing power inasmuch as the radiation of the newly appearing polarization component is output in one way or another from the resonator, making no contribution to the useful signal. In the case of large-scale double refraction the degree of depolarization and power losses become significant (lasing can even be curtailed). It is possible to avoid this, using the system proposed in [266], the meaning of which reduces to the fact that the resonator for emission of undesirable polarization "is blocked" -- this radiation returns, not reaching the part of the optical system which contains the shutter and the output mirror (Figure 5.2, b).

Even in cases where double refraction does not lead to power losses (in particular, in the absence of polarizers), a number of undesirable effects still remains both in the oscillators and in the amplifiers. In particular, the natural oscillations of the resonator with axisymmetric anisotropic medium cannot have a polarization state identical with respect to the entire cross section. As a rule, this leads to a sharp decrease in the spatial coherence of the generated radiation; in the best case the laser begins to operate on modes, the direction of the polarization of the radiation of which in each segment of the cross section is oriented along the radius or tangentially [267, 268]. From § 2.2 it is known that such polarization states are obtained only as a result of superposition of higher-order modes than zero (see Figure 2.14). In laser amplifiers the double refraction even in the single pulse mode can lead to nonuniform distribution of the radiation intensity with respect to cross section [269, 270]; it prevents the creation of highly efficient multipass amplifiers "decoupled" with respect to polarization [271].

FOR OFFICIAL USE ONLY

APPROVED FOR RELEASE: 2007/02/09: CIA-RDP82-00850R000500010010-4

APPROVED FOR RELEASE: 2007/02/09: CIA-RDP82-00850R000500010010-4

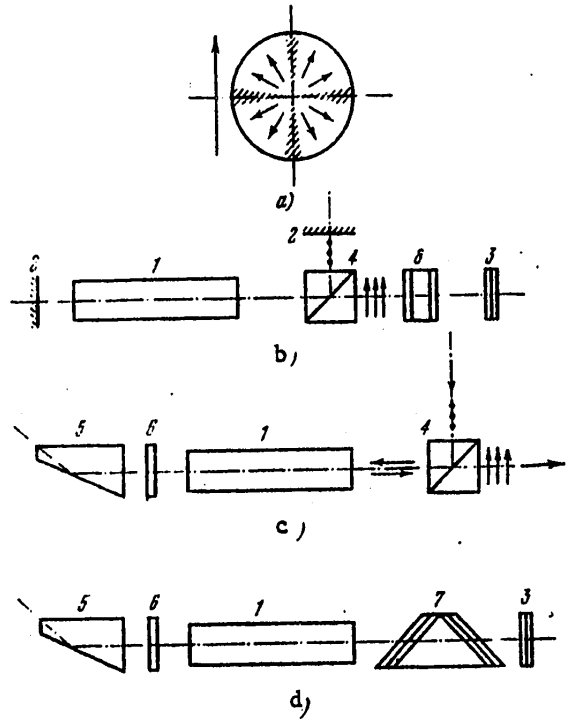

Figure 5.2. Birefringence in lasers based on circular active elements with axisymmetric temperature distribution: a) direction of local optical axes inside the active element (the zones are crosshatched in which the plane-polarized light with the direction of polarization indicated to the side by the large arrow does not undergo depolarization); b) the resonator for the plane-polarization radiation laser in which double refraction does not lead to energy losses; c) diagram of the double-pass amplifier with compensated double refraction; d) diagram of an analogous laser; 1 -- active element in the form of a circular cylinder, 2 -- completely reflecting mirror, 3 — output mirror (stacked), 4 — Glan prism (radiation of one polarization passes without losses, the other is reflected from the diagonal splicing plane), 5 — tetrahedral reflecting prism, 6 — quarter-wave phase plate, the principal direction of which is 45° with the plane of the figure, 7 — polarizer (conventional representation), the principal plane of which makes an angle of 45° with the plane of the figure, 8 -- electrooptical shutter.

All of these phenomena greatly complicate the construction of single-mode laser systems with small radiation divergence. Therefore the efforts to completely avoid the consequences of double refraction are of unquestioned interest, realizing 90-degree rotation of the polarization plane on the path between the two identical active elements. Then the radiation having r-polarization in the first element will have ϕ-polarization in the second element, and vice versa. Obviously, the phase shifts between the different polarization components in the two active elements are compensated for here, and the manifestations of double refraction

APPROVED FOR RELEASE: 2007/02/09: CIA-RDP82-00850R000500010010-4

APPROVED FOR RELEASE: 2007/02/09: CIA-RDP82-00850R000500010010-4

disappear [272]. It is possible to achieve the analogous effect also for one active element, rotating the polarization plane on the path from the element to the mirror and back (which can be achieved, for example, using a 45-degree Faraday rotator of the polarization plane installed between the element and the mirror).

A detailed analysis of the possible diagrams of two-pass amplifiers and lasers with compensated double refraction, two of which are presented in Figure 5.2, c, d, was performed in [273]. The experiments performed there demonstrated, on the one hand, that when using these systems, the double refraction actually does not lead to such a sharp decrease in power as in ordinary lasers; on the other hand they demonstrated that the required accuracy of all of the optical elements and their mutual orientation here are far from simply achieved. In addition, the compensation of the double refraction still turns out to be incomplete inasmuch as the beams pass through the active element nonparallel to its axis as a result of the presence of the same thermal aberrations.

Let us mention such a characteristic method of compensation of the thermal deformations as the creation in the active element of the correspondingly selected preliminary stresses by quenching it [274], and let us proceed to the efforts to decrease the deformations themselves.

Various Methods of Reducing Cavity Deformations. The most natural method of decreasing the thermal deformations of the resonator is the adoption of all possible measures to insure the maximum uniform temperature field with respect to the active sample. In the single pulse mode the decisive role is obviously played by uniformity of the pumping distribution with respect to the volume of the active element. Inasmuch as ideal uniformity is still not achieved, sometimes a temperature gradient is created in the active element which is inverse to the gradient occurring as a result of pumping. This can be achieved, varying the temperature of the coolant in time according to a given law [275] or heating the sample by an additional pumping pulse and waiting a defined time until the required temperature distribution is established in the cooling process [271]. In frequency lasers operating in a series of pulses, obviously it is best of all to cool the active element only in the gaps between the series, offering it the possibility of being freely heated during the series itself, which insures the minimum temperature gradients with respect to cross section [276].

From this list alone, the necessity for more radical methods of eliminating thermal deformations is clear. Actually, such methods exist. One of them consists in the fact that the lateral surfaces of the active element are made planar, and the light flux passes through the sample inclined to these surfaces and undergoes total internal reflection on them. Here each ray of the parallel beam crosses through all of the layers of the sample with different temperature and index of refraction, which leads to equalization of the optical paths, that is, the absence of thermal deformations.

The generation of radiation beams experiencing reflections from the side walls of the active elements of rectangular and octagonal cross sections was first observed by Vanyukov, et al., in 1963-1964 [18]. The different systems of lasers and amplifiers with total internal reflection in the active element were subjects of lively discussion in 1965-1968 [277, 139, 140]; two of them borrowed from [139, 140] are presented in Figure 5.3. It is true that the creators of these systems primarily pursued the goal of using sharp dependence of the reflection coefficient on

FOR OFFICIAL USE ONLY

APPROVED FOR RELEASE: 2007/02/09: CIA-RDP82-00850R000500010010-4

APPROVED FOR RELEASE: 2007/02/09: CIA-RDP82-00850R000500010010-4

the angle of incidence near the critical angle of total internal reflection for angular selection of the radiation (see § 2.6, Figure 2.24, d), but it turned out that the problem of thermal deformations is also solved simultaneously 140].

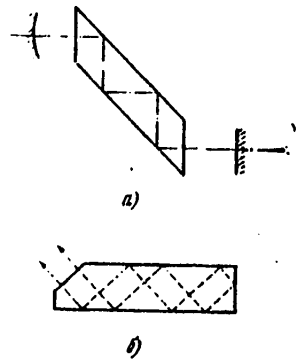

Figure 5.3. Diagrams of lasers with total internal reflection in the active element: a), b) diagrams proposed in [139, 140], respectively.

Finally, in 1970 attention was again attracted to this area by the papers of Mikaelyan and D'yachenko [278], who did not try to use the mentioned dependence of the reflection coefficient on the angle of incidence, but were only interested in the problem of thermal deformations. They classified the resonators which they called wave guide resonators and demonstrated the possibility of eliminating the thermal deformations experimentally. However, lasers of this type did not become widespread as a result of difficulty of manufacturing the active elements, complexity of their cooling and other similar causes.

The method consisting in transmission of plane-polarized light through active elements again inclined with respect to the plane side surfaces but at the Brewster angle so that the light is not reflected, but on the contrary, passes through the surfaces almost without losses turned out to be more vital. This method is used when constructing frequency lasers (for example, [279]) and also powerful output stages of the monopulse lasers [280, 281]. In the frequency lasers the elements are in a coolant, the presence of which decreases the Brewster angle and reduces unavoidable losses on transmission of the light through the surfaces to an extraordinarily small magnitude. This, in turn, creates the possibilities for placement of a large number of active elements in one resonator to which the form of thin disks is assigned (Figure 5.4, a). Small thickness of them implies a sharp decrease in the temperature gradients and promotes an increase in the uniformity of the pumping distribution.

In the terminal amplifiers of giant pulse lasers the cooling or immersion liquids are not used as a result of the low self-focusing threshold characteristic of them. Therefore such amplifiers are capable of operation only in single-pulse modes. There is a positive side here -- the thermal loads for small, and the thickness of the active elements can be made sufficiently large; thus, in [281] it was 30 mm. This permits us to limit ourselves to a moderate number of elements. The diameter of the light aperture here usually is very large and frequently reaches 200 mm [281]. Therefore it is necessary to realize the pumpings through the same lateral surfaces through which the amplified radiation is

APPROVED FOR RELEASE: 2007/02/09: CIA-RDP82-00850R000500010010-4

APPROVED FOR RELEASE: 2007/02/09: CIA-RDP82-00850R000500010010-4

transmitted and locate the element so that they do not shield each other from the pumping source (Figure 5.4, b). In spite of its unique characteristics, the disc amplifiers are used only in exceptional cases as a result of enormous dimensions and large labor consumption of manufacture.

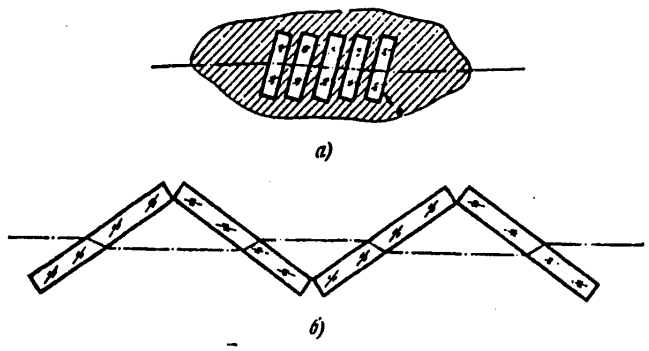

Figure 5.4. Diagram of the arrangement of the active elements: a) disc elements in the coolant (frequency laser); b) flat plates in the air (monopulse laser).

The most fruitful idea pertaining to the methods of controlling thermal operations in the resonator and amplified channels lies in a somewhat different area. It was first stated by Spitzer [71]; it pertains only to loss lasers and reduces to the fact that the thermal deformations can be significantly decreased by the selection of the glass composition. The fact is that the variations of the index of refraction as a result of the temperature gradient itself and the stresses arising here in practice are always in opposite directions — in the formula for P the terms with dn/dT and $\partial n/\partial\sigma$ are subtracted from each other ($\beta < 0$, $C_1 + 3C_2 < 0$). This is easily explainable: a decrease in the index of refraction with an increase in temperature is connected to a significant degree with reduction of the density of the medium, and the thermal stresses always prevent redistribution of the density in the nonuniformily heated part (see Figure 5.1 and the comments to it). At the same time the thermooptical properties of the medium depend, of course, not only on its density (which is indicated at least by the presence of double refraction), and there is a certain possibility of independent variation of some of the parameters entering into (1), (3). The thermal coefficient of the index of refraction β can vary within especially broad limits, and P also with it.

The experiments in this area quickly led to impressive progress in the field of neodymium glass lasers. Over the course of several years an entire series of so-called athermal laser glasses appeared in which one linear combination or another of thermooptical constants P and Q reduce to zero. In order to understand what the developers of laser glasses are striving for, let us return to expression (3).

The optimal version is, of course, equality of P and Q to zero. In this case the thermal deformations must be absent for any form of $T(r)$. In recent years it was actually possible to create glass in which P and Q are extremely small at room temperature [282] (the stipulation with respect to the temperature arose from the fact that the constants P and Q themselves are slowly varying functions of it [283], and athermalness is insured only in a narrow temperature range). However, such

FOR OFFICIAL USE ONLY

APPROVED FOR RELEASE: 2007/02/09: CIA-RDP82-00850R000500010010-4

APPROVED FOR RELEASE: 2007/02/09: CIA-RDP82-00850R000500010010-4

response can be achieved only for phosphate glass having much lower chemical stability and thermal strength than the most widespread silicate glasses. As for silicate glass, in different types of it, the value of Q is in practice the same; only P is subject to variation.

If $Q \neq 0$ the thermal deformations cannot be avoided for arbitrary form of T(r). When the temperature distribution is of a regular nature, some possibilities appear in this respect. In particular, for quadratic dependence of T on r characteristic of frequency and continuous lasers, formula (3) acquires the form

$$n_{r,\varphi} = n_0 + P\Delta T/2 - (P \pm Q/2)\Delta T(r/a)^2,$$

where ΔT is the total temperature gradient between the axis and the side surface, and a is the radius of the rod. Hence it follows that for $P \pm Q/2 = 0$ the thermal deformations for the r or ϕ polarization radiation are absent [284]. For frequency lasers $P - Q/2$ usually approach zero; the divergence of their radiation actually is sharply reduced as this value is decreased (see, for example, [257]). However, as has already been pointed out, double refraction in circular active elements prevents plane-polarized radiation lasing; therefore the maximum small divergence still remains unattainable.

Lasers Using Active Elements With Elongated Rectangular Cross Section. From everything that has been discussed it follows that even defined possibilities for controlling thermoelectrical characteristics of glass do not permit complete solution of the problem of thermal deformations in lasers based on traditional active elements of circular cross section. It is also obvious that the primary causes of all of the difficulties here are the following: 1. The form of the stress distribution near the circular element in the general case does not repeat the form of the temperature distribution (see (2)); therefore exact compensation for the variations of the index of refraction caused by its dependence on temperature and on the stresses it is possible only for certain specific forms of T(r). 2. Local optical axes of the anisotropic medium from which the circular axisymmetrically stressed rod consists are oriented along the radii and their directions are therefore different in different sections of the cross section which prevents plane-polarized radiation lasing.

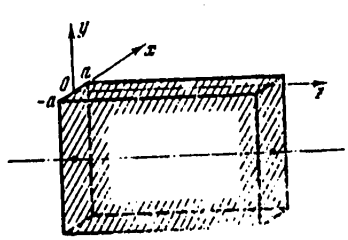

Figure 5.5. Active element in the form of a flat plate.

The origin of both of these phenomena is organically connected with the circular shape of the cross section, and on variation of the type of symmetry of the cross sections they can disappear. Actually, let us consider the optical properties of

FOR OFFICIAL USE ONLY

APPROVED FOR RELEASE: 2007/02/09: CIA-RDP82-00850R000500010010-4

APPROVED FOR RELEASE: 2007/02/09: CIA-RDP82-00850R000500010010-4

glass plate bounded by the planes $x = \pm a$ and heated symmetrically with the plane $x = 0$ (Figure 5.5). Obviously the local optical axes inside this plate together with the temperature gradient have the same direction in the entire volume. In addition, from elasticity theory it is known that the shape of the stress distribution in the absence of external forces here completely repeats the form of the temperature distribution [251]:

$$\sigma_x = 0, \quad \sigma_y = \sigma_z = \frac{\alpha E}{1-\mu}[T_0 - T(x)],$$

where $T_0 = \frac{1}{a}\int_0^a T(x)\,dx$ - is the average temperature. Substituting these formula in (1) and considering that the light is propagated through the plate along the z-axis, we obtain the following relations [200]:

$$n_{x,y} = n_0 + (P \pm Q)[T(x) - T_0], \tag{4}$$

where $n_{x,y}$ is the index of refraction for light polarized along the x and y-axes, respectively, n_0 is as before the index of refraction in the medium without stresses at a temperature of T_0.

Hence the obvious conclusion follows immediately: if the plate made of glass with $P + Q = 0$ or $P - Q = 0$ is used as the active element, the deformations of the resonator for plane-polarized radiation with one of the two directions of polarization must be absent for any temperature distribution. Let us only remember that this distribution must always remain symmetric with respect to the $x = 0$ plane; if this is not so, the plate will bend, and for description of the resonator deformations, a much more complex expression is required in which W will figure in addition to P and Q.

It remains only to discuss the edge effects and the polarization characteristics of the generated radiation. Let us begin with the simpler problem of edge effects. In exactly the same way as in the case of a circular cylinder, the width of the region adjacent to the edges of the plate inside which the stressed and strain pattern differs significantly from the pattern in an infinite plate does not exceed the plate thickness (which is confirmed by the results of the corresponding calculations [285]). However, here in contrast to the circular elements, this region borders the plate on all four sides (crosshatched in Figure 5.5). Whereas the zones adjacent to the ends of the element do not play a special role (for the same reasons as for circular rods), the situation is somewhat different with regard to the zones adjacent to the sides — the light passes crosswise through them, and the effect turns out to be significant along the entire length. Hence it follows that for large temperature gradient the radiation passing near the sides will deviate significantly from the rectilinear direction and will not make a contribution to the central peak of the radiation pattern. Thus, from the point of view of thermal deformations it is desirable that the thickness of the plate determining the width of the edge zones be as small as possible; on the other hand, as the thickness decreases, the vibrations of the active element [192] and its heating at pumping time increase.

FOR OFFICIAL USE ONLY

APPROVED FOR RELEASE: 2007/02/09: CIA-RDP82-00850R000500010010-4

APPROVED FOR RELEASE: 2007/02/09: CIA-RDP82-00850R000500010010-4

Now let us discuss the problem of the polarization of the stimulated radiation. Inasmuch as for $Q \neq 0$ the resonator deformations can be reduced to zero only for plane-polarized radiation with completely defined direction of polarization, it is necessary in some way to achieve a situation where the laser will operate on this radiation. Double refraction is not dangerous in this case: the required direction of polarization is parallel or perpendicular to the direction of the optical axis of the medium. The data of [264] and subsequent experimental papers indicate that certain other theoretically important reasons which could cause the decrease in power in the case of intraresonator polarization selection of the radiation are absent in the case of neodymium glass lasers.

Thus, the transition to elements with strongly elongated rectangular cross section permits the use of comparatively simple means to avoid thermal deformations without lowering the lasing power. Even the use of a polarizer is not mandatory in this case: it is possible to select conditions such that the "harmful" polarization component will be suppressed automatically. Let us explain this in the example of the single pulse mode.

In the case of symmetric two-sided illumination of the planar element, the minimum pumping density always falls to the central plane ($x = 0$); in the single pulse mode, the temperature obviously is normal at the pumping time. Let the composition of the glass be such that $P - Q = 0$; inasmuch as usually $Q > 0$, $P + Q$ in this case also turns out to be positive. From formula (4) it follows that in this case for radiation polarized along y, the index of refraction gradient is absent, and for the other polarization component the element is equivalent to a scattering lens. In planar or telescopic resonators this necessarily leads to an increase in losses; therefore the x-component can be present equally with the y-component only at the very beginning of the pumping pulse until a noticeable temperature gradient appears.

Spontaneous polarization of the laser emission with planar active elements must occur under certain other combinations of conditions and be actually observed in practice [284].

In spite of individual hopeful experiments with planar active elements to $40 \cdot 204 \cdot 600$ mm^3 in size [192], lasers of this type still have not become especially widespread. The reason for this is that for now for the majority of solid state lasers an effort is being made to consider the possibility of Q-switched operation. The large-cross section planar active elements are not too suitable for monopulsed lasers -- this configuration is highly unfavorable from the point of view of superluminescence which plays an extraordinarily important role in the "slave" operating mode. As for glass lasers with high output energy in the free lasing mode, the procedure discussed above for constructing them obviously is optimal [194].

In conclusion, let us briefly touch on the problems of thermal deformations of the liquid laser resonators. The value of dn/dT here is very large and as a result of the absence of static stresses is not compensated for any way; therefore the variations of the index of refraction turn out to be very large. The always available mixing of different layers of liquid leads to the fact that the temperature field is unstable, and the nonuniformities are irregularly distributed with respect to volume. For these reasons small angular divergence of the powerful liquid lasers almost unattainable. Therefore the liquid media are widely used only in

APPROVED FOR RELEASE: 2007/02/09: CIA-RDP82-00850R000500010010-4

APPROVED FOR RELEASE: 2007/02/09: CIA-RDP82-00850R000500010010-4

small lasers with tunable frequency, on the angular divergence of the emission of which as a rule special requirements are not imposed.

§ 5.2. Phase Correction of Wave Fronts. Dynamic Holography and Stimulated Scattering

Inasmuch as in the optical channels of lasers usually all possible nonuniformities are present, even an insignificant decrease in which frequently is extremely complicated, there is a natural effort to find methods permitting insurance of high output characteristics even when such inhomogeneities are present. A brief discussion of research for this purpose makes up the content of this and the following sections.

Optical-Mechanical Correction Systems. Let us begin with the possibilities which are related to purely mechanical displacements of certain elements with respect to the channel. First of all, the systems for automatic adjustment of laser resonators which are gradually entering into practice deserve attention. Their function is adjustment of the mutual arrangement of the mirrors in order to optimize any laser parameter. Without going into the technical details, let us only discuss the most theoretical problem of selecting a parameter, the magnitude of which is subject to optimization.

The output parameter of the laser which is quite "sensitive" to the resonator geometry and at the same time most simply controlled is its power. Therefore it is easy to create a self-adjustment system which maintains the maximum high level of output power. However, this operating algorithm can be far from always used: the pursuit of an insignificant gain in power can easily become enveloped in the large fluctuations in the position of the resonator axis, and, along with it, also the direction of the generated radiation. In addition, cases are possible where the shift of the resonator axis leading to an increase in power is accompanied not only by "drift" of direction, but also other undesirable consequences. We encountered one such example in § 4.2 — as the resonator axis of the flow laser approaches the point of entrance of the flow of medium into the resonator which is advantageous from the point of view of efficiency, the nonuniformity of the radiation distribution with respect to cross section of the lased beam and, consequently, the divergence increase sharply. Finally, it is necessary not to forget that the systems based on measuring output power can realize adjustment of the resonator only some time after lasing has started. Therefore for the overwhelming majority of pulsed lasers such systems are disadvantageous. It is also difficult to use them for certain continuous-action lasers, at the time of starting of which frequently such large misalignments occur that the laser in general does not begin to lase without resonator tuning.

For all these reasons, the most efficient operating algorithm for the autoadjustment systems is maintenance of the resonator axis in the given position. It is possible to deal with this problem by using the radiation of a low-power external source which will permit adjustment of the laser without beginning of its lasing.

A system for autoadjustment of unstable resonators investigated in the already-mentioned paper [217] was constructed by the same principle; the radiation of the auxiliary helium-neon laser is input to the resonator here along its axis through a small opening in the center of one of the mirrors. Undergoing multiple reflections, this radiation then "spreads" over the entire cross section. If the resonator was misaligned, the intensity distribution with respect to cross section turns out to be asymmetric, which is used for generating the error signal

FOR OFFICIAL USE ONLY

APPROVED FOR RELEASE: 2007/02/09: CIA-RDP82-00850R000500010010-4

APPROVED FOR RELEASE: 2007/02/09: CIA-RDP82-00850R000500010010-4

putting the corresponding automation circuits into operation. The system described in [217] permits insurance also of satisfactory precision of adjustment of the errors (~5") and "capture" of the initial misalignment (5'-7') in a sufficiently large range of angles. The application of an auxiliary laser and the receivers of its radiation operating on a frequency differing from the frequency of the basic laser permits possible interference caused by the lasing process in the latter to be avoided. The system with introduction of the auxiliary laser through the central opening is also convenient in that this radiation passes through the adjusted resonator on the same path as the generated radiation; therefore it can be used so that the radiation will be directed at the measuring devices and so on visually or automatically.

A further step in improving the methods of mechanical automatic tuning of lasers is the application of the so-called adaptive optical system. Linnik's idea [286] about the possibility of autocompensation of phase distortions of the wave front caused by a turbulent atmosphere and interfering with the observation of remote objects marked the beginning of this area of study. The typical method of solving this problem by the methods of adaptive optics consists in the following: one of the elements of the optical channel of the transceiving system, for example, the mirror objective of the shaping telescope is made up of many more small mirrors having the possibility of insignificant translational displacements. By using these displacements, compensation of the large-scale phase distortions is also insured.

When creating such devices it is most complicated to deal with the generation of error signals. Let, for example, the problem of the formation of a beam with divergence as small as possible be solved. The recording and analysis of the form of the intensity distribution in the far zone with invariant arrangement of the individual parts of the composite mirror still do not permit judgment of which of their displacements are needed to improve this form. Actually, the same distribution in the far zone can be observed for different forms of the wave front; thus, in § 1.1 we are dealing with the fact that the beams distinguished by the sign of the curvature of the spherical wave front had identical divergences.

In order to obtain the required information about the deviation of each individual mirror from its optimal position corresponding to the maximum axial luminous intensity of the devices as a whole, it is simplest to use the following fact. The dependence of total axial luminous intensity F on the coordinate of one of the mirrors x measured along the axis perpendicular to its surface is depicted in Figure 5.6. If this mirror undergoes oscillations with of amplitude h much shorter than a wavelength nears its optimal position x_0, the axial luminous intensity as is obvious in the figure, remains almost constant. If the average position of the mirror is shifted to any point x_1 noticeably remote from x_0, the magnitude of the axial luminous intensity begins to fluctuate with the same frequency as the mirror. The relation between the phases of these two fluctuations will obviously depend on the direction from optimal that the average mirror position is shifted.

Now, leaving only one of the mirrors stationary, let us force each of the remaining ones to oscillate with its individual frequency and let us carry out spectral expansion of the time dependence of the axial luminous intensity. Obviously, the presence in this expansion of components with frequencies equal to the frequencies of the oscillations of individual mirrors will indicate that the positions of the

FOR OFFICIAL USE ONLY

APPROVED FOR RELEASE: 2007/02/09: CIA-RDP82-00850R000500010010-4

APPROVED FOR RELEASE: 2007/02/09: CIA-RDP82-00850R000500010010-4

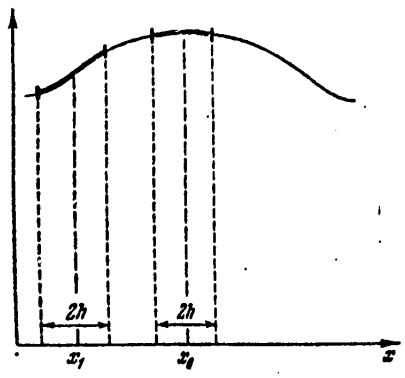

Figure 5.6. Axial luminous intensity as a function of the position of one of the parts of the composite mirror.

given mirrors are subject to adjustment. The phase relations provide information about the direction of the required shifts.

This principle was also proposed and realized in the known papers [287, 288]. In the first of them an adaptive system of seven elements was manufactured and successfully tested; in the second, a system of 18 elements. Later the possibilities of adaptive optics were unconditionally expanded. Instead of the set of individual mirrors now single flexible mirrors are beginning to be used — this corresponds to the transition from "step" approximation of the given phase distribution to more improved approximation using continuous functions. The number of independently adjustable parameters will also increase; familiarization with [334] gives a sufficiently good idea about the paths of development of adaptive optics.

In spite of all of these prospects it is difficult to count on broad application of adaptive optics directly in the laser resonators: the creation of a low-inertia adjustable mirror capable of operating under high beam load conditions is a highly complicated problem. In addition, the small phase aberrations and unstable resonators, as we have seen in Chapters 3, 4, cannot lead to either multimodal lasing or to large reduction in the output power, and they only cause phase distortions of the wave front of the generated radiation which can be entirely compensated for also outside of the resonator. Therefore the optimal location of the complex adjustable mirrors is the exit of the shaping system where the density of the radiation usually is many times less than the density inside the oscillator. As for resonators, among their mechanical correction devices probably only the simplest autoadjustment systems have become widespread which can be supplemented by very useful and not too complex systems for automatic compensation of the second-order wave aberrations which are variable in time (lenticularity).

Other methods of conversion of the wave front form are also of great interest. The most universal and common of them is obviously holography.

Holographic Correction Principles. Usually two mutually coherent light beams participate in the recording of the hologram depicted in Figure 5.7, a. In the case of standard use of holography for recording the image of real objects one of

FOR OFFICIAL USE ONLY

APPROVED FOR RELEASE: 2007/02/09: CIA-RDP82-00850R000500010010-4

APPROVED FOR RELEASE: 2007/02/09: CIA-RDP82-00850R000500010010-4

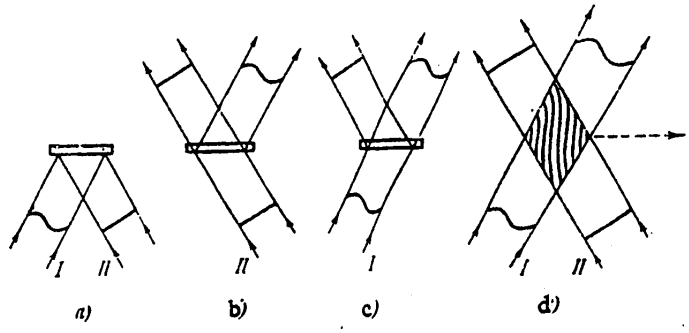

Figure 5.7. Problem of holographic corrections: a) recording of a thin hologram; b), c) reproduction of one of the beams on illumination of a hologram by the others; d) beams and three-dimensional hologram.

these beams -- I — is the light scattered from the object illuminated by the coherent radiation; its wave front has a complex shape which carries information about the image of the object. The beam II — the reference beam — has a regular, for example, planar shape of the wave front. When the hologram, which is an imprint of the interference pattern between these two beams is made and then illuminated by the reference beam itself II, the light scattered from it in the direction of one of the diffraction orders has, as is known, the same structure as the beam I has during the recording, that is, as before, it is the carrier of all of the information about the image of the object (Figure 5.7, b). However, the light beams of I and II are theoretically entirely equivalent. If the hologram is illuminated not by the reference beam, but by the object beam I the light scattered in the corresponding direction will have the same structure as beam II has during the recording, that is, it will have regular (planar) shape of the wave front. The given process is also depicted in Figure 5.7, c.

This property of a holograph also provides the basis for holographic methods of correcting the wave front of the wave emission first realized by Soskin, et al. [289]. The functions of the object beam of I here are performed by the laser radiation, the shape of the wave front of which is subject to correction. The coherent reference beams II with flat wave front can be formed, for example, from part of the same emission transmitted through an angle selector.

When using holography to decrease the convergence of the laser emission, the decisive role is played where the density of the efficiency of conversion — the fraction of the power of the beam illuminating the hologram which pertains to the required diffraction order. The lowest efficiency not exceeding a few percentages occurs for thin amplitude holograms which are obtained on ordinary processing of thin-layer photographic material. Bleaching converts the metallic silver to a transparent compound with a different index of refraction than for the emulsion gelatin, and the hologram is converted from an amplitude hologram to a phase hologram — the peaks and the minima of the recorded interference pattern on the hologram made correspond to sections of different optical thickness. The efficiency of thin phase holograms can theoretically approach 30%; such holograms were used when investigating the possibilities of the given correction method used by the same group of authors in 1969-1972 [289-291].

FOR OFFICIAL USE ONLY

APPROVED FOR RELEASE: 2007/02/09: CIA-RDP82-00850R000500010010-4

APPROVED FOR RELEASE: 2007/02/09: CIA-RDP82-00850R000500010010-4

Among the other results contained in the mentioned papers, the realization of phase correction of the radiation of the helium-neon laser generated on one transverse mode of the stable resonator TEM_{02} [290] deserves to be noted. Before correction, the lasing beam had a flat equiphasal surface in the hologram zone and just as the radiation of any nonzero mode of a stable resonator, it had sign-variable amplitude distribution (see § 2.1). It is possible to interpret the change in sign of the amplitude as a phase shift by π; as a result of the holographic correction such phase shifts disappear, and the wave front becomes genuinely planar (although the amplitude distribution naturally remains nonuniform). Under the conditions of [290] this has led to a fourfold decrease in divergence, and the axial luminous intensity increased noticeably although the energy efficiency of the conversion was a total of ~10% [291][1].

No less interesting experiments were performed with a ruby laser operating in the ordinary "spike" free lasing mode [291]. Here the gain in the divergence turned out to be still more significant. The possibility of realizing the correction itself in the free lasing mode which is more frequently multimodal when using a planar resonator is, generally speaking, connected with two facts. First, in the case of an optically nonuniform active medium the general distortion of the wave front caused by aberrations of the resonator characteristic of different transverse modes can prevail over the differences in the shape of the wave fronts of the individual modes (which, probably, occurred also in [291]). Secondly, although the spatial field distributions can vary from spike to spike, the peaks of these distributions naturally do not coincide; therefore the overlap of the holograms recorded by the radiation of the individual "spikes" is only partial. However, partial superposition of the holograms must lead to a reduction in energy efficiency of conversion; under the conditions of [291] it was a total of 3%.

The successful performance of the individual experiments could not free the given method of holographic correction of the serious deficiencies organically inherent in it. The use of thin-layer photographic materials alone immediately imposes rigid restrictions on the working wavelength and on the admissible radiation flux densities and, finally, the energy efficiency of conversion. It is still more important that the correction using the previously manufactured holograms is generally possible only in rare cases where the laser operates under exceptionally stable conditions, and the shape of the wave front of the generated radiation remains the same.

All of this dictates the transition to dynamic volumetric phase holography based on reversible changes in the index of refraction of certain nonlinear media in the radiation field; as a result of the presence of the known Bragg condition, the light incident on the three-dimensional hologram is scattered predominately in one diffraction procedure, and the efficiency of conversion can theoretically reach 100%.

All of the subsequent studies in the given field have proceeded along this path. The system which is used for correction by the methods of dynamic three-dimensional holography is depicted in Figure 5.7, d. The volumetric interference between two

---

[1] Having high energy efficiency, although less elegant, the procedure for realizing the correction in such cases with the help of a stationary phase plate was described after several years in [292].

FOR OFFICIAL USE ONLY

APPROVED FOR RELEASE: 2007/02/09: CIA-RDP82-00850R000500010010-4

APPROVED FOR RELEASE: 2007/02/09: CIA-RDP82-00850R000500010010-4

coherent light beams leads to the fact that a holographic phase lattice is formed in the nonlinear medium consisting of alternating layers with different index of refraction. If such a lattice is fixed in some way and then illuminated by one of the beams participating in the process of its formation, as a result of reflection from the lattice it acquires the structure of the second beam entirely similarly to how this occurs in the case of a thin hologram (see Figure 5.7, a-c). Reflection takes place without loss of intensity if the absorption in the medium is quite low, the lattice is sufficiently thick (the number of its periods along the direction of the incident beam must be significantly greater than one), and the condition $\Delta n/n \ll 4 \sin^2 \theta$ is satisfied [293, 294], where Δn is the modulation amplitude of the index of refraction, 2θ is the angle between the initial beams (see Figure 5.7, d). The meaning of the last condition reduces to the fact that the reflection from one lattice period taken separately must be quite small; only then does the three-dimensional nature of the lattice acquire a genuinely important role. Otherwise the light, just as with a thin lattice will be scattered also in other directions. Hereafter we shall consider that the conditions of three dimensionality are satisfied, and the scattering of the light in other directions is absent.

Now let us consider a real situation where both light beams exist simultaneously together with the three-dimensional hologram created by them. As a result of the interaction of each of these beams with the hologram, scattered (or, if one likes, reflected from the hologram) radiation appears. However, inasmuch as the shape of the wave front of the scattered radiation coincides with the shape of the wave front of another beam, the structure of the initial two beams remains unchanged; only redistribution of their intensities can occur.

The idea of the dynamic holographic correction is connected with this redistribution: if it actually occurs, the possibility appears for transmission of the energy of a powerful light beam, the shape of the wave front of which is subject to correction, to a reference beam with small initial intensity and plane wave front. This method of obtaining (more precisely, amplifying) narrowly directional irradiation is obviously applicable when the shape of the wave front of the powerful beam varies in time; it is only necessary that these changes be sufficiently small during the lattice relaxation time.

Conditions of Realizing the Process of Holographic "Transfer" and Its Energy Efficiency. "Transfer" on Thermal Gratings. In spite of the apparent "transparency" of the above-discussed idea of using dynamic holography, in reality it is not so simple. A more careful analysis indicates that under steady conditions and in an isotropic nonlinear medium redistribution of the energy between beams of identical frequency does not occur whatever the initial ratio of their intensities [295]. The reason for this is the following. Strictly defined phase relations exist between any of the two light beams and the radiation scattered in its direction as a result of interaction of the second beam with the volumetric hologram. These relations depend on how the holographic lattice is arranged relative to the interference pattern between the beams. Under the above indicated conditions the positions of the lattice and the interference pattern coincide — the extrema of the index of refraction are matched with the extrema of the total field intensity. It turns out that in this case the scattered radiation is phase shifted by $\pi/2$ with respect to the radiation of the beam to which it is added, and therefore it does not cause a change in its intensity. The phase shift and together with it the result of the interaction of the beams with the hologram, becomes different only when the holographic lattice is shifted for certain reasons by a fraction of a period in the transverse direction with respect to the interference pattern.

APPROVED FOR RELEASE: 2007/02/09: CIA-RDP82-00850R000500010010-4

APPROVED FOR RELEASE: 2007/02/09: CIA-RDP82-00850R000500010010-4

Initially we shall consider the hypothetical case where the radiation absorption in a nonliear medium is absent. For derivation of the corresponding equations let us represent the total field of two beams in the form

$$E(r) = A_1 \exp(ik_1 r) + A_2 \exp(ik_2 r),$$

where A_1 and A_2 are the complex amplitudes of beams I and II, k_1 and k_2 are the wave vectors of these beams where $k_1 = k_2 = k_0 = 2\pi n_0/\lambda$ where n_0 is the index of refraction of the nonlinear medium in the absence of a field. The index of refraction in the presence of the two beams will be considered equal

$$n = n_0[1 + \alpha|A_1 \exp(ik_1 r) + A_2 \exp(ik_2 r)\exp(i\delta)|^2]. \tag{5}$$

The value of the index of refraction averaged with respect to the lattice period obviously is $n_{mean} = n_0[1 + \alpha(|A_1|^2 + |A_2|^2)]$, and the modulation amplitude $\Delta n = 2|\alpha A_1 A_2|$. The introduction of the factor exp ($i\delta$) in one of the terms in the right-hand side of (5) leads, as is easy to see, to the fact that the holographic lattice described by this formula is shifted with respect to the interference pattern by a fraction of a period equal to $\delta/2\pi$; the direction of the shift for $\delta > 0$ is shown in Figure 5.7, d by the dotted arrow. If the conditions are steady state, and the medium is isotropic, $\delta = 0$; then the formula for n acquires a standard form $n = n_0(1 + \alpha|E|^2)$.

The calculation of the interaction of light beams with a nonlinear medium reduces to the solution of the wave equation $\nabla^2 E + k^2 E = 0$ considering the dependence of k^2 on the radiation field. Inasmuch as the terms with α play the role of a small correction in the formulas for n, the following approximate formula is valid for $k^2 = k_0^2(n/n_0)^2$:

$$k^2 \approx k_0^2[1 + 2\alpha|A_1 \exp(ik_1 r) + A_2 \exp(ik_2 r)\exp(i\delta)|^2].$$

Substituting this formula and the expression for E in the wave equation, as a result of the calculations analogous to those discussed in the known paper by Kogel'nik [296] by the theory of three-dimensional holograms we obtain the following differential equations relating A_1 and A_2:

$$\frac{1}{A_{1,2}}\frac{dA_{1,2}}{dl_{1,2}} = i\frac{2\pi}{\lambda}(n_{cp} - n_0) + ik_0\alpha|A_{2,1}|^2 \exp(\mp i\delta), \tag{6}$$

where $\ell_{1,2}$ are the distances along the directions of propagation of beams I and II, respectively.

The equations obtained have obvious meaning. The first terms in their right-hand sides are identical and do not depend on the lattice shift parameter δ; they describe the phase incursion occurring as a result of the fact that the average index of refraction n_{mean} in the presence of a field differs from n_0. The origin of the latter is explicitly related to the reflection from the lattice. This is

FOR OFFICIAL USE ONLY

APPROVED FOR RELEASE: 2007/02/09: CIA-RDP82-00850R000500010010-4

APPROVED FOR RELEASE: 2007/02/09: CIA-RDP82-00850R000500010010-4

indicated primarily by the presence of the "shift" factor exp ($\pm i\delta$). In addition, inasmuch as $\Delta n \sim |A_1A_2|$, the amplitude of the radiation scattered in the direction of beam I must be proportional to $|A_1A_2^2|$, and in the direction of the second beam $|A_1^2A_2|$; this dependence is also contained in (6).

From equations (6) it follows that for $\delta = 0$ the scattered radiation leads only to additional phase variations which turn out to be greater for the less intense beam. When $\delta \neq 0$ (the lattice is shifted) in addition to the imaginary terms real terms also appear in the right-sides of (6). Accordingly, the intensity of one of the beams begins to decrease as it is propagated and the other, to increase — so-called energy "transfer" takes place. The direction of the "transfer" is defined only by the sign of the product $\alpha \sin \delta$ and does not depend on the relation between the intensities of the interacting beams; therefore the energy of one of them can be transferred entirely to the other.

We have succeeded in drawing this optimistic conclusion after the authors of [294] only because, just as in [294], we introduced the lattice shift purely formally, not analyzing the natural situations in which it could really occur. Nevertheless, it will be seen later that the "transfer" will be realized in its classical version (the interacting beams have the same frequency) primarily in the presence of significant linear absorption in the medium. The corresponding theoretical analysis was performed in [297]. In the case of linear absorption (that is, when the absorbed power is proportional to the field intensity) the term $-\sigma/2$ is added to the right-hand side of each equation of system (6) where σ is the absorption coefficient. After transition from amplitudes to intensities $I_1 \equiv |A_1|^2$, $I_2 \equiv |A_2|^2$ the system acquires the form

$$\frac{1}{I_{1,2}}\frac{dI_{1,2}}{dl_{1,2}} = \pm 2k_0\alpha I_{2,1}\sin\delta - \sigma. \tag{7}$$

Hereafter, for determinacy we shall consider that $\alpha < 0$ (which is characteristic of the thermal lattices investigated later) and $\sin \delta > 0$. In this case the beam I is the donor, and the second is amplified. From (7) it is obvious that $-k_0\alpha I_1 \sin \delta$ has the meaning of the amplification coefficient in a medium for a second beam in the presence of the first. The density of the amplified beam increases while the condition $I_1 > I_0 \equiv \sigma/(2k_0|\alpha| \sin \delta)$ is satisfied.

It follows immediately from this that for maximum use of the energy of the donor beam it is desirable that its density decrease in the zone of interaction of the beams to a value of I_0. In the most favorable case where the densities of the two beams at the entrance to the medium I'_1, I'_2 are constant with respect to cross section, this condition can be satisfied by using the flat layer of the medium (Figure 5.8), the thickness of which must be correspondingly selected. In Figure 5.9, a, b, the data obtained by solution of the system (7) on the optimal thickness of the layer of medium for the cases depicted in Figure 5.8, a, b when the beams enter into the layer from one or different sides are presented[1]. Although for the same I'_1, I'_2 the optimal thickness of the layer in these two versions does not coincide, the attained density of the amplified beam $I_{2\ max}$ turns out to be the same;

[1]The calculations for the second of these cases were performed by V. D. Solov'yev.

APPROVED FOR RELEASE: 2007/02/09: CIA-RDP82-00850R000500010010-4

APPROVED FOR RELEASE: 2007/02/09: CIA-RDP82-00850R000500010010-4

the data on it are presented in Figure 5.9, c. It is obvious that high energy efficiency of the "transfer" (on the order of 50% or more) can be achieved only

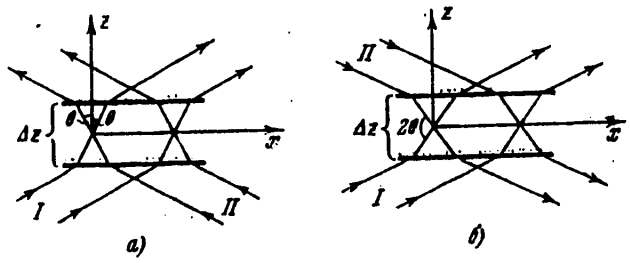

Figure 5.8. Geometry of the interaction of beams during "transfer" in a flat layer of medium: a) one-sided incidence of the beams on the layer; b) counterbeams.

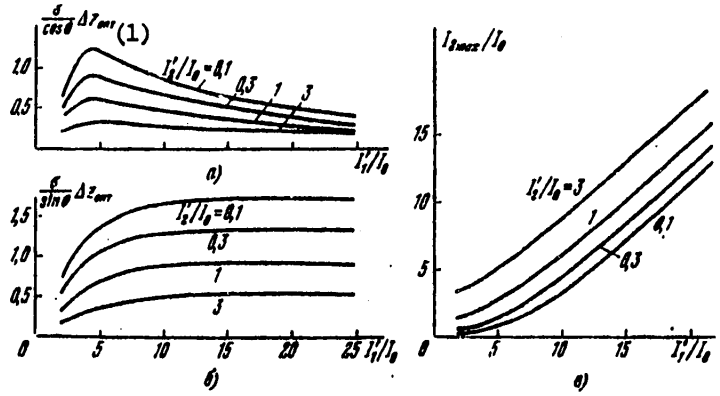

Figure 5.9. Optimal thicknesses of the layers of the medium and maximum attainable density of the amplified beam during "transfer": a), b) dependence of the thickness Δz of the layer of medium in the initial values of the beam densities I'_1, I'_2 in the diagram in Figure 5.8, a, b, respectively; c) dependence of the maximum attainable density of the amplified beam $I_{2\ max}$ I'_1, I'_2.

Key: 1. opt

when the initial density of the donor beam exceeds I_0 by at least several times; the initial density of the amplified beam also must not be too small.

Such is the theory of the interaction of beams with the holographic phase lattice created by them in the quasistationary mode in general outlines. Now we shall discuss the causes of the lattice shift with respect to the interference pattern required for energy "transfer."

In individual cases the shift occurs as a result of a natural anisotropic medium in which the hologram is created. The classical example of this is described in the well-known paper by Stabler and Amodei [298] devoted to the investigation of phase lattices in a lithium niobate crystal. On illumination of this material

FOR OFFICIAL USE ONLY

APPROVED FOR RELEASE: 2007/02/09: CIA-RDP82-00850R000500010010-4

APPROVED FOR RELEASE: 2007/02/09: CIA-RDP82-00850R000500010010-4

charge carriers are relaeased in it, which is the cause of local changes in the index of refraction. As a result of anisotropy of the given material, the drift of the free carriers here is directed in an entirely defined direction which also causes a shift of the lattice recorded in the presence of two coherent beams. The authors [298] observed noticeable redistribution of the beam intensities. It is true that they used the given phenomenon not for correction of the wave front, but for discovery of the previously unknown sign of the free charge carriers which can be established by comparing the direction of the energy transfer process with the direction of conductivity of the given crystal. This phenomenon can hardly be exemplary of the dynamic correction — the setup times here are tens of seconds.

In the general case of an isotropic medium a defined lattice shift can be obtained directly during interaction of the beams, obviously continuously shifting the medium in the direction perpendicular to the lattice planes. The shift must appear as a result of unavoidable inertia of the processes of recording and erasing it. Later it will be seen that it is possible to obtain the desired result in practice using this procedure only when using such comparatively slow recording mechanisms as thermal recordings. According to [297] let us consider this version.

For the geometry of the interaction of the beams depicted in Figure 5.8, a, the density of the thermal power dissipated as a result of absorption in the medium is $\sigma[I_1 + I_2 + 2\sqrt{I_1 I_2}\cos(2\pi x/\Lambda)]$, where $\Lambda = \lambda/2n \sin\theta$ is the period of the interference pattern, and the remaining notation was as before. The origin of the coordinates is matched with one of the peaks of the interference pattern (it is possible to neglect its small distortions along the Y and Z axes in the given investigation). A simple analysis shows that in the case of stationary medium the dependence of the temperature on x in the presence of such peak release sources has the form $T = T_{mean} + 2\sqrt{I_1 I_2}\frac{\sigma}{\varkappa} \times \left(\frac{\Lambda}{2\pi}\right)^2 \cos\left(\frac{2\pi x}{\Lambda}\right)$ with setup time of the spatial modulation $\tau = \frac{c\rho}{\varkappa}\left(\frac{\Lambda}{2\pi}\right)^2$,

where T_{mean} is the mean temperature of the medium slowly increasing with time, κ is the coefficient of thermal conductivity, c is the heat capacity and ρ is the density of the medium. This leads to the occurrence of the phase lattice with modulation amplitude $\Delta n = 2\sqrt{I_1 I_2}\frac{\sigma}{\varkappa}\left(\frac{\Lambda}{2\pi}\right)^2 \left|\frac{dn}{dT}\right|$.

If the medium is shifted continuously along the x-axis with a velocity V, the lattice setup time remains as before; its stationary position turns out to be shifted by $\Delta x = (\Lambda/2\pi)\operatorname{arctg}\omega\tau$, the depth of the modulation of the temperature and the index of refraction decreases in the ratio $(1 + \omega^2\tau^2)^{-1/2}$, where $\omega = 2\pi V/\Lambda$. A comparison of these data with (5) indicates that the parameters of the "transfer" theory under the investigated conditions assume the values

$$\alpha = \frac{\sigma}{\varkappa}\left(\frac{\Lambda}{2\pi}\right)^2 \frac{1}{n}\frac{dn}{dT}(1 + \omega^2\tau^2)^{-\frac{1}{2}}, \quad \delta = \operatorname{arctg}\omega\tau.$$

As the velocity of the medium increases, δ increases, approaching the optimal value of $\pi/2$ from the point of view of the "transfer," and on the other hand $|\alpha|$ decreases rapidly. From (7) it follows that the intensity of the energy transfer process from beam to beam is defined in the final analysis by the value of $|\alpha \sin\delta|$. This value reaches the maximum equal to $\frac{1}{2n}\frac{\sigma}{\varkappa}\left(\frac{\Lambda}{2\pi}\right)^2\left|\frac{dn}{dT}\right|$, for $\omega_0 = 1/\tau$; thus, the optimal

FOR OFFICIAL USE ONLY

APPROVED FOR RELEASE: 2007/02/09: CIA-RDP82-00850R000500010010-4

APPROVED FOR RELEASE: 2007/02/09: CIA-RDP82-00850R000500010010-4

speed of the meium is $V_0 = \left(\frac{1}{\tau}\right)\left(\frac{\Lambda}{2\pi}\right) = \frac{4\pi n}{\lambda}\frac{\varkappa}{c\rho}\sin\theta$. The density of the "donor" beam for which the amplification of the second beam as a result of "transfer" compensates for its absorption in the medium; for V_0 is equal to

$$I_0 = 4k\varkappa\sin^2\theta\Big/\left(\frac{1}{n}\left|\frac{dn}{dT}\right|\right). \tag{8}$$

All of the relations derived above are also valid for the case of "counter" beams (Figure 5.8, b) except here the index of refraction is not modulated along the x-axis, but along the z-axis; movement of the medium must be realized in the same direction.

Relation of the Idea of Dynamic Holography to the Phenomena of Stimulated Scattering. Lasers Based on Various Forms of Stimulated Scattering. Finally the time has come to explain what the logical development of the idea of holographic correction has led us to. For this purpose it is sufficient to compare two facts. First, when investigating the above-described "transfer" process in the coordinate system which is stationary with respect to not the interference pattern but the medium, the interacting beams acquire a defined frequency difference as a result of the Doppler effect. Its magnitude, as is easy to see, is ω, which explains why in this coordinate system the interference pattern is shifted at a velocity $-V$. Secondly, as follows from (7), the differential amplificaiton coefficient of the radiation with respect to beam II does not at all depend on its intensity and is completely determined by the density of beam I. Therefore when the latter has sufficient power that the "transfer" process takes place, in its presence not only the specially formed radiation is subject to application, but also the randomly scattered or "noise" radiation of proper frequency and direction.

The phenomenon consisting of the fact that on illumination of the proper medium by a powerful coherent beam amplification of the radiation takes place with frequency usually somewhat shifted with respect to the initial frequency is, as is known, called induced scattering of light. A specific amplification mechanism was described above connected with variation of the index of refraction as a result of heating of the medium during absorption of light. This type of induced scattering is actually known. It was discovered in 1967 and since that time has been called stimulated thermal scattering (STS) [299, 300]. In accordance with the above-presented calculations, the maximum amplification of the scattered radiation occurs on a frequency shift with respect to the initial frequency in the antistokes direction (that is, larger) by ω_0. The STS threshold on this frequency is defined by the formula (8); for other frequencies the threshold increases proportionally to $|\alpha \sin \delta|_{max}/|\alpha \sin \delta| = 1/2(\omega\tau + 1/\omega\tau)$.

The "transfer" observed in [298] in lithium niobate pertains to the phenomena of induced scattering on conduction electrons in semiconductors [301]. On the other hand, all types of induced scattering permit analogous "holographic" interpretation and are distinguished only by the mechanisms which cause variation of the index of refraction and shift of the phase lattice with respect to the position of the interference pattern. The reason for the shift almost always is movement of the interference pattern with respect to the medium as a result of the difference in frequencies of primary and scattered radiation (the source of the "seed" photons with shifted frequency for spontaneously occurring induced scattering which occurs predominately in the forward and return directions, usually is the scattering

FOR OFFICIAL USE ONLY

APPROVED FOR RELEASE: 2007/02/09: CIA-RDP82-00850R000500010010-4

APPROVED FOR RELEASE: 2007/02/09: CIA-RDP82-00850R000500010010-4

on the random dynamic fluctuations of the index of refraction). The fact that for STS the frequency of the scattered radiation is shifted with respect to the initial in the direction opposite to the usual shift direction for stimulated Mandelstam-Brillouin scattering on hypersonic waves (SMBS) and stimulated Raman scattering (SRS) are explained simply by the fact that the nonlinearity parameter α has different signs in these cases.

Thus, the dynamic holographic correction reduced to the well-known idea of solving the problem of divergence by constructing radiation converters based on induced scattering — no other is given. Our corrector on the thermal hologram in the moving medium is none other than the STS amplifier with frequency shift compensated as a result of the Doppler effect. Supplementing this amplifier by feedback — a resonator -- obviously we can construct the analogous laser.

For STS, the frequency shift is so small that it actually is easy to compensate, shifting the medium: according to the estimates of [297] if in the diagram in Figure 5.8, a the medium is a liquid of the type of an organic solvent, the required speed of its movement is a total of ~10 cm/sec. If the shift is compensated, it is possible to use the part of the initial beam transmitted through the shaper as the amplified. The first experiments with an amplifier of this type are described in [302]; the source of primary radiation split into two interacting beams was a single-mode ruby laser operating in the "spike" mode of free lasing. With a total lasing pulse duration of ~400 microseconds, the lattice relaxation time was ~100 microseconds, which, in turn, significantly exceeded the time interval between individual "spikes"; therefore for the extent of the greater part of the pulse the lattice was in practice quasistationary. The highest energy efficiency of "transfer" was achieved for the initial ratio of the beam intensities of 10:1; after passage of a liquid moving at a speed of 8 cm/sec, this ratio became equal to 1:3, and the amplified beam power was about 50% of the total power of the initial beams.

High inertia of the thermal processes permits observation of the phenomenon of nonsteady "transfer" predicted in [303] and consisting in the fact that for short-term interaction of the beams the energy transfer to the weaker one takes place even if the medium is stationary. This has the following explanation: when the unshifted lattice begins to be recorded and the scattered radiation appears, it, in accordance with (6), leads to additional phase incursions of the initial beams. As has already been noted, for a beam with lower intensity this incursion turns out to be larger; as a result, the interference pattern, while the processes of setting up the thermal lattice are taking place, moves through the medium which causes "transfer." The direction of the displacement is such that the weak beam is subjected to amplification. As applied to the problems of correction of the wave fronts this phenomenon was experimentally studied in references [302, 304, 305,335].

Although the papers studying the "transfer" on the thermal lattices turned out to be highly useful for understanding the possibilities of dynamic holography, it is not possible now to count on the fact that by using this process we will decrease the divergence by the radiation of real lasers. Here the mechanism of recording the lattice itself is unfavorable. The heat release required for its formation has, in addition to everything else, a negative effect on the optical quality of the medium. As a result of unavoidable nonuniformity of heating of the medium, variations of the index of refraction averaged over the lattice period appear; in the liquids, in addition, light scattering begins on the formed gas bubbles and so on.

FOR OFFICIAL USE ONLY

APPROVED FOR RELEASE: 2007/02/09: CIA-RDP82-00850R000500010010-4

APPROVED FOR RELEASE: 2007/02/09: CIA-RDP82-00850R000500010010-4

All of this, in turn, leads to an increase in the divergence of the beam itself into which the energy is "transferred." The effects of this type begin to be manifested in practice by comparatively small energy levels of the beams [335].

Now let us proceed to other types of induced scattering. For STS the energy "transfer" to a weaker beam with the same frequency is achieved without special difficulty even in the quasistationary mode. In the presence of SMBS and, in particular, for SRS everything looks somewhat different. The frequency shifts here are not so small, and the possibility of compensation for them using the Doppler effect is for a number of reasons for the most part speculative. It is already sufficient that in the former case the medium should be shifted at the speed of sound in it, and in the latter case, many times faster. Therefore by using the given forms of induced scattering having lower thresholds in the majority of media than STS, it is possible to construct only lasers and amplifiers of radiation with shifted frequency. Nevertheless, the "transfer" with splitting of the initial beam into the donor and amplified beams is realizable and in this case the required frequency shift of the later amplified beam can be obtained using the same induced scattering. When using this system [306] conversion on SMBS was obtained with transfer on the order of 80% of the donor beam power to the amplified beam. As a result of the conversion, the axial luminous intensity increased by more than 3 orders.

As for the SMBS and SRS lasers, their properties are quite well-known. These lasers have, of course, many specific peculiarities distinguishing them from standard inverted medium lasers. First of all here although the primary radiation frequently is called pumping radiation as before, theoretically different requirements are imposed on its coherence — the sources of the pumping of lasers based on induced scattering usually are other lasers with spectral radiation selection. Complex phenomena arise as a result of the fact that in the case of induced scattering the theoretical role is played only by the magnitude of the frequency different $\Delta\omega$, but not the exact absolute values. Therefore when the density of the converted radiation itself begins to exceed the induced scattering threshold, lasing is excited on a frequency $2\Delta\omega$ from the initial frequency, and so on. Finally, as already been mentioned in § 4.2, with respect to the nature of the interrelation between the excitation and the generated radiation fields the converters based on induced scattering more resemble flow lasers than standard lasers with a stationary medium.

In spite of all their peculiarities, the induced scattering lasers are, of course, the most genuine lasers. The principles of the selection of the type and parameters of the resonators remain the same as in ordinary lasers; the resonator deformations exist exactly the same, including those caused by heating of the medium. Being the basic, theoretically unavoidable source of heating, the Stokes losses in the SRS and SMBS lasers are much less than in the ordinary lasers which gives rise to the prospectiveness of this entire area. At the present time a number of experimental papers have already been published in which the conversion of the radiation with the help of SMBS and, in particular, SRS, has led to a decrease in the divergence (a broad bibliography exists, in particular, in [218, 306]). It is not appropriate to enumerate all of them; let us only mention one interesting area of research,

In 1973 when studying the properties of the SRS converters [307] and SMBS converters [308] with pumping by the radiation of multimode lasers, it was possible to

FOR OFFICIAL USE ONLY

APPROVED FOR RELEASE: 2007/02/09: CIA-RDP82-00850R000500010010-4

APPROVED FOR RELEASE: 2007/02/09: CIA-RDP82-00850R000500010010-4

observe significant amplification of narrowly directional light beams without significant variation of their spatial structure. The nontrivialness of the situation consists in the fact that the multimode pumping field is nonuniform and actually divided into a large number of randomly distributed spots with respect to volume, the characteristic dimensions of which are defined by the parameters of coherence and the geometry of the illumination. The theoretical analysis of the conditions under which the nonuniformity of the pumping field does not imply a change in the spatial structure of the amplified beam (as a result of the statistical averaging of the effect of a large number of small nonuniformities) was performed in references [309, 310]. The first purposeful experiment checking this model was described in [311].

§5.3. Method of Wave Front Reversal

The Idea and Theoretical Possibilities of the Method. In 1971 another method of obtaining narrowly directional laser emission was proposed [312]. The basis for it was the argument that it is better to realize wave front correction not at the exit of a powerful laser amplifier, but at its entrance, giving the wave front a form such that after passage through an optically nonuniform amplifying medium it becomes plane. Shifting the corrector from the exit to the entrance permits the requirements on the beam stability of its elements to be lowered; in addition, even if the correction process has low energy efficiency, the dissipated power will be small and will be felt little in the efficiency of the system as a whole.

In order to give the wave front of the beam coming to the amplifier exit the required shape, in [312] it was proposed that the procedure illustrated in Figure 5.10, a be used. The reference light wave 1 with plane (or other required) front shape is fed to the laser amplifier 2 containing optical nonuniformities from the direction of its exit and passes through it in the opposite direction, being amplified and simultaneously acquiring the phase distortions. Then this wave is somehow transformed to a so-called reversed (or complex-conjugate) wave 3 of the same frequency which has equiphasal surfaces common to the reference wave at the input to the amplifier and similar amplitude distribution with respect to cross section but is directed in the opposite direction. It is easy to show that on satisfaction of certain quite reasonable requirements imposed on a laser amplifier, coincidence of the equiphasal surfaces of these two waves with respect to one side of the amplifier guarantees their coincidence also with respect to the other side. Thus, the reversed wave, passing through an amplifier containing nonuniformities, acquires the required shape of its front (in the given case plane).

Actually, let us consider the interrelation between the spatial structure of the reference wave and the reversed wave. Although this interrelation is of the most universal nature, as usual we shall limit ourselves to the case where the scalar approximation is applicable. Let us represent the field of the reference and reversed waves in the form $E=A\exp(-ikz)$ and $E'=A'\exp(ikz)$, respectively, where A and A' are comparatively slowly varying functions of the coordinates, the direction of the z-axis is shown in the figure. Using the condition of similarity of the amplitude distribution with respect to cross section, it is easy to demonstrate that on any equiphasal surface common to two waves, the values of

APPROVED FOR RELEASE: 2007/02/09: CIA-RDP82-00850R000500010010-4

APPROVED FOR RELEASE: 2007/02/09: CIA-RDP82-00850R000500010010-4

A and A' are related by an expression of the type $A'=\gamma A^*$, where γ is a constant factor, the symbol * denotes complex conjugation (this is where the second name of the reversed wave finds its origin).

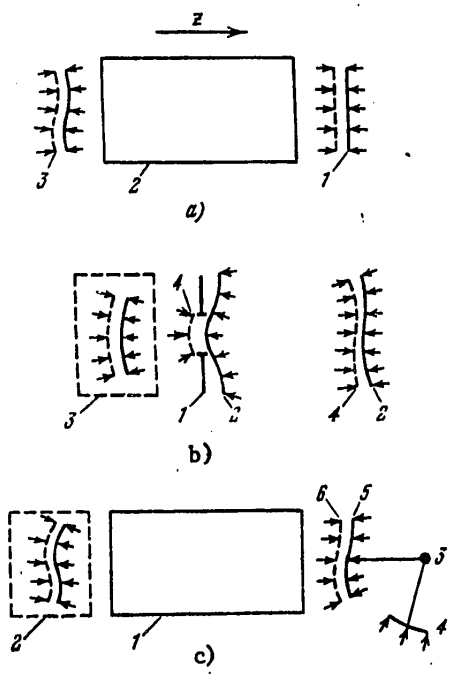

Figure 5.10. Correction of a wave front by the "reversal" method: a) scheme for compensation of phase distortions in a laser amplifier; 1 -- reference beam, 2 -- amplifier, 3 -- conjugate wave; b) effect of decreasing the conjugation precision in the presence of aperture irises; 1 -- screen with aperture, 2 -- reference wave, 3 -- assembly in which "reversal" takes place, 4 -- reversed wave; c) diagram of a laser with self-induction of emission; 1 -- laser amplifier, 2 -- assembly in which "reversal" takes place, 3 -- object, 4 -- auxiliary laser, 5 -- front of the emission scattered by the object, 6 -- front of the laser exit emission.

Substituting the expressions for E and E' in the wave equation $\nabla^2E+k^2E=0$, we arrive at the equations $\nabla^2A-2ik(\partial A/\partial z)=0$, $\nabla^2A'+2ik(\partial A'/\partial z)=0$. Let us write out another equation complex conjugate to the first: $\nabla^2A^*+2ik^*(\partial A^*/\partial z)=0$. It is obvious that in the absence of absorption or amplification, that is, when k is real, the values of A* and A' satisfy the same differential equation. Inasmuch as on a common equiphasal surface these values coincide with accuracy to a constant factor, the comparison must occur in the entire region of space where the reference and reversed wave do not go beyond the boundaries of the medium containing only phase nonuniformities. Hence, in turn, it follows that in the entire indicated region these waves have common equiphasal surfaces and similar distribution of the radiation intensity with respect to cross section.

APPROVED FOR RELEASE: 2007/02/09: CIA-RDP82-00850R000500010010-4

APPROVED FOR RELEASE: 2007/02/09: CIA-RDP82-00850R000500010010-4

The theoretical possibility of using this remarkable property of conjugate waves for autocompensation of purely phase inhomogeneities is unquestioned; in 1965, Kh. Kogel'nik demonstrated how, forming a reversed wave, it is possible to reproduce an undistorted holographic image of the subjected observed through an optically inhomogeneous medium [313]. On transition to the problem of correction of phase distortions in lasers, definite difficulties arise. The main one of them naturally is connected with the fact that the parameter k in the amplifying medium is complex and equations for A* and A' cease to coincide. It is primarily of interest that the presence of amplification uniformly distributed with respect to cross section involves only multiplication of the complex amplitude of the wave passing through the amplifier by some additional constant; the form of its distribution remains the same as in the absence of amplification (see §1.3). Hence, it follows that the presence of amplification under the condition of uniformity of its distribution with respect to cross section has no influence on the precision of coincidence of the equiphasal surfaces of the conjugate waves.

The case is also important where although the amplification is nonuniform with respect to cross section but varies little at distances on the order of the size of the Fresnel zone, the phase nonuniformities are not so large as to cause "mixing" of the radiation with respect to cross section inside the amplifier. Then the equiphasal surfaces of the reversed wave at the amplifier output continue approximately to coincide with the equiphasal surfaces of the reference beam; only the intensity distribution in them becomes different. Inasmuch as the intensity distribution has much less influence on the magnitude of the divergence than the radiation phase distribution (§1.1), the given correction method is unconditionally effective also in this situation. It can become meaningless only for the most unfavorable properties of the active medium.

The accuracy of reproduction of the initial structure of the reference wave at the amplifier output can also decrease as a result of the presence of certain aperture irises. This effect is explained by Figure 5.10, b. Let only part of the reference beam cross section 2 pass through the aperture in the screen 1. Then if radiation losses are absent until the reference beam hits the node 3 which realizes "reversal," the reversed wave 4 formed in this node passes entirely through the opening; conjugation in the vicinity of the aperture is complete. However, to the right of the screen the absence of radiation must be felt in the peripheral sections of the cross section of the reversed wave near the screen -- the wave somehow diffracts at the aperture, and on going away from the aperture, the exactness of coincidence of the equiphasal surfaces gradually decreases. Obviously, it is necessary to achieve the situation where the greatest possible part of the reference beam entering the amplifier reaches the node realizing the "reversal" operation. This must be done especially carefully when using amplifiers with long path length of the emission travel through the active medium, in particular, multipass amplifiers of the type described in §4.3.

The stipulations made cannot shake the general conclusion of the extraordinarily prospectiveness of the "reversal" method. Let us note another advantage of this method. Preamplification of the reference beam (before it hits the "reversal" node) makes it possible to get along with very small initial radiation intensities. This makes the idea of creating a laser with homing of emission on a given

APPROVED FOR RELEASE: 2007/02/09: CIA-RDP82-00850R000500010010-4

APPROVED FOR RELEASE: 2007/02/09: CIA-RDP82-00850R000500010010-4

object -- a remote target, a target in experiments in laser thermonuclear fusion and the like -- which is very popular at the present time, highly realistic. As was pointed out in [312], in order to provide the homing effect, it is sufficient to expose the target to the coherent radiation of an auxiliary laser and use the light scattered from the target in the range of the primary laser as a reference beam (see Figure 5.10, c; it possible to get along without the auxiliary laser, converting the basic emitter to the lasing mode for some period of time). In this case, the optical distortions turn out to be compensated not only in the laser medium and the shaping system, but also in the atmosphere (if, of course, the inhomogeneities do not change while the light travels the distance to the emitter and back). Obviously, this method can be used to solve the problems of automatic target tracking, and so on.

It is necessary to note that the possibilities of creating emitters with a wave front which is "reversed" with respect to the wave front of the emission scattered from the target, began to be discussed in the 1960's (primarily as applied to the microwave band). However, we are talking only about the corresponding correction of the phase distribution directly at the output of a complex multielement system using phase control of the individual elementary emitters making up the system. The development of analogous ideas as applied to the optical band became one of the principal areas of adaptive optics mentioned in the preceding section [334].

"Reversal" in Stimulated Backscattering. Let us proceed with the investigation of specific methods by means of which the "reversal" operation can be realized. Although historically the holographic methods of forming a complex-conjugate wave began to be discussed first, which we shall discuss somewhat later, general attention has been attracted to the "reversing" method on a somewhat different level. In 1972 it came to be known that a wave reflected back in an uncontrolled induced Brillouin scattering process under defined conditions turns out to be conjugate with respect to the initial wave [316]. Soon, by using the given effect, a ruby laser was built by the scheme presented in Figure 5.10, a [317].

Generally speaking, at that time a number of observations had already been published indicating that with forced backscattering frequently something similar to the process of formation of a conjugate wave takes place. In the experiment, the results of which were revealed by Bespalov and Kubarev in 1966 [339], the back-reflected beam had, just as the initial beam, diffraction divergence. Mentions of the fact that the backscattered beam has approximately the same divergence as the initial beam (or the same cross section at a noticeable distance from the cell with the medium in which scattering took place) can also be found in the papers by Rank, et al. on stimulated Brillouin scattering and stimulated Thomson scattering [318, 310], and reference [319] on stimulated Raman scattering.

Although the presence of an entire series of such observations indicated that they are not accidental, a clearcut conclusion regarding conjugation of the scattered and initial wave was formulated only in [316]; in the same paper the possibility of using this effect for autocompensation of phase distortions was clearly demonstrated. The experiment performed in [316] consisted in the following. Narrowly directional emission of a unimodal ruby laser was passed through an etched glass plate which naturally led to multiple increase in the divergence. Then the emission was focused on a hollow glass light guide with methane (Figure 5.11).

APPROVED FOR RELEASE: 2007/02/09: CIA-RDP82-00850R000500010010-4

APPROVED FOR RELEASE: 2007/02/09: CIA-RDP82-00850R000500010010-4

The beam "reflected" back as a result of stimulated Brillouin scattering through the same lens and scattering plate, acquired the initial structure with very small divergence.

Subsequent studies demonstrated that conjugation of the incident and reflected wave also occurs for other types of stimulated scattering [320, 321]. The mechanism of this phenomenon became understandable. This mechanism is explained as follows. When a beam, the average density of which greatly exceeds the induced scattering threshold, is incident on a nonlinear medium, a set of scattered light waves appears in the medium. On propagation through a region exposed to primary emission, these waves are amplified. The better the field distribution of any of them is "inscribed" in the outlines of this region, the more this wave is amplified. Obviously the waves, all of the field distribution peaks of which fall exactly at the initial radiation intensity peaks, are subject to the greatest amplification. Inasmuch as the propagation of all of the waves is described by like equations, only the waves with the same shape of front can have intensity distribution exactly coinciding inside a defined volume. Therefore a wave conjugate to the initial wave is isolated among the backscattered waves.

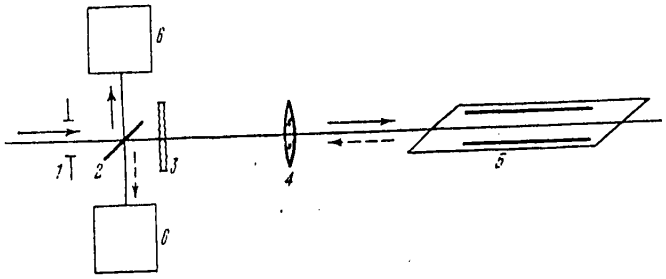

Figure 5.11. Diagram of the experiment in [316]:
1 -- iris 6×6 mm, 2 -- light dividing plate, 3 -- etched plate, 4 -- lens, 5 -- cell with light guide, 6 -- systems for measuring the parameters of the primary and reflected radiation.

From this primitive explanation, it becomes understandable that the degree of isolation of a conjugate wave against the general background of scattered emission must depend on the configuration of the exposed zone, the average density of the primary emission and the nature of its distribution inside this zone. The role of a lens and etched plate in the above-described experiment will also become understandable -- the lens and the etched plate provide the required average density and nature of distribution. Let us note that without the plate, the conjugation effect was not observed in [316] -- the scattered emission had much greater divergence than the primary emission.

On the other hand, if the initial beam has suitable characteristics immediately (or acquires them, on being propagated in a nonuniform scattering medium), the lens and special scattering medium can be unnecessary -- then the device realizing the "reversing" operation reduces to a cell with a nonlinear medium. As an example we have reference [321] -- no separate scattering medium was used there.

APPROVED FOR RELEASE: 2007/02/09: CIA-RDP82-00850R000500010010-4

APPROVED FOR RELEASE: 2007/02/09: CIA-RDP82-00850R000500010010-4

Those desiring to familiarize themselves in more detail with the theory of the process of formation of a conjugate wave during stimulated backscattering are referred to the articles [322, 323, 340], and so on; in this book we shall proceed with a brief discussion of the general advantages and disadvantages characterizing the given "reversing" procedure. Its basic advantage is, of course, simplicity: as we have seen, in addition to the cell with nonlinear medium one or two primitive optical elements may be needed. A theoretically important item is the absence of any requirements on the optical quality of the nonlinear medium -- neither the initial nor the induced inhomogeneities can decrease the conjugation precision.

Now let us proceed to the shadow aspects of using the "reversal" effect during stimulated backscattering. One of them should already be understandable to the reader: a conjugate wave is isolated from "noise" only with suitable nature of distribution of the emission in the interaction zone, which, in turn, is indifferent to the spatial structure of the initial beam. The fact that the differences between the thresholds of the stimulated scattering and destruction of the medium (caused by optical breakdown or something similar) are usually not too large imposes its restrictions also. As a result, the dynamic range of admissible radiation densities of the reference wave turns out to be small. This is especially inconvenient when solving the "homing" problem where the reference beam is formed from scattered light, the intensity of which, depending on the properties and degree of remoteness of the target, can vary within the broadest limits.

Finally, an important deficiency of stimulated scattering from the point of view of the possibilities of its use in lasers with wave front "reversal," which theoretically cannot be eliminated, is the presence of a frequency shift. The situation is especially bad with stimulated Raman scattering. Let us begin with the fact that all of our preceding arguments were based on at least example equality of the frequencies of the initial and the scattered light. For stimulated Raman scattering the frequencies are so different that even in the case of exact conjugation of the waves at the input of an amplifier containing significant phase inhomogeneities, coincidence of the fronts at its output can turn out to be far from ideal. In addition, the exactness of conjugation in the process of stimulated scattering itself decreases: coincidence of a large number of intensity peaks of two waves in a thick layer of nonlinear medium in general becomes impossible. Added to this fact is the fact that the frequency shift during stimulated Raman scattering greatly exceeds the band width of all of the active media used in powerful lasers; therefore in the diagram in Figure 5.10, a, c the light can be amplified only on one of two passes through the medium. On the basis of all of the mentioned facts, the work in the given area offers little promise.

The situation is much more favorable with stimulated Brillouin and Thomson scattering -- the frequency shifts are too small for them to have a real influence on the exactness of conjugation. They are also less than the amplification band widths of many active media; therefore amplification can be realized on both passes through the medium. However, other unfortunate situations arise -- in the final analysis the small frequency shift is the consequence of high inertia of the processes leading to stimulated scattering. Therefore for very rapidly varying wave fronts neither stimulated Brillouin nor Thomson scattering can be used.

APPROVED FOR RELEASE: 2007/02/09: CIA-RDP82-00850R000500010010-4

APPROVED FOR RELEASE: 2007/02/09: CIA-RDP82-00850R000500010010-4

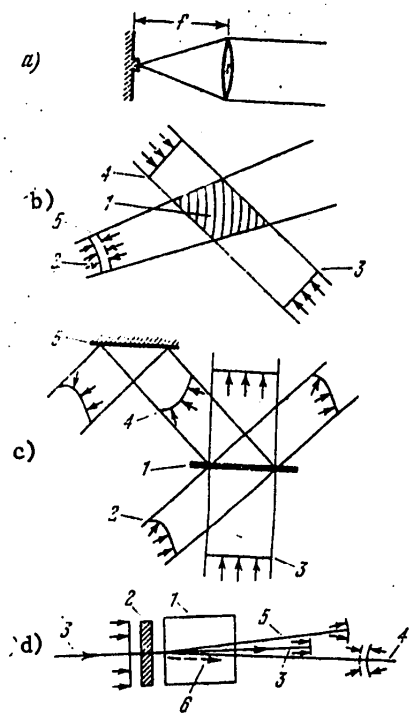

Figure 5.12. Methods of "reversal": a) "reversal" system for small deviations from plane shape of the wave front; b) four-wave interaction system (1 -- hologram, 2 -- beam subject to "reversal," 3, 4 -- reference beams with plane wave fronts, 5 -- desired conjugate beam); c) "reversal" system using additional diffraction procedure in the case of a thin hologram (1 -- thin flat hologram, 2 -- beam subject to "reversal," 3 -- reference beam with plane wave front, 4 -- beam scattered in one of the additional diffraction procedures, 5 -- mirror); d) conjugation with parametric amplification of light (1 -- nonlinear crystal, 2 -- light dividing mirror, 3 -- double frequency emission, 4 -- beam subject to "reversal," 5, 6 -- signal wave and idler wave).

"Reversal" by Methods of Classical Optics and Holography. Now let us proceed to other methods of "reversal," which, in contrast to the preceding one, can be called stimulated as a result of the uncontrolled stimulated scattering. Initially we shall mention one possibility of using the methods of classical optics, of interest but not having special practical significance [312]. The simplest device capable of performing the "reversal" operation with small deviations from a plane wave front is depicted in Figure 5.12, a; it consists of a lens, in the focal plane of which a mirror has been installed. On the system axis the mirror has a projection (or depression) of height $\lambda/4$ covering only the central peak of the diffraction pattern which appears on exposure of the lens to a parallel light beam. This

APPROVED FOR RELEASE: 2007/02/09: CIA-RDP82-00850R000500010010-4

APPROVED FOR RELEASE: 2007/02/09: CIA-RDP82-00850R000500010010-4

corrector operates as follows. Let an almost parallel beam incident on the lens from the right have amplitude distribution $A \exp(i\phi)$, where A=const, ϕ is the phase distortion which is variable with respect to the beam cross section. For $|\phi|<1$, the amplitude $A \exp(i\phi) \simeq A+iA\phi$. Two waves described by these terms are separated spatially in the focal plane of the lens: the greater part of the first of them is collected at the central peak of the diffraction pattern, the second is distributed primarily with respect to the remaining part of the plane. The presence of a projection leads to the fact that on reflection from the mirror, an additional phase difference equal to π occurs between these waves; as a result, the amplitude distribution after passage through the lens in the opposite direction acquires the form $A-iA\phi \simeq A\exp(-i\phi)$ -- the front becomes "reversed." Let us note that in the known method of Zoernicke contrast [7] an analogous procedure is used except the introduced phase shift is not π, but $\pi/2$. Then the same initial beam acquires amplitude distribution $A \exp(\phi)$ -- the phase variations are transformed to intensity variations.

The idea of a holographic "reversal" method for arbitrary phase distortions belongs to Denisyuk [331]; the version of the method of practical importance described in [313] is explained in Figure 5.12, b. The hologram 1, which can be both volumetric and thin, is recorded with the participation of the beam 2 subject to reversal and the reference beam 3 with plane wave front. If the hologram is exposed to beam 4 also with a plane wave front and opposite direction of propagation, then as a result of reflection of beam 4 from the hologram, the desired "reversed" beam 5 is formed.

Although the authors of the initial papers [331, 313] proposed hologram recording and "reading" processes separated in time, the same system can also be realized in the dynamic mode, that is, with simultaneous feed of beams 2, 3 and 4 to the nonlinear medium [341, 342, 297]. Moreover, here the situation is much better than in the case of the method of holographic "pumping" discussed in the preceding section. Actually, the basic difficulties there were connected with the necessity for the presence of a shift of the holographic grid with respect to the interference pattern between the interacting beams. This, in turn, was caused by the fact that the emission scattered by the hologram was added directly to the initial beams, varying their intensity only on satisfaction of defined phase relations. As for the system in Figure 5.12, b, here beam 5 which is of interest to us is formed wholly from scattered emission -- nothing is fed from the outside to the nonlinear medium in this direction, there are no phase conditions, and the grid shift is not required. Therefore in the given system beams of identical frequency and media with in practice any nonlinearity mechanism can be used.

With respect to the light beams participating in it this process now is called the four-wave interaction process. Analysis of spatial evolution of the intensities of the interacting beams can be made in the same approximation which was used in the preceding section when investigating "pumping," except, of course, it looks more complicated [324, 325]. The corresponding estimates show that here for high, but entirely reasonable densities of beams 3 and 4 which serve as the basic energy source, it is possible to obtain the transformation coefficient of the direct wave 2 to the reversed wave 5 on the order of 100% and even higher.

APPROVED FOR RELEASE: 2007/02/09: CIA-RDP82-00850R000500010010-4

APPROVED FOR RELEASE: 2007/02/09: CIA-RDP82-00850R000500010010-4

Whereas everything is all right with the energy efficiency of the "reversal" process in the case of four-wave interaction, the problem of optical uniformity of the nonlinear medium in which interaction takes place is quite serious. The situation is as follows: waves 2 and 5 turn out to be conjugate, generally speaking, only as a result of the fact that the "pumping" waves of the converter 3 and 4 are conjugate. From Figure 5.12, b, it is clear, however, that for conjugation of "pumping" waves it is necessary that they have plane fronts not only at the entrance to the nonlinear medium, but also after passes through it. Thus, in the case of four-wave interaction the precision of "reversal" depends directly on the optical quality of the medium.

If in the initial state the medium has quite high optical uniformity, it is necessary to consider the inhomogeneities caused by the light fields themselves. In addition to any type of side phenomena (of the type of the occurrence of gas bubbles in the absorbing centers in liquid media), the variations of the index of refraction themselves can lead to distortion of the wave front. These variations also are the cause for the existence of the holographic grid. Indeed, the superposition of coherent light beams in a nonlinear medium is accompanied not only by the appearance of spatial periodic modulation of the index of refraction, but also variation of its mean value with respect to period (usually this variation is proportional to the total light intensity). As a result, it can turn out to be necessary to impose defined, still quite rigid, requirements on the uniformity of the radiation density distribution with respect to cross section of interacting beams; this pertains, of course, primarily to intense "pumping" beams of the converter 3 and 4.

Another possible method of "reversal" by the methods of holography is explained by Figure 5.12, c. The beam 2 subject to "reversal" and the reference beam 3 with plane wave front parallel to the surface of the hologram participate in recording the thin flat hologram 1. When discussing Figure 5.7, we mentioned in passing that on illumination of a thin hologram, in addition to the reconstructed initial beams, beams also appear which are scattered in the direction of other diffraction orders. One of them -- beam 4 -- has a front shape that is mirror imaged with respect to the desired shape (it is possible to see this if we try to compare the wave fronts of beams 2 and 4); after reflection from the mirror 5, this beam finally becomes "reversed" with respect to beam 2. This system can also be used in the dynamic mode.

Although the theoretical possibilities of obtaining conjugate waves using dynamic holography became obvious quite long ago [341, 342, 312], the given direction began to be developed intensely only at the present time. In addition to the mentioned theoretical articles [324, 325], an entire series of new reports have appeared on experimental observation of "reversal" in the case of four-wave interaction. The first article [326] in which the realization of dynamic correction by holographic "reversal" in a ruby amplifier was recorded was published in Soviet literature. The system used was a combination of systems depicted in Figure 5.12, b, c; a thin dynamic hologram with time constant $\sim 5 \cdot 10^{-9}$ sec was recorded in a KdS semiconductor crystal (the variations of the index of refraction were caused by variations of the concentration of three charge carriers). It is true that the efficiency of conversion of a direct wave to a reversed one did not exceed 5%; indeed, the amplification on passage through the ruby rod was small.

APPROVED FOR RELEASE: 2007/02/09: CIA-RDP82-00850R000500010010-4

APPROVED FOR RELEASE: 2007/02/09: CIA-RDP82-00850R000500010010-4

Therefore the resultant amplification of the device as a whole (two passes through the rod plus the conjugation operation) did not reach one, but the fact that compensation of the inhomogeneities in the amplifier was present. Without any doubt, this is not the limit and we shall soon be witnesses to much more impressive experiments.

"Reversal" in Parametric Amplification of Light. Conclusion. The idea of another, highly prospective "reversal" method is connected with using long-known laws of the process of parametric amplification of light [327]. In contrast to stimulated scattering, parametric amplification is a three-wave process. In addition to the amplified wave and powerful high-coherent, high-frequency light beam playing the role of "pumping," in a nonlinear medium a so-called idler wave of difference frequency is formed. It is significant for us that the phase distribution with respect to cross section of the idler wave is equal to the difference of the phase distributions of the pumping emission and the amplified (signal) wave. If the pumping emission has a plane wave front and frequency twice the signal wave frequency, the idler wave obviously turns out to have the same frequency as the signal wave, and it has phase distribution that is opposite with respect to sign, that is, "reversed" front with respect to the signal wave (for example [328]).

One of the possible ideas of the parametric converter systems performing the conjugation operation is presented in Figure 5.12, d. The converter consists of a nonlinear crystal 1 and light dividing mirror 2 reflecting the emission of a frequency such as the signal and idler waves have, and the transmitted double-frequency emission. The specially formed double frequency beam 3 with plane wave front falls strictly normally on the surface of the mirror 2 and, passing through it, enters the crystal 1. The beam 4 subject to "reversal" reaches the crystal from the other side; after reflection from the mirror it acquires a suitable direction and becomes the signal wave 5 of the conversion process. The crystal is oriented so that synchrony of the interaction between this wave and the "pumping" emission 3 will be achieved. The "idler" wave 6 formed during parametric amplification of the signal wave has direction opposite to the direction of arrival of the initial beam 4 and a "reversed" wave front with respect to the initial beam.

Here the basic difficulties are connected with the fact that beams with frequencies that differ by two times participate in the process. It is known that such beams are capable of interacting properly with each other only in a narrow class of media with specific nature of nonlinearity. In addition, even if interaction theoretically exists, in order to obtain any noticeable conversion efficiency, it is necessary to provide for the above-mentioned synchrony (explanations of all of these problems can be found in any text on nonlinear optics). In the simplest case of collinear interaction (propagation directions of all three waves coincide the synchrony conditions reduce to the requirement of exact equality of the indices of refraction for the first and second harmonic emission.

Generally speaking, it is necessary to trace the observation of synchrony conditions even in the general case of four-wave interaction; however, in the above-investigated "degenerate" version of this process where the frequencies of all beams are identical, the synchrony conditions are satisfied automatically, which made it possible for us to ignore them. As for the three-wave process discussed

APPROVED FOR RELEASE: 2007/02/09: CIA-RDP82-00850R000500010010-4

APPROVED FOR RELEASE: 2007/02/09: CIA-RDP82-00850R000500010010-4

here, providing synchrony for this process becomes an integral problem. In the final analysis it turns out that efficient interaction between the radiation of the first and second harmonics can be realized only in very few, anisotropic crystals and with strictly defined orientation of them relative to the directions of the light beams; it is natural that restrictions are imposed on the magnitude of the angular divergence of the light beams.

Nevertheless, these difficulties are surmountable, which is indicated primarily by the experience of building second harmonic lasers (frequency doublers). Indeed, the same nonlinear crystals and satisfaction of the same synchrony condition are required for them, but this did not interfere long ago with achievement in practice of conversion coefficients of the first harmonic radiation to second amounting to several tens of percentages. Without going into details, it is worthwhile to note that in a parametric converter with interaction close to collinear, less rigid requirements are imposed on the angular divergence of the signal wave than on the divergence of the first harmonic emission in frequency doublers. It is also possible to show that in the system in Figure 5.12, d the optical inhomogeneity of the nonlinear medium is not so large as to disturb the synchrony of interaction, it influences the precision of the "reversal" much less than in the case of four-wave interaction (this advantage of the parametric converter disappears if the double frequency emission is fed to the crystal from the same side as the initial "reversed" beam arrives).

The results of the first experiments with autocompensation of the aberrations in a neodymium glass laser amplifier with parametric "reversal" are published in [329]. The basic structure was assembled by the diagram in Figure 5.10, a; in the operating mode the amplifier provided ten-fold amplification of the signal passing through it in one direction. The reference beam was part of the output emission of an auxiliary giant-pulse laser, the active medium of which was also neodymium glass; the remaining part of the emission was directed toward the frequency doubler, generating the second-harmonic emission required for the parametric process there. The nonlinear material in the parametric converter having the diagram shown in Figure 5.12, d, was a lithium iodate crystal; the magnitude of the angle between the signal and idler waves reached $2 \cdot 10^{-2}$ rads, which was entirely sufficient for the second of them only to reach the amplifier input.

The energy efficiency of conversion of the signal wave to an idler wave was ~10%; thus, considering the passage through the amplifier in both directions, the entire device insured approximately 10-fold amplification of the initial reference beam. Demonstration experiments with introduction of an optical wedge into the amplifier, the angle of deviation on passage through which was 10^{-3} rads demonstrated that total compensation of the introduced aberrations takes place here.

The list of methods by means of which the "reversal" can be realized clearly does not exhaust this. Let us also mention, for example, the phenomenon of so-called photon echo, which consists in the following: on feeding two light pulses separated by very short time interval to the appropriate medium, this medium emits a third pulse independently after an identical time interval [337]. If we give the second-pulse emission a plane wave front, then the fronts of the first and third pulses turn out to be conjugate. It is now difficult to say what all of this leads to. Only one thing is clear: the work in the field of angular divergence of laser emission will in the future lead not only to technical progress, but also to the discovery of new, interesting phenomena and laws of the behavior of powerful coherent light beams.

APPROVED FOR RELEASE: 2007/02/09: CIA-RDP82-00850R000500010010-4

APPROVED FOR RELEASE: 2007/02/09: CIA-RDP82-00850R000500010010-4

BIBLIOGRAPY

1. Prokhorov, A. M. "Submillimeter Molecular Amplifier and Smaser," ZHETF [Journal of Experimental and Theoretical Physics], Vol 34, 1958, p 1658.

2. Schawlow, A. L.; Townes, C. H. "Infrared and Optical Masers," PHYS. REV., Vol 112, 1958, p 1940.

3. Vaynshteyn, L. A. OTKRYTYYE REZONATORY I OTKRYTYYE VOLNOVODY [Open Resonators and Open Waveguides], Moscow, Sovetskoye radio, 1966.

4. Siegman, A. E. "Unstable Optical Resonators for Laser Application," PROC. IEEE, Vol 53, 1965, p 277.

5. Anan'yev, Yu. A.; Sventsitskaya, N. A.; Sherstobitov, V. Ye. "Selection of Transverse Types of Oscillations in Lasers with Convex Mirrors," DAN SSSR [Reports of the USSR Academy of Sciences], Vol 179, 1968, p 1304.

6. Born, M.; Wolf, E. OSNOVY OPTIKI [Fundamentals of Optics], Moscow, Nauka, 1970.

7. Goodman, J. VVEDENIYE V FURYE-OPTIKU [Introduction to Fourier Optics], Moscow, Mir, 1970.

8. Anan'yev, Yu. A. "Unstable Resonator for Lasers with Weakly Amplifying Media," PIS'MA V ZHTF [Letters to the Journal of Technical Physics], Vol 4, 1978, p 372.

9. Fox, A. G.; Li, T. "Resonant Modes in a Maser Interferometer," BELL SYST. TECHN. J., Vol 40, 19691, p 453.

10. Boyd, G. D.; Gordon, J. P. "Confocal Multimode Resonator for Millimeter Through Optical Wavelength Masers," BELL SYST. TECHN. J., Vol 40, 1969, p 489.

11. Boyd, G. D.; Kogelnik, H. "Generalized Confocal Resonator Theory," BELL SYST. TECHN. J., Vol 41, 1962, p 1347.

12. Collins, S. A. "Analysis of Optical Resonators Involving Focusing Elements," APPL. OPTICS, Vol 3, 1964, p 1263.

13. Kogelnik, H. "Imaging of Optical Modes-Resonators with Internal Lenses," BELL SYST. TECHN. J., Vol 44, 1965, p 455.

14. Kogelnik, H.; Li, T. "Laser Beams and Resonators," PROC. IEEE, Vol 54, 1966, p 1312; APPL. OPTICS, Vol 5, 1966, p 1550.

15. Kahn, W. K. "Unstable Optical Resonators," APPL. OPTICS, Vol 5, 1966, p 407.

APPROVED FOR RELEASE: 2007/02/09: CIA-RDP82-00850R000500010010-4

APPROVED FOR RELEASE: 2007/02/09: CIA-RDP82-00850R000500010010-4

16. Anan'yev, Yu. A. "Angular Divergence of the Emission of Solid-State Lasers," UFN [Progress in the Physical Sciences], Vol 103, 1971, p 705.

17. Mak, A. A.; Anan'yev, Yu. A.; Yermakov, B. A. "Solid-State Lasers," UFN, Vol 92, 1967, p 373.

18. Vanyukov, M. P.; Isayenko, V. I.; Serebryakov, V. A. "Study of a Laser Radiation Pattern," ZHETF, Vol 44, 1963, p 1493.

19. Vanyukov, M. P.; Isayenko, V. I.; Serebryakov, V. A. "Variation in Time of Stimulated Emission in Separate Side Modes," ZHETF, Vol 46, 1964, p 1182.

20. Suchkov, A. F. "Influence of Inhomogeneities on the Operation Conditions of Solid-State Lasers," ZHETF, Vol 49, 1965, p 1495.

21. Letokhov, V. S.; Suchkov, A. F. "Dynamics of Coherent Light Giant Pulse Lasing," ZHETF, Vol 50, 1966; p 1148; Vol 52, 1967, p 282.

22. Ambartsumyan, R. V.; Basov, N. G., et al. "Structure of a Giant Emission Pulse of an Instantaneous-Q Laser," ZHETF, Vol 51, 1966, p 406.

23. Korobkin, V. V.; Leontovich, A. M., et al. "Lasing Frequency and Field Dynamics in a Giant Pulse of a Passive-Gate Laser," PIS'MA V ZHETF [Letters to the Journal of Experimental and Theoretical Physics], Vol 3, 1966, p 301.

"Dynamics of the Lasing Field, Spectrum and Coherence in a Giant Pulse of a Ruby Laser," ZHETF, Vol 53, 1967, p 16.

24. Suchkov, A. F. "Electrodynamics of Lasers with an Open Resonator with Inhomogeneous Filling," TRUDY FIAN SSSR [Works of the Physics Institute of the USSR Academy of Sciences], Vol 43, 1968, p 161.

25. Letokhov, V. S.; Suchkov, A. F. "Dynamics of an Instantaneous-Q Laser," TRUDY FIAN SSSR, Vol 43, 1968, p 169.

26. Anan'yev, Yu. A.; Mak, A. A.; Sedov, B. M. "Angular Divergence of the Emission of a Solid-State Laser," ZHETF, Vol 52, 1967, p 12.

27. METODY RASCHETA OPTICHESKIKH KVANTOVYYH GENERATOROV [Methods of Calculating Lasers], Minsk, Nauka i tekhnika, edited by B. I. Stepanov, Vol 1, 1966.

28. Mikaelyan, A. L.; Ter-Mikaelyan, M. L.; Turkov, Yu. G. OPTICHESKIYE GENERATORY NA TVERDOM TELE [Solid-State Lasers], Moscow, Sov. radio, 1967.

29. Anan'yev, Yu. A.; Yegorova, V. F., et al. "Operation of a Four-Level Laser," ZHETF, Vol 44, 1963, p 1884.

30. Rigrod, W. "Gain Saturation and Output Power of Optical Masers," J. APPL. PHYS., Vol 34, 1963, p 2602.

APPROVED FOR RELEASE: 2007/02/09: CIA-RDP82-00850R000500010010-4

APPROVED FOR RELEASE: 2007/02/09: CIA-RDP82-00850R000500010010-4

31. Anan'yev, Yu. A.; Shorokhov, O. A. "Pumping Energy Conversion Efficiency in Laser Resonators," OPTIKO-MEKHANICHESKAYA PROMYSHLENNOST' [Optico-mechanics Industry], No 11, 1977, p 12.

32. Anan'yev, Yu. a.; Balashov, I. F.; Mak, A. A. "Theory of Giant-Pulse Operation of Lasers," DAN SSSR, Vol 166, 1966, p 825.

33. TEKHNIKA SUBMILLIMETROVYKH VOLN. [Submillimeter Wave Engineering], edited by R. A. Valitov, Moscow, Sov. radio, 1969.

34. Lyubimov, V. V.; Orlova, I. B. "Approximate Calculation of Oscillations in Resonators with Concave Mirrors," OPT. I SPEKTR. [Optics and Spectroscopy], Vol 29, 1970, p 581.

35. Vaynshteyn, L. A. DIFRAKTSIYA I METOD FAKTORIZATSII [Diffraction and the Factorization Method], Moscow, Sov. radio, 1964.

36. Herriott, D. R. "Optical Properties of Continuous Helium Neon Optical Masers," J. OPT. SOC. AMERICA, Vol 52, 1962, p 31.

37. Hughes, T. P.; Young, K. M. "Mode Sequences in Ruby Laser Emission," NATURE, Vol 196, 1962, p 332.

38. Evtuhov, V.; Neeland, J. K. "Observations Relating to the Transverse and Longitudinal Modes of a Ruby Laser," APPL. OPTICS, Vol 1, 1962, p 517.

39. Stickley, C. M. "Optical Quality and Radiation Patterns of Ruby Lasers," APPL. OPTICS., Vol 2, 1963, p 855.

40. Jaseja, T. S.; Dheer, M. K.; Madhavan, D. "Beam Characteristics of Ruby Optical Masers," APPL. OPTICS., Vol 4, 1965, p 1643.

41. Tatuoka, S. "Higher Oscillation Modes in Nd-Glass Laser," APPL. OPTICS, Vol 3, 1964, p 986.

42. Dayhoff, E. S. "Emission Patterns of Ruby Lasers," PROC. IRE., Vol 50, 1962, p 1684.

43. Dayhoff, E. S.; Kessler, B. "High-Speed Sequence Photography of a Ruby Laser," APPL. OPTICS, Vol 1, 1962, p 339.

44. Lippsett, M. S.; Strandberg, M. P. W. "Mode Control in Ruby Optical Masers by Means of Elastic Deformation," APPL. OPTICS., Vol 1, 1962, p 343.

45. Evtuhov, N.; Neeland, J. K. "Measurements and Interpretation of Laser Beam Divergence," APPL. OPTICS, Vol 2, 1963, p 319'

46. Leontovich, A. M.; Veduta, A. P. "Node Excitation and Explanation of Beam Divergence in a Ruby Laser," ZHETF, Vol 46, 1964, p 71.

APPROVED FOR RELEASE: 2007/02/09: CIA-RDP82-00850R000500010010-4

APPROVED FOR RELEASE: 2007/02/09: CIA-RDP82-00850R000500010010-4

47. Anan'yev, Yu. A.; Korolev, Ye. A. "Density Distribution of Pumping Emission in a Laser Crystal," OPTIKA I SPEKTROSKOPIYA [Optics and Spectroscopy], Vol 16, 1964, p 702.

48. METODY RASCHETA OPTICHESKIKH KVANTOVYKH GENERATOROV [Methods of Calculating Lasers], edited by B. I. Stepanov, Minsk, Nauka i tekhnika, Vol 2, 1968.

49. Rigrod, W. W. "Isolation of Axisymmetrical Optical-Resonator Modes," PROC. THIRD INTERN. CONGRESS OF QUANT. ELECTR., New York, Columbia Univ. Press, 1964, p 1285.

50. Röss, D.; Zeidler, G. "Modenselection und Rinschwingverhaften eines konfokalen kontinuierlichen Rubinlasers," Z. NATURF., Vol 21a, 1966, p 340.

51. Bonch-Bruyevich, A. M., et al. "Study of a Neodymium Glass Laser with Spherical Mirror Resonator," ZHTF, Vol 36, 1966, p 2175.

52. Rom-Krichevskaya, I. A.; Ratner, A. M. "Angular Distribution of Emission in an Optical Resonator with Lenses," OPTIKA I SPEKTROSKOPIYA, Vol 22, 1967, p 653.

53. Mak, A. A.; Soms, L. N., et al. "Angular Divergence and Transverse Oscillation Modes of a Neodymium Glass Laser with Spherical Resonator," OPTIKA I SPEKTROSKOPIYA, Vol 26, 1969, p 793.

54. Roess, D. "Analysis of a Room Temperature CW Ruby Laser of 10 mm Resonator Length: the Ruby Laser as a Thermal Lens," J. APPL. PHYS., Vol 37, 1966, p 3587.

55. Sventsitskaya, N. A.; Khazov, L. D. "Some Results of Comparing a Ruby Laser with Plane-Parallel and Confocal Resonators," ZH. PRIKL. SPEKTROSKOPII [Journal of Applied Spectroscopy], Vol 4, 1966, p 345.

56. Muzhdaba, A. A.; Tikhonova, N. P.; Korolev, Ye. A. "Light Dispersion in Corundum Crystals," OPTIKO-MEKHANICHESKAYA PROMYSHLENNOST', No 1, 1968, p 14.

57. Abella, J. D.; Townes, C. H. "Mode Characteristics and Coherence in Optical Ruby Masers," NATURE, Vol 192, 1961, p 957.

58. Galanin, M. D.; Leontovich, A. M.; Chizhikova, Z. D. "Coherence and Radiation Pattern of a Ruby Laser," ZHETF, Vol 43, 1962, p 347.

59. Korobkin, V. V.; Leontovich, A. M. "Coherence and Time Base of the Radiation Spectra of a Ruby Laser," ZHETF, Vol 44, 1963, p 1847.

60. Stoicheff, B. P.; Scabo, A. "Interference Rings in Ruby Maser Beams," APPL. OPTICS, Vol 2, 1963, p 811.

61. Vanyukov, M. P.; Isayenko, V. I., et al. "Pumping of Additional Extra-axial Stimulated Emission Beams," ZHETF, Vol 48, 1965, p 3.

62. Anan'yev, Yu. A.; Sedov, B. M. "Spectral and Time Characteristics of $CaF_2:Sm^{2+}$ Stimulated Emission," ZHETF, Vol 48, 1965, p 782.

APPROVED FOR RELEASE: 2007/02/09: CIA-RDP82-00850R000500010010-4

APPROVED FOR RELEASE: 2007/02/09: CIA-RDP82-00850R000500010010-4

63. Bortfeld, D. P.; Congleton, R. S., et al. "Influence of Optical Quality on Ruby Laser Oscillators and Amplifiers," J. APPL. PHYS., Vol 35, 1964, p 2267.

64. Kellington, C. M.; Katzman, M. "Beam Divergence and Far-Field Patterns of Rubies of Varying Optical Quality," J. APPL. PHYS., Vol 36, 1965, p 2910.

65. Korolev, Ye. A.; Bondarchuk, V. A.; Tikhonova, N. P. "Influence of Ruby Crystal Flaws on Laser Emission Characteristics," OPTIKO-MEKHANICHESKAYA PROMYSHLENNOST', No 3, 1967, p 9.

66. Akulenok, Ye. M.; Bagdasarov, Kh. S., et al. "Influence of Modular Structure on Ruby Laser Emission Divergence," KRISTALLOGRAFIYA [Crystallography], Vol 12, 1967, p 286.

67. Danileyko, Yu, K.; Manenkov, A. A., et al. "Optical Homogeneity of Ruby Crystals and Its Relation to Laser Emission Divergence," FTT [Solid-State Physics], Vol 10, 1968, p 2738.

68. Danileiko, Yu. K.; Khaimov-Mal'kov, V. Ya., et al. "Surface and Volume Scattering Surface Damages, and Optical Homogeneity Studies of Ruby Crystals and Their Connections with Laser Emission Characteristics," IEEE J. OF QUANT. ELECTR., Vol QE-5, 1969, p 87.

69. Arisonis, P. V.; Doss, T. T.; Heimlich, R. "Measurement of Beam Divergence of Q-Switched Ruby Laser Rods," REV. SCI. INSTR, Vol 38, 1967, p 334.

70. Quelle, W. "Thermal Distortion of Diffraction-Limited Optical Elements," APPL. OPTICS., Vol 5, 1966, p 633.

71. Snitzer, E. "Glass Lasers," PROC. IEEE, Vol 54, 1966, p 1249.

72. Anan'yev, Yu. A.; Mak, A. A. "Variation of Laser Resonator Characteristics in the Lasing Process," OPTIKA I SPEKTROSKOPIYA, Vol 16, 1964, p 1065.

73. Schmidt, U. J. "Change of the Refractive Index of Ruby During Optical Pumping," J. APPL. PHYS., Vol 35, 1964, p 259.

74. Anan'yev, Yu. A.; Kozlov, N. A., et al. "Thermal Deformation of a Solid-State Laser Resonator," ZH. PRIKL. SPEKTROSKOPII, Vol 5, 1966, p 51.

75. Grishmanova, N. I.; Sventsitskaya, N. A.; Khazov, L. D. "Investigation of Thermal Deformations of Ruby Laser Crystals," ZH. PRIKL. SPEKTROSKOPII, Vol 7, 1967, p 340.

76. Vanyukov, M. P.; Isayenko, V. I., et al. "Study of Thermal Distortions in Samples of Glass Generating Stimulated Emission," ZH. PRKL. SPEKTROSKOPII, Vol 2, 1965, p 295.

77. Vanyukov, M. P.; Isayenko, V. I., et al. "Effect of the Resonator Mirror Alignment on the Lasing Mode of Neodymium-Doped Glass," ZH. PRKL. SPEKTROSKOPII, Vol 2, 1965, p 415.

APPROVED FOR RELEASE: 2007/02/09: CIA-RDP82-00850R000500010010-4

APPROVED FOR RELEASE: 2007/02/09: CIA-RDP82-00850R000500010010-4

78. Broude, V. L.; Zaika, V. V., et al. "Operation of a Ruby Laser with Tilted Mirrors," ZH. PRKL. SPEKTROSKOPII, Vol 3, 1965, p 225.

79. Kalinin, V. P.; Lyubimov, V. V. "Effect of Misalignment of Laser Resonator Mirrors on Angular Distribution of the Laser Emission," OPTIKA I SPEKTROSKOPII, Vol 22, 1967, p 123.

80. Kravchenko, V. I.; Soskin, M. S. "Imperfections of the Active Media, Aberrations of Resonators and Oscillation Modes of Solid-State Lasers," KVANTOVAYA ELEKTRONIKA (TRUDY RESPUBLIKANSKOGO SEMINARA) [Quantum Electronics (Proceedings of the Republic Seminar)], Kiev, Naukova dumka, No 4, 1969, p 42.

81. Kalinin, Yu. A., et al. "Influence of Inverse Population Distribution on Transverse Laser Oscillation Modes," ZHTF, Vol 38, 1968, p 1108.

82. Kuznetsova, T. I.; Rautian, S. G. "Instability of the Monochromatic Lasing Conditions in Solid-State Lasers," FTT, Vol 5, 1963, p 2105.

83. Tang, C. L.; Statz, de Mars, G. A. "Spiking Behavior of Solid-State Lasers," J. APPL. PHYS., Vol 34, 1963, p 2289.

84. Statz, H.; Tang, C. L. "Multimode Oscillation in Solid State Masers," J. APPL. PHYS., Vol 35, 1964, p 1377.

85. Livshits, B. L.; Tsikunov, V. N. "Spectral Properties of Forced Emission in a Broad Pumping Range," ZHETF, Vol 49, 1965, p 1843.

86. Anan'yev, Yu. A. "Emission Intensity Distribution of a Solid-State Laser with Plane Mirrors with Respect to Transverse Oscillation Modes," ZHTF, Vol 37, 1967, p 139.

87. Tang, C. L.; Statz, H., et al. "Spectral Properties of a Single-Mode Ruby Laser: Evidence of Homogeneous Broadening of the Zero Phonon Lines in Solids," PHYS. REV., Vol 136A, 1964, p 1.

88. Livshits, B. L.; Nazarov, V. P., et al. "Spectral Composition of Forced Emission as a Function of the Speed of a Crystal," PIS'MA V ZHETF, Vol 1, 1965, p 23.

89. Evtuhov, V.; Siegman, A. E. "A Twisted-Mode Technique for Obtaining Axially Uniform Energy Density in a Laser Cavity," APPL. OPTICS, Vol 4, 1965, p 142.

90. Fox, A. G.; Li, T. "Effect of Gain Saturation on the Oscillating Modes of Optical Masers," IEEE J. QUANT. ELECTR., Vol QE-2, 1966, p 774.

91. Belousova, I. M.; Vinokurov, G. N., et al. "Interaction of Oscillation Modes in a Gas Laser with Spherical Mirror Resonator," ZHETF, Vol 52, 1967, p 1146.

92. Kalinin, Yu. A.; Mak, A. A. "Influence of the Inverse Population Density on the Angular Divergence of Solid-State Laser Emission," OPTIKO-MEKHANICHESKAYA PROMYSHLENNOST', No 5, 1969, p 61.

APPROVED FOR RELEASE: 2007/02/09: CIA-RDP82-00850R000500010010-4

APPROVED FOR RELEASE: 2007/02/09: CIA-RDP82-00850R000500010010-4

93. Livshits, B. L. "Traveling-Medium Laser," UFN, Vol 98, 1969, p 393.

94. Vinokurov, G. N.: Galaktionova, N. M., et al. "Spiking Behavior of Solid-State Lasers," ZHETF, Vol 60, 1971, p 489.

95. Gloge, D. "Calculation of Fabry-Perot Resonators for Lasers Using Scattering Matrices," KVAZIOPTIKA [Quasioptics], Moscow, Mir, 1966, p 264; "General Method of Calculating Optical Cavities and Periodic Lens Systems," Ibid., p 280 (also published in ARCH. ELECTR. UBERTRAG, Vol 18, 1964, p 197; Vol 19, 1965, p 13).

96. Averbakh, V. S.; Vlasov, S. N.; Talanov, V. M. "Effect of First and Second Order Aberrations on Open Resonator Characteristics," RADIOTEKHNIKA I ELEKTRONIKA [Radio Engineering and Electronics], Vol 10, 1965, p 1150.

97. Anan'yev, Yu. A.; Lyubimov, V. V.; Orlova, I. B. "Mode Deformation in Open Resonators with Mirrors," ZHTF, Vol 39, 1969, p 1872.

98. Belousova, I. M.; Danilov, O. B. "Study of Various Types of Resonators to Obtain a Single-Mode Laser with Optimal Parameters," ZHTF, Vol 37, 1967, p 1519.

99. Sanderson, R. L.; Streifer, W. "Laser Resonators with Tilted Reflectors," APPL. OPTICS, Vol 8, 1969, p 2241.

100. Statz, H.; Tang, C. L. "Problem of Mode Deformation in Optical Masers," J. APPL. PHYS., Vol 36, 1965, p 1816.

101. Li, T.; Skinner, J. G. "Oscillating modes in Ruby Lasers with Nonuniform Pumping Energy Distribution," J. APPL. PHYS., Vol 36, 1965, p 2595.

102. Ogura, H.; Yoshida, Y.; Ikenoue, J. "Theory of Deformed Fabry Perot Resonator," J. PHYS. SOC., Japan, Vol 20, 1965, p 598.

103. Lyubimov, V. V. "Obtaining Laser Emission with Extremely Narrow Directionality," OPTIKA I SPEKTROSKOPIYA, Vol 21, 1966, p 224.

104. Fox, A. G.; Li, T. "Modes in a Maser Interferometer with Curved and Tilted Mirrors," PROC. IEEE, Vol 51, 1963, p 80.

105. Wells, W. H. "Modes of a Tilted-Mirror Optical Resonator for the Far Infrared," IEEE J. OF QUANT. ELECTR., Vol QE-2, 1966, p 94.

106. Lyubimov, V. V.; Orlova, I. B. "Estimating the Influence of Misalignment of Resonator Mirrors on Losses and Angular Distribution," ZHTF, Vol 39, 1969, p 2183.

107. Schaack, G. "Modes in a Deformed Laser Resonator," IEEE J. OF QUANT. ELECTR., Vol QE-3, 1967, p 130.

APPROVED FOR RELEASE: 2007/02/09: CIA-RDP82-00850R000500010010-4

APPROVED FOR RELEASE: 2007/02/09: CIA-RDP82-00850R000500010010-4

108. Kuznetsova, T. I. "Eigen Solutions of the Wave Equation for an Inhomogeneous Laser," ZHTF, Vol 34, 1964, p 419; "Influence of Nonuniformity of Dielectric Constant on the Properties of Natural Oscillations in Resonators," ZHTF, Vol 36, 1966, p 58.

109. Tang, C. L.; Statz, H. "Effects of Intensity Dependent Anomalous Dispersion on the Mode Shapes of the Fabry-Perot Oscillators," J. APPL. PHYS., Vol 38, 1967, p 886.

110. Riedel, E. P.; Baldwin, G. D. "Theory of Dynamic Optical Dispersion in Isotropic Laser Materials," J. APPL. PHYS., Vol 38, 1967, p 2720.

111. Anisimov, N. A.; Kononchuk, G. L. "Variation of the Index of Refraction of a Ruby as a Result of Inverse Population," FTT, Vol 10, 1968, p 3150.

112. Anan'yev, Yu. A. "Losses in a Nonuniformly Pumped Solid-State Laser," ZH. PRIKL. SPEKTROSKOPII, Vol 7, 1967, p 825.

113. Soskin, M. S. "Linear Phase Distortions of a Resonator and Forced Emission Lasing by a Ruby Crystal," KVANTOVAYA ELEKTRONIKA (TRUDY RESPUBLIKANSKOGO SEMINARA), Kiev, Naukova dumka, No 1, 1966, p 107.

114. Lyubimov, V. V. "Estimating the Width of the Angular Distribution of Laser Emission in the Presence of Inhomogeneity in a Plane Mirror Resonator," OPTIKA I SPEKTROSKOPIYA, Vol 24, 1968, p 815.

115. Anan'yev, Yu. A.; Lyubimov, V. V.; Sedov, B. M. "Effect of Light Scattering on Laser Properties," ZH. PRKL. SPEKTROSKOPII, Vol 8, 1968, p 955.

116. Anan'yev, Yu. A.; Grishmanova, N. I.; Sventsitskaya, N. A. "Properties of a Laser with a Grating Used as the Resonator Exit Mirror," ZHTF, Vol 43, 1973, p 1530.

117. Kalinin, V. P.; Lyubimov, V. V.; Orlova, I. B. "Effect of Mirror Deformation on the Angular Distribution of the Emission of Lasers with Flat Mirrors," ZH. PRKL. SPEKTROSKOPII, Vol 12, 1970, p 1019.

118. Kirillov, G. A.; Kormer, S. B., et al. "Study of the Emission Divergence of a Photodissociation Laser with Inhomogeneous Active Medium," ZH. PRKL. SPEKTROSKOPII, Vol 12, 1970, p 1019.

119. Landau, D. D.; Lifshits, Ye. M. ELEKTRODINAMIKA SPLOSHNYKH SRED [Electrodynamics of Continuous Media], Moscow, Gostekhizdat, 1957, Chapter 10.

120. Toraldo di, Francia G. "Flat-Roof Resonators, APPL. OPTICS, Vol 4, 1965, p 1267.

121. Soncini, G.; Svelto, O. "Single Transverse Mode Pulsed Ruby Laser," APPL. PHYS. LETT., Vol 11, 1967, p 261; "Single Mode Passive Q-Switched Ruby Laser," IEEE J. QUANT. ELECTR., Vol QE-4, 1968, p 422.

APPROVED FOR RELEASE: 2007/02/09: CIA-RDP82-00850R000500010010-4

APPROVED FOR RELEASE: 2007/02/09: CIA-RDP82-00850R000500010010-4

122. Averbakh, V. S.; Vlasov, S. N. "Experimental Study of a He-Ne-Laser with Nonspherical Mirrors," RADIOTEKHNIKA I ELEKTRONIKA, Vol 14, 1969, p 1709.

123. Maslov, V. P.; Vorob'yev, Ye. M. "Unimodal Open Resonators," DAN SSSR, Vol 179, 1968, p 558.

124. Mikaelyan, A. L.; Korovitsyn, A. V.; Naumova, L. V. "Laser with Diffraction Width of the Radiation Pattern," PIS'MA V ZHETF, Vol 2, 1965, p 37.

125. Troitskiy, Yu. V. "Nonuniform Energy Emission of Higher Transverse Oscillation Modes in a Gas Laser," KVANTOVAYA ELEKTRONIKA [Quantum Electronics], Vol 1, 1974, p 124.

126. Baker, J. A.; Peters, C. V. "Mode Selection and Enhancement with a Ruby Laser," APPL. OPTICS, Vol 1, 1962, p 674.

127. Skinner, J. G.; Geusik, J. E. "Diffraction-Limited Ruby Oscillator," J. OPT. SOC. AMERICA, Vol 52, 1962, p 1319.

128. Li, T. "Mode Selection in an Aperture-Limited Concentric Maser Interferometer," BELL SYST. TECHN. J., Vol 42, 1963, p 2609.

129. Hagen, W. F. "Diffraction-Limited High-Radiance Nd-glass Laser System," J. APPL. PHYS., Vol 40, 1969, p 511.

130. Stein, A. "Mode Selection for Giant Pulse Ruby Lasers," APPL. OPTICS, Vol 6, 1967, p 2193.

131. Collins, S. A.; White, G. R. "Interferometer Laser Mode Selection," APPL. OPTICS, Vol 2, 1963, p 448.

132. Gehrer, G.; Ross, D. "Modenselective Eigenschaften einer planparallelen dielektrischen Platte als Reflektor eines Laserresonators," Z. NATURFORSCH., Vol 20a, 1965, p 701.

133. Daly, R.; Sims, S. D. "An Improved Method of Mechanical Q-Switching Using Total Internal Reflection," APPL. OPTICS, Vol 3, 1964, p 1063.

134. Giordmaine, J. A.; Kaiser, W. "Mode-Selecting Prism Reflector for Optical Masers," J. APPL. PHYS., Vol 35, 1964, p 3446.

135. Kruzhilin, Yu. I. "Anisotropic Reflector for a Laser," OPTIKA I SPEKTROSKOPIYA, Vol 20, 1966, p 713.

136. Lyubimov, V. V.; Nilov, Ye. V. "Optical-Mechanical Shutter for Q-Switching of a Laser Resonator," OPTIKO-MEKHANICHESKAYA PROMYSHLENNOST', No 2, 1967, p 32.

137. De Shazer, L. G.; Maunders, E. A. "Laser Mode Selection by Internal Reflection Prisms," APPL. OPTICS, Vol 6, 1967, p 431.

APPROVED FOR RELEASE: 2007/02/09: CIA-RDP82-00850R000500010010-4

APPROVED FOR RELEASE: 2007/02/09: CIA-RDP82-00850R000500010010-4

138. Ishchenko, V. N.; Starunskiy, V. N. "Application of Lummer-Gehrcke Plates in a Ruby Laser," IZV. VUZOV, RADIOFIZIKA [News of the Institutions of Higher Learning, Radio Physics], Vol 10, 1967, p 1189.

139. Bondarenko, N. G.; Yeremina, I. V.; Talanov, V. I. "Solid-State Laser with Mode Selection Inside the Active Element," PIS'MA V ZHETF, Vol 6, 1967, p 459.

140. Boyko, B. B.; Petrov, N. S., et al. "Laser with Two-Dimensional Resonator," ZH. PRIKL. SPEKTROSKOPII, Vol 3, 1968, p 351.

141. Lyubimov, V. V.; Orlova, I. B. "Consideration of the Influence of the Angular Distribution Selector on the Oscillation Modes of Open Resonators with Flat Mirrors and Constriction of the Angular Distribution of the Emission," ZH. PRKL. SPEKTROSKOPII, Vol 9, 1968, p 54.

142. Talanov, V. I. "Suppression of Nonaxial Modes in Open Resonators with Broad Wave Beams by the Combined Selection Method," IZV. VUZOV, RADIOFIZIKA, Vol 10, 1967, p 298.

143. La Tourette, J. T.; Jacobs, S. F.; Rabinowitz, R. "Improved Laser Angular Brightness Through Diffraction Coupling," APPL. OPTICS, Vol 3, 1964, p 981.

144. Evtuhov, V.; Neeland, J. K. "Study of the Output Spectra of Ruby Lasers," IEEE J. OF QUANT. ELECTR., Vol QE-1, 1965, p 7.

145. Kalinin, Yu. A.; Mak, A. A., et al. "Laser With Cross Sectionally Variable Transmission of the Resonator Mirrors," ZHETF, Vol 56, 1969, p 1161.

146. Vakhitov, N. G. "Open Resonators with Mirrors Having Variable Reflection Coefficient," RADIOTEKHNIKA I ELEKTRONIKA, Vol 10, 1965, p 1676.

147. Sventsitskaya, N. A.; Khazov, L. D. "Increasing the Ruby Laser Emission Directionality by Using a Remote Reflector," ZH. PRIKL. SPEKTROSKOPII, Vol 3, 1966, p 230.

148. Anan'yev, Yu. A.; Belousova, I. M., et al. Angular Characteristics of the Emission of Lasers with High Effective-Length Resonator," KVANTOVAYA ELEKTRONIKA, Vol 1, 1974, p 296.

149. Okaya, A. "Off-Axial Mode Rejection of Ruby Laser Using Ball Mirror," PROC. IEEE, Vol 51, 1963, p 1033.

150. Nash, D. I.; Panulovskiy, V. F.; Chirina, L. P. "Experimental Study of the Beam Divergence in He-Ne-Lasers," OPTIKA I SPEKTROSKOPIYA, Vol 18, 1965, p 866.

151. Anan'yev, Yu. A.; Sherstobitov, V. Ye. "Influence of Edge Effects on the Properties of Unstable Resonators," KVANTOVAYA ELEKTRONIKA, edited by N. G. Basov, No 3, 1971, p 82.

APPROVED FOR RELEASE: 2007/02/09: CIA-RDP82-00850R000500010010-4

APPROVED FOR RELEASE: 2007/02/09: CIA-RDP82-00850R000500010010-4

152. Anan'yev, Yu. A.; Sventsitskaya, N. A.; Sherstobitov, V. Ye. "Properties of Lasers with Unstable Resonator," ZHETF, Vol 55, 1968, p 130.

153. Anan'yev, Yu. A.; Vinokurov, G. N., et al. "Laser with Telescopic Resonator," ZHETF, Vol 58, 1970, p 786.

154. Anan'yev, Yu. A. "Unstable Resonators and Their Applications," KVANTOVAYA ELEKTRONIKA, edited by N. G. Basov, No 6, 1971, p 3.

155. Vasil'yev, L. A.; Demkin, V. K., et al. "Calculating the Angular Distribution of the Emission of a Laser with Inhomogeneous Medium and Telescopic Resonator," KVANTOVAYA ELEKTRONIKA, Vol 2, 1975, p 51.

156. Rogov, V. S.; Rikenglaz, M. M. "Numerical Investigation of the Influence of Optical Nonuniformities of the Active Medium on the Operation of an Unstable Telescopic Resonator," KVANTOVAYA ELEKTRONIKA, Vol 4, 1977, p 35.

157. Siegman, A. E.; Arrathoon, R. "Modes in Unstable Optical Resonators and Lens Waveguides," IEEE J. OF QUANT. ELECTR., Vol QE-3, 1967, p 156.

158. Streifer, W. "Unstable Optical Resonators and Waveguides," IEEE J. OF QUANTUM ELECTRONICS, Vol QE-4, 1968, p 229.

159. Bergstein, L. "Modes of Stable and Unstable Optical Resonators," APPL. OPTICS, Vol 7, 1968, p 495.

160. Sanderson, R. L.; Streifer, W. "Unstable Laser Resonator Modes," APPL. OPTICS, Vol 8, 1969, p 2129.

161. Siegman, A. E.; Miller, H. Y. "Unstable Optical Resonator Loss Calculations Using the Prony Method," APPL. OPTICS, Vol 9, 1970, p 2729.

162. Vinokurov, G. N.; Lyubimov, V. V., et al. PRIBLIZHENNYY RASCHET KOLEBANIY V OTKRYTYKH REZONATORAKH S VYPUKLYMI ZERKALAMI (TRUDY V VSESOYUZNOGO SIMPOZIUMA PO DIFRAKTSII I RASPROSTRANENIYU VOLN) [Approximate Calculation of Oscillations in Open Resonators with Convex Mirrors (Proceedings of the 5th All-Union Symposium on Wave Propagation and Diffraction)], Leningrad, Nauka, 1971, p 72.

163. Vinokurov, G. N.; Lyubimov, V. V.; Orlova, I. B. "Study of the Selective Properties of Open Unstable Resonators," OPTIKA I SPEKTROSKOPIYA, Vol 34, 1973, p 741.

164. Santana, C.; Felsen, L. B. "Unstable Open Resonators: Two-Dimensional and Three-Dimensional Losses by Waveguide Analyses," APPL. OPTICS, Vol 15, 1976, p 1478.

165. Sommerfeld, A. OPTIKA [Optics], Moscow, IIL, 1953.

166. Sherstobitov, V. Ye.; Vinokurov, G. N. "Properties of Unstable Resonators with Large Equivalent Fresnel Number," KVANTOVAYA ELEKTRONIKA, edited by N. G. Basov, No 3(9), 1972, p 36.

APPROVED FOR RELEASE: 2007/02/09: CIA-RDP82-00850R000500010010-4

APPROVED FOR RELEASE: 2007/02/09: CIA-RDP82-00850R000500010010-4

167. Siegman, A. E. "Stabilizing Output with Unstable Resonators," LASER FOCUS, No 5, 1971, p 42.

168. Anan'yev, Yu. A.; Sherstobitov, V. Ye. "Unstable Resonators with Central Coupling Hole in Lasers and Amplifiers," ZHTF, Vol 43, 1973, p 1013.

169. Lyubimov, V. V.; Nevgenen, N. N.; Petrov, V. F. "Asymmetric Unstable Resonators," OPTIKA I SPEKTROSKOPIYA, Vol 35, 1973, p 1132.

170. Netrun'kin, Yu. V.; Yesepkina, N. A., et al. "Problem of Obtaining the Traveling Wave Mode in a Complex Optical Resonator," RADIOTEKHNIKA I ELEKTRONIKA, Vol 12, 1967, p 146.

171. Anan'yev, Yu. A.; Vinokurov, G. N. "Some Properties of Unstable Ring Cavities with Emission Angle Selection," ZHTF, Vol 39, 1969, p 1327.

172. Smirnov, V. I. KURS VYSSHEY MATEMATIKI [Course in Higher Mathematics], Moscow, Gostekhizdat, Vol 4, 1957.

173. Freiberg, R. J.; Chenausky, P. P.; Buczek, C. J. "Unidirectional Unstable Ring Lasers," APPL. OPTICS, Vol 12, 1973, p 1140.

174. Lyubimov, V. V.; Orlova, I. B. "Unstable Resonator with Angular Distribution Selector," OPTIKA I SPEKTROSKOPIYA, Vol 33, 1972, p 138.

175. Anan'yev, Yu. A. "Prism Unstable Resonators," KVANTOVAYA ELEKTRONIKA, edited by N. G. Basov, No 1(13), 1973, p 105.

176. Molchanov, V. Ya.; Skrotskiy, G. V. "Matrix Method of Calculating the Natural Polarization States of Anisotropic Resonators," KVANTOVAYA ELEKTRONIKA, edited by N. G. Basov, No 4, 1971, p 3.

177. Peck, E. R. "Polarization Properties of Corner Reflectors and Cavities," J. OPT. SOC. OF AMERICA, Vol 52, 1962, p 253.

178. Lyubimov, V. V. USSR Author's Certificate No 357875, priority as of 31 August 1970, BYULLETEN' [Bulletin], No 34, 1972.

179. Arnaud, J. A. "Degenerate Optical Cavities," APPL. OPTICS, Vol 8, 1969, p 189.

180. Nogarev, G. V. OPTICHESKIYE YUSTIROVOCHNYYE ZADACHI [Optical Alignment Problems], Leningrad, Mashinostroyeniye, 1974.

181. Anan'yev, Yu. A.; Kuprenyuk, V. I.; Sherstobitov, V. Ye. "Properties of Unstable Resonators with Field Reversal, I, Theoretical Elements," KVANTOVAYA ELEKTRONIKA, Vol 6, 1979, p 1871.

182. Danileyko, Yu. K.; Lobachev, V. A. "New Resonator for Lasers -- Resonator with Rotating Field," KVANTOVAYA ELEKTRONIKA, Vol 1, 1974, p 668.

APPROVED FOR RELEASE: 2007/02/09: CIA-RDP82-00850R000500010010-4

APPROVED FOR RELEASE: 2007/02/09: CIA-RDP82-00850R000500010010-4

183. Kytina, I. G.; Nesterenko, V. M. "Laser with Increased Uniformity of Emission Field," KVANTOVAYA ELEKTRONIKA, Vol 1, 1974, p 721.

184. Anan'yev, Yu. A. USSR Author's Certificate No 530606, priority as of 4 April 1975.

185. Anan'yev, Yu. A.; Sventsitskaya, N. A.; Sherstobitov, V. Ye. USSR Author's Certificate No 274254, priority as of 18 March 1968, BYULLETEN', No 24, 1970, p 63.

186. Anan'yev, Yu. A.; Mak, A. A.; Sedov, B. M. "Light Gain by Four-Level Quantum Systems," ZHETF, Vol 48, 1965, p 7.

187. Anan'yev, Yu. A.; Sherstobitov, V. Ye.; Shorokhov, O. A. "Calculating the Efficiency of Lasers with Large Emission Losses," KVANTOVAYA ELEKTRONIKA, edited by N. G. Basov, No 1, 1971, p 91.

188. Anan'yev, Yu. A.; Koval'chuk, L. V., et al. "Procedure for Calculating the Efficiency of Lasers with Unstable Resonators," KVANTOVAYA ELEKTRONIKA, Vol 1, 1974, p 1201.

189. Anan'yev, Yu. A.; Sventsitskaya, N. A.; Sherstobitov, V. Ye. "Characteristics of Giant-Pulse Laser with Unstable Resonator," ZHTF, Vol 39, 1969, p 1325.

190. Anan'yev, Yu. A.; Chernov, V. N.; Sherstobitov, V. Ye. "High Spatial-Coherence Solid-State Laser," KVANTOVAYA ELEKTRONIKA, edited by N. G. Basov, No 4, 1971, p 112.

191. Anan'yev, Yu. A.; Grishmanova, N. I., et al. "Possibility of Controlling the Emission of Lasers with Telescopic Resonators," KVANTOVAYA ELEKTRONIKA, edited by N. G. Basov, No 2(8), 1972, p 85.

192. Anan'yev, Yu. A.; Sirazetdinov, V. S., et al. "Emission Direction Stabilization Effect in Unstable Prism Resonators," KVANTOVAYA ELEKTRONIKA, edited by N. G. Basov, No 3(15), 1973, p 115.

193. Anan'yev, Yu. A.; Zavgorodneva, S. I., et al. "Possibility of Spectral Selection in Unstable-Resonator Lasers," LAZERY S PERESTRAIVAYEMOY CHASTOTOY [Frequency-Tunable Lasers], Kiev, Izd-vo AN USSR, 1973, p 41.

194. Alekseyev, V. N.; Anan'yev, Yu. A.; Dauengauer, E. F. "Solid-State Telescopic-Resonator Lasers," DAN SSSR, Vol 214, 1974, p 535.

195. Anan'yev, Yu. A.; Grishmanova, N. I., et al. "Comparison of the Emission Divergence of a Multistage System and Laser with Telescopic Resonator," KVANTOVAYA ELEKTRONIKA, Vol 1, 1974, p 1247.

196. Anan'yev, Yu. A.; Grishmanova, N. I., et al. "Spectral Selection of the Emission of Unstable-Resonator Lasers," KVANTOVAYA ELEKTRONIKA, Vol 2, 1975, p 738.

FOR OFFICIAL USE ONLY

APPROVED FOR RELEASE: 2007/02/09: CIA-RDP82-00850R000500010010-4

APPROVED FOR RELEASE: 2007/02/09: CIA-RDP82-00850R000500010010-4

197. Anan'yev, Yu. A.; Grishmanova, N. I., et al. "Reflecting Surfaces Inside Unstable Resonators," KVANTOVAYA ELEKTRONIKA, Vol 2, 1975, p 1952.

198. Anan'yev, Yu. A.; Buzhinskiy, I. M., et al. "Highly Efficient Neodymium-Glass Laser," OPTIKO-MEKHANICHESKAYA PROMYSHLENNOST', No 9, 1968, p 26.

199. Krupke, W. E.; Sooy, W. R. "Properties of an Unstable Confocal Resonator CO_2 Laser System," IEEE J. OF QUANT. ELECTRONICS, Vol QE-5, 1969, p 575.

200. Anan'yev, Yu. A.; Grishmanova, N. I. "Deformations of the Active Elements of Interferometers and Thermal Optical Constants of Neodymium Glass," ZH. PRIKL. SPEKTROSKOPII, Vol 12, 1970, p 668.

201. Sinclair, D. C.; Cottrell, T. N. E. "Transverse Mode Structure in Unstable Optical Cavities," APPL. OPTICS, Vol 6, 1967, p 845.

202. Reilly, J. P. "Single-Mode Operation of a High-Power Pulsed N_2/CO_2 Laser," IEEE J. OF QUANT. ELECTR., Vol QE-8, 1972, p 136.

203. Dyer, P. E.; James, D. J.; Ramsden, S. A. "Single Transverse Mode Operation of a Pulsed Volume Excited Atmospheric Pressure CO_2 Laser Using an Unstable Resonator," OPTICAL COMMUN., Vol 5, 1972, p 236.

204. Vanyukov, M. P.; Gorlanov, A. V., et al. "Multichannel Giant-Pulse Neodymium Glass Laser," KVANTOVAYA ELEKTRONIKA, edited by N. G. Basov, No 4, 1971, p 117.

205. Vanyukov, M. P.; Serebryakov, V. A., et al. "Powerful Giant-Pulse Unstable-Resonator Laser," OPTIKO-MEKHANICHESKAYA PROMYSHLENNOST', No 1, 1972, p 58.

206. Datskevich, N. P.; Karlova, Ye. K., et al. "Powerful Pulsed CO_2-Laser with Unstable Resonator," KVANTOVAYA ELEKTRONIKA, Vol 4, 1977, p 457.

207. Zemskov, K. I.; Isayev, A. A., et al. "Application of Unstable Resonators to Obtain Diffraction Divergence of the Emission of Pulsed High-Gain Gas Lasers," KVANTOVAYA ELEKTRONIKA, Vol 1, 1974, p 863.

208. Isayev, A. A.; Kazaryan, M. A., et al. "Pinched Beams in Telescopic and Stable Resonators," KVANTOVAYA ELEKTRONIKA, Vol 1, 1974, p 1379.

209. Isayev, A. A.; Kazaryan, M. A., et al. "Evolution of Gaussian Beams and Pulsed Lasing in Unstable-Resonator Lasers," KVANTOVAYA ELEKTRONIKA, Vol 2, 1975, p 1125.

210. Anan'yev, Yu. A. "Setting Up Oscillations in Unstable Resonators," KVANTOVAYA ELEKTRONIKA, Vol 2, 1975, p 1138.

211. Locke, E. V.; Hella, R. A.; Westra, L. "performance of an Unstable Oscillator on a 30-kw CW Gas Dynamic Laser," IEEE J. OF QUANT. ELECTR., Vol QE-7, 1971, p 581.

APPROVED FOR RELEASE: 2007/02/09: CIA-RDP82-00850R000500010010-4

APPROVED FOR RELEASE: 2007/02/09: CIA-RDP82-00850R000500010010-4

212. Freiberg, R. J.; Chenausky, P.; Buczek, C. J. "An Experimental Study of Unstable Confocal CO_2 Resonators," IEEE J. OF QUANT. EL., Vol QE-8, 1972, p 882.

213. Wisner, G. R.; Foster, M. C.; Blausuk, P. R. "Unstable Resonators of CO_2 Electric-Discharge Convection Lasers," APPL. PHYS. LETT., Vol 22, 1973, p 14.

214. Mansell, D. N.; Love, J. A.; Snell, W. L. "Investigations of an Unstable Confocal Resonator and Chemical Laser System," IEEE J. OF QUANT. ELECTR., Vol QE-7, 1971, p 177.

215. Chodzko, R. A.; Mirels, H., et al. "Application of a Single-Frequency Unstable Cavity to a CW HF Laser," IEEE J. OF QUANT. ELECTR., Vol QE-9, 1973, p 523.

216. Siegman, A. E. "Unstable Optical Resonators," APPL. OPTICS, Vol 13, 1974, p 353.

217. Kuprenyuk, V. I., Rybalko, I. O., et al. "Possibility of Creating Automatic Alignment Systems for Lasers with Unstable Resonators," OPTIKO-MEKHANICHESKAYA PROMYSHLENNOST', No 9, 1976, p 3.

218. Grasyuk, A. Z. "Raman Lasers," KVANTOVAYA ELEKTRONIKA, Vol 1, 1974, p 485.

219. Alekseyev, V. D.; Sobel'man, I. I. "Conversion of Laser Emission in the Case of Stimulated Raman Scattering," ZHETF, Vol 54, 1968, p 1834.

220. Dreyzin, Yu. A.; Dykhne, A. M. "Autooscillatory Lasing Instability of High-Flow Lasers Using Unstable Resonators," PIS'MA V ZHETF, Vol 19, 1974, p 718.

221. Alme, M. L. "Temporal Oscillations in the Output from a Gas-Dynamic Laser with an Unstable Resonator," APPL. PHYS. LETT., Vol 29, 1976, p 1.

222. Karamzin, Yu. N.; Konev, Yu. B. "Numerical Investigation of Unstable Telescopic Resonators Considering Diffraction and the Saturation Effect in the Active Medium," KVANTOVAYA ELEKTRONIKA, Vol 2, 1975, p 256.

223. Rench, D. B.; Chester, A. N. "Iterative Diffraction Calculations of Transverse Mode Distributions in Confocal Unstable Laser Resonators," APPL. OPTICS, Vol 12, 1973, p 997.

224. Chester, A. N. "Three-Dimensional Diffraction Calculations of Laser Resonator Modes," APPL. OPTICS, Vol 12, 1973, p 2352.

225. Mamzer, A. F.; Rogov, V. S. CHISLENNYY METOD ISSLEDOVANIYA ENERGETICHESKIKH KHARAKTERISTIK OKG S NEUSTOYCHIVYM REZONATOROM [Numerical Method of Studying the Energy Characteristics of a Laser with Unstable Resonators], Moscow, preprint of the Nuclear Power Institute, No 2449, 1974.

APPROVED FOR RELEASE: 2007/02/09: CIA-RDP82-00850R000500010010-4

APPROVED FOR RELEASE: 2007/02/09: CIA-RDP82-00850R000500010010-4

226. Breyev, V. V.; Mamzer, A. F.; Rogov, V. S. METOD ISSLEDOVANIYA KHARAKTERISTIK BYSTROPROTOCHNOGO CO_2-LAZERA S NEUSTOYCHIVYM REZONATOROM [Method of Studying the Characteristics of a High-Flow CO_2-Laser with Unstable Resonator], Moscow, preprint of the Nuclear Power Institute, No 2450, 1974.

227. Siegman, A. E.; Sziklas, E. A. "Mode Calculations in Unstable Resonators with Flowing Saturable Gain. I. Hermite-Gaussian Expansion," APPL. OPTICS, Vol 13, 1974, p 2775;"II. Fast Fourier Transform Method," APPL. OPTICS, Vol 14, 1975, p 1875.

228. Anan'yev, Yu. A.; Trusov, V. P.; Sherstobitov, V. Ye. "Selection of an Unstable Resonator for a Gas Dynamic Laser," KVANTOVAYA ELEKTRONIKA, Vol 3, 1976, p 1715.

229. Konyukhov, V. K.; Prokhorov, A. M. USSR Author's Certificate No 223954 with priority as of 19 June 1966.

230. Konyukhov, V. K. OPTICHESKIY REZONATOR GAZODINAMICHESKOGO LAZERA [Optical Cavity of a Gas Dynamic Laser], Moscow, Otchet FIAN SSSR, 1971; preprint FIAN SSSR, No 141, 1976.

231. Aleksandrov, B. S.; Anan'yev, Yu. A., et al. "Model of a Medium for Calculating the Resonators of Gas Dynamic CO_2-Lasers," KVANTOVAYA ELEKTRONIKA, Vol 4, 1977, p 1460.

232. Anan'yev, Yu. A.; Kuprenyuk, V. I., et al. "Study of the Properties of an Unstable Resonator with Two-Faced Corner Reflector in a Continuous-Action CO_2-Laser," KVANTOVAYA ELEKTRONIKA, Vol 4, 1977, p 1456.

233. Anan'yev, Yu. A.; Sherstobitov, V. Ye. "Cylindrical Mirror with Adjustable Curvature," KVANTOVAYA ELEKTRONIKA, Vol 1, 1974, p 2636.

234. Zavgorodneva, S. I.; Kuprenyuk, V. I., et al. "Measurement of the Spatial Gain Distribution in Infrared Lasers," KVANTOVAYA ELEKTRONIKA, Vol 3, 1976, p 1124.

235. Zavgorodneva, S. I.; Kuprenyuk, V. I.; Sherstobitov, V. Ye. "Unstable Resonator with Field Reversal," KVANTOVAYA ELEKTRONIKA, Vol 4, 1977, p 1383.

236. Casperson, L. W.; Romero, C. "Properties of a Radial Mode CO_2-Laser," IEEE J. OF QUANT. ELECTR., Vol QE-9, 1973, p 484.

237. Gorlanov, A. V.; Lyubimov, V. V.; Petrov, V. F. "Neodymium Laser in the Quasicontinuous Mode," KVANTOVAYA ELEKTRONIKA, edited by N. G. Basov, No 4, 1971, p 116.

238. Mikaelyan, A. L.; Kuprishov, V. F., et al. "New Method of Giant-Pulse Lasing," PIS'MA V ZHETF, Vol 11, 1970, p 224; "Study of the Lasing of an Automatic Q-Switching Laser," KVANTOVAYA ELEKTRONIKA, edited by N. G. Basov, No 1, 1971, p 102.

APPROVED FOR RELEASE: 2007/02/09: CIA-RDP82-00850R000500010010-4

APPROVED FOR RELEASE: 2007/02/09: CIA-RDP82-00850R000500010010-4

239. Anan'yev, Yu. A.; Shorokhov, O. A. USSR Author's Certificate No 282542 with priority as of 19 March 1969, BYULLETEN', No 30, 1970, p 86.

240. Bondarenko, A. N.; Folin, K. G., et al. "Lasing of a Q-Switching Ruby Laser Under the Effect of an External Signal," PIS'MA V ZHETF, Vol 6, 1967, p 692.

241. De Shazer, L. G.; Maunders, E. A. "Spectral Control of Laser Oscillators by Secondary Light Sources," IEEE J. OF QUANT. ELECTR., Vol QE-4, 1968, p 642.

242. Bondarenko, A. N.; Krivoshchekov, G. V.; Smirnov, V. A. "Nd^{3+}-Doped Giant-Pulse Laser under the Effect of an External Stimulating Signal," IZV. VUZOV, RADIOFIZIKA [News of the Institutions of Higher Learning, Radiophysics], Vol 12, 1969, p 1895.

243. Prilezhayev, D. S.; Dukhovnyy, A. M., et al. "Controlled Neodymium-Glass Giant-Pulse Laser," OPTIKA I SPEKTROSKOPIYA, Vol 33, 1972, p 733.

244. Buczek, C. J.; Freiberg, R. J.; Scolnik, M. L. "Laser Injection Locking," PROC. IEEE., Vol 61, 1973, p 1411.

245. Anan'yev, Yu. A.; Koval'chuk, L. V.; Sherstobitov, V. Ye. "Calculating the Energy Characteristics of Multipass Telescopic Amplifiers," KVANTOVAYA ELEKTRONIKA, Vol 3, 1976, p 1412.

246. Koval'chuk, L. V.; Sherstobitov, V. Ye. "Effect of Small-Scale Phase Non-uniformities on the Properties of Unstable Resonators," KVANTOVAYA ELEKTRONIKA, Vol 4, 1977, p 2174.

247. Andreyev, R. B.; Volosov, V. D., et al. "Powerful Giant-Pulse Laser with Stabilized Spectrum and Emission Directionality Close to Diffraction," ZH. PRIKL. SPEKTROSKOPII, Vol 17, 1972, p 355.

248. Dukhovnyy, A. M., Mak, A. A., et al. "High-Coherence Neodymium-Glass Laser," KVANTOVAYA ELEKTRONIKA, Vol 2, 1975, p 2521.

249. Gorlanov, A. V.; Kalinina, A. A., et al. "Study of the Possibilities of Building High-Gain Telescopic Amplifiers," ZH. PRIKL. SPEKTROSKOPII, Vol 17, 1972, p 617.

250. Cocker, E.; Fylon, L. OPTICHESKIY METOD ISSLEDOVANIYA NAPRYAZHENIY [Optical Method of Studying Stresses], Moscow-Leningrad, ONTI, 1936.

251. Timoshenko, S. P. TEORIYA UPRUGOSTI [Elasticity Theory], Moscow-Leningrad, GTTI, 1934.

252. GOST 13659-68 "STEKLO OPTICHESKOYE BESTSVETNOYE. FIZIKO-KHIMICHESKIYE SVOYSTVA. PARAMETRY" [All-Union State Standard 13659-68 "Colorless Optical Glass. Physical-Chemical Properties. Parameters"].

253. Buzhinskiy, I. M.; Dianov, Ye. M., et al. "Thermooptical Characteristics of Neodymium-Doped Glass," DAN SSSR, Vol 190, 1970, p 558.

APPROVED FOR RELEASE: 2007/02/09: CIA-RDP82-00850R000500010010-4

APPROVED FOR RELEASE: 2007/02/09: CIA-RDP82-00850R000500010010-4

254. BUBNOV, M. M.; Buzhinskiy, I. M., et al. "Brightening of Neodymium-Glass Lasers by Selecting the Active Element Matrix Composition," KVANTOVAYA ELEKTRONIKA, edited by N. G. Basov, No 4(16), 1973, p 113.

255. Anan'yev, Yu. A.; Grishmanova, N. I.; Zabelin, A. A. "Use of the Jamin Interferometer in a Shear Interferometer System," OPTIKO-MEKHANICHESKAYA PROMYSHLENNOST', No 7, 1970, p 68.

256. Mak, A. A.; Mit'kin, V. M., et al. "Thermooptical Constants of Neodymium Glass," OPTIKO-MEKHANICHESKAYA PROMYSHLENNOST', No 9, 1971, p 42.

257. Mit'kin, V. M.; Shchavelev, O. S.; Bunkina, N. N. "Selecting the Temperature of a Neodymium Glass Laser," ZH. PRIKL. SPEKTR., Vol 23, 1975, p 248.

258. Mit'kin, V. M.; Shchavelev, O. S. "Problem of Athermanality Criteria of Doped Glass for Lasers," ZH. PRIKL. SPEKTROSKOPII, Vol 26, 1977, p 667.

259. Zeidler, G. "Abschätzung des Temperaturgradienten in thermisch stationär betriebenen Festkörpenlasern," Z. NATURF., Vol 22a, 1967, p 909.

260. Voron'ko, O. N.; Kozlov, N. A., et al. "A Possibility of Increasing the Q-Factor of a Resonator for a Neodymium Laser," DAN SSSR, Vol 173, 1967, p 542.

261. Sticley, C. M. "Laser Brightness Gain and Mode Control by Compensation for Thermal Distortion," IEEE J. OF QUANT. ELECTR., Vol QE-2, 1966, p 511.

262. McMahon, J. M. "A Correlation Between Passive and Active Test of the Beam Divergence of a Ruby Laser," APPL. OPTICS, Vol 6, 1967, p 2191.

263. Anan'yev, Yu. A.; Grishmanova, N. I. "A Possibility of Dynamic Compensation for Thermal Deformations of a Laser Resonator," ZH. PRKL. SPEKTROSKOPII, Vol 12, 1970, p 1109.

264. Anan'yev, Yu. A.; Grishmanova, N. I., et al. "Energy Characteristics of a Neodymium Glass Laser with Polarized Emission," ZH. PRIKL. SPEKTROSKOPII, Vol 13, 1970, p 227.

265. Alekseyev, V. N.; Gorokhov, A. A. "Energy and Polarization Characteristics of a Neodymium Glass Laser Using Flat and Telescopic Cavities," KVANTOVAYA ELEKTRONIKA, Vol 2, 1975, p 733.

266. DiShington, R. H.; Hook, W. R.; Hilbert, R. P. "A Polarized Laser Cavity which Is Insensitive to Birefringence in the Laser Rod," PROC. IEEE, Vol 55, 1967, p 2038.

267. Mak, A. A.; Mit'kin, V. M.; Soms, L. N. "Excitation of Type E^{r}_{mnq} and E^{ϕ}_{mnq} Modes in Optical Cavities," OPTIKA I SPEKTROSKOPIYA, Vol 33, 1972, p 996.

268. Vinokurov, G. N.; Mak, A. A.; Mit'kin, V. M. "Generation of Tangentially Polarized Higher-Order Modes in the Optical Band," KVANTOVAYA ELEKTRONIKA, Vol 1, 1974, p 1890.

APPROVED FOR RELEASE: 2007/02/09: CIA-RDP82-00850R000500010010-4

APPROVED FOR RELEASE: 2007/02/09: CIA-RDP82-00850R000500010010-4

269. Kertes, I.; Kononkov, Ye. A., et al. "Influence of Birefringence Arising in Neodymium Glass During Pumping on Laser Operation," ZHETF, Vol 59, 1970, p 1115.

270. Vanyukov, M. P.; Mit'kin, V. M., et al. "Giant-Pulse Neodymium Glass Lasers with Diffraction Beam Divergence," KVANTOVAYA ELEKTRONIKA, edited by N. G. Basov, No 1(13), 1973, p 85.

271. Kryzhanovskiy, V. I.; Serebryakov, V. A.; Starikov, A. D. "Depolarization of the Emission of Giant-Pulse Neodymium Glass Lasers," OPTIKO-MEKHANICHESKAYA PROMYSHLENNOST', No 8, 1973, p 14.

272. Scott, W. C.; Wit, M. "Birefringence Compensation and TEM_{00} Mode Enhancement in a Nd:YAG Laser," APPL. PHYS. LETT., Vol 18, 1971, p 3.

273. Yevdokimova, V. G.; Mak, A. A., et al. "Compensation of Induced Birefringence in Laser Systems by Passive Anisotropic Elements," KVANTOVAYA ELEKTRONIKA, Vol 2, 1975, p 1915.

274. Mak, A. A.; Mit'kin, V. M., et al. "A Possibility for Brightness Gain of a Neodymium Glass Laser," KVANTOVAYA ELEKTRONIKA, Vol 2, 1975, p 850.

275. Bradford, J. N.; Eckart, R. C. "Compensating for Pump-Induced Distortion in Glass Laser Rods," APPL. OPTICS, Vol 7, 1968, p 2418.

276. Buchenkov, V. A.; Kolesnikov, B. N., et al. "Investigation of a Neodymium Glass Periodic Laser in the Transient Thermal Mode," KVANTOVAYA ELEKTRONIKA, Vol 2, 1975, p 728.

277. DeMaria, A. J. "A Multiple Internal-Reflection Folded-Path Optical Maser Geometry," PROC. IEEE, Vol 53, 1965, p 1757.

278. Mikaelyan, A. L.; L'yachenko, V. V. "Phenomenon of Maintaining a Wave Front in Sharply Deformed Solid Media," PIS'MA V ZHETF, Vol 16, 1972, p 25; "Waveguide Type Optical Cavities," KVANTOVAYA ELEKTRONIKA, edited by N. G. Basov, No 5(11), 1972, p 97.

279. Buchenkov, V. A.; Mak, A. A., et al. "Study of Periodic Disk Lasers," KVANTOVAYA ELEKTRONIKA, Vol 2, 1975, p 2037.

280. Swain, J. E.; Kidder, R. E., et al. "Large-Aperture Glass Disk Laser System," J. APPL. PHYS., Vol 40, 1969, p 3973.

281. Simmons, W. W.; Speck, D. R.; Hunt, J. T. APPL. OPTICS, Vol 17, 1978, p 999.

282. Shchavelev, O. S.; Babkina, V. A., et al. "Glass with Small Thermooptical Characteristics P and Q," OPTIKO-MEKHANICHESKAYA PROMYSHLENNOST', No 7, 1976, p 32.

283. Shchavelev, O. S.; Mit'kin, V. M., et al. "Thermooptical Characteristics of Glass as a Function of Temperature," OPTIKO-MEKHANICHESKAYA PROMYSHLENNOST', No 1, 1975, p 30.

APPROVED FOR RELEASE: 2007/02/09: CIA-RDP82-00850R000500010010-4

APPROVED FOR RELEASE: 2007/02/09: CIA-RDP82-00850R000500010010-4

284. Mak, A. A.; Soms, L. N., et al. "Influence of Induced Anisotropy of the Active Element on the Operation of a Neodymium Glass Laser," OPTIKA I SPEKTROSKOPIYA, Vol 30, 1971, p 1081.

285. Libik, L. P.; Koval'chuk, L. V. 'VLIYANIYE KRAYEVYKH EFFEKTOV NA TERMICHESKIYE DEFORMATSII AKTIVNYKH ELEMENTOV PRYAMOUGOL'NOY FORMY. TEZISY DOKLADOV NA I VSESOYUZNOY KONFERENTSII "OPTIKA LAZEROV" [Influence of Edge Effects on Thermal Deformations of Rectangular Active Elements. Topics of Reports at the First All-Union Conference on Laser Optics], Leningrad, 1976, p 38.

286. Linnik, V. P. "Theoretical Possibility of Decreasing the Influence of the Atmosphere on Star Imaging," OPTIKA I SPEKTROSKOPIYA, Vol 3, 1957, p 401.

287. Bridges, W. B.; Brunner, P. T., et al. "Coherent Optical Adaptive Techniques," APPL. OPTICS, Vol 13, 1974, p 291.

288. Pearson, J. E.; Bridges W. B., et al. "Coherent Optical Adaptive Techniques: Design and Performance of an 18-Element Visible Multidither COAT System," APPL. OPTICS, Vol 15, 1976, p 611.

289. Bondarenko, M. D.; Gnatovskiy, A. V.; Soskin, M. S. "Holographic Method of Transformation of Coherent Light Fields," DAN SSSR, Vol 187, 1969, p 538.

290. Soskin, M. S.; Bondarenko, M. D.; Gnatovskiy, A. V. "Holographic Method of Phase-Amplitude Correction of Laser Beams," PIS'MA V ZHETF, Vol 14, 1971, p 27.

291. Bondarenko, M. D.; Gnatovskiy, A. V.; Soskin, M. S. "Holographic Method of Controlling Laser Emission Divergence," KVANTOVAYA ELEKTRONIKA, Kiev, Naukova dumka, No 6, 1972, p 71.

292. Casperson, L. W.; Kincheloe, N. K.; Stafsudd, O. M. Phase Plate for Laser Beam Compensation," OPT. COMMUN., Vol 21, 1977, p 1.

293. Klein, W. R.; Cook, B. D. "Unified Approach to Ultrasonic Light Diffraction," IEEE TRANS. ON SONICS AND ULTRASONICS, Vol SU-14, 1967, p 123.

294. Stasel'ko, D. I.; Sidorovich, V. G. "Light Beam Conversion Efficiency Using Dynamic Volumetric Phase Holograms," ZHTF, Vol 44, 1974, p 580.

295. Zel'dovich, B. Ya. "Nonlinear Optical Effects and Conservation Laws," KRATKIYE SOOBSHCHENIYA PO FIZIKE [Brief Reports on Physics], FIAN SSSR, No 5, 1970, p 20.

296. Kogelnik, H. "Coupled Wave Theory for Thick Hologram Gratings," BELL SYST. TECHN. J., Vol 48, 1969, p 2909.

297. Anan'yev, Yu. A. "Possibility of Dynamic Wave Front Correction," KVANTOVAYA ELEKTRONIKA, Vol 1, 1974, p 1669.

APPROVED FOR RELEASE: 2007/02/09: CIA-RDP82-00850R000500010010-4

APPROVED FOR RELEASE: 2007/02/09: CIA-RDP82-00850R000500010010-4

298. Staebler, D. L.; Amodei, J. J. "Coupled-Wave Analysis of Holographic Storage in $LiNbO_3$," J. APPL. PHYS., Vol 43, 1972, p 1042.

299. Herman, R. M.; Gray, M. A. "Theoretical Prediction of the Stimulated Thermal Rayleigh Scattering in Liquids," PHYS. REV. LETT., Vol 19, 1967, p 824.

300. Wiggins, T. A.; Cho, C. W., et al. "Stimulated Thermal Rayleigh Scattering," PHYS. REV. LETT., Vol 19, 1967, p 828.

301. Wolff, P. A. Theory of Stimulated Light Scattering from Electrons in Semi-Conductors," PROC. 2ND CONF. INT. CONF. LIGHT SCAT. SOL., Paris, 1971, p 180.

302. Bryskin, V. Z.; Groznyy, A. V., et al. "Effective Gain of Weak Light Beams Using Dynamic Volumetric Holograms with Thermal Recording Mechanism," PIS'MA V ZHTF, Vol 2, 1976, p 561.

303. Rother, W.; Pohl, D.; Kaiser, W. "Time and Frequency Dependence of Stimulated Thermal Rayleigh Scattering," PHYS. REV. LETT., Vol 22, 1969, p 915.

304. Dukhovnyy, A. M.; Stasel'ko, D. I. "Efficient Conversion of a Diverging Light Beam to a Plane Wave by a Volumetric Dynamic Hologram with Thermal Mechanism of Recording," PIS'MA V ZHTF, Vol 4, 1978, p 354.

305. Gorlanov, A. V.; Grishmanova, N. I., et al. Nonsteady Self-Diffusion of Laser Beams in an Absorbing Liquid," KVANTOVAYA ELEKTRONIKA, Vol 6, 1979, p 856.

306. Ragul'skiy, V. V. LAZERY NA VYNUZHDENNOM RASSEYANII MANDEL'SHTAMA - BRILLYUENA, TRUDY FIAN SSSR [Stimulated Brillouin Scattering Lasers. Works of the Physics Institute of the USSR Academy of Sciences], Moscow, Nauka, Vol 85, 1976, p 3.

307. Grasyuk, A. Z.; Zubarev, I. P., et al. "Light Gain and Lasing Dynamics in Stimulated Raman Scattering," KVANTOVAYA ELEKTRONIKA, edited by N. G. Basov, No 5(17), 1973, p 27.

308. Kovalev, V. I.; Popovichev, V. I., et al. "Influence of Saturation on Light Gain During Stimulated Brillouin Scattering," ZHETF, Vol 64, 1973, p 2028.

309. Pasmanik, G. A. "Raman Interaction in Incoherent Pumping Beam Field," IZV. VUZOV, RADIO FIZIKA, Vol 17, 1974, p 970.

310. Bespalov, V. I.; Pasmanik, G. A. "Parametric Conversion and Stimulated Incoherent Light Scattering," IZV. VUZOV, RADIOFIZIKA, Vol 19, 1976, p 634.

311. Betin, A. A.; Pasmanik, G. A. "Maintenance of Spatial Coherence of Stokes Beams During Amplification in a Multimodal Pumping Field," PIS'MA V ZHETF, Vol 23, 1976, p 577.

312. Anan'yev, Yu. A. "Author's Claim No 1705404 with Priority as of 12 October 1971, Author's Certificate No 414935."

APPROVED FOR RELEASE: 2007/02/09: CIA-RDP82-00850R000500010010-4

APPROVED FOR RELEASE: 2007/02/09: CIA-RDP82-00850R000500010010-4

313. Kogelnic, H. "Holographic Image Projection Inhomogeneous Media," BELL SYST. TECHN. J., Vol 44, 1965, p 2451.

314. Wang, V.; Giuliano, C. R. "Correction of Phase Distortion via Nonlinear Optical Techniques," IEEE J. OF QUANT.ELECTR., Vol QE-13, 1977, p 83D.

315. Kruzhilin, Yu. I. "Adaptive Laser-Target System for Laser Thermonuclear Fusion," KVANTOVAYA ELEKTRONIKA, Vol 5, 1978, p 625.

316. Zel'dovich, B. Ya.; Popovichev, V. I., et al. "Relation Between Wave Fronts of Reflected and Stimulating Light During Stimulated Brillouin Scattering," PIS'MA V ZHETF, Vol 15, 1972, p 160.

317. Nosach, O. Yu.; Popovichev, V. I., et al. "Compensation of Phase Distortions in an Amplifying Medium Using a 'Brillouin Mirror'," PIS'MA V ZHETF, Vol 16, 1972, p 617.

318. Wiggins, T. A.; Wick, P. V.; Rank, D. H. "Stimulated Effects in N_2 and CH_4 Gases," APPL. OPTICS, Vol 5, 1966, p 1069.

319. Kudryavtseva, A. D.; Sokolovskaya, A. I.; Sushchinskiy, M. M. "Stimulated Raman Scattering and Self-Focusing of Light in Liquid Nitrogen," ZHETF, Vol 59, 1970, p 1557.

320. Zel'dovich, B. Ya.; Mel'nikov, N. A., et al. "Observation of the Effect of Wave Front Inversion During Stimulated Raman Scattering of Light," PIS'MA V ZHETF, Vol 25, 1977, p 41.

321. Sokolovskaya, A. I., Brekhovskikh, G. L.; Kudryavtseva, A. D. "Wave Front Reconstruction of Light Beams with Induced Raman Scattering of Light," DAN SSSR, Vol 233, 1977, p 356.

322. Sidorovich, V. G. "Brillouin Mirror Theory," ZHTF, Vol 46, 1976, p 2168.

323. Zel'dovich, B. Ya.; Shkunov, V. V. "Limits of the Existence of the Wave Front Reversal Effect During Induced Scattering of Light," KVANTOVAYA ELEKTRONIKA, Vol 5, 1978, p 36.

324. Hellwarth, R. W. "Generation of Time-Reversed Wave Fronts by Nonlinear Refraction," JOSA, Vol 67, 1977, p 1.

325. Yariv, A.; Pepper, D. M. "Amplified Reflection, Phase Conjugation and Oscillation in Degenerate Four-Wave Mixing," OPTICS LETT., Vol 1, 1977, p 16.

326. Odulov, S. G.; Sal'kova, Ye. N., et al. "Elimination of Laser Beam Distortions Induced in Amplifiers by the Methods of Dynamic Holography," UKR. FIZICH. ZH. [Ukrainian Physics Journal], Vol 23, 1978, p 562.

327. Akhmanov, S. A.; Khokhlov, R. V. PROBLEMY NELINEYNOY OPTIKI [Problems of Nonlinear Optics], Moscow, Nauka, 1964.

APPROVED FOR RELEASE: 2007/02/09: CIA-RDP82-00850R000500010010-4

APPROVED FOR RELEASE: 2007/02/09: CIA-RDP82-00850R000500010010-4

328. Yariv, A. "Compensation for Atmospheric Degradation of Optical Beam Transmission by Nonlinear Optical Mixing," OPT. COMMUN., Vol 21, 1977, p 49.

329. Shostko, S. N.; Podoba, Ya. G.; Anan'yev, Yu. A., et al. "A Possibility of Compensating Optical Nonuniformities in Lasers," PIS'MA V ZHTF, Vol 5, 1979, p 29.

330. Hunf, J. T.; Renard, P. A.; Simmons, W. W. "Improved Performance of Fusion Lasers Using the Imaging of Multiple Spatial Filters," APPL. OPTICS, Vol 16, 1977, p 779.

331. Denisyuk, Yu. N. "Imaging of the Optical Properties of an Object in the Wave Field of Emission Scattered by the Object," OPTIKA I SPEKTROSKOPIYA, Vol 15, 1963, p 522.

332. Isayev, A. A.; Kazaryan, M. A., et al. "Process of Formation of the Output Beam in a Pulsed Gas Laser with Unstable Resonator," KVANTOVAYA ELEKTRONIKA, Vol 4, 1977, p 1325.

333. Goryachkin, D. A.; Kalinin, V. P., et al. "Properties of Unstable Resonators with Field Reversal. III. Experimental Results," KVANTOVAYA ELEKTRONIKA, Vol 6, 1979, p 1880.

334. "Adaptive Optics," JOSA, Vol 67, 1977, pp 269-409.

335. Anan'yev, Yu. A.; Gorlanov, A. V., et al. "Phenomenon of Nonsteady Self-Diffraction of Coherent Light Beams in an Absorbing Fluid," KVANTOVAYA ELEKTRONIKA, Vol 6, 1979, p 1813.

336. Anan'yev, Yu. A.; Goryachkin, D. A., et al. "Study of the Properties of a Laser with Unstable Resonator and Additional Feedback," KVANTOVAYA ELEKTRONIKA, Vol 6, 1979, p 1773.

337. Allen, L.; Aberly, J. OPTICHESKIY REZONANS I DVUKHUROVNEVYYE ATOMY. [Optical Resonance and Two-Level Atoms], Moscow, Mir, 1978.

338. Lyubimov, V. V.; Orlova, I. B. "Influence of the Shape of the Edge of Mirrors on the Selective Characteristics of Unstable Resonators," OPTIKA I SPEKTROSKOPIYA, Vol 41, 1976, p 288.

339. Bespalov, V. I.; Kubarev, A. M. "Report at the Second All-Union Symposium on Nonlinear Optics," Novosibirsk, 1966, NELINEYNAYA OPTIKA [Nonlinear Optics], Novosibirsk, Nauka, 1968.

340. Bespalov, V. I.; Betin, A. A.; Pasmanik, G. A. IZV. VUZOV. RADIOFIZIKA [News of the Institutions of Higher Learning. Radio Physics], Vol 20, 1977, p 791; Vol 21, 1978, p 961.

341. Woerdman, J. P. OPT. COMMUN., Vol 2, 1970, p 212; PHILIPS RES. REPTS SUPPL., No 7, 1971, p 58.

APPROVED FOR RELEASE: 2007/02/09: CIA-RDP82-00850R000500010010-4

APPROVED FOR RELEASE: 2007/02/09: CIA-RDP82-00850R000500010010-4

342. Stepanov, B. I.; Ivakin, Ye. V.; Rubanov, A. S. "Recording Two and Three-Dimensional Dynamic Holograms in Transparent Substances," DAN SSSR, Vol 196, 1971, p 567.

COPYRIGHT: "Nauka" Glavnaya redaktsiya fizikomatematicheskoy literatury, 1979

10845
CSO: 8144/1776

- END -

APPROVED FOR RELEASE: 2007/02/09: CIA-RDP82-00850R000500010010-4